

**SYNTHETIC STUDIES ON NOVEL BRYOSTATIN ANALOGUES AND
THEIR INTERACTION WITH THE CRD2 OF PROTEIN KINASE C**

by

Mark Frigerio

A thesis presented to the University of London in part fulfilment of the
requirements for the degree of Doctor of philosophy

September 2003

The Christopher Ingold Laboratories
Department of Chemistry
University College London

UMI Number: U602790

All rights reserved

INFORMATION TO ALL USERS

The quality of this reproduction is dependent upon the quality of the copy submitted.

In the unlikely event that the author did not send a complete manuscript and there are missing pages, these will be noted. Also, if material had to be removed, a note will indicate the deletion.



UMI U602790

Published by ProQuest LLC 2014. Copyright in the Dissertation held by the Author.
Microform Edition © ProQuest LLC.

All rights reserved. This work is protected against
unauthorized copying under Title 17, United States Code.



ProQuest LLC
789 East Eisenhower Parkway
P.O. Box 1346
Ann Arbor, MI 48106-1346

Dedicated with love to my parents

ACKNOWLEDGEMENTS

I would like to express my sincere thanks to Professor Karl J. Hale for his invaluable help and excellent guidance throughout this study. His willingness to make time for you in a busy schedule, and his eagerness to explain problems will not be forgotten.

I would also like to thank my colleagues in the chemistry department for their help, advice and support, and for their friendship over the years, especially Marc, Pascal, Gurpreet, Shahid, Linos, Marcus, Maxine, Sven, Ying and Soraya.

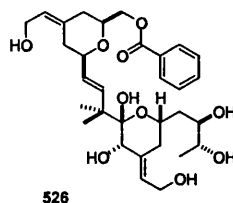
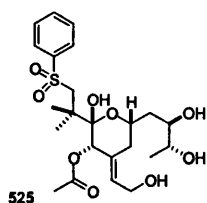
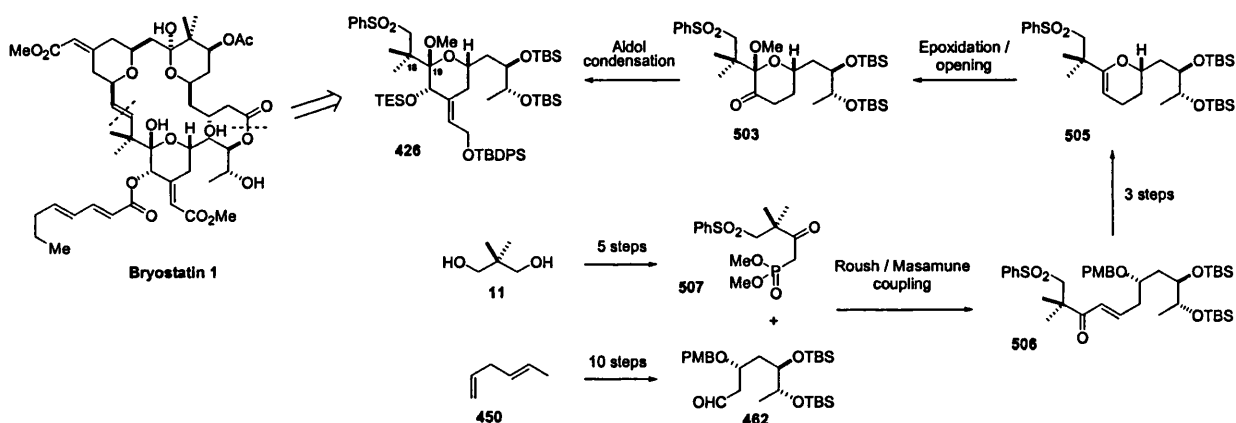
I am also grateful to all the technical staff for all their help and advice, especially Dr Abil Aliev, David Knapp and Mike Cocksedge and staff at the London School of Pharmacy for HRMS.

Finally a special thanks to all my friends and family who gave me both advice and encouragement, and for their patience with me, especially Abbe, Jessica, Freya, Amit, Paddy, Ivan, Luisa, Matthew, Susie, Alex, and most importantly my parents to whom this thesis is dedicated.

ABSTRACT

A fully stereocontrolled asymmetric synthesis of the Southern Hemisphere intermediate **426** for the bryostatin family of antitumour agents is described in this thesis. It details how the strategy evolved from (*E*)-1,4-hexadiene **450** including a Roush-Masamune coupling between **462** and **507**, cyclisation to glycal **505**, selective epoxidation and in-situ Fischer glycosidation to **503** and an aldol / dehydration sequence to establish the (*E*)-exocyclic olefin. We also document a rare example of slow bond rotation in the C(18)-C(19)-bond of **426** and provide an explanation of this phenomenon.

In addition, the synthesis of two truncated bryostatin analogs **525** and **526** is described, and the interaction of **525** with the CRD2 of human PKC- α discussed.

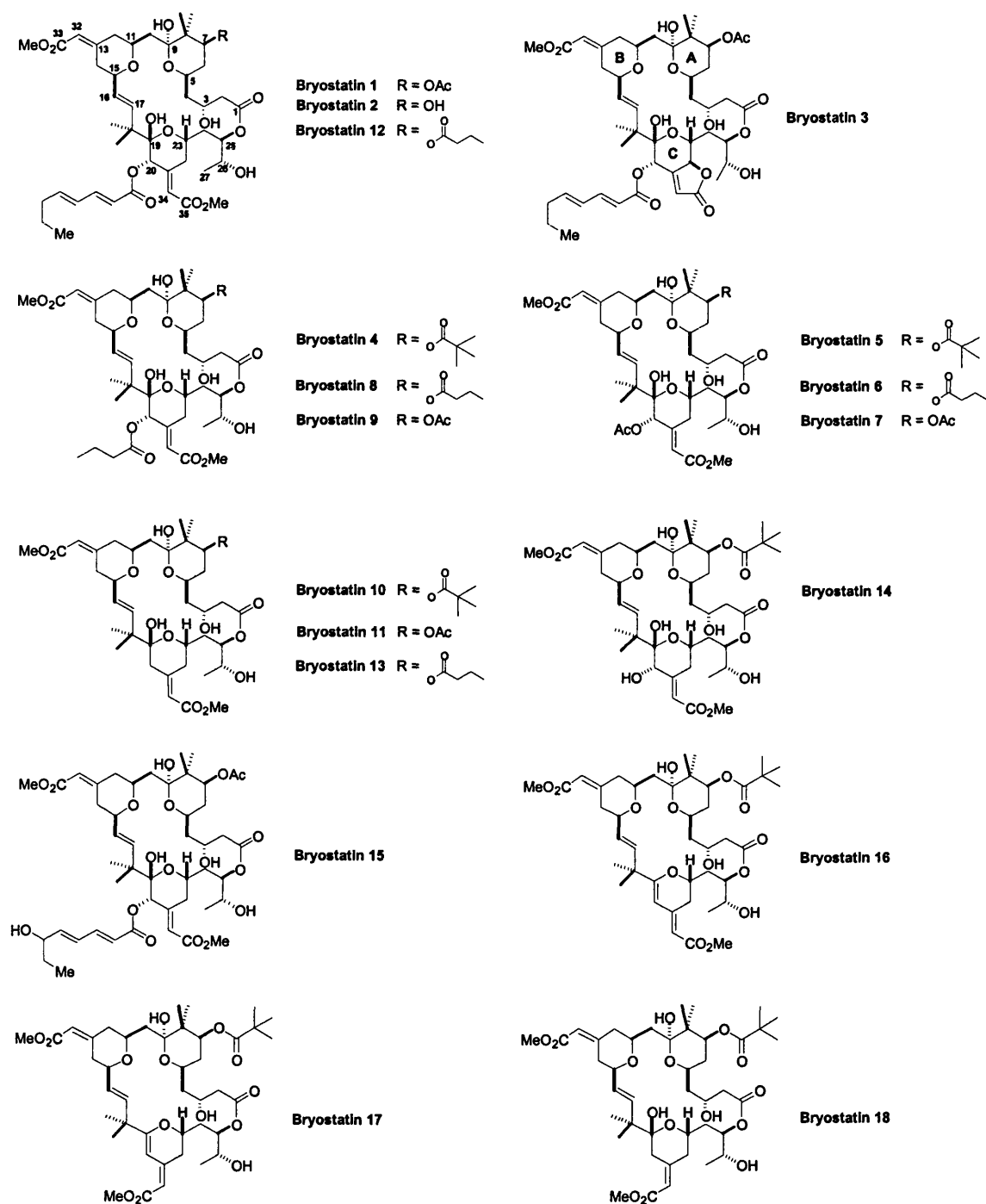


CONTENTS

Acknowledgements	i
Abstract	ii
Contents	iii
1. INTRODUCTION	
1.1 Biosynthesis of bryostatin 1	2
1.2 Bryostatin biology	3
1.3 Bryostatin total synthesis	8
1.3.1 Masamune's enantioselective total synthesis of bryostatin 7	8
1.3.2 The Evans enantioselective total synthesis of bryostatin 2	14
1.3.3 The Nishiyama-Yamamura total synthesis of bryostatin 3	22
1.4 Synthetic studies on the bryostatins	28
1.4.1 Thomas's synthetic route to bryostatin 11	28
1.4.2 Vandewalle's synthetic studies on bryostatin 11	32
1.4.3 R. W. Hoffmann's racemic route to the C(1)-C(9) segment 267	37
1.4.4 The Kalesse enantioselective route to the C(1)-C(9)-segment 257	38
1.4.5 The Kiyooka reagent-controlled asymmetric route to the C(1)-C(9)-segment	38
1.4.6 Roy's synthetic studies on bryostatin 1	39
1.4.7 The H.M.R. Hoffmann route to the C(1)-C(16) AB-segment of bryostatin	41
1.4.8 Janda's polymer-supported synthesis of the bryostatin 1 C(21)-C(27)-sector	44
1.4.9 Yadav's synthesis of the bryostatin "Northern Hemisphere"	45
1.5 Synthesis of bryostatin analogues	49
1.5.1 Wender's analogue work	49
1.6 Mendola's aquaculture solution to the bryostatin 1 supply problem	55
1.7 Hale's synthetic work on the bryostatins	56
2.0 DISCUSSION	
2.1 Continuation of the first generation synthesis	62
2.2 Modified retrosynthetic analysis of the bryostatin C-ring	66

2.3	An alternative approach to the bryostatin C-ring	73
2.4	Synthesis of bryostatin analogues	85
2.5	Synthetic studies on bryostatin 7	95
3.0	EXPERIMENTAL	
3.1	Detailing the synthetic routes described in Schemes 53 and 54	100
References		
Abbreviations		
Appendices		

1. INTRODUCTION



Scheme 1 The bryostatin family of antitumour macrolides.

The bryostatins (Scheme 1) are a structurally novel family of marine macrolides whose prototype, bryostatin 1, was first isolated in 1968 from the bryozoan invertebrate *Bugula neritina* Linnaeus by Pettit and

coworkers, in their search for new anti-cancer drugs ¹. Several years later a number of other family members were isolated from *Amathia convulata*. Both marine animals are colonial filter feeders, known for their ability to attach to ships hulls. So far 18 members of the bryostatin family have been isolated from collections of both organisms. These bryozoans are found in the Gulf's of Mexico, California and Sagami off Japan.

It was not until 1982, that the structure of bryostatin 1 was eventually deduced by detailed spectroscopic and X-ray crystallographic analysis. This revealed some interesting functionality embedded in the bryostatin array. All of the bryostatins possess a 20-membered macrolactone containing three pyran rings and an (*E*)-disubstituted olefin. Two of the pyrans also contain hemiketals in the A and C rings, and always, the A and B pyrans are bridged by a methylene unit. Geminal dimethyl groups at C(8) and C(18) are always present, as is the C(24)-C(27) side chain. B- and C-ring exocyclic methyl enoates are also present in all but bryostatin 3, which has an extra stereocentre at C(22) which ties up the enoate as a butanolide. Most of the differences between the various bryostatin family members lie in the remote ester functionality at the C(7) and C(20) positions. Further structural differences can be found in bryostatins 16 and 17 which have a glycol at C(19)-C(20). Also bryostatins 17 and 18 have opposite methyl enoate geometry in the C-ring.

1.1 Biosynthesis of bryostatin 1

Through radiolabelling experiments, Kerr and coworkers ² have shown that acetate, glycerol and *S*-adenosylmethionine (SAM) are all key building blocks in the biosynthesis of bryostatin 1; Propionate, *n*-butyrate, isobutyrate and succinate are not required for its biosynthesis. The geminal dimethyl groups are thought to originate from series of a SAM methylations on the corresponding acetate units, as was observed for the biosynthesis of lankacidin and aplasmomycin. The exocyclic olefin units possibly arise from the addition of acetate to a polyketide chain, followed by dehydration. The exact sites where the radiolabelled precursors are being incorporated are presently under investigation by Kerr, and further are eagerly awaited.

1.2 Bryostatin biology^{3,4}

1.2.1 The antitumour profile of bryostatin 1

Bryostatin 1 shows remarkable *in vitro* and *in vivo* antitumour effects against a range of mouse cancer cell lines that include P388 lymphocytic leukaemia, ovarian sarcoma⁵, B16 melanoma^{6, 7}, and M5076 reticulum cell sarcoma. Moreover when bryostatin 1 was administered alongside auristatin PE and dolastatin 10, a successful cure of 7/10 SCID mice, with chronic human lymphocytic leukaemia xenographs was achieved⁸.

Bryostatin 1 has recently completed a large number of anticancer trials in man^{9, 10}. Its most noteworthy anticancer effects were seen against ovarian cancer and relapsed non-Hodgkin's lymphoma. Its total cure of a 41 year old woman with stage 4 follicular small-cell-cleaved non-Hodgkin's lymphoma was of particular interest. This patients disease had recurred at multiple sites five years after originally having been brought into remission with alkylator drug therapy. The treatment regime that elicited this cure consisted of eight fortnightly cycles of bryostatin 1 by 72 h intravenous infusion at a dose of 120 $\mu\text{g m}^{-2}$. Although this represents the only cure to date, bryostatin 1 has brought about many partial remissions. The main side-effect of bryostatin 1 treatment is myalgia¹¹.

1.2.2 Mechanisms of antitumour action

The antitumour effects of bryostatin 1 have been linked to its ability to selectively modulate the functioning of protein kinase C (PKC) isozymes within cells¹². PKC's are serine and threonine kinases that play a pivotal role in the O-phosphorylation of proteins involved in the signal transduction pathways^{13, 14} that control cell growth and proliferation. Their over- or under- expression is linked with the transition of some tissues into malignancy. This observation was first made by Mushinski and coworkers, when they noticed that over-expression of η -PKC- ϵ in NIH 3T3 cells made them highly neoplastic and tumourigenic towards mice¹⁵. The elevation of η -PKC- ϵ levels in rat fibroblasts¹⁶ also renders them malignant and tumourogenic, while over-expression of PKC- β makes them highly susceptible to transformation with the Ha-*ras* oncogene. Both Ha-*ras* and c-*myc* oncogenes serve to increase PKC- β II levels in the cotransfection of human small-cell lung carcinoma, and this has been correlated to their conversion to a

much more malignant large-cell phenotype. It has also been reported that in human A549 lung cancer cells, cPKC- α levels are higher than in healthy neighbouring tissue ¹⁷, suggesting that up-regulation of PKC might be contributing to onset of this particular cancer. PKC activity is also significantly raised in human breast cancer tissue when compared to nearby normal tissue. Collectively, these results strongly suggest that the up-regulation of PKC signalling could be contributing to the onset of a range of tumours.

Because bryostatin 1's ability to inhibit human A549 lung and MCF-7 breast cancer cells correlates closely with its down-regulation of PKC- α , an extrapolation to the PKC isozymes of many other cell types seemed logical for explaining its mechanism of action. However, that this extrapolation cannot be made can be seen from bryostatin 1's protection of some PKC- δ s from down-regulation; this leading to tumour growth inhibition. PKC- δ levels appear to play a decisive role in determining whether cells become cancerous; their degree of expression frequently deciding whether a cell undergoes growth-arrest and proliferation. This is evident from the over-expression of PKC- δ in mouse keratinocytes which result in apoptosis ¹⁸, and in its overexpression in NIH 3T3 cells which halts their proliferation ¹⁹. Here PKC- δ is believed to function as an efficient tumour suppresser. PKC- δ can also nullify the effects of an over-expressed c-src-proto-oncogene in 3Y1 fibroblasts, preventing them from undergoing transformation ²⁰. By way of contrast, PKC- δ under-expression in some cells has been correlated with a greatly enhanced rate of growth ²¹. The fact that bryostatin can prevent PKC- δ from undergoing down-regulation in mouse keratinocytes and human fibroblasts ²² suggests that bryostatin might be inhibiting the growth of some tumours via a PKC- protective, or stabilising mechanism ²³.

Thus it would appear that bryostatin acts upon the individual PKC isozymes in a highly tissue-specific manner and this therefore complicates our ability to rationalise many of its observed antitumour effects by a single, all-encompassing, and general mechanism.

Bryostatin 1 competitively binds to the phorbol ester-diacylglycerol binding sites of PKC isozymes at two highly conserved regions known as the cysteine-rich domains 1 and 2 (CRD's 1 and 2). The three-dimensional structures of several CRD's have now been elucidated. There is an NMR solution structure for a murine PKC- α CRD2 construct ²⁴, and a 2.2 Å resolution X-ray crystal structure of phorbol-13-acetate complexed PKC- δ CRD2 ²⁵. The crystallographic data have confirmed that the tumour promoting phorbol ester sits in a polar groove that exists between two opened β -strands at one tip of the CRD, and that this complexation does not produce significant conformational changes in the PKC activator domain. It appears

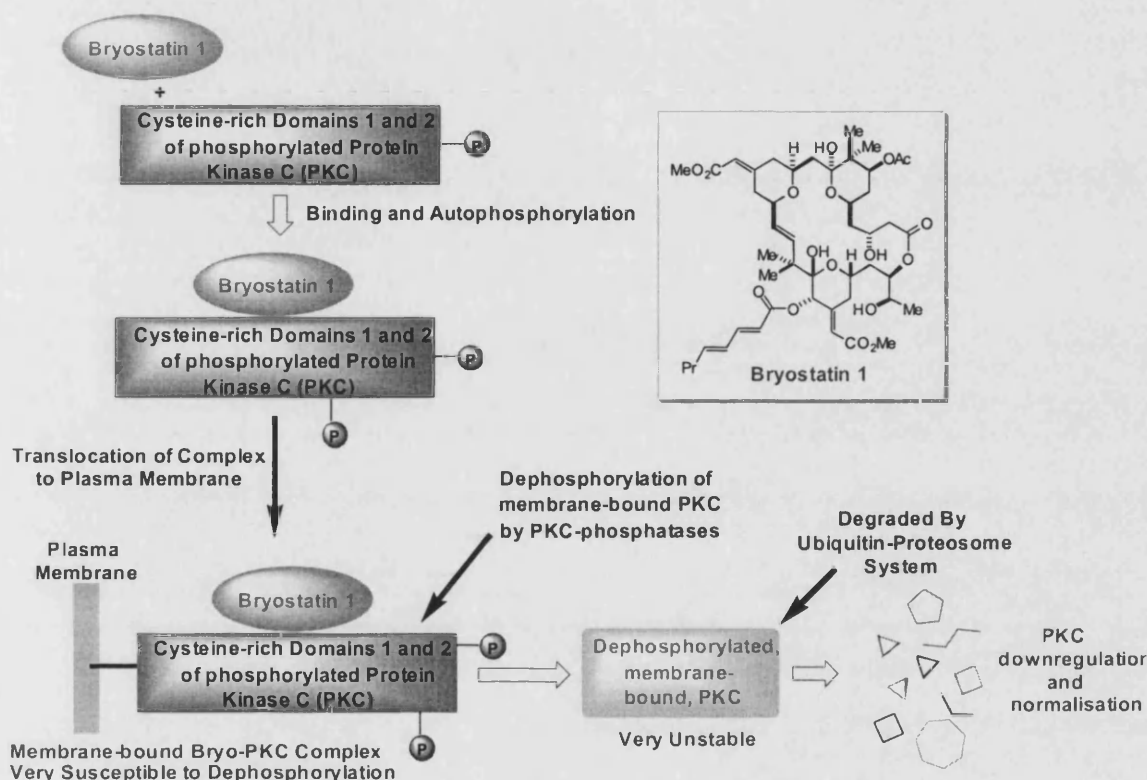
that once the phorbol ester is bound to the protein, it creates a long continuous hydrophobic surface that covers approximately one third of the protein. The enhanced hydrophobicity of the phosphorylated PKC- δ -phorbol ester complex has led to the proposal that this promotes its translocation from the cytoplasm plasma and nuclear membranes to mediate specific signals within the cell that include tumour propagation. Similar increases in lipophilicity are also thought to occur when bryostatin 1 becomes bound to the CRDs of PKCs, although in this case it is likely that different conformational changes are elicited in the target in the PKCs compared with the phorbol esters. It is thought that when bryostatin 1 binds to PKC- δ s, it induces a “stabilising” conformational change in the enzymes that prevents them being degraded by the ubiquitin proteasome. However, when bound to phosphorylated PKCs that are down-regulated by bryostatin, the complexation is thought to induce a conformational change that favours the insertion of the protein into the cell, and subsequent ubiquitination.

In this regard, the way in which bryostatin down-modulates PKC- α in renal epithelial cells, and PKC- α and PKC- ϵ in human fibroblasts, has been elucidated by Bingham Smith and coworkers ²⁶, elegant ³²P-labelling studies. They have shown that for these two cell lines, PKC down-modulation proceeds through the ubiquitin-proteasome pathway (Scheme 2). Soon after bryostatin 1 complexes to PKC, autophosphorylation occurs, resulting in the translocation of the drug-protein complex from the cytosol into the plasma membrane. Once embedded, the complex is apparently rendered susceptible to dephosphorylation by the membrane bound alkaline phosphatases, yielding a catalytically inactive form of the PKC protein. The inactive membrane-bound PKC is then degraded by the ubiquitin-proteasome causing PKC down-regulation.

The ability of bryostatin 1 to bind selectively to different PKC isoforms and therefore to render them susceptible or non-susceptible to undergoing down-regulation within cells is probably central to many of its observed antitumour effects. For some cancers, the down-regulatory ability of bryostatin 1 to arrest a particular up-regulated PKC pathway might be the critical requirement; for others, a bryostatin-mediated PKC-up-regulation might be all that is needed to correct the tumourigenic state.

It has been recently demonstrated that PKC- β isozyme levels can greatly affect whether some cells rest or proliferate. This is significant because bryostatin 1 is capable of selectively targeting PKC- β IIs in both human erythroleukaemia (K562) and promyelocytic (HL60) cells. After complexation, bryostatin-PKC- β complexes selectively insert into the nuclear membrane and phosphorylate lamin B at the Ser-395

and Ser-405 residues²⁷. This phosphorylation is associated with the disassembly and increased solubilisation of the nuclear lamina network during mitosis. It causes a breakdown of the nuclear envelope, and enhances proliferation of these cells. Thus, in some cell types bryostatin might prove to be tumourogenic.



Scheme 2 Mechanism by which bryostatin downregulates PKC- α and PKC- ϵ in human fibroblasts.

The majority of the biological research on bryostatin 1 has attributed its antitumour effects to its interactions with various PKC isozymes, although there is gathering evidence which suggests that bryostatin 1 is able to function as a powerful immunostimulant. Indeed, it has been suggested that this might be the primary means by which bryostatin 1 exerts its antitumour properties in some patients²⁸. Bryostatin 1 readily activates resting human T-cells and neutrophils²⁹ both *in vitro* and *in vivo*³⁰, and in a number of patients, it has also been shown to raise the levels of tumour-necrosis factor (TNF); a powerful tumouricide produced by the body in response to immunostimulation. Bryostatin 1 can also induce the rapid release of TNF from MONO-MAC-6 cells³¹. It can also significantly increase TNF mRNA expression and production in the murine macrophage ANA-1 cell line. This enabled bryostatin 1 to synergise with INF in the

production of $[\text{NO}_2]^-$ and in the expression of the nitric oxide synthase (*i*-NOS) gene, which catalyses the *in vivo* production of NO from L-arginine. In turn, this confers powerful tumouricidal effects upon murine macrophages. The production of NO is known to induce apoptosis in tumour cells³². These results very clearly support the idea that bryostatin 1 could be exerting some of its antitumour effects via an immunostimulatory mechanism.

While C(20)-oxygenated bryostatins 1, 3, 8 and 9 are all capable of activating neutrophil chemiluminescence and the cytotoxic killing of K562 cells, no such data exists for a member of the C(20)-deoxy class. Bryostatin 13, which is reported to be amongst the most potent antitumour agents in the bryostatin family, is incapable of mimicking their ability to stimulate colony formation from bone marrow progenitor cells³³. This suggests that while an immunostimulatory antitumour mechanism might be significant for the C(20)-O-acyl bryostatins, a similar mode of action is unlikely for the C(20)-deoxygenated bryostatins.

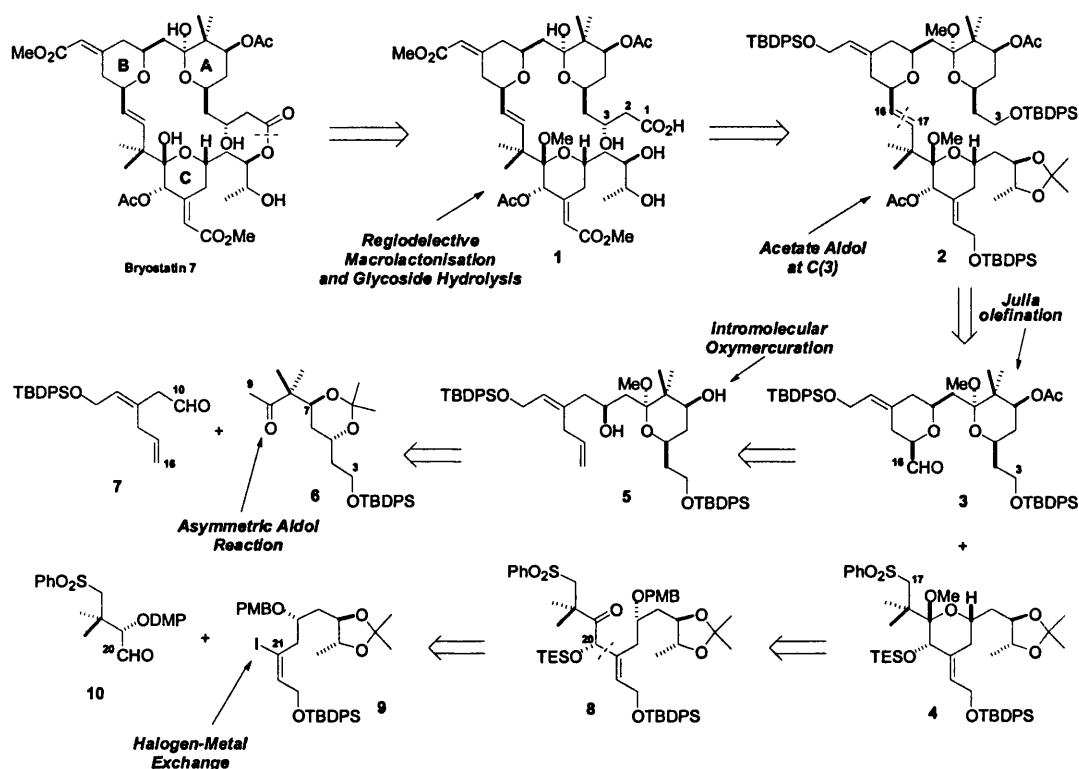
The many divergent actions of the bryostatins on the numerous PKCs, along with the ability of certain family members to function as immunostimulants, mean that a singular, overall mechanism of antitumour action is unlikely to ever be proposed. The data gathered from the numerous human trials has suggested that the efficacy of bryostatin 1 varies from patient to patient, it depending both on the cancer cell type and on the PKC content of the patients cell.

This overall somewhat contradictory behaviour of bryostatin towards PKCs can be exploited in a clinical programme that would involve initial *in vitro* screening of the patients before therapy is commenced. This could establish whether bryostatin 1 would have a realistic chance of success.

There is an urgent need for significant quantities of the bryostatins, due to the scarcity of a natural supply, and this has attracted significant interest in their chemical synthesis. To date only three members of the bryostatin class have succumbed to total synthesis, although in the myriad of chemical transformations carried out in the name of bryostatin research, much headway has been made in the probing of the bryostatin mode of action.

1.3 Bryostatin total synthesis ³⁴1.3.1 Masamune's enantioselective total synthesis of bryostatin 7 (1990) ³⁵

1.3.1.1 Masamune's retrosynthetic strategy for bryostatin 7



Scheme 3 Masamune's retrosynthetic planning for bryostatin 7.

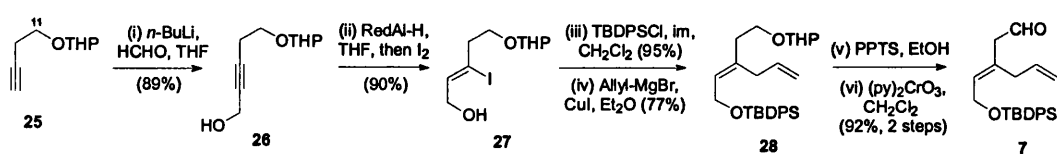
There were a number of key elements in the tactical planning employed by Masamune and coworkers for their proposed approach to bryostatin 7 (Scheme 3). Their strategy was predicted upon the regioselective macrolactonisation of seco-acid **1** for 20-membered macrolide ring assembly. It also called for installation of the C(3)-hydroxyl via the use of a reagent-controlled acetate aldol reaction, which would also serve to introduce the C(1) and C(2) carbons of the polyketide framework. Connection of the three pyran segments and construction of the sterically inhibited C(16)-C(17)-*trans*-alkene would be accomplished by Julia olefination ³⁶. Assembly of the B-ring would rely upon a chemoselective oxymercuration of the less hindered olefin ³⁷ in diene **5**, and a borolane-mediated asymmetric aldol reaction was envisioned for uniting the A- and B-ring sections. Sulfone **4** looked accessible from the open chain ketone **8** by addition of a vinylmetallic to the chiral α -alkoxy aldehyde **10**. Central to this plan, of course,

11 $\xrightarrow[\text{(ii) CrO}_3, \text{Py, CH}_2\text{Cl}_2 \text{ (50\%)}]{\text{(i) NaH, DMF, BnCl, RT, 14 h (52\%)}}$ 12 $\xrightarrow[\text{(iv) DIBAL-H}]{\text{(iii) (EtO)}_2\text{(P=O)CH}_2\text{CO}_2\text{Et, NaH}}$ 13 $\xrightarrow[\text{(vii) Ph}_3\text{P=CHCHO, C}_6\text{H}_6]{\text{(vi) (COCl)}_2, \text{Me}_2\text{SO, -78}^\circ\text{C, Et}_3\text{N, then } 0^\circ\text{C}}$ 14 $\xrightarrow{\text{(x) RedAl-H}}$ 15 $\xrightarrow[\text{(xi) PPTS, (OMe)}_2\text{CMe}_2]{\text{(xi) TBDPSCI, Imidazole}}$ 16 $\xrightarrow[\text{(xiv) (COCl)}_2, \text{Me}_2\text{SO, -78}^\circ\text{C, Et}_3\text{N, then } 0^\circ\text{C}]{\text{(xiii) Na, liquid NH}_3}$ 17 $\xrightarrow[\text{(xvi) (COCl)}_2, \text{Me}_2\text{SO, -78}^\circ\text{C, Et}_3\text{N, then } 0^\circ\text{C}]{\text{(xv) MeLi (45\% for 5 steps)}}$ 18 $\xrightarrow[\text{(R,R) 18}]{\text{(xvii) (R,R) 18, } i\text{-Pr}_2\text{NEt, Et}_2\text{O}}$ 19 $\xrightarrow[\text{(xix) Hg(OAc)}_2, \text{THF, MeOH, then KCl}]{\text{(xviii) (MeO)}_3\text{CH, MeOH, PPTS}}$ 20 $\xrightarrow[\text{(xx) Ac}_2\text{O, py, DMAP}]{\text{(xxi) NaBH}_4, \text{O}_2, \text{DMF/CH}_2\text{Cl}_2}$ 21 $\xrightarrow[\text{(xxii) (COCl)}_2, \text{Me}_2\text{SO, -78}^\circ\text{C; then Et}_3\text{N, } 0^\circ\text{C}]{\text{(xxiii) Al}_2\text{O}_3 \text{ (3\% H}_2\text{O), CH}_2\text{Cl}_2}$ 22 $\xrightarrow[\text{(xxiv) Al}_2\text{O}_3 \text{ (3\% H}_2\text{O), CH}_2\text{Cl}_2]{\text{(xxv) (MeO)}_3\text{CH, MeOH, PPTS}}$ 23 $\xrightarrow[\text{(xxvi) (MeO)}_3\text{CH, MeOH, PPTS}]{\text{(xxvii) (MeO)}_3\text{CH, MeOH, PPTS}}$ 24 $\xrightarrow[\text{(xxviii) (MeO)}_3\text{CH, MeOH, PPTS}]{\text{(xxviii) (MeO)}_3\text{CH, MeOH, PPTS}}$ 3

For the preparation of methyl ketone **6** (Scheme 4), an expedient pathway for constructing the 1,3,5- hydroxy array was the primary concern. Previously, during their work on the antifungal agent amphotericin B ³⁹, Masamune and Sharpless had devised a powerful solution for this general synthetic problem. Their protocol generated an appropriate chiral 2,3,4,5-*bis*-epoxy alcohol via the AE, and thereafter implemented a regioselective ring-opening at the C(2) and C(4) positions with REDAL ⁴⁰. The desired

epoxide **14**, required for assembly of the A-ring was prepared in nine steps from 2,2-dimethylpropane-1,3-diol **11** (Scheme 4). Diol **11** was converted to the aldehyde **12** by selective O-benzoylation and oxidation. A Wadsworth-Horner-Emmons (WHE) olefination, DIBAL ester reduction and Sharpless AE delivered the 2,3-epoxy alcohol **13** in 92% ee. Swern oxidation of **13**, chain extension via a Wittig olefination, and borohydride reduction delivered the desired allylic alcohol substrate. A second AE was performed, which enhanced the de of the bis-epoxide **14** to 99%. As expected, treatment with REDAL promoted a regiospecific alkoxide-directed ring-opening to deliver **15** as a single reaction product. Primary O-silylation and acetonide formation completed triol protection to yield **16**. A Birch O-benzyl reduction followed by Swern oxidation, methyllithium addition, and a second Swern oxidation concluded the sequence to methyl ketone **6**.

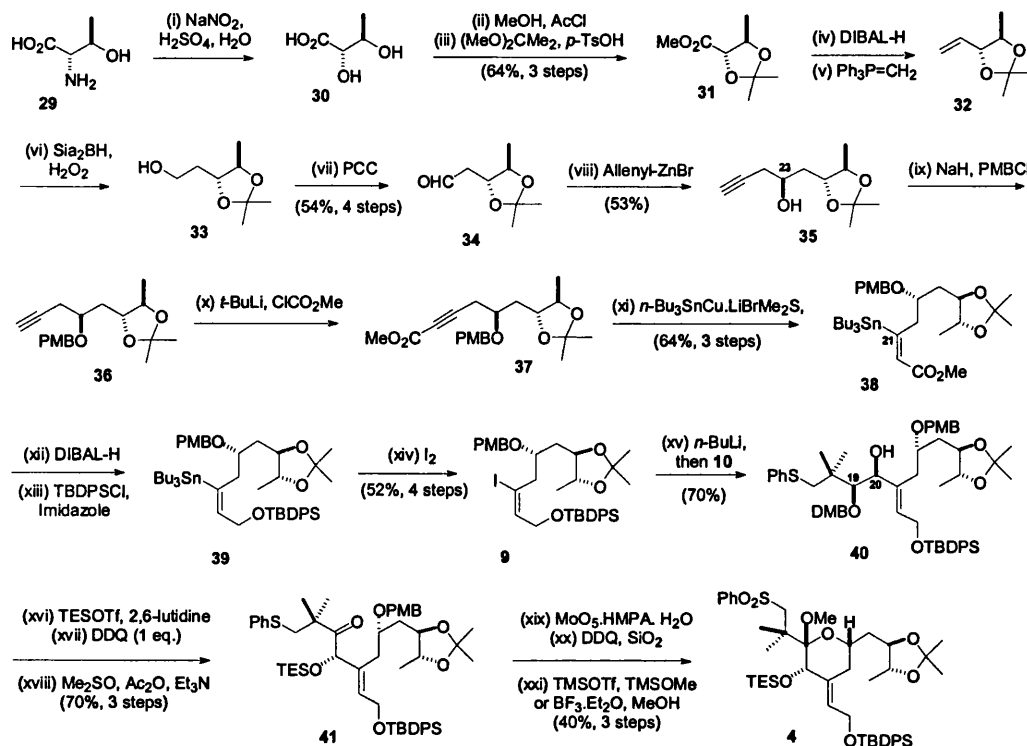
The chiral boron enolate **19** was produced by treatment of ketone **6** with the (*R,R*)-borolane triflate **18** and Hunigs base. It combined readily with the dienyl aldehyde **7** to furnish the desired β -hydroxy ketone **20** with 8:1 selectivity. Fischer glycosidation of **20** with MeOH, PPTS and trimethylorthoformate isopropylidene cleavage and instigated pyran formation to deliver the α -methyl glycoside **5**. An intramolecular oxymercuration, C(7) O-acetylation, and free radical oxidative demercuration aided B-ring cyclisation. Unfortunately this resulted in a 1:1 mixture of alcohols **23**, epimeric at C(15). This adverse stereochemical outcome could, however, be redressed by Swern oxidation to aldehyde epimers **24**, and equilibration with alumina, which thus provided **3** as the major component of a 9:1 mixture at C(15).



Scheme 5 Masamune's synthesis of the C(11)-C(16) B-ring fragment **7**.

The route to aldehyde **7** (Scheme 5) began with addition of **25** to formaldehyde, which subsequently allowed a Corey trisubstituted olefin synthesis⁴¹ to be applied to obtain the (*Z*)-iodo allylic alcohol **27**. After O-silylation, copper catalysed allyl Grignard addition formulated the requisite C(11)-C(16) segment **28**. Cleavage of the THP protecting group, followed by a Collins oxidation, yielded **7**.

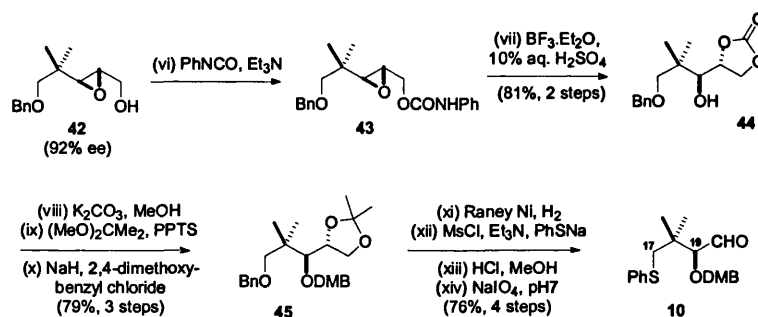
1.3.1.3 Synthesis of the C(17)-C(27) segment 4



Scheme 6 Masamune's route to the bryostatin 7 "Southern Hemisphere".

The coupling strategy proposed for **4** utilised fragments **9** and **10** as important intermediates (Schemes 6 and 7). Firstly the vinyl iodide **9** was assembled from L-threonine **29**. The desired C(25)-C(26) hydroxy stereocentres were set after amine diazotisation; this was followed by O-esterification and O-isopropylidination to acquire methyl ester **31**⁴². DIBAL reduction to the aldehyde next facilitated a carbon homologation via Wittig olefination with methylenetriphenylphosphorane. Conversion of alkene **32** into alcohol **33** was achieved by hydroboration and oxidative work-up; this was then further oxidised to aldehyde **34**. A chelation-controlled coupling with allenylzinc bromide elaborated the necessary acetylenic unit required for manipulation to the exocyclic olefin, and also set the C(23) stereocentre with 8:1 selectivity. The influence of coordination to the C(26) alkoxy group in order to achieve high levels of selectivity is of note, as β -alkoxy aldehydes are not normally considered good substrates for the chelation-controlled nucleophilic additions of organometallic reagents.

Protection of the hydroxyl in **35** as a PMB ether allowed the alkyne to be homologated with *t*-BuLi and methyl chloroformate to produce the alkynyl ester **37**. The (*E*)-vinyl-stannane was prepared by stereoselective stannylcupration⁴³. Ester reduction of **38** with DIBAL and protection provided **39**, which then underwent a halogen-metal exchange with iodine to yield vinyl iodide **9**. Treatment of **9** with *n*-BuLi afforded a vinyl lithium species that added readily to aldehyde **10** providing a 6:1 mixture of alcohols at C(20), enhanced in the desired chelation-controlled product **40**. An *O*-triethylsilylation, followed by selective removal of the DMP group and oxidation yielded the ketone **41**. MoOPH oxidation of the thioether introduced the sulfone unit under conditions which left the double bond intact. Removal of the PMB group released the δ -hydroxy ketone and cyclisation to the hemiketal was achieved via mild acid treatment. Final conversion to the methyl glycoside **4** was accomplished by exposing the hemiketal mixture to Me₃SiOMe and Me₃SiOTf⁴⁴. The pathway used to aldehyde **10** is described in Scheme 7. A Sharpless AE and a phenylurethane mediated intramolecular epoxide ring-opening featured as key steps. Subsequent protecting group interchange and thiophenyl installation completed the sequence to **10**.

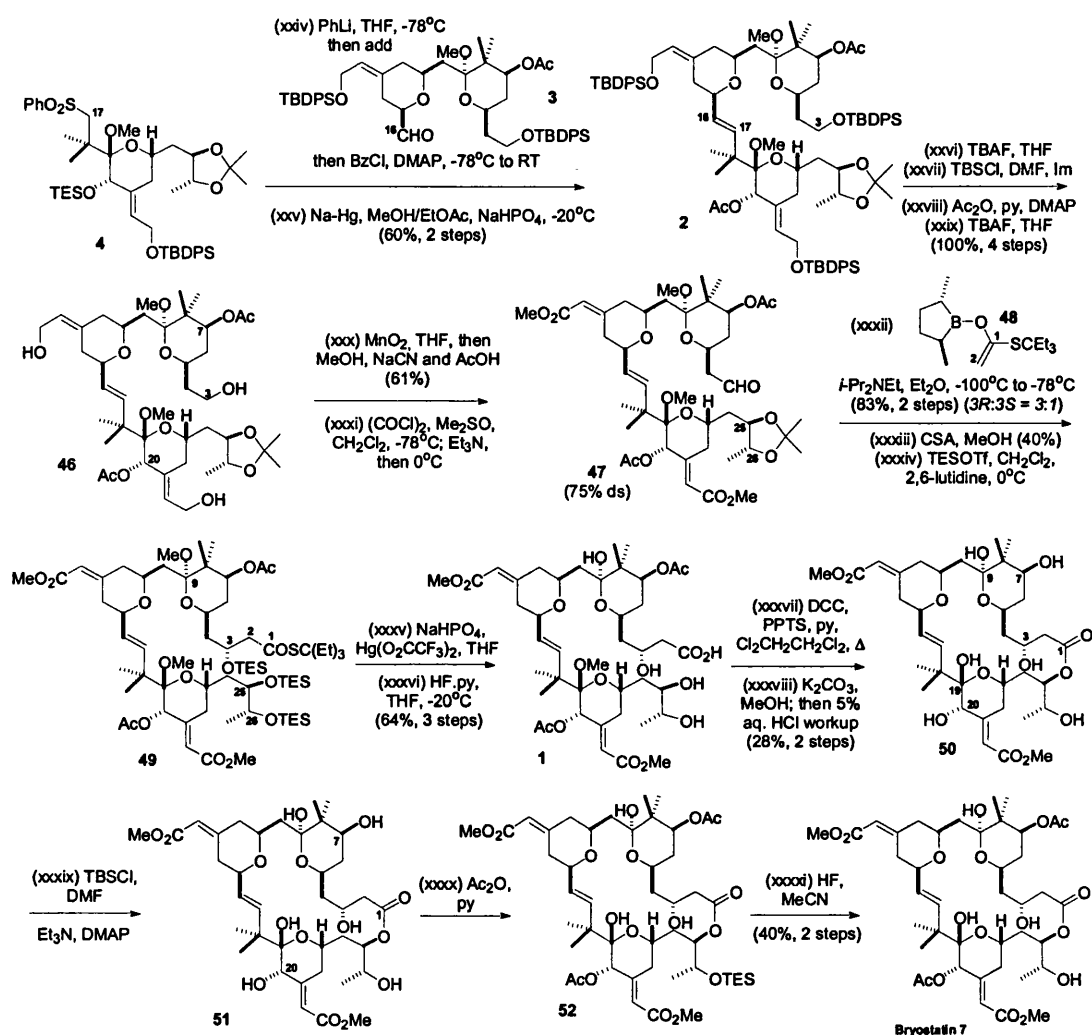


Scheme 7 Synthetic pathway to aldehyde **10**.

1.3.1.4 The Masamune bryostatin **7** endgame

The AB- and C-rings **3** and **4** were connected together via a Julia olefination (Scheme 8). This also set the C(16)-C(17) disubstituted olefin stereochemistry with good stereocontrol (*E:Z* 6.2:1). An *O*-desilylation / resilylation tactic allowed selective *O*-acetylation of the C(20)- and C(7)- hydroxyls. Further *O*-desilylation with TBAF secured triol **46** and this was then oxidised with MnO₂ in THF. The procedure

employed by Corey for oxidising enals to methyl enoates⁴⁵ was then used to obtain the *bis*-methyl enoate which underwent a Swern oxidation of the primary alcohol to give aldehyde **47**.



Scheme 8 Masamune's synthetic route to bryostatin 7.

Installation of the C(1)-C(2) unit was accomplished by aldol addition with enolate **48**. The required alcohol was obtained with 3:1 selectivity. Treatment of the product with CSA-MeOH released the C(25)-C(26) diol array, and a global O-silylation subsequently procured **49**. Deprotection apparently aided the hydrolysis of the C(1)-thioester. Global O-desilylation subsequently released the *seco*-acid **1** which underwent a highly regioselective macrolactonisation at the OH(25)-hydroxy group mediated by DCC and PPTS in pyridine/dichloroethane at reflux⁴⁶. These conditions also caused a selective glycoside hydrolysis

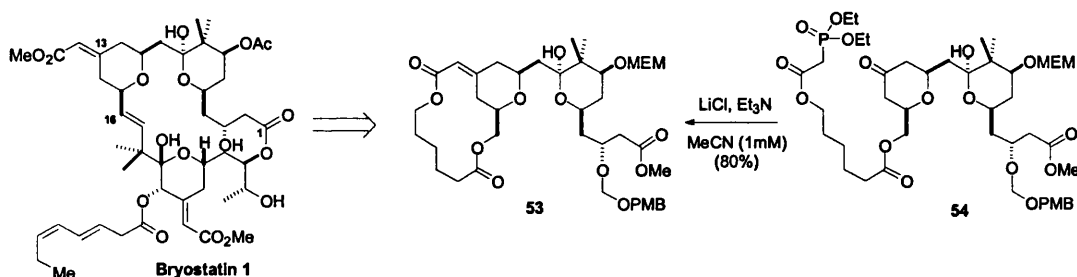
at C(9). However the C(19)-glycoside remained intact, presumably because of the electron withdrawing C(20) O-acetate which makes the anomeric OMe less basic and susceptible to protonation. Such a grouping would further disfavour hydrolysis.

This proved to be an inconvenience as double glycoside hydrolysis had been called for in the original synthetic plan. A great deal of work was carried out to effect C(19)- glycoside hydrolysis, under conditions which did not also cause destruction of the remainder of the molecule.

The solution to this problem was to cleave both the C(20) and C(7)-O-acetates with catalytic KOMe, which increased the acid lability of the C(19)-OMe, and resulted in the formation of the labile hemiketal **50**. This strategy was adventurous so far on in the synthesis as these acetates were required in the target compound, and the lactones could have undergone transesterification; that it survived was of particular note. Distinguishing the remaining hydroxyls was now called for. Transient blocking of the C(26)-OH as its O-triethylsilyl ether **51** allowed the re-positioning of the O(7) and O(20) acetates in **52**. Completion of this landmark total synthesis was accomplished by O-desilylation with aqueous HF, to yield bryostatin 7. This was the first bryostatin family member ever to be synthesised.

1.3.2 The Evans enantioselective total synthesis of bryostatin 2 (1999) ⁴⁷

1.3.2.1 Model work by Evans (1990) ⁴⁸

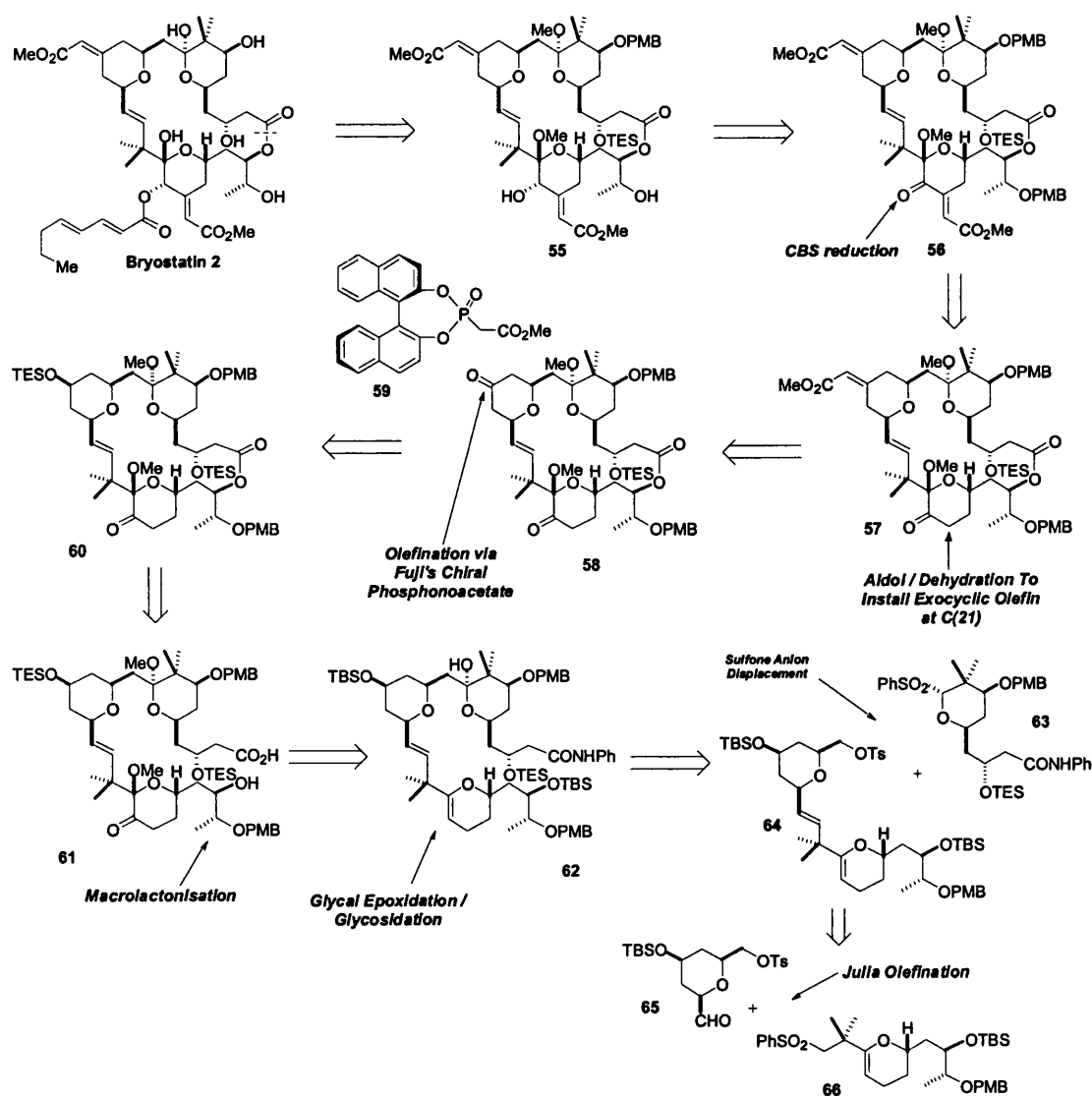


Scheme 9 The tethered phosphonoacetate strategy for exocyclic olefin construction in the bryostatins.

Evans' first synthetic endeavours in the bryostatin field led to him evaluating the potential of tethered phosphonoacetates for stereoselective control of the remote enoate geometry *via* the intramolecular WHE macro-olefination process ⁴⁹. Models suggested that a six-carbon tether could be ideal for controlling olefin geometry in the bryostatin B-ring, and molecular mechanics calculations further indicated a difference of more than 10 kcal mol⁻¹ between the two possible (*E*)- and (*Z*)-alkene 14-

membered macrocycles that could potentially be produced with the desired (*E*)- form being favoured. Under high dilution conditions, Evans and Carreira found that treatment of the tethered phosphonoacetate **54** with a large excess of lithium chloride and triethylamine in acetonitrile produced only the desired (*E*) olefin **53** in a modest 60% yield (Scheme 9). Previous model studies had indicated that these diester dilactone tethers could be successfully cleaved via a transesterification without competing olefin isomerisation. However, such a cleavage was not actually reported for **53** itself. This strategy, although not used in the final bryostatin synthesis, still remains an important method for future assembly of related olefinic arrays.

1.3.2.2 Evans' retrosynthetic analysis of bryostatin 2 (1999)



Scheme 10

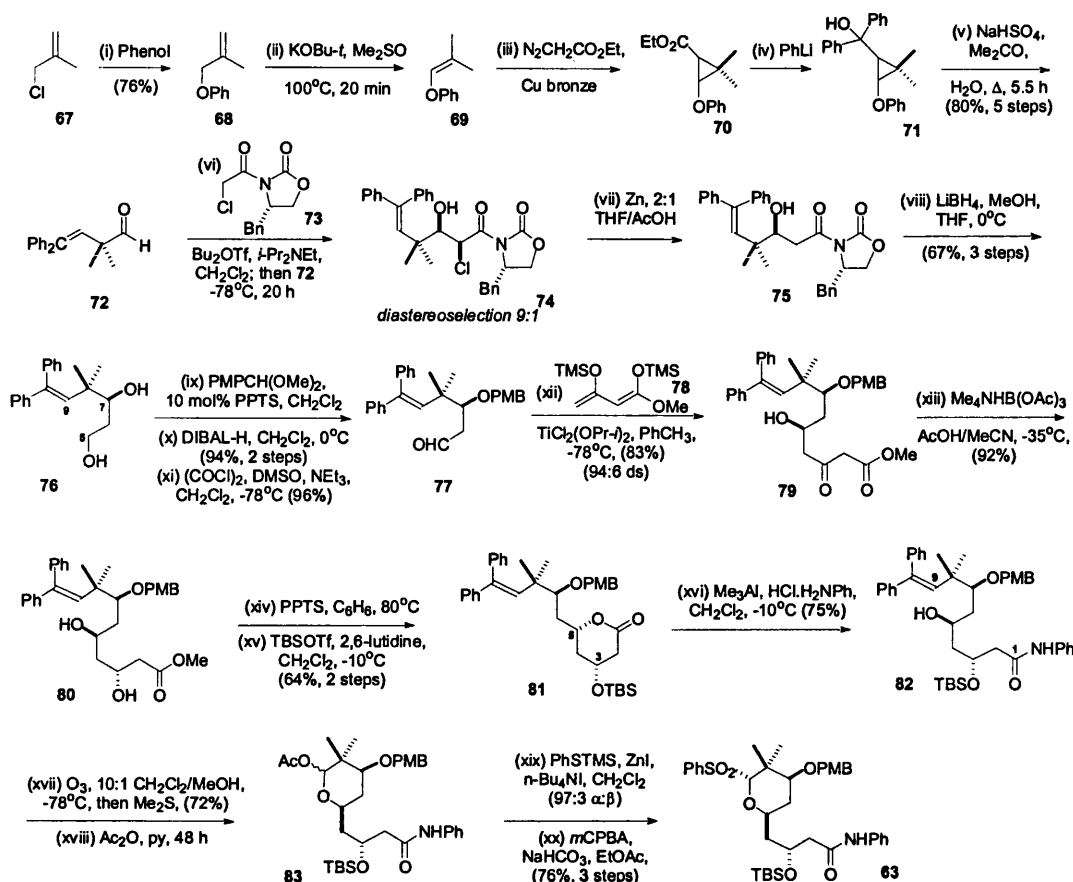
Evans' retrosynthetic analysis of bryostatin 2.

Having tackled the bryostatin problem over a number of years and learnt much about the idiosyncrasies that lay within its boundaries, Evans' final overall strategy for bryostatin 2 (Scheme 10) relied upon delaying the introduction of the exocyclic olefins until late-on in the projected synthesis. Installation of the C(13)-C(34) B-ring enoate would be accomplished via an asymmetric WHE involving Fuji's chiral phosphonate **59**⁵⁰ and the advanced macrocyclic diketone **58**. The C(21)-C(35) olefin positioned would be positioned via an aldol-dehydration sequence on **57**. The latter would be accessible from the addition of methyl glyoxalate to an appropriate C(20)-ketone intermediate.

A stereoselective reduction of this keto-enoate addition product would then be required to furnish the desired C(20)- stereochemistry for **55**. The requisite diketone **58** would be available from the tris-pyran *seco*-acid **61**, itself derived from glycal **62**. Implicit in the bryostatin planning was the ability to distinguish the more electron-rich C(19)-C(20) enol ether double bond in **62** in a regioselective epoxidation reaction which would subsequently allow methyl glycosidation at C(19) on route to **61**, with the positioning of the requisite C(20) hydroxyl. Finally, a C(1) anilide to acid conversion would have to be grappled with prior to macrolactonisation. The pyran linking sequence would involve a Beau-Sinay alkylative C-glycosidation⁵¹ between sulfone **63** and triflate **64** as a key step, and the BC-fragment would be assembled via a Julia olefination between **65** and **66**, in a notably more convergent synthesis than Masamune.

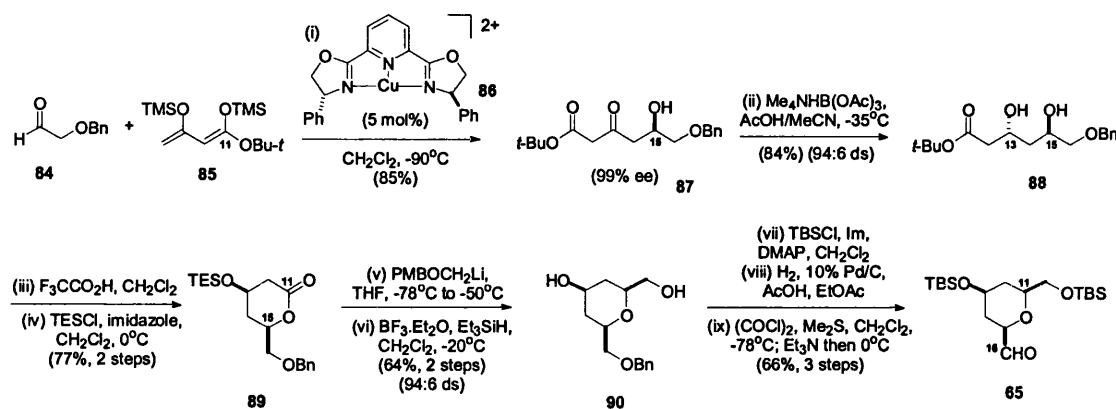
1.3.2.3 Asymmetric synthesis of the C(1)-C(9) glycosulfone **63**

The synthesis of A-ring **63** began with the conversion of methallyl chloride **67** to aldehyde **72** in five straightforward steps, one of which included the acid-induced cyclopropylmethanol rearrangement of **71** (Scheme 11)⁵². Aldehyde **72** underwent an Evans asymmetric aldol reaction⁵³ with oxazolidinone **73** to produce the *syn*-aldol adduct **74** after dehalogenation. This sequence set the C(7)-hydroxyl stereocentre with 9:1 (*S*:*R*) selectivity to favour the desired diol intermediate **76** after reductive removal of the auxiliary. For differentiating between the two hydroxyls, an *O-p*-methoxy-benzylidenation and a regioselective reductive acetal opening⁵⁴ was used to position a PMB group on O(7). The primary alcohol that remained was thereafter oxidised under Swern conditions to aldehyde **77**, and an acetoacetate aldol reaction performed with the disilyl enol ether **78** to effect the homologation to **79**.

Scheme 11 Evans' synthesis of the A-ring glycosyl phenylsulfone **63**.

The diastereocontrol achieved in this Lewis acid mediated aldol condensation⁵⁵ greatly depended upon the reaction solvent employed, with dichloromethane delivering a modest 6:1 selectivity in favour of **79**, which increased to 94:1 when upon the reaction was carried out in toluene. Hydroxy-directed reduction of the β -keto ester **79**⁵⁶ was accomplished with 91:9 selectivity under Saksena-Evans conditions and set the final C(3) stereocentre present in synthon **80**. A mild acid catalysed lactonisation was next effected in order to temporarily block the C(5) hydroxyl. O-Silylation and lactone opening aniline hydrochloride and trimethylaluminium furnished **82**. Ozonolytic cleavage of **82** produced a 3:2 mixture of the (β/α)-lactols and the C(9)-epoxide. The undesired epoxide by-product arose from an end-on approach of ozone to the sterically-demanding alkene⁵⁷. The desired hemiacetals were readily O-acetylated, and a Hanessian-Guindon thioglycosidation reaction⁵⁸ was applied on **83** to access the thioether. Exhaustive oxidation of the thioether unit with buffered *m*-CPBA completed the synthesis of phenylsulfone **63**.

1.3.2.4 Evans' asymmetric route to C(1)-C(16)-B-ring fragment 65



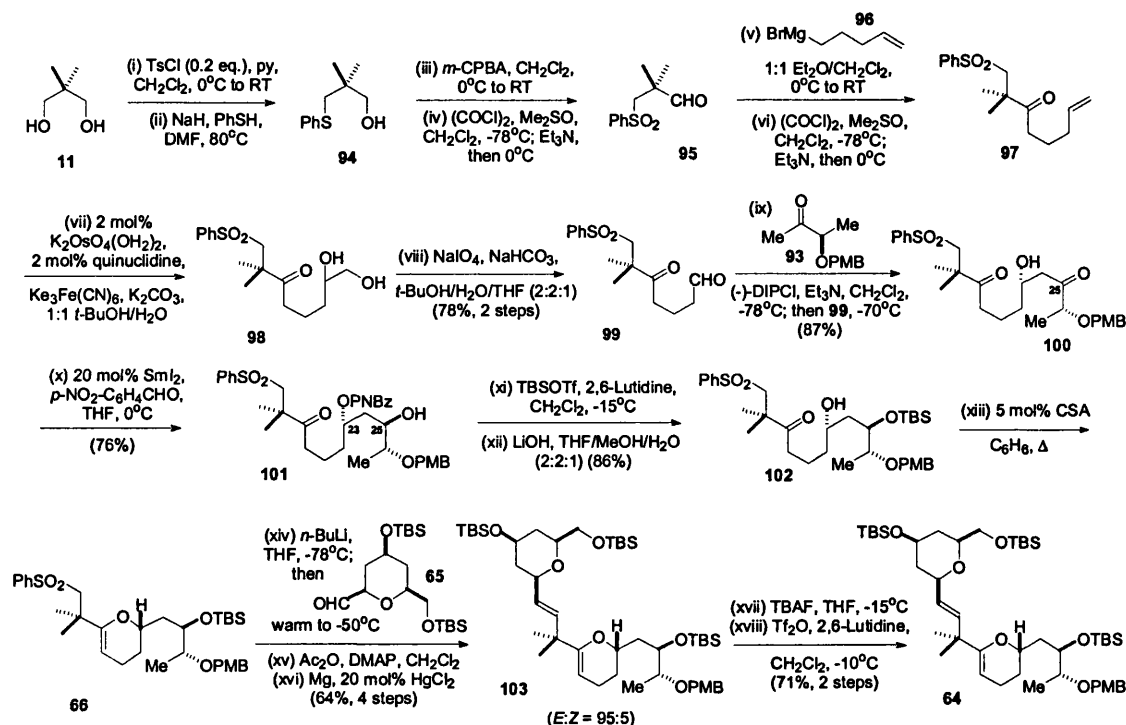
Scheme 12 Evans' B-ring synthesis.

The catalytic asymmetric acetoacetate aldol reaction of Evans, Murry and Koslowski⁵⁹ constitutes a powerful method for the construction of 1,3-diol subunits when combined with the stereoselective reduction of β -hydroxy ketones. Together these technologies look tailor-made for use in the bryostatin field, and they were employed by Evans for his assembly of the B-ring synthon **65**. The critical aldol process was effected with aldehyde **84** and disilyl enol ether **85** (Scheme 12), and delivered the β -hydroxy ketone **87** in 99% ee when the C_2 -symmetric copper(II) complex $([\text{Cu}(\text{R}, \text{R})\text{-Ph-pybox}]) (\text{SbF}_6)$ **86** was used as the chiral catalyst. A subsequent Saksena-Evans reduction⁵⁸ ceded the diol **88** as a 94:6 (*anti:syn*) mixture enriched in the desired isomer. A two-step lactonisation and protection strategy next delivered the δ -lactone that underwent a one-carbon homologation with *p*-methoxybenzyl lithium⁶⁰ proceeded by ionic reduction of the resulting α -lactols⁶¹, to finalise the desired carbon framework of **90**. The positioning of the final stereocentre at C(11) was completed in a favourable 94:6 ds, and the resulting diol underwent O-silylation, benzyl removal and Swern oxidation to conclude this expedient route to **65**.

1.3.2.5 Synthesis of the C-ring sector and elaboration into the BC-segment 64

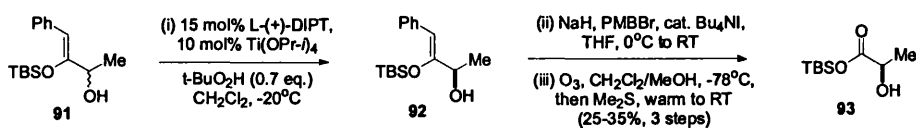
In his route to the C-ring glycal **66**, Evans began prepared sulfone **95** in a four-step procedure involving diol **11** (Scheme 13). Aldehyde **95** was then chain elongated with pentylmagnesium bromide to

deliver **97** after Swern oxidation. A two-step dihydroxylation and oxidative cleavage thereafter converted **97** to aldehyde **99**.



Scheme 13 Evans' synthesis of the bryostatin 2 BC-ring synthon **64**.

A Brown-Patterson DIP-Cl-mediated asymmetric aldol reaction⁶² with the pre-prepared ketone **93** produced the desired β -hydroxy-ketone **100** with 93:7 ds in favour of the desired adduct. Scheme 14 details the route taken to ketone **93**, which involved a Sharpless kinetic resolution⁴⁰, a protection and an ozonolysis.



Scheme 14 Asymmetric synthesis of methyl ketone **93**.

Fortuitously, the samarium-catalysed Tischenko reduction⁶³ of **100** not only installed the requisite stereochemistry for the C(25)-hydroxy, it also positioned a *p*-nitrobenzoate group on O(23) in **101** (Scheme 13). Subsequent silylation set the stage for dehydration to the phenylsulfone glycal **66**. A Julia

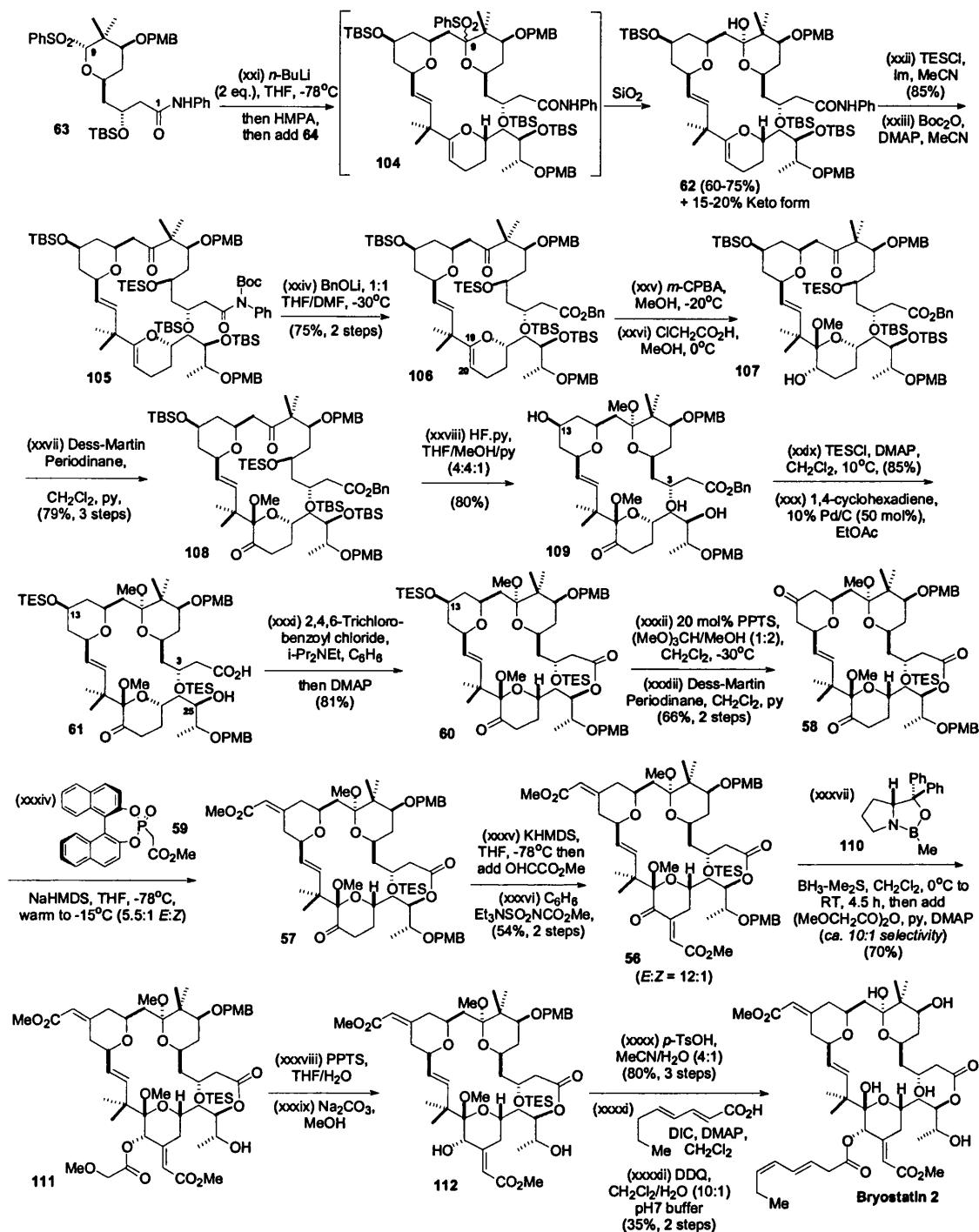
olefination³⁶ between **65** and **66** forged the C(16)-C(17) double bond with high geometric control (*E:Z* = 95:5) procuring **63** in a reasonable 64% yield. Selective *O*-desilylation of the primary silyl protecting group and exposure to triflic anhydride and 2,6-lutidine subsequently delivered the triflate ester **64**.

1.3.2.6 Completion of the bryostatin 2 synthetic venture

The cornerstone of Evans' the synthetic strategy for bryostatin 2 was his linking of the aforementioned A- and BC- segments via a Beau-Sinay glycosulfone C-alkylation reaction⁵¹ (Scheme 15). The coupling of the anion derived from **63** with **64** initially produced a glycosyl sulfone mixture **104** which underwent ready hydrolysis to the hemiketals **62**, which existed as alongside a small amount (15-20%) of the open-chain hydroxy ketone isomer. The high-yield of this alkylation was indeed impressive given the severe steric hindrance around the C(9) anionic site, and the electronically deactivating B-ring pyran oxygen that was present in the triflate component. The next step of the synthesis was ring-opening of the hemiketal in **62** with TESCI, and conversion of the anilide to a benzyl ester.

The anilide protecting group cleavage was best performed by protecting the anilide nitrogen, with a Boc prior to treatment with LiOBn. The protected ester **106** then underwent a selective epoxidation of the more electron-rich glycal double bond at C(19)-C(20) and an acid-catalysed epoxide ring-opening with methanol acquired the methyl glycoside **107**. Dess-Martin oxidation⁶⁴ at C(20), and a global *O*-desilylation with HF-MeOH also brought about a Fischer glycosidation, which delivered the triol **109** in good yield.

A selective *O*-triethylsilylation was now performed at hydroxyls -3 and -13, followed by hydrogenative cleavage of the benzyl group using a Pd/C catalyst in cyclohexa-1,4-diene⁶⁵. The *seco*-acid **61**, then underwent macrolactonisation under the conditions developed by Yamaguchi⁶⁶. Ketone **60** was then selectively *O*-desilylated at O(13) and oxidised to the diketone **58**. Positioning of the required (*E*)-olefin at C(13)-C(34) was accomplished with Fuji's chiral phosphonoacetate **59**⁵⁰ and delivered an isomeric mix of 5.5:1 in favour of the correct geometry to yield **57**. Interestingly, steric hindrance in the vicinity of C(19) resulted in no olefination occurring at the adjacent C(20) position. The second exocyclic olefin was installed in a slightly better 12:1 (*E:Z*) isomeric mix, via an aldol/dehydration sequence with methylglyoxalate to obtain **56**. Here, a CBS-reduction completed the installation of the final stereocentre at C(20). The isolation of **111** was aided by the trapping of the unstable alcohol as an *O*-methoxyacetate.



Scheme 15 Unification of the A- and BC-ring systems and the final stages of Evans' bryostatin 2 synthesis.

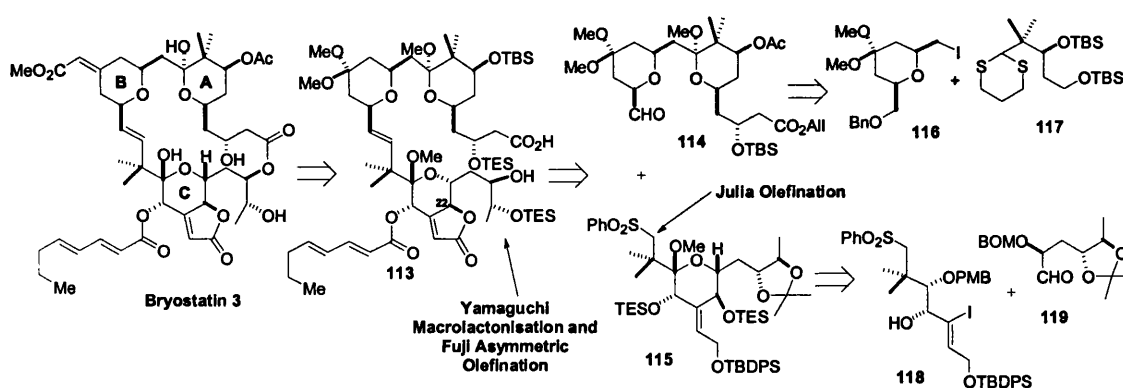
Selective hydrolysis of the C(9) methyl glycoside and desilylation at O(3) was achieved with PPTS in aqueous THF. As had previously been pointed out by Masamune³⁵ in his synthesis of bryostatin 7, hydrolysis of the C(19)-methyl glycoside under mildly acidic conditions was hampered by the presence of a

C(20)-O-acyl protecting group. The Masamune O-deacylation tactic overcame this problem allowing the glycoside to be hydrolysed with *p*-TsOH in aqueous MeCN, without any product decomposition. To complete of this elegant synthesis of bryostatin 2, the C(20) acid side-chain was installed via a selective esterification with octadienoic acid and the PMB at C(7) was deprotected with DDQ³⁸.

1.3.3 The Nishiyama-Yamamura total synthesis of bryostatin 3 (2000)⁶⁷

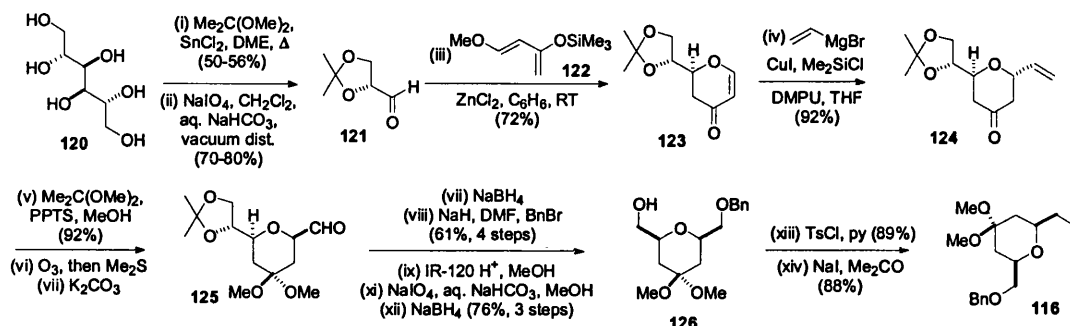
1.3.3.1 The retrosynthetic planning for bryostatin 3

Bryostatin 3 is unique amongst all the bryostatin family members, by virtue of its C(22)-stereocentre being involved in an α - β -unsaturated γ -lactone system. This extra feature clearly adds to the synthetic challenge of these molecules. Nishiyama's initial plan for this molecule called for a macrolactonisation of the *seco*-acid **113** under Yamaguchi conditions to establish its 20-membered macrolide ring (Scheme 16).



Scheme 16 The Nishiyama-Yamamura retrosynthetic analysis of bryostatin 3.

Final introduction of the B-ring exocyclic olefin would be accomplished with Fuji's chiral phosphonoacetate⁵⁰, although the greater complexity of the ketone on which this would be attempted offered considerably greater uncertainty for acquiring the desired (*E*)-geometry. Disconnection across the C(16)-C(17) trans olefin next led to AB-ring segment **114** and the C-ring segment **115** which would be conjoined via a Julia olefination³⁶. For the "Northern Hemisphere" **114**, a dithiane coupling between **117** and iodide **116** was envisioned while for the "Southern Hemisphere", a chelation-controlled addition between vinyl iodide **118** and aldehyde **119** would set the C(22) stereocentre.

1.3.3.2 Preparation of the enantiopure B-ring iodide **116** from D-mannitolScheme 17 The Nishiyama-Yamamura synthesis of the B-ring synthon **116**.

At the outset of their synthetic venture, Nishiyama and Yamamura's plan was to utilise materials emanating from the chiral pool, with construction of the requisite B-ring iodide **116** commencing with the known conversion of D-mannitol into protected aldehyde **121**⁶⁸. This then underwent a zinc-mediated hetero-Diels-Alder (HDA) reaction⁶⁹ with Danishefski's diene **122** to produce the enone **123** as the single (S)-isomer.

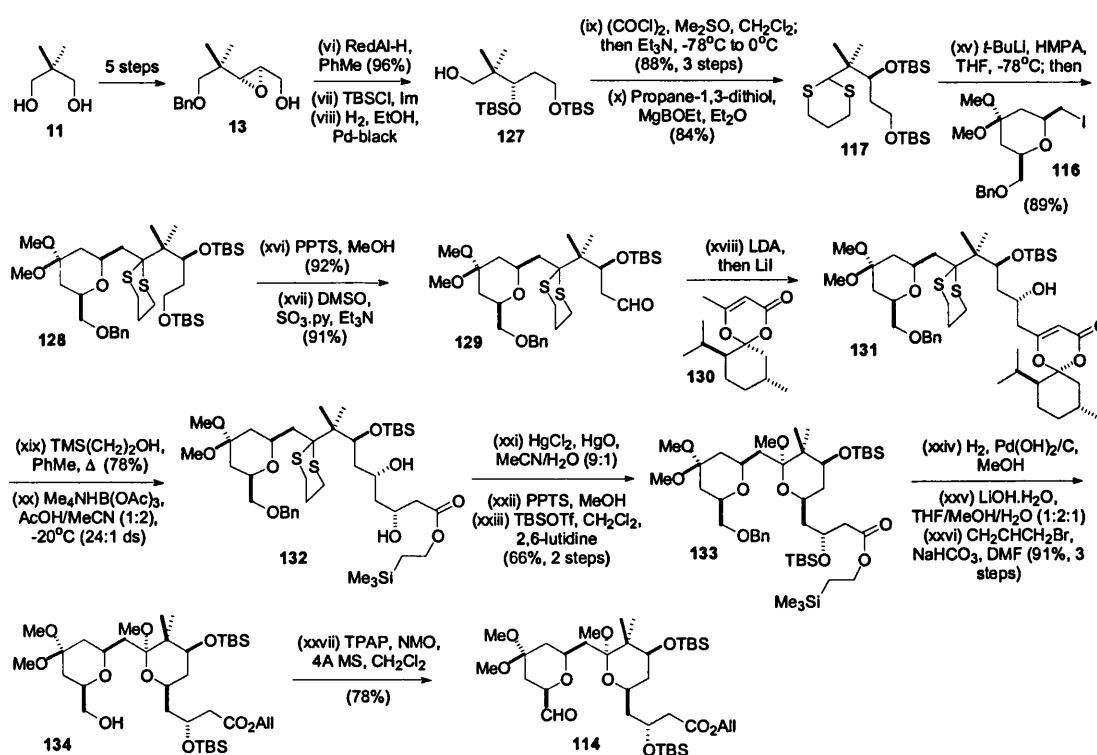
The stereospecific addition of a vinyl anion at the glycosidic position was carried out via a copper-mediated Grignard coupling to yield **124**, allowing protection of the keto unit as its O-dimethyl acetal, under conditions that preserved the existing O-isopropylidene acetal. This opened the gateway to ozonolytic cleavage of the terminal olefin to produce the axial aldehyde. However this undesired stereochemical situation could quickly be rectified by a base-induced epimerisation to the more stable, desired equatorial aldehyde **125**. A borohydride reduction of this aldehyde then allowed O-benzylation, acetonide removal, and manipulation of the diol into alcohol **126**. A primary tosylation / halide displacement sequence furnished the B-ring synthon **116**.

1.3.3.3 Preparation of the AB-ring intermediate **114**

In the synthesis of the dithiane coupling partner **117** with iodide **116**, the Keio group employed some of the chemistry described by Masamune in his work for the AB-ring sector (see Scheme 4). Epoxide **13** readily underwent regioselective reductive ring opening, O-silylation and O-debenzylation to yield **127**. A

Swern oxidation to the aldehyde then allowed dithiane installation to give **117** with no loss of the acid-labile silyl ethers.

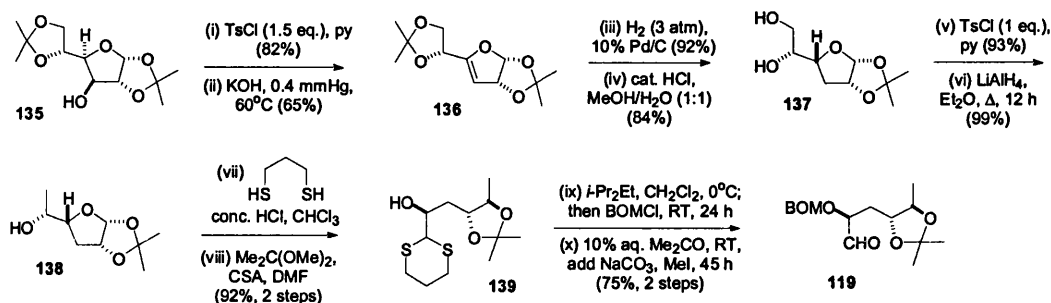
The 2-lithio-anion of **117** underwent addition to the iodide **116** to set the C(5)-C(16) carbon chain, and a selective O-desilylation and oxidation yielded the aldehyde **129**. The aldol addition of the C(1)-C(4) spiroacetal protected synthon **130** delivered the C(5) stereocentre in **131**, when the acetal unit was cleaved to reveal the β -hydroxy ketone allowing a hydroxyl-directed reduction⁵⁶ and completing the final chiral centre array in **132** at C(3).



Scheme 18 Nishiyama-Yamamura synthetic strategy for the AB-aldehyde synthon **114**.

After removal of the dithiane moiety with mercuric-chloride, Fischer glycosidation and O-silylation afforded the methyl glycoside **133**. Hydrogenolytic cleavage of the benzyl ether and protecting group interchange next yielded the allyl ester **134**, and TPAP oxidation of the C(16) alcohol completed the synthesis of the AB-ring synthon **114**.

1.3.3.4 Synthesis of the C-ring sulfone 115



Scheme 19 Synthesis of the C(22)-C(27) aldehyde segment 119.

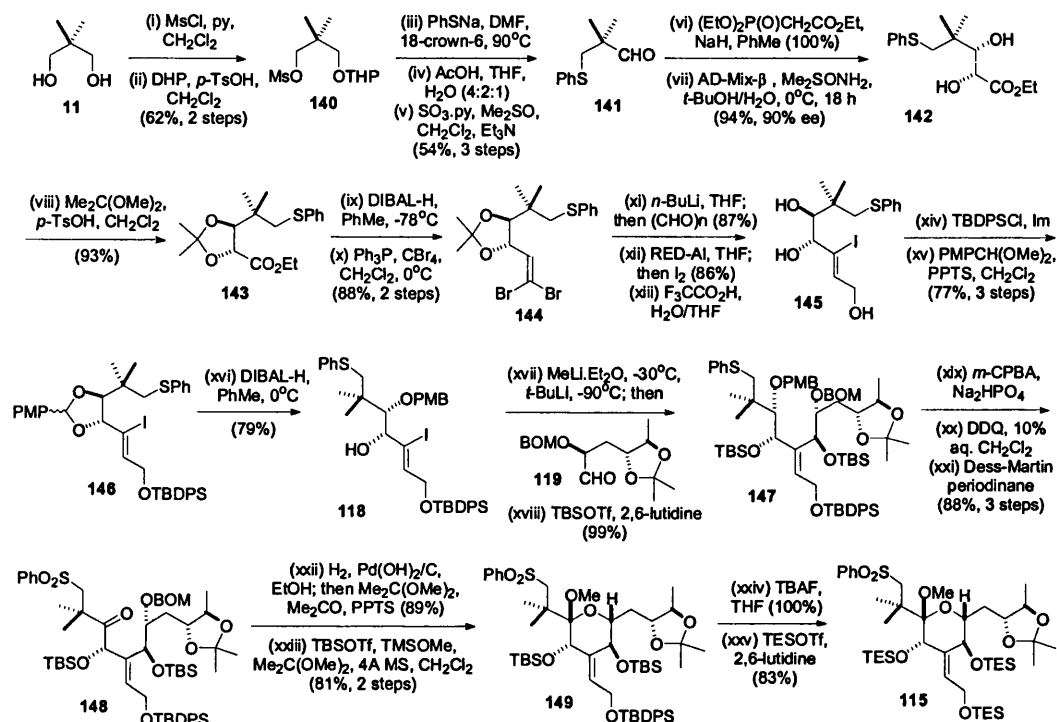
The chiral building block selected for the synthesis of the C(22)-C(27) aldehyde **119** was the carbohydrate derivative diacetone D-galactose, as this precursor possessed two of the required stereocentres. It is available from diacetone D-glucose **135** by O-tosylation at OH(3), base-catalysed elimination with KOH, and face-selective hydrogenation of **136**⁷⁰. After conversion to **137** a two-step deoxygenation of the hydroxyl via tosylation and LiAlH₄ reduction delivered the *bis*-acetonide **138**.

The furanose ring was then opened with 1,3-propanedithiol, and a re-protection of the 1,2-diol formed alcohol **139** in excellent yields. The aldehyde precursor **119** was completed by a BOM etherification and thioketal hydrolysis.

The synthesis of vinyl iodide **118** (Scheme 20), again began from diol **11**. After conversion to the thiophenyl aldehyde **142**, Wittig olefination and Sharpless asymmetric dihydroxylation⁷¹ collectively permitted installation of the C(20)-stereocentre. Acetal protection of the diol array in **142** gave **143**, and set the stage for ester reduction and subsequent dibromo olefination under Corey-Fuchs conditions⁷² to furnish **144**. Conversion to the lithium acetylide with *n*-BuLi and exposure to paraformaldehyde next resulted in the expected propargylic alcohol. Hydroxyl directed hydroalumination of the alkene, and *in-situ* trapping with iodine delivered the required vinylic iodide, and acid cleavage of the acetonide yielded the triol **145**.

Selective O-silylation and diol differentiation led to **118**, to complete the synthesis of the desired coupling target. The crucial union of **118** and **119** was accomplished by halogen-metal exchange with a mixture of methyl- and *t*-butyl lithium, and proceeded with 3:1 selectivity in favour of the desired alcohol. O-Silylation subsequently procured **147**. Thioether oxidation to the corresponding sulfone, DDQ mediated cleavage of the PMB group and C(19) oxidation⁶⁴ delivered the ketone **148** in excellent yield. The BOM

ether was then cleaved by hydrogenation without damage to the alkene functionality. A novel Fischer glycosidation⁴⁴ was then carried out to yield the methyl glycoside **149**. Silyl group interchange then delivered the phenyl sulfone **115**.

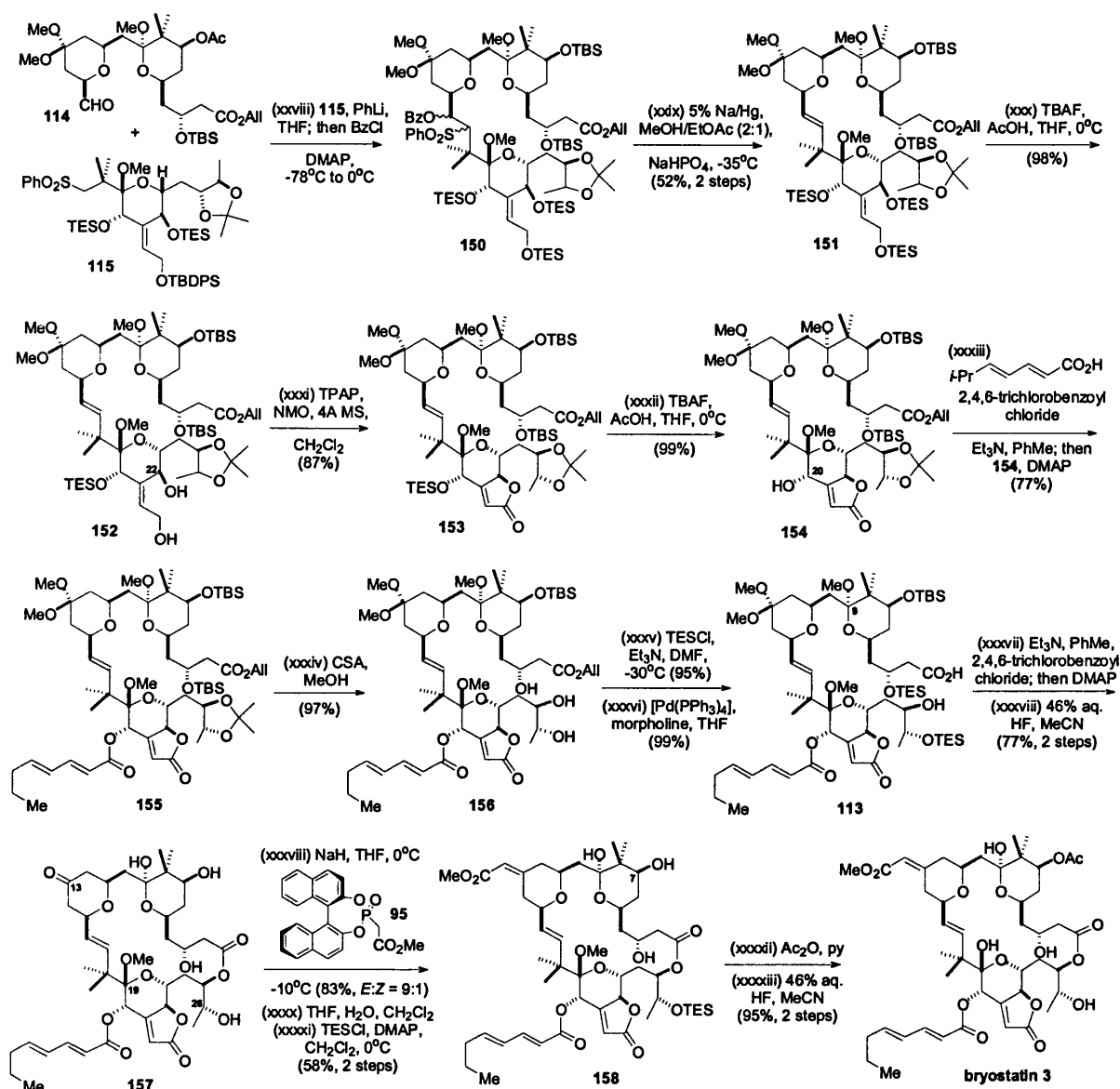


Scheme 20 The Nishiyama-Yamamura synthetic pathway to the bryostatin 3 C-ring synthon **15**.

1.3.3.5 Union of the AB- and C-ring intermediates and synthesis of bryostatin 3

As had been described by Masamune with a similar related C-ring intermediate, a successful Julia olefination³⁶ could be effected between the lithiated sulfone **114** and the aldehyde **115**. *In-situ* benzoylation yielded the expected benzoyl sulfone mixture **150**, which then underwent Na/Hg elimination to yield the desired (*E*)-olefin **151** (Scheme 21).

The different labilities of the various silyl ethers was exploited first by a selective cleavage of the allylic and C(22)-OTES ethers to give diol **152**. Selective oxidation of the allylic primary OH then followed; it was accomplished by hemi-acetal formation and further oxidation to the butanolide unit. Selective removal of the C(20)-OTES subsequently afforded **154**.



Scheme 21 The union of the AB- and C-ring intermediates **114** and **115** in the synthesis of bryostatin **3**.

The octadienyl ester side-chain was appended to **154** under the Yamaguchi esterification conditions⁶⁶. Compound **155** then underwent acetonide cleavage to the diol **156**. The C(3) and C(26)-hydroxyls were then selectively silylated, for steric reasons, and the *seco*-acid **113** unveiled by cleavage of the allyl ester with tetrakis palladium (0).

A Yamaguchi macrolactonisation was then performed on **113**, under conditions of high dilution. A global O-desilylation in aqueous HF not only cleaved the silyl groups, it also brought about hydrolysis of the C(9) glycoside and C(13) ketal to yield **157**. Olefination at C(13) was then effected using Fuji's chiral

phosphonoacetate **95**⁵⁰. Although this reaction was potentially problematic and very high risk, it resulted in a favourable 9:1 (*E*:*Z*) ratio of the product, in good yield. This system gave much better *E/Z* selectivity than Evans' much simpler system (**58** in scheme 15). As had been reported in the previous total syntheses, the lability of the C(19) glycoside was problematic with the C(20) ester flanking functionality present, however by using aqueous TFA at room temperature, it was found that desired C(19) hydrolysis could be accomplished without the need for ester cleavage.

The final hydroxyl elaboration to position an acetal at C(7) was accomplished by a transient protection of the C(26) hydroxyl as its silyl ether **158**, and installation upon exposure to acetic anhydride. Interestingly, the C(3), hydroxyl was left untouched in this manipulation, and this was assumed from a hydrogen-bond network involving the C(9) and C(19)- hemiketals to render this position locked inside the macrolide ring. The final step in the synthesis was the removal of the silyl ether at C(26) to secure bryostatin 3 in a remarkable synthesis, and the synthetic efforts in this area opens the potential for future commercial applications.

1.4 Synthetic studies on the bryostatins

In conjunction with the three total syntheses reported to date, there has been significant work in bryostatin synthetic programmes from a number of groups. This considerable effort has led to the publication of a number of individual pyran ring sections capable of further manipulation.

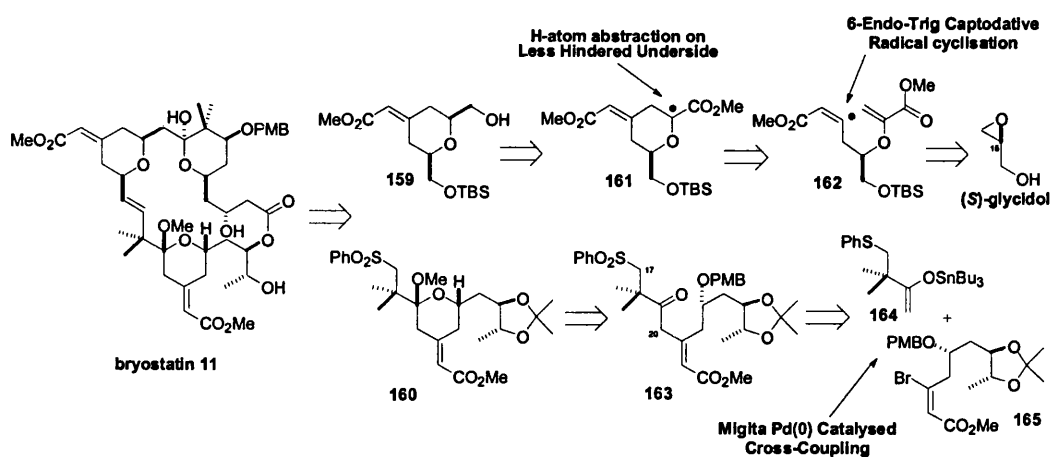
1.4.1 Thomas's synthetic route to bryostatin 11⁷³

1.4.1.1 Thomas's retrosynthetic strategy for bryostatin 11

In his synthetic efforts towards members of the C(20)-deoxy class of bryostatins, Thomas has described an approach to the of a B-ring synthon **159**, and the C-ring phenylsulfone **160** (Scheme 22).

Thomas' plan for procuring the C(10)-C(16) B-ring intermediate **159** would exploit a vinyl radical cyclisation to establish the pyran ring-system and simultaneously set the exocyclic enoate and C(11) stereocentre. They postulated that the (*Z*)- vinyl radical **162** would lie in the equilibrium with its (*E*)-

counterpart, and that the (*Z*)- radical would cyclise more rapidly, due to its transition state for addition being less hindered than that for the (*E*)-isomer.



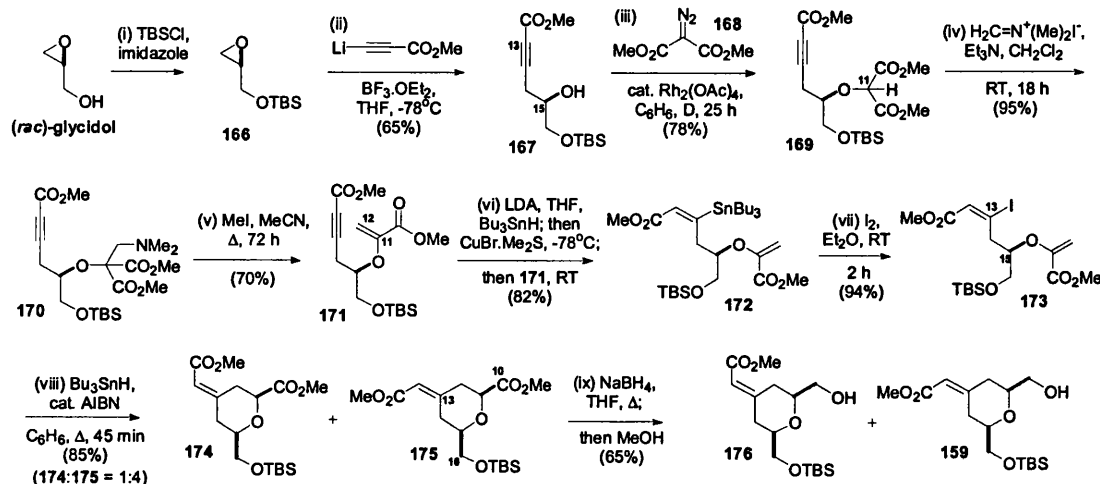
Scheme 22 Thomas's retrosynthetic plan for the bryostatin 11 B- and C- ring intermediates.

A sterically favourable hydrogen abstraction from Bu_3SnH from the α -face of the ring in **161** would thereafter place the carboxymethyl substituent equatorial. Further retrosynthetic analysis of **162** led to (*S*)-glycidol being selected as an appropriate starting material as it exhibited a stereochemical match with the C(15) stereocentre of **159**. For construction of the C-ring synthon **163**, the cross-coupling of vinyl bromide **165** with enol stannane **164** was envisaged; further underlining the range of strategies that can potentially be employed in the bryostatin field.

1.4.1.2 Thomas's racemic free-radical routes to the bryostatin B-ring (1989 and 2000)

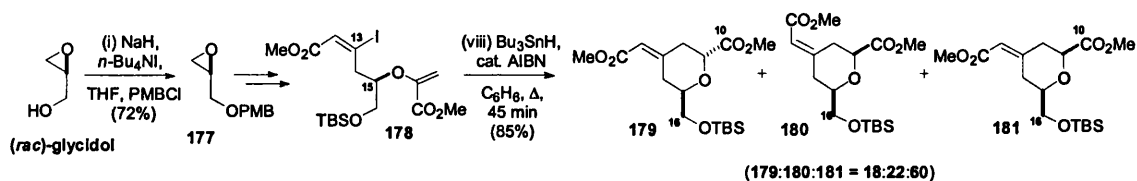
To validate his proposed synthetic route, Thomas initially employed racemic glycidol (Scheme 23) in his synthesis of the B-ring synthon **159**. The route commenced with the O-silylation of \pm glycidol to obtain **166**, and a ring opening with the lithiated methyl propiolate to access alcohol **167**. A rhodium catalysed carbene insertion of **168** into the hydroxyl of **167** thereafter led to the alkoxymalonate **169**⁷⁴, and subsequent alkylation⁷⁵ yielded the aminomalonate **170**. The latter underwent quaternisation and decarboxylative elimination upon exposure to methyl iodide in acetonitrile at reflux, to furnish the enol ether **171** in 70% yield.

To access the desired precursor **172** for the proposed radical cyclisation, a tributyltin hydride free radical mediated addition to the acetylene of **171** was effected under carefully monitored conditions. The vinyl stannane **172** was then subjected to a halogen-metal exchange to obtain the vinyl iodide **173**.



Scheme 23 Thomas's free radical cyclisation to control the B-ring olefin geometry.

It was found that by heating **173** with tributyltin hydride and AIBN in refluxing benzene, the desired cyclisation proceeded to give a mixture of the B-ring enoates **175** and **174** in a 4:1 ratio in favour of the desired (*E*)-exocyclic enoate. The enhanced electrophilicity of the C(10) ester was then exploited for a selective borohydride reduction to deliver the final B-ring synthon **159** in a creditable 9 steps. In an attempt to improve the observed selectivity in the cyclisation process, the synthetic route was repeated with a PMB ether positioned at OH(16) (Scheme 24).

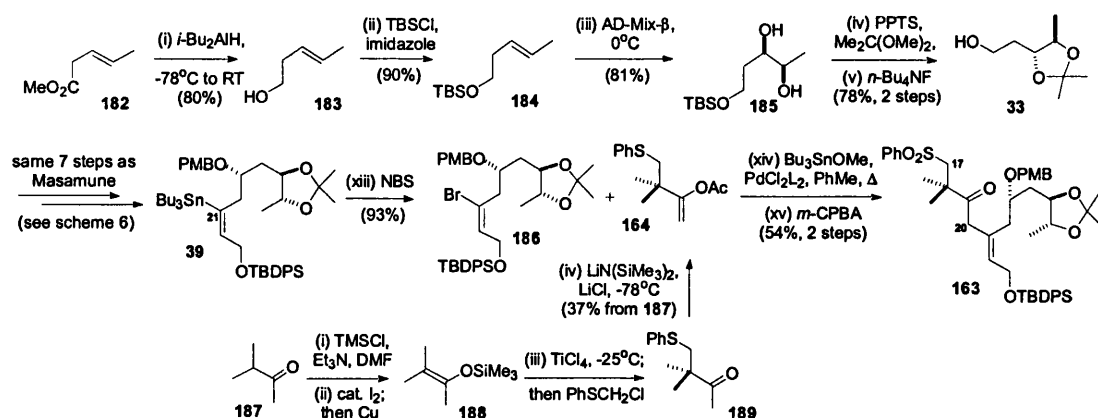


Scheme 24 Alternative protecting group strategy in the bryostatin B-ring synthesis.

Initial etherification of the racemic epoxide to **177** followed by conversion to the vinyl iodide **178** as before allowed this ring cyclisation to be studied. Although the 6-endo addition to the (*E*)-enoate was carried

out in a comparable 4:1 ratio, the stereochemical integrity at C(10) of the products was diminished considerably. It was suggested that this unfavourable outcome was the result of intramolecular hydrogen abstraction from the benzylic position of the protecting group rather than from the stannane.

1.4.1.3 Thomas's asymmetric synthesis of the C-ring sulfone **163** (2000)



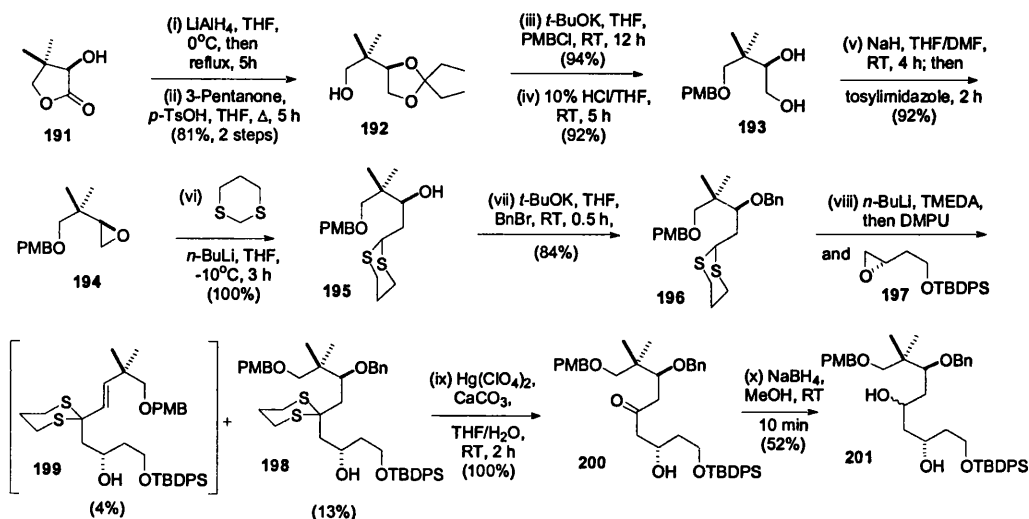
Scheme 25 Thomas's palladium (0) catalysed coupling strategy for the bryostatin 11 C-ring.

The route to vinylic bromide **186** set off from the α - β -unsaturated ester **182** and featured a reduction to the allylic alcohol **183** and an O-silylation as the first two steps in the synthesis. A Sharpless asymmetric dihydroxylation on olefin **184** positioned the C(25) and C(26) stereocentres in **185** which were then O-isopropylidened; subsequently desilylation yielded the Masamune intermediate **33**. An oxidation and conversion to the vinyl stannane **39** was accomplished under the conditions previously reported by Masamune^{35/} (see Scheme 6).

The final halogen-metal exchange with *N*-bromosuccinimide delivered the required C(21)-C(27) synthon **186**. Its cross-coupling with the enol acetate **190** was readily implemented with palladium (0)⁷⁶ to establish the C(17)-C(27) carbon backbone. A thioether to sulfone oxidation with *m*-CPBA completed the C-ring synthon **163**. The coupling partner **190** was readily acquired from the ketone **187** in four steps (see Scheme 25).

1.4.2 Vandewalle's synthetic studies on bryostatin 11 (1990's) ⁷⁷

1.4.2.1 Attempted construction of the C(1)-C(9) backbone via a dithiane coupling strategy

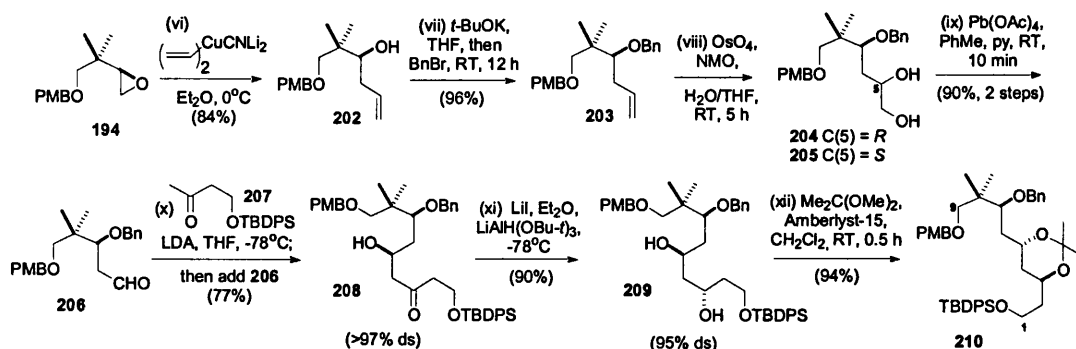


Scheme 26 Vandewalle's attempted dithiane strategy for assembly of the C(1)-C(9)-sector.

Vandewalle's strategy for the A-ring employed a dithiane / epoxide coupling strategy to assemble the requisite C(1)-C(9) carbon framework. This entailed the epoxide precursors **194** and **197** with the appropriate dithiane partners. The former epoxide was secured from (*R*)-pantalactone **191** in five steps by a pathway developed by Lavalée ⁷⁸. Commencing with the reduction of **191**, the placement of an acetal on the 1,2-diol function allowed the primary hydroxyls to be differentiated. After a PMB etherification, removal of the acetal, diol **193** was obtained and connected to the terminal epoxide **194** via base-induced elimination.

Oxirane **197** was readily prepared in three steps from (*L*)-malic acid ⁷⁹. The first of the proposed couplings, with the lithio-anion of 1,3-dithiane provided **195** quantitatively. Although **195** underwent O-benzylation at C(7) fairly readily, the resulting dithiane **196** performed poorly in the second coupling with epoxide **197**, with only a disappointingly low yield of the desired alkylated product **198** being isolated along with a small amount of the β -eliminated side-product **199**. This first generation synthesis was completed by a mercury-induced cleavage of the dithiane unit, and reduction of the resulting ketone **200** to **201**. However due to the significant impasse encountered in the aforementioned late coupling step, this synthetic strategy was later abandoned in favour of the one shown below.

1.4.2.2 Synthesis of the C(1)-C(9)-segment of the bryostatins (1991)



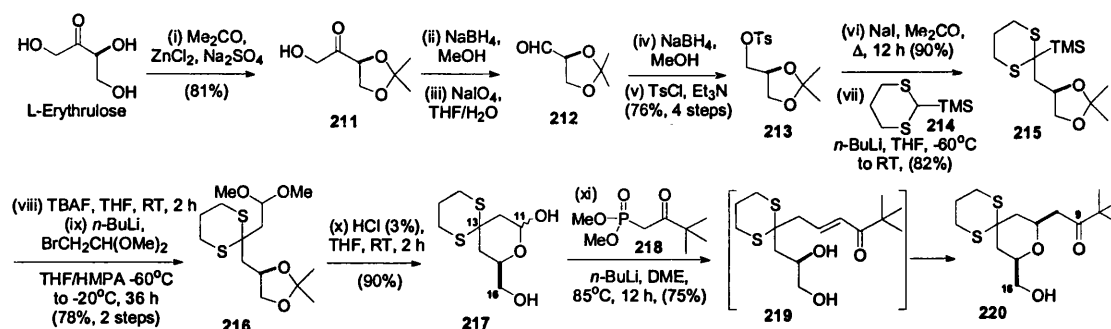
Scheme 27 Vandewalle's stereocontrolled route to the C(1)-C(9) segment of the bryostatins.

An alteration of the synthesis led to the opening of epoxide **194** with the Lipschutz vinylcuprate⁸⁰ to access the allylic alcohol **202** which was then O-benzylated and oxidatively cleaved to the aldehyde **206**. An aldol addition between ketone **207** and **206** served to not only set the required C(5) stereocentre in excellent control, but also the C(1)-C(4) sector to be introduced in one fell swoop. The presence of the β -hydroxyketo unit in **208** lent itself to a hydroxyl-directed reduction, and literature precedent suggested good 1,3-anti-selectivity would be achieved with the Evans reagent $\text{Me}_4\text{NBH}(\text{OAc})_3$ ⁵⁶. However, this turned out not to be the case. After numerous reagents were evaluated, $\text{Li}(\text{t-BuO})_3\text{AlH}$ in the presence of LiI ⁸¹ effected the desired *anti*-reduction, positioning the C(3)OH stereocentre in **209** with 95% ds. Subsequent protection as an acetonide produced the target synthon **210**. Further elaboration of this late-stage intermediate will be needed in order to deliver a synthon capable of being further advanced towards the bryostatins. However, as yet, no additional results in this area have been published.

1.4.2.3 Model studies on the bryostatin B-ring (1991)

Vandewalle and coworkers have also reported a model study for obtaining the bryostatin B-ring system. The crux of Vandewalle's B-ring strategy lies in a sterically-controlled, Wittig-Horner-Emmons olefination tandem intramolecular Michael sequence being applied on an appropriate hemiketal precursor to setup the pyran ring and C(11) centre. The C(15) centre emanates from (*L*)-erythrose as shown in Scheme 28. After various manipulations, this chiral triol was converted to protected aldehyde **212**, and then

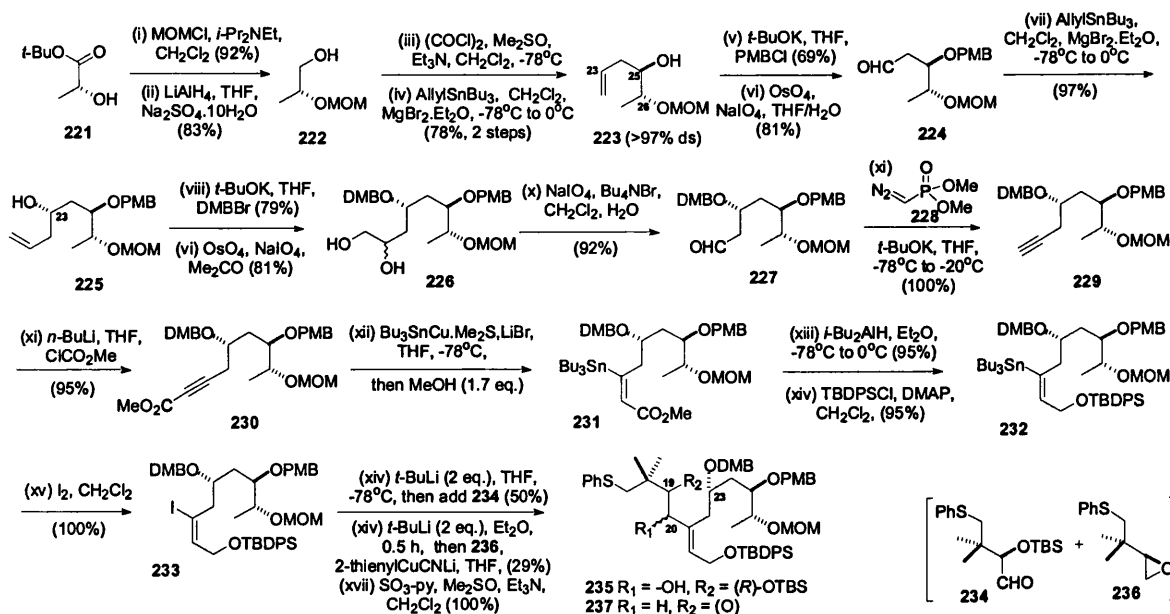
reduced, tosylated and alkylated with 2-TMS-1,3-dithiane **214**. C-Desilylation, chain homologation, and treatment with mild acid led to the α -lactols **217** which then engaged in the proposed Michael addition to deliver the pyran **220**.



Scheme 28 Vandewalle's synthesis of a C(9)-C(16) B-ring synthon **220**.

Although Vandewalle's group have reported no further work in this direction, Jadav's group later used this type of approach in their route to a bryostatin AB fragment (see section 1.4.9).

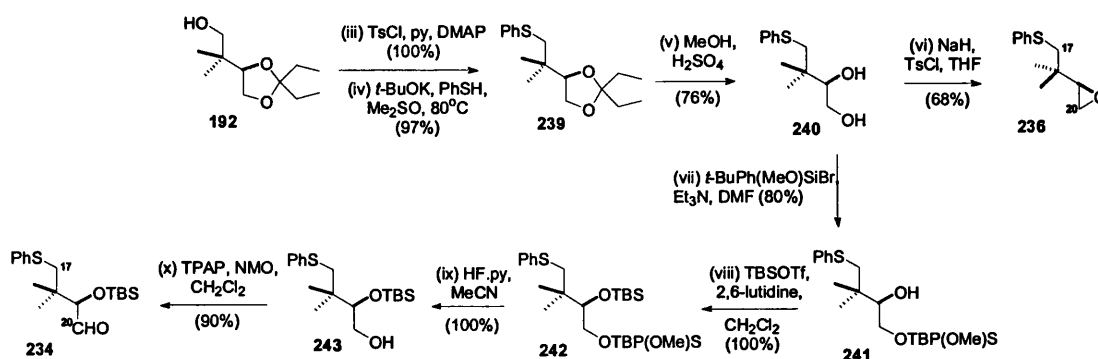
1.4.2.4 Vandewalle's strategy for the C-ring in bryostatins 1 and 11 (1994)



Scheme 29 The bryostatin C-ring synthesis of Vandewalle and coworkers

Vandewalle's group have also reported a convergent strategy to the C-ring intermediates **235** and **237**. Vandewalle's routes to these compounds relied upon the addition of a common vinyl iodide **233** to either the aldehyde **234** or the epoxide **236** respectively. The synthesis of **233** began with the protection and reduction of D-isobutyl lactate **221** to obtain **222** (Scheme 29). After Swern oxidation, the C(26) stereocentre in the product aldehyde was used to direct stereochemical outcome of a Keck allylation⁸² with allylstannane which delivered **223** in high stereocontrol.

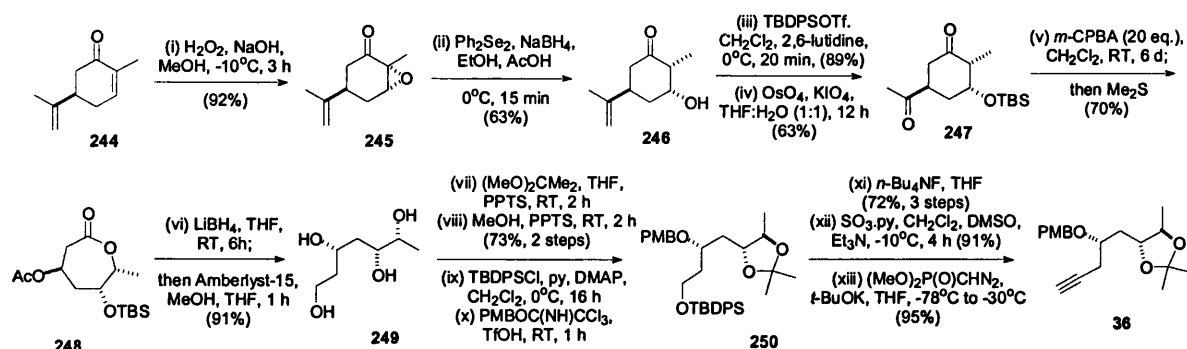
A *p*-methoxybenzyl etherification of the resulting hydroxyl allowed an oxidative cleavage of the terminal olefin to give an aldehyde **224**, which then underwent a second Keck allylation to install the C(23)-hydroxy stereochemistry, again, with high stereocontrol. Subsequent protection of alcohol **225** as its *O*-dimethoxybenzyl ether permitted a two-step oxidative degradation to yield aldehyde **227** which was alkynylated with the Seyferth-Gilbert diazo-phosphonate **228**⁸³. The lithio-anion of the resulting alkyne **229** was then trapped with methylchloroformate, and the resulting alkynyl ester **230** subjected to a Piers conjugate addition. Vinyl stannane **231** was now reduced and *O*-silylated, and **232** converted to the vinyl iodide **233** by halogen-metal exchange. The coupling of aldehyde **234** with the vinyl lithium obtained from **233** delivered the C(20) hydroxylated intermediate **235** as a mixture of epimers. The coupling of the corresponding vinylcuprate with epoxide **236** also produced the C(20) non-hydroxylated intermediate **237**, after Swern oxidation. The latter stages of the synthesis to **235** mirrored those carried out by Masamune³⁵ (Scheme 6). However, the selectivity in the crucial vinyl iodide addition step was eroded significantly when compared to that achieved by Masamune.



Scheme 30 Vandewalle's route to the aldehyde **234** and epoxide **236**.

The routes developed to the addition precursors **234** and **236** are shown in scheme 30, and proceed from the common intermediate **240** (Scheme 30).

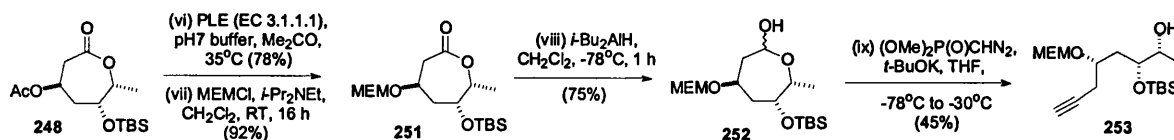
1.4.2.5 Vandewalle's use of (*R*)-carvone for a the synthesis of Masamune's C(27)-C(34)-alkyne fragment (1994)



Scheme 31 Vandewalle's alternative route to the Masamune C-ring synthon **36** from (*R*)-carvone

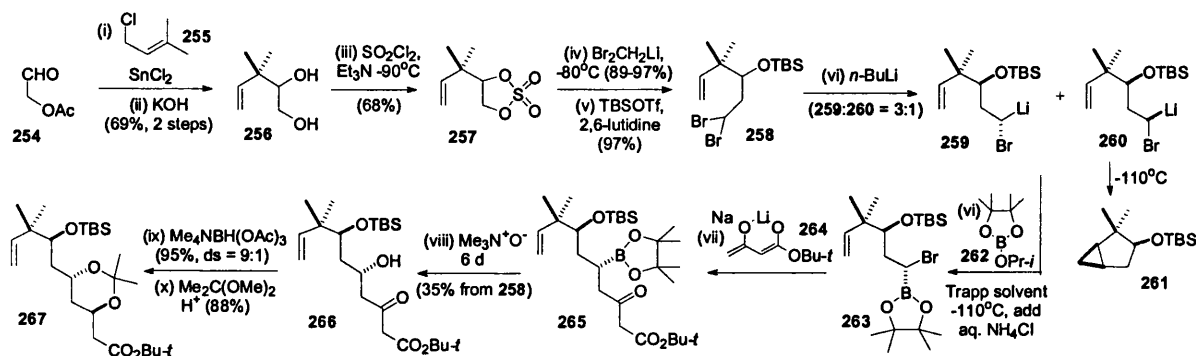
A novel approach has been adopted by Vandewalle for construction of Masamune's C(27)-C(34) alkyne intermediate **36** which utilises (*R*)-carvone as the chiral starting material. An initial face-selective epoxidation with basic hydrogen peroxide⁸⁴ afforded **245** which was then regioselectively opened in an organoselenium-mediated reduction⁸⁵ to produce **246** along with its C(2) epimer in an easily separable 4:1 ratio.

An O-silylation on the remaining hydroxyl, and oxidative cleavage of the terminal olefin subsequently yielded diketone **247**. A double Bayer-Villiger oxidation was next performed using an excess of *m*-CPBA; this installed the C(26) hydroxyl in masked form, and its identity was revealed after conversion the tetraol **249**. A series of protecting group manipulations yielded the differentially protected C(21)-C(27) subsection **250**, and the protected terminal alcohol to alkyne employed a Seyferth-Gilbert chain extension to deliver the desired Masamune intermediate **36**. The increased number of operations required in this route compared with Masamune's pathway detract from the worth of this sequence. Vandewalle has also reported an alternative synthetic pathway, that leads to **253**; it is shown in Scheme 32.



Scheme 32 Vandewalle's synthesis of the alkyne intermediate **253** from (*R*)-carvone

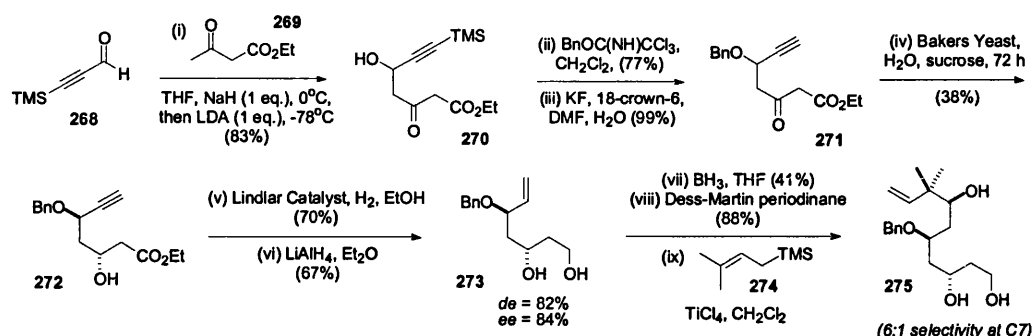
1.4.3 R. W. Hoffmann's racemic route to the C(1)-C(9) segment **267**(1995)⁸⁶



Scheme 33 R. W. Hoffmann's pathway to a racemic C(1)-C(9) bryostatin fragment.

For his synthesis of an advanced bryostatin A-ring synthon **267**, R. W. Hoffmann demonstrated the utility of the Matteson haloboronate displacement technology⁸⁷ for the efficient construction of the carbon framework (Scheme 33). Tin(II)-mediated addition of prenol chloride **255** to aldehyde **254** and subsequent hydrolysis led to the racemic diol **256** which could be converted to the cyclic sulfate **257**. After nucleophilic displacement of **257** with the lithium anion of methylenedibromide, TBS- protection of the liberated alcohol yielded the intermediate dibromide **258**.

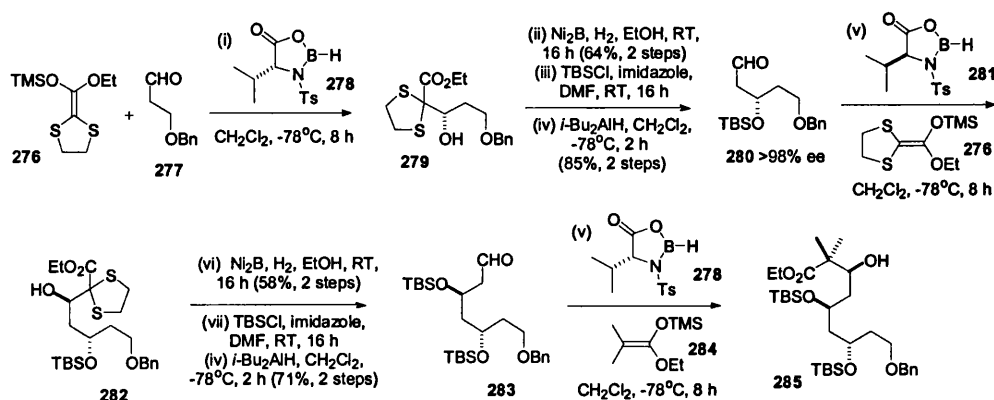
When treated with base, **258** gave rise to two carbenoid intermediates **259** and **260** with 3:1 selectivity. Whilst **260** underwent spontaneous ring closure to the [3.5]bicyclo- system **261**, it proved possible to selectively trap the desired organolithium **259** with the cyclic boronate **262**, and react the product of this union, **263**, with the di-enolate **264** to assemble the C(1)-C(9) chain in **265**. Oxidative removal of the boronic ester was achieved by extended exposure to trimethylamine-*N*-oxide and revealed the β-hydroxy ketone **266**. After a Saksena-Evans *anti*-reduction⁵⁶, the 1,3-diol array was protected as an isopropylidene acetal to yield the desired precursor **267**.

1.4.4 The Kalesse enantioselective route to the C(1)-C(9)-segment 257 (1996) ⁸⁸

Scheme 34 Kalesse's chemoenzymatic approach to C(1)-C(9) assembly for the bryostatins.

In his efforts towards the bryostatins, Kalesse has reported an A-ring synthon for the C(1)-C(9) framework that employed a biotransformation to induce the chirality present in the target (Scheme 34).

An acetoacetate aldol reaction between the propargylic aldehyde **268** and ethyl acetoacetate **269** formed the β -hydroxyketone **270**. O-Benzoylation and O-desilylation delivered β -keto ester **271** possessing the required array for kinetic resolution by stereoselective reduction with Baker's yeast; a process that furnished alcohol **272** in 82% de and 84% ee. Manipulation of the terminal moieties by alkyne hydrogenation with Lindlar catalyst, and ester reduction procured **273**, which then underwent a hydroboration and Dess-Martin oxidation. A chelation-controlled Sakurai reaction, under Lewis acid conditions thereafter resulted in an inseparable 6:1 mixture of alcohols enriched in **275**.

1.4.5 The Kiyooka reagent-controlled asymmetric route to the C(1)-C(9)-segment (1997) ⁸⁹

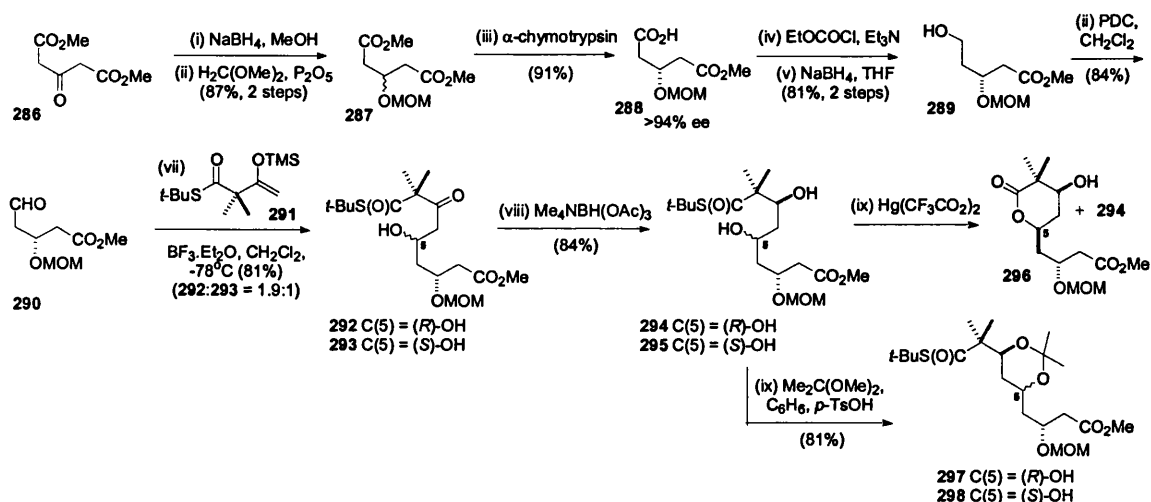
Scheme 35 Kiyooka's asymmetric aldol approach to C(1)-C(9) segment of the bryostatins.

The presence of a partially masked 1,3,5 *anti-anti* hydroxyl array in the C(1)-C(9) section of the bryostatins led Kiyooka to investigate a catalytic asymmetric aldol approach to the synthon **285**, using the valine derived boranes **278** and **281** as chiral Lewis acids (Scheme 35). By employing the mixed silylketene thioacetal **276** for a series of boron-mediated aldol reactions with aldehydes **277** and **280**, the required acetate aldol products were isolated after desulfurisation with nickel-boride.

The desired A-ring synthon **285** was produced as the sole product of a final aldol addition between **283** and **284**. The excellent levels of stereocontrol evident in this synthesis, coupled with the expedience of the route is testament to the utility of this strategy.

1.4.6 Roy's synthetic studies on bryostatin 1 (1989, 1990)⁹⁰

1.4.6.1 The synthetic path to the C(1)-C(9) fragment of bryostatin 1

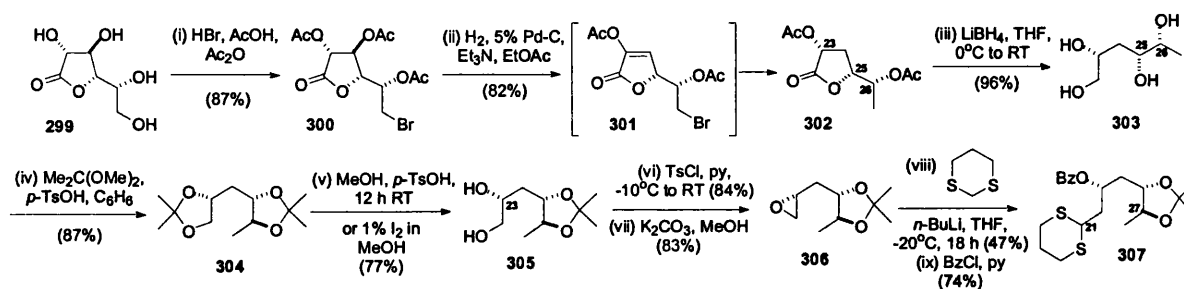


Scheme 36 Roy's chemoenzymatic route to the bryostatin A-ring.

Roy's synthesis of two potential bryostatin A-ring synthons has also exploited an enzyme mediated transformation for asymmetric induction. After a non-selective reduction of dimethyl 3-ketoglutarate **286** and subsequent MOM etherification of the resulting racemate **287** (Scheme 36), the key enzyme-catalysed step was the enantioselective hydrolysis of the pro-*S* ester, performed with α-chymotrypsin to yield the monoacid **288** in 94% ee⁹¹.

A borohydride reduction of the mixed anhydride derived from **288**, and partial re-oxidation led to the aldehyde **290**, which readily participated in a Mukaiyama aldol condensation⁹² with the silyl enoether **291**. Considerable effort was expended before $\text{BF}_3 \cdot \text{Et}_2\text{O}$ was found to deliver the desired *anti*-product **293** as the predominant isomer of an inseparable 1.9:1 mixture of *anti:syn* C(5) epimers. The two β -hydroxy ketones **292** and **293** were next subjected to a hydroxyl-directed reduction under Saksena-Evans conditions to yield the diols **294** and **295**, which could be separated after lactonisation as only one isomer lactonised. It was possible to isopropylidenate and then separate out the desired C(1)-C(9) fragment **297**.

1.4.6.2 Roy's enantiospecific route to a C(21)-C(27) synthon **307**



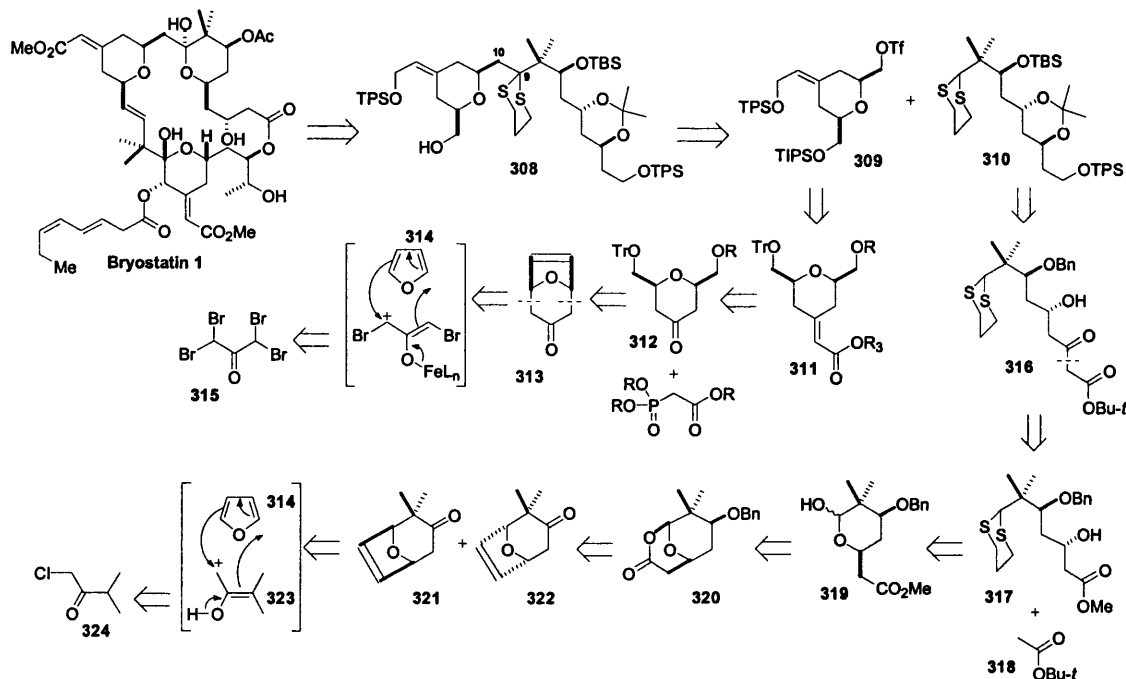
Scheme 37 Roy's synthesis of a C(21)-C(27)-dithiane intermediate for the bryostatins.

Roy's analysis of the C(21)-C(27) section of bryostatin **1** indicated that there was matching of the C(23), C(25) and C(26) hydroxyl stereochemistry of D-galactose. Conceptually a selective deoxygenation of the C(3) and C(6) positions of D-galactose is required followed by chain extension at C(11). With this in mind, Roy selected the chiral building block D-galactono-1,4-lactone **299** as the starting material for the synthesis of **307**.

After bromination and acetylation to yield the *tris*-acetate **300**, elimination and stereospecific hydrogenolysis were employed for the deoxygenation of C(3). This was followed by in-situ dehalogenation to deliver the acetoxy-lactone **302**, which underwent exhaustive reduction with lithium borohydride to reveal the bare tetraol **303**. A series of acetonide manipulations⁹³ then afforded diol **305**. Selective tosylation of **305** was followed by formation of the epoxide **306**. Completion of **307** involved selective opening of **306** with the lithio-anion of 1,3-dithiane. No further work on the elaboration of **307** has been reported.

1.4.7 The H.M.R. Hoffmann route to the C(1)-C(16) AB-segment of bryostatin (2000) ⁹⁴

1.4.7.1 H.M.R. Hoffmann's retrosynthetic analysis of the AB-ring 308



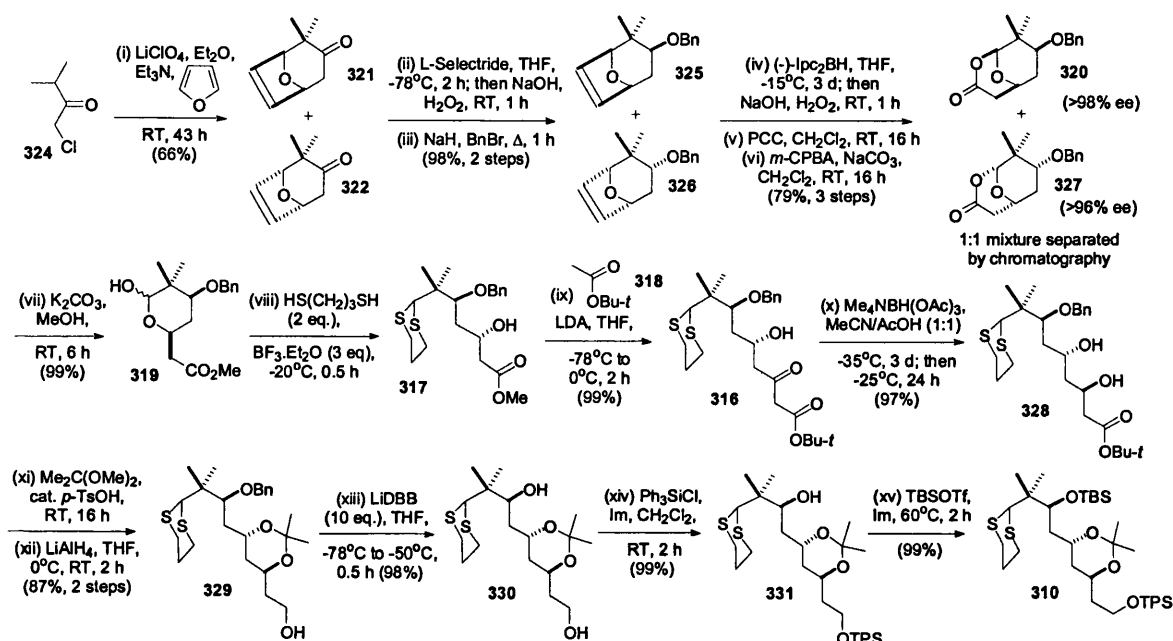
Scheme 38 H. M. R. Hoffmann's retrosynthetic plan for the bryostatin northern hemisphere 308.

Hoffmann's retrosynthetic strategy for the top-half of bryostatin 1 is shown in Scheme 38. He envisioned generating the AB system 308 from the union of the B-ring triflate 309 with the A-ring dithiane 310. The triflate 309 was thought derivable from the enoate 311 via a WHE exocyclic olefination ⁴⁹ on ketone 312. It was speculated that the steric hindrance from the bulky C(11)-trityl protecting group might shield one side of the pyran, and lead to production of the thermodynamically favoured (*E*)-olefin 311. Potentially this could be derived from the alkene 313 via ozonolysis and enzymatic desymmetrisation. Ketone 313 itself could be potentially be prepared from an iron-mediated furan [4+3] cycloaddition to the tetrabromide 315; a technology that had originally been devised by Hoffmann's and Noyori's groups ^{95, 96}.

The furan addition tactic was also thought applicable to the construction of the A-ring dithiane subsection; on this occasion the addition would be between enol 323 and furan 314 to deliver the racemic pyranones 321 and 322. The important alkene to lactone transmutation was thought possible via ketone reduction, alcohol protection and a Brown asymmetric hydroboration ⁹⁷, the latter step proceeding selectively on the more electron-rich double bond. A subsequent Bayer-Villiger oxidation would then yield

320. Reduction of **320** to the hemiketal **319**, and dithiane installation would then provide the linear-chain **317**. A chain homologation, and selective reduction would complete the desired C(1)-C(9)-synthon **310**. With this as background, we will now discuss the Hoffmann route to **308** in more detail.

1.4.7.2 H.M.R. Hoffmann's asymmetric synthesis of the C(19)-C(9)-dithiane **310**



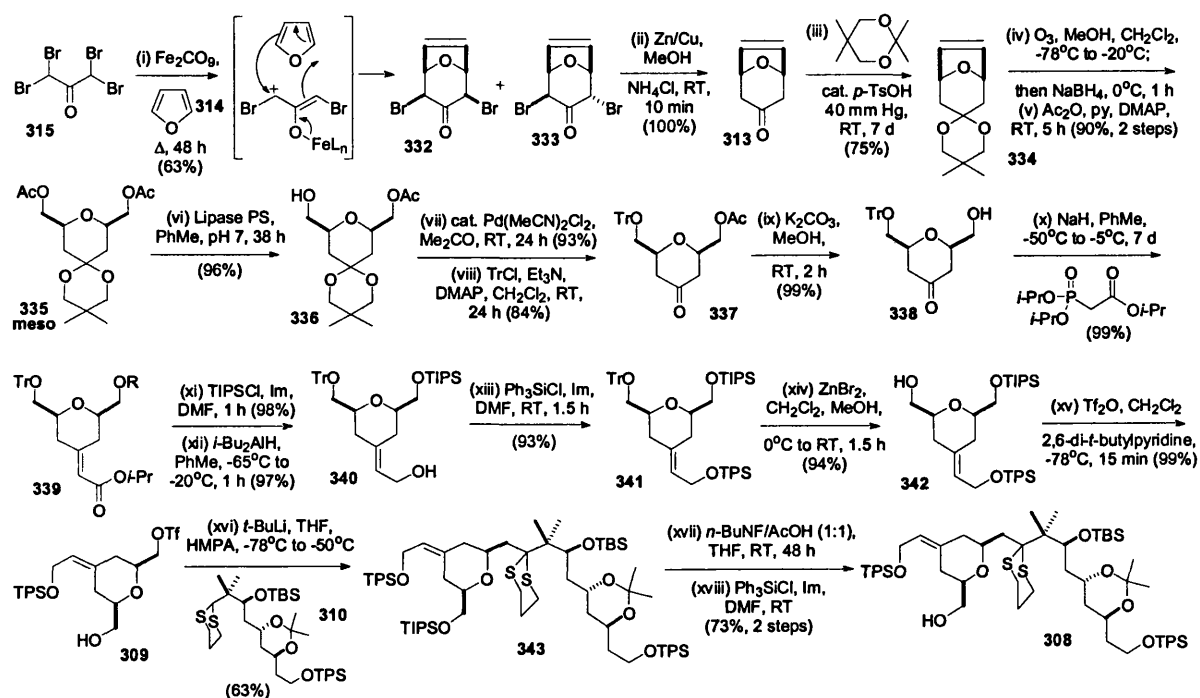
Scheme 39 H. M. R. Hoffmann's asymmetric synthesis of the A-ring dithiane synthon **310**.

In a modification of Hoffmann's original [4+3]- cycloaddition process, Fohlisch⁹⁶ⁱⁱⁱ has shown that by reacting the α -chloromethylketone **324** with furan and lithium perchlorate, the racemic ketones **321** and **322** are produced in 66% yield (Scheme 38). Hoffmann utilised this method in his outset to **310** (Scheme 39). He subjected the addition products **321** and **322** to a stereoselective reduction with L-Selectride and an O-benzoylation to obtain the alkenes **325** and **326**. Asymmetric hydroboration was then carried out with (-)-Ipc₂BH, but was not regioselective. However this impasse could be overcome by a PCC and Bayer-Villiger oxidation which allowed the lactones **320** and **327** to be easily separated by chromatography.

Transesterification of **320** provided a mixture of the hemiacetals **319** which were ring-opened with BF₃·Et₂O and propane dithiol. Dithiane **317** then underwent a Claisen condensation with the enolate derived from **318** to yield the β -hydroxy ketone **316**.

An Evans hydroxyl-directed reduction of the β -hydroxy ketone introduced the final stereocentre needed for the A-ring synthon, and the 1,3-*anti* diol array in **328** was protected as an acetonide, and the ester reduced to obtain alcohol **329**. Removal of the benzyl ether is of particular note due to the labile dithiane moiety⁹⁸, followed by selective positioning of a triphenylsilyl ether at OH(1) led to **331**, and a final O-silylation resulted in the orthogonally protected C(1)-C(9) A-ring synthon **310**.

1.4.7.3 H.M.R. Hoffmann's construction of the AB-system 308 via the B-ring triflate 310



Scheme 40 H. M. R. Hoffmann's B-ring synthesis and formation of a bryostatin "Northern Hemisphere".

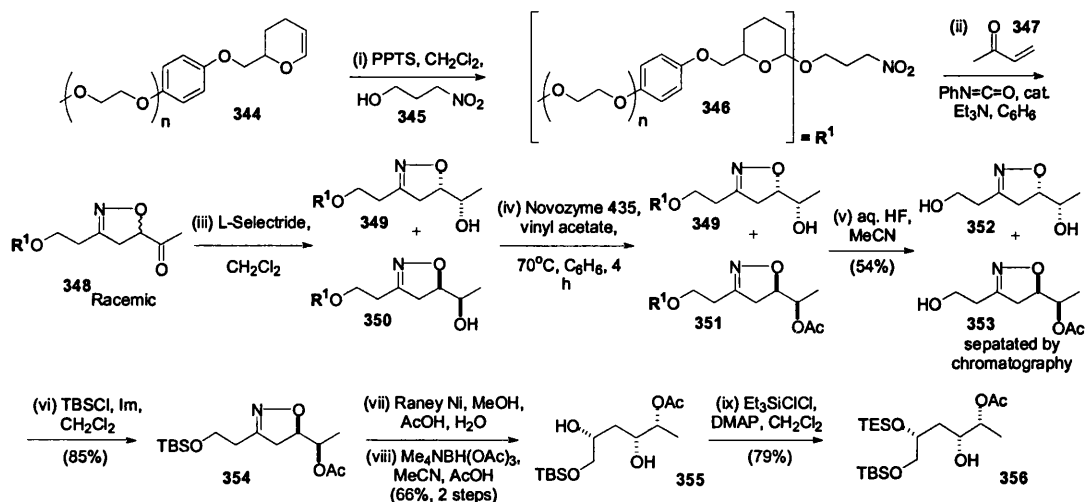
The synthesis of the *meso*-ketone **313** had been previously reported by Noyori and coworkers⁹⁶ from tetrabromo-acetone and furan in the presence of diiron nonacarbonyl catalyst. Initially this [4+3]-cycloaddition affords the dibromo adducts **332** and **333** (Scheme 40). A zinc-mediated reduction of the pyranones then produces the desired intermediate **313** quantitatively. Hoffmann protected ketone **313** as the acetal **324**, thereby avoiding potential problems in the reduction of the *bis*-aldehyde formed from the ozonolytic cleavage of the alkene.

Acetylation of **334** yielded the meso-diacetate intermediate **335** required for enzymatic differentiation of the two enantiotopic acetoxymethyl groups, which was best accomplished with lipase PS at neutral pH; the desired alcohol **336** was obtained with excellent stereoselectivity. Removal of the cyclic acetal was accomplished with catalytic palladium(II) and protection of the C(10) hydroxyl followed. Trityloxymethyl ether **337** then underwent acetal deprotection to give **338**. The planned olefination was next investigated, and as expected, the trityl ether had a most beneficial effect on directing the stereochemical outcome of this reaction. It was found that by exposing **338** to isopropyl phosphonoacetate for extended periods, the exocyclic olefin **339** was formed in superb (98%) ee. An O-silylation at OH(16) and ester reduction furnished **340**, which was then further silylated, this time, with triphenylsilyl chloride. Selective removal of the trityl ether from **341** was accomplished with zinc-bromide, and did not cause concomitant loss of the potentially labile allylic protecting group. Alcohol **342** was then converted to triflate **309**, the requisite intermediate needed for dithiane coupling.

This union was best achieved by adding the triflate **309** to a solution of the lithio-anion of dithiane **310** in THF/HMPA. This produced the desired C(1)-C(16) carbon framework in reasonable yields. Hoffmann had also shown that by altering the protecting group at C(16), dramatic effects can ensue on the coupling yield. In completion of the synthetic route, a protecting group interchange was carried out to free the C(16)-hydroxyl in preparation for the coupling to a suitable bryostatin C-ring synthon. The expediency of this pathway is most noteworthy.

1.4.8 Janda's polymer-supported synthesis of the bryostatin 1 C(21)-C(27)-sector (2000)⁹⁹

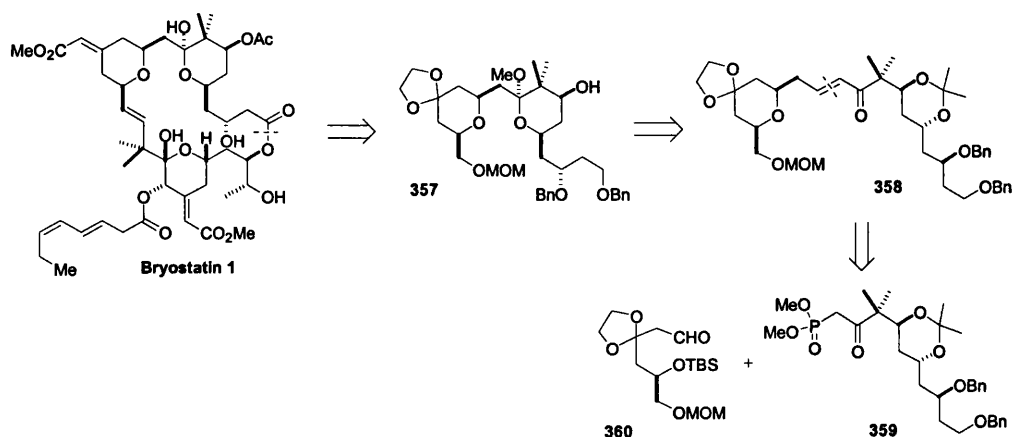
In a novel solid phase synthesis of a bryostatin C-ring synthon **356**, Janda has explored the use of a polymer support **344** (synthesised in four steps from dihydroquinone). This was attached to nitro-propanol **345** at the dihydropyran position (Scheme 41), and an intermolecular nitrile oxide cycloaddition reaction effected with methyl vinylketone **347**, yielded the racemic isoxazolines **348**. Keto reduction with L-selectride thereafter produced the diastereomeric alcohols **349** and **350**. In order to facilitate the separation these intermediates, treatment with Novozyme-435 and vinyl acetate as an acyl donor, delivered the requisite protected **351** and unreacted **349** in excellent selectivity, although in diminished yields.



Scheme 41 Janda's soluble-supported polymer pathway to a bryostatin C-ring synthon **419**.

Cleavage of the polymer was completed by exposure to aqueous HF; the alcohols **352** and **353** were readily separated by conventional methods. O-Silylation of **352** yielded **354** which was then reduced to the β -hydroxy ketone with Ra-Ni. A Saksena-Evans reduction and selective protection of the more nucleophilic C(23)-hydroxyl completed the route **356**, which could potentially be used in a convergent strategy similar to those previously reported.

1.4.9 Yadav's synthesis of the bryostatin "Northern Hemisphere" (2001)¹⁰⁰

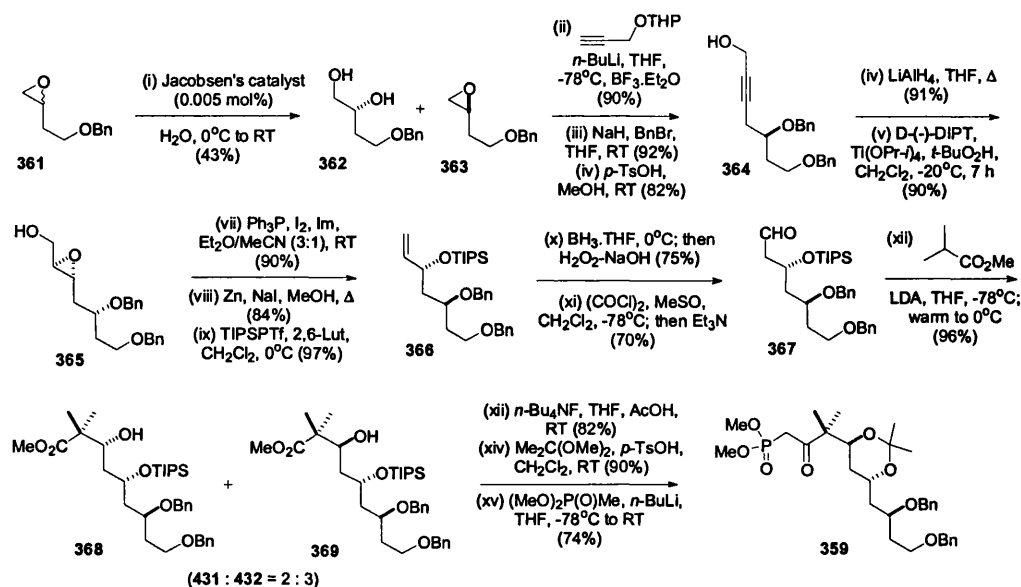


Scheme 42 Yadav's retrosynthetic planning for the bryostatin "Northern Hemisphere" **357**.

In their synthetic efforts towards the bryostatins, Yadav and coworkers have described the synthesis of an AB-ring segment **357** (Scheme 42) that has considerable for being further developed using the exocyclic olefination tactic employed by Nishiyama in their bryostatin 3 synthesis.

Their plan for the closure of the B-ring relied upon the Vandewalle intramolecular Michael addition tactic being applied to the enone **358**. The latter would be available through a WHE olefination. A Fischer glycosidation would be employed to close the A-ring. The precursors for the requisite WHE coupling were the phosphonate **359** and the aldehyde **360**.

1.4.9.1 Yadav's asymmetric synthesis of the ketophosphonate 359



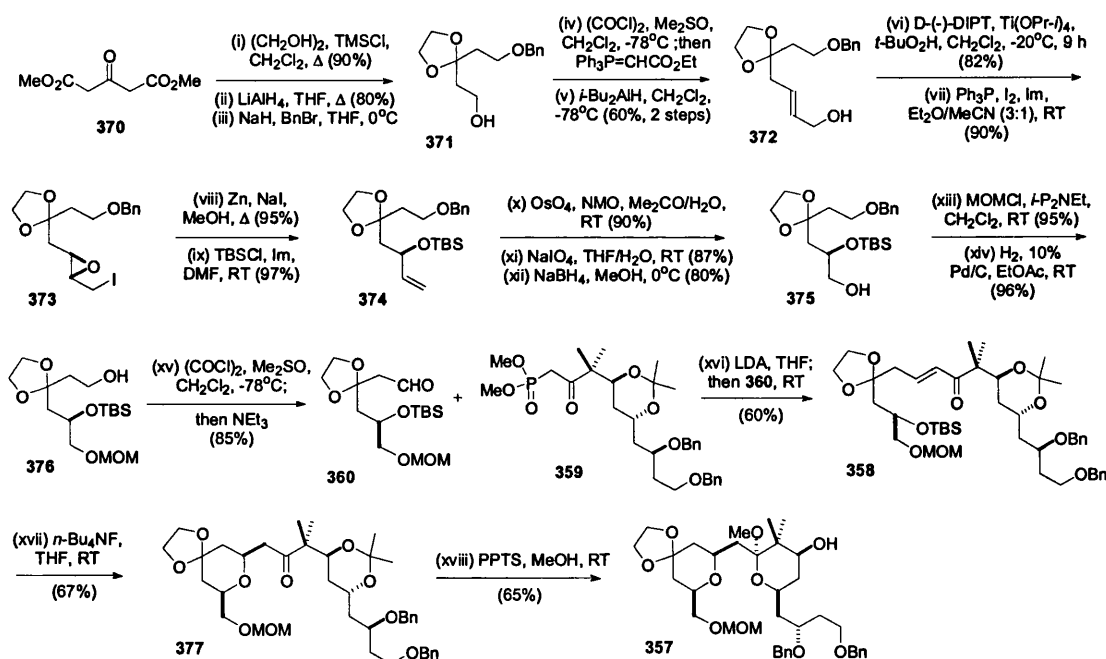
Scheme 43 Yadav's synthesis of the C(1)-C(10)-ketophosphonate **359**.

An initial kinetic resolution of the homochiral epoxide **361** using Jacobsen's procedure¹⁰¹ reliably produced a mixture of **362** and **363** that were separated (Scheme 43). Epoxide **363** was ring-opened under BF₃-catalysis with the lithio anion of a propargyl synthon. An O-benylation and THP deprotection then ensued to procure the known alcohol **364**, which underwent reduction to the allylic alcohol with LAH. A Sharpless AE helped position the C(5)-stereocentre with good levels of control. However, the surplus O-functionality in **365** needed to be removed.

For this, the epoxyalcohol **365** needed to be iodinated, and the iodohydrin reduced with Zn dust. Protection of the remaining hydroxyl as a TIPS ether then delivered the terminal olefin **366**. Hydroboration and Swern oxidation reaction subsequently yielded the aldehyde **367** which was condensed with the anion derived from methyl isobutyrate.

A 2:3 mixture of alcohols emerged from this addition in favour of the desired **369**. O-Desilylation and O-isopropylidination now protected the OH(5)-OH(7) array. The phosphonate unit was elaborated by condensation of **369** with the lithio-anion of dimethyl methylphosphonate which gave **359** in 74% yield.

1.4.9.2 Completion of the AB-intermediate 357



Scheme 44 Yadav's synthetic route to the bryostatin 1 "Northern Hemisphere".

For aldehyde **357**, the diester **370** served as the starting material. Ketone protection, ester reduction and mono-benzoylation were the first steps implemented to obtain **371** (Scheme 44). A Wittig / Sharpless AE sequence next ensued, and halogenation/elimination and O-silylation subsequently led to alkene **374**. A three-step procedure oxidatively degraded the extra carbon atom to yield the primary alcohol **375**. Protecting group rearrangement released the C(10)-hydroxy for the final Swern oxidation needed to obtain the required aldehyde **360**. The critical WHE olefination between **360** and **359** produced the desired

(*E*)-enone **358** in moderate yields, and desilylation at C(15) induced the in-situ pyran formation to place the C(9)-side-chain in **377** in an equatorial configuration. Fischer glycosidation finally removed the acetonide and closed the A-ring thereby completing the bryostatin C(1)-C(16)-synthon **357**.

1.5 Synthesis of bryostatin analogues

1.5.1 Wender's analogue work (1998, 2000)^{3, 102}

The early difficulties associated with isolating large quantities of bryostatin from natural sources have led to a number of synthetic groups embarking on the synthesis of simplified bryostatin analogues that will function as antitumour agents by an identical PKC-modulating mechanism. Many of these groups have also hoped to identify more potent analogues that could be administered orally. So far, only Wender's group has made any in-roads into the development of analogues.

The early analogue studies of Pettit and Wender had shown that alterations could be made to the northern hemisphere that did not interfere with the PKC binding activity, whereas slight structural changes to the southern hemisphere resulted in substantial loss of PKC modulatory and anticancer activity. Therefore Wender's later strategy for analogue design was to dispense with as much of the AB-ring segment as possible. To aid in the design of the analogues, molecular modelling was used in an effort to identify compounds that appeared capable of mimicking the hydrogen-bonding present in the natural bryostatins (Figure 1).

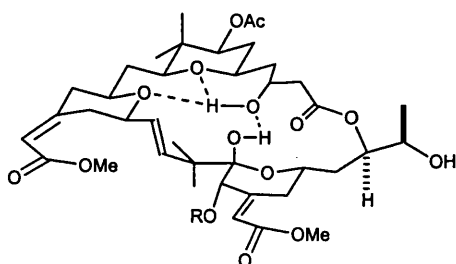
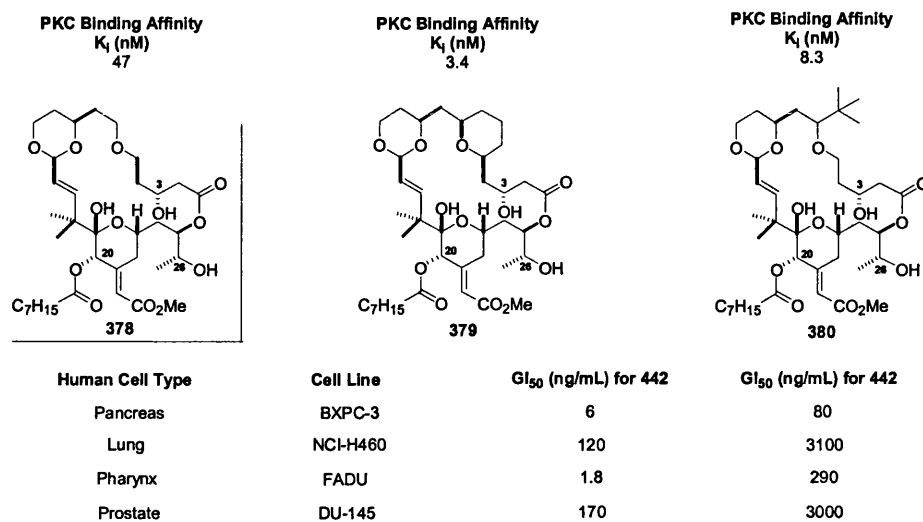


Figure 1 The bryostatin intramolecular hydrogen-bond network

These internal H-bonds are formed by interactions between the C(3)-OH and the O(5) and O(11) pyran oxygens, and also with the OH(19) hemiketal. This analogue search led to a number of candidates being proposed for synthesis, that had undergone sweeping changes to the C(3)-C(15) motif of the bryostatin framework. Indeed some of these targets possessed a relatively bare carbon chain but retained the crucial C(5) and C(15) pyran ring oxygens needed for maintaining the internal hydrogen bonding network. Significantly some of the compounds prepared have exhibited potent *in vitro* activity against a

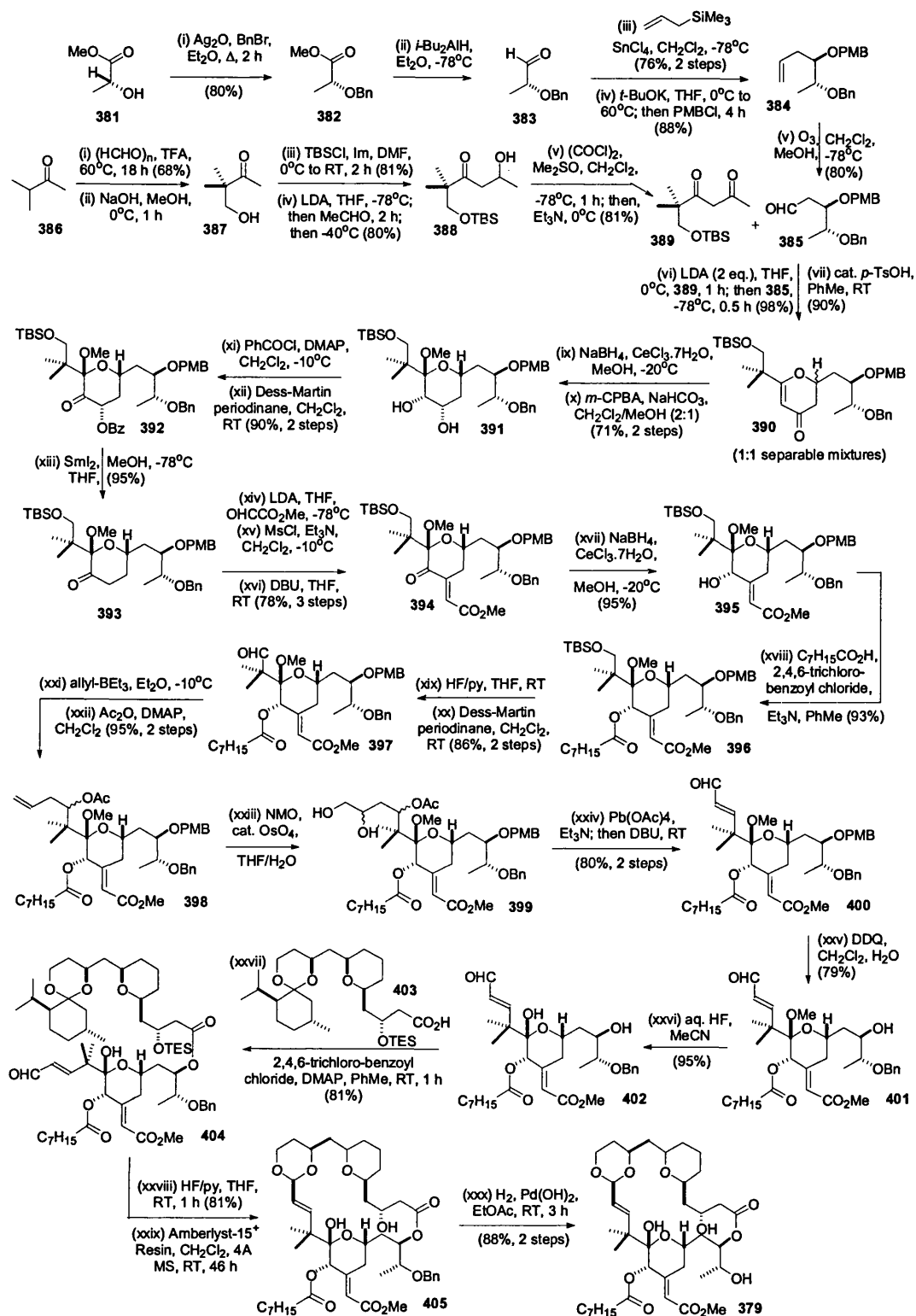
range of human cancer cell lines (Scheme 45), and similar PKC binding activities to bryostatin 1 have been found.



Scheme 45 Some examples of Wender's bryostatin analogues and their antitumour activities.

Wender's analogue work to date has suggested the need for certain structural features in all such analogues to ensure potency in their binding to PKC. These features include the presence of a 20-membered macrolactone containing the free C(3)- and C(26)-hydroxy groups of (*R*)- configuration. Significantly the B-ring enoate and A-ring pyran can be totally deleted^{3, 116}.

The central intermediate used in the assembly of Wender's bryostatin analogues was the C-ring aldehyde **402**, referred to as the recognition domain; which was prepared in 25 steps from methyl (*R*)-lactate **381** (Scheme 46). Its deployment in the synthesis of one representative analogue **379** will now be illustrated. After an initial Ag(I)-mediated benzylation, partial reduction of ester **382** to the aldehyde **383** permitted a Sakurai reaction to be effected with allyl trimethylsilane and tin(IV) chloride. Following protection of the newly generated hydroxyl as a PMB ether, the olefin in **384** was ozonolytically cleaved to give the aldehyde **385**. A non-stereoselective aldol condensation with the diketone **389**, and acid-catalysed ring cyclisation / dehydration, thereafter yielded the glycal pyranones **390** as a 1:1 mixture of epimers. The two pyranones were separated, and the desired pyranone subjected to a Luche reduction¹¹⁰ to set the C(21) equatorial hydroxyl.



Scheme 46

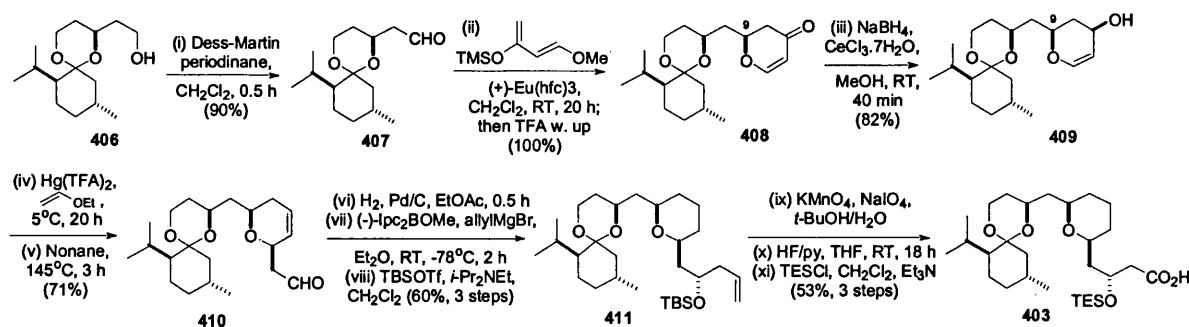
Wender's asymmetric synthesis of the simplified bryostatin analogue 442.

This served to direct the stereochemical outcome of the following epoxidation with *m*-CPBA in CH₂Cl₂ and MeOH; the acidity of the reaction mixture was sufficient to bring about methanolysis to yield the methyl glycoside **391**. A careful differentiation of the ring hydroxyls was accomplished by an equatorial benzoate protection, and an axial oxidation, to yield the ketone **392**.

This allowed deoxygenation to be effected at C(21) with samarium diiodide, and an aldol addition to be performed with methyl glyoxalate. A two step mesylation / dehydration procedure was required to set up the desired ketoenoate **394** as a single isomer, in good yields. A second Luche reduction now followed; it very efficiently set the C(20)-stereochemistry of **395**. Due to the ready availability of caprylic acid, and its potential for mimicking the bryostatin 1 C(20) side-chain, an esterification was performed with this acid under Yamaguchi conditions⁶⁶ to yield **396**. All that now remained was development of the C(17) alkene moiety. For this, an *O*-desilylation and subsequent oxidation to the aldehyde **397** was implemented. An allylboration and acetylation next procured **398**, whose olefin moiety was oxidatively cleaved and subjected to β -elimination to reveal the α - β -unsaturated aldehyde **400**. Removal of the PMB ether at OH(25) now furnished **401**, and it was considered prudent at this stage, to cleave the C(19) glycoside, as a later stage removal could have been problematic.

The desired glycoside hydrolysis could be accomplished with aqueous HF despite the flanking ester functionality, in an improvement over previous attempts at hydrolysis. The alcohol in **402** was then esterified with the AB-ring synthon **403** by the Yamaguchi protocol. After tethering of the AB-ring section had been accomplished, a desilylation and treatment with mild acid closed the 20-membered macrolactone to form the cyclic acetal **405**. The final step in the synthesis of **379** involved *O*-debenzylation by hydrogenation over Pearlman's catalyst. Amazingly, notwithstanding the presence of the olefin and enoate motifs, this selective deprotection succeeded, to yield one of the most biologically potent analogues so far synthesised by Wender.

The synthesis of the AB-ring synthon **403** is shown in Scheme 47. In this, the *spiro*-acetal **406** was oxidised to the aldehyde **407** and a hetero-diels-alder (HDA) reaction was performed with Danishefski's diene to produce the α - β -unsaturated δ -pyranone **408** in excellent yields. Luche reduction next introduced the equatorial hydroxyl of **409**, and this was then protected with ethyl vinyl ether. In the presence of *n*-nonane, a Claisen rearrangement could then be effected by heating at 145°C to obtain **410**.



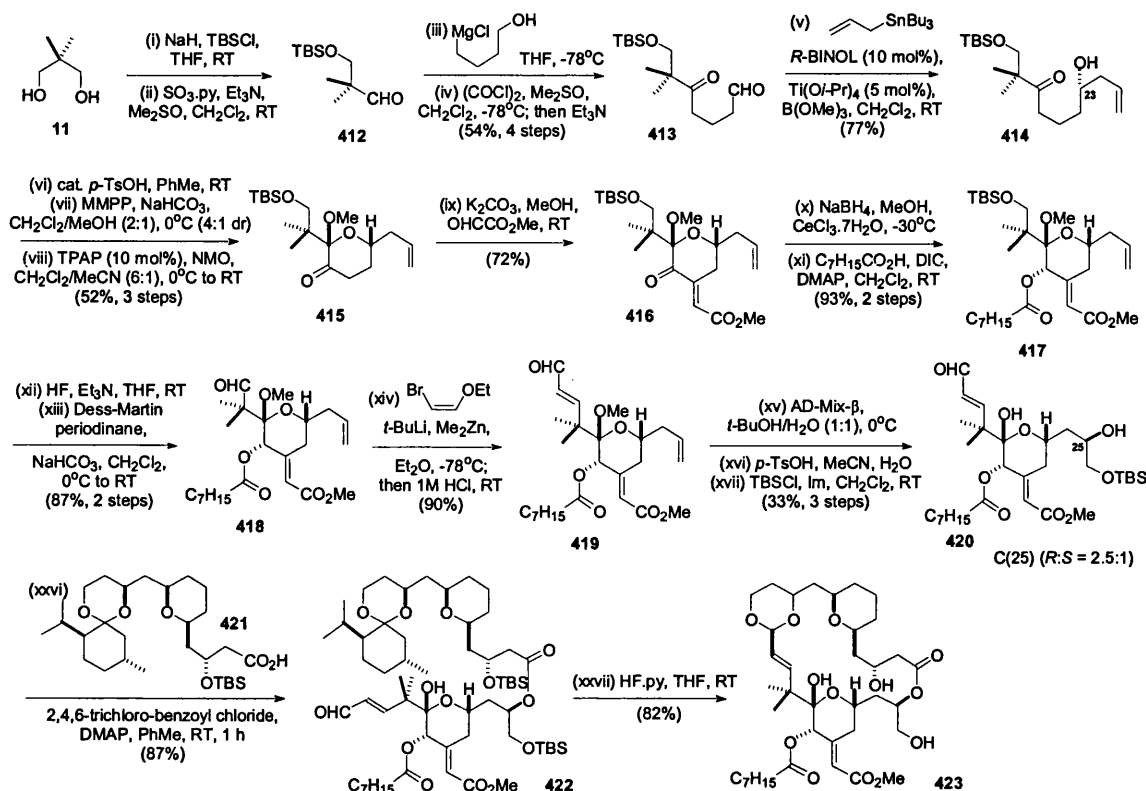
Scheme 47 Wender's asymmetric synthesis of the "Spacer Domain" of analogue **403**.

Hydrogenation of the alkene was followed by a second allylboration, and a subsequent O-silylation to yield the protected olefin **411**. The remainder of the synthesis consisted of an oxidative cleavage of the alkene to the seco-acid, and a silyl ether exchange delivered the acid **403**.

Wender's route to the analogue **379** was completed in a total of 43 steps, and had a longest linear sequence of 31 steps. Although this represents a significant reduction in steps when compared to the three bryostatin total syntheses, its great length and lack of stereocontrol in some places may prevent future commercial exploration. It does however serve to demonstrate that it is possible to greatly simplify the bryostatin framework without destroying the biological activity, allowing potential for further removal of functionality in related intermediates.

1.5.2 Wender's refinement of the simplified bryostatin analogues (2002) ¹⁰³

In his quest to improve potency and still further reduce structural complexity, Wender identified a related analogue that replaced the C(27) methyl group with a H-atom (Scheme 48). A very economic strategy has been devised to **423** starting from neopentyl glycol **11**. It was selectively monosilylated and oxidised to the aldehyde **412**, and a chain homologation effected with *bis*(chloromagnesium)butoxide; a double oxidation was then executed to obtain the *bis*-carbonyl **413**. Introduction of the C(23)-hydroxy stereocentre was completed via a Keck allylation in the presence of trimethoxyboron in 92% ee. Closure of the δ -hydroxy ketone **414** to the pyran was next accomplished by treatment with mild acid. The resulting glycal was then epoxidised and ring opened to position the methyl glycoside. The 4:1 mixture of isomers at C(20) was then oxidised to the ketone **415** using catalytic TPAP.



Scheme 48 Wender's synthesis of the modified analogue **423**.

The condensation with methyl glyoxalate was carried out in relatively mild conditions, and the resulting enone **416** was stereospecifically reduced under Luche conditions. Addition of the caprylic acid side-unit furnished the protected olefin **417**. An O-desilylation followed by oxidation gave the aldehyde **418** which was readily converted to the enal **419** by a coupling with the organozinc reagent derived from bromoethoxy-ethane. A Sharpless AD was then performed on the alkene, yielding a 2.5:1 mixture in favour of the desired diol. Its terminal hydroxyl was then selectively protected as a TBS ether, to produce the C-ring synthon **420**, and it was at this juncture that the isomers were separated.

The AB-ring segment **421** was coupled to alcohol **420** under the Yamaguchi esterification procedure to afford **422**. A global protecting group removal served to release the C(3)- and C(26)-hydroxyls, and close the lactone to deliver **423** in a remarkably efficient synthesis. The significance of removing the C(27) methyl unit served to increase the potency dramatically, when compared to the previously synthesised analogue **379**, and indeed showed over a 100-fold increase in potency over bryostatin 1.

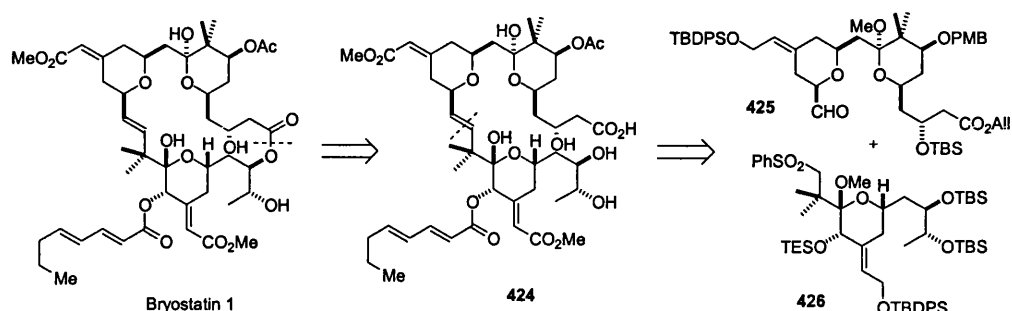
1.6 Mendola's aquaculture solution to the bryostatin 1 supply problem (2000) ¹⁰⁴

Before departing fully from our introductory discussion, a truly significant contribution has come from Dominic Mendola's laboratory with regard to bryostatin aquaculture. In an attempt to cultivate meaningful quantities of *Bugula neritina*, Mendola has developed a marine aquaculture method in which colonies of bryozoan larvae are established, and cultivated at sea over a number of months. Gratifyingly, it is found that upon harvesting, the isolated yields of the bryostatins match those typically acquired from natural sources, meaning a large-scale production could possibly deliver the large amounts needed of between 100-200 g per annum for ca. \$800,000. The aquaculture method of obtaining bryostatin 1 has the added advantage of being able to deliver the natural product at much lower cost than synthetic routes, although the limiting factor is still the relatively arduous task of isolation.

In an effort to impart an even greater degree of control over the colony production, Mendola investigated the possibility of using sea-water tanks. Unfortunately, this relied on the availability of large amounts of cultured plankton as food-stock, and since this was difficult to obtain, only limited quantities of the bryostatins were isolated. Other artificial sources of food were also investigated, however these were poorly received, and this route was therefore abandoned.

1.7 Hale's synthetic work on the bryostatins (1995, 2000) ¹⁰⁵

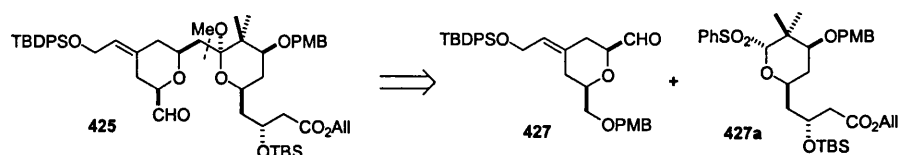
1.7.1 Hale's retrosynthetic planning for bryostatin 1



Scheme 48 The Hale retrosynthetic analysis of bryostatin 1.

A total synthesis programme towards the bryostatins has been undertaken by our group, which has so far culminated in the development of some advanced intermediates and some novel PKC- α binding analogues. Our most recent retrosynthetic analysis of the bryostatin 1 array (shown in Scheme 48) has a chemoselective macrolactonisation on **424** delivering the final target. Further disconnection across the trans olefin suggested a Julia coupling ³⁶ between the phenyl sulfone **426** and aldehyde **425** as a major fragment-joining step. Given the past precedents set by Masamune ³⁵, Evans ⁴⁷ and Nishiyama ⁶⁷ in their respective endeavours, we anticipated that this would successfully install the desired (*E*)-geometry.

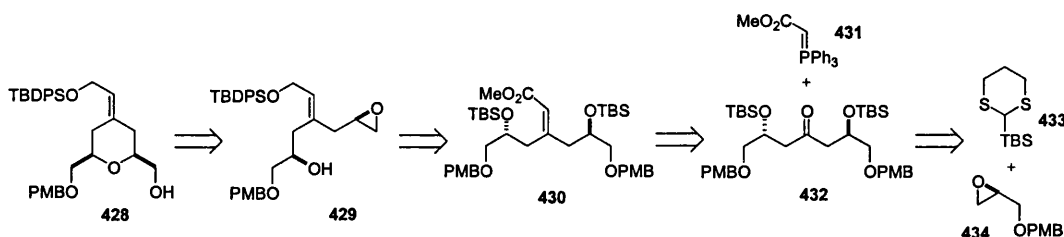
Aldehyde **425** appeared accessible from the union of the B- ring aldehyde **427** with the glycosyl sulfone **427a**, in a modified Julia olefination (Scheme 49). One could easily imagine that this would afford an exocyclic glycal capable of undergoing conversion to the methyl glycoside under mild conditions (PPTS/MeOH). Subsequent selective PMB benzyl ether removal and oxidation would then yield **425**.



Scheme 49 Our retrosynthetic plan for the "northern hemisphere" of bryostatin 1.

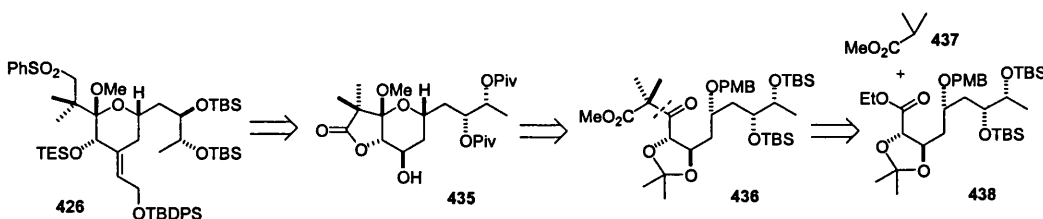
Our original retrosynthetic proposal for the B- ring aldehyde **427** (Scheme 50) called for the acid-mediated Williamson intramolecular ring closure ¹⁰⁶ of **429**. Epoxy alcohol **429** itself looked accessible from

the methyl enoate **430** via a series of hydroxy-differentiating steps. Retrosynthetic cleavage across the olefin, in turn, revealed the C₂-symmetric ketone **432**. Installation of the enoate either through a Wittig, WHE, or Peterson olefination would potentially allow complete control of the alkene geometry due to the C₂-symmetry of the substrate. This key intermediate could itself potentially be formed via a Smith-Tietze bis-alkylation reaction¹⁰⁷ between TBS-dithiane **433** and the protected epoxide **434**.



Scheme 50 Our tactics for complete control of the B-ring olefin geometry.

Retrosynthetic analysis of the C- ring phenyl sulfone **426** suggested that it could be prepared from the bicyclic lactone **435** (Scheme 51). An acid-catalysed *bis*-ring closure was proposed for the construction of this array on β -keto ester **436**. It, in turn, could potentially be derived from a Claisen condensation between methyl isobutyrate **437** and ester **438**. A series of Sharpless catalytic AD reactions were planned for introducing the requisite C(23)- C(25)- and C(26)- hydroxy stereocentres.

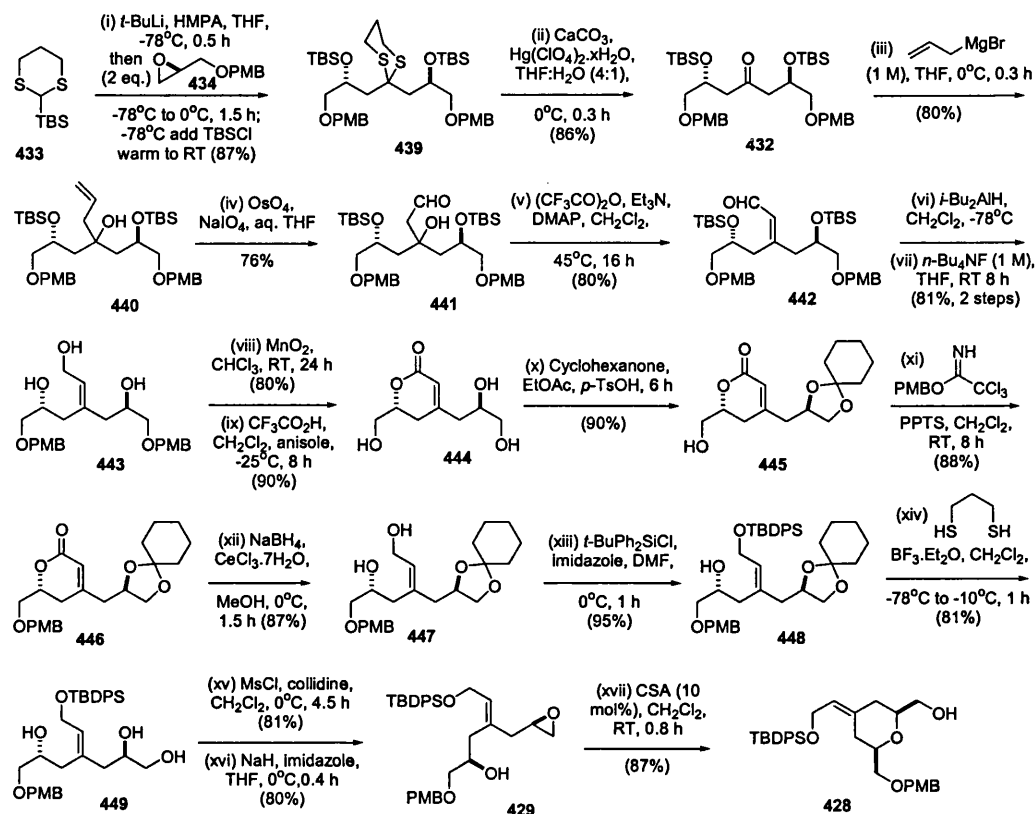


Scheme 51 Retrosynthetic tactics for the C-ring of bryostatin 1.

1.7.2 Hale's C₂-symmetry breaking olefination tactic for the construction of the B-ring^{105/}

The synthesis of the bryostatin B-ring synthon **428** commenced with the proposed Smith-Tietze *bis*-alkylation (Scheme 52) between 2-lithio-2-TBS-dithiane **433** and the protected epoxide **434**¹⁰⁸ (obtained in one step from (*S*)-glycidol). The inclusion of HMPA was critical to ensure clean TBS C- to O- migration, to generate the new monoalkylated 1,3-dithianyl anion capable of reacting with a second equivalent of epoxide

434. Trapping of the resulting alkoxide as its TBS ether led to the formation of the desired dithiane **439** in good yield.



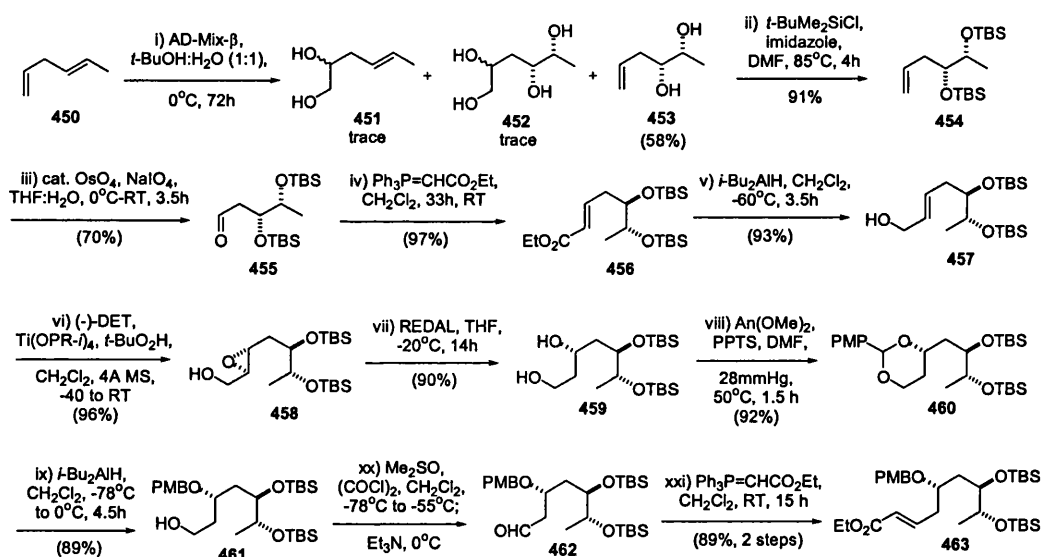
Scheme 52 Hale's fully stereocontrolled asymmetric synthesis of the B-ring **428**.

The most favourable conditions for the removal of this thioketal involved treating **439** with mercuric perchlorate in aqueous THF. Frustratingly, however all our subsequent efforts to implement olefination via Wittig, WHE or Peterson methods on **432** were unsuccessful. However, an alternative less direct method for olefination employing allyl magnesiumbromide proved more fruitful. This addition led to alcohol **440** which then underwent facile oxidative cleavage to give **441**. After trifluoroacetic anhydride- induced β -elimination to yield the enal **442**, 1,2-aldehyde reduction with DIBAL and O-desilylation revealed triol **443**. Due to the similarities of the hydroxyls present in **443** there was little room for manoeuvre in their differentiation.

However, allylic oxidation with MnO₂ proved most versatile for this purpose, it allowing the δ -lactone to be generated. Cleavage of the terminal O-PMB ethers with trifluoroacetic acid and anisole¹⁰⁹ thereafter formed **444**. Selective protection of the 1,2-diol as its cyclohexylidene acetal **445** enabled the remaining OH to be protected as a PMB ether, the lactone to subsequently be reduced under Luche

conditions ¹¹⁰ to afford the diol **447**. A selective O-silylation of the primary OH with TBDPSCI then provided **448** which underwent a Lewis-acid catalysed chemoselective removal of the acetal with propane-1,3-dithiol ¹¹¹ to triol **449**. The mesyl chloride-collidine system of Burke and O'Donnell ¹¹² was next employed for regioselective O-mesylation, and the resulting hydroxy mesylate treated with two equivalents of NaH. It was thought that epoxide formation might be followed by an in-situ ring-opening to yield the target. However only δ -hydroxy epoxide **429** was ever isolated from this reaction. The desired pyran was obtained after **429** was exposed to mild acid ¹⁰⁶. This totally stereocontrolled route to the requisite B-ring synthon was achieved in 6.3% overall yield from epoxide **434**, and is amenable to the production of **428** on multigram scale.

1.7.3 Hale's early studies on the synthesis of the "Southern Hemisphere" of bryostatin 1.



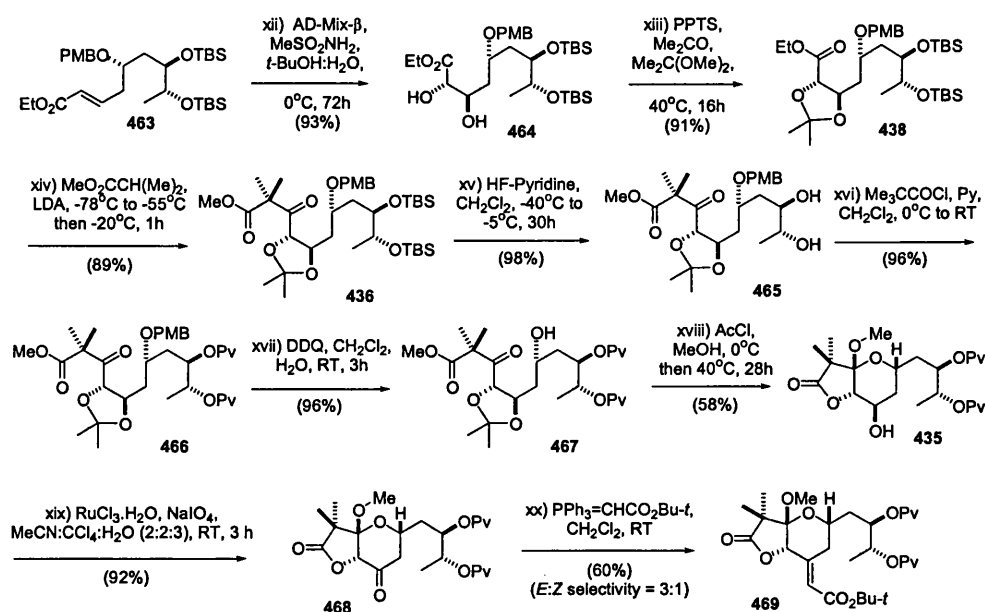
Scheme 53 Hale's synthetic studies on the C-ring of bryostatin 1.

Our plan for creating the C-ring synthon **426** was based on a series of Sharpless asymmetric oxidation reactions ¹¹³ (Scheme 53) which began with the asymmetric dihydroxylation (AD) of (*E*)-1,4-hexadiene **450** at its more electron-rich double bond. This installed the required C(25) and C(26)-hydroxy stereocentres with high stereocontrol (94% ee). By employing 0.6 equivalents of AD-mix- β , only a slight amount of the undesired diol **451** and the over-oxidised tetraol **452** were ever produced; the predominant product was always **453**. O-Silylation of the resulting diol gave **454** which then underwent oxidative

degradation with NaIO_4 and catalytic OsO_4 to give aldehyde **455**, which readily participated in a Wittig olefination and a DIBAL reduction to secure the allylic alcohol **457**.

A Sharpless asymmetric epoxidation was now performed with (-)-diethyl tartrate to set the C(23) oxygen stereocentre. The epoxy alcohol **458** was then regioselectively opened with REDAL³⁹ to yield **459**. Positioning of a PMB ether protecting group at OH(23) was accomplished by *p*-methoxybenzylidination and selective reduction to alcohol **461**. Oxidation at C(25) followed by a second Wittig olefination delivered the chain-elongated α - β -unsaturated ester **463**. A second AD was then performed on **463** with AD-mix- β to introduce the C(20) hydroxy stereocentre (Scheme 54), and an acetal protection of the diol motif was completed with 2,2-dimethoxypropane. Implementation of a Claisen condensation with the anion from methyl isobutyrate delivered the β -keto ester **436**, and the *bis*-ring formation now looked within reach.

This desired ring closure would have to be carried out under acidic conditions; conditions that would almost certainly cause O-desilylation. Therefore it was reasoned that by converting these silyl ethers into more acid-stable pivaloyl esters, ring closure could be achieved cleanly. Dipivaloate **466** was easily accessed; it underwent cleavage of the PMB ether with DDQ to form the requisite δ -hydroxy ketone **467**. Treatment of **467** with methanolic HCl then led to cleavage of the acetonide and effected an *in-situ* butyrolactonisation upon the C(20)-hydroxyl, yielding the methyl glycoside **435**. This cyclisation nicely differentiated between OH-(20) and OH-(21)¹¹⁴.



Scheme 54

Continuation of Hale's synthesis of the bryostatin 1 C-ring.

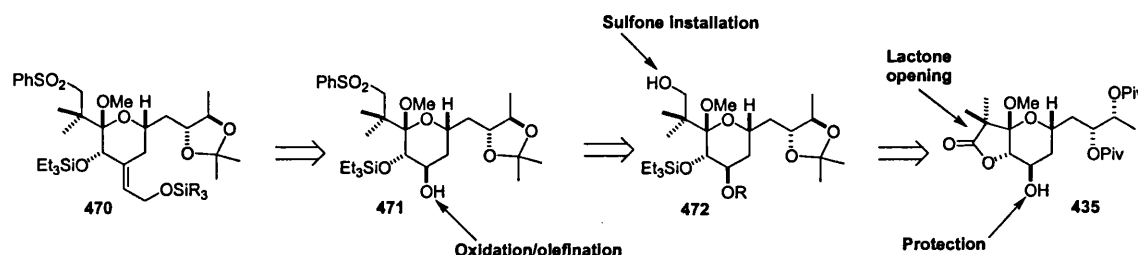
Oxidation of the resulting hydroxyl ¹¹⁵ delivered ketone **468** which was then reacted with the phosphonate $\text{Ph}_3\text{P}=\text{CHCO}_2\text{Me}$. Unfortunately, this led only to a 1:1 mixture of exocyclic olefins, with similar results being obtained under WHE conditions. The butyrolactone unit was clearly not exhibiting enough of a steric influence to favour the desired (*E*)-enoate, so an increase in the steric bulk of the ylid component from OMe to *O**t*-Bu was examined. This led to a 3:1 mixture enriched in the desired olefin and completed the synthesis of the late-stage synthon **469**.

It was at this point that I began my involvement in the project; my aim was to complete the synthesis of the desired C-ring synthon **426** via manipulation of **435**.

2.0 DISCUSSION

2.1 Continuation of the first generation synthesis

Given the poor selectivity encountered in the olefinations of **468**, we decided to now position a more sterically demanding group on the C(20) hydroxyl; something that would clearly be much bigger and bulkier than the γ -lactone. Our hope was to induce a much greater level of selectivity in the Wittig olefination than was previously encountered. A triethylsilyl ether was deemed suitable in this capacity, and one could readily envision such a system reacting in the desired way (Scheme 55). We envisioned that the cardinal intermediate in our new plan would be **471** and that it could readily be derived from **435**.



Scheme 55 Overall retrosynthetic planning for completing the Bryostatin C(17)-C(27) C-ring.

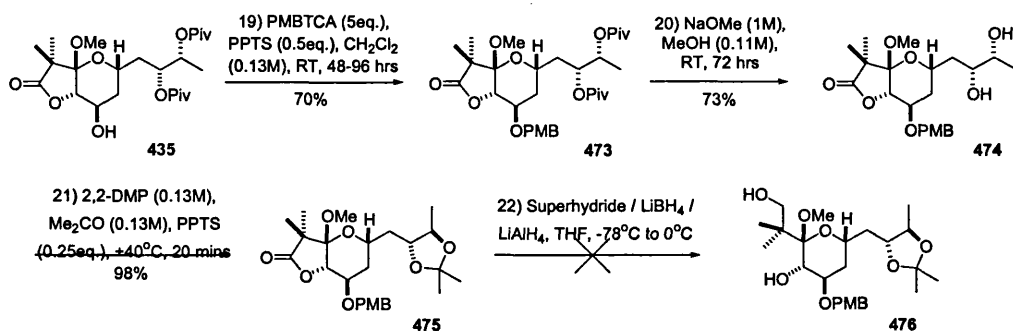
Our strategy was first to position a suitable protecting group on the free hydroxyl at C(21), and then to exchange the pivaloyl esters at OH(25)/OH(26) for an acetonide. The likely ease with which a *p*-methoxybenzyl ether could be differentiated from the other functionality present in **435** led to its selection for blocking the C(21)-OH.

Treatment of **435** with excess PMB-trichloroacetimidate¹¹⁶ in CH_2Cl_2 and a catalytic amount of pyridinium-*p*-toluene sulfonate (Scheme 56) led to **473** in 70% yield, but extended reaction times were required. The slow rate of benzylation was presumably due to the unfavourable 1,3-diaxial interaction encountered with the anomeric OMe, and the steric bulk of the imidate. Saying this, any starting material that remained in this reaction could always be recovered.

Purification of the PMB ether **473** was usually hampered by the fact that an excess of the imidate had to be used, and it degraded to by-products possessing very similar R_f values to the product. Successful etherification was confirmed by the appearance of aromatic AX doublets at δ 7.20 and 6.82 ppm which

exhibited a J coupling of 8.6 Hz in the 500 MHz ^1H NMR spectrum in CDCl_3 , with accompanying loss of the broad OH doublet at δ 2.34 ppm.

Ether **473** was then subjected to hydrolysis using a large excess of a freshly made 1M sodium methoxide solution in MeOH at room temperature for 3 days. This served only to remove the remote pivaloate ester functionalities, leaving the lactone unit intact, possibly due to shielding from the adjacent geminal dimethyl entity, or to a Thorpe-Ingold effect favouring butyrolactonisation after initial ring-opening.



Scheme 56 Protecting group manipulation followed by attempts at lactone opening.

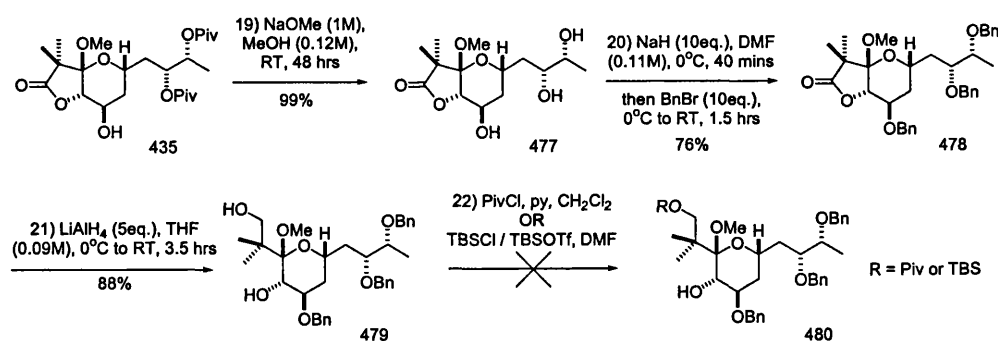
Amberlite IR-120 H^+ neutralisation and work-up allowed the isolation of diol **474** in 73% yield. The loss of the two O-pivaloates was confirmed by the disappearance of the two t-Bu singlets at δ 1.17 and 1.15 ppm in the 500 MHz ^1H NMR spectrum in CDCl_3 . The ester carbonyl peaks which resonated at δ 177.5 and 177.3 ppm in the 125 MHz ^{13}C NMR spectrum of **473** in CDCl_3 were also absent. A broad OH stretching absorption appeared at 3446 cm^{-1} in the IR spectrum of **474**, and its HRMS confirmed our structural assignment, it showing an $[\text{M}+\text{Na}]^+$ ion at m/e 447.1995 suggesting an empirical formula of $\text{C}_{22}\text{H}_{32}\text{O}_8$.

Gentle heating of the *cis* 1,2-diol in a 1:1 mixture of acetone and 2,2-dimethoxypropane containing a catalytic amount of PPTS caused rapid acetonide formation to give **475** typically in quantitative yield. The presence of two methyl singlets at δ 1.35 and 1.32 ppm in the 500 MHz ^1H NMR of **475** in CDCl_3 , together with the loss of the broad OH resonance in the IR spectrum confirmed that protection had been successful. This now meant that the critical butanolide ring-opening could be attempted.

In our efforts to achieve this goal, a number of differing reducing agents were examined, including an excess of Superhydride[®] [$\text{LiB}(\text{Et})_3\text{H}$] or sodium borohydride in THF at -78°C . To our dismay, these served only to generate a large number of products according to TLC analysis. However, encouragement

came when a 1M solution of lithium aluminium hydride (LAH) in Et₂O at room temperature was employed for the reduction. It generated a mixture of the desired intermediate lactols, and although relatively small yields of product were seen, the reaction did occur cleanly and was associated with no other decomposition by-products. We reasoned therefore that if some protecting group changes were made, then the pivotal lactone opening could be achieved in higher yield under similar conditions.

We now judged benzyl ethers to be acceptable protecting group alternatives at this juncture, and therefore adopted a comprehensive benzylation stratagem. With this intention, the pivaloyl esters in **435** were again hydrolysed with an excess of 1M sodium methoxide, yielding triol **477** in quantitative yield (Scheme 57). HRMS again provided the evidence for product formation, it showing an [M+Na]⁺ ion at *m/e* 327.1420 suggesting an empirical formula of C₁₄H₂₄O₇. O-Benzoylation was now effected by treatment with an excess of sodium hydride (60% dispersion in mineral oil) in DMF at 0°C for 40 mins, followed by addition of excess benzyl bromide and warming to room temperature. The *tris*-O-benzyl ether **478** was isolated in 76% yield after SiO₂ chromatography. The appearance of a large 15 proton multiplet at δ 7.21 ppm in the 500 MHz ¹H NMR spectrum (CDCl₃) confirmed the presence of the 3 phenyl rings. The 6 benzylic proton doublets at δ 4.62 - 4.41 ppm were also readily discerned. Together with the disappearance of the broad OH signal at 3394 cm⁻¹ in the IR spectrum, the available evidence suggested that protection had gone to plan.

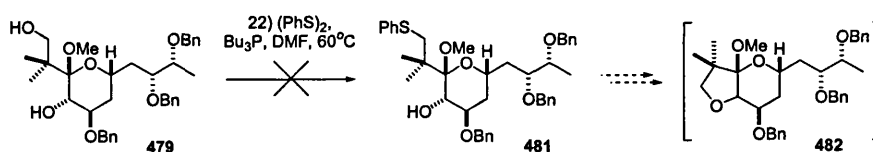


Scheme 57 Protecting group reorganisation allowing a successful lactone opening.

Although this route circumvented the cumbersome PMB etherification, and its associated purification problems, it did now necessitate a later-stage deprotection / reprotection strategy. To our satisfaction, treatment of **478** with 5 equivalents of a 1M solution of LAH in Et₂O at 0°C in THF, and slow warming to ambient temperature over 3.5 hours led to the starting lactone and intermediate lactol being

consumed according to TLC analysis. On re-cooling to 0°C and quenching with MeOH, the crude product was vigorously stirred with a 10% aqueous solution of Rochelle salt prior to extraction. This helped remove all the aluminium salts. The subsequent purification of the unstable diol **479** was best achieved by rapid SiO₂ flash chromatography; it provided **479** as a viscous oil in a pleasing 88% yield. The appearance of a new AB quartet at δ 3.53 ppm in the 500 MHz ¹H NMR spectra in CDCl₃ for the C17 protons confirmed the CH₂OH group was present.

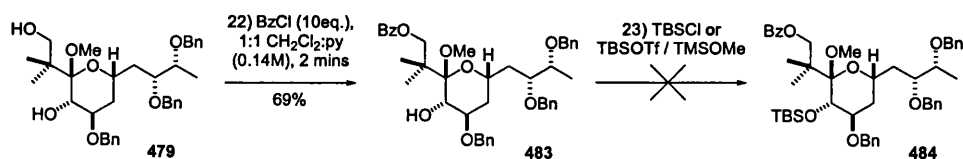
Due to the greater nucleophilicity and reactivity of the primary alcohol over the secondary, we were confident in our rationale that we could selectively protect the newly formed C(17)- and C(20)- hydroxyls in **479**. Disappointingly, problems were encountered when selective primary silyl etherification or pivaloyl esterification methods were employed, due to competing elimination reactions both at the glycosidic position. Difficulties were also met when we tried to effect a selective thioetherification of the primary alcohol in **479** using diphenyl disulfide as the phenylthiolate anion source (Scheme 58). Although a clean reaction took place according to TLC, purification of the resulting product showed no thiophenyl signals, and mass spectral analysis confirmed that a tetrahydrofuran had formed, possibly again due to a favourable Thorpe-Ingold effect from the geminal dimethyl groups which would clearly favour intramolecular displacement of the phosphonium ion intermediate.



Scheme 58 Attempted selective thioetherification of intermediate diol **479**.

Gratifyingly, we later found that by subjecting the unstable diol **479** to rapid treatment with 10 equivalents of benzoyl chloride at 0°C in a 0.04M solution of 1:1 CH₂Cl₂ and pyridine, only the primary benzoate **483** was formed (69% yield) (Scheme 59). Confirmation of this result came from the appearance of the carbonyl resonance at δ 172.3 ppm in the 125 MHz ¹³C NMR spectrum, and the HRMS which showed an [M+Na]⁺ ion at *m/e* 705.3403 suggesting an empirical formula of C₄₂H₅₀O₈.

The major source of instability of these intermediates was always found to be the great ease of which the anomeric methoxy group underwent elimination to either the glycal or the hemiketal, principally when the C20 hydroxyl was left unprotected.

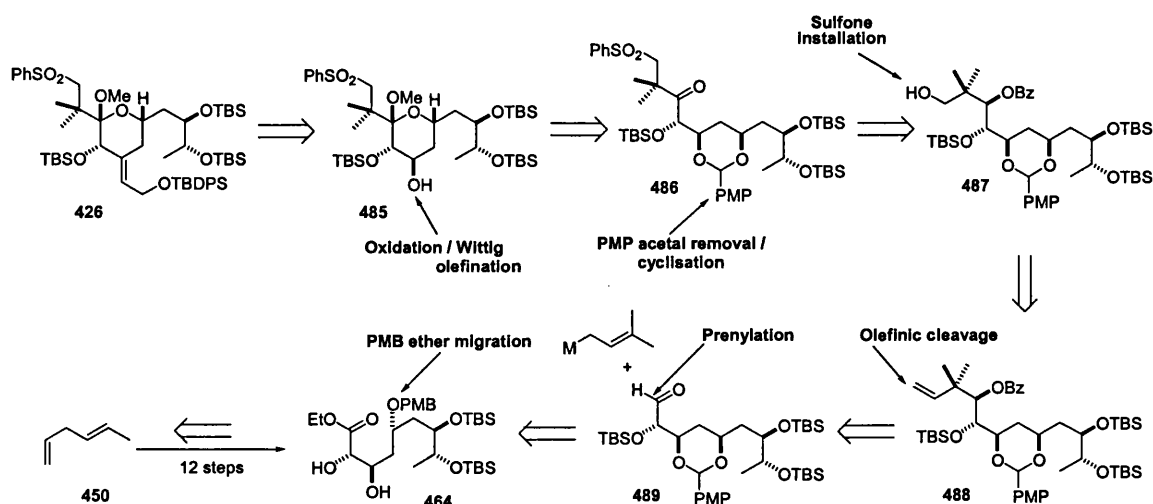


Scheme 59 Attempted silyl etherification at C(20).

This elimination meant that all our endeavours at trying to position a silyl ether protecting group at OH(20) on **483** were unsuccessful, even when a methoxide source was added to the reaction mixture, which we thought would alleviate this misfortune¹¹⁷.

In view of these unforeseen setbacks, and also due to the large and ever increasing number of steps required to complete the synthesis of the target, we elected to abandon this strategy in favour of a potentially more facile route, that involved fewer transformations. However, we did not want to abandon the chemistry developed by Lennon entirely, and so a suitable intermediate was sought on his route that would allow us to deviate and access our target **426** more economically. Again, our original postulate of positioning a bulky protecting group at OH(20) was the conceptual driving-force behind our new approach.

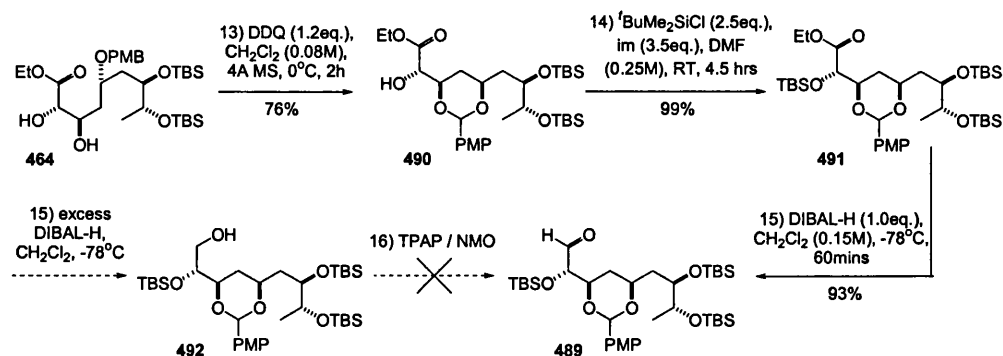
2.2 Modified retrosynthetic analysis of the bryostatin C-ring



Scheme 60 Modified retrosynthetic analysis employing a linear backbone strategy.

The intermediate diol **464** was now singled out as a potentially useful starting point for the new approach, as it already contained the requisite C(26)/C(25)/C(23) and C(20) stereocentres, and so our modified retrosynthetic analysis began from this point (Scheme 60). By inducing a PMB migration, a subsequent O-silylation and partial ester reduction could allow a prenylation reaction to be performed on aldehyde **489** to yield the protected benzoate **488**. Olefin degradation towards the primary alcohol **437** would then allow the sulfone unit to be anchored. Debenzoylation and hydroxyl oxidation would then lead us to intermediate **486** that could undergo Fischer glycosidation to give **485**. Oxidation and olefination could then yield **426**.

It was found that by subjecting the diol **464** to 1.2 equivalents of DDQ in CH₂Cl₂ in the presence of flame activated 4Å molecular sieves, a clean C- to O- benzylic migration could be accomplished to give **490** in 76% yield (Scheme 61). Sometimes lower yields (65%) were encountered and attributed to the fact that DDQ could act as a PMB ether cleavage reagent when traces of H₂O were present. The disappearance of the benzylic AB quartet and the appearance of a high-field singlet at δ 5.44 ppm in the 500 MHz ¹H NMR spectrum of **490** in CDCl₃ indicated that the desired migration had occurred. As expected, HRMS showed the loss of two hydrogens, thus being an [M+Na]⁺ ion at *m/e* 635.3411 indicative of an empirical formula of C₃₁H₅₆O₈Si₂.



Scheme 61 Formation of the aldehyde **489** via a PMB migration tactic.

Although in our initial retrosynthetic analysis we had envisioned positioning a triethylsilyl ether at OH(20) (**426** in scheme 48), further reasoning concluded that a TBS ether could be subjected to a greater array of intermediate transformations due to its increased stability. To this end, O-silylation of the C(20) hydroxyl in **490** was achieved by treatment with 2.5 equivalents of *tert*-butyldimethylsilyl chloride and 3.5 equivalents of imidazole in DMF for 4.5 hours, in typically quantitative yields. Final confirmation of product

synthesis came from the HRMS which showed the addition of a $C_6H_{15}Si$ unit, with an $[M+Na]^+$ ion at m/e 749.4276, indicative of an empirical formula of $C_{37}H_{70}O_8Si_3$.

Our next objective was the ester to aldehyde conversion, and our initial planning had involved a two-step procedure involving exhaustive reduction of the ester followed by partial alcohol oxidation. Work was investigated along these lines, however poor yields of the product were often encountered, as well as a disproportionate amount of degradation material. A one-step partial ester reduction looked a viable alternative, and indeed, treatment of the ester **491** with a equimolar quantity of Superhydride® in THF effected this transformation.

This method was superseded, however, by treating **491** with an equimolar amount of a 1.5M solution of diisobutylaluminiumhydride in toluene at low temperature. After 1 hour the reaction mixture was quenched with MeOH and on warming to 0°C the crude product was vigorously stirred with a 10% aqueous solution of Rochelle salt. Isolation of the desired aldehyde **489** was completed in a credible 93% yield with only trace amounts of the over-reduced alcohol being formed. This advantageous result could be explained by the internal chelation of the alkoxyaluminium species preventing its ready breakdown, thereby limiting the amount of the desired aldehyde present in our mixture, until aqueous work-up was completed.

The observation of an aldehyde proton resonance at δ 9.73 ppm in the 1H NMR spectrum of **489** in $CDCl_3$, and of the aldehyde carbon at δ 202.9 ppm in the 125 MHz ^{13}C NMR spectrum confirmed we had been successful. Moreover the HRMS of **489** showed that the OEt unit had been lost with the $[M+Na]^+$ ion at m/e 683.4195 which was suggestive of a correct product analysis.

Attention now turned towards the important prenylation reaction that would introduce the C(18)-C(17) segment of our linear chain. To probe the possible selectivity issues that might be raised in this addition, we carried out some crude studies using Grignard tactics, and found that methyl- / allyl- / and prenyl- magnesium bromide additions occurred in reasonably high yields, albeit in diminished selectivities. Even though a selective stereochemical outcome for these transformations was not called for in our target analysis, loss of stereointegrity would hamper our overall strategy, and make the subsequent olefin manipulation problematical. Indeed from these findings, an undesirable oxidation at the newly formed C(19) hydroxyl looked the only option open at this point, and so alternative methods were sought to alleviate this problem.

Our interest turned to some work carried out by Paquette *et al* using crotyl and allyl indiums as reagents for C-C bond formation ¹¹⁸. They had shown that allylic indium bromides readily add to numerous aldehydes in a 1:1 mixture of H₂O and THF, in a predictive asymmetric manner.

The added advantage of utilising their chemistry meant that the reactions could be carried out at ambient temperatures, and in aqueous media. Following the protocol developed by Paquette, aldehyde **489** was dissolved in a 0.2 M solution of 1:1 H₂O:THF and stirred with 2 equivalents of indium powder. Upon addition of prenyl bromide, a rapid addition of the allylic unit was observed and upon purification, a single isomer **493** was isolated, in 59% yield. The observation of a single product agreed with the findings reported, where a bulky OTBS was positioned α to the aldehyde. Such groups were suggested to exist in the more stable equatorial position in the transition state analysis (Figure 2), with the bulky R group residing in the more stable equatorial position

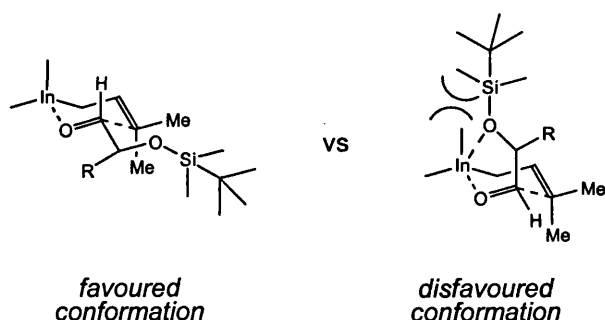


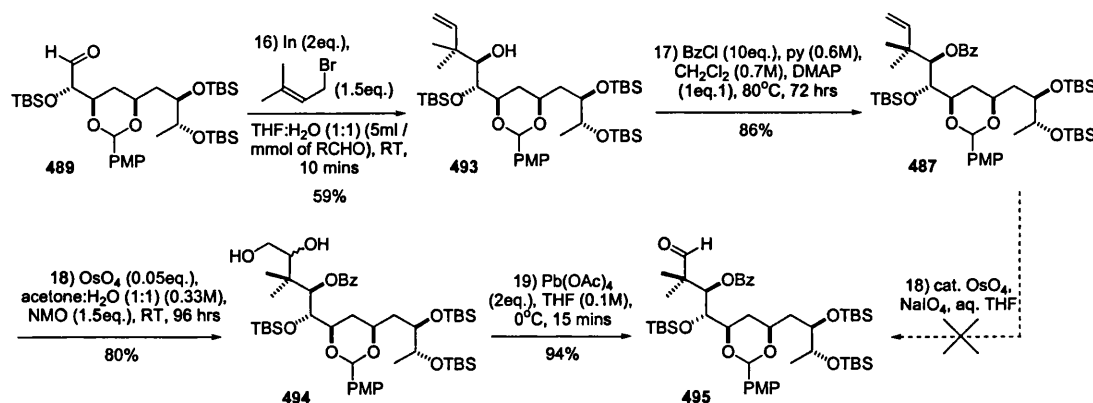
Figure 2 Analysis of the transition state indium prenylation of **489**.

The TBS protected alkoxy group is suggested not to partake in any secondary coordination to the indium centre. Confirmation of the terminal olefination was provided by the 500 MHz ¹H NMR spectrum of **493** in CDCl₃, which contained a two hydrogen multiplet at δ 4.99 ppm and a single hydrogen double doublet at δ 5.83 ppm, with *cis*- and *trans*- *J* couplings of 10.4, 18.0 Hz with the C(17) proton across the other side of the double bond.

It was felt prudent as this stage to protect the hydroxyl and carry out the olefin installation later (Scheme 62). Initial attempts at O-pivaloylation were found to be slow and so an alternative acid chloride was sought. It was found that by reacting the alcohol **493** with an excess of benzoyl chloride in a CH₂Cl₂ / py mix, with one equivalent of DMAP and heating at 80°C, the secondary benzoate **487** was formed in 86% yield after 72 hours. The extended reaction times were needed due to the severe steric crowding around

the C(19)-OH exerted by the geminal dimethyl group and the α -TBS ether. The product identity was confirmed by the appearance of an ester carbonyl peak at δ 166.0 ppm in the 125 MHz ^{13}C NMR spectrum of **487**, and its LRMS which showed that the a $\text{C}_7\text{H}_4\text{O}$ unit had been added ($[\text{M}]^+$ ion at m/e 857).

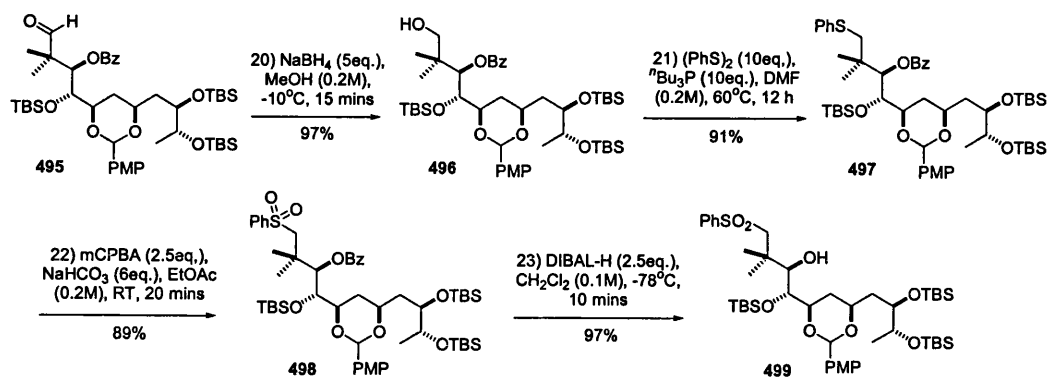
To position a CH_2OH at C(17), the olefin would now need to be oxidatively degraded. Dihydroxylation via OsO_4 and in-situ cleavage with NaIO_4 looked a viable procedure. This method was, however, found to be unsatisfactory, and although the consumption of starting alkene **487** was seen, only a number of undesired degradation by-products were formed. It was then postulated that by performing the initial dihydroxylation, and isolating the product at this point, that we might get better results in the vicinal glycol cleavage using $\text{Pb}(\text{OAc})_4$.



Scheme 62 Chain elongation via an indium catalysed addition.

The desired diol intermediate **494** was obtained in a reliable way by dissolving **487** in a 1:1 mixture of acetone: H_2O and exposing it to 10 mol% of a 0.04 M solution of OsO_4 . To aid the solubility of the olefin, a small amount of *tert*-butanol was added. 1.5 Equivalents of methyl morpholine-*N*-oxide (NMO) was also added as a co-oxidant. Prolonged reaction times were necessary in order to maximise the product yield, and addition of a large excess of Na_2SO_3 was needed for the osmate ester reduction; a 1:1 mixture of diols was isolated. The appearance of a large broad OH stretching vibration at 3424 cm^{-1} in the IR spectrum of **494** confirmed that dihydroxylation had indeed taken place. To our great delight, exposure of diol **494** to two equivalents of $\text{Pb}(\text{OAc})_4$ in THF caused a clean and rapid conversion to the aldehyde **495** in 94% yield.

The desired olefin to alcohol conversion was completed by reducing the aldehyde **495** with five equivalents of sodium borohydride in methanol, and typically proceeded in quantitative yield (Scheme 63).



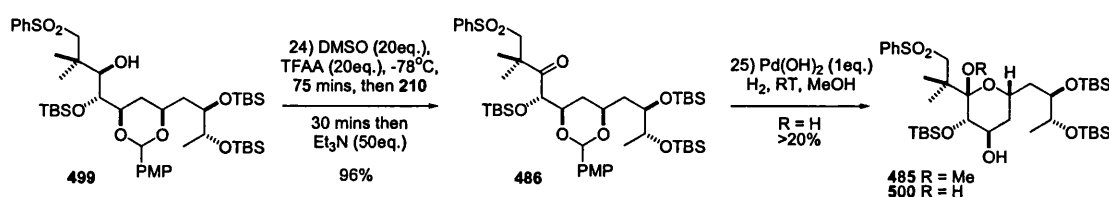
Scheme 63 Installation of the sulfone unit at C(17).

With alcohol **495** now in hand, the ensuing thioetherification became the next synthetic hurdle to traverse. After much experimentation, it was eventually found that by heating **495** with 10 equivalents of diphenyl disulfide and tri-*n*-butyl phosphine in DMF for 14 hours, the required thioether **496** was obtained in 91% yield. Loss of the broad OH resonance at 3472 cm^{-1} in the IR spectrum of **496**, and the appearance of 5 phenyl protons between $\delta\ 7.30 - 7.10\text{ ppm}$ in the 500 MHz ^1H NMR spectrum of **496** in CDCl_3 indicated that thio-etherification had been a success.

Thioether oxidation was carried out by treating **497** with 6 equivalents of sodium bicarbonate and 2.5 equivalents of *meta*-chloroperbenzoic acid in expeditious fashion, and reasonable yield. Due to the enhanced acidity generated at the α -sulfone position, the C(17) protons exhibited a shift of $\delta\ 0.27\text{ ppm}$ in the 500 MHz ^1H NMR spectrum of **498**.

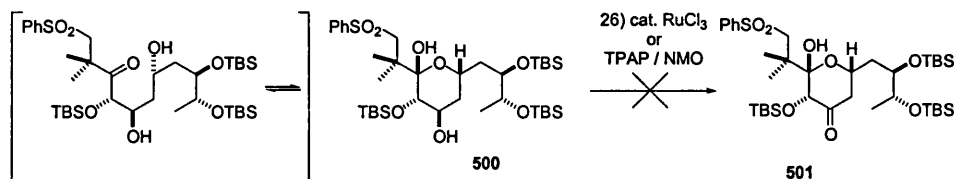
Removal of the benzoate ester protecting group from **498** was accomplished by the low temperature addition of 2.2 equivalents of a 1.5 M solution of diisobutylaluminium hydride in toluene and dry dichloromethane. After 10 minutes, the mixture was quenched with methanol and stirred with saturated aqueous Rochelle salt to aid the extractive work-up; the secondary alcohol **499** was isolated in quantitative yield. The absence of any acetal opening was attributed to the enhanced electrophilicity of the ester functionality and the slow conversion rate of the undesired benzylic C-O cleavage. The absence of all benzoate protons in the 500 MHz ^1H NMR spectrum, and the disappearance of the carbonyl ester resonance at $\delta\ 165.7\text{ ppm}$ in the 125 MHz ^{13}C NMR spectrum in CDCl_3 , indicated complete ester reduction. Finally the HRMS revealed an $[\text{M}+\text{Na}]^+$ ion at $m/e\ 903.4729$ suggesting the empirical formula $\text{C}_{45}\text{H}_{80}\text{O}_9\text{Si}_3\text{S}$.

A Swern oxidation to deliver the requisite C(19) ketone **485** looked a feasible operation, and work along these lines using trifluoroacetic anhydride (TFAA) as the electrophilic component was investigated (Scheme 64). The oxidation of the β -hydroxy sulfone **499** produced the ketone **486** in excellent yields, as shown by the appearance of a carbonyl resonance at δ 209.7 ppm in the ^{13}C NMR spectrum, and by a large C=O stretching vibration at 1717 cm^{-1} in the IR spectrum, with concomitant loss of the broad OH resonance at 3509 cm^{-1} . HRMS also confirmed the loss of two protons with an $[\text{M}+\text{Na}]^+$ ion at m/e 901.4572 suggesting the empirical formula $\text{C}_{45}\text{H}_{76}\text{O}_9\text{Si}_3\text{S}$.



Scheme 64 Attempted ring cyclisation to the Fischer glycoside **485**.

Now that the linear framework was in place, all that remained was for us to remove the PMP acetal and perform a Fischer glycosidation to install the anomeric methoxy and access the crucial pyran **485**. Our first attempts at Fischer glycosidation used mild acids in methanol (PPTS, 10 mol%, MeOH; TsOH, 10 mol%, MeOH) and resulted only in complex reaction mixtures, which we attribute to the acid sensitive silyl ether moieties undergoing non-selective cleavage. We now attempted a catalytic hydrogenation protocol involving Pearlman's catalyst to remove the PMP acetal, and although this delivered what we presumed was the hemiketal **500** it was formed only in low yields, making purification difficult to achieve. A chemoselective oxidation was therefore attempted on the axial C(21) hydroxyl with ruthenium based oxidants (Scheme 65) but due to the significant amount of the open chain form that existed in solution, the production of ketone **501** was hampered.

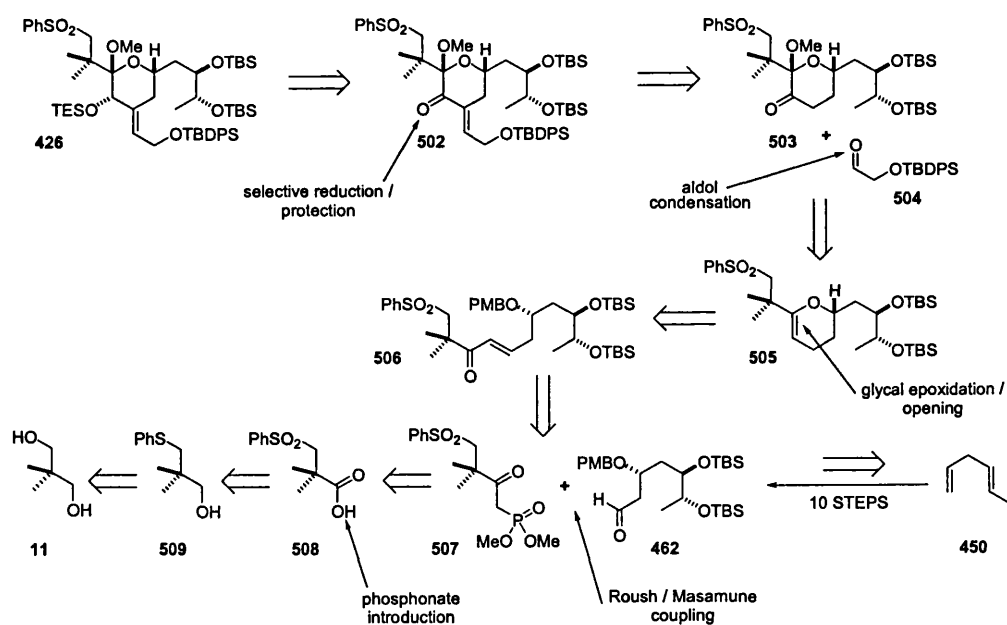


Scheme 65 Attempted oxidation at OH-(21) to ketone **501**.

Another avenue open to us was the catalytic DDQ removal of the PMP acetal in an aqueous acetonitrile mix, but again our efforts were thwarted; the reaction producing many products according to TLC. Not to be rebuffed easily, we hydrogenated **486** with a large excess of $\text{Pd}(\text{OH})_2$ in EtOH; consumption of the acetal occurred with little evidence of degradation. After filtration of the catalyst, and removal of the solvent, the cyclisation was attempted with methanol and catalytic PPTS, but unfortunately this served only to produce hemiketal **500**, albeit in slightly improved yields.

Continuation along this synthetic course seemed futile at this juncture, but we had significantly added to our knowledge of how the late-stage intermediates needed to be handled. We now thought it necessary to rethink our overall strategy for accessing target **426**.

2.3 An alternative approach to the bryostatin C-ring¹¹⁹

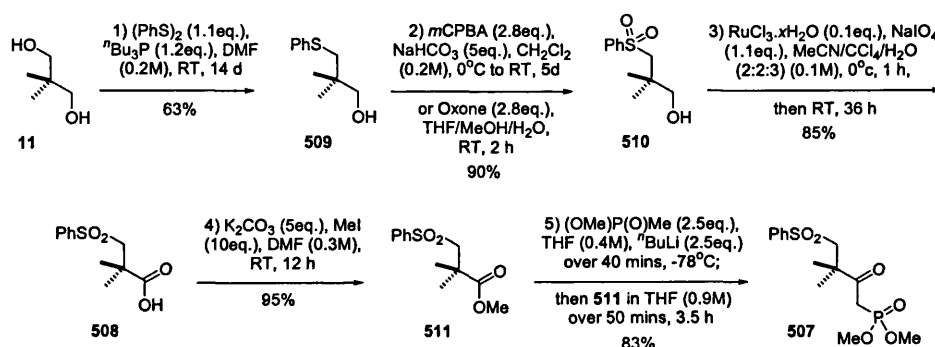


Scheme 66 Modified retrosynthetic analysis via a late-stage aldol condensation tactic.

In our remodelled retrosynthetic analysis (Scheme 66), we envisioned uniting the aldehyde **462** with the phosphonate **507**, to form the C(17)/C(27) backbone intermediate **506**. The phosphonate itself would potentially be accessible from 2,2-dimethyl-propane-1,3-diol **11**. Dehydrative ring-closure of **506** should furnish the glycal **505** which could potentially be converted to **503** by glycal epoxidation, methanolysis, and oxidation. Ketone **503** could then be used in an aldol / dehydration sequence involving

504. Selective enone reduction and O-silylation should then furnish the target **426**. The advantage of this new strategy was its potential for leading to a considerably abridged pathway to **426**, if successful. It also used the first 10 steps of the original Lennon route ¹⁰⁵ⁱⁱⁱ.

Our new synthetic pathway to **507** began with the thioetherification of 2,2-dimethylpropane-1,3-diol **11** with 1.1 equivalents of diphenyldisulfide and 1.2 equivalents of tri-*n*-butyl phosphine in DMF ¹²⁰ at room temperature, for an extended period (Scheme 67). It was subsequently found that the reaction time could be reduced considerably by heating the reactants at 70°C for 12 h ¹²¹. After aqueous work-up, the room temperature protocol delivered the mono thioether **509** in 63% yield. None of the *bis*-thioether was seen, presumably because of the unfavourable steric influence exerted by the thiophenyl constituent.



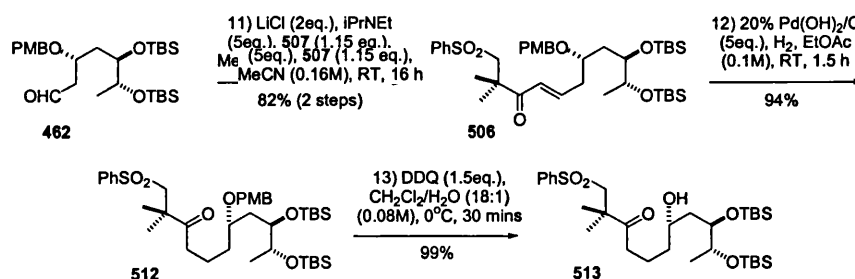
Scheme 67 Synthesis of the C(17)-C(20) sulfone phosphonate **507**.

Oxidation to the sulfone **510** was accomplished with *m*-CPBA and sodium bicarbonate in CH₂Cl₂ at 0°C, for extended reaction times in 90% yield. The very long time required for this transformation could be significantly shortened by using 2.8 equivalents of Oxone™ in a mixture of MeOH/THF/H₂O at room temperature; the oxone protocol only required 2 h at room temperature to reach completion, and delivered alcohol **510**. Alcohol to acid oxidation was accomplished with ruthenium trichloride and sodium-*meta*-periodate in MeCN/CCl₄/H₂O (2:2:3) for 12 h; this led to the acid **508** in 85% yield.

Methylation of the acid **508** was achieved by exposure to a large excess of methyl iodide and potassium carbonate in DMF ¹²² over a period of 12 hours, with the resulting methyl ester **511** being isolated in 95% yield. Treatment of **511** with an excess of the lithio anion derived from methyl dimethylphosphonate (2.5 equivalents) ¹²³ allowed a clean condensation to occur, and resulted in the C(17)/C(20) subsection **507** being formed in 5 steps and 38% overall yield from diol **11**. The β-keto

phosphonate exhibited an absorption at 1709 cm^{-1} in its IR spectrum attributable to the keto C=O group. HRMS also confirmed product formation with an $[M+H]^+$ ion at m/e 349.0875, which indicated an empirical formula $C_{14}H_{21}O_6SP$.

Crucial to the continuation of our route was the union of aldehyde **462** with phosphonate **507**, and the WHE conditions developed by Masamune / Roush¹²⁴ looked applicable to the situation at hand. We found that by treating a slight excess of phosphonate **507** with the crude aldehyde **462**, in the presence of flame-activated lithium chloride and dry diisopropylethylamine in acetonitrile, a single (*E*)-enone **506** could be obtained in 82% yield from alcohol **461** (Scheme 68). The newly formed olefinic proton at C(20) resonated at δ 6.55 ppm as a doublet with a J_3 coupling of 15.3 Hz, confirming the *trans* relationship with H(21). The strongly deshielded C(21) olefin proton resonated at δ 7.00 ppm as a doublet of triplets with J_3 couplings of 7.4 and 15.3 Hz. The increased down-field is presumably because this proton sits inside the deshielding cone of the ketone carbonyl.



Scheme 68 Installation of the C(17)-C(27) carbon framework via a Roush / Masamune coupling.

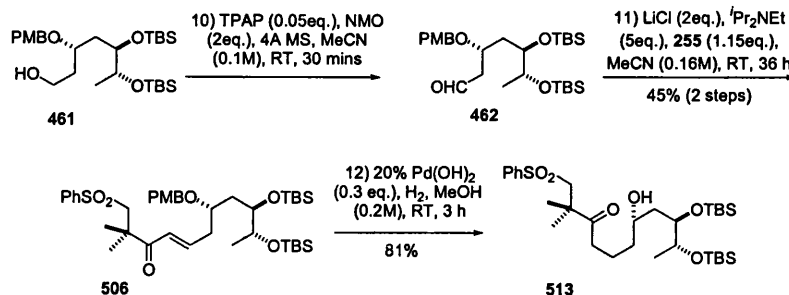
The IR spectrum of **506** showed the expected C=O and C=C resonances at 1693 and 1621 cm^{-1} respectively, again consistent with the conjugated system present. The addition was also confirmed by HRMS with an $[M+Na]^+$ ion at m/e 755.3809, which confirmed an empirical formula of $C_{39}H_{64}O_7Si_2S$. The saturated δ -hydroxy ketone **513** was our next synthetic target. It looked as though it could be prepared by the exhaustive hydrogenation of the olefin and PMB ether moieties in **506**. However, our initial efforts along these lines using 10% palladium on carbon in ethyl acetate proved fruitless. Typically a large number of products were formed according to TLC analysis. To circumvent this problem, a successive olefin saturation and PMB deprotection protocol was investigated.

It was found that by hydrogenating enone **506** in EtOAc with 20% palladium hydroxide for 1.5 h at 1 atmosphere, the ketone **512** was isolated in 94% yield very cleanly. The loss of the olefin resonances in the 500 MHz ^1H NMR spectrum of **512**, and the down-field shift of the C=O resonance by 12 ppm in the ^{13}C NMR spectrum in CDCl_3 , confirmed enone reduction. In the IR spectrum of **512**, the C=O absorption was at a frequency 16 cm^{-1} higher than for **506**, consistent with the C=C bond now no longer being in conjugation.

We had previously proved the validity of utilising a DDQ-mediated PMB cleavage in the synthesis of the precursor to the *bis*-pyran lactone **435**, and similar conditions were again employed here¹²⁵. By dissolving **512** in an 18:1 $\text{CH}_2\text{Cl}_2:\text{H}_2\text{O}$ solvent mix and adding 1.5 equivalents of DDQ, rapid generation of the expected δ -hydroxy ketone **513** resulted in near quantitative yield. The *p*-methoxy singlet at δ 3.77 ppm and the arene AX system at δ 7.25 and 6.83 ppm in the 500 MHz ^1H NMR spectrum of **512** in CDCl_3 had now disappeared from the corresponding spectrum of **513**. The appearance of a broad OH resonance at 3538 cm^{-1} in the IR spectrum further confirmed our assignment. The loss of a *p*-MeOC₆H₄CH unit in the HRMS confirmed that the desired overall transformation had been successful.

Of note at this point was the ^1H and ^{13}C NMR spectrum for **513**. When recorded in CDCl_3 , what initially appeared to be an impurity was evident, however these minor resonances were unobserved when the spectrum were recorded in C_6D_6 . Further analysis showed the deuterated chloroform to be of acidic enough in nature to effect a small amount of the hemiketal form, whereas the more neutral solvent C_6D_6 had this equilibria firmly in the open chain form. This could again be seen with the small hemiketal C(19) peak resonating at $\sim 94\text{ ppm}$ in the ^{13}C NMR for CDCl_3 .

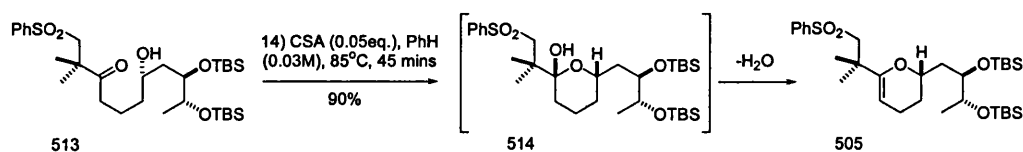
Later work showed that the fundamental reason why the advantageous one-step PMB cleavage and olefin hydrogenation was unsuccessful most likely lay in our method for oxidising the requisite aldehyde **462**. The Swern residues apparent in this procedure were invariably carried through, and even though they were present in very small quantities, they were sufficient to poison the catalyst thereby halting the PMB ether removal and favouring O-desilylation. We then discovered an alternative oxidation that used catalytic amounts of tetrapropylammonium perruthenate (TPAP) to produce the aldehyde **462**. Again, coupling of this crude material with the phosphonate **507** produced the single (*E*)-isomer **506** but in slightly reduced yields (Scheme 69). On hydrogenation with 20% $\text{Pd}(\text{OH})_2$ in MeOH the δ -hydroxyketone **513** was now isolated successfully in 81% yield.



Scheme 69 Modified one-step hydrogenation procedure to produce the δ -hydroxy ketone **513**.

The lower yields of **513** from the modified one-step synthesis from **506**, when compared to the higher yields achieved by the two-step methodology, meant that although it added an extra element to our synthetic route, the latter protocol was the more desirable.

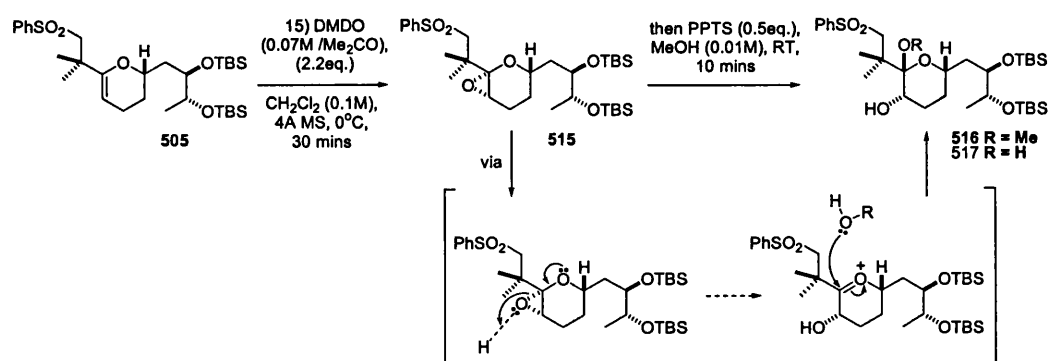
Having arrived at the δ -hydroxyketone **513**, ring closure to the glycal was our next aim. In this work on the southern hemisphere of bryostatin **2**⁴⁷ⁱⁱ, Evans had shown the efficiency of forming a glycal precursor with camphorsulfonic acid (CSA) in C_6H_6 at reflux (**66** in scheme 13). By applying similar conditions to **513**, a rapid ring closure to **514** ensued, followed by dehydration; the desired glycal **505** was isolated in a creditable 90% yield (Scheme 70). The successful outcome of this reaction was confirmed by the appearance of the newly-formed vinylic C(20) proton which resonated as a double doublet at δ 4.43 ppm in the 500 MHz 1H NMR spectrum in C_6D_6 , which showed J_3 couplings with the $H(22)_{eq}$ and $H(22)_{ax}$ of 2.5 and 4.7 Hz also consistent with the imposed rigid ring system. In the 125 MHz ^{13}C NMR spectrum in C_6D_6 , the ketone resonance at δ 211.7 ppm had now disappeared and the anomeric C(19) carbon now resonated at δ 94.2 ppm. The IR spectrum of **505** conferred a strong the C=C stretching vibration for the glycal at 1670 cm^{-1} . HRMS data gave final confirmation for pyran formation, there being an $[M+Na]^+$ ion at m/e 619.3285, consistent with an empirical formula of $C_{31}H_{56}O_5Si_2S$. Our planning now called for the implementation of a three-step sequence to secure the ketone **503**, with glycal epoxidation with DMDO at its heart.



Scheme 70 Ring closure and dehydration sequence to the glycal **505**.

In the formation of oligosaccharides, Danishefsky had shown the potential of using dimethyldioxirane (DMDO) over conventional methods to epoxidise glycosidic C=C double bonds ¹²⁶, due to its high electrophilicity, its generation of acetone as the only by-product, and its neutrality. We reasoned that if we could epoxidise glycal **505** then the problematic methyl glycoside might be installed by opening selectively at the anomeric position with added methanol.

Generation of the DMDO was carried out according to the procedure described by Adam *et al* ¹²⁷, which is useful for producing large quantities of an approximately 0.07 M solution in acetone. The determination of molarity is carried out by its slow addition to *trans* stilbene. Our initial foray in this area started by employing a two-step procedure, first isolating the epoxide **515** and then subjecting it to *trans*-diaxial ring-opening with PPTS in MeOH (Scheme 71). It was found that treatment of the glycal **505** in dry CH₂Cl₂ with a 0.07 M solution in acetone of redistilled DMDO in the presence of flame activated 4Å molecular sieves, gave rise to a very clean and almost totally stereospecific epoxidation on the α -face of the alkene, after only 10 mins.



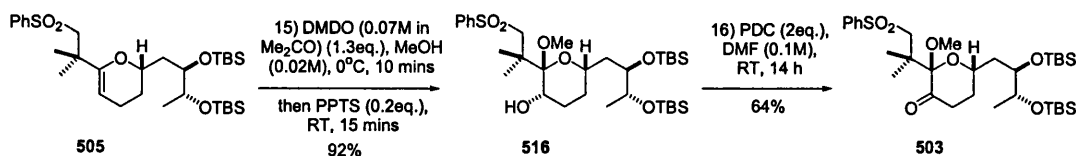
Scheme 71 Epoxidation sequence of glycal **505**.

TLC analysis at this stage reveals that all the starting material is consumed; however, several products are observed to be formed on the TLC plate due to the high lability of **515** on SiO₂. Concentration of the mixture after 10 minutes, followed by dilution with methanol and addition of a catalytic amount of PPTS unfortunately delivered a number of undesired side-products along with the required methyl glycoside **516**. This was attributed to the trace amounts of water that were always present in our redistilled DMDO / acetone solutions, which, during the concentration process, inevitability caused a significant amount of epoxide hydrolysis to form the unstable hemiketal mixture **517**.

While ordinarily, this side-reaction is not problematical with less-reactive aldose-type glycols, it was seriously detrimental here where a more reactive ketose-type glycol was being epoxidised. Reasoning that a limiting amount of desired material was still being produced, we believed that an in-situ epoxide opening might circumvent this complication, and allow an efficient one-pot procedure. To our delight, it was found that by treating a solution of the glycol **505** in MeOH with a 0.07 M solution of DMDO in acetone in the presence of 4Å molecular sieves at 0°C, a rapid stereospecific epoxidation occurred on the α -face of the double bond. When the consumption of glycol had occurred, a catalytic amount of PPTS was added and the mixture allowed to warm to room temperature. As the reaction mixture warmed, in-situ *trans*-diaxial ring opening occurred with the large excess of methanol that was present, which was present in substantially higher amount than any H₂O present in the original DMDO solution. This sequence yielded only the desired product **516** in a predictable and less cumbersome fashion.

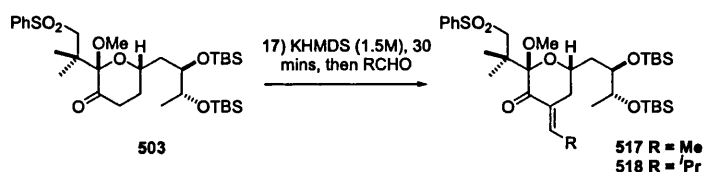
As our earlier experiences had shown, substrates possessing the methyl glycoside and an unprotected C(20) hydroxyl were extremely labile. However the unstable intermediate **516** could be purified if it was rapidly subjected to conventional SiO₂ flash chromatography. It was obtained as a crystalline solid, even if in slightly diminished yield. Confirmation that **516** had been formed was provided by its ¹H NMR spectrum in C₆D₆. The C(20) olefinic proton now resonated at δ 3.55 ppm, and methoxy protons resonated as a singlet at δ 3.32 ppm. In the 125 MHz ¹³C NMR spectrum, C(19) now appeared at 100.7 ppm, as expected for a pyranoside; C(20) peak that appeared at 94.2 ppm in **505** was also now absent. The IR spectra showed the appearance of a broad peak at 3492 cm⁻¹ associated with the newly formed OH. Clearly our new modification of the Danishefsky-Murray epoxidation method offers distinct advantages for the preparation of "simple" ketose-type glycosides from reactive trisubstituted glycols.

Once the epoxidation / opening sequence had been successfully negotiated, the alcohol at C(20) was oxidised. Exposure to 2 equivalents of pyridinium dichromate (PDC) in dry DMF at room temperature was the method of choice (Scheme 72). The oxidation could also be performed on the crude **516**, avoiding the potentially risky purification step. This two-step procedure to ketone **503** could be achieved in good overall yield from the glycol; typically 60-85% yield. The resonance at δ 207.4 ppm in the ¹³C NMR spectrum of **503** in C₆D₆ confirmed the presence of the C=O. The very strong absorption at 1724 cm⁻¹ in the IR spectrum of **503** confirmed this assignment. Final verification of the identity of **503** was provided by the HRMS, which showed an [M+Na]⁺ ion at *m/e* 665.3340, indicative of the empirical formula C₃₂H₅₈O₇Si₂S.



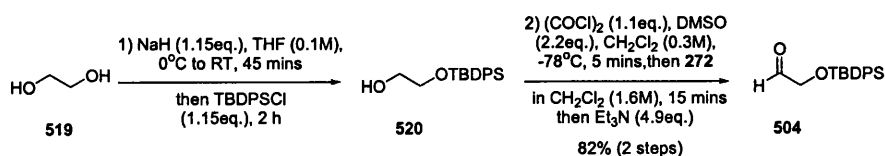
Scheme 72 In-situ epoxidation of glycal and oxidation to ketone **503**.

We now set about introducing the desired exocyclic olefin via an aldol / dehydration sequence. Initial model studies were investigated along these lines with a non-nucleophilic base. Treatment of ketone **503** with 1.5 equivalents of a 0.5 M solution of potassium hexamethyl disilazide (KHMDs) in THF at -78°C for 30 minutes and subsequent exposure to either acetaldehyde or isobutylaldehyde produced a single isomeric product in good overall yields, with no addition taking place α - to the sulfone (Scheme 73). Preliminary investigations into the geometry of the methyl or isopropyl side unit suggested that it had the (*E*)- stereochemistry.



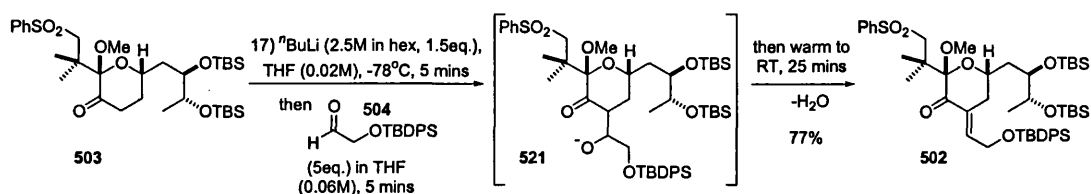
Scheme 73 Investigative studies of aldehyde addition to ketone **503**.

This led us to conclude that the desired exocyclic olefin geometry could also be achieved Marshall's' aldehyde **504** if could be employed. Marshall's' aldehyde ¹²⁸ **504** is available in two steps from ethylene glycol **519** via a mono silylation and Swern oxidation. Product yields are typically 85% over the two steps (Scheme 74).



Scheme 74 Formation of Marshall's aldehyde **273**.

After screening a range of experimental conditions for effecting the desired aldol conversion of **503** to **521**, we eventually found that the best results in terms of yield and cleanliness of reaction utilised the lithium enolate obtained from treating **503** with *n*-BuLi in hexanes and THF for 5 mins at -78°C . This was then transferred to a pre-cooled -78°C solution of the aldehyde **504** in THF, whereupon a rapid addition occurred. The elimination took place *in-situ* after the reactants were warmed to room temperature (Scheme 75); the resulting enone was typically isolated in a pleasing 77% yield.

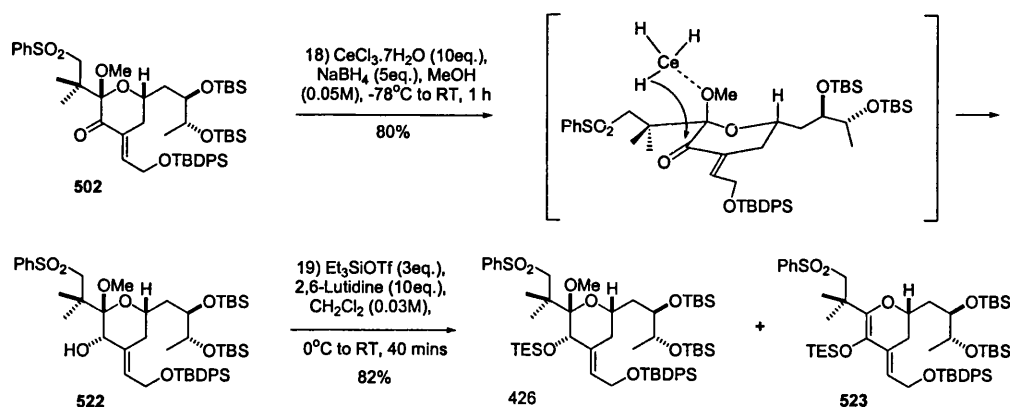


Scheme 75 Aldol addition and in situ dehydration to enone **502**.

To confirm that the correct (*E*)-stereochemistry had been achieved, detailed 2-D NMR studies were undertaken with **502**. Of special relevance was the 500 MHz ^1H NMR 2D nOe spectrum in C_6D_6 which showed cross-peaks between the C(22) ring protons and the C(35) methylenic protons. The C(19) OMe also showed a strong correlation with the C(23) axial ring proton, indicating that they had a *cis* relationship to one another. The carbonyl resonance shifted by 12 ppm to δ 195.4 ppm in the 125 MHz ^{13}C NMR spectrum in C_6D_6 which was consistent with enone conjugation. The new olefinic carbons appeared at δ 140.7 and 135.9 ppm. We now had all the required heteroatoms in place and past precedent in Wenders' and Evans' work^{102, 47} suggested that good selectivity could be attained in a stereospecific reduction of the enone **502** using a multitude of reducing agents. However the Luche¹¹⁰ conditions looked the easiest and most convenient to effect.

It was found that vigorous stirring of the **502** with 10 equivalents of cerium trichloride heptahydrate in methanol at room temperature over 45 minutes ensured coordination of the metal. On cooling to -78°C , 1 equivalent of sodium borohydride was added every 5 minutes for 25 minutes to avoid a large excess of the reducing agent being present in the mixture. The reaction was then warmed to 0°C . This unstable intermediate was isolated as a single isomer in 80% yield after rapid purification by SiO_2 flash chromatography. The 125 MHz ^{13}C NMR spectrum of **522** showed a shift of the C(20) carbon resonance

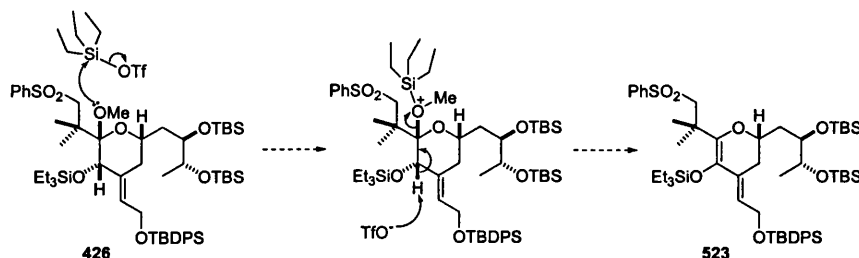
from δ 195.4 ppm to δ 72.6 ppm. The C=O stretch at 1698 cm^{-1} in the IR spectrum of **522** was now replaced by a broad OH peak at 3478 cm^{-1} (Scheme 76).



Scheme 76 Completion of the C(17)/C(27) bryostatin C-ring "Southern Hemisphere" **426**.

Protection of the newly formed hydroxyl as its triethylsilyl ether was accomplished with TES-triflate in dichloromethane (Scheme 76). The addition of an excess of 2,6-lutidine was required to buffer the triflic acid that was generated which would destroy the sensitive product **426**.

Small amounts of a side product, tentatively assigned as the elimination product **523**, were also formed, making the total purification of **426** difficult to achieve. It was thought that this by-product was induced by the anomeric oxygen displacing the labile triflate from the silyl moiety with the resulting triflate stripping the H(20) causing elimination across C(19)/C(20) (Scheme 77). A transient oxonium ion species could also contribute to this elimination mechanism, and this by-product would also be stabilised by the double bond conjugation; unfortunately **523** was inseparable from **426** by conventional SiO_2 flash or prep. thin layer chromatography.



Scheme 77 Proposed mechanism for the formation of the eliminated by-product **523**.

To ascertain if the correct stereochemistry had been installed at C(20) in **426**, a series of 1-D and 2-D NMR experiments were performed. It was found that the 1D 500 MHz spectra of **426** in C_6D_6 and toluene- d_8 were temperature dependent, suggesting that the rate of internal rotation for the sterically congested C(18)-C(19) bond was slow on the NMR time scale (Figure 3).

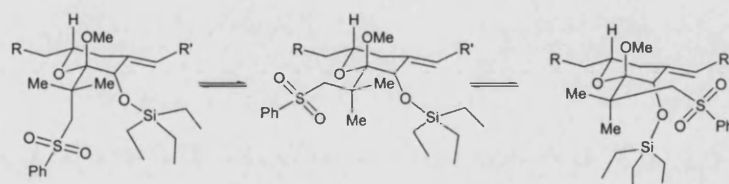


Figure 3 Slow bond rotational forms about the C(18)-C(19) bond for **426**.

There were seen many broadened resonances in benzene- d_6 and toluene- d_8 at room temperature. At elevated temperatures (70°C for benzene- d_6 and 90°C for toluene- d_8) these spectra sharpened quite dramatically as a result of the increased rate of C(18)-C(19) bond rotation, which now became fast on the NMR time scale. Under these conditions the rotationally averaged spectrum of **426** was observed.

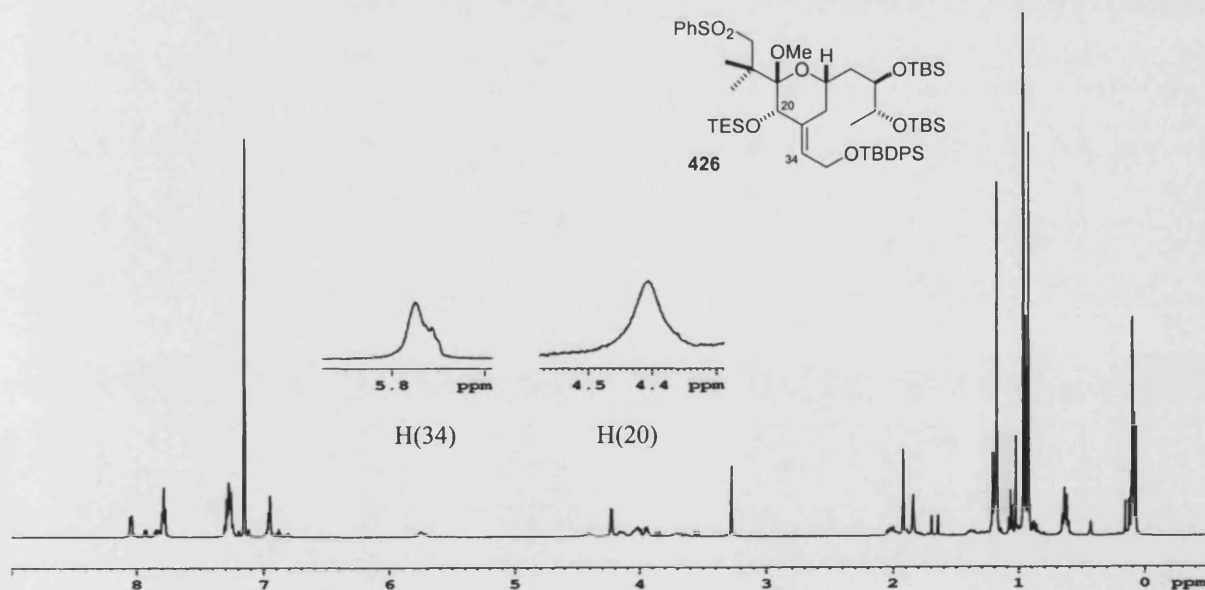


Figure 4 1H NMR spectra in C_6D_6 at 0°C for **426**.

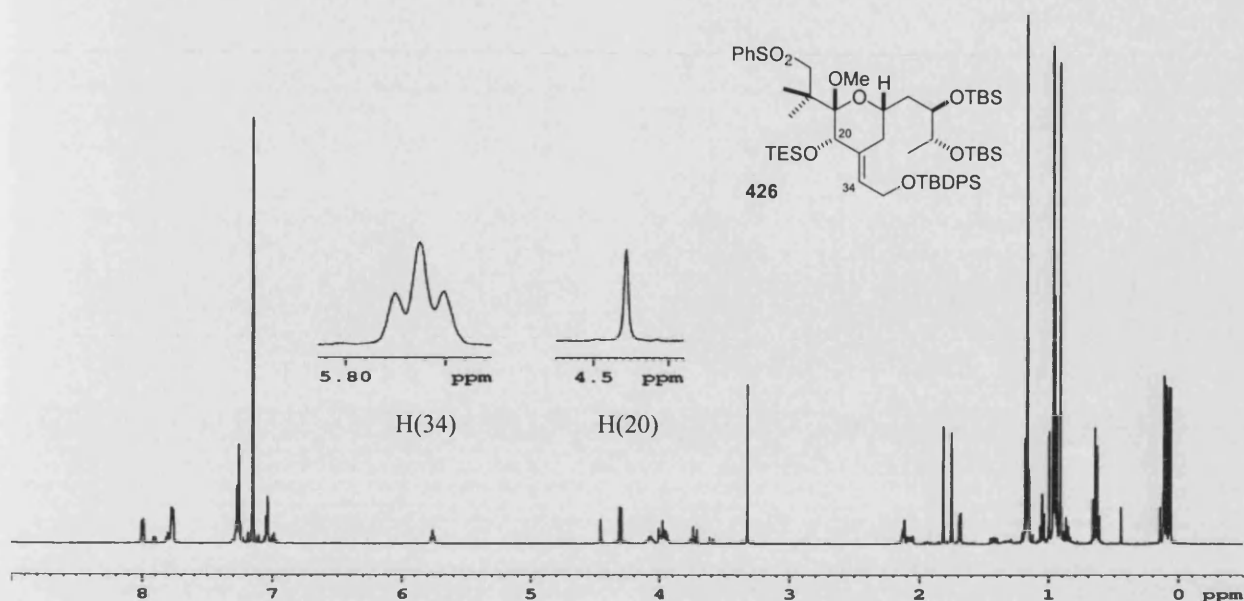


Figure 5 ^1H NMR spectra in C_6D_6 at 70°C for **426**.

A 2-D nOe NMR experiment, in toluene- d_8 at 90°C , revealed cross-peaks between the H(20) singlet at δ 4.38 ppm and the C(18) geminal dimethyl singlets at δ 1.64 and 1.58 ppm - as was expected, and also with the C(19)-OMe resonating at δ 3.27 ppm confirming their *cis*- relationship (Figure 6). H(20) also gave rise to an nOe cross-peak with the C(34) exocyclic triplet at δ 5.68 ppm, while the allylic C(35) methylenes at δ 4.26 and 4.23 ppm showed nOe's with the equatorial H(22) which appeared as a multiplet at δ 2.10 ppm. The combination of these results enabled us to confidently assign the C(20)-alkoxy and olefin stereochemistry.

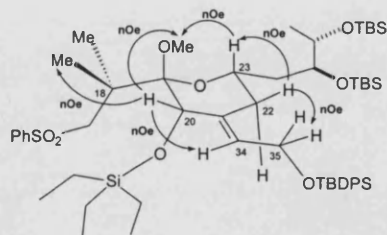


Figure 6 Rotationally averaged conformation at 70°C in C_6D_6 , with relevant nOe data for **426**.

The desired C-ring target **426** was produced in 4.02% overall yield from diene **450** for the 19 step longest linear sequence, and 3.45% for the 18 step longest linear synthesis, in an overall 25 / 26 step

sequence. Confirmation of the identity of **426** came from the HRMS showing an $[M+Cs]^+$ ion at m/e 1171.4801 suggesting an empirical formula of $C_{56}H_{94}O_8Si_4S$. This is the shortest route so far to a fully-elaborated, appropriately protected, bryostatin 1 "Southern Hemisphere".

2.4 Synthesis of bryostatin analogues ¹²⁹

Although a significant amount of our synthetic effort in the bryostatin area has been concerned with bryostatin total synthesis, a significant amount of work has also been concerned with the design and synthesis of simplified analogues for evaluation as antitumour agents and probes of PKC enzyme activity. Given the availability of the CRD2-phorbol ester X-ray crystal structure, we removed the phorbol ester from the crystal structure and attempted the computer assisted docking of some potential C-ring analogue structures within the phorbol-ester / bryostatin 1 binding site of the CRD2 domain. We identified three key analogues from these studies, two of which were based solely on the C-ring (**524** and **525**), and a third more elaborate analogue structure **526** based on the bryostatin B/C-ring array (Figure 7).

These analogue structures contained many of the key criteria lay down by Wender ³ in his postulates for potency in the PKC-binding of simplified bryostatin molecules ¹⁰². Whilst the phenylsulfone intermediate **524** possessed the desired exocyclic enoate, the C(20)-acyloxy substituent, the C(19) hemiketal and the C(26)-hydroxyl of bryostatin 1, it lacked the 30-membered macrolactone bearing the (3*R*)-OH.

Analogue **525** looked as though it would benefit from significant H-bonding between the allylic OH and the C(25)-OH, which would restrict rotation of the side-chain. Modelling within the CRD2 suggested that it would form 4-H-bonds within the PKC-d bryostatin binding site and so bind potently. Our initial decision to model these phenylsulfone analogues **524** and **525** stemmed from the notion that they might themselves serve as useful precursors to more elaborate analogues, in particular **526**. We reasoned that if these simplified designs were unable to bind to the CRD2, the potential for further elaboration to analogues possessing a greater congruence with the bryostatin structure would give us a greater chance of observing potent binding to the CRD2, without the macrolactone.

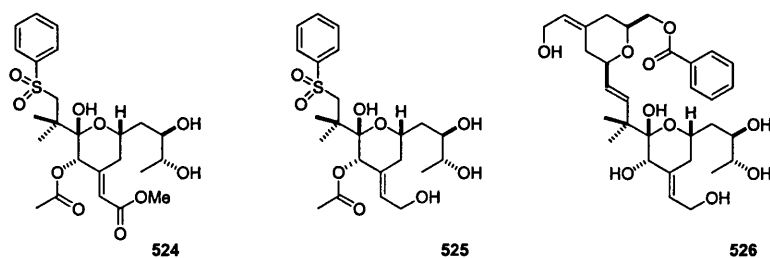
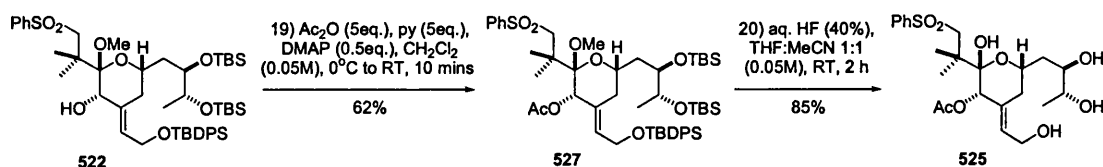


Figure 7 Modelled target intermediates with potential for PKC binding.

Analogue **525** was readily prepared from **522** in 2 steps, by acetylation and treatment with aq. HF, which not only caused O-desilylation but also glycoside hydrolysis. The acetylation of **522** was best effected with 5 equivalents of acetic anhydride and pyridine in 0.05 M CH₂Cl₂, and a catalytic amount of DMAP (Scheme 78). The OAc group gave rise to a singlet at δ 1.69 ppm in the 500 MHz ¹H NMR spectrum of **527** in C₆D₆. The ester carbonyl resonated at δ 169 ppm in the 125 MHz ¹³C NMR spectrum in C₆D₆, and **527** also gave rise to an [M+Na]⁺ ion at *m/e* 989.4885 confirming the empirical formula of C₅₂H₈₂O₉Si₃S.

Of special note at this point was the appearance of a sharp clearly defined 500 MHz ¹H NMR spectrum for **527** toluene-*d*₆, which indicated that the slow room temperature C(18)-C(19) bond rotation in **426** was a direct consequence of steric crowding exerted by the bulky OTES group at C(20).

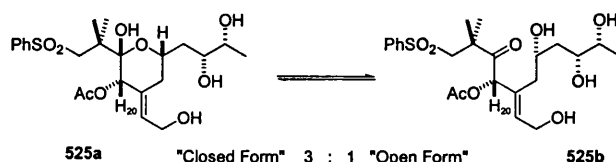
In their efforts towards bryostatin 3, Nishiyama and Yamamura had effected a key desilylation and ketal hydrolysis step utilising HF in aqueous acetonitrile. In an attempt to mimic this transformation, the acetate **527** was diluted with a 0.05 M solution of 1:1 THF:MeCN, with subsequent addition of 4 equivalents of a 40% aqueous HF solution. After two hours, basic work-up allowed the highly polar tetraol **525** to be purified via conventional flash chromatography in a gratifying 85% yield as a crystalline solid.



Scheme 78 Formation of the truncated bryostatin 1 C-ring analogue **525**.

The 500 MHz ¹H NMR spectrum for **525** in methanol-*d*₄ indicated that it existed as an approximate 3.6:1 mixture of ring-closed:open forms (Scheme 79); the same was true in benzene-*d*₆. In methanol-*d*₄, the

H(20) resonated at δ 5.14 ppm in the closed form **525a** and at δ 6.03 ppm in the open form **525b** due to the increased ketone electronegativity. The ketone carbonyl peak at δ ~208 ppm was also evident in the 125 MHz ^{13}C NMR spectrum for **525b**. Final confirmation of the structure of **525** came from the HRMS which showed an $[\text{M}+\text{Na}]^+$ ion at m/e 509.1821 suggesting an empirical formula of $\text{C}_{23}\text{H}_{34}\text{O}_9\text{S}$.



Scheme 79 Equilibrium structures for the C-ring analogue **525**.

The interaction of **525** was studied with the human PKC- α CRD2 by 600 MHz ^1H NMR spectroscopy. The CRD2 construct of human PKC- α that we had used had been very kindly prepared by Dr Peter Parker of the CRUK Laboratories at Lincoln's Inn Fields. Its sequence and folding were verified by comparing its 1D ^1H spectrum in $^2\text{H}_2\text{O}$ with the previously published resonance assignments of Ichikawa and Hommel¹³⁰. To our great dismay, upon the addition of phorbol-12,13-acetate (PA) or phorbol-12,13-butyrate (PB) to our CRD2 in $^2\text{H}_2\text{O}$, our ligand-protein complexes immediately precipitated. Following a suggestion in the literature¹³¹, 25% $\text{C}^2\text{H}_3\text{CN}$ was added to the complexes, and this was found to markedly improve their solubility. A careful examination of the 1D and 2D spectra of the CRD2 in this solvent system confirmed that the structure of the protein had not been significantly affected by the addition of the organic solvent, which suggests that this mixed NMR solvent system will be generally useful for studying the binding of very hydrophobic ligands to this protein.

Residues that appeared to be most affected by the binding of PA and PB corresponded to those observed in the binding pocket of the PA-PKC- δ CRD2 X-ray crystal structure. Bryostatin 1 was also found to affect several of these residues but clearly interacted much more tightly than PA or PB. Our observations conclusively prove for the first time ever that the binding site for bryostatin 1 does indeed overlap with that of PA and PB.

The binding of our simplified analogue **525** also affected some, but not all, of the residues bound to PA, suggesting that **525** occupies a part of the same binding pocket. Chemical shift changes in the amide region were apparent for **525** and for the PA and PB over similar concentration ranges, showing that their

binding constants must indeed be very similar under these conditions. Our combined data proves that it is possible to design bryostatin C-ring analogues that bind specifically to the human PKC- α CRD2, in a novel manner, and with an affinity of the same order of magnitude as those of the phorbol esters. An evaluation of the antitumour properties is therefore awaited with great interest.

This is elegantly shown in figure 8¹³² where the docking of **525** was modelled in the cavity of the CRD2 of PKC- δ . The space filled diagrams show that the allylic alcohol sits in the bottom of the cavity, and the phenyl and dimethyl units create a hydrophobic outer surface that extends across the surface of the protein.

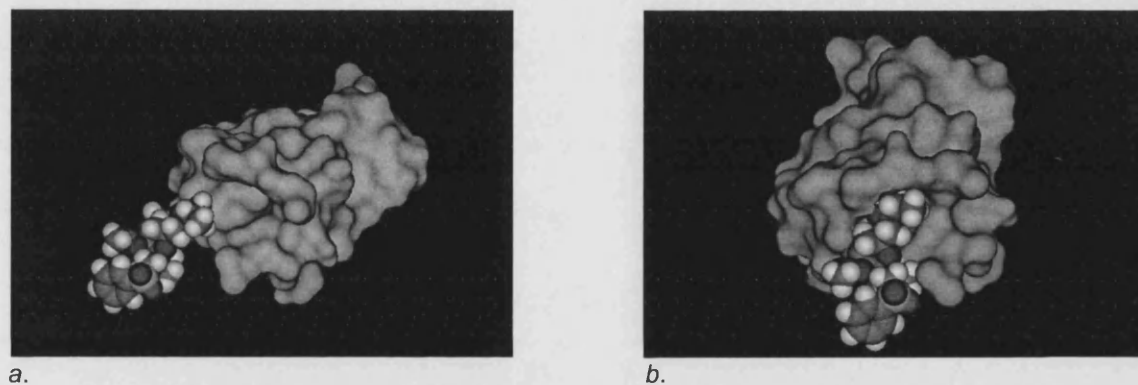
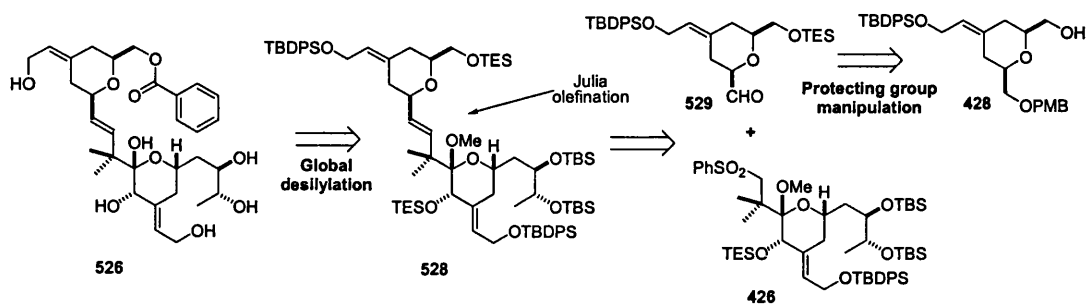


Figure 8 Undocked (a) and docked (b) analogue **525** to the CRD2 of PKC- δ .

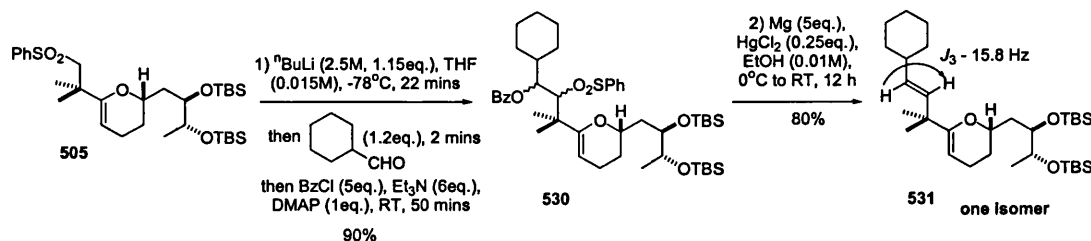
Given these extremely encouraging NMR binding studies with **525**, we embarked on the much more formidable task of acquiring the BC target **526**. Retrosynthetic analysis had suggested a late-stage global desilylation / glycoside hydrolysis for accessing **528** (Scheme 80), similar to that executed for **525**. Disconnection across the C(16)-C(17) trans olefin led to the selection of a Julia olefination between the C-ring sulfone **426** and the B-ring aldehyde **529** for creating **526**.

Due to the significant number of transformations needed to acquire both these B- and C- ring intermediates, we reasoned that the critical Julia olefination sequence could be explored using less valued material. The glycal **505** was identified as a suitable starting point from where to commence such model studies, and cyclohexanecarboxaldehyde suggested itself as a useful B-ring mimetic. It was found that deprotonation α - to the sulfone could be readily achieved with *n*-butyl lithium, and cyclohexanecarboxaldehyde readily combined with the resulting anion.



Scheme 80 Retrosynthetic analysis for the formation of the B/C analogue 282.

The diastereomeric β -hydroxy sulfone mixture that was produced could be isolated as a white solid by conventional flash chromatography. However, to our disappointment, all attempts at acetylating or benzoylating the resulting alcohols were unsuccessful. We therefore decided on an *in-situ* esterification, and subsequently found that by treating the intermediary alkoxides with an excess of benzoyl chloride and triethylamine, and an equimolar amount of DMAP, the desired α -benzoyl sulfone **530** could be obtained after stirring for 50 minutes at RT (Scheme 81).

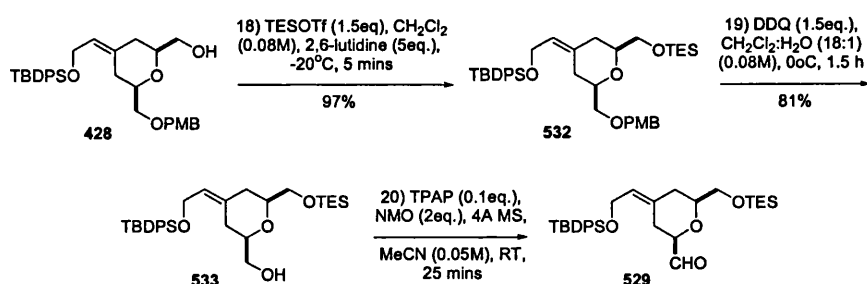


Scheme 81 Initial attempts for the Julia olefination of the glycol **505**.

Due to the large number of diastereoisomers now present, NMR data was of minimal value, although it did serve to confirm the loss of the C(17) AB quartet. Compelling evidence for the formation of **530** came from the HRMS which showed an $[M+H]^+$ ion at m/e 813.4616 suggesting an empirical formula of $C_{45}H_{72}O_7Si_2S$. It was thought that a magnesium / mercuric chloride mix¹³³, forming an *in situ* magnesium amalgam similar to that described by Evans⁴⁷ⁱⁱ, could effect the key benzoyloxysulfone elimination step, and a number of solvent systems were investigated. It turned out that by subjecting **530** to an excess of mercury (II) chloride and a catalytic amount of magnesium powder (~50 mesh) in dry ethanol at 0°C and allowing to warm slowly to room temperature, produced a single product.

NMR analysis confirmed the loss of all aromatic signals, and to our satisfaction showed the newly-formed C(16)-C(17) double bond protons were mutually coupled, possessing a J_3 coupling of 15.8 Hz in the 500 MHz ^1H NMR, indicating that the desired *trans* stereochemistry had been achieved. Further confirmation of the structure of **531** came from its HRMS which showed an $[\text{M}+\text{H}]^+$ ion at m/e 551.4316 suggesting the loss of the O_2SPh and OBz groups, and an empirical formula of $\text{C}_{32}\text{H}_{62}\text{O}_3\text{Si}_2$.

With a reasonable amount of information to hand regarding the Julia olefination, our attention now focussed on the all-important union of the B- and C-ring intermediates **529** and **426**. Since the B-ring intermediate **428** needed to be further elaborated to reach the requisite aldehyde **529**, we set off from this point. Firstly, O-triethylsilylation was completed by treating the primary alcohol **428** with a slight excess of triethylsilyl triflate in dichloromethane and 2,6-lutidine; this caused a clean and rapid protection in essentially quantitative yield (Scheme 82). 500 MHz ^1H NMR analysis of **532** in CDCl_3 now revealed a triplet at δ 0.95 ppm which integrated to nine hydrogens, and a six hydrogen quartet at δ 0.60 ppm that was coupled, to the former signal, indicating that installation of the triethylsilyl group had been achieved.



Scheme 82 Further manipulation of the B-ring alcohol **428** to facilitate the Julia coupling.

Utilising our previous protocol for DDQ-mediated PMB ether removal, **532** was subjected to 1.5 equivalents of DDQ in an 18:1 dichloromethane:water solvent mix, which procured the C(16) primary alcohol **533** in reasonable yields. The loss of the multiplet signals at δ 7.21, 6.85 and the OMe resonance at δ 3.78 ppm in the 500 MHz ^1H NMR spectrum in CDCl_3 confirmed the desired PMB ether protecting group cleavage. The released hydroxyl also showed a broad resonance at 3395.2 cm^{-1} in the IR spectrum of **533**.

All that remained to complete this sequence was oxidation of the primary alcohol in **533** to the aldehyde. Initial efforts using Swern methodology proved disappointingly fruitless, with a number of products being produced as seen by TLC. This hurdle was overcome, however, by employing a catalytic

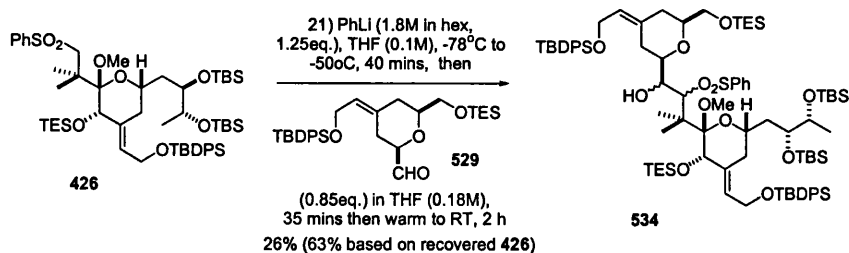
amount of TPAP and an excess of NMO for oxidation in dry acetonitrile - aided by the addition of flame activated molecular sieves. This led to complete consumption of starting alcohol. The newly formed crude aldehyde **529** was generally used immediately to avoid any partial degradation occurring.

Following the reports of Masamune³⁵ and Nishiyama⁶⁷, we had anticipated that deprotonation at the C(17) α -sulfone position of **426** might be a formidable obstacle. However given the past success of Masamune and Nishiyama, we elected to use the deprotonation methodology developed by these workers to effect the union of **426** with **529** (Scheme 83). In developing this methodology towards the key bryostatin B/C- ring coupling, Masamune had investigated a number of different bases to effect the desired deprotonation. It was found that the use of weak bases such as $i\text{-Pr}_2\text{NLi}$ and Et_2NLi resulted in insufficient deprotonation, and that stronger bases such as $t\text{-BuLi}$ and $n\text{-BuLi}$ formed aryl anion species, possibly from the greater ease with which the aryl protons could be accessed. To circumvent this problem, phenyllithium was investigated and found to effect the desired deprotonation.

It was with all this information in mind that we embarked on the crucial pyran coupling. Initial attempts at this addition proved remarkably unsuccessful when undertaken at -78°C with bases such as $t\text{-BuLi}$ and $n\text{-BuLi}$, resulting in complete recovery of the sulfone **426** and concomitant loss of all aldehyde **529** traces. This led us to believe that the required sulfone deprotonation was not occurring, and that the resulting base remaining in the solutions was itself adding to the aldehyde.

When the deprotonation was initiated at -78°C with 1.5 equivalents of a 1.8 M solution of phenyllithium in THF, and the reactants allowed to warm slowly to -50°C over 20 minutes, the familiar sulfone yellow / green anion colour was finally seen for the first time (Scheme 83). After a period of 20 mins, the resulting sulfone anion was re-cooled to -78°C and a solution of aldehyde **529** in THF added. A number of spots were apparent by TLC along with a significant amount of starting sulfone. The reaction mixture was then allowed to warm to ambient temperature, although little change was seen by TLC. This was presumably due to insufficient deprotonation occurring and the quenching of any base still present by the aldehyde. Fortunately any unreacted sulfone could be recovered, but again all aldehyde residues were destroyed.

Due to the inconclusive information we received from TLC, we thought it prudent to isolate the α -hydroxysulfone **534** in a measured, stepwise procedure. The sulfone mixture **534** was isolated as a viscous oil, and as in our earlier efforts towards **530**, it was difficult to obtain relevant NMR data.

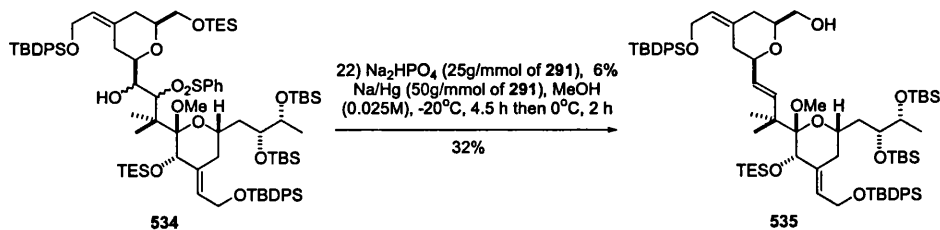


Scheme 83 Julia coupling of sulfone **426** and aldehyde **529**.

The yield of this two step procedure was 26% based on the aldehyde. As much of the unreacted sulfone could be recovered, a 63% yield could also be calculated based on the amount of sulfone **426** recovered.

In some earlier model work on the union of benzaldehyde with sulfone **426**, the desulfurisation / elimination of the α -hydroxy sulfone could be achieved directly with 6% sodium-mercury amalgam. This protocol was therefore used for the elimination of the α -hydroxysulfones **534**. The best conditions used an excess of 6% sodium-mercury amalgam in a 2:1 methanol:ethyl acetate solvent mix at reduced temperatures (Scheme 84), in the presence of disodium hydrogen orthophosphate to buffer the basic nature of the reactants. To our great delight, these conditions produced a single alkene product spot as judged by TLC.

After filtration of the metallic residues, purification of the resulting product **535** was carried out by SiO₂ flash chromatography. The yield of **535** was somewhat disappointing, however. Fortunately though, the correct (*E*)-olefination had been achieved, with proof coming from the 500 MHz ¹H NMR spectrum of **535** in C₆D₆. The H(17) resonance appeared as a doublet at δ 6.40 ppm, whilst H(16) resonated as a double-doublet at δ 5.58 ppm, with the large J_3 coupling value of 15.9 Hz between them confirming their *trans* relationship.



Scheme 84 Desulfurisation / elimination to deliver the *trans* C(16)/C(17) olefin.

In an extremely fortuitous event, the ^1H NMR spectrum also showed that the C(10) primary triethyl silyl group had been selectively cleaved, whilst all other silyl protecting groups had been left intact. This could be explained by the greater acid lability of the TES group over both the TBS and TBDPS groups, and also from the enhanced lability of the C(10) primary over C(20) secondary position due to the steric crowding around C(20). Confirmation that it was indeed the primary TES group that had undergone cleavage came from the 2-D NMR NOESY spectrum, with the H(20) singlet showing cross-peaks with the 3 x CH_2 ethyl quartets (Figure 9).

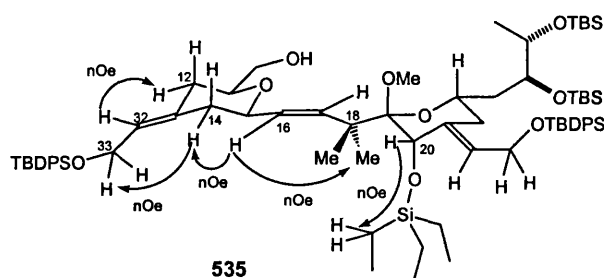
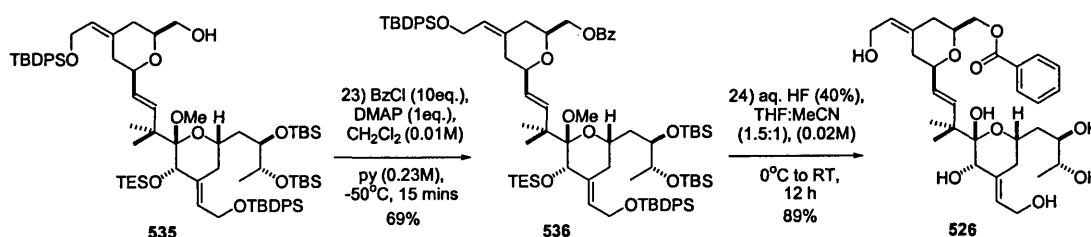


Figure 9 Relevant nOe data for the B/C coupled trans olefin **535**.

The NOESY spectrum also served to solidify our postulate of the correct olefination, with H(16) showing a cross peak with the geminal dimethyl unit, and also with H(14)_{ax}. The HRMS also confirmed the unification of the two pyran rings with the additional loss of the single TES group, there being an $[\text{M}+\text{Na}]^+$ ion at m/e 1327.7676 in the spectrum, suggesting an empirical formula of $\text{C}_{75}\text{H}_{120}\text{O}_9\text{Si}_5$.

The primary hydroxyl in **535** was now exposed to a large excess of benzoyl chloride at low temperatures to introduce the requisite OBz group. This produced the desired benzoate **536** in expedient fashion and reasonable yields (Scheme 85).



Scheme 85 Completion of the C(10)/C(27) B/C-ring analogue **526**.

The ester carbonyl now resonated at δ 167.5 ppm in the 125 MHz ^{13}C NMR spectrum of **536** in C_6D_6 and 500 MHz ^1H NMR spectrum in the same solvent also showed a new phenyl ring system resonating between δ 8.07 and 7.05 ppm. The disappearance of the OH stretch at 3481 cm^{-1} in the IR spectrum and the HRMS further confirmed the addition of a $\text{C}_6\text{H}_5\text{C}=\text{O}$ benzoyl unit.

All that remained was the global desilylation / hemiketalisation, and similar conditions to that employed in our synthesis of the C-ring analogue **525** again proved advantageous. The benzoate **536** was stirred in a 3:2 mix of THF:acetonitrile, followed by the addition of 6 equivalents of a 40% aqueous solution of hydrogen fluoride. The cooled solution was allowed to warm to 0°C and stirred for a further 12 hours, whereafter mildly basic work-up revealed the hexanol **526** in a pleasing 89% yield as a white crystalline solid.

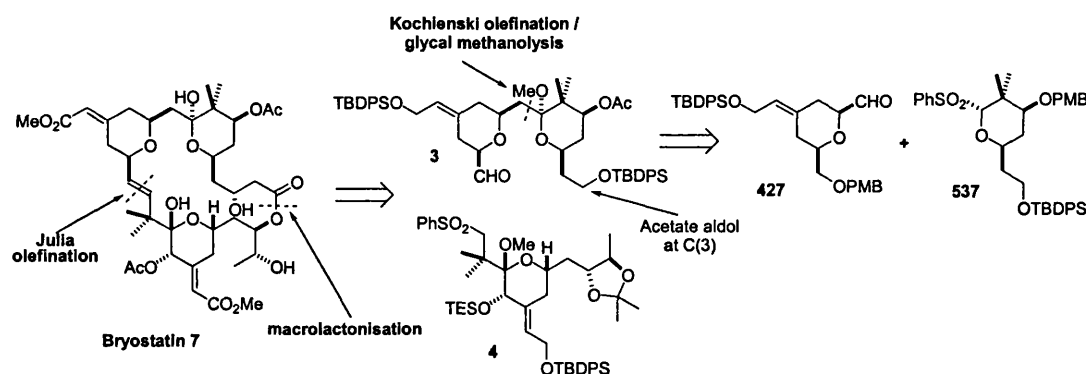
The 500 MHz ^1H NMR spectrum in methanol- d_4 confirmed the total loss of all silyl residues and the anomeric methoxide singlet at δ 3.37 ppm. Interestingly, **526** exhibited only the "closed form" for the C-ring hemiketal. The HRMS also served to confirm product formation had been successful, although due the high stability of the tertiary oxonium ion formed from the loss of H_2O at one of the hemiketals an $[\text{M}+\text{Na}-\text{H}_2\text{O}]^+$ ion was now observed at m/e 581.2727 suggesting the empirical formula $\text{C}_{31}\text{H}_{44}\text{O}_{10}$. Unfortunately due to a lack of time, analogue **526** has not yet had its interaction with the PKC CRD2 investigated by NMR.

The synthesis of **526** has a longest linear sequence of 24 steps and proceeds in 0.62% overall yield, with 43 synthetic operations being required overall. Although we had had some successes in this area, limiting time factors, as well as the limiting amount of material available did not allow us to optimise the synthetic transformations en route to **526**.

In the synthesis of both bryostatin **7** and bryostatin **3**, Masamune and Nishiyama were far more successful than us in their Julia olefination steps; 60% and 52% respectively for their two step procedures, compared with our modest 26% (see schemes 8 and 23). Crude molecular modelling studies showed that by changing the C(25)/C(26) di-silyl ether to its acetonide altered the way in which the C-ring positioned itself, and it became apparent that the acetonide protected synthon **4** caused a greater degree of planarity of the ring compared to **426**, presumably from the decrease in steric repulsion. At first sight this might not serve to radically alter the reactivity of the molecule, however this slight modification was thought to possibly allow an easier access to the sulfone methylene protons thereby increasing the degree of deprotonation available.

2.5 Synthetic studies on bryostatin 7 ¹³⁴

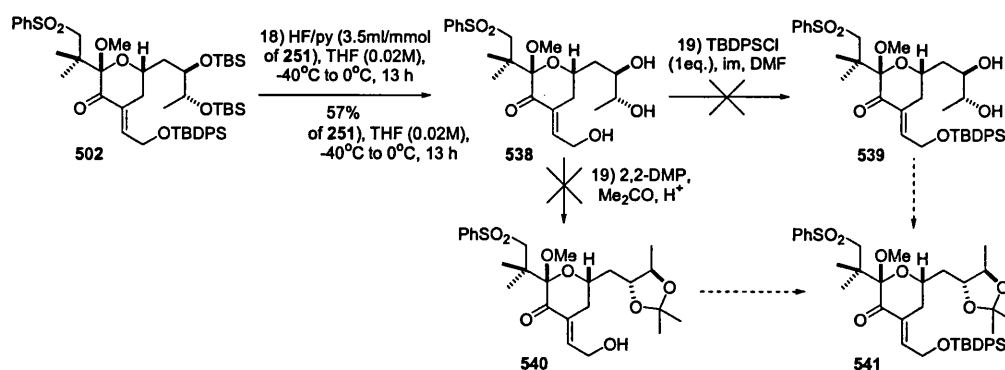
In light of these observations on the Julia reactions with phenylsulfone **426**, our attention now focussed on the use of compound **4** for our total synthesis work, as this previously had given good results in Julia couplings in the bryostatin field. It will be recalled that this intermediate had previously been employed by Masamune ³⁵ in his total synthesis of bryostatin 7. However, his synthesis of **4** required 34 steps. We felt that this could be shortened considerably by adapting our previous synthesis of **426**.



Scheme 86 Modified retrosynthetic analysis of bryostatin 7.

Our first attempts towards **4** were initiated from the enone **502** (Scheme 87) where we considered a *tris*-silyl deprotection followed by an allylic hydroxyl re-protection and an *O*-isopropylidination might yield the requisite enone **541**. Subsequent Luche reduction and *O*-triethyl silylation would complete the target **4**. It was found that by treating the enone **502** with HF/py complex (3.5 ml per mmol of **502**) in dry THF at -40°C and warming to 0°C for 13 hours, compound **538** was formed in 57% yield. All traces of the silyl resonances in the ¹H NMR spectrum were removed, and the IR spectrum now showed a large broad OH stretch at 3388 cm⁻¹. The HRMS showed an [M+Na]⁺ ion at *m/e* 479.1716 suggesting an empirical formula of C₂₂H₃₂O₈S where no silyl protecting groups were present.

We had good reason to believe that a selective TBDPS protection could now be accomplished on the allylic alcohol, but to our disappointment we found that this always resulted in either degradation of the starting material or no reaction at all. An alternative whereby the *cis*-1,2 diol of **538** was isopropylidinated at the outset was then investigated.

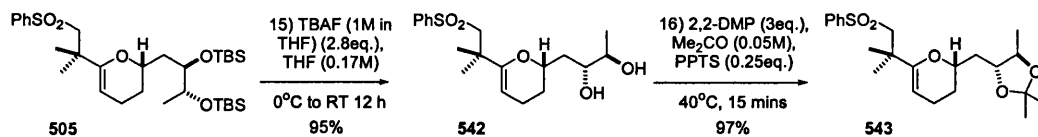


Scheme 87 Attempted desilylation and protecting group manipulation tactics of **502**.

However, it was discovered that Me₂C(OMe)₂ reacted with all the free hydroxyl sites, when treated under our standard acetonide formation conditions. Slight modifications did nothing to solve this impediment, so we realised this was an unsuitable approach.

Retreating somewhat in our efforts to acquire **4**, we sought to complete the DMDO epoxidation / aldol sequence with the acetonide already installed, and the glycal **505** presented itself as a credible foundation. By effecting an O-silyl to acetonide interchange, the chemistry developed for the synthesis of our initial target **426** might then be applied to the new route.

Therefore at the outset, the silyl ethers of **505** were removed in almost quantitative yields by treatment with tetrabutylammonium fluoride (TBAF) at ambient temperature (Scheme 88). The IR spectrum clearly showed the formation of a large OH resonance at 3489 cm⁻¹; NMR analysis showed loss of both silyl residues, and HRMS confirmed the loss of the two TBS groups with the presence of an [M+Na]⁺ ion at *m/e* 369.1736 which confirmed the empirical formula C₁₉H₂₈O₅S.



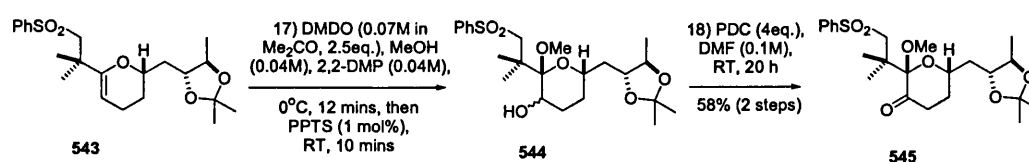
Scheme 88 Silyl to acetonide protecting group change to **543**.

Immediate reprotection using the same procedure as for **475** meant mild heating with acetone and 2,2-dimethoxypropane along with 25 mol% of PPTS. This caused a rapid, and again high yielding reaction.

The methyl units of the acetonide now resonated at δ 1.30 and δ 1.23 ppm in the 500 MHz ^1H NMR spectrum of **543** in C_6D_6 , and the IR showed the loss of the OH resonance.

In our first attempts at effecting the DMDO / opening sequence, we found that consumption of the glycal occurred readily. However, upon addition of PPTS under our original conditions, and warming to room temperature, we discovered that the acetonide was being cleaved. We reasoned this problem was not insurmountable, and sought to alleviate the undesired acid mediated transketalisation by introducing an isopropylidene source so that if cleavage still occurred, there would be an equal chance of re-introducing the same group.

Thankfully this turned out to be the case, for it was subsequently found that after dissolving the glycal **505** in a cooled 1:1 solution of methanol and 2,2-dimethoxypropane, (containing flame activated molecular sieves), the addition of our freshly distilled DMDO solution caused its rapid consumption (Scheme 89). After addition of a stock solution of PPTS in methanol – which allowed the addition of only 1 mol % of acid, and warming to room temperature, the formation of the product **544** was seen. From our earlier work on this procedure, we had shown that the alcohol could undergo crude oxidation to the much more stable ketone, so **544** was dissolved in dry DMF and stirred with an excess of PDC at room temperature.

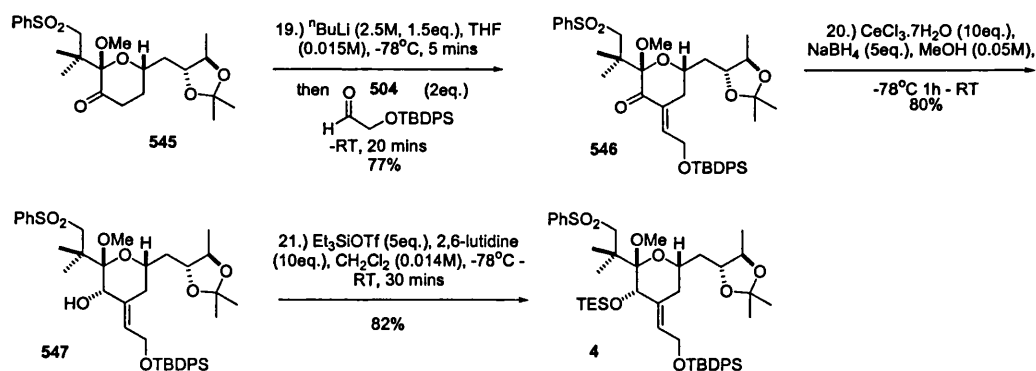


Scheme 89 Modified glycal epoxidation sequence to ketone **545**.

We had noticed the formation of two closely separated major products for the epoxide opening step. However, after oxidation a single product was obtained. This could be explained by epoxidation step being less stereoselective. The anomeric opening with MeOH would still occur from the favoured axial position due to a transient oxonium ion species. It was also interesting to note that the oxidation step proceeded at a decreased rate, as seen by the slow consumption of one of the two spots, presumably from the less favourable axial hydroxyl position.

The newly formed C=O resonated at δ 204.9 ppm in the 125 MHz ^{13}C NMR spectrum of **545** in C_6D_6 , consistent with a ketone carbonyl. There was also a sharp peak at 1722 cm^{-1} in the IR spectrum. HRMS confirmed the desired manipulation had taken place there being an $[\text{M}+\text{Na}]^+$ ion at m/e 474.1923 suggesting an empirical formula $\text{C}_{23}\text{H}_{34}\text{O}_7\text{S}$. The ketone **545** was then diluted with dry THF at low temperature, and *n*-butyllithium added to effect enolisation (Scheme 90). The naked lithium enolate added to aldehyde **504** in THF as before and the desired dehydration was again observed when the reaction mixture was warmed. The enone **546** was isolated in 77% yield. HRMS showed the addition of the exocyclic olefin unit there being an $[\text{M}+\text{Cs}]^+$ ion at m/e 867.2363 suggesting an empirical formula of $\text{C}_{41}\text{H}_{54}\text{O}_8\text{SSi}$.

In continuation of our route, the acetonide enone **546** was subjected to a Luche reduction. Metal coordination with the anomeric methoxide over 45 minutes at room temperature and subsequent cooling to -78°C followed by the addition of sodium borohydride in three equal portions delivered the unstable β -hydroxy alkene **547**. This was used directly for the next step to avoid any potential loss of product.



Scheme 90 Completion of Masamunes C- ring synthon **4**.

On exposure to an excess of triethylsilyl triflate in 0.06 M dichloromethane and 10 equivalents of 2,6-lutidine at 0°C and allowing to warm to room temperature, the synthesis of the modified target **4** was completed in 57% yield over the two steps. This was completed in 3.06 % yield for the 21 step sequence, and 2.67% yield for the 20 step sequence from (*E*)-1,4-hexadiene **450**. Although the overall synthesis required a longest linear synthesis of 25 steps and 27 synthetic transformations, this compared favourably with the route Masamune used in the synthesis of bryostatin **7**³⁵, which had a longest linear synthesis of 21 steps and 40 synthetic transformations.

As was seen in **426**, acetal **4** also showed slow bond rotation about C(18)/C(19) bond, significantly broadening the peaks at room temperature. At elevated temperatures however, it could be seen that these sharpened quite dramatically, and a high temperature 2-D NMR NOESY spectrum confirmed once again the desired stereochemistry. The C(34) exocyclic olefin triplet at δ 5.61 ppm showed significant correlation with the H(20) singlet at δ 4.68 ppm, and not the H(22) ring protons, however it was also interesting to note that there was a decrease in the correlation between the H(20) singlet and the anomeric methoxide. This could be a consequence of the slight change in the conformation of the ring, positioning H(20) in a more equatorial confirmation. HRMS confirmed that the reduction / protection sequence had been successful with an $[M+Na]^+$ ion at m/e 873.4228 suggesting an empirical formula of $C_{47}H_{70}O_8Si_2S$.

It was interesting to note that even though Masamune and Nishiyama had both previously prepared structurally related O(20)-triethylsilylated C-ring phenylsulfone intermediates (**4** and **115**), neither had documented the occurrence of this restricted bond-rotational effect.

In conclusion, the shortest route to a fully elaborated and functionalised C-ring intermediate **426** so far in existence has been developed, with interesting slow bond rotation effects apparent. We have shown its usefulness in constructing a bare C-ring analogue **525** that has exhibited binding to the PKC- α CRD2 in similar concentrations to phorbol ester. The value of **525** has also been demonstrated in the construction of a more elaborate bryostatin analogue **526** that has yet to undergo biological NMR testing. Finally in our efforts towards the formal synthesis of bryostatin 7, the formation of the requisite C-ring synthon **4** has been completed.

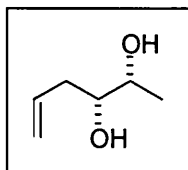
3.0 EXPERIMENTAL

Materials and Methods

Reactions were carried out under a nitrogen atmosphere with freshly distilled solvents unless otherwise noted. Hexanes refer to the distillate fraction of petroleum spirit that is collected at 40-60 °C and was distilled prior to use. All solvents were reagent grade. Dichloromethane, toluene, benzene and acetonitrile were distilled from calcium hydride under nitrogen. Diethyl ether and THF were distilled from sodium under nitrogen. All other reagents were used 'as supplied' from manufacturers unless otherwise stated. Flash chromatography was carried out according to Still *et al.*¹³⁴ with Kieselgel 60 40/60A (220-240 mesh) silica gel. Precoated silica gel plates (250 µm) with a fluorescent indicator (E. Merck) were used for analytical thin layer chromatography. The plates were initially examined under UV light and then developed with either a sulfuric acid stain [EtOH:H₂SO₄:*p*-MeOC₆H₄CHO (95:4:1)] or iodine unless otherwise stated. Evaporation refers to the removal of solvents at ≤ 40 °C on a Büchi rotary evaporator. ¹H NMR spectra were acquired at 500 MHz with a Bruker DRX 500 and ¹³C NMR spectra were acquired at 125 MHz with a Bruker DRX 500. 2-D NMR spectra were also recorded on a Bruker DRX 500. Chemical shifts are reported in δ-values relative to tetramethylsilane (¹H and ¹³C) and all NMR spectra were recorded in deuterated solvent solutions. All infrared spectra were recorded on a Perkin-Elmer 1605 FT-IR spectrophotometer. Optical rotations were measured on an Optical Activity, Polaar 2000 automatic polarimeter. High resolution mass spectra were measured at the London School of Pharmacy on a V.G. 7070H or VG-ZAB instrument with a Finnigan Incos II data system.

3.1 Detailing the synthetic routes described in Schemes 53 and 54¹³⁵

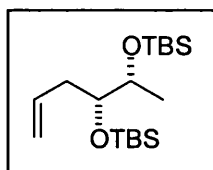
In the following sub-section, compounds **450** to **435** had previously been prepared by Dr John Lennon¹⁰⁵ⁱⁱⁱ. However, the scale upon which he conducted many of his preparations of these compounds was often much smaller. The procedures described herein were all carried out on a larger scale or were adapted and improved in some way.

(2R,3R)-hex-5-ene-2,3-diol 453

A 3 L conical flask equipped with an overhead mechanical stirrer was charged with H₂O (1.2 L), *t*-butanol^a (1.2 L) and AD-mix- β ^a (400 g, 0.6 eq). After 10 min of vigorous stirring at room temperature, the mixture was cooled to 0 °C when *trans*-1,4-hexadiene^a **450** (40.0 g, 490 mmol) was added in one portion. After 72 h at 0 °C the reaction was quenched with solid sodium sulfite (145 g) and vigorously stirred at room temperature for 1 h. The organic layer was separated and aqueous layer extracted with EtOAc (9 x 200 mL). The combined organic layers were washed with brine (1 x 200 mL), dried over MgSO₄, filtered, and concentrated *in vacuo*. Purification of the residue by SiO₂ flash chromatography using hexanes/Et₂O (2:1) as eluent afforded the volatile diol **453** (17.2 g, 51%) as a colourless free-flowing oil.

Spectral data agreed with those previously reported by Lennon¹⁰⁵ⁱⁱⁱ.

Literature yield: 45-58%

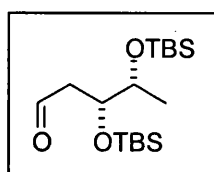
(4R,5R)-4,5-Bis-(*t*-butyl-dimethylsilanyloxy)-hex-1-ene 454

To a stirred solution of diol **453** (7.46 g, 64.2 mmol) and imidazole^c (13.12 g, 192 mmol) in dry DMF^a (65 mL) was added *t*-butyldimethylchlorosilane^c (24.2 g, 161 mmol) in one portion and the reactants heated at 85 °C. After 4 h, the reaction mixture was cooled to 0 °C, diluted with Et₂O (50 mL) and quenched with solid NaHCO₃ followed by saturated aq. NaHCO₃. It was then extracted with Et₂O (5 x 75 mL), the combined organic extracts washed with H₂O (1 x 200 mL) and brine (1 x 200 mL), dried over MgSO₄, filtered, and concentrated *in vacuo*. Purification of the residue by SiO₂ flash chromatography using neat hexanes as eluent afforded disilyl ether **454** (20.2 g, 91%) as a colourless free-flowing oil.

Spectral data agreed with those previously reported by Lennon ¹⁰⁵ⁱⁱⁱ.

Literature yield: 84%

(3*R*,4*R*)-3,4-Bis-(*t*-butyl-dimethylsilanyloxy)-pentanal 455

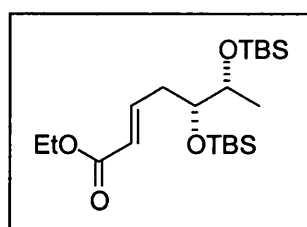


To a cooled (0 °C) solution of alkene **454** (44.9 g, 130 mmol) in dry THF (200 mL) was added osmium tetroxide^o (0.04 M solution in 1:1 acetone:H₂O, 53 mL, 2.10 mmol). After 5 min sodium *meta*-periodate^c (167 g, 782 mmol) was added in one portion and after a 0.5 h at 0 °C, the reaction mixture was allowed to warm to RT. After 3.5 h, H₂O (80 mL) was added, and the reaction mixture extracted with EtOAc (6 x 200 mL). The combined organic extracts were washed with brine (1 x 200 mL), dried over MgSO₄, filtered, and concentrated *in vacuo*. Purification of the residue by SiO₂ flash chromatography using hexanes/EtOAc (150:1) as eluent afforded aldehyde **455** (29.6 g, 65%) as a colourless oil.

Spectral data agreed with those previously reported by Lennon ¹⁰⁵ⁱⁱⁱ.

Literature yield: 72%

(*E*)-(5*R*,6*R*)-5,6-Bis-(*t*-butyl-dimethylsilanyloxy)-hept-2-enoic acid ethyl ester 456



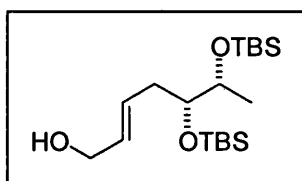
To a stirred solution of aldehyde **455** (24.0 g, 69.3 mmol) in dry CH₂Cl₂ (70 mL) was added carbethoxymethylene triphenylphosphorane^c (35.0 g, 101 mmol) in one portion. After 48 h at room temperature the reaction mixture was concentrated *in vacuo*. Et₂O (~100 ml) was then added to precipitate

the $\text{Ph}_3\text{P}=\text{O}$ solid by-product which was then removed by filtration. The filtrate was then concentrated *in vacuo*, and the residue purified by SiO_2 flash chromatography using hexanes/EtOAc (20:1) as eluent to afford allylic ester **456** (28.0 g, 97%) as a colourless oil.

Spectral data agreed with those previously reported by Lennon¹⁰⁵ⁱⁱⁱ.

Literature yield: 93-95%

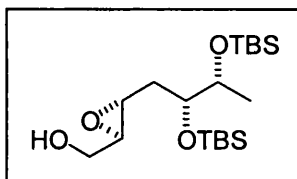
(E)-(5R,6R)-5,6-Bis-(*t*-butyl-dimethylsilanyloxy)-hept-2-en-1-ol 457



To a cooled (-78 °C) solution of allylic ester **456** (28.0 g, 67.2 mmol) in dry CH_2Cl_2 (335 mL) was added diisobutylaluminiumhydride^a (1.5 M solution in PhMe, 99 mL, 148 mmol) dropwise over 0.5 h. The reaction mixture was allowed to warm to -60 °C over 1 h and maintained at this temperature for 2.5 h. It was then quenched by the careful dropwise addition of MeOH until all gas evolution ceased. The mixture was then diluted with CH_2Cl_2 (300 mL) and allowed to warm to 0 °C whereupon 10% aq. sodium potassium tartrate solution (300 mL) was added. After vigorous stirring at 0 °C for 1 h the solution was then stirred at room temperature for 1 h. The organic layer was separated and aqueous layer extracted with CH_2Cl_2 (5 x 300 mL), then EtOAc (5 x 400 mL). The combined organic layers were dried over MgSO_4 , filtered and concentrated *in vacuo*. Purification of the crude residue by SiO_2 flash chromatography using hexanes/EtOAc (9:1) as eluent afforded allylic alcohol **457** (23.8 g, 95%) as a viscous light yellow oil.

Spectral data agreed with those previously reported by Lennon¹⁰⁵ⁱⁱⁱ.

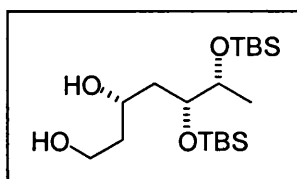
Literature yield: 87%

{{(2*R*,3*R*)-3-[(2*R*,3*R*)-2,3-Bis-(*t*-butyl-dimethylsilanyloxy)-butyl]-oxiranyl}-methanol 458

To a cooled (-35 °C) solution of diethyl D-tartrate^a (1.63 mL, 9.60 mmol) in dry CH₂Cl₂ (120 mL) and flame activated 4Å molecular sieves^a (20 g) was added titanium(IV) isopropoxide^a (2.31 mL, 7.76 mmol) and *t*-butyl hydroperoxide (8.8 M solution in CH₂Cl₂, 50.4 mL) sequentially. After ageing for 1 h, a solution of allylic alcohol **457** (18.0 g, 48.0 mmol) in dry CH₂Cl₂ (25 mL) was added dropwise over 18 mins and the mixture was stored at -33 °C for 7 d. The mixture was then warmed to 0 °C, and quenched by pouring in a solution of iron(II) sulfate heptahydrate^b (80 g) and citric acid^a (18.1 g) in H₂O (178 mL) and stirring vigorously for 0.5 h. The organic layer was removed and aqueous layer extracted with Et₂O (4 x 200 mL) and the combined organic layers were vigorously stirred with 15% NaOH in brine (260 mL) at 0 °C for 1.5 h. The organic layer was separated and the aqueous layer again extracted with Et₂O (5 x 50 mL). The combined organic layers were dried over MgSO₄, filtered, and concentrated *in vacuo*. Purification of the residue by SiO₂ flash chromatography using hexanes/EtOAc (40:1) as eluent afforded epoxy alcohol **458** (18.1 g, 96%) as a colourless viscous oil.

Spectral data agreed with those previously reported by Lennon ¹⁰⁵ⁱⁱⁱ.

Literature yield: 89%

(3*S*,5*R*,6*R*)-5,6-Bis-(*t*-butyl-dimethylsilanyloxy)-heptane-1,3-diol 459

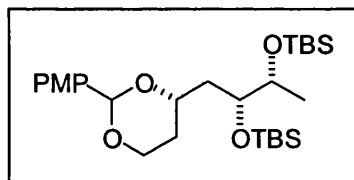
To a cooled (-40 °C) solution of epoxy alcohol **458** (19.04 g, 48.7 mmol) in dry THF (10 mL) was added sodium *bis*(methoxyethoxy)aluminium hydride^f (3.5 M solution in PhMe, 70 mL, 244 mmol) diluted

with THF (20 mL) dropwise over 19 min and the mixture was stored at -33 °C for 96 h. The mixture was then cooled to -78 °C, diluted with CH₂Cl₂ (200 mL) and quenched by the careful addition of MeOH until effervescence ceased. The mixture was warmed to 0 °C whereupon 10% aq. sodium potassium tartrate solution (200 mL) was added with vigorous stirring for 1.5 h. The organic layer was separated and the aqueous layer successively extracted with CH₂Cl₂ (5 x 150 mL). The combined organic layers were washed with brine (1 x 60 mL), dried over MgSO₄, filtered, and concentrated *in vacuo*. Purification of the residue by SiO₂ flash chromatography using hexanes/EtOAc (elution gradient 9:1, then 6:1) as eluent afforded 1,3-diol **459** (16.5 g, 86%) as a white solid.

Spectral data agreed with those previously reported by Lennon ¹⁰⁵ⁱⁱⁱ.

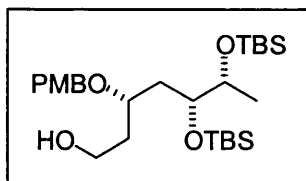
Literature yield: 83%

(S)-4-[(2R,3R)-2,3-Bis-(*t*-butyl-dimethylsilanyloxy)-butyl]-2-(4-methoxy-phenyl)-[1,3]dioxane 460



A mixture of 1,3-diol **459** (16.3 g, 41.6 mmol), *p*-anisaldehyde dimethylacetal⁹ (10.6 mL, 62.4 mmol) and pyridinium *p*-toluenesulfonate^a (1.9 g, 7.5 mmol) in dry DMF^a (275 mL) were heated at 50 °C on a rotary evaporator under reduced pressure (28 mmHg) for 25 min. The reaction mixture was then cooled to room temperature and quenched by the slow addition of saturated aq. NaHCO₃ (~50 mL) and extracted with Et₂O (6 x 150 mL). The combined organic layers were washed with brine (1 x 150 mL), dried over MgSO₄, filtered, and concentrated *in vacuo*. Purification of the residue by SiO₂ flash chromatography using hexanes/EtOAc (9:1) as eluent afforded *p*-methoxybenzylidene acetal **460** (19.6 g, 92 %) as a colourless viscous oil.

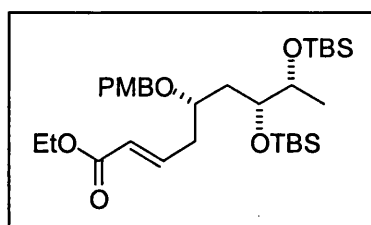
Spectral data agreed with those previously reported by Lennon ¹⁰⁵ⁱⁱⁱ.

(3S,5R,6R)-5,6-Bis-(*t*-butyl-dimethylsilanyloxy)-3-(4-methoxy-benzyloxy)-heptan-1-ol 461

To a cooled (-78 °C) solution of *p*-methoxybenzylidene acetal **460** (5.6 g, 11.0 mmol) in dry CH₂Cl₂ (10 mL) was added diisobutylaluminiumhydride^a (1.5 M solution in PhMe, 21.8 mL, 26.3 mmol) dropwise over 8 min and the reaction was allowed to warm to 0 °C over 4 h. After 30 min at 0 °C it was re-cooled to -78 °C, diluted with CH₂Cl₂ (60 mL) and quenched by the careful dropwise addition of MeOH until effervescence ceased. The mixture was warmed to 0 °C whereafter 10% aq. sodium potassium tartrate solution (90 mL) was added. After vigorous stirring for 1 h, the organic layer was separated and the aqueous layer extracted with CH₂Cl₂ (9 x 100 mL). The combined organic layers were washed with brine (1 x 200 mL), dried over MgSO₄, filtered, and concentrated *in vacuo*. Purification of the crude residue by SiO₂ flash chromatography using hexanes/EtOAc (40:1) as eluent afforded primary alcohol **461** (5.0 g, 89%; or 82% for 2 steps) as a colourless viscous oil.

Spectral data agreed with those previously reported by Lennon¹⁰⁵ⁱⁱⁱ.

Literature yield: 60-69% (2 steps)

(*E*)-(5S,7R,8R)-7,8-Bis-(*t*-butyl-dimethyl-silanyloxy)-5-(4-methoxy-benzyloxy)-non-2-enoic acid ethyl ester 463

To a cooled (-78 °C) solution of oxalyl chloride^a (4.8 mL, 55.4 mmol) in dry CH₂Cl₂ (34 mL) was added DMSO^a (7.86 mL, 110.8 mmol) dropwise over 8 min with concomitant gas evolution. After 50 min at -78 °C, a solution of **461** (5.7 g, 11.1 mmol) in dry CH₂Cl₂ (25 mL) was added dropwise over 13 min, and the

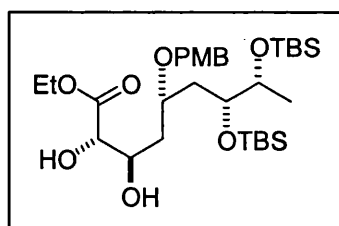
reaction mixture then allowed to warm to $-55\text{ }^{\circ}\text{C}$ over 2 h. After 45 min at this temperature, Et_3N (23.15 mL, 166 mmol) was added dropwise over 11 min and the mixture stirred vigorously for 10 min. Dry CH_2Cl_2 (60 mL) was then added and the reactants allowed to warm to RT. The reaction mixture was washed with brine (1 x 70 mL), dried over MgSO_4 , filtered, and concentrated *in vacuo* to yield a thick dark yellow oil. The crude aldehyde **462** was azeotropically dried from C_6H_6 (1 x 15 mL) and used for the next step without further purification.

To the crude aldehyde **462** (5.7 g, 11.1 mmol, assuming 100% conversion) in dry CH_2Cl_2 (11.2 mL) was added carbethoxymethylene triphenylphosphorane^c (7.7 g, 22.2 mmol) in one portion. After 15 h at room temperature, SiO_2 (~10 g) was added and the solvents removed *in vacuo*. Flash chromatography was then performed with hexanes/ EtOAc (20:1) as eluent to afford α,β -unsaturated ester **463** (5.8 g, 89%, 2 steps) as a colourless viscous oil.

Spectral data agreed with those previously reported by Lennon¹⁰⁵ⁱⁱⁱ.

Literature yield: 70-75% (2 steps)

(2S,3R,5S,7R,8R)-7,8-Bis-(*t*-butyl-dimethyl-silanyloxy)-2,3-dihydroxy-5-(4-methoxy-benzyloxy)-nonanoic acid ethyl ester **464**



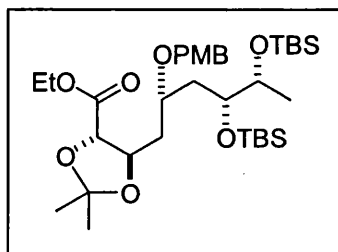
To a stirred suspension of H_2O (50.0 mL) and *t*-butanol^a (60.0 mL) was added AD-mix β^a (55.7 g, 4.0 eq.) and methanesulfonamide^c (3.8 g, 39.6 mmol). After 10 min of vigorous stirring at room temperature, the mixture was cooled to $0\text{ }^{\circ}\text{C}$ whereupon a solution of α,β -unsaturated ester **463** (5.8 g, 9.9 mmol) in *t*-butanol^a (10 mL) was added in one portion. After 20 h the reaction was quenched with solid sodium sulfite (59.6 g) and vigorously stirred at room temperature for 1 h. The organic layer was separated and the aqueous layer extracted with hot EtOAc (8 x 30 mL). The combined organic layers were dried over MgSO_4 , filtered, and concentrated *in vacuo*. Purification of the crude residue by SiO_2 flash chromatography using

hexanes/EtOAc (elution gradient 20:1, then 3:1) as eluent afforded 1,2-diol **464** (5.7 g, 93%) as a light yellow viscous oil.

Spectral data agreed with those previously reported by Lennon ¹⁰⁵ⁱⁱⁱ.

Literature yield: 86%

(4S,5R)-5-[(2S,4R,5R)-4,5-Bis-(*t*-butyl-dimethyl-silanyloxy)-2-(4-methoxy-benzyloxy)-hexyl]-2,2-dimethyl-[1,3]dioxolane-4-carboxylic acid ethyl ester 438

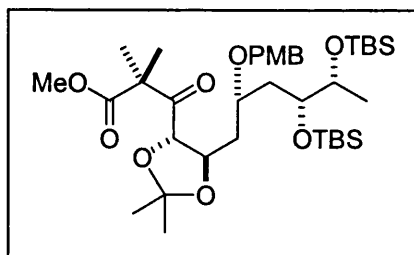


To a stirred solution of 1,2-diol **464** (13.7 g, 22.3 mmol) in acetone^b (48 mL) and 2,2-dimethoxypropane^a (48 mL) was added pyridinium *p*-toluenesulfonate^c (1.4 g, 5.6 mmol) in one portion, a condenser was fitted and the mixture heated to 40 °C. After 16 h the solvent was removed *in vacuo*. Purification of the residue by SiO₂ flash chromatography using hexanes/EtOAc (20:1) as eluent afforded acetone **438** (13.7 g, 94%) as a colourless viscous oil.

Spectral data agreed with those previously reported by Lennon ¹⁰⁵ⁱⁱⁱ.

Literature yield: 85-90%

3-[(4S,5R)-5-[(2S,4R,5R)-4,5-Bis-(*t*-butyl-dimethyl-silanyloxy)-2-(4-methoxy-benzyloxy)-hexyl]-2,2-dimethyl-[1,3]dioxolan-4-yl]-2,2-dimethyl-3-oxo-propionic acid methyl ester 436

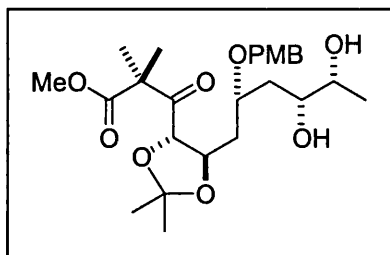


To a cooled (-78°C) solution of dry diisopropylamine (7.9 mL, 56.0 mmol) and dry THF (8.5 mL) was added *n*-butyllithium^a (2.5 M solution in hexanes, 22.4 mL, 56.0 mmol) dropwise over 7 min. After 45 min methyl isobutyrate^a (6.80 mL, 59.2 mmol) was added in one portion. After a further 40 min a solution of acetone **438** (5.24 g, 8.0 mmol) in dry THF (19 mL) was added over 12 min. After 0.5 h the mixture was warmed to -20°C and stirred for 1 h. The mixture was diluted with Et₂O (80 mL), quenched by dropwise addition of saturated NH₄Cl (aq.) (~30 mL) and stirred for 20 min at room temperature. The organic layer was separated and the aqueous layer extracted with EtOAc (9 x 60 mL). The combined organic layers were washed with brine (1 x 50 mL), dried over MgSO₄, filtered, and concentrated *in vacuo*. Purification of the residue by SiO₂ flash chromatography using hexanes/EtOAc (4:1) as eluent afforded β -keto ester **436** (5.4 g, 95%) as a light yellow viscous oil.

Spectral data agreed with those previously reported by Lennon¹⁰⁵ⁱⁱⁱ.

Literature yield: 85%

3-((4*S*,5*R*)-5-[(2*R*,4*R*,5*R*)-4,5-Dihydroxy-2-(4-methoxy-benzyloxy)-hexyl]-2,2-dimethyl-[1,3]dioxolan-4-yl)-2,2-dimethyl-3-oxo-propionic acid methyl ester **465**



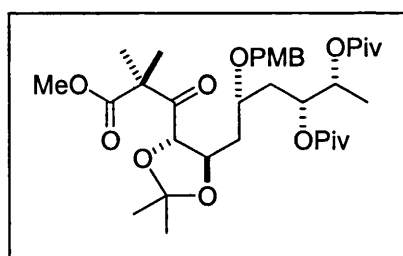
To a cooled (-40°C) solution of β -keto ester **436** (5.4 g, 7.6 mmol) in dry THF (64 mL) in a polyethylene bottle was added hydrogen fluoride-pyridine complex (20 mL) dropwise via a polyethylene

syringe over 5 min and the mixture was allowed to warm to -5 °C over 4 h. After a further 26 h at -5 °C, the reaction was quenched by the sequential addition of solid NaHCO₃, and saturated aq. NaHCO₃ solution, and diluted with EtOAc (20 mL). The organic layer was then separated and aqueous layer was extracted with EtOAc (10 x 50 mL). The combined organic layers were dried over MgSO₄, filtered, and concentrated *in vacuo*. Purification of the residue by SiO₂ flash chromatography using hexanes/EtOAc (3:2, then 1:1) as eluent afforded diol **465** (3.25 g, 89%) as a colourless viscous oil.

Spectral data agreed with those previously reported by Lennon ¹⁰⁵ⁱⁱⁱ.

Literature yield: 98%

3-[(4*S*,5*R*)-5-[(2*S*,4*R*,5*R*)-4,5-Bis-(2,2-dimethyl-propionyloxy)-2-(4-methoxy-benzyloxy)-hexyl]-2,2-dimethyl-[1,3]dioxolan-4-yl]-2,2-dimethyl-3-oxo-propionic acid methyl ester **466**

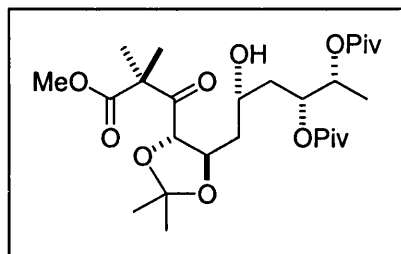


To a cooled (0 °C) solution of diol **465** (702 mg, 1.5 mmol) in dry pyridine^a (2.4 mL) and dry CH₂Cl₂ (2.1 mL) was added trimethylacetylchloride^c (1.8 mL, 15.0 mmol) dropwise over 2 min, and the mixture was allowed to warm to room temperature. After 10 d the mixture was quenched by the addition of saturated aq. NaHCO₃ solution (~5 mL) and extracted with EtOAc (6 x 10 mL). The combined organic layers were washed with brine (1 x 15 mL), dried over MgSO₄, filtered, and concentrated *in vacuo*. The excess pyridine was then azeotropically removed with PhMe (2 x 10 mL). Purification of the residue by SiO₂ flash chromatography using hexanes/EtOAc (12:1) as eluent afforded the dipivaloate **466** (820 mg, 87%) as a colourless viscous oil.

Spectral data agreed with those previously reported by Lennon ¹⁰⁵ⁱⁱⁱ.

Literature yield: 92%

3-((4*S*,5*R*)-5-[(2*S*,4*R*,5*R*)-4,5-Bis-(2,2-dimethyl-propionyloxy)-2-hydroxy-hexyl]-2,2-dimethyl-[1,3]-dioxolan-4-yl)-2,2-dimethyl-3-oxo-propionic acid methyl ester 467

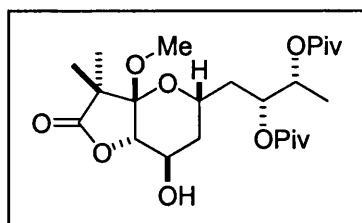


To a stirred solution of dipivaloate **466** (5.73 g, 8.81 mmol) in CH₂Cl₂ (68 mL) and H₂O (3.8 mL) was added 2,3-dichloro-5,6-dicyanobenzoquinone^a (4.0 g, 17.6 mmol) in one portion. After 85 min at room temperature the mixture was quenched with saturated aq. NaHCO₃ solution and filtered through a plug of CELITETM with subsequent CH₂Cl₂ washings, then H₂O washings. The organic layer was separated and aqueous layer extracted with CH₂Cl₂ (4 x 50 mL). The combined organic layers were dried over MgSO₄, filtered, and concentrated *in vacuo*. Purification of the crude residue by SiO₂ flash chromatography using hexanes/EtOAc (10:1) as eluent afforded δ -hydroxy ketone **467** (4.2 g, 89%) as a light yellow viscous oil.

Spectral data agreed with those previously reported by Lennon¹⁰⁵ⁱⁱⁱ.

Literature yield: 89-94%

2,2-Dimethyl-propionic acid (1*R*,2*R*)-2-(2,2-dimethyl-propionyloxy)-3-((3*aS*,5*S*,7*R*,7*aS*)-7-hydroxy -3*a*-methoxy-3,3-dimethyl-2-oxo-hexahydro-furo[3,2-*b*]pyran-5-yl)-1-methyl-propyl ester 435



To a 50 mL flask containing dry MeOH^a (6.2 mL) was added acetyl chloride^a (0.9 mL, 12.1 mmol). After 4 h at RT the solution of methanolic HCl was added to δ -hydroxy ketone **467** (552 mg, 1.1 mmol). The mixture was heated at 40 °C for 96 h, whereafter it was cooled to 0 °C and quenched by the addition of solid

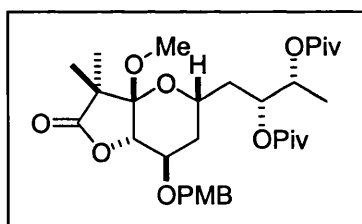
NaHCO₃ (~5 g). After CO₂ evolution had subsided, the mixture was diluted with EtOAc (10 mL) and H₂O (10 mL). The organic layer was separated and the aqueous layer extracted with EtOAc (8 x 15 mL). The combined organic layers were washed with brine (1 x 15 mL), dried over MgSO₄, filtered, and concentrated *in vacuo*. Purification of the crude residue by SiO₂ flash chromatography using hexanes/EtOAc (20:1, then 5:1) as eluent afforded methyl glycoside **435** (280 mg, 58%) as a clear viscous oil.

Spectral data agreed with those previously reported by Lennon¹⁰⁵ⁱⁱⁱ.

Literature yield: 56% (for 2 step procedure)

2,2-Dimethyl-propionic acid (1*R*,2*R*)-2-(2,2-dimethyl-propionyloxy)-1-[(3*aS*,5*S*,7*R*,7*aS*)-3*a*-methoxy-7-(4-methoxy-benzyloxy)-3,3-dimethyl-2-oxo-hexahydro-furo[3,2-*b*]pyran-5-ylmethyl]-propyl ester

473



To a stirred solution of methyl glycoside **435** (306 mg, 0.66 mmol) in dry CH₂Cl₂ (2.0 mL) was added a solution of *p*-methoxybenzyl trichloroacetimidate (940 mg, 3.3 mmol) in dry CH₂Cl₂ (3.0 mL) in one portion. Pyridinium-*p*-toluene sulfonate^c (83 mg, 0.33 mmol) was then added in one portion. After 14 d of stirring, the mixture was diluted with CH₂Cl₂ (13 mL) and quenched by dropwise addition of saturated aq. NaHCO₃ (~2 mL). The organic layer was separated and aqueous layer extracted with CH₂Cl₂ (4 x 5 mL). The combined organic layers were washed with brine (1 x 10 mL), dried over MgSO₄, filtered, and concentrated *in vacuo*. Purification of the residue by SiO₂ flash chromatography using hexanes/EtOAc (gradient elution with neat hexanes, then 400:1, then 100:1, then 10:1) as eluent afforded *p*-methoxybenzyl ether **473** (272 mg, 70%) as a colourless viscous oil.

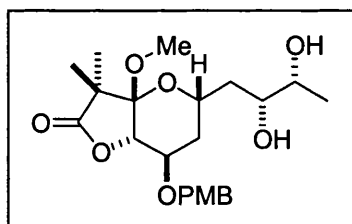
IR (neat film): 2975 (m), 2937 (m), 2910 (m), 2873 (w), 1791 (s), 1730 (s), 1613 (w), 1514 (m), 1480 (w), 1464 (w), 1391 (w), 1368 (w), 1281 (m), 1249 (m), 1210 (w), 1155 (s), 1099 (m), 1059 (m), 1037 (m), 993 (w), 823 (w) cm^{-1} .

^1H NMR (500 MHz in CDCl_3): δ 7.20 (d, J = 8.6 Hz, 2H), 6.82 (d, J = 8.6 Hz, 2H), 5.18 (m, 1H), 4.92 (m, 1H), 4.51 (dd, J = 11.8, 19.4 Hz, 2H), 4.15 (d, J = 2.0 Hz, 1H), 3.94 (m, 1H), 3.86 (m, 1H), 3.76 (s, 3H), 3.27 (s, 3H), 1.73-1.61 (complex m, 3H), 1.51 (m, 1H), 1.30 (s, 3H), 1.19 (s, 3H), 1.17 (s, 9H), 1.15 (s, 9H), 1.12 (d, J = 6.5 Hz, 3H) ppm.

^{13}C NMR (125 MHz in CDCl_3): δ 178.8, 177.5, 177.3, 159.2, 129.7, 129.0, 113.7, 102.0, 73.1, 70.6, 70.4, 70.2, 69.5, 61.7, 55.2, 49.9, 48.6, 38.8, 38.7, 36.5, 30.2, 27.1, 27.0, 20.1, 18.2, 15.5 ppm.

HRMS (FAB, MNOBA matrix): for $\text{C}_{32}\text{H}_{48}\text{O}_{10}\text{Na}$ ($\text{M}+\text{Na}$) $^+$, Calcd: 615.3180, Found: 615.3145.

(3a*S*,5*R*,7*R*,7a*S*)-5-((2*R*,3*R*)-2,3-Dihydroxy-butyl)-3a-methoxy-7-(4-methoxy-benzyloxy)-3,3-dimethyl-hexahydro-furo[3,2-*b*]pyran-2-one **474**



To a stirred solution of *p*-methoxybenzyl ether **473** (500 mg, 0.86 mmol) in MeOH^a (7.8 mL) was added a fresh solution of sodium methoxide (1 M solution in MeOH , 28 mL, 11.9 mmol) in one portion. After 72 h the mixture was neutralised (pH 7) by the slow addition of pre-washed (in MeOH) Amberlite 120 H^+ resin. The resin was filtered off and the solvent removed *in vacuo*. Purification of the residue by SiO_2 flash chromatography using hexanes/ EtOAc (2:1, then neat EtOAc) as eluent afforded 1,2-diol **474** (276 mg, 73%) as a colourless oil.

$[\alpha]_D^{20}$: +37.2 $^\circ$ (c 0.18, CH_2Cl_2).

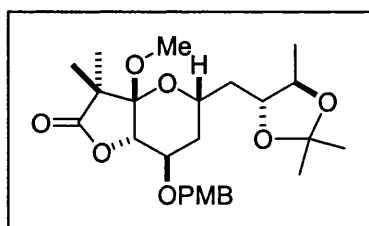
IR (neat film): 3446 (br), 2950 (s), 1783 (s), 1613 (m), 1514 (s), 1463 (m), 1390 (m), 1248 (s), 1037 (s), 914 (m), 823 (m), 732 (s) cm^{-1} .

^1H NMR (500 MHz in CDCl_3): δ 7.24 (d, J = 8.6 Hz, 2H), 6.85 (d, J = 8.6 Hz, 2H), 4.54 (s, 2H), 4.28 (t, J = 10.5 Hz, 1H), 4.17 (d, J = 1.6 Hz, 1H), 3.87 (m, 1H), 3.77 (s, 3H), 3.63 (m, 1H), 3.55 (m, 1H), 3.39 (s, 3H), 2.27 (broad s, 2H), 1.68 (d, J = 14.3 Hz, 1H), 1.59-1.48 (complex m, 3H), 1.30 (s, 3H), 1.24 (s, 3H), 1.17 (d, J = 6.2 Hz, 3H) ppm.

^{13}C NMR (125 MHz in CDCl_3): δ 179.1, 159.3, 130.0, 129.5, 113.9, 101.8, 73.3, 72.0, 71.2, 70.7, 69.4, 62.0, 55.2, 50.0, 48.6, 39.1, 30.1, 20.1, 19.7, 18.3 ppm.

HRMS (FAB, MNOBA matrix): for $\text{C}_{22}\text{H}_{32}\text{O}_8\text{Na}$ ($\text{M}+\text{Na}$) $^+$, Calcd: 447.2006, Found: 447.1995.

(3a*S*,5*S*,7*R*,7a*S*)-3a-Methoxy-7-(4-methoxy-benzyloxy)-3,3-dimethyl-5-((4*R*,5*R*)-2,2,5-trimethyl-[1,3]-dioxolan-4-ylmethyl)-hexahydro-furo[3,2-*b*]pyran-2-one **475**



To a stirred solution of 1,2-diol **474** (56 mg, 0.13 mmol) in acetone^b (0.95 mL) and 2,2-dimethoxypropane^a (0.95 mL) was added pyridinium *p*-toluenesulfonate^c (8 mg, 30 μmol) in one portion, a condenser was fitted and the mixture was heated to 40 $^{\circ}\text{C}$. After 20 min the solvent was removed *in vacuo*. Purification of the residue by SiO_2 flash chromatography using hexanes/EtOAc (gradient elution 4:1, then 3:1) as eluent afforded acetone **475** (60 mg, 98%) as a colourless oil.

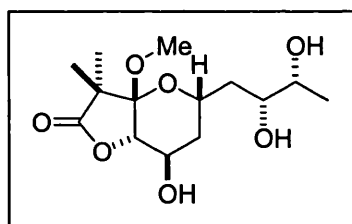
IR (neat film): 2981 (m), 1789 (s), 1613 (w), 1514 (m), 1464 (w), 1378 (w), 1247 (s), 1099 (m), 1039 (m) cm^{-1} .

¹H NMR (500 MHz in CDCl₃): δ 7.25 (d, *J* = 8.3 Hz, 2H), 6.86 (d, *J* = 8.6 Hz, 2H), 4.55 (dd, *J* = 12.2, 14.8 Hz, 2H), 4.21 (m, 1H), 4.16 (d, *J* = 1.4 Hz, 1H), 3.86 (dd, *J* = 2.4, 4.9 Hz, 1H), 3.79 (m, 1H), 3.78 (s, 3H), 3.63 (m, 1H), 3.38 (s, 3H), 1.73 (d, *J* = 14.3 Hz, 1H), 1.62-1.44 (complex m, 3H), 1.35 (s, 3H), 1.320 (s, 3H), 1.316 (s, 3H), 1.24 (s, 3H), 1.21 (d, *J* = 6.0 Hz, 3H) ppm.

¹³C NMR (125 MHz in CDCl₃): δ 179.0, 159.3, 129.7, 129.3, 113.8, 107.8, 101.8, 77.9, 76.8, 73.3, 70.7, 69.4, 62.3, 55.2, 49.6, 48.6, 37.8, 30.3, 27.3, 27.0, 20.1, 18.4, 16.9 ppm.

HRMS (FAB, MNOBA matrix): for C₂₅H₃₆O₈Na (M+Na)⁺, Calcd: 487.2330, Found: 487.2308.

(3a*S*,5*R*,7*R*,7a*S*)-5-((2*R*,3*R*)-2,3-Dihydroxy-butyl)-7-hydroxy-3a-methoxy-3,3-dimethyl-hexahydro-furo[3,2-*b*]pyran-2-one 477



To a stirred solution of dipivaloate **435** (2.3 g, 4.8 mmol) in MeOH^a (40 mL) was added a fresh solution of sodium methoxide (1 M solution in MeOH, 170 mL, 72 mmol) in one portion. After 48 h the mixture was neutralised (pH 7) by the slow addition of pre-washed (in MeOH) Amberlite 120 H⁺ resin. The resin was filtered off, SiO₂ added and the solvent removed *in vacuo*. It was then added to a pre-packed column of SiO₂ and the column eluted using hexanes/EtOAc (1:2, then 20:1 EtOAc:MeOH). Triol **477** (1.4 g, 99%) was obtained as a white crystalline solid.

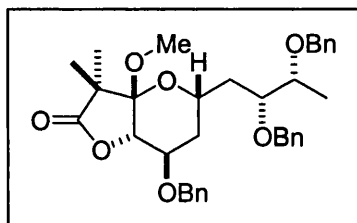
IR (neat film): 3394 (br), 2977 (m), 2948 (m), 1768 (s), 1650 (w), 1461 (m), 1391 (m), 1285 (m), 1245 (m), 1213 (m), 1157 (s), 1131 (s), 1096 (s), 1038 (s), 922 (m) 730 (m) cm⁻¹.

¹H NMR (500 MHz in CDCl₃): δ 4.26 (m, 2H), 4.13 (d, J = 2.6 Hz, 1H), 3.64 (m, 1H), 3.57 (m, 1H), 3.41 (s, 3H), 2.54 (broad s, 3H), 1.68 (m, 2H), 1.64-1.47 (complex m, 2H), 1.32 (s, 3H), 1.25 (s, 3H), 1.19 (d, J = 6.22 Hz, 3H) ppm.

¹³C NMR (125 MHz in CDCl₃): δ 178.8, 102.2, 73.8, 71.8, 71.3, 64.0, 61.0, 50.1, 48.6, 39.0, 32.9, 19.8, 18.3 ppm.

HRMS (FAB, MNOBA matrix): for C₁₄H₂₄O₇Na (M+Na)⁺, Calcd: 327.1407, Found: 327.1420.

(3a*S*,5*R*,7*R*,7a*S*)-7-Benzoyloxy-5-((2*R*,3*R*)-2,3-bis-benzoyloxy-butyl)-3a-methoxy-3,3-dimethyl-hexahydro-furo[3,2-*b*]pyran-2-one 478



To a cooled (0 °C) solution of triol **477** (500 mg, 1.64 mmol) in dry DMF^a (15 mL) was added sodium hydride^c (60% dispersion in mineral oil, 660 mg, 16.4 mmol) in 3 portions over a 2 min period, to avoid excess foaming. After 40 min, benzyl bromide^a (1.95 mL, 16.4 mmol) was added dropwise over 2 min and 10 min later, the mixture was allowed to warm to room temperature. After a further 1.5 h at RT the mixture was re-cooled to 0 °C and quenched by adding solid NaHCO₃ (~2 g) and dropwise addition of H₂O (~30 mL). The mixture was extracted with Et₂O (9 x 20 mL) and the combined organic layers were dried over MgSO₄, filtered, and concentrated *in vacuo*. Purification of the crude residue by SiO₂ flash chromatography using hexanes/EtOAc (gradient elution with neat hexanes, then 20:1, then 10:1, then 5:1) as eluent afforded *tris*-benzyl ether **478** (713 mg, 76%) as a colourless oil.

[α]_D: +1.6° (c 1.865, CH₂Cl₂).

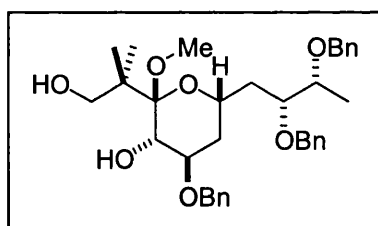
IR (neat film): 2976 (m), 2876 (m), 1786 (s), 1496 (w), 1455 (m), 1389 (m), 1211 (m), 1101 (s), 1061 (s), 738 (s) cm^{-1} .

^1H NMR (500 MHz in CDCl_3): δ 7.23 (m, 15H), 4.62 (d, J = 11.4 Hz, 1H), 4.56 (m, 3H), 4.47 (d, J = 11.8 Hz, 1H), 4.41 (d, J = 11.4 Hz, 1H), 4.22 (dt, J = 2.3, 9.3 Hz, 1H), 4.16 (d, J = 1.7 Hz, 1H), 3.86 (m, 1H), 3.80 (m, 1H), 3.74 (m, 1H), 3.23 (s, 3H), 1.80-1.73 (complex m, 2H), 1.59-1.48 (complex m, 2H), 1.30 (s, 3H), 1.21 (s, 3H), 1.13 (d, J = 6.3 Hz, 3H) ppm.

^{13}C NMR (125 MHz in CDCl_3): δ 179.0, 138.5, 137.8, 128.1, 127.7, 127.6, 127.4, 101.9, 77.4, 74.7, 73.6, 72.0, 71.1, 70.9, 70.0, 62.6, 49.6, 48.6, 35.7, 30.0, 20.2, 18.4, 14.4 ppm.

HRMS (FAB, MNOBA matrix): for $\text{C}_{35}\text{H}_{42}\text{O}_7\text{Na}$ ($\text{M}+\text{Na}$) $^+$, Calcd: 597.2807, Found: 597.2828.

(2S,3S,4R,6S)-4-Benzoyloxy-6-[(2R,3R)-2,3-bis-benzyloxy-butyl]-2-(2-hydroxy-1,1-dimethyl-ethyl)-2-methoxy-tetrahydro-pyran-3-ol 479

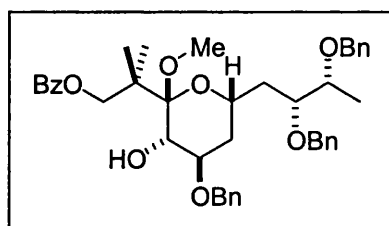


To a cooled (0 °C) solution of lithium aluminium hydride^a (1 M solution in Et_2O , 1.74 mL, 1.74 mmol) in dry THF (4 mL) was added a solution of *tris*-benzyl ether **478** (200 mg, 0.35 mmol) in dry THF (800 μL) dropwise over 2 min. After 5 min, the reaction mixture was allowed to warm to room temperature and stirred for 3.5 h. It was then re-cooled to 0 °C and EtOAc (5 mL) was added. Final quenching was accomplished by dropwise addition of MeOH until H_2 gas evolution visibly ceased. The mixture was then stirred vigorously with saturated aq. sodium potassium tartrate^c (10 mL) for 45 min. The organic layer was separated and the aqueous layer extracted with EtOAc (8 x 10 mL). The combined organic layers were dried over MgSO_4 , filtered, and concentrated *in vacuo*. The residue was purified by rapid SiO_2 flash

chromatography using hexanes/EtOAc (2:1) as eluent. Diol **479** (176 mg, 88%) was obtained as a colourless viscous oil, that proved rather unstable.

¹H NMR (500 MHz in C₆D₆): δ 7.41-7.04 (complex m, 15H), 4.59-4.42 (complex m, 6H), 4.30 (d, J = 11.7 Hz, 1H), 4.07 (m, 2H), 3.70 (m, 2H), 3.53 (q, J = 10.8 Hz, 2H), 3.28 (s, 3H), 1.95 (complex m, 2H), 1.62 (complex m, 2H), 1.20 (s, 3H), 1.17 (d, J = 6.3 Hz, 3H), 1.09 (s, 3H) ppm.

Benzoic acid 2-[(2S,3S,4R,6S)-4-benzyloxy-6-((2R,3R)-2,3-bis-benzyloxy-butyl)-3-hydroxy-2-methoxy-tetrahydro-pyran-2-yl]-2-methyl-propyl ester **483**

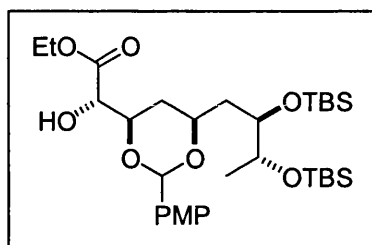


To a cooled (0 °C) solution of diol **479** (50 mg, 0.09 mmol) in dry CH₂Cl₂ (1.2 mL) and pyridine^a (1.2 mL) was added benzoyl chloride⁹ (100 μ L, 0.9 mmol) dropwise over 1 min. After 2 min the mixture was diluted with CH₂Cl₂ (~1 mL) and quenched by dropwise addition of saturated aq. NaHCO₃. The organic layer was separated and aqueous layer extracted with CH₂Cl₂ (4 x 2 mL). The combined organic layers were dried over MgSO₄, filtered, and concentrated *in vacuo*. Purification of the residue by SiO₂ flash chromatography using hexanes/EtOAc (gradient elution with neat hexanes, then 6:1, then 3:1) as eluent afforded primary benzoate **483** (41 mg, 69%) as a colourless viscous oil.

¹³C NMR (125 MHz in C₆D₆): δ 172.3, 167.0, 148.4, 139.5, 133.6, 130.5, 130.0, 128.6, 128.5, 128.3, 127.8, 127.7, 127.5, 102.6, 77.4, 76.8, 75.2, 72.4, 71.2, 70.8, 67.5, 65.0, 51.3, 46.4, 36.8, 31.8, 30.4, 21.6, 21.0, 14.6 ppm.

HRMS (FAB, MNOBA matrix): for C₄₂H₅₀O₈Na (M+Na)⁺, Calcd: 705.3373, Found: 705.3403.

(S)-[(4*R*,6*S*)-6-[(2*R*,3*R*)-2,3-Bis-(*t*-butyl-dimethyl-silanyloxy)-butyl]-2-(4-methoxy-phenyl)-[1,3]dioxan-4-yl]-hydroxy-acetic acid ethyl ester 490



To a cooled (0 °C) solution of 1,2-diol **464** (5.7 g, 9.4 mmol) in dry CH₂Cl₂ (115 mL) and flame activated 4Å molecular sieves^a (8 g) was added 2,3-dichloro-5,6-dicyanobezoquinone^a (2.6 g, 11.3 mmol) in one portion. After 2.5 h the mixture was diluted with CH₂Cl₂ (100 mL), filtered through CELITETM with CH₂Cl₂ washings, and then washed with H₂O (2 x 30 mL). The aqueous layers were back-extracted with CH₂Cl₂ (2 x 20 mL), and the combined organic layers were dried over MgSO₄, filtered, and concentrated *in vacuo*. Purification of the residue by SiO₂ flash chromatography using hexanes/EtOAc (gradient elution 100:1, then 20:1) as eluent afforded *p*-methoxybenzylidene acetal **490** (4.4 g, 76%) as a light yellow viscous oil.

[α]_D: +26.6° (c 1.22, CH₂Cl₂).

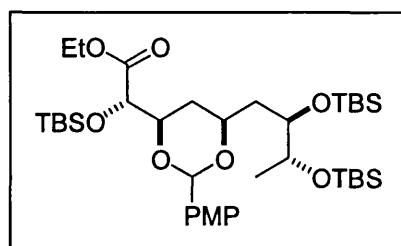
IR (neat film): 3524 (br), 2996 (s), 2857 (s), 1744 (m), 1616 (w), 1589 (w), 1518 (m), 1472 (m), 1389 (m), 1302 (m), 1250 (s), 1105 (s), 1007 (m), 836 (s), 775 (s) cm⁻¹.

¹H NMR (500 MHz in CDCl₃): δ 7.32 (d, *J* = 8.7 Hz, 2H), 6.83 (d, *J* = 8.7 Hz, 2H), 5.44 (s, 1H), 4.28 (q, *J* = 7.1 Hz, 2H), 4.19 (dt, *J* = 2.3, 11.5 Hz, 1H), 4.11 (dd, *J* = 2.4, 8.7 Hz, 1H), 3.96 (m, 2H), 3.81 (m, 1H), 3.78 (s, 3H), 2.91 (d, *J* = 8.8 Hz, 2H), 1.92 (m, 2H), 1.53-1.42 (complex m, 2H), 1.30 (t, *J* = 7.1 Hz, 3H), 1.05 (d, *J* = 6.3 Hz, 3H), 0.87 (s, 9H), 0.85 (s, 9H), 0.021 (s, 3H), 0.016 (s, 6H), 0.00 (s, 3H) ppm.

¹³C NMR (125 MHz in CDCl₃): δ 172.2, 159.7, 130.9, 127.2, 113.3, 99.9, 77.3, 76.7, 73.1, 72.4, 70.3, 70.2, 61.7, 55.2, 36.1, 32.6, 25.8, 18.2, 18.0, 16.2, 14.3, -4.3, -4.6, -4.7, -4.8 ppm.

HRMS (FAB, MNOBA matrix): for $C_{31}H_{56}O_8Si_2Na$ ($M+Na$)⁺, Calcd: 635.3430, Found: 635.3411.

(S)-[[(4R,6S)-6-[(2R,3R)-2,3-Bis-(*t*-butyl-dimethyl-silanyloxy)-butyl]-2-(4-methoxy-phenyl)-[1,3]dioxan-4-yl]-(*t*-butyl-dimethyl-silanyloxy)-acetic acid ethyl ester 491



To a solution of α -hydroxy ester **490** (1.6 g, 2.6 mmol) in dry DMF^a (10 mL) was added *t*-butyldimethylchlorosilane^c (1.0 g, 6.6 mmol) and imidazole^c (630 mg, 9.3 mmol) in one portion each sequentially. After 4.5 hrs the mixture was cooled to 0 °C, diluted with Et₂O (20 mL) and quenched by dropwise addition of saturated aq. NaHCO₃ solution (~10 mL). The organic layer was separated and aqueous layer extracted with Et₂O (5 x 5 mL). The combined organic layers were washed with H₂O (1 x 10 mL) then brine (1 x 10 mL), dried over MgSO₄, filtered, and concentrated *in vacuo*. Purification of the residue by SiO₂ flash chromatography using hexanes/EtOAc (100:1) as eluent afforded trisilyl ether **491** (1.9 g, 99%) as a colourless oil.

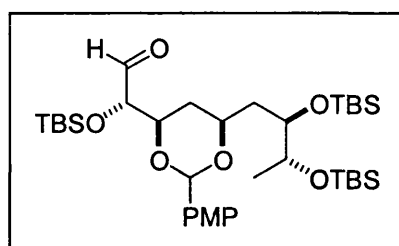
$[\alpha]_D^{25}$: +22.6° (c 0.7, CH₂Cl₂).

¹H NMR (500 MHz in CDCl₃): δ 7.36 (d, *J* = 8.7 Hz, 2H), 6.82 (d, *J* = 8.8 Hz, 2H), 5.42 (s, 1H), 4.23 (d, *J* = 6.0 Hz, 2H), 4.20 (q, *J* = 7.2 Hz, 3H), 4.05 (ddd, *J* = 2.3, 6.0, 11.4 Hz, 1H), 3.95 (d, *J* = 1.8, 4.4, 10.3 Hz, 1H), 3.89 (t, *J* = 10.7 Hz, 1H), 3.78 (s, 3H), 3.77 (overlapping m, 1H), 1.88 (ddd, *J* = 1.7, 10.5, 13.9 Hz, 1H), 1.59 (m, 2H), 1.41 (m, 2H), 1.27 (t, *J* = 7.1 Hz, 3H), 1.04 (d, *J* = 6.3 Hz, 3H), 0.87 (s, 9H), 0.86 (s, 9H), 0.84 (s, 9H) ppm.

¹³C NMR (125 MHz in CDCl₃): δ 171.2, 159.6, 131.3, 127.5, 113.1, 100.3, 78.4, 76.2, 75.5, 72.3, 70.3, 70.2, 60.9, 55.2, 36.1, 32.7, 25.8, 25.7, 18.2, 18.1, 18.0, 16.2, 14.2, -4.3, -4.6, -4.7, -4.8, -4.96, -5.04 ppm.

HRMS (FAB, MNOBA matrix): for $C_{37}H_{70}O_8Si_3Na$ ($M+Na$)⁺, Calcd: 749.4300, Found: 749.4276.

(S)-[(4*R*,6*S*)-6-[(2*R*,3*R*)-2,3-Bis-(*t*-butyl-dimethyl-silanyloxy)-butyl]-2-(4-methoxy-phenyl)-[1,3]dioxan-4-yl]-(*t*-butyl-dimethyl-silanyloxy)-acetaldehyde **489**



To a cooled (-78 °C) solution of trisilyl ether **491** (1.9 g, 2.6 mmol) in dry CH_2Cl_2 (18.0 mL) was added diisobutylaluminiumhydride^a (1.5 M in PhMe, 2.2 mL, 2.6 mmol) dropwise over 5 min. After 1 h the mixture was quenched by the dropwise addition of MeOH (~10 mL) and warmed to 0 °C when 10% aq. sodium potassium tartrate solution (20 mL) and solid NaCl (5 g) were added with vigorous stirring. After 15 min the organic layer was separated and aqueous layer was extracted with CH_2Cl_2 (6 x 10 mL). The combined organic layers were washed with brine (1 x 10 mL), dried over $MgSO_4$, filtered, and concentrated *in vacuo*. Purification of the residue by SiO_2 flash chromatography using hexanes/EtOAc (100:1) as eluent afforded aldehyde **489** (1.7 g, 93%) as a colourless viscous oil, that proved rather unstable.

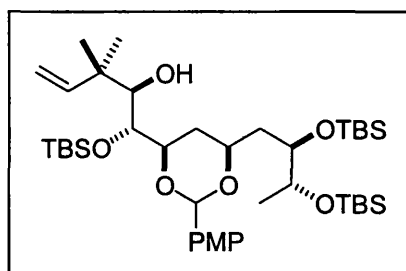
IR (neat film): 2955 (s), 2931 (s), 2888 (s), 2857 (s), 1738 (m), 1617 (m), 1591 (w), 1518 (m), 1469 (m), 1440 (w), 1386 (m), 1343 (m), 1303 (m), 1252 (s), 1105 (s), 1068 (s), 1041 (s), 1008 (s), 939 (m), 880 (m), 836 (s), 809 (m), 777 (s) cm^{-1} .

¹H NMR (500 MHz in $CDCl_3$): δ 9.73 (d, J = 0.6 Hz, 1H), 7.36 (m, 2H), 6.83 (m, 2H), 5.41 (m, 1H), 4.22 (m, 1H), 4.12 (m, 1H), 3.96-3.86 (complex m, 2H), 3.78 (s, 3H), 3.77 (overlapping m, 1H), 1.88 (m, 1H), 1.61-1.54 (complex m, 2H), 1.43 (m, 1H), 1.04 (d, J = 6.2 Hz, 3H), 0.87 (m, 27H), 0.03 (m, 18H) ppm.

¹³C NMR (125 MHz in $CDCl_3$): δ 202.9, 171.1, 159.7, 131.4, 127.6, 113.1, 100.6, 79.4, 77.3, 72.5, 72.3, 70.3, 55.2, 36.1, 32.7, 25.8, 18.4, 18.0, 16.1, 14.2, -4.4, -4.7, -4.8, -5.0, -5.1 ppm.

HRMS (FAB, MNOBA matrix): for $C_{35}H_{67}O_7Si_3$ ($M+H$)⁺, Calcd: 683.4222, Found: 683.4195.

(1*R*,2*R*)-1-[(4*R*,6*S*)-6-[(2*R*,3*R*)-2,3-Bis-(*t*-butyl-dimethyl-silanyloxy)-butyl]-2-(4-methoxy-phenyl)-[1,3]-dioxan-4-yl]-1-(*t*-butyl-dimethyl-silanyloxy)-3,3-dimethyl-pent-4-en-2-ol **493**



To a solution of aldehyde **489** (1.7 g, 2.4 mmol) in THF (6.1 mL) and H₂O (6.1 mL) was added indium powder^a (560 mg, 4.9 mmol) in one portion. Then prenyl bromide^a (0.42 mL, 3.6 mmol) was added dropwise over 1 min. After 10 min the mixture was diluted with CH₂Cl₂ (10 mL), the organic layer was separated and aqueous layer was extracted with CH₂Cl₂ (5 x 5 mL). The combined organic layers were washed with brine (1 x 5 mL), dried over MgSO₄, filtered, and concentrated *in vacuo*. Purification of the residue by SiO₂ flash chromatography using hexanes/EtOAc (100:1) as eluent afforded β-hydroxy alkene **493** (1.1 g, 59%) as a colourless syrup.

$[\alpha]_D^{25}$: +26.3° (c 0.49, CH₂Cl₂).

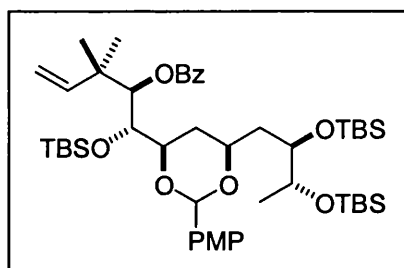
IR (neat film): 2956 (s), 2929 (s), 2858 (s), 1617 (w), 1518 (m), 1472 (m), 1389 (w), 1250 (s), 1098 (s), 1006 (m), 835 (s), 775 (s) cm⁻¹.

¹H NMR (500 MHz in CDCl₃): δ 7.35 (d, *J* = 8.7 Hz, 2H), 6.84 (d, *J* = 8.8 Hz, 2H), 5.83 (dd, *J* = 10.4, 18.0 Hz, 1H), 5.38 (s, 1H), 4.99 (m, 2H), 3.93 (d, *J* = 5.0 Hz, 1H), 3.90 (ddd, *J* = 1.4, 4.4, 10.3 Hz, 1H), 3.84-3.74 (overlapping m, 3H), 3.80 (s, 3H), 3.51 (d, *J* = 8.6 Hz, 1H), 3.07 (d, *J* = 8.6 Hz, 1H), 1.89 (m, 1H), 1.63-1.50 (complex m, 2H), 1.39 (m, 1H), 1.03 (d, *J* = 6.3 Hz, 3H), 1.00 (s, 3H), 0.98 (s, 3H), 0.88 (s, 9H), 0.87 (s, 9H), 0.83 (s, 9H), 0.09 (s, 3H), 0.06 (s, 3H), 0.02 (s, 3H), 0.00 (s, 3H), -0.01 (s, 3H), -0.03 (s, 3H) ppm.

^{13}C NMR (125 MHz in CDCl_3): δ 159.6, 145.3, 131.5, 127.5, 113.1, 112.3, 100.5, 78.7, 73.6, 72.9, 70.8, 70.4, 70.3, 55.2, 41.7, 36.3, 31.6, 26.0, 25.8, 24.3, 22.3, 18.3, 18.04, 17.99, 16.3, -3.2, -4.2, -4.6, -4.7, -4.76, -4.79 ppm.

HRMS (FAB, MNOBA matrix): for $\text{C}_{35}\text{H}_{67}\text{O}_7\text{Si}_3$ ($\text{M}+\text{H}$) $^+$, Calcd: 753.4969, Found: 753.4977.

Benzoic acid (*R*)-1-[(*S*)-[(4*R*,6*S*)-6-[(2*R*,3*R*)-2,3-bis-(*t*-butyl-dimethyl-silanyloxy)-butyl]-2-(4-methoxy-phenyl)-[1,3] dioxan-4-yl]-(*t*-butyl-dimethyl-silanyloxy)-methyl]-2,2-dimethyl-but-3-enyl ester **487**



To a stirred solution of β -hydroxy alkene **493** (1.5 g, 2.0 mmol) in dry CH_2Cl_2 (2.9 mL) and dry pyridine^a (3.4 mL) was added 4-dimethylaminopyridine^c (247 mg, 2.0 mmol) in one portion followed by dropwise addition of benzoyl chloride⁹ (2.3 mL, 20.2 mmol) over 1 min. A condenser was fitted and mixture heated to 80 °C for 72 h. The mixture was then allowed to cool to room temperature, diluted with CH_2Cl_2 (10 mL) and quenched by dropwise addition of saturated aq. NaHCO_3 solution (~5 mL) with vigorous stirring. After 15 min the organic layer was separated and aqueous layer was extracted with CH_2Cl_2 (5 x 10 mL). The combined organic layers were washed with brine (1 x 10 mL), dried over MgSO_4 , filtered, and concentrated *in vacuo*. Purification of the residue by SiO_2 flash chromatography using hexanes/EtOAc (100:1) as eluent afforded alkene **487** 1.5 g (86%) as a colourless oil.

$[\alpha]_D^{20}$: +21.0° (c 0.39, CH_2Cl_2).

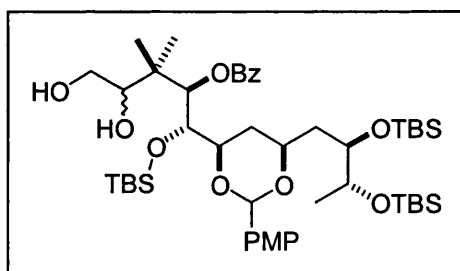
IR (neat film): 2956 (s), 2931 (s), 2888 (s), 2857 (s), 1720 (s), 1618 (m), 1518 (s), 1469 (s), 1385 (s), 1363 (m), 1339 (m), 1311 (m), 1250 (s), 1173 (s), 1100 (s), 1007 (s), 912 (m), 830 (s), 776 (s), 710 (s) cm^{-1} .

^1H NMR (500 MHz in CDCl_3): δ 8.11 (dd, J = 1.2, 8.3 Hz, 2H), 7.55 (t, J = 7.4 Hz, 1H), 7.44 (t, J = 7.7 Hz, 2H), 7.37 (d, J = 8.7 Hz, 2H), 6.84 (d, J = 8.8 Hz, 2H), 6.04 (dd, J = 10.8, 17.5 Hz, 1H), 5.32 (s, 1H), 5.08 (m, 2H), 5.05 (d, J = 1.5 Hz, 1H), 4.03 (dd, J = 1.9, 6.8 Hz, 1H), 3.89 (m, 1H), 3.84 (complex m, 2H), 3.80 (s, 3H), 3.77 (m, 1H), 1.81 (m, 2H), 1.43 (m, 2H), 1.16 (s, 3H), 1.14 (s, 3H), 1.05 (d, J = 6.3 Hz, 3H), 0.88 (s, 9H), 0.85 (s, 9H), 0.79 (s, 9H), 0.00 (s, 6H), -0.01 (s, 3H), -0.02 (s, 6H), -0.10 (s, 3H) ppm.

^{13}C NMR (125 MHz in CDCl_3): δ 166.0, 159.6, 145.0, 132.8, 131.5, 130.5, 129.9, 128.3, 128.0, 113.1, 112.7, 101.1, 79.4, 76.7, 73.5, 72.4, 70.3, 70.1, 55.1, 41.3, 36.2, 33.3, 26.1, 25.9, 25.8, 24.7, 23.9, 18.5, 18.1, 18.0, 16.3, -3.3, -4.3, -4.4, -4.6, -4.7, -4.8 ppm.

LRMS (FAB, MNOBA matrix): for $\text{C}_{47}\text{H}_{80}\text{O}_8\text{Si}_3$, $[\text{M}]^+$ 857.

Benzoic acid (*R*)-1-[(*S*)-[(4*R*,6*S*)-6-[(2*R*,3*R*)-2,3-bis-(*t*-butyl-dimethyl-silanyloxy)-butyl]-2-(4-methoxy-phenyl)-[1,3]dioxan-4-yl]-(*t*-butyl-dimethyl-silanyloxy)-methyl]-3,4-dihydroxy-2,2-dimethyl-butyl ester
494



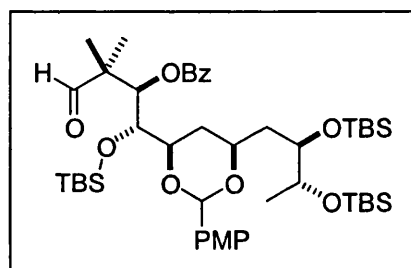
To a stirred solution of alkene **487** (1.2 g, 1.4 mmol) in acetone^b (4.2 mL) and H_2O (4.2 mL) was added osmium tetroxide^e (3.5 mL, 0.14 mmol of a 0.04 M solution in (1:1) acetone: H_2O) in one portion. Then 4-methylmorpholine-*N*-oxide^a (244 mg, 2.1 mmol) was added in one portion followed by addition of *t*-butanol^a (10 mL) in one portion. After 96 h the mixture was quenched by addition of sodium sulfite (25 g) with vigorous stirring. After 1.5 h the organic layer was separated and aqueous layer was extracted with EtOAc (9 x 20 mL). The combined organic layers were dried over MgSO_4 , filtered, and concentrated *in vacuo*. Purification of the residue by SiO_2 flash chromatography using hexanes/EtOAc (6:1) as eluent afforded 1,2-diol **494** (991 mg, 80%) as a white foam.

$[\alpha]_D$: +22.3° (c 0.965, CH₂Cl₂).

IR (neat film): 3424 (br), 2955 (s), 2931 (s), 2887 (s), 2857 (s), 1719 (s), 1617 (s), 1518 (s), 1470 (s), 1391 (s), 1249 (s), 1100 (s), 1007 (s), 910 (s), 829 (s), 777 (s), 734 (s) cm⁻¹.

LRMS (FAB, MNOBA matrix): for C₄₇H₈₂O₁₀Si₃, [M+Na-H⁺]⁺ 913.

Benzoic acid (R)-1-[(S)-[(4R,6S)-6-[(2R,3R)-2,3-bis-(*t*-butyl-dimethyl-silanyloxy)-butyl]-2-(4-methoxy-phenyl)-[1,3]dioxan-4-yl]-(*t*-butyl-dimethyl-silanyloxy)-methyl]-2,2-dimethyl-3-oxo-propyl ester 495

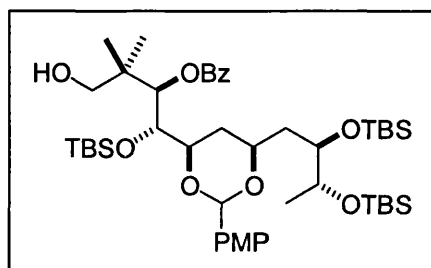


To a cooled (0 °C) solution of 1,2-diol **494** (1.2 g, 1.3 mmol) in dry THF (10 mL) was added lead tetraacetate^a (1.2 g, 2.6 mmol) in one portion. After 10 min the bright yellow solution was diluted with Et₂O (10 mL) followed by addition of solid NaHCO₃ (~1.2 g) then dropwise addition of saturated aq. NaHCO₃ solution (~5 mL). The organic layer was separated and aqueous layer was extracted with Et₂O (4 x 5 mL). The combined organic layers were dried over MgSO₄, filtered, and concentrated *in vacuo*. Purification of the residue by SiO₂ flash chromatography using hexanes/EtOAc (9:1) as eluent afforded aldehyde **495** (1.1 g, 94%) as a white crystalline solid.

IR (neat film): 3422 (br), 2955 (s), 2931 (s), 2888 (s), 2857 (s), 1721 (s), 1700 (s), 1601 (s), 1579 (m), 1512 (m), 1471 (s), 1386 (m), 1317 (m), 1264 (s), 1160 (s), 1106 (s), 1031 (s), 836 (s), 776 (s), 711 (s) cm⁻¹.

LRMS (FAB, MNOBA matrix): for C₄₆H₇₈O₉Si₃, [M]⁺ 861.

Benzoic acid (*R*)-1-[(*S*)-[(4*R*,6*S*)-6-[(2*R*,3*R*)-2,3-bis-(*t*-butyl-dimethyl-silanyloxy)-butyl]-2-(4-methoxy-phenyl)-[1,3]dioxan-4-yl]-(*t*-butyl-dimethyl-silanyloxy)-methyl]-3-hydroxy-2,2-dimethyl-propyl ester 496



To a cooled ($-10\text{ }^{\circ}\text{C}$) solution of aldehyde **495** (616 mg, 720 μmol) in MeOH^{a} (3.6 mL) was added sodium borohydride^c (136 mg, 3.6 mmol) in 3 equal portions to avoid excess foaming. After 15 min the mixture was quenched by dropwise addition of H_2O ($\sim 10\text{ mL}$), diluted with EtOAc (10 mL) and stirred vigorously for 10 min. The organic layer was separated and aqueous layer was extracted with EtOAc (5 x 15 mL). The combined organic layers were washed with brine (1 x 15 mL), dried over MgSO_4 , filtered, and concentrated *in vacuo*. Purification of the residue by SiO_2 flash chromatography using hexanes/ EtOAc (elution gradient 40:1, then 15:1) as eluent afforded alcohol **496** (601 mg, 97%) as a white foam.

$[\alpha]_{\text{D}}^{25} +15.1^{\circ}$ (c 0.425, CH_2Cl_2).

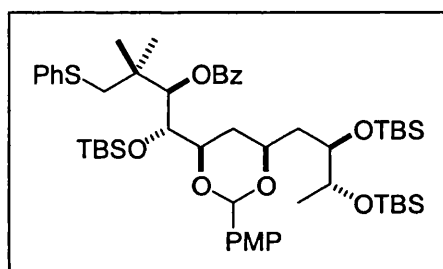
IR (neat film): 34712 (br), 2955 (s), 2888 (s), 2857 (s), 1720 (m), 1617 (w), 1518 (m), 1470 (m), 1389 (m), 1251 (s), 1100 (s), 1065 (s), 1008 (s), 832 (s), 776 (s), 711 (m) cm^{-1} .

^1H NMR (500 MHz in CDCl_3): δ 8.09 (dd, $J = 1.2, 8.3\text{ Hz}$, 2H), 7.58 (t, $J = 7.4\text{ Hz}$, 1H), 7.45 (t, $J = 7.8\text{ Hz}$, 2H), 7.33 (d, $J = 8.7\text{ Hz}$, 2H), 6.82 (d, $J = 8.8\text{ Hz}$, 2H), 5.31 (s, 1H), 5.17 (d, $J = 1.9\text{ Hz}$, 1H), 4.13 (dd, $J = 1.6, 6.9\text{ Hz}$, 1H), 3.89 (m, 1H), 3.83 (ddd, $J = 1.5, 4.4, 10.3\text{ Hz}$, 1H), 3.79 (s, 3H), 3.74 (complex m, 2H), 3.28 (q, $J = 11.9\text{ Hz}$, 2H), 1.78 (m, 1H), 1.69 (m, 1H), 1.45-1.33 (complex m, 2H), 1.10 (s, 3H), 1.00 (d, $J = 6.3\text{ Hz}$, 3H), 0.97 (s, 3H), 0.85 (s, 9H), 0.82 (s, 18H), 0.05 (s, 3H), -0.03 (s, 6H), -0.06 (s, 9H) ppm.

^{13}C NMR (125 MHz in CDCl_3): δ 166.6, 159.6, 133.1, 131.1, 129.9, 128.5, 128.0, 113.1, 101.4, 79.1, 75.1, 73.8, 72.4, 70.2, 70.1, 69.5, 55.2, 40.0, 36.2, 33.3, 26.0, 25.7, 21.7, 18.3, 18.0, 17.9, 16.3, -3.4, -4.2, -4.4, -4.6, -4.7, -4.8 ppm.

LRMS (FAB, MNOBA matrix): for $\text{C}_{46}\text{H}_{80}\text{O}_9\text{Si}_3$, $[\text{M}]^+$ 861.

Benzoic acid (*R*)-1-[(*S*)-[(4*R*,6*S*)-6-[(2*R*,3*R*)-2,3-bis-(*t*-butyl-dimethyl-silanyloxy)-butyl]-2-(4-methoxy-phenyl)-[1,3]dioxan-4-yl]-(*t*-butyl-dimethyl-silanyloxy)-methyl]-2,2-dimethyl-3-phenylsulfanyl-propyl ester **497**



To a stirred solution of alcohol **496** (839 mg, 997 μmol) in dry DMF^{a} (5.0 mL) was added phenyl disulfide^a (2.18 g, 10.0 mmol) in one portion followed by addition of tri-*n*-butylphosphine^c (2.5 mL, 10.0 mmol) in one portion. A condenser was fitted and mixture heated to 75 $^{\circ}\text{C}$. After 14 h the mixture was cooled to room temperature, diluted with Et_2O (10 mL) and quenched by dropwise addition of H_2O (~10 mL). The organic layer was separated and aqueous layer extracted with Et_2O (5 x 10 mL). The combined organic layers were washed with brine (1 x 15 mL), dried over MgSO_4 , filtered, and concentrated *in vacuo*. Purification of the residue by SiO_2 flash chromatography using hexanes/ EtOAc (elution gradient neat Hexanes then 20:1, then 9:1) as eluent afforded thiophenyl ether **497** (846 mg, 91%) as a white foam.

$[\alpha]_{\text{D}}^{25}$: +54.0 $^{\circ}$ (c 0.48, CH_2Cl_2).

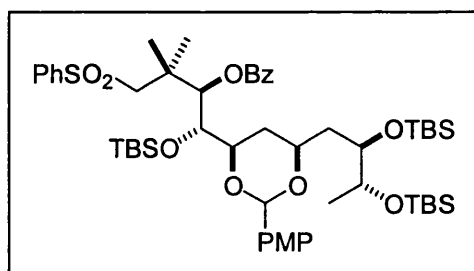
IR (neat film): 2955 (s), 2930 (s), 2889 (s), 2856 (s), 1720 (s), 1617 (w), 1584 (w), 1519 (w), 1470 (m), 1388 (w), 1251 (s), 1101 (s), 1066 (m), 1007 (m), 832 (s), 776 (s) cm^{-1} .

¹H NMR (500 MHz in CDCl₃): δ 8.07 (dd, *J* = 1.2, 8.2 Hz, 2H), 7.55 (t, *J* = 7.4 Hz, 1H), 7.43 (t, *J* = 7.8 Hz, 2H), 7.33 (d, *J* = 8.7 Hz, 2H), 7.30 (dd, *J* = 1.1, 8.3 Hz, 2H), 7.18 (t, *J* = 7.6 Hz, 2H), 7.10 (t, *J* = 7.3 Hz, 1H), 6.81 (d, *J* = 8.8 Hz, 2H), 5.27 (s, 1H), 5.14 (d, *J* = 1.5 Hz, 1H), 4.08 (dd, *J* = 1.3, 7.1 Hz, 1H), 3.87-3.78 (complex m, 3H), 3.79 (s, 3H), 3.73 (m, 1H), 3.10 (q, *J* = 12.6 Hz, 2H), 1.82 (m, 2H), 1.43 (m, 2H), 1.17 (s, 3H), 1.15 (s, 3H), 1.03 (d, *J* = 6.3 Hz, 3H), 0.84 (s, 9H), 0.83 (s, 9H), 0.75 (s, 9H), -0.02 (s, 3H), -0.04 (s, 3H), -0.05 (s, 3H), -0.06 (s, 6H), -0.13 (s, 3H) ppm.

¹³C NMR (125 MHz in CDCl₃): δ 165.9, 159.2, 137.7, 132.9, 131.4, 130.2, 129.9, 129.6, 129.1, 128.3, 128.2, 125.8, 113.0, 101.3, 79.5, 76.1, 73.9, 73.0, 70.3, 70.0, 55.2, 44.9, 39.8, 36.2, 33.5, 29.7, 25.9, 25.8, 24.2, 24.0, 18.5, 18.2, 18.0, 16.2, -3.2, -4.3, -4.4, -4.6, -4.7, -4.8 ppm.

LRMS (FAB, MNOBA matrix): for C₅₂H₈₄O₈Si₃S, [M+H]⁺ 953.

Benzoic acid (*R*)-3-benzenesulfonyl-1-[(*S*)-[(4*R*,6*S*)-6-[(2*R*,3*R*)-2,3-bis-(*t*-butyl-dimethyl-silanyloxy)-butyl]-2-(4-methoxy-phenyl)-[1,3]dioxan-4-yl]-(*t*-butyl-dimethyl-silanyloxy)-methyl]-2,2-dimethyl-propyl ester 498



To a stirred solution of thiophenyl ether **497** (846 mg, 906 μmol) in EtOAc^b (4.5 mL) was added sodium hydrogencarbonate^b (457 mg, 5.4 mmol) in one portion. Then 3-chloroperoxy-benzoic acid^a (543 mg, 2.3 mmol) was added in one portion. After 20 min the reaction mixture was diluted with Et₂O (10 mL) and quenched by dropwise addition of saturated aq. NaHCO₃ solution (~5 mL). The organic layer was then washed with saturated aq. NaHCO₃ solution (1 x 10 mL), brine (1 x 10 mL) and the combined aqueous layers were washed with Et₂O (5 x 5 mL). The combined organic layers were dried over MgSO₄, filtered,

and concentrated *in vacuo*. Purification of the residue by SiO₂ flash chromatography using hexanes/EtOAc (9:1) as eluent afforded phenyl sulfone **498** (778 mg, 89%) as a white foam.

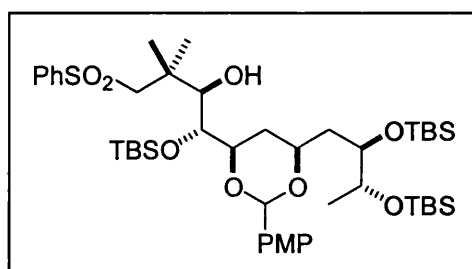
$[\alpha]_D^{20}$: +22.0° (c 0.92, CH₂Cl₂).

IR (neat film): 2955 (s), 2930 (s), 2887 (s), 2857 (s), 1722 (s), 1617 (s), 1518 (s), 1470 (s), 1392 (s), 1317 (s), 1257 (s), 1151 (s), 1104 (s), 1008 (s), 912 (s), 8289 (s), 777 (s), 733 (s), 687 (s) cm⁻¹.

¹H NMR (500 MHz in CDCl₃): δ 8.04 (dd, J = 1.2, 8.2 Hz, 2H), 7.78 (d, J = 7.6 Hz, 2H), 7.57 (m, 2H), 7.46 (m, 4H), 7.32 (d, J = 8.7 Hz, 2H), 6.82 (d, J = 8.8 Hz, 2H), 5.25 (s, 1H), 5.02 (d, J = 1.2 Hz, 1H), 4.06 (d, J = 6.3 Hz, 1H), 3.84 (ddd, J = 1.5, 4.4, 10.3 Hz, 1H), 3.79 (s, 3H), 3.75 (m, 3H), 3.37 (q, J = 14.3 Hz, 2H), 1.80 (m, 1H), 1.72 (m, 1H), 1.43 (s, 3H), 1.39 (s, 3H), 1.39 (overlapping m, 2H), 1.01 (d, J = 6.3 Hz, 3H), 0.83 (s, 9H), 0.82 (s, 9H), 0.61 (s, 9H), -0.03 (s, 3H), -0.06 (s, 6H), -0.07 (s, 3H), -0.12 (s, 3H), -0.15 (s, 3H) ppm.

¹³C NMR (125 MHz in CDCl₃): δ 165.7, 159.7, 141.9, 133.3, 133.2, 131.2, 129.9, 129.8, 129.1, 128.5, 128.1, 127.6, 113.1, 101.3, 77.7, 73.9, 72.3, 70.2, 70.0, 62.8, 55.2, 39.6, 36.1, 33.4, 25.8, 25.7, 24.7, 24.2, 18.3, 18.0, 17.9, 16.2, -3.3, -4.3, -4.4, -4.7, -4.8, -4.9 ppm.

(1*R*,2*R*)-4-Benzenesulfonyl-1-[(4*R*,6*S*)-6-[(2*R*,3*R*)-2,3-bis-(*t*-butyl-dimethyl-silanyloxy)-butyl]-2-(4-methoxy-phenyl)-[1,3]dioxan-4-yl]-1-(*t*-butyl-dimethyl-silanyloxy)-3,3-dimethyl-butan-2-ol **499**



To a cooled (-78 °C) solution of phenyl sulfone **498** (488 mg, 495 μ mol) in dry CH₂Cl₂ (5.0 mL) was added diisobutylaluminiumhydride^a (1.5 M solution PhMe, 0.73 mL, 1.1 mmol) dropwise over 2 min. After 10 min the mixture was quenched by dropwise addition of MeOH (~5 mL), diluted with CH₂Cl₂ (5.0 mL) and

warmed to 0 °C. The mixture was then vigorously stirred with 10% aq. sodium potassium tartrate^c solution (10 mL) for 0.5 h then warmed to room temperature and stirred for a further 0.5 h. The organic layer was separated and aqueous layer extracted with CH₂Cl₂ (9 x 10 mL). The combined organic layers were dried over MgSO₄, filtered, and concentrated *in vacuo*. Purification of the residue by SiO₂ flash chromatography using hexanes/EtOAc (30:1, then 20:1) as eluent afforded β-hydroxy sulfone **499** (422 mg, 97%) as a white crystalline solid.

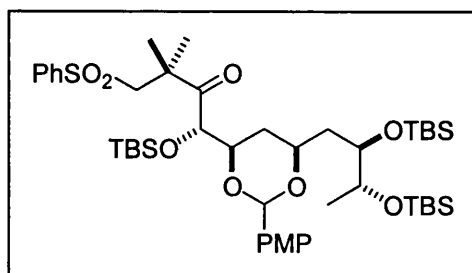
IR (neat film): 3509 (m), 2955 (s), 2931 (s), 2857 (s), 1617 (s), 1589 (w), 1518 (s), 1469 (s), 1392 (s), 1317 (s), 1252 (s), 1102 (s), 1006 (s), 838 (s), 777 (s), 733 (s), 687 (m) cm⁻¹.

¹H NMR (500 MHz in CDCl₃): δ 7.86 (dd, *J* = 1.2, 8.4 Hz, 2H), 7.56 (t, *J* = 7.5 Hz, 1H), 7.46 (t, *J* = 7.7 Hz, 1H), 7.33 (d, *J* = 8.7 Hz, 2H), 6.84 (d, *J* = 8.9 Hz, 2H), 5.38 (s, 1H), 3.98 (d, *J* = 5.1 Hz, 1H), 3.90 (ddd, *J* = 1.3, 4.4, 10.4 Hz, 1H), 3.84-3.76 (complex m, 3H), 3.79 (s, 3H), 3.47 (d, *J* = 7.5 Hz, 1H), 3.17 (q, *J* = 14.2 Hz, 2H), 3.14 (d, *J* = 8.0 Hz, 1H), 1.87 (m, 1H), 1.45 (m, 2H), 1.37 (m, 1H), 1.29 (s, 3H), 1.14 (s, 3H), 1.02 (d, *J* = 6.3 Hz, 3H), 0.87 (s, 9H), 0.83 (s, 9H), 0.81 (s, 9H), 0.08 (s, 3H), 0.06 (s, 3H), 0.02 (s, 3H), 0.01 (s, 3H), 0.00 (s, 3H), -0.02 (s, 3H) ppm.

¹³C NMR (125 MHz in CDCl₃): δ 159.6, 142.0, 133.2, 131.1, 129.1, 127.7, 127.3, 113.2, 100.4, 78.1, 77.2, 73.2, 72.7, 70.5, 70.3, 69.6, 63.4, 55.1, 39.7, 36.1, 31.2, 25.8, 25.6, 22.9, 22.0, 18.1, 18.0, 16.2, -3.2, -4.2, -4.6, -4.7, -4.8, -4.9 ppm.

HRMS (FAB, MNOBA matrix): for C₄₅H₈₀O₉Si₃SNa (M+Na)⁺, Calcd: 903.4748, Found: 903.4729.

(S)-4-Benzenesulfonyl-1-[(4*R*,6*S*)-6-[(2*R*,3*R*)-2,3-bis-(*t*-butyl-dimethyl-silanyloxy)-butyl]-2-(4-methoxy-phenyl)-[1,3]dioxan-4-yl]-1-(*t*-butyl-dimethyl-silanyloxy)-3,3-dimethyl-butan-2-one **486**



To a cooled ($-78\text{ }^{\circ}\text{C}$) solution of dry CH_2Cl_2 (6.0 mL) and DMSO^a (0.70 mL, 9.6 mmol) was added trifluoroacetic anhydride^a (1.35 mL, 9.6 mmol) dropwise over 3 min. After 75 min a solution of β -hydroxy sulfone **499** (422 mg, 429 μmol) in dry CH_2Cl_2 (4.0 mL) was added dropwise over 8 min. After 0.5 h dry Et_3N (3.4 mL, 23.9 mmol) was added dropwise over 4 min and the reaction mixture was warmed to $0\text{ }^{\circ}\text{C}$ when Et_2O (20 mL) and H_2O (10 mL) were added. The organic layer was separated and aqueous layer extracted with Et_2O (6 x 10 mL). The combined organic layers were dried over MgSO_4 , filtered, and concentrated *in vacuo*. Purification of the residue by SiO_2 flash chromatography using hexanes/ EtOAc (10:1) as eluent afforded β -keto sulfone **486** (406 mg, 96%) as a white foam.

$[\alpha]_D^{25}$: $+38.3^{\circ}$ (c 0.815, CH_2Cl_2).

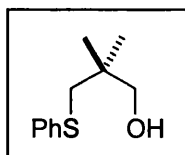
IR (neat film): 2955 (s), 2931 (s), 2888 (s), 2857 (s), 1717 (m), 1617 (m), 1518 (m), 1469 (m), 1390 (m), 1361 (m), 1315 (m), 1253 (s), 1150 (s), 1104 (s), 1005 (s), 836 (s), 777 (s), 734 (m), 687 (w) cm^{-1} .

^1H NMR (500 MHz in CDCl_3): δ 7.81 (d, $J = 7.2\text{ Hz}$, 2H), 7.59 (t, $J = 7.4\text{ Hz}$, 1H), 7.50 (t, $J = 7.7\text{ Hz}$, 2H), 7.33 (d, $J = 8.7\text{ Hz}$, 2H), 6.82 (d, $J = 8.8\text{ Hz}$, 2H), 5.35 (s, 1H), 4.75 (d, $J = 6.2\text{ Hz}$, 1H), 4.10 (ddd, $J = 2.3, 6.2, 11.3\text{ Hz}$, 1H), 3.85 (complex m, 2H), 3.80 (s, 3H), 3.74 (m, 1H), 3.44 (q, $J = 14.1\text{ Hz}$, 2H), 1.82 (m, 1H), 1.56 (s, 3H), 1.53 (m, 1H), 1.45 (s, 3H), 1.42 (m, 2H), 1.01 (d, $J = 6.3\text{ Hz}$, 3H), 0.85 (s, 9H), 0.83 (s, 9H), 0.82 (s, 9H), 0.04 (s, 3H), 0.00 (s, 3H), -0.02 (s, 3H), -0.03 (s, 3H), -0.04 (s, 3H) ppm.

^{13}C NMR (125 MHz in CDCl_3): δ 209.7, 159.8, 141.7, 133.4, 131.1, 129.2, 127.8, 127.5, 113.2, 101.1, 78.7, 76.1, 72.5, 70.3, 70.0, 64.0, 55.2, 47.2, 36.1, 32.7, 26.0, 25.8, 24.3, 24.2, 18.4, 18.0, 16.2, -4.1, -4.3, -4.4, -4.5, -4.6, -4.7 ppm.

HRMS (FAB, MNOBA matrix): for $C_{45}H_{78}O_9Si_3SNa$ ($M+Na$)⁺, Calcd: 901.4585, Found: 901.4572.

2,2-Dimethyl-3-phenylsulfanyl-propan-1-ol 509

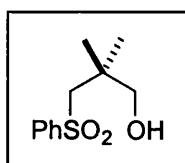


To a stirred solution of 2,2-dimethyl-1,3-propane diol^g **11** (13.0 g, 125 mmol) and phenyl disulfide^a (30.0 g, 137 mmol) in dry DMF^a (625 mL) was added tri-*n*-butylphosphine^c (40.1 mL, 150 mmol) dropwise over 8 min and the mixture was stirred vigorously for 14 d. The reaction mixture was then cooled to 0 °C and quenched by addition of H₂O (500 mL). The organic layer was separated and aqueous layer extracted with EtOAc (7 x 250 mL). The combined organic layers were washed with brine (2 x 100 mL), dried over Na₂SO₄, filtered and concentrated *in vacuo*. Purification of the residue by SiO₂ flash chromatography using hexanes/EtOAc (elution gradient neat hexanes, then 10:1, then 5:1) as eluent afforded thioether **509** (15.4 g, 63%) as a light orange free-flowing oil.

Data agreed with those previously reported⁴⁷ⁱⁱ.

Literature yield: 85% (for a 2-step procedure).

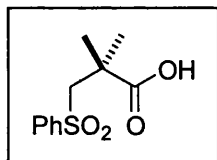
3-Benzenesulfonyl-2,2-dimethyl-propan-1-ol 510



To a stirred solution of thioether **509** (15.4 g, 78.2 mmol) in dry CH₂Cl₂ (390 mL) was added sodium bicarbonate^b (32.9 g, 391 mmol) in one portion with vigorous stirring. After 15 min the mixture was cooled to 0 °C when 4-chloroperoxybenzoic acid^a (52.5 g, 219 mmol) was added in 6 equal portions with vigorous stirring, and after 1 h the mixture was allowed to warm to 0 °C. After 5 d the mixture was quenched

by pouring into a solution of aq. $\text{Na}_2\text{S}_2\text{O}_3$ (200 mL) with vigorous stirring for 2 h. Then EtOAc (2 L) was added, the organic layer was separated and aqueous layer extracted with CH_2Cl_2 (7 x 250 mL). The combined organic layers were dried over Na_2SO_4 , filtered, and concentrated *in vacuo*. Purification of the residue by SiO_2 flash chromatography using hexanes/EtOAc (elution gradient 10:1, then 4:1) as eluent afforded sulfone **510** (16.0 g, 90%) as a light orange viscous oil.

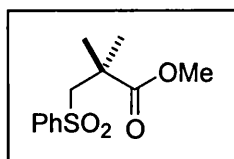
3-Benzenesulfonyl-2,2-dimethyl-propionic acid **508**



To a cooled (0 °C) solution of sulfone **510** (8.4 g, 36.6 mmol) in MeCN (100 mL), CCl_4^a (100 mL) and H_2O (150 mL) was added sodium-*meta*-periodate^c (8.6 g, 40.3 mmol) and ruthenium trichloride^c (760 mg, 3.7 mmol) in one portion each sequentially. After 1 h the mixture was allowed to warm to room temperature, and after a further 12 h, sodium-*meta*-periodate^c (3.9 g, 20.2 mmol) was added in one portion. After 24 h the mixture was quenched by diluting with H_2O (200 mL) and extracted with CH_2Cl_2 (6 x 250 mL). The combined organic layers were dried over Na_2SO_4 , filtered, and concentrated *in vacuo*. Purification of the residue by SiO_2 flash chromatography using hexanes/EtOAc (elution gradient 2:1, then 1:1, then 1:2) as eluent afforded acid **508** (7.5 g, 85%) as a white solid.

Data agreed with those previously reported¹³⁶.

3-Benzenesulfonyl-2,2-dimethyl-propionic acid methyl ester **511**

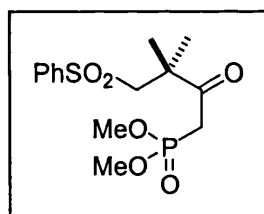


To a stirred solution of acid **508** (13.1 g, 54.3 mmol) in dry DMF^a (185 mL) was added potassium carbonate^b (37.4 g, 271 mmol) in one portion. After 5 min of vigorous stirring, methyl iodide^a (33.7 mL, 542 mmol) was added dropwise over 5 min. After 12 h the reaction was diluted with H₂O (350 mL), the organic layer was separated and aqueous layer extracted with EtOAc (5 x 200 mL). The combined organic layers were dried over Na₂SO₄, filtered, and concentrated *in vacuo*. Purification of the residue by SiO₂ flash chromatography using hexanes/EtOAc (elution gradient neat hexanes, then 2:1) as eluent afforded methyl ester **511** (13.2 g, 95%) as a viscous light yellow oil.

Data agreed with those previously reported by ³.

Literature yield: 83% (for a 2-step procedure).

(4-Benzenesulfonyl-3,3-dimethyl-2-oxo-butyl)-phosphonic acid dimethyl ester 507



To a cooled (-78 °C) of dimethyl methylphosphonate^a (4.6 mL, 42.3 mmol) in dry THF (40 mL) was added *n*-butyl lithium^a (1.6 M in hexanes, 26.5 mL, 42.3 mmol) via a dropping funnel over 40 min. After 50 min, a solution of methyl ester **511** (4.3 g, 16.9 mmol) in dry THF (19 mL) was added to the mixture via a dropping funnel over 40 min. After 3.5 h the mixture was quenched by dropwise addition of saturated aq. NH₄Cl (~50 mL), and warmed to room temperature. The organic layer was separated and aqueous layer extracted with EtOAc (4 x 25 mL). The combined organic layers were washed with brine (1 x 20 mL), dried over MgSO₄, filtered, and concentrated *in vacuo*. Purification of the residue by SiO₂ flash chromatography using hexanes/EtOAc (elution gradient 5:1, then 1:1) as eluent afforded phosphonate **507** (4.9 g, 83%) as a viscous light yellow oil.

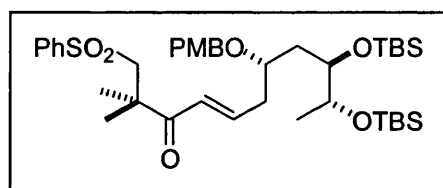
IR (neat film): 3424 (br), 2959 (m), 1709 (m), 1641 (w), 1448 (m), 1307 (m), 1248 (m), 1150 (m), 1032 (s) cm⁻¹.

^1H NMR (500 MHz in CDCl_3): δ 7.76 (d, J = 7.2 Hz, 2H), 7.54 (t, J = 7.5 Hz, 1H), 7.45 (t, J = 7.7 Hz, 2H), 3.71 (s, 3H), 3.69 (s, 3H), 3.39 (s, 2H), 3.28 (d, J = 21.6 Hz, 2H), 1.37 (s, 6H) ppm.

^{13}C NMR (125 MHz in CDCl_3): δ 204.9, 140.8, 133.5, 129.2, 127.4, 65.1, 52.9, 49.4, 47.4, 36.7, 35.3, 24.8 ppm.

HRMS (FAB, MNOBA matrix): for $\text{C}_{14}\text{H}_{22}\text{O}_6\text{SP}$ ($\text{M}+\text{H}$) $^+$, Calcd: 349.0869, Found: 349.0875.

(*E*)-(7*S*,9*R*,10*R*)-1-Benzenesulfonyl-9,10-bis-(*t*-butyl-dimethyl-silanyloxy)-7-(4-methoxy-benzyloxy)-2,2-dimethyl-undec-4-en-3-one 506



To a stirred solution of phosphonate **507** (5.8 g, 16.5 mmol) in dry MeCN (45 mL) and lithium chloride^d (1.22 g, 28.7 mmol) was added diisopropylethylamine^a (12.5 mL, 71.8 mmol) dropwise over 5 min. After a further 5 min, a solution of crude aldehyde **462** (assumed 100% yield, 7.34 g, 14.4 mmol) in dry MeCN (45 mL) was added dropwise over 5 min. After 48 h the mixture was cooled to 0 °C, diluted with EtOAc (200 mL) and quenched by dropwise addition of 10% aq. HCl (~200 mL) until the pH reached 7. The organic layer was separated and aqueous layer extracted with EtOAc (5 x 50 mL). The combined organic layers were washed with brine (1 x 100 mL), dried over MgSO_4 , filtered, and concentrated *in vacuo*. Purification of the residue by SiO_2 flash chromatography using hexanes/EtOAc (elution gradient 9:1, then 5:1) as eluent afforded enone **506** (8.6 g, 82%, 2 steps based on alcohol **461**) as a viscous light orange oil.

$[\alpha]_D^{20}$: +13.2° (c 0.635, CH_2Cl_2).

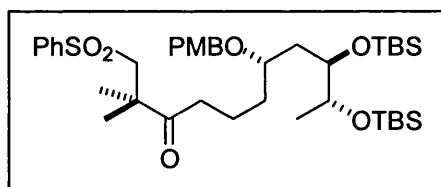
IR (neat film): 2931 (s), 2857 (s), 1693 (m), 1621 (m), 1513 (m), 1469 (m), 1388 (w), 1317 (m), 1250 (s), 1152 (s), 1039 (s), 934 (s), 775 (s) cm^{-1} .

¹H NMR (500 MHz in CDCl₃): δ 7.88 (d, *J* = 7.6 Hz, 2H), 7.59 (t, *J* = 7.4 Hz, 1H), 7.51 (t, *J* = 7.5 Hz, 2H), 7.21 (d, *J* = 8.5 Hz, 2H), 7.00 (dt, *J* = 7.4, 15.2 Hz, 1H), 6.82 (d, *J* = 8.5 Hz, 2H), 6.55 (d, *J* = 15.3 Hz, 1H), 4.43 (q, *J* = 11.0 Hz, 2H), 3.83 – 3.71 (complex multiplet, 3H), 3.76 (s, 3H), 3.45 (s, 2H), 2.51 (t, *J* = 6.4 Hz, 2H), 1.93 (dd, *J* = 8.8, 14.1 Hz, 1H), 1.42 (s, 3H), 1.41 (s, 3H), 1.37 (multiplet, 1H), 1.02 (d, *J* = 6.2 Hz, 3H), 0.85 (s, 9H), 0.84 (s, 9H), 0.02 (s, 3H), 0.01 (s, 6H), 0.00 (s, 3H) ppm.

¹³C NMR (125 MHz in CDCl₃): δ 200.2, 158.9, 146.0, 141.4, 133.4, 130.8, 129.2, 128.9, 128.7, 127.6, 124.8, 113.8, 113.6, 74.9, 70.4, 69.7, 63.7, 55.2, 45.8, 37.9, 35.1, 25.9, 25.7, 24.5, 24.4, 17.9, 16.1, -4.4, -4.6, -4.7, -4.8 ppm.

HRMS (FAB, MNOBA matrix): for C₃₉H₆₄O₇Si₂SNa (M+Na)⁺, Calcd: 755.3827, Found: 755.3809.

(7*S*,9*R*,10*R*)-1-Benzenesulfonyl-9,10-bis-(*t*-butyl-dimethyl-silanyloxy)-7-(4-methoxy-benzyloxy)-2,2-dimethyl-undecan-3-one 512



To a stirred solution of enone **506** (8.0 g, 10.9 mmol) in EtOAc^b (110 mL) was added palladium hydroxide^a (20% on carbon) (1.5 g, 2.2 mmol) in one portion, then the reaction flask was evacuated and filled with a hydrogen atmosphere. After 1.5 h the mixture was filtered to remove the carbon particulates, with subsequent MeOH washes, and the residue was concentrated *in vacuo*. Purification of the residue by SiO₂ flash chromatography using hexanes/EtOAc (elution gradient 9:1, then 7:1, then 5:1) as eluent afforded ketone **512** (7.6 g, 94%) as a viscous colourless oil.

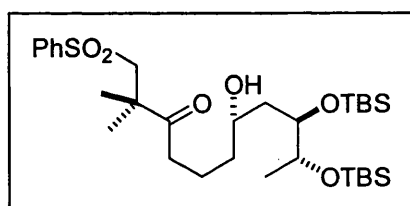
IR (neat film): 2855 (s), 2857 (s), 1709 (m), 1613 (w), 1513 (m), 1469 (m), 1387 (w), 1315 (m), 1250 (s), 1152 (s), 1088 (s), 983 (s), 775 (s), cm⁻¹.

¹H NMR (500 MHz in CDCl₃): δ 7.87 (d, *J* = 7.2 Hz, 2H), 7.60 (t, *J* = 7.4 Hz, 1H), 7.52 (t, *J* = 7.6 Hz, 2H), 7.25 (d, *J* = 8.6 Hz, 2H), 6.83 (d, *J* = 8.7 Hz, 2H), 4.40 (q, *J* = 11.1 Hz, 2H), 3.83 (m, 1H), 3.78 (m, 1H), 3.77 (s, 3H overlapping multiplet), 3.59 (m, 1H), 3.47 (s, 2H), 2.60 (t, *J* = 6.9 Hz, 2H), 1.91 (dd, *J* = 9.1, 14.1 Hz, 1H), 1.68 – 1.53 (m, 4H), 1.39 (m, 1H), 1.373 (s, 3H), 1.366 (s, 3H), 1.04 (d, *J* = 6.2 Hz, 3H), 0.86 (s, 9H), 0.85 (s, 9H), 0.02 (s, 3H), 0.010 (s, 6H), 0.008 (s, 3H) ppm.

¹³C NMR (125 MHz in CDCl₃): δ 212.3, 158.7, 141.3, 133.5, 131.5, 129.2, 128.7, 127.6, 113.7, 113.5, 75.6, 72.1, 70.5, 68.9, 64.6, 55.2, 46.5, 37.2, 34.6, 33.4, 25.8, 24.9, 19.1, 18.0, 16.3, -4.4, -4.6, -4.7, -4.8 ppm.

HRMS (FAB, MNOBA matrix): for C₃₉H₆₆O₇Si₂SNa (M+Na)⁺, Calcd: 757.3991, Found: 757.3966.

(7*S*,9*R*,10*R*)-1-Benzenesulfonyl-9,10-bis-(*t*-butyl-dimethyl-silanyloxy)-7-hydroxy-2,2-dimethyl-undecan-3-one 513



To a cooled (0 °C) solution of ketone **512** (270 mg, 367 μmol) in CH₂Cl₂ (4.9 mL) and H₂O (270 μL) was added 2,3-dichloro-5,6-dicyanobenzoquinone^a (125 mg, 551 μmol) in one portion turning mixture green. After 0.5 h the now orange mixture was quenched by dropwise addition of saturated aq. NaHCO₃ (~30 mL) and filtered through CELITETM with subsequent CH₂Cl₂ washes. The organic layer was separated and aqueous layer extracted with CH₂Cl₂ (3 x 15 mL). The combined organic layers were washed with brine (1 x 15 mL), dried over MgSO₄, filtered, and concentrated *in vacuo*. Purification of the residue by SiO₂ flash chromatography using hexanes/EtOAc (elution gradient 10:1, then 5:1) as eluent afforded δ-hydroxy ketone **513** (224 mg, 99%) as a viscous colourless oil.

[α]_D: +18.9° (c 1.25, CH₂Cl₂).

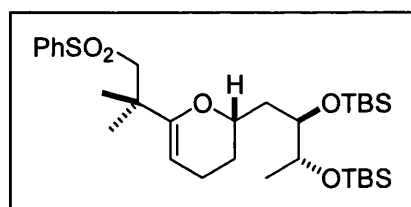
IR (neat film): 3538 (m), 3460 (m), 2954 (s), 2857 (s), 1708 (s), 1472 (s), 1390 (m), 1308 (s), 1255 (s), 1155 (s), 1095 (s), 908 (s), 779 (s) cm^{-1} .

^1H NMR (500 MHz in C_6D_6): δ 7.83 (d, J = 6.6 Hz, 2H), 6.93 (m, 3H), 4.07 (dt, J = 4.4, 8.6 Hz, 1H), 3.97 (m, 1H), 3.85 (m, 1H), 3.15 (s, 3H), 2.50 (d, J = 4.2 Hz, 1H), 2.41 (m, 2H), 1.94–1.78 (complex m, 3H), 1.63 (ddd, J = 1.8, 7.7, 14.2 Hz, 1H), 1.47 (m, 1H), 1.25 (d, J = 6.3 Hz, 3H), 1.11 (s, 6H), 0.98 (s, 9H), 0.97 (s, 9H), 0.16 (s, 3H), 0.126 (s, 3H), 0.117 (s, 3H), 0.07 (s, 3H) ppm.

^{13}C NMR (125 MHz in C_6D_6): δ 211.7, 142.4, 133.0, 129.0, 128.5, 127.5, 73.4, 71.6, 68.4, 65.0, 46.5, 39.3, 37.9, 37.0, 26.0, 25.9, 25.0, 24.9, 20.1, 18.2, 16.7, -4.1, -4.3, -4.6, -4.8 ppm.

HRMS (FAB, MNOBA matrix): for $\text{C}_{31}\text{H}_{58}\text{O}_6\text{Si}_2\text{SNa}$ ($\text{M}+\text{Na}$) $^+$, Calcd: 637.3369, Found: 637.3390.

(S)-6-(2-Benzenesulfonyl-1,1-dimethyl-ethyl)-2-[(2R,3R)-2,3-bis-(*t*-butyl-dimethyl-silanyloxy)-butyl]-3,4-dihydro-2H-pyran 505



To a solution of δ -hydroxy ketone **513** (2.3 g, 3.7 mmol) in C_6H_6 (125 mL) was added camphorsulfonic acid^a (43 mg, 184 μmol) in one portion when Dean-Stark apparatus was fitted and mixture was heated to 85 $^\circ\text{C}$. After 45 min the mixture was allowed to cool to room temperature then quenched by dropwise addition of pyridine (~ 0.5 mL) and the crude mixture was concentrated *in vacuo*. Purification of the residue by SiO_2 flash chromatography using hexanes/EtOAc (10:1) as eluent afforded glycal **505** (1.97 g, 90%) as a white solid.

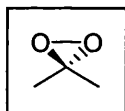
IR (neat film): 2954 (s), 2940 (s), 2856 (s), 1670 (m), 1470 (m), 1382 (m), 1314 (m), 1254 (m), 1134 (m), 1058 (s), 1008 (m), 833 (s), 776 (s) cm^{-1}

¹H NMR (500 MHz in C₆D₆): δ 7.84 (d, *J* = 7.9 Hz, 2H), 6.99 (m, 3H), 4.43 (dd, *J* = 2.5, 4.7 Hz, 1H), 3.96 (m, 1H), 3.86 (m, 2H), 3.27 (q, 14.1 Hz, 2H), 1.93 (m, 1H), 1.80 (m, 1H), 1.62 (m, 1H), 1.47 (s, 3H), 1.38 (s, 3H), 1.33 (m, 2H), 1.14 (d, *J* = 6.3 Hz, 3H), 1.00 (m, 1H), 0.95 (s, 9H), 0.91 (s, 9H), 0.09 (s, 3H), 0.07 (s, 3H), 0.04 (s, 3H), 0.02 (s, 3H) ppm.

¹³C NMR (125 MHz in C₆D₆): δ 157.1, 142.9, 132.8, 128.8, 127.9, 94.2, 72.2, 71.9, 70.8, 64.2, 38.9, 36.1, 28.1, 26.7, 26.0, 25.5, 20.6, 18.2, 16.4, -4.1, -4.4, -4.5 ppm

HRMS (FAB, MNOBA matrix): for C₃₁H₅₆O₅Si₂SNa (M+Na)⁺, Calcd: 619.3273, Found: 619.3285.

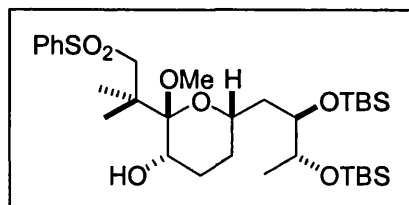
Preparation of dimethyldioxirane



To a cooled solution (0 °C) of H₂O (191 mL, 10.6 mol) and acetone^b (144 mL, 1.96 mol) was added sodium hydrogen carbonate^b (43.5 g, 0.52 mol) with vigorous stirring. Then Oxone^{TM a} (90 g, 0.15 mol) was added in 5 equal portions in 3-4 minute intervals. The mixture was then allowed to warm to room temperature and the apparatus placed under reduced pressure. The DMDO solution was then collected at -78 °C using a cold finger. When no more solution was removed the mixture was dried over K₂CO₃, filtered into a cooled (0°C) flask and stored at -33 °C as a pale yellow solution, smelling of bleach.

Typical yields 120-130 mL ¹²⁶.

(2S,3S,6S)-2-(2-Benzenesulfonyl-1,1-dimethyl-ethyl)-6-[(2R,3R)-2,3-bis-(*t*-butyl-dimethyl-silanyloxy)-butyl]-2-methoxy-tetrahydro-pyran-3-ol 516



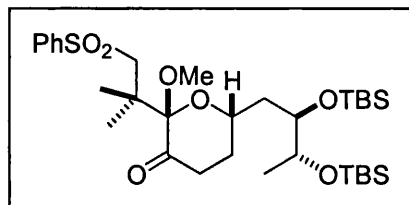
To a cooled (0 °C) solution of glycal **505** (1.47 g, 2.5 mmol) in MeOH^a (120 mL) was added flame activated 4Å molecular sieves^g (20 g). Then freshly distilled DMDO (~0.07 M in acetone, 45.8 mL, 3.2 mmol) was added dropwise over 5 min. After 10 min, pyridinium-*p*-toluenesulfonate^c (124 mg, 493 μmol) was added in one portion and mixture was allowed to warm to room temperature. After 15 min the mixture was quenched by the dropwise addition of saturated aq. NaHCO₃ (~50 mL) then diluted with EtOAc (50 mL) and H₂O (200 mL). The organic layer was separated and aqueous layer extracted with EtOAc (3 x 50 mL). The combined organic layers were washed with brine (1 x 50 mL), dried over Na₂SO₄, filtered, and concentrated *in vacuo*. Rapid purification of the residue by SiO₂ flash chromatography using hexanes/EtOAc (elution gradient 6:1, then 4:1) as eluent afforded alcohol **516** (1.46 g, 92%) as a white foam.

IR (neat film): 3492 (br), 2955 (s), 2657 (s), 1472 (m), 1389 (m), 1305 (m), 1257 (m), 1148 (s), 1097 (s), 836 (s), 775 (m) cm⁻¹.

¹H NMR (500 MHz in C₆D₆): δ 7.94 (dd, *J* = 1.9, 7.7 Hz, 2H), 6.91 (m, 3H), 4.07 (d, *J* = 14.4 Hz, 1H), 3.93 (m, 2H), 3.62 (m, 1H), 3.55 (dt, *J* = 5.2, 11.1 Hz, 1H), 3.45 (d, *J* = 14.4 Hz, 1H), 3.32 (s, 3H), 1.98 (ddd, *J* = 2.6, 8.2, 14.1 Hz, 1H), 1.84 (s, 3H), 1.61 (s, 3H), 1.50–1.35 (complex multiplet, 5H), 1.14 (d, *J* = 6.0 Hz, 3H), 0.97 (m, 1H), 0.97 (s, 9H), 0.95 (s, 9H), 0.09 (s, 6H), 0.07 (s, 3H), 0.06 (s, 3H) ppm.

¹³C NMR (125 MHz in C₆D₆): δ 143.8, 132.6, 129.1, 128.5, 100.7, 73.0, 70.8, 68.8, 63.9, 51.3, 44.7, 37.7, 31.7, 29.9, 26.05, 25.97, 25.8, 23.2, 18.3, 18.2, 16.3, -3.5, -4.4, -4.6, -4.7 ppm

(2*S*,6*S*)-2-(2-Benzenesulfonyl-1,1-dimethyl-ethyl)-6-[(2*R*,3*R*)-2,3-bis-(*t*-butyl-dimethyl-silanyloxy)-butyl]-2-methoxy-dihydro-pyran-3-one **503**



To a solution of alcohol **516** (338 mg, 524 μmol) in dry DMF^a (5.2 mL) was added pyridinium dichromate^a (394 mg, 1.05 mmol) in one portion. After 14 h the mixture was diluted with H_2O (5 mL), the organic layer was separated and aqueous layer extracted with EtOAc (3 x 10 mL). The combined organic layers were dried over Na_2SO_4 , filtered, and concentrated *in vacuo*. Purification of the residue by SiO_2 flash chromatography using hexanes/ EtOAc (15:1) as eluent afforded ketone **503** (216 mg, 64%) as a light yellow oil.

$[\alpha]_D^{25}$: +3.1° (c 0.8, CH_2Cl_2).

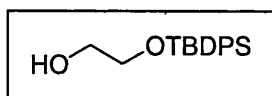
IR (neat film): 2955 (s), 2657 (s), 1724 (s), 1470 (m), 1388 (w), 1327 (m), 1256 (m), 1411 (s), 1008 (m), 996 (s), 776 (s) cm^{-1} .

^1H NMR (500 MHz in CDCl_3): δ 7.89 (d, J = 7.2 Hz, 2H), 7.59 (t, J = 7.2 Hz, 1H), 7.51 (t, J = 7.4 Hz, 2H), 4.13 (m, 1H), 3.77 (m, 2H), 3.55 (d, J = 14.4 Hz, 1H), 3.30 (s, 3H), 3.27 (d, J = 14.5 Hz, 1H), 2.46 (m, 2H), 2.03–1.87 (complex multiplet, 3H), 1.42 (s, 3H), 1.39 (m, 1H), 1.33 (s, 3H), 1.03 (d, J = 6.1 Hz, 3H), 0.85 (s, 9H), 0.84 (s, 9H), 0.02 (s, 6H), 0.00 (s, 6H) ppm.

^{13}C NMR (125 MHz in CDCl_3): δ 207.4, 142.4, 133.1, 129.4, 129.1, 127.5, 102.9, 71.8, 70.3, 69.4, 61.2, 53.2, 43.9, 37.9, 36.8, 30.2, 25.8, 25.7, 21.7, 21.5, 17.99, 17.96, 16.0, -4.0, -4.5, -4.76, -4.84 ppm.

HRMS (FAB, MNOBA matrix): for $\text{C}_{32}\text{H}_{58}\text{O}_7\text{Si}_2\text{SNa}$ ($\text{M}+\text{Na}$)⁺, Calcd: 665.3363, Found: 665.3340.

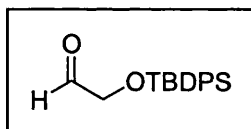
2-(*t*-Butyl-diphenyl-silanyloxy)-ethanol 520



To a cooled (0 °C) solution of dry THF (155 mL) and sodium hydride^c (60% dispersion in mineral oil, 741 mg, 18.5 mmol) was added ethylene glycol^b **519** (900 µL, 16.1 mmol) dropwise over 5 min and the mixture was allowed to warm to room temperature over 45 min. Then *t*-butyl-diphenylchlorosilane^c (4.8 mL, 18.5 mmol) was added dropwise over 1 min. After 2 h the mixture was quenched by the dropwise addition of saturated aq. NH₄Cl (~20 mL), the organic layer was separated and the aqueous layer was extracted with Et₂O (3 x 15 mL). The combined organic layers were dried over MgSO₄, filtered, and concentrated *in vacuo*. Purification using Kugelrohr distillation afforded alcohol **520** as a colourless viscous oil.

Data agreed with those previously reported by Marshall ¹²⁷.

(*t*-Butyl-diphenyl-silanyloxy)-acetaldehyde 504

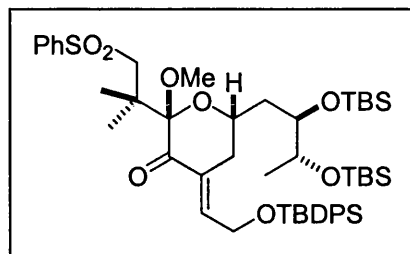


To a cooled (-78 °C) solution of dry CH₂Cl₂ (61 mL) and oxalyl chloride^a (1.6 mL, 17.7 mmol) was added DMSO^a (2.5 mL, 35.4 mmol) over 2 min. After 5 min a solution of alcohol **520** (assumed 100%, 4.84 g, 16.1 mmol) in CH₂Cl₂ (10 mL) was added dropwise over 6 min. After a further 15 min, Et₃N (11.0 mL, 79 mmol) was added dropwise over 4 min and the reaction was allowed to warm to room temperature. The solvent was removed *in vacuo* and then triturated with a solution of 4:1 hexanes/EtOAc (3 x 250 mL). The combined organic washings were filtered through a plug of SiO₂ then concentrated *in vacuo*. Purification using Kugelrohr distillation afforded aldehyde **504** (3.93 g, 82%, 2 steps) as a colourless free-flowing oil.

Data agreed with those previously reported by Marshall ¹²⁷.

Literature yield: 84% (for 2 steps)

(2S,6S)-2-(2-Benzenesulfonyl-1,1-dimethyl-ethyl)-6-[(2R,3R)-2,3-bis-(*t*-butyl-dimethyl-silanyloxy)-butyl]-4-[2-(*t*-butyl-methyl-phenyl-silanyloxy)-eth-(*E*)-ylidene]-2-methoxy-dihydro-pyran-3-one 502



To a cooled (-78 °C) solution of ketone **503** (495 mg, 770 μ mol) in dry THF (38 mL) was added *n*-butyllithium^a (2.5 M in hexanes, 0.46 mL, 1.12 mmol) dropwise over 2 min turning the reaction bright yellow. After 5 min a pre-cooled (-78 °C) solution of aldehyde **504** (1.15 g, 3.85 mmol) in dry THF (12 mL) was added to the mixture via a cannula over 1 min. After 5 min the flask was warmed to room temperature and after a further 20 min the mixture was re-cooled to 0 °C and quenched by the dropwise addition of saturated aq. NH₄Cl solution (~10 mL) and diluted with H₂O (10 mL) and EtOAc (10 mL) with vigorous stirring. After 5 min, the organic layer was separated and aqueous layer was extracted with EtOAc (1 x 20 mL). The combined organic layers were washed with brine (1 x 20 mL), dried over Na₂SO₄, filtered, and concentrated *in vacuo*. Purification of the residue by SiO₂ flash chromatography using hexanes/EtOAc (elution gradient 20:1, then 10:1, then 5:1) as eluent afforded enone **502** (547 mg, 77%) as a colourless oil.

[α]_D: -18.9° (c 0.38, CH₂Cl₂).

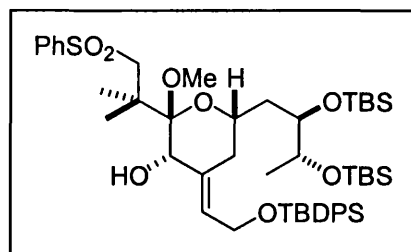
IR (neat film): 3074 (w), 2955 (s), 2930 (s), 2857 (s), 1698 (w), 1619 (w), 1472 (m), 1428 (m), 1306 (w), 1258 (w), 1147 (m), 1112 (s), 823 (m), 701 (s) cm⁻¹

¹H NMR (500 MHz in C₆D₆): δ 7.85 (d, *J* = 8.2 Hz, 2H), 7.71 (m, 4H), 7.22 (m, 6H), 7.11 (m, 1H), 6.86 (m, 3H), 4.13 (dd, *J* = 4.7, 14.3 Hz, 2H), 4.08 (m, 1H), 3.99 (m, 1H), 3.93 (m, 2H), 3.69 (d, *J* = 14.4 Hz, 1H), 3.21 (s, 3H), 2.02–1.88 (complex multiplet, 3H), 1.80 (s, 3H), 1.64 (s, 3H), 1.33 (m, 1H), 1.16 (d, *J* = 6.2 Hz, 3H), 0.97 (s, 9H), 0.89 (s, 9H), 0.09 (s, 3H), 0.072 (s, 3H), 0.069 (s, 3H), 0.01 (s, 3H) ppm.

^{13}C NMR (125 MHz in C_6D_6): δ 195.4, 143.5, 140.7, 135.9, 133.5, 133.3, 132.6, 130.4, 130.2, 129.0, 128.3, 104.2, 72.3, 70.5, 69.7, 61.7, 61.5, 53.6, 44.9, 37.3, 33.7, 26.8, 26.00, 25.96, 21.9, 21.7, 19.6, 18.20, 18.19, 16.3, -3.6, -4.58, -4.62 ppm.

HRMS (FAB, MNOBA matrix): for $\text{C}_{50}\text{H}_{78}\text{O}_8\text{Si}_3\text{SNa}$ ($\text{M}+\text{Na}$) $^+$, Calcd: 945.4633, Found: 945.4623.

(2*S*,3*S*,6*S*)-2-(2-Benzenesulfonyl-1,1-dimethyl-ethyl)-6-[(2*R*,3*R*)-2,3-bis-(*t*-butyl-dimethyl-silanyloxy)-butyl]-4-[2-(*t*-butyl-methyl-phenyl-silanyloxy)-eth-(*E*)-ylidene]-2-methoxy-tetrahydro-pyran-3-ol 522



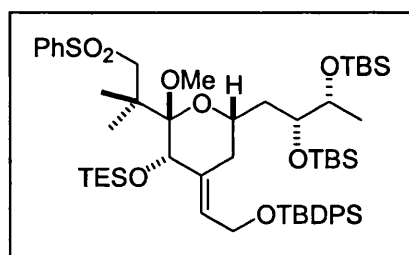
To a stirred solution of enone **502** (100 mg, 108 μmol) in dry methanol^a (2.2 mL) was added ceriumtrichloride heptahydrate^a (403 mg, 1.1 mmol) in one portion with vigorous stirring. After 45 min the mixture was cooled to $-78\text{ }^\circ\text{C}$ when sodium borohydride^c (20 mg, 542 μmol) was added in one portion with associated gas evolution. After 15 min the mixture was warmed to $-20\text{ }^\circ\text{C}$ and after a further 10 min the mixture was stirred at room temperature. After 10 min, the mixture was re-cooled to $-20\text{ }^\circ\text{C}$ and quenched by dropwise addition of saturated aq. NaHCO_3 (~3 mL) and diluted with EtOAc (5 mL). The organic layer was separated and aqueous layer extracted with EtOAc (2 x 5 mL). The combined organic layers were washed with brine (1 x 10 mL), dried over Na_2SO_4 , filtered, and concentrated *in vacuo*. The boronic acid residues were then azeotropically removed with MeOH (1 x 10 mL). Rapid purification of the residue by SiO_2 flash chromatography using hexanes/EtOAc (elution gradient 10:1, then 5:1) as eluent afforded α -hydroxy alkene **522** (80 mg, 80%) as a white foam, that proved rather unstable.

IR (neat film): 3478 (br), 2955 (s), 2856 (s), 1472 (m), 1389 (m), 1305 (m), 1256 (m), 1145 (m), 1112 (s), 836 (m), 775 (m), 703 (m) cm^{-1}

¹H NMR (500 MHz in C₆D₆): δ 7.97 (m, 2H), 7.76 (m, 4H), 7.26 (m, 6H), 6.96 (m, 3H), 5.60 (t, J = 6.0 Hz, 1H), 4.20 (m, 3H), 4.03 (d, J = 4.4 Hz, 1H), 3.96 (m, 3H), 3.60 (d, J = 14.4 Hz, 1H), 3.24 (s, 3H), 1.98 (dd, J = 9.6, 12.9 Hz, 1H), 1.86 (m, 2H), 1.74 (s, 6H), 1.51 (m, 1H), 1.33 (m, 1H), 1.18 (s, 3H), 1.16 (s, 9H), 0.96 (s, 9H), 0.92 (s, 9H), 0.109 (s, 3H), 0.09 (s, 3H), 0.07 (s, 3H), 0.06 (s, 3H) ppm.

¹³C NMR (125 MHz in C₆D₆): δ 143.9, 136.9, 135.9, 134.0, 132.5, 130.06, 130.04, 129.0, 128.5, 126.5, 102.7, 72.6, 72.3, 70.8, 68.2, 63.2, 60.2, 52.8, 45.4, 36.8, 30.6, 27.0, 26.07, 26.05, 23.6, 22.7, 19.3, 18.3, 16.4, -3.9, -4.3, -4.5, -4.6 ppm.

(2S,3S,6S)-2-(2-Benzenesulfonyl-1,1-dimethyl-ethyl)-6-[(2R,3R)-2,3-bis-(*t*-butyl-dimethyl-silanyloxy)-butyl]-4-[2-(*t*-butyl-methyl-phenyl-silanyloxy)-eth-(*E*)-ylidene]-2-methoxy-3-triethylsilanyloxy-tetrahydro-pyran 426



To a cooled (0 °C) solution of α -hydroxy alkene **522** (104 mg, 112 μ mol) in dry CH₂Cl₂ (4.0 mL) and freshly 2,6-lutidine (130 μ L, 1.12 mmol) was added triethylsilyl triflate^a (80 μ L, 337 μ mol) dropwise over 2 min and the mixture was allowed to warm to room temperature. After 40 min, the mixture was cooled to 0 °C and quenched by dropwise addition of saturated aq. NaHCO₃ (~5 mL) then solid NaHCO₃ and diluting with EtOAc (10 mL). The organic layer was separated and aqueous layer extracted with EtOAc (2 x 5 mL). The combined organic layers were washed with brine (1 x 5 mL), dried over Na₂SO₄, filtered, and concentrated *in vacuo*. Purification of the residue by SiO₂ flash chromatography using hexanes/EtOAc (12:1) as eluent afforded triethylsilylether **426** (96 mg, 82%) as a very light yellow oil.

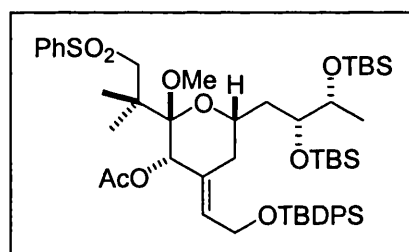
[α]_D: +2.9° (c 0.855, CH₂Cl₂).

IR (neat film): 3051 (w), 2955 (s), 2931 (s), 2856 (s), 1730 (w), 1589 (w), 1469 (s), 1427 (m), 1385 (m), 1314 (m), 1255 (s), 1149 (s), 1110 (s), 1085 (s), 1006 (m), 959 (m), 831 (s), 776 (m), 740 (m), 704 (m) cm^{-1}

^1H NMR (500 MHz in C_6D_6 at $+70^\circ\text{C}$): (data quoted for major isomer) δ 8.00 (d, $J = 7.5$ Hz, 2H), 7.77 (m, 4H), 7.26 (m, 6H), 7.04 (m, 3H), 5.76 (t, $J = 6.2$ Hz, 1H), 4.46 (s, 1H), 4.30 (d, $J = 6.2$ Hz, 2H), 4.07 (m, 1H), 3.99 (d, $J = 14.2$ Hz, 1H), 3.96 (overlapping m, 2H), 3.73 (d, $J = 14.2$ Hz, 1H), 3.32 (s, 3H), 2.13-2.04 (complex m, 3H), 1.81 (s, 3H), 1.75 (s, 3H), 1.16 (s, 9H), 0.96 (s, 9H), 0.94 (complex m, 12H), 0.91 (s, 9H), 0.64 (q, $J = 7.9$ Hz, 6H), 0.11 (s, 3H), 0.09 (s, 3H), 0.07 (s, 3H), 0.06 (s, 3H) ppm.

HRMS (FAB, MNOBA matrix): for $\text{C}_{56}\text{H}_{94}\text{O}_8\text{Si}_4\text{SCs}$ ($\text{M}+\text{Cs}$) $^+$, Calcd: 1171.4840, Found: 1171.4801.

Acetic acid (2S,3S,6S)-2-(2-benzenesulfonyl-1,1-dimethyl-ethyl)-6-[(2R,3R)-2,3-bis-(*t*-butyl-dimethyl-silanyloxy)-butyl]-4-[1-(*t*-butyl-diphenyl-silanyloxy)-meth-(*E*)-ylidene]-2-methoxy-tetrahydro-pyran-3-yl ester 527



To a cooled (0°C) solution of alcohol **522** (48 mg, 52 μmol) in dry CH_2Cl_2 (1.0 mL) and pyridine^a (20 μL , 259 μmol) was added acetic anhydride^a (25 μL , 259 μmol) dropwise over 1 min. Then dimethylaminopyridine^c (30 mg, 26 μmol) was added in one portion and the mixture was removed from the ice bath. After 10 min the mixture was re-cooled to 0°C and quenched by the addition of solid NaHCO_3 followed by dropwise addition of saturated aq. NaHCO_3 (~2 mL), diluted with CH_2Cl_2 (~5 mL) and stirred vigorously for 10 min. The organic layer was separated and aqueous layer extracted with EtOAc (3 x 5 mL). The combined organic layers were washed with brine (1 x 5 mL), dried over Na_2SO_4 , filtered, and concentrated *in vacuo*. Purification of the residue by SiO_2 flash chromatography using hexanes/EtOAc (10:1) as eluent afforded acetate **527** (31 mg, 62%) as a very light orange oil.

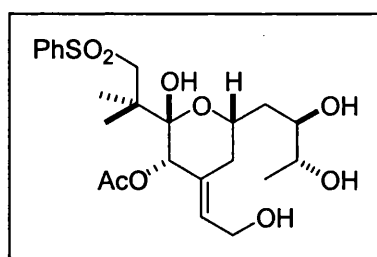
IR (neat film): 2955 (s), 2857 (s), 1747 (s), 1470 (m), 1428 (m), 1372 (m), 1315 (m), 1255 (m), 1227 (m), 1149 (m), 1109 (s), 961 (m), 833 (m), 777 (m), 705 (m) cm^{-1}

^1H NMR (500 MHz in C_6D_6): δ 7.93 (m, 2H), 7.73 (m, 4H), 7.25 (m, 6H), 6.97 (m, 3H), 6.04 (t, $J = 5.5$ Hz, 1H), 5.80 (s, 1H), 4.15 (ddd, $J = 6.1, 13.1, 26.1$ Hz, 2H), 4.05 (m, 1H), 3.91 (m, 3H), 3.52 (d, $J = 14.3$ Hz, 1H), 3.19 (s, 3H), 1.94 (m, 2H), 1.84 (m, 1H), 1.78 (s, 3H), 1.76 (s, 3H), 1.69 (s, 3H), 1.31 (m, 1H), 1.15 (d, $J = 6.1$ Hz, 3H), 1.13 (s, 9H), 0.92 (s, 9H), 0.90 (s, 9H), 0.06 (s, 3H), 0.05 (s, 3H), 0.04 (s, 3H), 0.03 (s, 3H) ppm.

^{13}C NMR (125 MHz in C_6D_6): δ 168.6, 143.6, 135.9, 134.0, 133.9, 132.8, 130.0, 129.9, 129.1, 128.3, 102.4, 72.2, 72.0, 70.6, 68.0, 63.1, 60.1, 53.0, 45.2, 36.6, 31.2, 30.1, 26.9, 26.0, 25.9, 23.5, 22.6, 21.0, 19.3, 18.23, 18.19, 16.3, -4.3, -4.4, -4.55, -4.64 ppm.

HRMS (FAB, MNOBA matrix): for $\text{C}_{52}\text{H}_{82}\text{O}_9\text{Si}_3\text{SNa}$ ($\text{M}+\text{Na}$) $^+$, Calcd: 989.4904, Found: 989.4885.

Acetic acid (2S,3S,6S)-2-(2-benzenesulfonyl-1,1-dimethyl-ethyl)-6-((2R,3R)-2,3-dihydroxy-butyl)-2-hydroxy-4-[2-hydroxy-eth-(E)-ylidene]-tetrahydro-pyran-3-yl ester 525



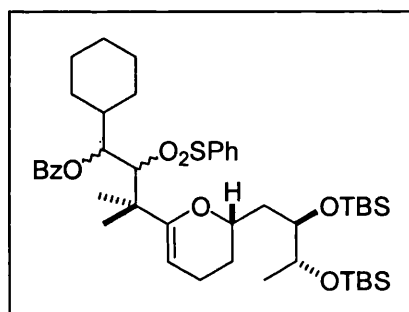
To a stirred solution of acetate **527** (163 mg, 170 μmol) in MeCN (1.8 mL) and THF (1.8 mL) in a polyethylene container was added hydrogen fluoride^b solution (40% aq., 1.8 mL, 0.7 mmol) dropwise over 1 min. After 2 h the mixture was quenched by slow addition of solid NaHCO_3 and saturated aq. NaHCO_3 solution (~2 mL), diluted with EtOAc (~5 mL) and stirred vigorously until gas evolution ceased. The organic layer was separated and aqueous layer extracted with EtOAc (3 x 5 mL). The combined organic layers were dried over Na_2SO_4 , filtered, and concentrated *in vacuo*. Purification of the residue by SiO_2 flash

chromatography using chloroform/ethanol (10:1) as eluent afforded tetraol **525** (70 mg, 85%) as a white crystalline solid. Due to the existence of two forms of the product, spectral data was difficult to achieve.

$[\alpha]_D^{25}$: +31.7° (c 0.375, CH₂Cl₂).

HRMS (FAB, MNOBA matrix): for C₂₃H₃₄O₉SNa (M+Na)⁺, Calcd: 509.1803, Found: 509.1821.

Benzoic acid 2-benzenesulfonyl-3-{6-[(2*R*,3*R*)-2,3-bis-(*t*-butyl-dimethyl-silanyloxy)-butyl]-5,6-dihydro-4*H*-pyran-2-yl}-1-cyclohexyl-3-methyl-butyl ester **530**

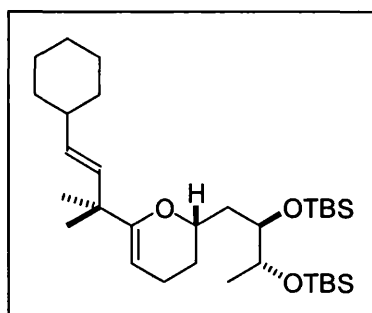


To a cooled (-78 °C) solution of glycal **505** (200 mg, 335 μmol) in dry THF (2.7 mL) was added *n*-butyl lithium^a (2.5 M in hexanes, 155 μL, 390 μmol) dropwise over 1 min turning the mixture bright yellow. After 22 min cyclohexanecarboxaldehyde^a (50 μL, 400 μmol) was added dropwise over 1 min turning mixture colourless. Immediately benzoyl chloride^g (190 μL, 1.68 mmol) was added in one portion followed by addition of dry Et₃N (280 μL, 2.01 mmol) and dimethylaminopyridine^c (410 mg, 340 μmol) in one portion each sequentially. The mixture was then warmed to 0 °C and after 10 min warmed to room temperature. After a further 40 min the mixture was re-cooled to 0 °C and quenched by dropwise addition of saturated aq. NaHCO₃ (~2 mL), diluted with EtOAc (10 mL) and H₂O (15 mL) and stirred vigorously for 10 min. The organic layer was separated and aqueous layer extracted with EtOAc (3 x 10 mL). The combined organic layers were washed with brine (1 x 15 mL), dried over Na₂SO₄, filtered, and concentrated *in vacuo*. Purification of the residue by SiO₂ flash chromatography using hexanes/EtOAc (20:1) as eluent afforded benzoyl sulfones **530** (246 mg, 90%) as a light yellow oil.

The compound was then used directly for the next without full characterisation.

HRMS (FAB, MNOBA matrix): for $C_{45}H_{73}O_7Si_2S$ ($M+H$)⁺, Calcd: 813.4645, Found: 813.4616.

2-[(2*R*,3*R*)-2,3-Bis-(*t*-butyl-dimethyl-silanyloxy)-butyl]-6-[(*E*)-3-cyclohexyl-1,1-dimethyl-allyl]-3,4-dihydro-2*H*-pyran 531



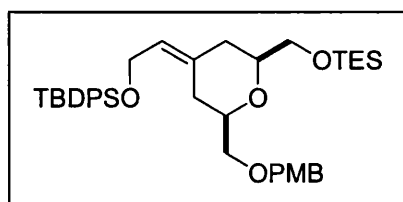
To a cooled (0 °C) solution of benzoyl sulfones **530** (267 mg, 330 μ mol) in EtOH^b (32.8 mL) was added magnesium powder^a (~50 mesh) (40 mg, 1.64 mmol) and mercury(II) chloride^h (22 mg, 82 μ mol) in one portion each sequentially, and mixture allowed to warm to room temperature. After 12 h the mixture was quenched by addition of solid NaHCO₃ then dropwise addition of saturated aq. NaHCO₃ (~5 mL), and stirred vigorously for 15 min. The organic layer was separated and aqueous layer extracted with EtOAc (3 x 15 mL). The combined organic layers were washed with brine (1 x 10 mL), dried over Na₂SO₄, filtered, and concentrated *in vacuo*. Purification of the residue by SiO₂ flash chromatography using hexanes/EtOAc (9:1) as eluent afforded alkene **531** (144 mg, 80%) as a colourless viscous oil.

¹H NMR (500 MHz in C₆D₆): δ 5.77 (dd, J = 1.1, 15.8 Hz, 1H), 5.50 (dd, J = 6.9, 15.8 Hz, 1H), 4.66 (dd, J = 2.4, 4.6 Hz, 1H), 4.20 (ddd, J = 1.3, 4.3, 10.3 Hz, 1H), 4.08 (m, 1H), 2.14 (m, 1H), 2.00 (m, 2H), 1.88 (m, 1H), 1.77 (m, 2H), 1.69 (m, 2H), 1.62-1.41 (complex m, 4H), 1.39 (s, 3H), 1.37 (s, 3H), 1.34 (m, 1H), 1.28 (m, 1H), 1.22 (d, J = 6.3 Hz, 3H), 1.19-1.04 (complex m, 3H), 1.01 (s, 9H), 0.99 (s, 9H), 0.21 (s, 3H), 0.17 (s, 6H), 0.11 (s, 3H) ppm.

¹³C NMR (125 MHz in C₆D₆): δ 160.1, 136.0, 132.7, 128.5, 93.0, 72.0, 71.8, 71.0, 41.3, 40.7, 36.2, 33.75, 33.69, 28.9, 26.65, 26.59, 26.5, 26.4, 26.3, 26.1, 21.0, 18.3, 18.2, 16.5, -4.1, -4.2, -4.3, -4.5 ppm.

HRMS (FAB, MNOBA matrix): for $C_{32}H_{63}O_3Si_2$ ($M+H$)⁺, Calcd: 551.4333, Found: 551.4316.

(2R,6S)-4-[2-(*t*-Butyl-diphenyl-silanyloxy)-eth-(E)-ylidene]-2-(4-methoxy-benzyloxymethyl)-6-triethylsilanyloxymethyl-tetrahydro-pyran **532**



To a cooled (-20 °C) solution of primary alcohol **428** (190 mg, 350 μ mol) in dry CH_2Cl_2 (4.4 mL) and 2,6-lutidine (20 μ L, 1.74 mmol) was added triethylsilyl triflate^a (120 μ L, 520 μ mol) dropwise over 2 min. After 5 min, the mixture was quenched by the dropwise addition of saturated aq. $NaHCO_3$ (~2 mL) then solid $NaHCO_3$, diluted with EtOAc (10 mL) and vigorously stirred for 10 min. The organic layer was separated and aqueous layer extracted with EtOAc (3 x 5 mL). The combined organic layers were dried over $MgSO_4$, filtered, and concentrated *in vacuo*. Purification of the residue by SiO_2 flash chromatography using hexanes/EtOAc (20:1) as eluent afforded triethylsilylether **532** (224 mg, 97%) as a light yellow oil.

$[\alpha]_D^{25}$: +6.2° (c 1.57, CH_2Cl_2).

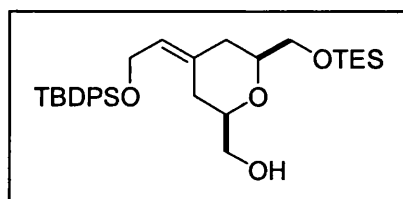
IR (neat film): 3070 (w), 2955 (s), 2876 (s), 1613 (m), 1588 (w), 1513 (s), 1461 (m), 1427 (m), 1360 (m), 1302 (m), 1248 (s), 1175 (m), 1110 (s), 1040 (s), 823 (m), 741 (s), 704 (s), 613 (m) cm^{-1} .

1H NMR (500 MHz in $CDCl_3$): δ 7.66 (d, J = 6.5 Hz, 4H), 7.37 (m, 6H), 7.21 (d, J = 8.7 Hz, 2H), 6.85 (d, J = 8.7 Hz, 2H), 5.46 (t, J = 6.5 Hz, 1H), 4.45 (q, J = 11.8 Hz, 2H), 4.20 (m, 2H), 3.78 (s, 3H), 3.72 (dd, J = 5.1, 10.3 Hz, 1H), 3.53 (dd, J = 5.9, 10.3 Hz, 1H), 3.41-3.31 (complex m, 4H), 2.21 (d, J = 13.5 Hz, 2H), 1.94 (t, J = 12.5 Hz, 1H), 1.63 (t, J = 12.3 Hz, 1H), 1.03 (s, 9H), 0.95 (t, J = 7.9 Hz, 9H), 0.60 (q, J = 8.0 Hz, 6H) ppm.

^{13}C NMR (125 MHz in CDCl_3): δ 159.1, 135.6, 133.9, 130.3, 129.6, 129.5, 129.3, 127.6, 123.5, 113.7, 78.7, 76.6, 73.0, 72.8, 66.1, 60.0, 55.2, 38.4, 31.5, 26.8, 19.1, 6.7, 4.4 ppm.

LRMS (FAB, MNOBA matrix): for $\text{C}_{39}\text{H}_{56}\text{O}_5\text{Si}_2$, $[\text{M}-2\text{H}]^+$ 659.

{(2*R*,6*S*)-4-[2-(*t*-Butyl-diphenyl-silanyloxy)-eth-(*E*)-ylidene]-6-triethylsilanyloxymethyl-tetrahydro-pyran-2-yl}-methanol **533**



To a cooled (0 °C) solution of triethylsilylether **532** (224 mg, 340 μmol) in CH_2Cl_2 (4.2 mL) and H_2O (230 μL) was added 2,3-dichloro-5,6-dicyanobenzoquinone^a (115 mg, 510 μmol) in one portion turning mixture green. After 1.5 h the now orange mixture was quenched by dropwise addition of saturated aq. NaHCO_3 (~5 mL), filtered through CELITETM with subsequent CH_2Cl_2 washes. The organic layer was separated and aqueous layer extracted with CH_2Cl_2 (3 x 5 mL). The combined organic layers were washed with brine (1 x 5 mL), dried over MgSO_4 , filtered, and concentrated *in vacuo*. Purification of the residue by SiO_2 flash chromatography using hexanes/EtOAc (gradient elution 40:1, then 30:1, then 20:1, then 5:1) as eluent afforded primary alcohol **533** (153 mg, 81%) as a light yellow oil.

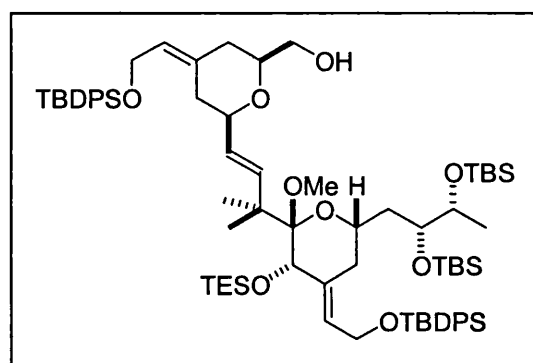
IR (neat film): 3395 (br), 2955 (s), 2877 (s), 1460 (w), 1427 (m), 1110 (s), 1068 (s), 823 (m), 787 (m), 741 (m), 703 (s), 612 (m), 505 (m) cm^{-1} .

^1H NMR (500 MHz in CDCl_3): δ 7.66 (d, J = 7.5 Hz, 4H), 7.42-7.34 (m, 6H), 5.47 (t, J = 6.5 Hz, 1H), 4.20 (m, 2H), 3.66 (dd, J = 5.6, 10.6 Hz, 1H), 3.53 (m, 2H), 3.41 (m, 2H), 3.23 (m, 1H), 2.14 (d, J = 13.4 Hz, 1H), 2.09 (d, J = 13.5 Hz, 1H), 1.94 (t, J = 12.4 Hz, 1H), 1.62 (t, J = 12.6 Hz, 1H), 1.62 (underlying m, 1H), 1.02 (s, 9H), 0.95 (t, J = 7.9 Hz, 9H), 0.59 (q, J = 8.0 Hz, 6H) ppm.

^{13}C NMR (125 MHz in CDCl_3): δ 135.6, 135.3, 133.8, 129.6, 127.6, 123.8, 78.8, 77.5, 66.1, 65.9, 60.0, 38.2, 30.5, 26.9, 19.1, 6.7, 4.4 ppm.

LRMS (FAB, MNOBA matrix): for $\text{C}_{31}\text{H}_{48}\text{O}_4\text{Si}_2$, $[\text{M}-\text{OH}]^+$ 539.

(2S,3S,6S)-6-[(2R,3R)-2,3-Bis-(*t*-butyl-dimethyl-silanyloxy)-butyl]-4-[2-(*t*-Butyl-diphenyl-silanyloxy)-eth-(*E*)-ylidene]-2-[(*E*)-3-[(2R,6S)-4-[2-(*t*-Butyl-diphenyl-silanyloxy)-eth-(*E*)-ylidene]-6-hydroxymethyl-tetrahydro-pyran-2-yl)-1,1-dimethyl-allyl]-2-methoxy-3-triethylsilanyloxy-tetrahydro-pyran 535



To a solution of primary alcohol **533** (90 mg, 160 μmol) in dry MeCN (3.25 mL) and flame activated 4Å molecular sieves (~1 g) was added tertapropylammonium perruthenate^c (6 mg, 16 μmol) and 4-methylmorpholine *N*-oxide^a (38 mg, 320 μmol) sequentially. After 25 min the mixture was diluted with CH_2Cl_2 (~10 mL), then filtered through a pad of CELITE™, then a pad of SiO_2 with CH_2Cl_2 washings. The crude aldehyde **529** was then concentrated *in vacuo* and used immediately without further purification.

To a cooled (-78 °C) solution of phenylsulfone **426** (200 mg, 193 μmol) in double distilled THF (1.9 mL) was added phenyllithium^a (1.8 M in hexanes, 140 μL , 240 μmol) dropwise over 1 min turning mixture lime green. The reaction was allowed to warm to -50 °C over 20 min, and after a further 20 min at -50 °C the mixture was re-cooled to -78 °C when a solution of freshly aldehyde **529** (assumed 100%, 90 mg, 160 μmol) in double distilled THF (1.1 mL) was added to the mixture dropwise over 3 min. After 35 min the reaction was allowed to warm to room temperature and after a further 2 h the mixture was re-cooled to -78 °C, quenched by the dropwise addition of saturated aq. NH_4Cl (~5 mL) solution and diluted with and EtOAc (5 mL) and H_2O (5 mL) with vigorous stirring. The organic layer was separated and aqueous layer was extracted with

EtOAc (3 x 5 mL). The combined organic layers were washed with brine (1 x 5 mL), dried over Na₂SO₄, filtered, and concentrated *in vacuo*. Purification of the residue by SiO₂ flash chromatography using hexanes/EtOAc (30:1, then neat EtOAc) as eluent afforded α -hydroxysulfones **534** (80 mg, 26%) (63% based on recovered starting material) as a light yellow oil. Due to the diastereomeric mixture of products, the material was used without full characterisation.

To a cooled (-20 °C) solution of α -hydroxysulfones **534** (80 mg, 50 μ mol) in MeOH^b (2.0 mL) and EtOAc^b (1.0 mL) was added freshly made sodium-mercury amalgam (6%, 500 mg), and disodium hydrogen orthophosphate (250 mg) in one portion each sequentially. After 1 h sodium-mercury amalgam (6%, 1.0 g) and disodium hydrogen orthophosphate (500 mg) were added in one portion each sequentially. After a further 3.5 h a third addition of sodium-mercury amalgam (6%, 1.0 g) and disodium hydrogen orthophosphate (500 mg) was carried out in one portion each sequentially, and the mixture was allowed to warm to 0 °C over 0.5 h. After 1.5 h the mixture was filtered through a pad of CELITE™ with subsequent EtOAc washings, transferred to a separating funnel and washed with saturated aq. NH₄Cl solution (1 x 5 mL). The aqueous layer was then back-extracted with EtOAc (1 x 5 mL), and the combined organic layers were washed with saturated brine solution (1 x 10 mL), dried over Na₂SO₄, filtered, and concentrated *in vacuo*. Purification of the residue by SiO₂ flash chromatography using hexanes/EtOAc (20:1) as eluent afforded primary alcohol **535** (21 mg, 32%) as a colourless oil.

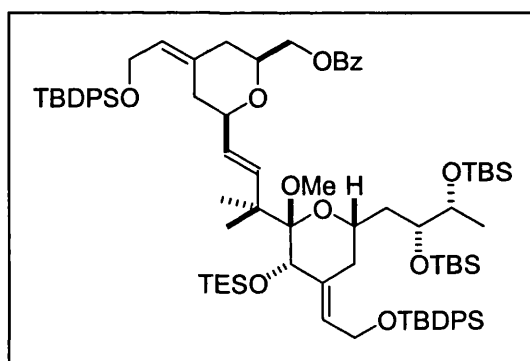
IR (neat film): 3481 (w), 2955 (s), 2931 (s), 2857 (s), 1472 (m), 1428 (m), 1378 (m), 1360 (w), 1256 (m), 1111 (s), 1006 (m), 825 (m), 808 (m), 775 (m), 739 (m), 702 (s), 614 (w) cm⁻¹.

¹H NMR (500 MHz in C₆D₆): δ 7.81 (m, 8H), 7.27 (m, 12H), 6.40 (d, *J* = 15.9 Hz, 1H), 5.81 (t, *J* = 5.4 Hz, 1H), 5.58 (dd, *J* = 6.5, 22.6 Hz, 1H), 5.56 (overlapping m, 1H), 4.44 (s, 1H), 4.37 (t, *J* = 6.2 Hz, 2H), 4.32 (d, *J* = 6.3 Hz, 2H), 4.16 (dd, *J* = 3.9, 9.1 Hz, 1H), 4.11 (t, *J* = 10.4 Hz, 1H), 3.99 (m, 1H), 3.79 (dd, *J* = 6.3, 10.1 Hz, 1H), 3.46 (complex m, 2H), 3.36 (s, 3H), 3.35 (overlapping m, 1H), 2.40 (d, *J* = 13.7 Hz, 1H), 2.19 (complex m, 2H), 2.08 (dd, *J* = 2.8, 13.9 Hz, 1H), 1.98 (t, *J* = 12.3 Hz, 1H), 1.75 (m, 3H), 1.51 (overlapping m, 1H), 1.50 (s, 3H), 1.46 (s, 3H), 1.23 (d, *J* = 6.2 Hz, 3H), 1.20 (s, 9H), 1.19 (s, 9H), 1.04 (t, *J* = 8.0 Hz, 9H), 1.00 (s, 9H), 0.97 (s, 9H), 0.71 (q, *J* = 7.7 Hz, 6H), 0.19 (s, 3H), 0.18 (s, 3H), 0.16 (s, 3H), 0.11 (s, 3H) ppm.

¹³C NMR (125 MHz in C₆D₆): δ 140.1, 137.7, 136.0, 135.9, 134.3, 130.0, 128.5, 128.3, 128.1, 127.9, 127.6, 127.1, 123.9, 103.3, 78.9, 78.8, 74.9, 72.3, 70.9, 68.0, 66.1, 60.4, 52.0, 46.2, 37.6, 37.5, 31.6, 30.2, 27.1, 27.0, 26.1, 25.3, 24.9, 19.4, 18.3, 16.5, 7.4, 5.5, -3.8, -4.3, -4.4, -4.5 ppm.

HRMS (FAB, MNOBA matrix): for C₇₅H₁₂₀O₉Si₅Na (M+Na)⁺, Calcd: 1327.7640, Found: 1327.7676.

Benzoic acid (2*S*,6*R*)-6-((*E*)-3-((2*S*,3*S*,6*S*)-6-((2*R*,3*R*)-2,3-Bis-(*t*-butyl-dimethyl-silanyloxy)-butyl)-3-triethylsilanyloxy -4-[2-(*t*-Butyl-diphenyl-silanyloxy)-eth-(*E*)-ylidene]-2-methoxy-tetrahydro-pyran-2-yl)-3-methyl-but-1-enyl)-4-[2-(*t*-Butyl-diphenyl-silanyloxy)-eth-(*E*)-ylidene]-tetrahydro-pyran-2-yl-methyl ester **536**



To a cooled (-50 °C) solution of primary alcohol **535** (15 mg, 12 μmol) in dry CH₂Cl₂ (750 μL) and dry pyridine^a (50 μL) was added 4-dimethylaminopyridine^c (1 mg, 12 μmol) in one portion followed by dropwise addition of benzoyl chloride^g (25 μL, 12 μmol) over 0.5 min. After 15 min the mixture was quenched by dropwise addition of saturated aq. NaHCO₃ solution (~2 mL) and diluted with EtOAc (5 mL) with vigorous stirring. After 5 min the organic layer was separated and aqueous layer was extracted with EtOAc (3 x 5 mL). The combined organic layers were washed with brine (1 x 5 mL), dried over Na₂SO₄, filtered, and concentrated *in vacuo*. Purification of the residue by SiO₂ flash chromatography using hexanes/EtOAc (20:1) as eluent afforded primary benzoate **536** (11 mg, 69%) as a light yellow oil.

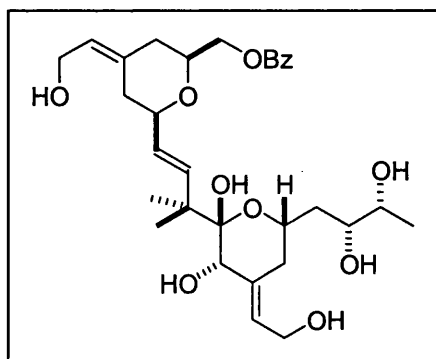
IR (neat film): 2956 (s), 2931 (s), 2857 (s), 1725 (s), 1472 (m), 1428 (m), 1379 (w), 1360 (w), 1272 (s), 1112 (s), 1027 (m), 1006 (m), 825 (m), 807.7 (m), 776 (m), 740 (m), 702 (s), 614 (w) cm⁻¹.

¹H NMR (500 MHz in C₆D₆): δ 8.17 (d, J = 7.2 Hz, 2H), 7.81 (m, 8H), 7.28 (m, 12H), 7.11 (t, J = 7.3 Hz, 1H), 7.05 (t, J = 7.5 Hz, 2H), 6.43 (d, J = 16.1 Hz, 1H), 5.81 (t, J = 5.7 Hz, 1H), 5.61 (dd, J = 5.9, 16.0 Hz, 1H), 5.56 (t, J = 6.3 Hz, 1H), 4.46 (s, 1H), 4.42-4.26 (complex m, 6H), 4.16 (dd, J = 3.8, 9.4 Hz, 1H), 4.11 (t, J = 10.4 Hz, 1H), 3.99 (m, 1H), 3.79 (dd, J = 5.9, 10.4 Hz, 1H), 3.62 (m, 1H), 3.37 (s, 3H), 2.40 (d, J = 13.4 Hz, 1H), 2.22 (t, J = 12.7 Hz, 1H), 2.15 (dd, J = 9.9, 13.3 Hz, 1H), 2.07 (dd, J = 2.4, 13.7 Hz, 1H), 1.98 (t, J = 12.5 Hz, 1H), 1.76 (t, J = 12.4 Hz, 3H), 1.58 (m, 1H), 1.49 (s, 3H), 1.45 (s, 3H), 1.23 (d, J = 6.3 Hz, 3H), 1.20 (s, 9H), 1.18 (s, 9H), 1.03 (t, J = 8.0 Hz, 9H), 1.00 (s, 9H), 0.96 (s, 9H), 0.71 (m, 6H), 0.18 (s, 6H), 0.15 (s, 3H), 0.10 (s, 3H) ppm.

¹³C NMR (125 MHz in C₆D₆): δ 167.5, 166.1, 139.6, 136.0, 135.9, 132.9, 130.7, 130.0, 129.0, 128.5, 128.1, 127.9, 127.1, 124.3, 103.3, 78.8, 76.2, 74.8, 72.3, 70.9, 68.0, 67.9, 67.5, 60.4, 52.0, 46.1, 39.2, 38.3, 35.7, 30.8, 29.3, 27.1, 27.0, 26.2, 26.1, 25.2, 24.1, 23.3, 19.4, 18.3, 16.5, 14.2, 11.1, 7.4, 5.5, -3.9, -4.3, -4.4, -4.5 ppm.

HRMS (FAB, MNOBA matrix): for C₈₂H₁₂₄O₁₀Si₅Na (M+Na)⁺, Calcd: 1431.7987, Found: 1431.7939.

Benzoic acid (2*S*,6*R*)-6-((*E*)-3-((2*S*,3*S*,6*S*)-6-((2*R*,3*R*)-2,3-dihydroxy-butyl)-2,3-dihydroxy-4-[2-hydroxy-eth-(*E*)-ylidene]-tetrahydro-pyran-2-yl)-3-methyl-but-1-enyl)-4-[2-hydroxy-eth-(*E*)-ylidene]-tetrahydro-pyran-2-yl-methyl ester **526**



To a cooled (-20 °C) solution of primary benzoate **536** (11 mg, 8 μ mol) in MeCN (130 μ L) and THF (200 μ L) in a polyethylene container was added hydrogen fluoride^b solution (40% aq., 130 μ L, 47 μ mol) dropwise over 1 min and the mixture was allowed to warm to 0 °C over 45 min. After 12 h the mixture was

quenched by slow addition of solid NaHCO_3 and saturated aq. NaHCO_3 solution (~2 mL), diluted with EtOAc (5 mL) and stirred vigorously, until gas evolution ceased. The organic layer was separated and aqueous layer extracted with EtOAc (3 x 5 mL). The combined organic layers were dried over Na_2SO_4 , filtered, and concentrated *in vacuo*. Purification of the residue by SiO_2 flash chromatography using $\text{CHCl}_3/\text{EtOH}$ (elution gradient 7:1 then 3:1) as eluent afforded hexanol **526** (4 mg, 89%) as a white crystalline solid.

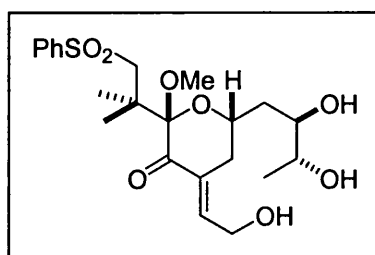
$[\alpha]_D^{25}$: +23.9° (c 0.046, CH_2Cl_2).

^1H NMR (500 MHz in CD_3OD): δ 8.02 (dd, J = 1.3, 8.4 Hz, 2H), 7.60 (t, J = 7.5 Hz, 1H), 7.47 (t, J = 7.8 Hz, 2H), 6.14 (dd, J = 0.9, 16.0 Hz, 1H), 5.88 (t, J = 6.9 Hz, 1H), 5.51 (dd, J = 6.6, 16.0 Hz, 1H), 5.51 (overlapping m, 1H), 4.38 (ddd, J = 3.7, 6.7, 12.3 Hz, 1H), 4.34 (d, J = 4.9 Hz, 2H), 4.24 (m, 2H), 4.20-4.08 (complex m, 4H), 3.83 (m, 1H), 3.76 (m, 1H), 3.49 (qu, J = 6.5 Hz, 1H), 2.75 (d, J = 15.1 Hz, 1H), 2.65 (d, J = 13.7 Hz, 1H), 2.50 (m, 1H), 2.24 (d, J = 12.4 Hz, 1H), 2.17 (t, J = 13.0 Hz, 1H), 1.88 (m, 1H), 1.75 (dt, J = 5.4, 12.5 Hz, 1H), 1.19 (s, 3H), 1.12 (s, 3H), 1.03 (d, J = 6.4 Hz, 3H) ppm.

^{13}C NMR (125 MHz in CD_3OD): δ 167.9, 142.6, 140.9, 137.9, 134.3, 131.4, 130.6, 129.6, 128.0, 124.7, 121.0, 101.4, 80.6, 77.4, 73.3, 72.5, 68.4, 58.9, 58.3, 45.9, 39.0, 36.1, 33.2, 31.4, 23.8, 23.4, 18.0 ppm.

HRMS (FAB, MNOBA matrix): for $\text{C}_{31}\text{H}_{42}\text{O}_9\text{Na}$ ($\text{M}+\text{Na}-\text{H}_2\text{O}$) $^+$, Calcd: 581.2719, Found: 581.2727.

(2*S*,6*S*)-2-(2-Benzenesulfonyl-1,1-dimethyl-ethyl)-6-((2*R*,3*R*)-2,3-dihydroxy-butyl)-4-[2-hydroxy-eth-(*E*)-ylidene]-2-methoxy-dihydro-pyran-3-one **538**



To a cooled (-40 °C) solution of enone **502** (314 mg, 340 µmol) in dry THF (17 mL) in a polyethylene bottle was added hydrogen fluoride-pyridine complex (5.4 mL) dropwise via a polyethylene syringe over 3 min and the mixture was allowed to warm to 0 °C over 1 hr. After a further 12 h the reaction was quenched by addition of solid NaHCO₃ and saturated aq. NaHCO₃ (~50 mL), diluted with EtOAc (35 mL) and stirred vigorously until effervescence ceased. The organic layer was separated and aqueous layer was extracted with EtOAc (7 x 25 mL). The combined organic layers were dried over Na₂SO₄, filtered, and concentrated *in vacuo*. Purification of the residue by SiO₂ flash chromatography using CHCl₃/MeOH (7:1) as eluent afforded triol **538** (88 mg, 57%) as a viscous light orange oil.

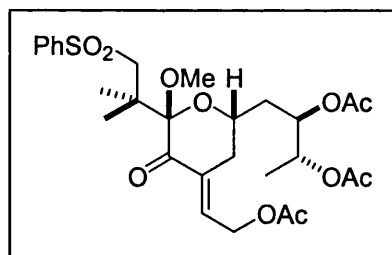
IR (neat film): 3388 (br), 2976 (w), 2936 (w), 1696 (m), 1621 (m), 1448 (m), 1304 (s), 1145 (s), 1065 (s), 726 (m), 688 (m) cm⁻¹.

¹H NMR (500 MHz in CD₃OD): δ 7.88 (d, *J* = 7.2 Hz, 2H), 7.70 (t, *J* = 7.4 Hz, 1H), 7.62 (t, *J* = 7.6 Hz, 2H), 6.76 (m, 1H), 4.32-4.15 (complex m, 3H), 3.70 (m, 1H), 3.59 (m, 1H), 3.40 (d, *J* = 2.2 Hz, 2H), 3.26 (s, 3H), 2.64 (d, *J* = 16.4 Hz, 1H), 2.51 (m, 1H), 1.77-1.63 (complex m, 2H), 1.28 (s, 3H), 1.18 (s, 3H), 1.15 (d, *J* = 6.4 Hz, 3H) ppm.

¹³C NMR (125 MHz in CD₃OD): δ 197.9, 143.5, 141.9, 135.2, 134.7, 130.5, 128.6, 105.1, 72.2, 71.9, 71.7, 62.2, 59.7, 52.9, 45.2, 39.8, 34.4, 21.81, 21.76, 18.9 ppm.

HRMS (FAB, MNOBA matrix): for C₂₂H₃₂O₈SNa (M+Na)⁺, Calcd: 479.1730, Found: 479.1716.

Acetic acid (1*R*,2*R*)-2-acetoxy-1-[(2*S*,6*S*)-4-[2-acetoxy-eth-(*E*)-ylidene]-6-(2-benzene-sulfonyl-1,1-dimethyl-ethyl)-6-methoxy-5-oxo-tetrahydro-pyran-2-ylmethyl]-propyl ester **538a**

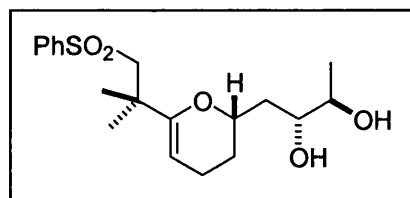


To a cooled (0 °C) solution of alcohol **538** (5 mg, 11 μmol) in dry CH₂Cl₂ (1.0 mL) and pyridine^a (13 μL, 160 μmol) was added acetic anhydride^a (16 μL, 160 μmol) dropwise over 1 min. Then dimethylaminopyridine^c (1 mg, 5 μmol) was added in one portion and the mixture was removed from the ice bath. After 1.5 h the reaction was re-cooled to 0 °C and quenched by the dropwise addition of saturated aq. NaHCO₃ (~2 mL), diluted with EtOAc (10 mL) and stirred vigorously for 10 min. The organic layer was separated and aqueous layer extracted with EtOAc (3 x 5 mL). The combined organic layers were washed with brine (1 x 5 mL), dried over Na₂SO₄, filtered, and concentrated *in vacuo*. Purification of the residue by SiO₂ flash chromatography using hexanes/EtOAc (1:1) as eluent afforded *tris*-acetate **538a** (4 mg, 63%) as a colourless viscous oil.

HRMS (FAB, MNOBA matrix): for C₂₈H₃₈O₁₁SNa (M+Na)⁺, Calcd: 605.2050, Found: 605.2033.

(2*R*,3*R*)-1-[(*S*)-6-(2-Benzenesulfonyl-1,1-dimethyl-ethyl)-3,4-dihydro-2*H*-pyran-2-yl]-butane-2,3-diol

542



To a cooled (0 °C) solution of glycol **505** (1.97 g, 3.3 mmol) in THF (19.4 mL) was added tetrabutylammonium fluoride^a (1 M in THF, 9.2 mL, 9.2 mmol) dropwise over 2 min and mixture was allowed to warm slowly to room temperature. After 12 h, SiO₂ was added and the solvent removed *in vacuo*. It was then added to a pre-packed column of SiO₂ and the column eluted using hexanes/EtOAc (elution gradient 1:2, then 1:4, then neat EtOAc) as eluent afforded diol **542** (1.16 g, 95%) as a viscous colourless oil.

$[\alpha]_D^{25}$: +34.3° (c 0.705, CH₂Cl₂).

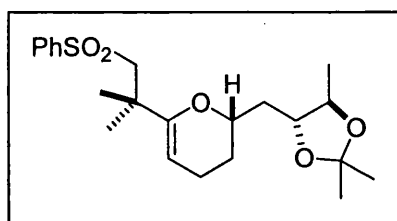
IR (neat film): 3489 (br, s), 2970 (s), 2924 (s), 1670 (s), 1447 (s), 1386 (m), 1307 (s), 1232 (m), 1149 (s), 1086 (s), 812 (m), 751 (m) cm⁻¹.

¹H NMR (500 MHz in C₆D₆): δ 7.89 (d, *J* = 8.0 Hz, 2H), 7.07 (m, 3H), 4.56 (dd, *J* = 2.2, 4.5 Hz, 1H), 4.03 (t, *J* = 10.6 Hz, 1H), 3.97 (d, *J* = 3.8 Hz, 1H), 3.85 (m, 1H), 3.69 (m, 1H), 3.45 (s, 1H), 3.31 (d, *J* = 14.0 Hz, 1H), 2.86 (d, *J* = 14.0 Hz, 1H), 1.89 (m, 1H), 1.74 (m, 1H), 1.59-1.49 (complex m, 2H), 1.41 (m, 1H), 1.28 (m, 1H), 1.28 (s, overlapping m, 3H), 1.22 (d, *J* = 6.3 Hz, 3H), 1.11 (s, 3H) ppm.

¹³C NMR (125 MHz in C₆D₆): δ 156.2, 142.1, 133.2, 129.2, 128.3, 95.5, 72.6, 72.1, 71.3, 64.1, 39.3, 38.6, 28.6, 28.1, 25.6, 21.1, 19.5 ppm.

HRMS (FAB, MNOBA matrix): for C₁₉H₂₉O₅S (M+H)⁺, Calcd: 369.1748, Found: 369.1736.

(S)-6-(2-Benzenesulfonyl-1,1-dimethyl-ethyl)-2-((4*R*,5*R*)-2,2,5-trimethyl-[1,3]dioxolan-4-ylmethyl)-3,4-dihydro-2*H*-pyran **543**



To a stirred solution of 1,2-diol **542** (1.16 g, 3.15 mmol) in acetone^b (24.2 mL) and 2,2-dimethoxypropane^a (24.2 mL, 9.4 mmol) was added pyridinium *p*-toluenesulfonate^c (198 mg, 780 μmol) in one portion and the mixture was heated to 40 °C. After 15 min the mixture was cooled to room temperature and the solvent was removed *in vacuo*. Purification of the residue by SiO₂ flash chromatography using hexanes/EtOAc (2:1) as eluent afforded acetone **543** (1.25 g, 97%) as a viscous colourless oil.

$[\alpha]_D$: +42.2° (c 1.72, CH₂Cl₂).

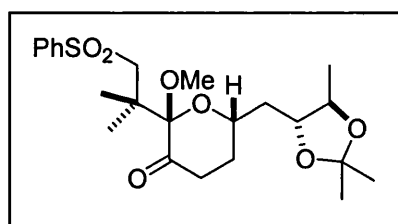
IR (neat film): 3065 (m), 2981 (s), 2932 (s), 1670 (s), 1447 (s), 1378 (s), 1308 (s), 1236 (s), 1151 (s), 1090 (s), 1003 (m), 931 (m), 846 (m), 750 (m) cm⁻¹.

¹H NMR (500 MHz in C₆D₆): δ 7.82 (d, *J* = 7.9 Hz, 2H), 7.03 (m, 3H), 4.42 (t, *J* = 3.6 Hz, 1H), 3.69 (m, 1H), 3.58 (m, 1H), 3.51 (m, 1H), 3.27 (d, *J* = 14.3 Hz, 1H), 3.14 (d, *J* = 14.3 Hz, 1H), 1.66 (m, 2H), 1.44-1.33 (complex m, 2H), 1.37 (s overlapping m, 3H), 1.36 (s overlapping m, 3H), 1.30 (s, 3H), 1.25 (m, 1H), 1.23 (s, overlapping m, 3H), 1.07 (m, 1H), 1.07 (d overlapping m, *J* = 6.0 Hz, 3H) ppm.

¹³C NMR (125 MHz in C₆D₆): δ 156.0, 142.4, 132.8, 128.8, 137.9, 107.8, 94.8, 79.0, 77.2, 72.4, 63.8, 63.7, 38.4, 38.2, 27.6, 27.5, 26.9, 25.7, 20.3, 17.2 ppm.

HRMS (FAB, MNOBA matrix): for C₂₂H₃₃O₅S (M+H)⁺, Calcd: 409.2054, Found: 409.2049.

(2*S*,6*S*)-2-(2-Benzenesulfonyl-1,1-dimethyl-ethyl)-2-methoxy-6-((4*R*,5*R*)-2,2,5-trimethyl-[1,3]dioxolan-4-ylmethyl)-dihydro-pyran-3-one 545



To a cooled (0 °C) solution of glycal **543** (30 mg, 70 μmol) in MeOH^a (1.8 mL) and 2,2-dimethoxypropane^a (1.8 mL) was added flame activated 4Å molecular sieves^g (~2 g). Then freshly distilled DMDO (~0.07 M in acetone, 2.6 mL, 180 μmol) was added dropwise over 2 min. After 12 min, a stock solution of pyridinium-*p*-toluenesulfonate^c (46 mg in 50 mL) (0.2 mL) was added in one portion and mixture was warmed to room temperature. After 10 min the reaction was re-cooled to 0 °C, quenched by the dropwise addition of saturated aq. NaHCO₃ (~5 mL) then diluted with EtOAc (10 mL) and H₂O (10 mL). The organic layer was separated and aqueous layer extracted with EtOAc (4 x 5 mL). The combined organic

layers were dried over Na_2SO_4 , filtered, and concentrated *in vacuo*. Due to the unstable nature of this intermediate, we were unable to obtain analytical data, instead using the compound directly for the next step.

To a solution of crude alcohol **544** (assumed 100%, 34 mg, 70 μmol) in dry DMF^a (750 μL) was added pyridinium dichromate^a (83 mg, 220 μmol) in one portion. After 12 h a second addition of pyridinium dichromate^a (28 mg, 70 μmol) was added in one portion. After a further 8 h the mixture was diluted with H_2O (5 mL) and Et_2O (5 mL). The organic layer was separated and aqueous layer extracted with Et_2O (5 x 3 mL). The combined organic layers were washed with brine (1 x 5 mL), dried over NaSO_4 , filtered, and concentrated *in vacuo*. Purification of the residue by SiO_2 flash chromatography using hexanes/ EtOAc (elution gradient 10:1, then 5:1, then 2:1, then 1:1) as eluent afforded ketone **545** (19 mg, 58%, 2 steps) as a light yellow oil.

$[\alpha]_D$: +23.2° (c 1.52, CH_2Cl_2).

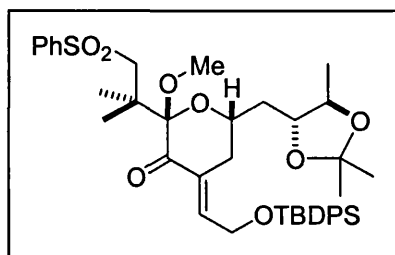
IR (neat film): 2984 (s), 2937 (s), 1722 (s), 1447 (m), 1379 (m), 1307 (s), 1235, (m), 1149 (s), 1114 (s), 1087 (s), 1046 (s), 996 (m), 841 (m), 724 (s), 690 (m) cm^{-1} .

^1H NMR (500 MHz in C_6D_6): δ 7.81 (d, J = 6.9 Hz, 2H), 6.93 (t, J = 7.3 Hz, 1H), 6.88 (t, J = 7.3 Hz, 2H), 3.93 (m, 1H), 3.88 (d, J = 14.4 Hz, 1H), 3.80 (m, 1H), 3.51 (m, 1H), 3.45 (d, J = 14.3 Hz, 1H), 3.17 (s, 3H), 2.17-2.05 (complex m, 2H), 1.62 (s, 3H), 1.59 (s, 3H), 1.53 (m, 1H), 1.44 (m, 1H), 1.36 (s, 3H), 1.31 (s, 3H), 1.31-1.22 (complex m, 2H), 1.16 (d, J = 6.0 Hz, 3H) ppm.

^{13}C NMR (125 MHz in C_6D_6): δ 204.9, 143.1, 132.5, 128.8, 128.3, 107.5, 102.6, 78.4, 76.9, 70.6, 62.0, 51.6, 43.9, 38.2, 37.3, 29.9, 27.2, 27.1, 22.5, 22.1, 16.9 ppm.

HRMS (FAB, MNOBA matrix): for $\text{C}_{23}\text{H}_{34}\text{O}_7\text{SNa}$ ($\text{M}+\text{Na}$)⁺, Calcd: 474.1940, Found: 474.1923.

(2S,6S)-2-(2-Benzenesulfonyl-1,1-dimethyl-ethyl)-4-[2-(*t*-butyl-diphenyl-silanyloxy)-eth-(*E*)-ylidene]-2-methoxy-6-((4*R*,5*R*)-2,2,5-trimethyl-[1,3]dioxolan-4-ylmethyl)-dihydro-pyran-3-one **546**



To a cooled (-78 °C) solution of ketone **545** (88 mg, 190 μmol) in dry THF (9.7 mL) was added *n*-butyllithium^a (2.5 M in hexanes, 150 μL, 390 μmol) dropwise over 1 min turning mixture bright yellow. After 13 min a solution of aldehyde **504** (144 mg, 480 μmol) in dry THF (3.2 mL) was added to the mixture dropwise over 1 min. After 15 min the reaction was warmed to 0 °C and after a further 10 min the mixture was quenched by the dropwise addition of saturated aq. NH₄Cl (~5 mL) and diluted with EtOAc (5 mL) with vigorous stirring. The organic layer was separated and aqueous layer was extracted with EtOAc (3 x 5 mL). The combined organic layers were washed with brine (1 x 5 mL), dried over Na₂SO₄, filtered, and concentrated *in vacuo*. Purification of the residue by SiO₂ flash chromatography using hexanes/EtOAc (elution gradient 10:1, then 5:1) as eluent afforded enone **546** (107 mg, 75%) as a light yellow oil.

[α]_D: -16.7° (c 0.57, CH₂Cl₂).

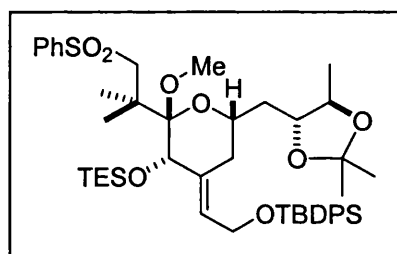
IR (neat film): 3070 (w), 2934 (m), 2858 (m), 1699 (m), 1625 (m), 1472 (m), 1430 (m), 1378 (m), 1316 (m), 1237 (m), 1148 (s), 1112 (s), 704 (s) cm⁻¹.

¹H NMR (500 MHz in C₆D₆): δ 7.82 (d, *J* = 8.3 Hz, 2H), 7.74 (m, 4H), 7.24 (m, 6H), 7.08 (t, *J* = 5.6 Hz, 1H), 6.88 (t, *J* = 7.3 Hz, 1H), 6.82 (7.4 Hz, 2H), 4.15 (ddd, *J* = 5.7, 15.9, 30.5 Hz, 2H), 3.95 (m, 1H), 3.78 (m, 1H), 3.76 (Abq overlapping m, *J* = 14.5 Hz, 2H), 3.51 (m, 1H), 3.19 (s, 3H), 1.93-1.79 (complex m, 2H), 1.73 (s, 3H), 1.62 (s, 3H), 1.35 (s, 3H), 1.34 (m, 1H), 1.30 (s, 3H), 1.15 (m, 1H), 1.13 (s overlapping m, 9H), 1.09, (d, *J* = 6.0 Hz, 3H) ppm.

^{13}C NMR (125 MHz in C_6D_6): δ 195.6, 143.4, 139.8, 135.9, 133.5, 132.6, 130.3, 129.2, 128.5, 127.6, 108.0, 104.4, 78.5, 77.2, 71.0, 61.6, 61.5, 52.2, 44.6, 38.5, 33.4, 27.5, 27.4, 26.8, 22.0, 21.6, 19.3, 17.1 ppm.

HRMS (FAB, MNOBA matrix): for $\text{C}_{41}\text{H}_{54}\text{O}_8\text{SSiCs}$ ($\text{M}+\text{Cs}$) $^+$, Calcd: 867.2386, Found: 867.2363.

(2S,3S,6S)-2-(2-Benzenesulfonyl-1,1-dimethyl-ethyl)-4-[2-(*t*-butyl-diphenyl-silanyloxy)-eth-(*E*)-ylidene]-2-methoxy-3-triethylsilanyloxy-6-((4*R*,5*R*)-2,2,5-trimethyl-[1,3]dioxolan-4-ylmethyl)-tetrahydro-pyran **4**



To a stirred solution of enone **546** (120 mg, 160 μmol) in dry MeOH^{a} (10 mL) was added ceriumtrichloride heptahydrate $^{\text{a}}$ (610 mg, 1.6 mmol) in one portion with vigorous stirring. After 45 min the mixture was cooled to $-78\text{ }^{\circ}\text{C}$ when sodium borohydride $^{\text{c}}$ (31 mg, 820 μmol) was added in 3 equal portions in 6 min intervals, with associated gas evolution. After 20 min the reaction was allowed to warm to room temperature. After a further 15 min, the mixture was re-cooled to $0\text{ }^{\circ}\text{C}$ and quenched by dropwise addition of saturated aq. NaHCO_3 (~5 mL) and diluted with H_2O (10 mL) and EtOAc (10 mL) with vigorous stirring. The organic layer was separated and aqueous layer extracted with EtOAc (3 x 5 mL). The combined organic layers were washed with brine (1 x 5 mL), dried over Na_2SO_4 , filtered, and concentrated *in vacuo*. Rapid purification of the residue by SiO_2 flash chromatography using hexanes/ EtOAc (elution gradient 5:1, then 3:1) as eluent afforded α -hydroxy alkene **547** (83 mg, 69%) as a white foam. Due to the unstable nature of this intermediate, we were unable to obtain analytical data, instead using the compound directly for the next step.

To a cooled ($0\text{ }^{\circ}\text{C}$) solution of α -hydroxy alkene **547** (83 mg, 110 μmol) in dry CH_2Cl_2 (2.0 mL) and freshly distilled 2,6-lutidine (130 μL , 1.1 mmol) was added triethylsilyl triflate $^{\text{a}}$ (80 μL , 340 μmol) dropwise over 1 min and the mixture was allowed to warm to room temperature. After 1.5 h, the reaction was re-

cooled to 0 °C and quenched by dropwise addition of saturated aq. NaHCO₃ (~5 mL) then solid NaHCO₃ and diluting with EtOAc (5 mL). The organic layer was separated and aqueous layer extracted with EtOAc (3 x 5 mL). The combined organic layers were washed with brine (1 x 5 mL), dried over Na₂SO₄, filtered, and concentrated *in vacuo*. Purification of the residue by SiO₂ flash chromatography using hexanes/EtOAc (neat hexane, then 10:1) as eluent afforded triethysilylether **4** (79 mg, 82%) as a very light yellow oil.

Spectral data agreed with those previously reported by Masamune ³⁵ⁱⁱ.

HRMS (FAB, MNOBA matrix): for C₄₇H₇₀O₈Si₂SNa (M+Na)⁺, Calcd: 873.4254, Found: 873.4228.

References

1. (i) Bryostatin 1 isolation and structure determination: Pettit G. R.; Herald, C. L.; Clardy, J.; Arnold, E.; Doubek, D. L.; Herald, D. L., *J. Am. Chem. Soc.*, **1982**, *104*, 6848; (ii) Bryostatin 2: Pettit, G. R.; Herald, C. L.; Kamano, Y.; Gust, D.; Aoyagi, R., *J. Nat. Prod.*, **1983**, *46*, 528; (iii) Bryostatins 1-3: Pettit, G. R.; Herald, C. L.; Kamano, Y.; *J. Org. Chem.*, **1983**, *48*, 5354; Bryostatin 3: Schaufelberger, D. E.; Chmurny, G. N.; Beutier, J. A.; Koleck, M. P.; Alvarado, A. B.; Schaufelberger, B. W.; Muschik, G. M., *J. Org. Chem.*, **1991**, *56*, 2895; Chmurny, G. N.; Koleck, M. P.; Hilton, B. D., *J. Org. Chem.*, **1992**, *57*, 5260; (iv) Bryostatin 4: Pettit, G. R.; Kamano, Y.; Herald, C. L.; Tozawa, M., *J. Am. Chem. Soc.*, **1984**, *106*, 6768; (v) Bryostatins 4-7: Pettit, G. R.; Kamano, Y.; Herald, C. L.; Tozawa, M., *Can. J. Chem.*, **1985**, *63*, 1204; (vi) Bryostatin 8: Pettit, G. R.; Kamano, Y.; Aoyagi, R.; Herald, C. L.; Doubek, D. L.; Schmidt, J. M.; Rudloc, J. J., *Tetrahedron*, **1985**, *41*, 985; (vii) Bryostatin 9: Pettit, G. R.; Kamano, Y.; Herald, C. L., *J. Nat. Prod.*, **1986**, *49*, 661; (viii) Bryostatins 10 and 11: Pettit, G. R.; Kamano, Y.; Herald, C. L., *J. Org. Chem.*, **1987**, *52*, 2848; (ix) Bryostatins 12 and 13: Pettit, G. R.; Leet, J. E.; Herald, C. L.; Kamano, Y.; Boettner, F. E.; Baczynskyj, L.; Nieman, R. A., *J. Org. Chem.*, **1987**, *52*, 2845; (x) Bryostatins 14 and 15: Pettit, G. R.; Gao, F.; Sengupta, D.; Coll, J. C.; Herald, C. L.; Doubek, D. L.; Schmidt, J. M.; Van Camp, J. R.; Rudloe, J. J.; Nieman, R. A., *Tetrahedron*, **1991**, *47*, 3601; (xi) Bryostatins 16-18: Pettit, G. R.; Gao, F.; Blumberg, P. M.; Herald, C. L.; Coll, J. C.; Kamano, Y.; Lewin, N. E.; Schmidt, J. M.; Chapuis, J.-C., *J. Nat. Prod.*, **1996**, *59*, 286.
2. Kerr, R. G.; Lawry, J.; Gush, K. A., *Tetrahedron Lett.*, **1996**, *37*, 8305.
3. Wender, P. A.; Hinkle, K. W.; Koehler, M. F. T.; Lippa, B., *Med. Chem. Rev.*, **1999**, *19*, 388.
4. Mutter R.; Wills, M., *Bioorg. Med. Chem.*, **2000**, *8*, 1841.
5. G. R. Pettit, The bryostatins, in *Progress in the Chemistry of Organic Natural Products*, eds. Herz, W.; Kirby, G. W.; Steglich, W.; Tamm, C., **1991**, *57*, 154, Springer-Verlag, Vienna.
6. (i) Szallasi, Z.; Du, L.; Levine, R.; Lewin, N. E.; Nguyen, P. N.; Williams, M.; Pettit, G. R.; Blumberg, P. M., *Cancer Res.*, **1996**, *56*, 2105; (ii) Schuchter, L. M.; Esa, A. H.; Stratford May, W.; Laulis, M. K.; Pettit, G. R.; Hess, A. D., *Cancer Res.*, **1991**, *51*, 682.
7. Hornung, R. L.; Pearson, J. W.; Beckwith, M.; Longo, D. L., *Cancer Res.*, **1992**, *52*, 101.
8. Mohammad, R. M.; Varterasian, M.; Almatchy, V P.; Hannoudi, G. N.; Pettit, G. R.; Al-Katib, A., *Clin. Cancer Res.*, **1998**, *4*, 1337.

9. (i) Phase 1 clinical trials with bryostatin 1: Philip, P. A.; Rea, D.; Thavas, P.; Carmichael, J.; Sturat, N. S. A.; Rockett, H.; Talbot, D. C.; Ganesan, T.; Pettit, G. R.; Balkwill, F.; Harris, A. L., *J. Natl. Cancer Inst.*, **1993**, *85*, 1812; (ii) Scheid, C.; Prendiville, J.; Jayson, G.; Crowther, D.; Fox, B.; Pettit, G. R.; Stem, P. L., *Cancer Immunol. Immunother.*, **1994**, *39*, 223; (iii) Jayson, C. G.; Crowther, D.; Prendiville, J.; McGown, A. T.; Scheid, C.; Stern, P.; Young, R.; Brenchley, P.; Owens, S.; Pettit, G. R., *Br. J. Cancer*, **1995**, *72*, 461; (iv) Varterasian, M. L.; Mohammad, R. M.; Eilander, D. S.; Hulburd, K.; Rodriguez, D.; Pemberton, P. A.; Pluda, J.; Dan, M. D.; Pettit, G. R.; Chen, B.; Al-Katib, A., *J. Clin. Oncol.*, **1998**, *16*, 56; (v) Propper, D. J.; Macaulay, V.; O'Byrne, K. J.; Braybrooke, J. P.; Wilner, S. M.; Ganesan, T. S.; Talbot, D. C.; Harris, A. L., *Br. J. Cancer*, **1998**, *78*, 1337; (vi) Varterasian, M. L.; Mohammad, R. M.; Eilander, D. S.; Hulburd, K.; Rodriguez, D.; Pemberton, R. A.; Pluda, J.; Dan, M. D.; Pettit, G. R.; Chen, B.; Al-Katib, A., *J. Clin. Oncol.*, **1998**, *16*, 56.
10. (i) Phase 2 clinical studies: Propper, D. J.; Macaulay, V.; O'Byrne, K. J.; Braybrooke, J. P.; Wilner, S. M.; Ganesan, T. S.; Talbot, D. C.; Harris, A. L., *Br. J. Cancer*, **1998**, *78*, 1337; (ii) Gonzalez, R.; Ebbinghaus, S.; Henthorn, T. K.; Miller, D.; Kraft, A. S., *Melanoma Res.*, **1999**, *9*, 599; (iii) Varterasiani, M. L.; Mohammad, R. M.; Shurafa, M. S.; Hulburd, K.; Pemberton, P. A.; Rodriguez, D. H.; Spadoni, V.; Eilander, D. S.; Murgo, A.; Wall, N.; Dan, M.; Al-Katib, A. M., *Clin. Cancer Res.*, **2000**, *6*, 825; (iv) Blackhall, F. H.; Ranson, M.; Radford, J. A.; Hancock, B. W.; Soukop, M.; McGown, A. T.; Robbins, A.; Halbert, G.; Jayson, G. C., *Br. J. Cancer*, **2001**, *84*, 465.
11. (i) Hickman, P. F.; Kemp, G. J.; Thompson, C. H.; Salisbury, A. J.; Wade, K.; Harris, A. L.; Radda, G. K., *Br. J. Cancer*, **1995**, *72*, 998; (ii) Thompson, C. H.; Macaulay, V. M.; O'Byrne, K. J.; Kemp, G. J.; Wilner, S. M.; Talbot, D. C.; Harris, A. L.; Radda, G. K., *Br. J. Cancer*, **1996**, *73*, 1161.
12. Gescher, A.; Stanwell, C.; Dale, I., *Cancer Top.*, **1994**, *9*(10), 3.
13. Nishizuka, Y., *Science*, **1992**, *258*, 607.
14. Caponigro, F.; French, R. C.; Kaye, S. B., *Anti-Cancer Drugs*, **1997**, *8*, 26.
15. Mischak, H.; Goodnight, J.; Kolch, W.; Martiny-Baron, G.; Schaehtle, C.; Kazanietz, M. G.; Blumberg, P. M.; Pierce, J. H.; Mushinski, J. F., *J. Biol. Chem.*, **1993**, *268*, 6090.
16. Cacace, A. M.; Nichols, S.; Guadagno, S.; Krauss, R. S.; Fabbro, D.; Weinstein, I. B., *Oncogene*, **1993**, *8*, 2095.

17. Stanwell, C.; Gescher, A.; Bradshaw, T. D.; Pettit, G. R., *Int. J. Cancer*, **1994**, *56*, 585.
18. Deacon, E. M.; Pongracz, J.; Griffiths, G.; Lord, J. M., *Mol. Pathol.*, **1997**, *50*, 124.
19. (i) Wang, Q.J.; Acs, P.; Goodnight, J.; Giese, T.; Blumberg, P. M.; Mischak, H.; Musliinski, J. F., *Oncogene*, **1997**, *16*, 53; (ii) Acs, P.; Wang, Q. J.; Bogi, K.; Marquez, A. M.; Lorenzo, R. S.; Biro, T.; Szallasi, Z.; Mushinski, J. F.; Blumberg, P. M., *J. Biol. Chem.*, **1997**, *272*, 2879.
20. Lu, Z.; Hornia, A.; Jiang, Y. W.; Zang, Q.; Ohno, S.; Foster, D. A., *Mol. Cell. Biol.*, **1997**, *17*, 3418.
21. Fukumoto, S.; Nishizawa, Y.; Hosoi, M.; Koyama, H.; Yamakawa, K.; Ohno, S.; Morii, H., *J. Biol. Chem.*, **1997**, *272*, 13816.
22. (i) Szallasi, Z.; Denning, M. F.; Smith, C. B.; Dlugosz, A. A.; Yuspa, S. H.; Pettit, G. R.; Blumberg, P. M., *Mol. Pharmacol.*, **1994**, *46*, 840; (ii) Heit, I.; Weiser, R. J.; Herget, T.; Faust, D.; Borchert-Stuhltrager, M.; Oesch, F.; Dietrich, C., *Oncogene*, **2001**, *20*, 5143.
23. Wang, Q. J.; Bhattacharyya, D.; Garfield, S.; Nacro, K.; Marquez, V. E.; Blumberg, P. M., *J. Biol. Chem.*, **1999**, *274*, 37233.
24. (i) liommel, U.; Zurini, M.; Luyten, M., *Nat. Struct. Biol.*, **1994**, *1*, 383; (ii) Ichikawa, S.; Hatanaka, H.; Takeuchi, Y.; Ohno, S.; Inagaki, F., *J. Biochem.*, **1995**, *117*, 566.
25. Zhang, G.; Kazanietz, M. G.; Blumberg, P. M.; Hurley, J. H., *Cell*, **1995**, *81*, 917.
26. (i) Lee, H.-W.; Smith, L.; Pettit, G. R.; Vinitsky, A.; Bingham Smith, J., *J. Biol. Chem.*, **1996**, *271*, 20973; (ii) Lee, H.-W.; Smith, L.; Pettit, G. R.; Bingham Smith, J., *Am. J. Physiol.*, **1996**, *271*, C304; (iii) Lee, H.-W.; Smith, L.; Pettit, G. R.; Bingham Smith, J., *Mol. Pharmacol.*, **1997**, *51*, 439.
27. (i) Hocevar, B. A.; Fields, A. R., *J. Biol. Chem.*, **1991**, *266*, 28; (ii) Hocevar, B. A.; Morrow, D. M.; Tykocinski, M. L.; Fields, A. P., *J. Cell. Sci.*, **1992**, *101*, 671; (iii) Hocevar, B. A.; Burns, D. J.; Fields, A. P., *J. Biol. Chem.*, **1993**, *269*, 7545.
28. (i) Trenn, G.; Pettit, G. R.; Takayama, H.; Hu-Li, J.; Sitkovsky, M. V., *J. Immunol.*, **1988**, *140*, 433; (ii) Hess, A. D.; Silanskis, M. K.; Esa, A. H.; Pettit G. R.; Stratford May, W., *J. Immunol.*, **1988**, *141*, 3263; (iii) Esa, A. H.; Warren, J. T.; Hess A. D.; Stratford May, W., *Res. Immunol.*, **1995**, *146*, 351.
29. Stratford May, W.; Sharkis, S. J.; Esa, A. H.; Gebbia, V.; Kraft, A. S.; Pettit G. R.; Sensenbrenner, L. L., *Proc. Natl. Acad. Sci.*, **1987**, *84*, 8483.
30. Berkow, R. L.; Schlabach, L.; Dodson, R.; Benjamin, Jr., W. H.; Pettit, G. R.; Rustagi, P.; Kraft, A. S., *Cancer Res.*, **1993**, *53*, 2810.

31. Steube, K. G.; Drexler, G., *Biochem. Biophys. Res. Commun.*, **1995**, 214, 1197.
32. Taylor, L. S.; Cox, G. W.; Melillo, G.; Bosco, M. C.; Espinoza-Delgado, I., *Cancer Res.*, **1997**, 57, 2468.
33. Esa, A. H.; Warren, J. T.; Hess, A. D.; May, W. S.; *Res. Immunol.*, **1995**, 146, 351.
34. For bryostatin synthesis reviews see: (i) Norcross, R. D.; Paterson, I., *Chem. Rev.*, **1995**, 95, 2401; (ii) Hale, K. J.; Hummersone, M. G.; Manaviazar, S.; Frigerio, M., *Nat. Prod. Rep.*, **2002**, 413.
35. (i) Masamune, S., *Pure Appl. Chem.*, **1988**, 60, 1587; (ii) Kageyama, M.; Tamura, T.; Nantz, M.H.; Roberts, J. C.; Somfai, P.; Whritenour, D.C.; Masamune, S., *J. Am. Chem. Soc.* **1990**, 112, 7407; (iii) Blanchette, M. A.; Malamas, M.S.; Nantz, M. H.; Roberts, J. C.; Somfai, P.; Whritenour, D.C.; Masamune, S.; Kageyama, M.; Tamura, T., *J. Org. Chem.*, **1989**, 54, 2817.
36. (i) Julia, M.; Paris, J. M., *Tetrahedron Lett.*, **1973**, 14, 4833; (ii) Kocienski, P. J.; Lythgoe, B.; Ruston, S., *J. Chem. Soc., Perkin Trans. 1*, **1978**, 829; (iii) Julia, M., *Pure Appl. Chem.*, **1985**, 57, 763; (iv) Kocienski, P. J., *Phosphorous Sulfur Relat. Elem.*, **1985**, 24, 97.
37. Hill, C. L.; Whitesides, G. M., *J. Am. Chem. Soc.* **1974**, 96, 870.
38. Horita, K.; Yoshioka, T.; Tanaka, T.; Oikawa, Y.; Yonemitsu, O., *Tetrahedron*, **1986**, 42, 3021.
39. Ma, P.; Martin, V. S.; Masamune, S.; Sharpless, K. B.; Viti, S. M., *J. Org. Chem.*, **1982**, 47, 1378.
40. Katsuki, T.; Sharpless, K. B.; *J. Am. Chem. Soc.* **1980**, 102, 5974; (ii) Rossiter, B. E.; Katsuki, T.; Sharpless, K. B.; *J. Am. Chem. Soc.* **1981**, 103, 464; (iii) Gao, Y.; Hanson, R. M.; Klunder, J. M.; Ko, S. K.; Masamune, S.; Sharpless, K. B., *J. Am. Chem. Soc.*, **1987**, 109, 5765; (iv) Pfenninger, A., *Synthesis*, **1986**, 89.
41. Corey, E. J.; Katzenellenbogen, J. A.; Posner, G. H., *J. Am. Chem. Soc.*, **1967**, 89, 4245.
42. Servi, S., *J. Org. Chem.*, **1985**, 50, 5865.
43. Piers, E.; Morton, H. E., *J. Org. Chem.*, **1980**, 45, 4263.
44. Tsunoda, T.; Suzuki, M.; Noyori, R., *Tetrahedron Lett.*, **1980**, 21, 1357.
45. Corey, E. J.; Gilman, N. W.; Ganem, B. E., *J. Am. Chem. Soc.*, **1968**, 90, 5616.
46. Boden, E. P.; Keck, G. E., *J. Org. Chem.*, **1985**, 50, 2394.
47. (i) Evans, D. A.; Carter, P. H.; Carreira, E. M.; Prunet, J. A.; Charette, A. B.; Lautens, M., *Angew. Chem., Int. Ed.*, **1998**, 37, 2354; (ii) Evans, D. A.; Carter, P. H.; Carreira, E. M.; Charette, A. B.;

- Prunet, J. A.; Lautens, M., *J. Am. Chem. Soc.* **1999**, *121*, 7540; (iii) Evans, D. A.; Gauchet-Prunet, J. A.; Carreira, E. M.; Charette, A. B., *J. Org. Chem.*, **1991**, *56*, 741.
48. Evans, D. A.; Carreira, E. M., *Tetrahedron Lett.*, **1990**, *31*, 4703.
49. For reviews on the WHE reaction: (i) Maryanoff, B. E.; Reitz, A. B., *Chem. Rev.*, **1989**, *89*, 863 (ii) Vedejs, E.; Peterson, M. J., *Top. Stereochem.*, **1994**, *24*, 1.
50. (i) Tanaka, K.; Ohta, Y.; Fuji, K.; Taga, T., *Tetrahedron Lett.*, **1993**, *34*, 4071; (ii) Tanaka, K.; Otsubo, K.; Fuji, K., *Tetrahedron Lett.*, **1996**, *37*, 3735.
51. (i) Beau, J. M.; Sinay, P., *Tetrahedron Lett.*, **1985**, *26*, 6185; (ii) Beau, J. M.; Sinay, P., *Tetrahedron Lett.*, **1985**, *26*, 6189; (iii) Beau, J. M.; Sinay, P., *Tetrahedron Lett.*, **1985**, *26*, 6193; see also: (iv) Ley, S. V.; Lygo, B.; Sternfeld, F.; Wonnacott, A., *Tetrahedron*, **1986**, *42*, 4333; (v) Greck, C.; Grice, P.; Ley, S. V.; Wonnacott, A., *Tetrahedron Lett.*, **1986**, *27*, 5277.
52. (i) Zimmerman, H. E.; Pratt, A.C., *J. Am. Chem. Soc.* **1970**, *92*, 6259; (ii) Julia, M.; Baillarge, *Bull. Soc. Chim. Fr.*, **1966**, 734.
53. Evans, D. A.; Sjogren, E. B.; Weber, A. E.; Conn, R. E., *Tetrahedron Lett.*, **1987**, *28*, 39.
54. Takano, S.; Akiyama, M.; Sato, S.; Ogasawara, K., *Chem. Lett.*, **1983**, 1539.
55. Evans, D. A.; Black, W. C., *J. Am. Chem. Soc.* **1993**, *115*, 4497.
56. Evans, D. A.; Chapman, K. T.; Carreira, E. M., *J. Am. Chem. Soc.* **1988**, *110*, 3560.
57. Bailey, P. S., *Ozonation in Organic Chemistry*, Acad. Press, New York, **1978**, vol. 1, ch. 11.
58. (i) Hanessian, S.; Guindon, Y., *Carbohydr. Res.*, **1980**, *86*, C3; (ii) Nicolaou, K. C.; Daines, R. A.; Ogawa, Y.; Chakraborty, T. K., *J. Am. Chem. Soc.* **1988**, *110*, 4696.
59. (i) Evans, D. A.; Murry, J. A.; Kozlowski, M. C., *J. Am. Chem. Soc.* **1996**, *118*, 5814; (ii) Evans, D. A.; Kozlowski, M. C.; Murry, J. A.; Burgey, C. S.; Campos, K. R.; Connell, B. T.; Staples, R. J., *J. Am. Chem. Soc.* **1999**, *121*, 669.
60. Still, W. C., *J. Am. Chem. Soc.* **1978**, *100*, 1481.
61. Lewis, M. D.; Cha, J. K.; Kishi, Y., *J. Am. Chem. Soc.* **1982**, *104*, 4976.
62. (i) Ramachandran, P. V.; Xu, W. C.; Brown, H. C., *Tetrahedron Lett.*, **1996**, *37*, 4911; (ii) Paterson, I.; Goodman, J. M.; Lister, M. A.; Schumann, R. C.; McClure, C. K.; Norcross, R. D., *Tetrahedron*, **1990**, *46*, 4663; (iii) For a review of chiral enolate chemistry see: Hale, K. J.; Manaviazar, S., *Advanced Asymmetric Synthesis*, ed. Stephenson, Chapman and Hall, London, **1996**, ch. 3, 27.

63. Evans, D. A.; Hoveyda, A. H., *J. Am. Chem. Soc.* **1990**, *112*, 6447.
64. (i) Dess, D. B.; Martin, J. C., *J. Am. Chem. Soc.* **1991**, *113*, 7277; (ii) Ireland, R. E.; Liu, L., *J. Org. Chem.*, **1993**, *58*, 2899.
65. Felix, A. M.; Heimer, E. P.; Lambros, T., J.; Tzougraki, C.; Meienhofer, J., *J. Org. Chem.*, **1978**, *43*, 4194.
66. Inanaga, J.; Hirata, K.; Saeki, H.; Katsuki, T., Yamaguchi, M., *Bull. Chem. Soc. Jpn.*, **1979**, *52*, 1989.
67. (i) Ohmori, K.; Ogawa, Y.; Obitsu, T.; Ishikawa, Y.; Nishiyama, S.; Yamamura, S., *Angew. Chem., Int. Ed.*, **2000**, *39*, 2290; (ii) Obitsu, T.; Ohmori, K.; Ogawa, Y.; Hosomi, H.; Ohba, S.; Nishiyama, S.; Yamamura, S., *Tetrahedron Lett.*, **1998**, *39*, 7349; (iii) Ohmori, K.; Suzuki, T.; Nishiyama, S.; Yamamura, S., *Tetrahedron Lett.*, **1995**, *36*, 6515; (iv) Ohmori, K.; Nishiyama, S.; Yamamura, S., *Tetrahedron Lett.*, **1995**, *36*, 6519; (v) Ohmori, K.; Suzuki, T.; Miyazawa, K.; Nishiyama, S.; Yamamura, S., *Tetrahedron Lett.*, **1993**, *34*, 4981.
68. Schmid, C. R.; Bryant, J. D.; McKennon, M. J.; Meyers, A. I., *Org. Synth.*, **1993**, *72*, 6.
69. Danishefsky, S.; Kobayashi, S.; Kerwin, J. F., *J. Org. Chem.*, **1982**, *47*, 19.
70. (i) Trost, B. M.; Klun, T. P., *J. Am. Chem. Soc.* **1981**, *103*, 1864; (ii) Copeland, C.; Stick, R. V., *Aust. J. Chem.*, **1977**, *30*, 1269.
71. Kolb, H. C.; VanNieuwenhze, M. S.; Sharpless, K. B., *Chem. Rev.*, **1994**, *94*, 2483.
72. Corey, E. J.; Fuchs, P. L., *Tetrahedron Lett.*, **1972**, *13*, 3769.
73. (i) Munt, S. P.; Thomas, E. J.; *J. Chem. Soc. Chem. Commun.*, **1989**, 480; (ii) Gracia, J.; Thomas, E. J.; *J. Chem. Soc. Perkin Trans. 1*, **1998**, 2865; (iii) Baxter, J.; Mata, E. G.; Thomas, E. J., *Tetrahedron*, **1998**, *54*, 14359; (iv) Maguire, R. J.; Munt, S. P.; Thomas, E. J.; *J. Chem. Soc. Perkin Trans. 1*, **2001**, 1473.
74. Ganem, B.; Ikota, N.; Muralidharan, V. B.; Wadee, W. S.; Young, S. D.; Yukimoto, Y., *J. Am. Chem. Soc.* **1982**, *104*, 6787.
75. (i) Bryson, T. A.; Bonitz, G. H.; Reichel, C. J.; Dardis, R. E., *J. Org. Chem.*, **1980**, *45*, 524; (ii) Schreiber, J.; Maag, H.; Hashimoto, N.; Eshenmoser, A., *Angew. Chem., Int. Ed.*, **1971**, *10*, 330.
76. (i) Kosugi, M.; Hagihara, H.; Sumiya, T.; Migita, T., *Bull. Chem. Soc. Jpn.*, **1984**, *57*, 242; (ii) Kosugi, M.; Hagihara, H.; Sumiya, T.; Migita, T., *Chem. Lett.*, **1982**, 939; (iii) Kosugi, M.;

- Hagihara, H.; Sumiya, T.; Migita, T., *Chem. Lett.*, **1983**, 839; (iv) Kosugi, M.; Hagihara, H.; Sumiya, T.; Migita, T., *J. Chem. Soc. Chem. Commun.*, **1983**, 344.
77. (i) De Brabander, J.; Vanhessche, K.; Vandewalle, M., *Tetrahedron Lett.*, **1991**, 32, 2821; (ii) De Brabander, J.; Vandewalle, M., *Synlett*, **1994**, 231; (iii) De Brabander, J.; Vandewalle, M., *Synthesis*, **1994**, 855; (iv) De Brabander, J.; Kulkarni, A.; Garcia-Lopez, R.; Vandewalle, M., *Tetrahedron: Asymmetry*, **1997**, 8, 1721.
78. Lavellee, P.; Ruel, R.; Grenier, L.; Bissonnette, M., *Tetrahedron Lett.*, **1986**, 27, 679.
79. (i) Hungerbuhler, E.; Seebach, D.; Wasmuth, D., *Helv. Chim. Acta*, **1981**, 64, 1467; (ii) Mori, Y.; Takeuchi, A.; Kageyama, H.; Suzuki, M., *Tetrahedron Lett.*, **1988**, 29, 5423.
80. Lipschutz, B. H., *Organometallics in Synthesis, A Manual*, Wiley, Chichester, **1994**, ch. 4, 283.
81. Mori, Y.; Suzuki, M., *Tetrahedron Lett.*, **1989**, 30, 4383.
82. Keck, G. E.; Abbott, D. E.; Boden, E. P.; Enholm, E. J., *Tetrahedron Lett.*, **1984**, 25, 3927.
83. (i) Seyferth, D.; Marmor, R. S.; Hilbert, P., *J. Org. Chem.*, **1971**, 36, 1379; (ii) Gilbert, J. C.; Weerasooriya, U., *J. Org. Chem.*, **1979**, 44, 4997; (iii) Gilbert, J. C.; Weerasooriya, U., *J. Org. Chem.*, **1982**, 47, 1837.
84. Baggiolini, E. G.; Iacobelli, J. A.; Hennessy, B. M.; Batcho, A. D.; Sereno, J. F.; Uskocovic, M. R., *J. Org. Chem.*, **1986**, 51, 3098.
85. Miyashita, M.; Suzuki, T.; Yoshikoshi, A., *Tetrahedron Lett.*, **1987**, 28, 4293.
86. Hoffmann, R. W.; Stiasny, H. C., *Tetrahedron Lett.*, **1995**, 36, 4595.
87. Matteson, D. S.; Michnick, J. T., *Organometallics*, **1990**, 9, 3171.
88. Kalesse, M.; Eh, M., *Tetrahedron Lett.*, **1996**, 37, 1767.
89. Kiyooka, S.; Maeda, H., *Tetrahedron: Asymmetry*, **1997**, 8, 3371.
90. (i) Roy, R.; Rey, A. W.; Charron, M.; Molino, R., *J. Chem. Soc. Chem. Commun.*, **1989**, 1308; (ii) Roy, R.; Rey, A. W., *Synlett*, **1990**, 448.
91. Roy, R.; Rey, A. W., *Tetrahedron Lett.*, **1987**, 28, 4935.
92. Kobayashi, T.; Mukaiyama, T., *Chem. Lett.*, **1986**, 1805.
93. (i) Bock, K.; Lundt, I.; Pederson, C., *Acta Chem. Scand. Ser. B*, **1981**, 35, 155; Westphal, O.; (ii) Luderitz, O., *Angew. Chem.*, **1960**, 72, 881.
94. (i) Lampe, T. F. J.; Hoffmann, H. M. R., *J. Chem. Soc. Chem. Commun.*, **1996**, 1931; (ii) Lampe, T. F. J.; Hoffmann, H. M. R., *J. Chem. Soc. Chem. Commun.*, **1996**, 2637; (iii) Lampe, T. F. J.;

- Hoffmann, H. M. R., *Tetrahedron Lett.*, **1996**, 37, 7695; (iv) Weiss, J. M.; Hoffmann, H. M. R., *Tetrahedron: Asymmetry*, **1997**, 8, 3913; (v) Vakalopoulos, A.; Lampe, T. F. J.; Hoffmann, H. M. R., *Org. Lett.*, **2001**, 6, 929.
95. (i) Hoffmann, H. M. R.; Clemens, K. E.; Smithers, R. H., *J. Am. Chem. Soc.* **1972**, 94, 3940; (ii) Hoffmann, H. M. R.; Iqbal, M. N., *Tetrahedron Lett.*, **1975**, 16, 4487.
 96. (i) Noyori, R.; Hayakawa, Y.; Takaya, H.; Murai, S.; Kobayashi, R. Sonoda, N., *J. Am. Chem. Soc.* **1978**, 100, 1759; (ii) Takaya, H.; Makino, S.; Hayakawa, Y.; Noyori, R., *J. Am. Chem. Soc.* **1978**, 100, 1765; (iii) Fohlisch, B.; Herter, R., *Synthesis*, **1982**, 976.
 97. Brown, H. C.; Joshi, N. N., *J. Org. Chem.*, **1988**, 53, 4059.
 98. Freeman, P. K.; Hutchinson, L. L., *J. Org. Chem.*, **1980**, 45, 1924.
 99. Lopez-Pelegrin, J. A.; Wentworth, Jr., P.; Sieber, F.; Metz, W. A.; Janda, K. D., *J. Org. Chem.*, **2000**, 65, 8527.
 100. Yadav, J. S.; Bandyopadhyay, A.; Kunwar, A. C., *Tetrahedron Lett.*, **2001**, 42, 4907.
 101. Tokunaga, T.; Iarrow, J. F.; Kakiuchi, F.; Jacobsen, E. N., *Science*, **1997**, 277, 936.
 102. (i) Wender, P. A.; De Brabander, J.; Harran, P. G.; Jimenez, J. -M.; Koehler, M. F. T.; Lippa, B.; Park, C. -M.; Shiozaki, M., *J. Am. Chem. Soc.*, **1998**, 120, 4534; (ii) Wender, P. A.; De Brabander, J.; Harran, P. G.; Hinkle, K. W.; Lippa, B.; Pettit, G. R., *Tetrahedron Lett.*, **1998**, 39, 8625; (iii) Wender, P. A.; Lippa, B., *Tetrahedron Lett.*, **2000**, 41, 1007.
 103. (i) Wender, P. A.; Baryza, J. L.; Bennett, C. E.; Bi, F. C.; Brenner, S. E.; Clarke, M. O.; Horan, J. C.; Kan, C.; Lacote, E.; Lippa, B.; Nell, P. G.; Turner, T. M., *J. Am. Chem. Soc.*, **2002**, 124, 13648; (ii) Wender, P. A.; Mayweg, A. V. W.; VanDeusen, C. L., *Org. Lett.*, **2003**, 5, 277.
 104. Mendola, D., *Drugs from the sea*, ed. Fusetani, Karger, Basel, **2000**, pp. 20.
 105. (i) Hale, K. J.; Hummersone, M. G.; Bhatia, G. S., *Org. Lett.*, **2000**, 2, 2189; (ii) Hale, K. J.; Hummersone, M. G.; Cai, J.; Manaviazar, S.; Bhatia, G. S.; Lennon, J. A.; Frigerio, M.; Delisser, V. M.; Chumnongsaksarp, A.; Jogia, N.; Lemaitre, A., *Pure Appl. Chem.*, **2000**, 72, 1659; (iii) Hale, K. J.; Lennon, J. A.; Manaviazar, S.; Javaid, M. H.; Hobbs, C. J., *Tetrahedron Lett.*, **1995**, 95, 2041.
 106. (i) Paterson, I.; Boddy, I.; Mason, I., *Tetrahedron Lett.*, **1987**, 28, 5205; (ii) Wei, A.; Kishi, Y., *J. Org. Chem.*, **1994**, 59, 88.

107. (i) Smith, III, A. B.; Boldi, A. M., *J. Am. Chem. Soc.*, **1997**, *119*, 6925; (ii) Smith, III, A. B.; Zhuang, L.; Brook, C. S.; Lin, Q.; Moser, W. H.; Trout, R. E. L.; Boldi, A. M., *Tetrahedron Lett.*, **1997**, *38*, 8671; (iii) Tietze, L. F.; Geissler, H.; Gewert, J. A.; Jakobi, U., *Synlett.*, **1994**, 511; (iv) Corey, E. J.; Seebach, D., *Angew. Chem., Int. Ed. Engl.*, **1965**, *4*, 1075.
108. Smith, III, A. B.; Zhuang, L.; Brook, C. S.; Boldi, A. M.; McBriar, M. D.; Moser, W. H.; Murase, H.; Nakayama, K.; Verhoest, P. R.; Lin, Q., *Tetrahedron Lett.*, **1997**, *38*, 8667.
109. De Medeiros, E. F.; Herbert, J. M.; Taylor, R. J. K., *J. Chem. Soc., Perkin Trans. 1*, **1991**, 2725.
110. Luche, J. L.; Rodriguez-Hahn, L.; Crabbe, P., *J. Chem. Soc., Chem. Commun.*, **1978**, 601.
111. Smith, III, A. B.; Chen, K.; Robinson, D. J.; Laakso, L. M.; Hale, K. J., *Tetrahedron Lett.*, **1994**, *35*, 4271.
112. O'Donnell, C. J.; Burke, S. D., *J. Org. Chem.*, **1998**, *63*, 8614.
113. (i) Sharpless, K. B.; Amberg, W.; Bennani, Y. L.; Crispino, G. A.; Hartung, J.; Jeong, K. S.; Kwong, H. L.; Morikawa, K.; Wang, Z. M.; Xu, D.; Xhang, X. L., *J. Org. Chem.*, **1992**, *57*, 2768; (ii) Xu, D.; Crispino, G. A.; Sharpless, K. B., *J. Am. Chem. Soc.*, **1992**, *114*, 7570.
114. Boons, G. J.; Hale, K. J., *Organic Synthesis with Carbohydrates*, Sheffield Acad. Press, Sheffield, **2000**, 19.
115. Carlson, P. H. J.; Katsuki, T.; Martin, V. S.; Sharpless, K. B., *J. Org. Chem.*, **1981**, *46*, 3936.
116. The formation of PMB-trichloroacetimidate was routinely performed on 70 mmol scale by deprotonation of PMB-alcohol with NaH, and subsequent exposure to trichloroacetonitrile. Purification was carried out by rapid SiO₂ flash chromatography, in typically 60% yield.
117. The use of TESOTf and TMSOMe was successfully used by Masamune in the synthesis of his C-ring intermediate to install the anomeric methoxide in **4**.
118. (i) Paquette, L. A.; Mitzel, T. M., *J. Org. Chem.*, **1996**, *61*, 8799; (ii) Paquette, L. A.; Rothaar, R. R., *J. Org. Chem.*, **1999**, *64*, 217.
119. Hale, K. J.; Frigerio, M.; Manaviazar, S., *Org. Lett.*, **2001**, *3*, 3791.
120. Hale, K. J.; Bhatia, G. S.; Peak, S. A.; Manaviazar, S., *Tet. Lett.*, **1993**, *34*, 5343.
121. Hale, K. J.; Manaviazar, S., unpublished results.
122. Smith, III, A. B.; Hale, K. J., *Tet. Lett.*, **1989**, *30*, 1037.
123. Nicolaou, K. C.; Daines, R. A.; Chakraborty, T. K.; Ogawa, Y., *J. Am. Chem. Soc.*, **1988**, *110*, 4685.

124. Blanchette, M. A.; Choy, W.; Davis, J. T.; Essenfield, A. P.; Masamune, S.; Roush, W. R.; Sakai, T., *Tet. Lett.*, **1984**, 25, 2183.
125. Horita, K.; Yoshioka, T.; Tanaka, T.; Oikawa, Y.; Yonemitsu, O., *Tetrahedron*, **1986**, 42, 3021.
126. Halcomb, R. L.; Danishefsky, S. J., *J. Am. Chem. Soc.*, **1989**, 111, 6661.
127. Adam, W.; Bialas, J.; Hadjiarapoglou, L., *Chem. Ber.*, **1991**, 124, 2377.
128. Marshall, J.A.; Garofalo, A.W., *J. Org. Chem.*, **1996**, 61, 8732.
129. Hale, K.J.; Frigerio, M.; Manaviazar, S.; Hummersone, M. G.; Fillingham, I. J.; Barsukov, I. G.; Damblon, C. F.; Gescher, A.; Roberts, G. C. K., *Org. Lett.*, **2003**, 5, 499.
130. (i) Ichikawa, S.; Hatanaka, H.; Takeuchi, Y.; Ohno, S.; Inagaki, F., *J. Biochem.*, **1995**, 117, 566;
(ii) Hommel, U.; Zurini, M.; Luytenm, M., *Nature Struct. Biol.*, **1994**, 1, 383.
131. Groves, P.; Searle, M. S.; Waltho, J. P.; Williams, D. H., *J. Am. Chem. Soc.*, **1995**, 117, 7958.
132. The modelling of **525** was carried out using Chem 3-D by S. Iqbal.
133. Lee, G. H.; Lee, H. K.; Choi, E. B.; Kim, B. T.; Pak, C. S., *Tet. Lett.*, **1995**, 36, 5067.
134. Hale, K.J.; Frigerio, M.; Manaviazar, S., *Org. Lett.*, **2003**, 5, 503.
135. Still, W.C.; Kahn, M.; Mitra, A., *J. Org. Chem.*, **1978**, 43, 2923.
136. To denote the origination of the reagents: *a* = aldrich; *b* = bdh; *c* = avocado; *d* = fisons; *e* = alfa aesar; *f* = acros; *g* = lancaster.
137. Parham, W.E.; McKown, W.D.; Nelson, V.; Kajigaeshi, S.; Ishikawa, N., *J. Org. Chem.*, **1973**, 38, 1361.

Common Abbreviations Used in the Text

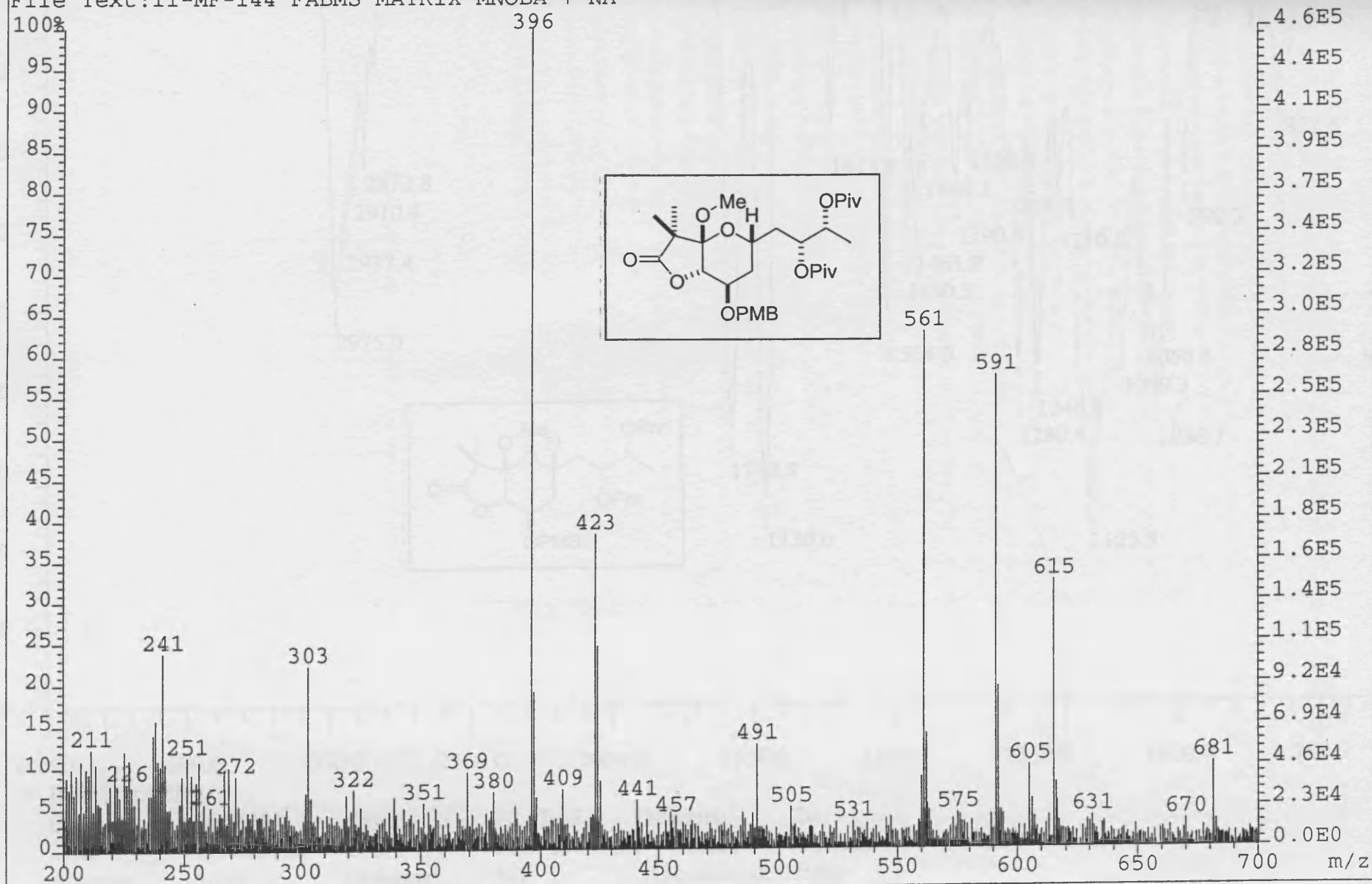
AD	Asymmetric dihydroxylation
AE	Asymmetric epoxidation
AIBN	α , α -Azoisobutyronitrile
AlI	Allyl
BINAP	2,2'-Bis(diphenylphosphino)-1,1'-binaphthyl
Bn	Benzyl
Boc	<i>t</i> -Butoxycarbonyl
BOM	Benzyloxymethyl
BOM	Benzyloxymethyl
Bz	Benzoyl
CAN	Ceric ammonium nitrate
CBS	Corey-Bakshui-Shibata
CRD	Cysteine rich domain
CSA	Camphorsulfonic acid
DBU	1,8-Diazobicyclo[5.4.0]undec-7-ene
DCC	1,3-Dicyclohexylcarbodiimide
DDQ	2,3-Dichloro-5,6-dicyanobenzoquinone
DEAD	Diethyl azodicarboxylate
DHP	Dihydropyran
DIBAL	Diisobutylaluminium hydride
DIC	Diisopropylcarbodiimide
DIP-CI	Chlorodiisopenylcamphenylborane
DMAP	4-Dimethylaminopyridine
DMB	3,5-Dimethoxybenzyl
DMDO	Dimethyldioxirane
DMF	Dimethylformamide
DMP	3,5-Dimethoxyphenyl
DMSO	Dimethylsulfoxide
FAB	Fast atom bombardment
Fmoc	9-Fluorenylmethoxycarbonyl
HDA	Hetero-Diels-Alder
HMPA	Hexamethylphosphoramide
HRMS	High resolution mass spectrometry
Ipc	Isopenylcamphenyl
IR	Infra red
KHMDS	Potassiumhexamethyl disilylamide
LDA	Lithium diisopropylamine
LRMS	Low resolution mass spectrometry
M	Molar
<i>m</i> -CPBA	<i>meta</i> -Chloroperoxybenzoic acid
MEM	2-Methoxyethoxymethyl
MHz	Megahertz
MMPP	Magnesium monoperoxyphthalate hexahydrate
Ms	Methanesulphonyl
MS	Molecular sieves
NaH	Sodium hydride
NaHMDS	Sodiumhexamethyl disilylamide
NMO	<i>N</i> -Methylmorpholine- <i>N</i> -oxide
NMR	Nuclear magnetic resonance
nOe	Nuclear overhauser effect
<i>o</i> -Tol	<i>o</i> -Toluyyl
PA	Phorbol-13-acetate
PB	Phorbol-12,13-butyrate
Ph	Phenyl

Piv	Pivaloyl
PKC	Protein kinase C
PMB	<i>p</i> -Methoxybenzyl
PMP	<i>p</i> -Methoxyphenyl
ppm	Parts per million
PPTS	Pyridinium <i>p</i> -toluene sulfonate
<i>p</i> -TsOH	<i>p</i> -Toluenesulfonic acid
Py	Pyridine
REDAL	Sodium bis(2-methoxyethoxy) aluminium hydride
SAM	S-adenosylmethionine
SEMICl	[2-(Trimethylsilyl)ethoxy]methyl chloride
TBAF	tetrabutylammonium fluoride
TBDPS	<i>t</i> -Butyldiphenylsilyl
TBS	<i>t</i> -Butyldimethylsilyl
TES	Triethylsilyl
Tf	Trifluoromethane sulfonate
TFA	Trifluoroacetic acid
TFAA	Trifluoroacetic anhydride
THF	Tetrahydrofuran
THP	Tetrahydropyran
TLC	Thin layer chromatography
TMS	Trimethylsilyl
TMSOMe	Trimethylsilyl methoxide
TMSOTf	Trimethylsilyl triflate
Tol	<i>p</i> -Tolyl
TPAP	Tetra- <i>n</i> -propylammonium perruthenate
Tr	Trityl
Ts	Toluenesulfonyl
WHE	Wadsworth-Horner-Emmons

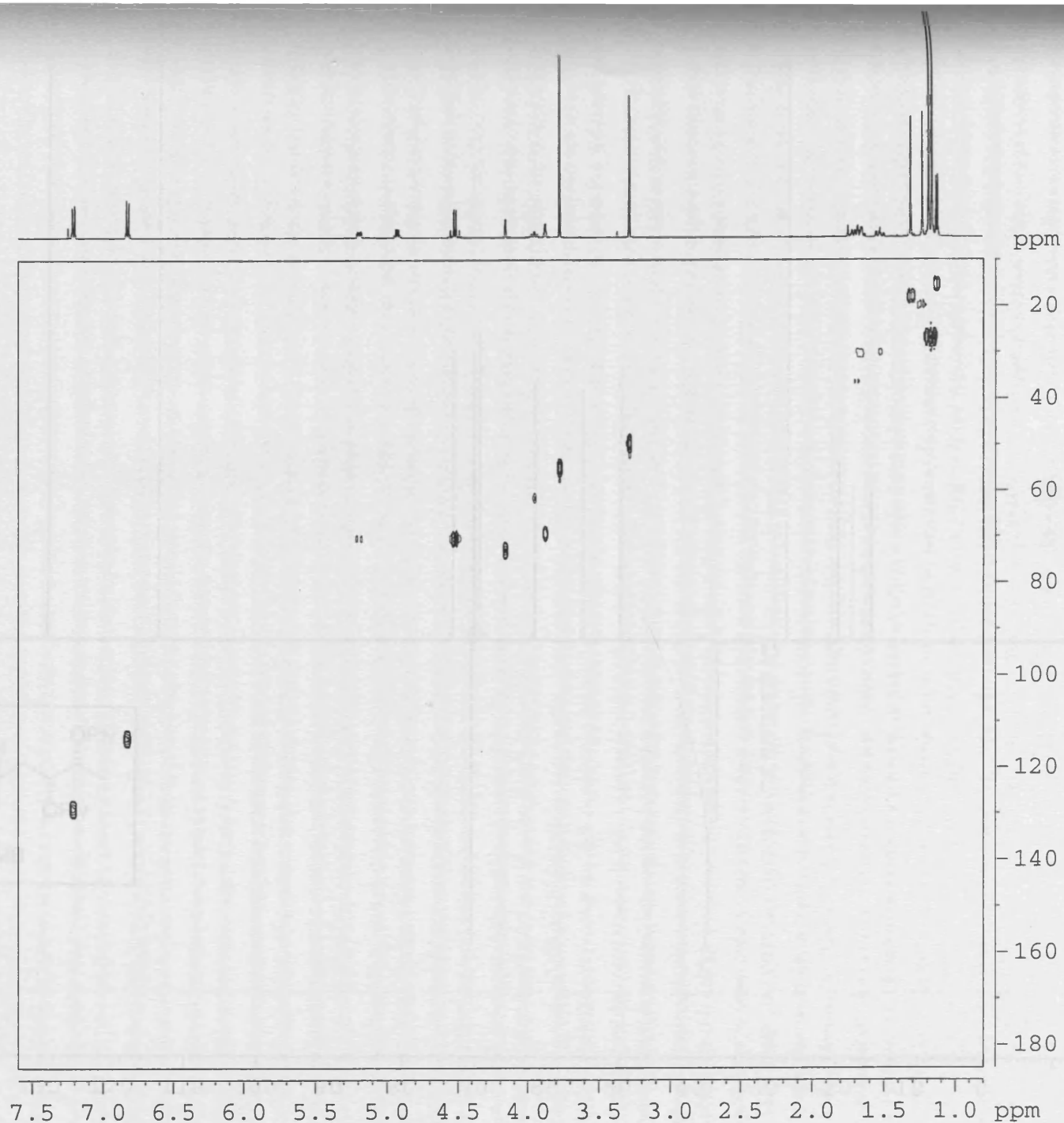
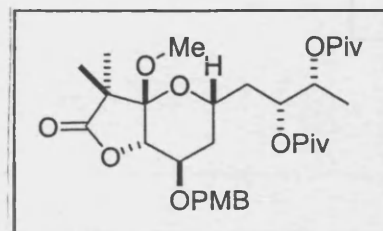
Appendix 1

The following pages contain the spectral data for compounds described in the experimental section on pages 100 to 164.

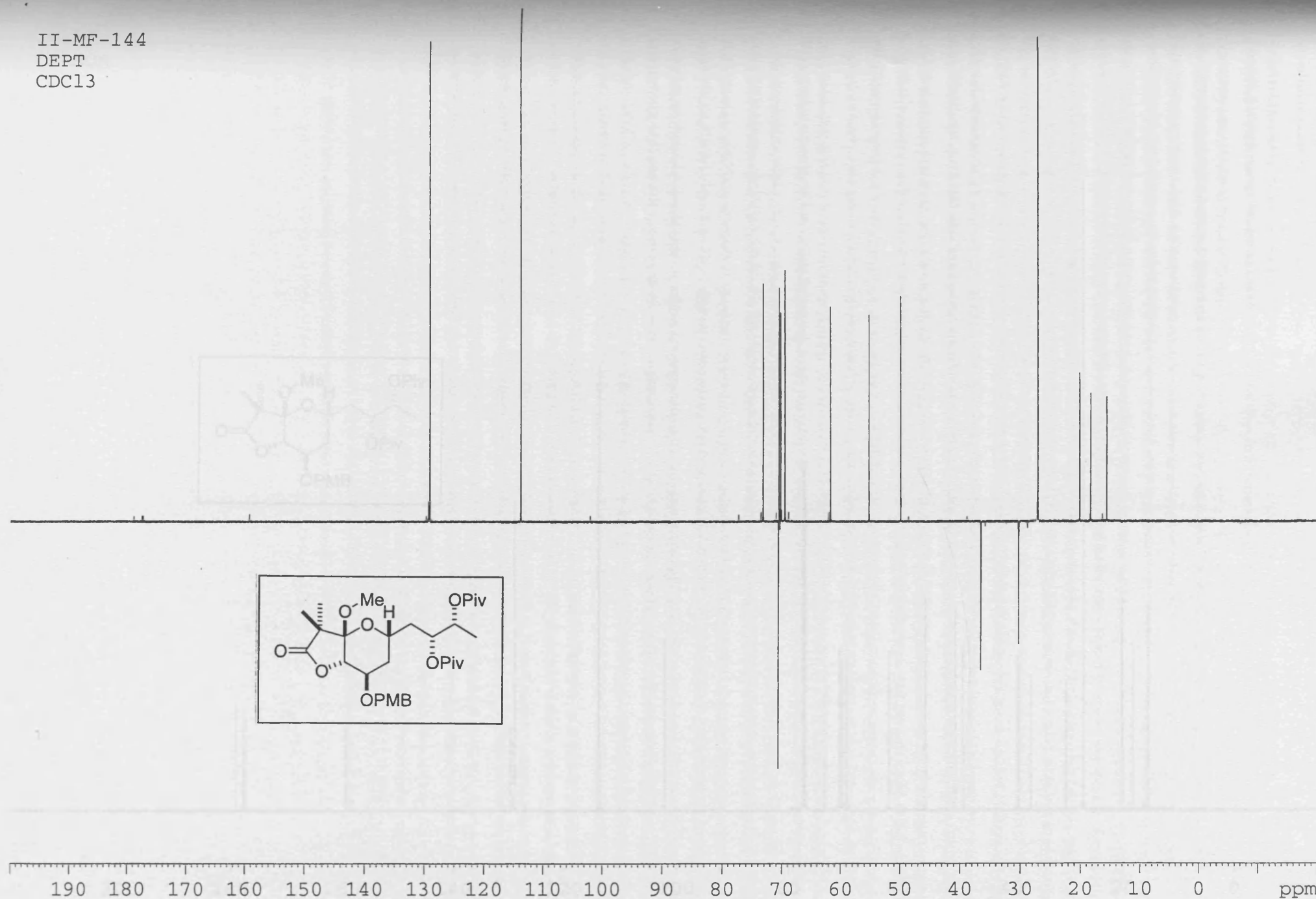
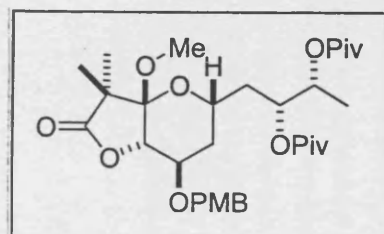
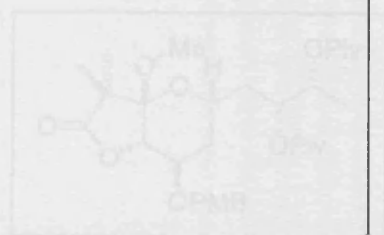
File:01SE442 Ident:36_38 Win 1000PPM Acq:12-FEB-2001 14:50:50 +2:00 Cal:FABLM080201_1
ZAB-SE4F FAB+ Magnet BpM:121 BpI:16657067 TIC:52518444 Flags:HALL
File Text:II-MF-144 FABMS MATRIX MNOBA + NA



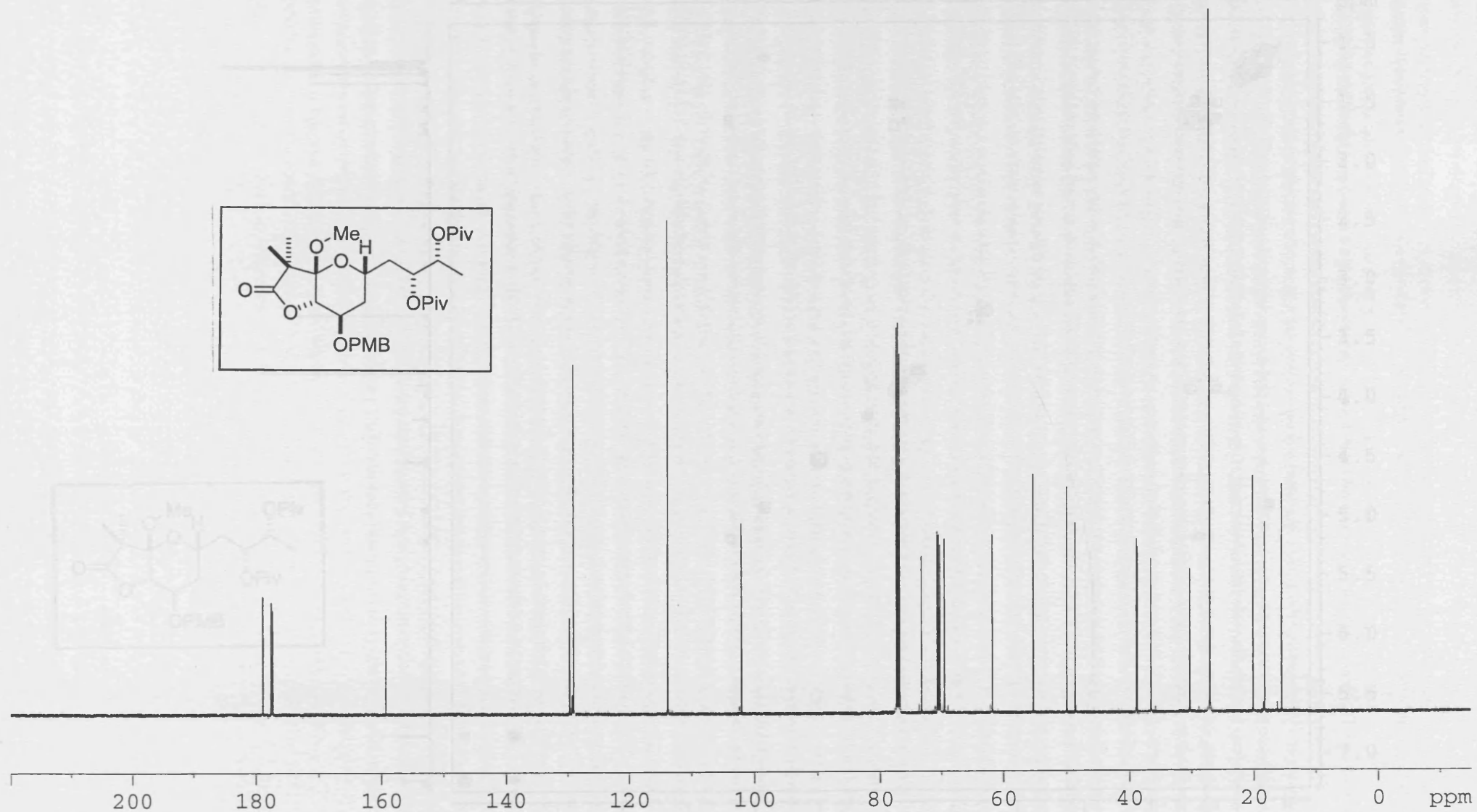
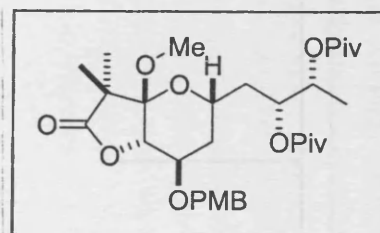
II-MF-144
HMQC
CDCl₃



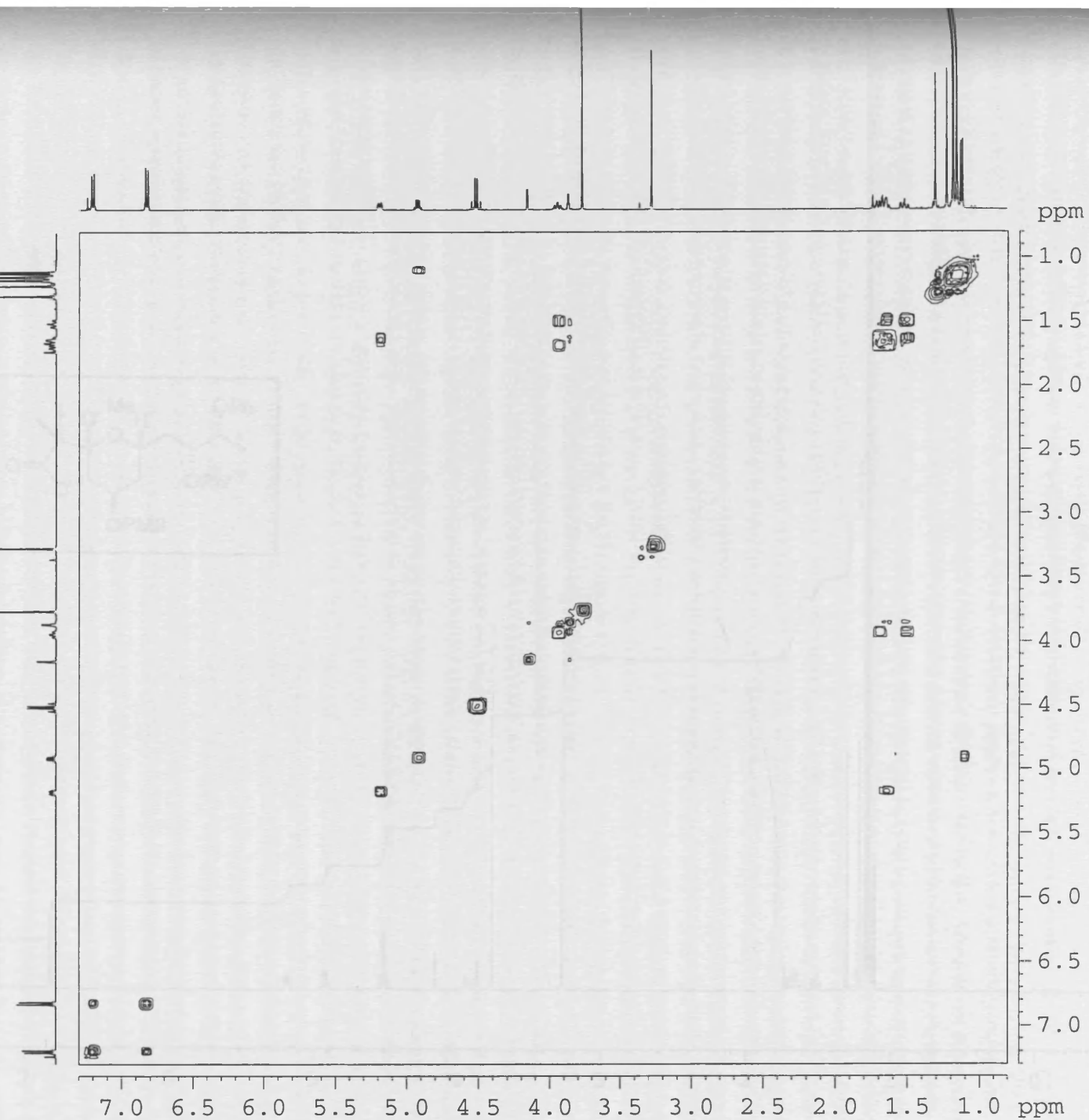
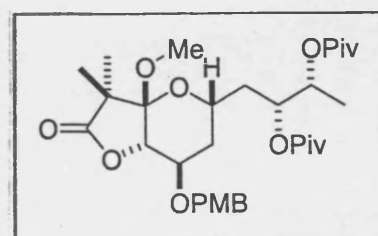
II-MF-144
DEPT
CDCl₃



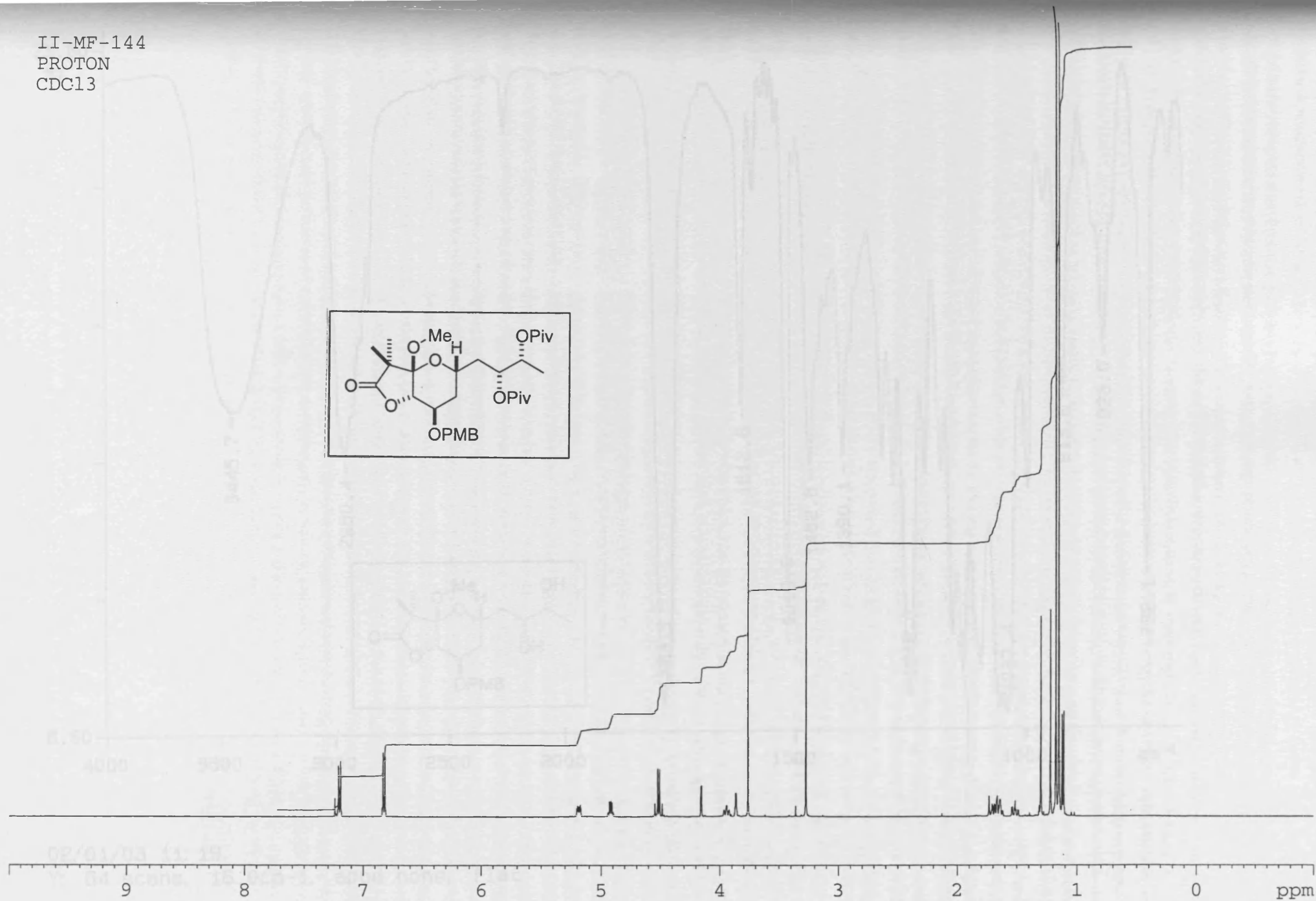
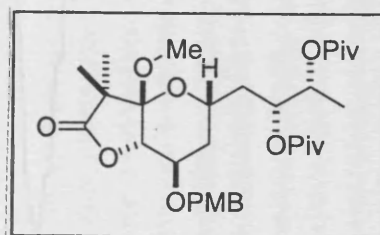
II-MF-144
CARBON
CDCl₃

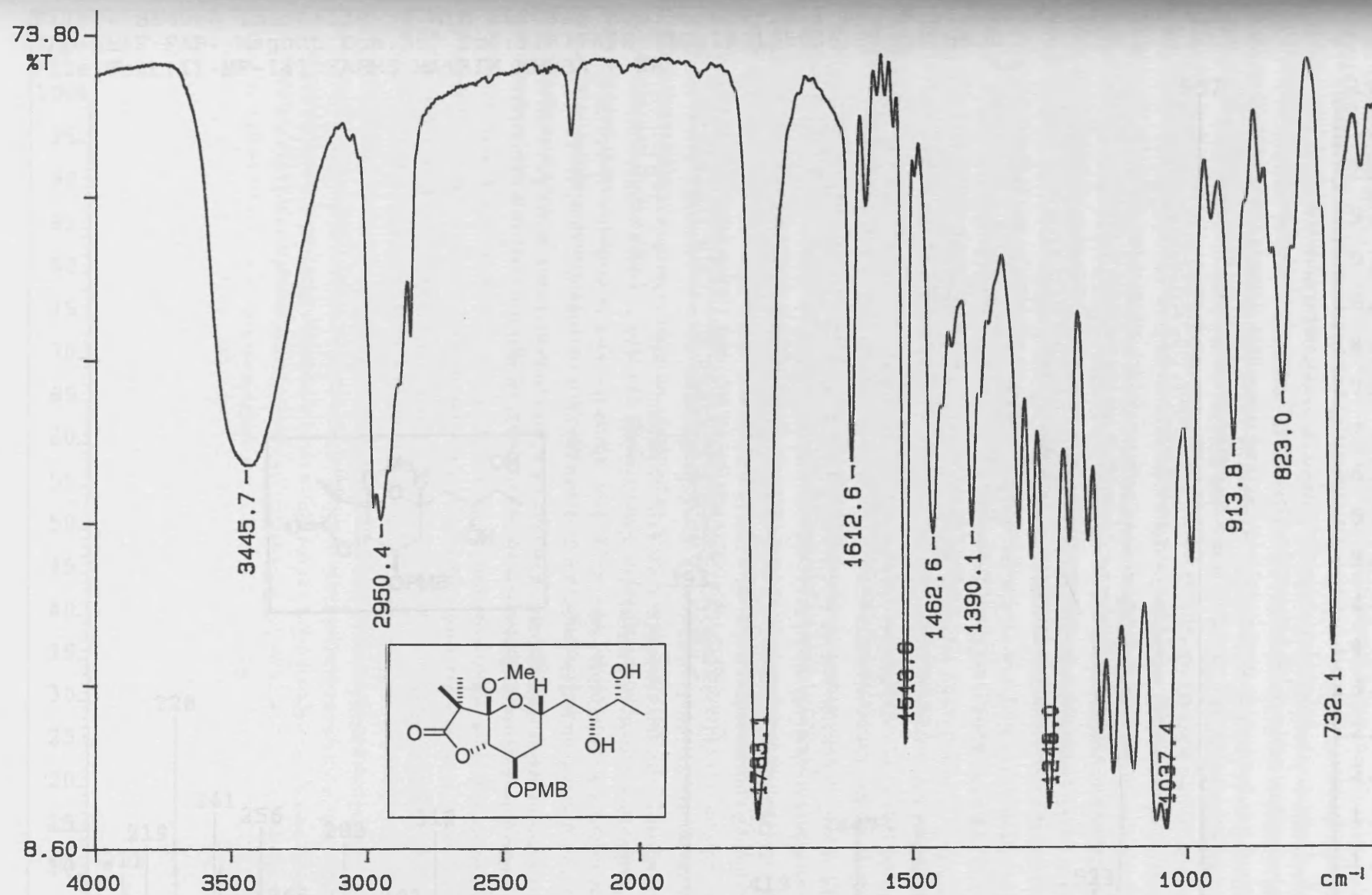


II-MF-144
COSY
CDCl₃



II-MF-144
PROTON
CDCl₃





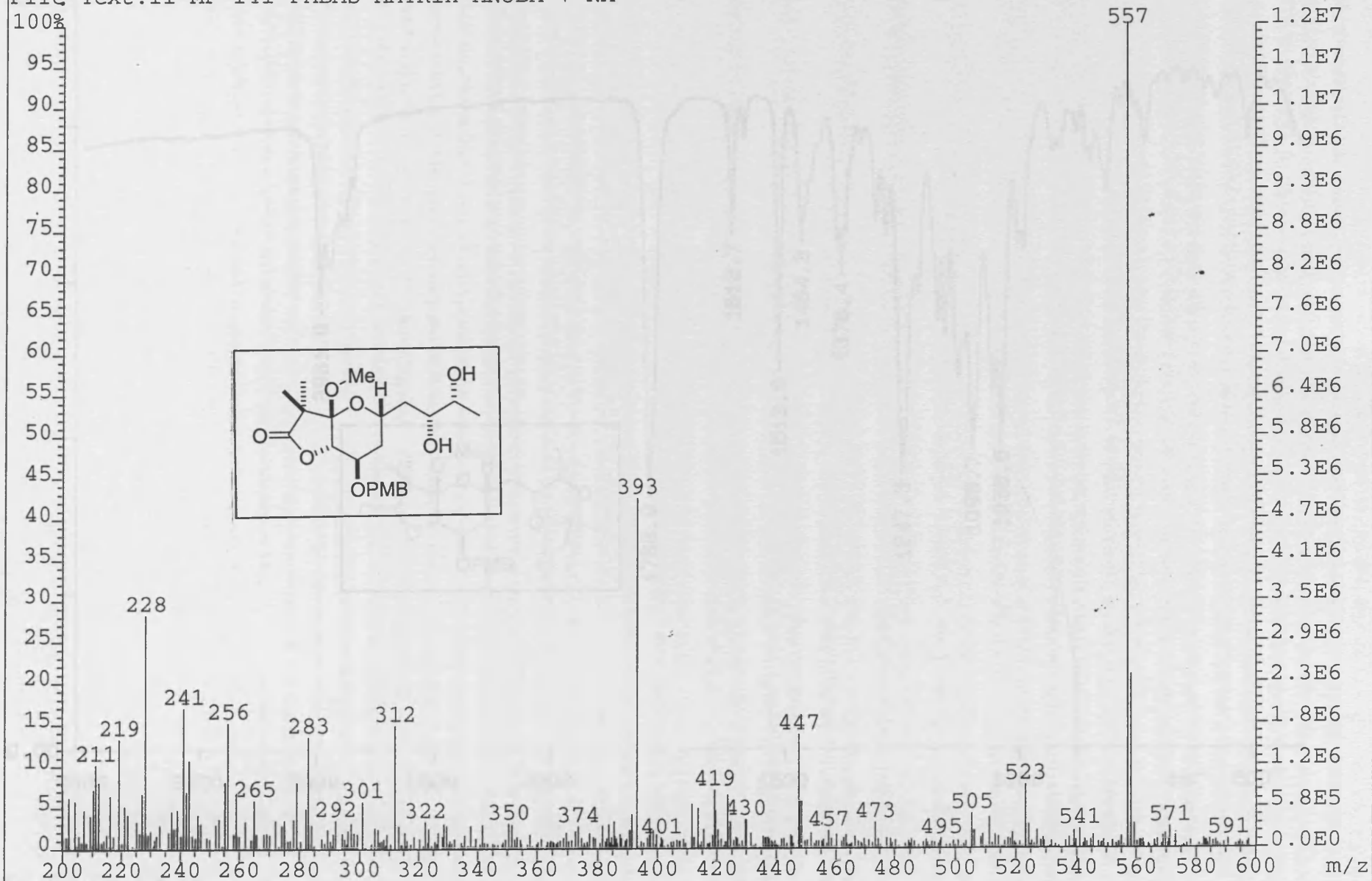
02/01/03 11:19

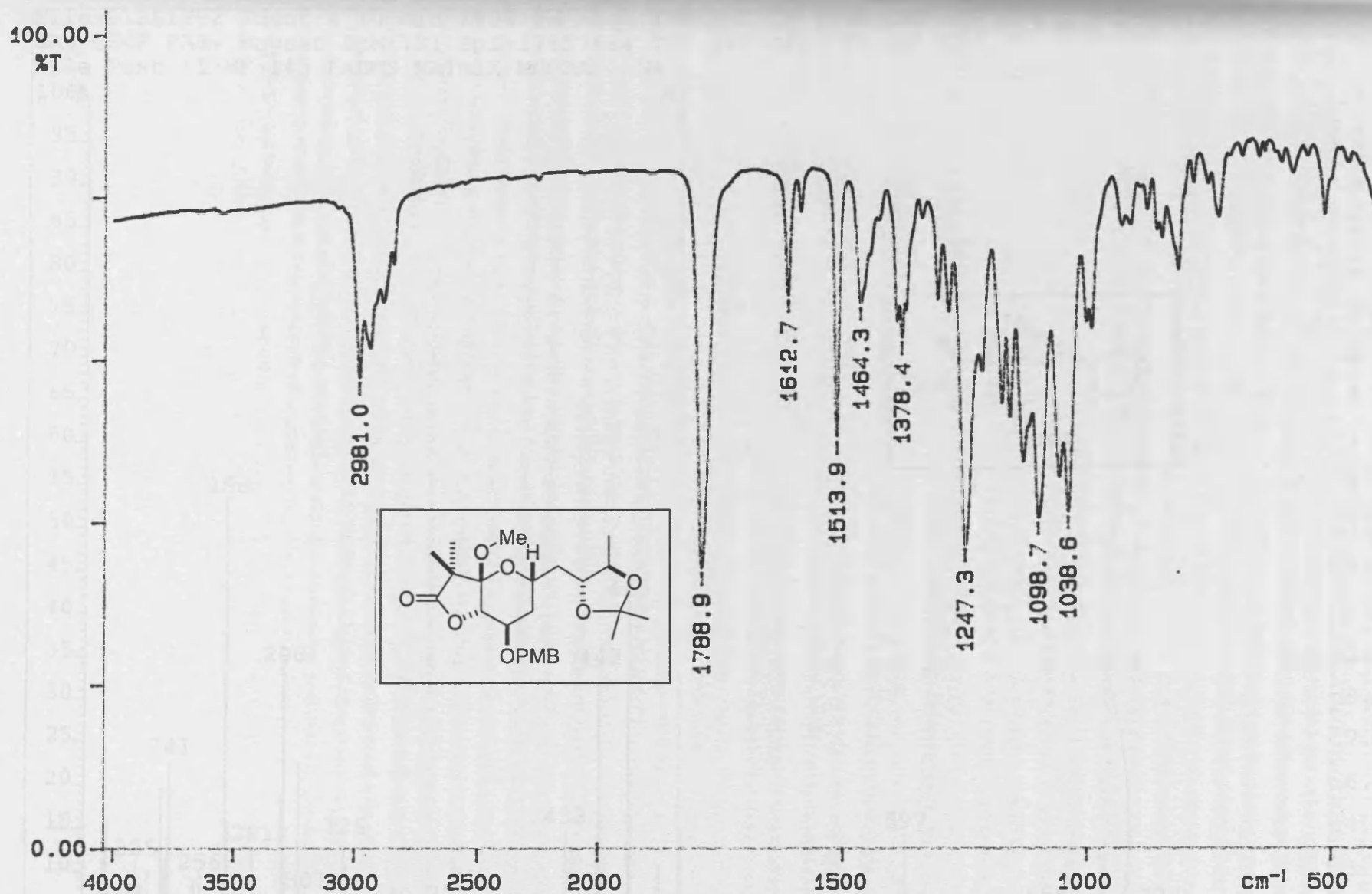
Y: 64 scans, 16.0cm⁻¹, apod none, flat

File:01SE4060 Ident:138-58 Win 1000PPM Acq: 1-NOV-2001 09:49:37 Cal:FABLM011101_1

ZAB-SE4F FAB+ Magnet BpM:557 BpI:11677696 TIC:189155936 Flags:HALL

File Text:II-MF-141 FABMS MATRIX MNOBA + NA





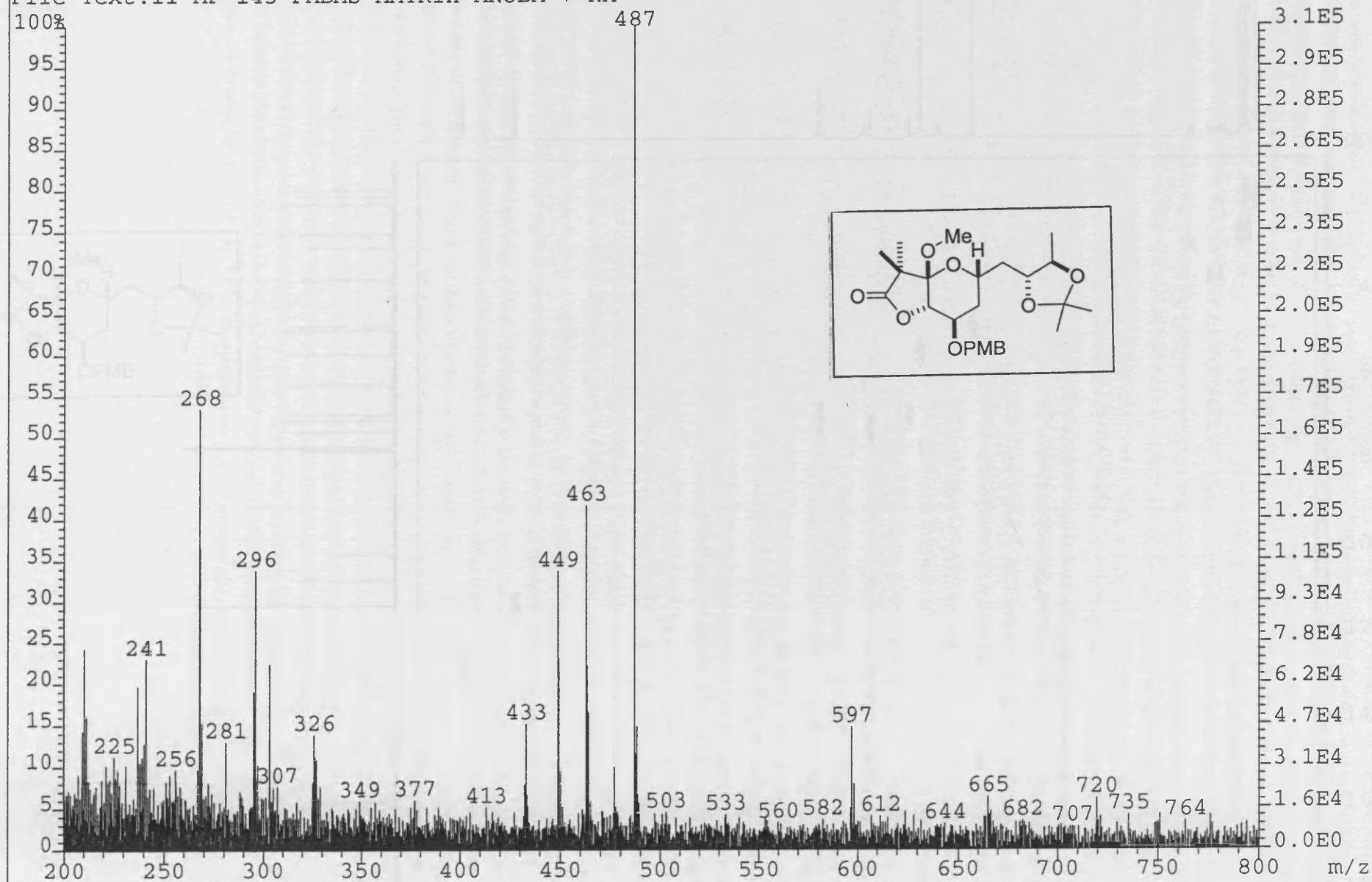
01/03/05 12:15

Y: 64 scans, 4.0cm⁻¹

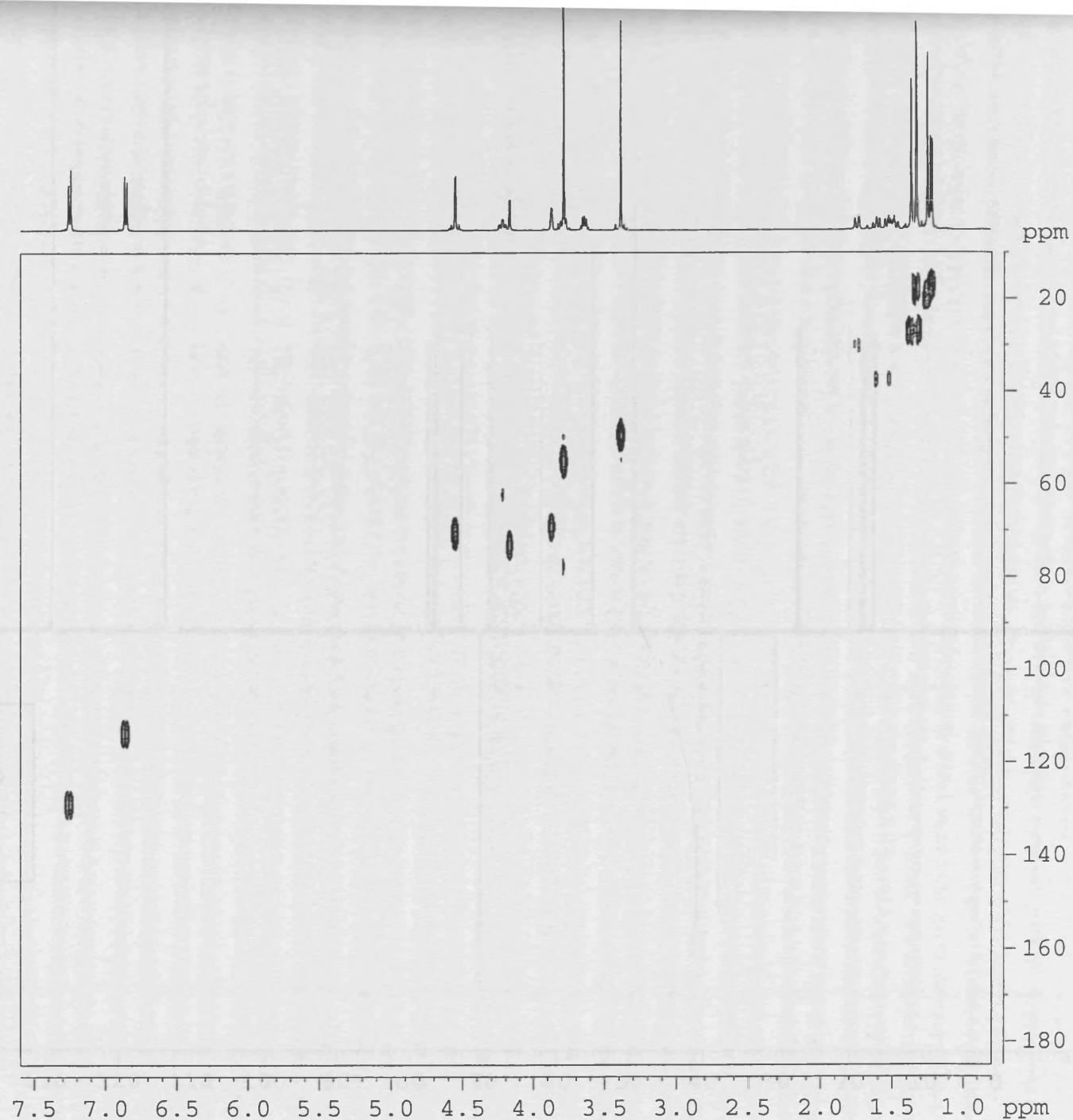
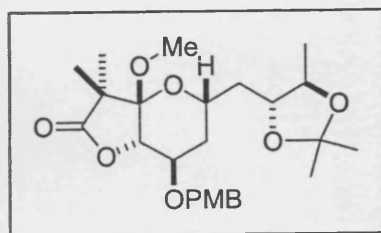
File:01SE1692 Ident:4_10 Win 1000PPM Acq: 1-MAY-2001 11:49:49 +0:25 Cal:FABMM010501_1

ZAB-SE4F FAB+ Magnet BpM:121 BpI:17857684 TIC:54860280 Flags:HALL

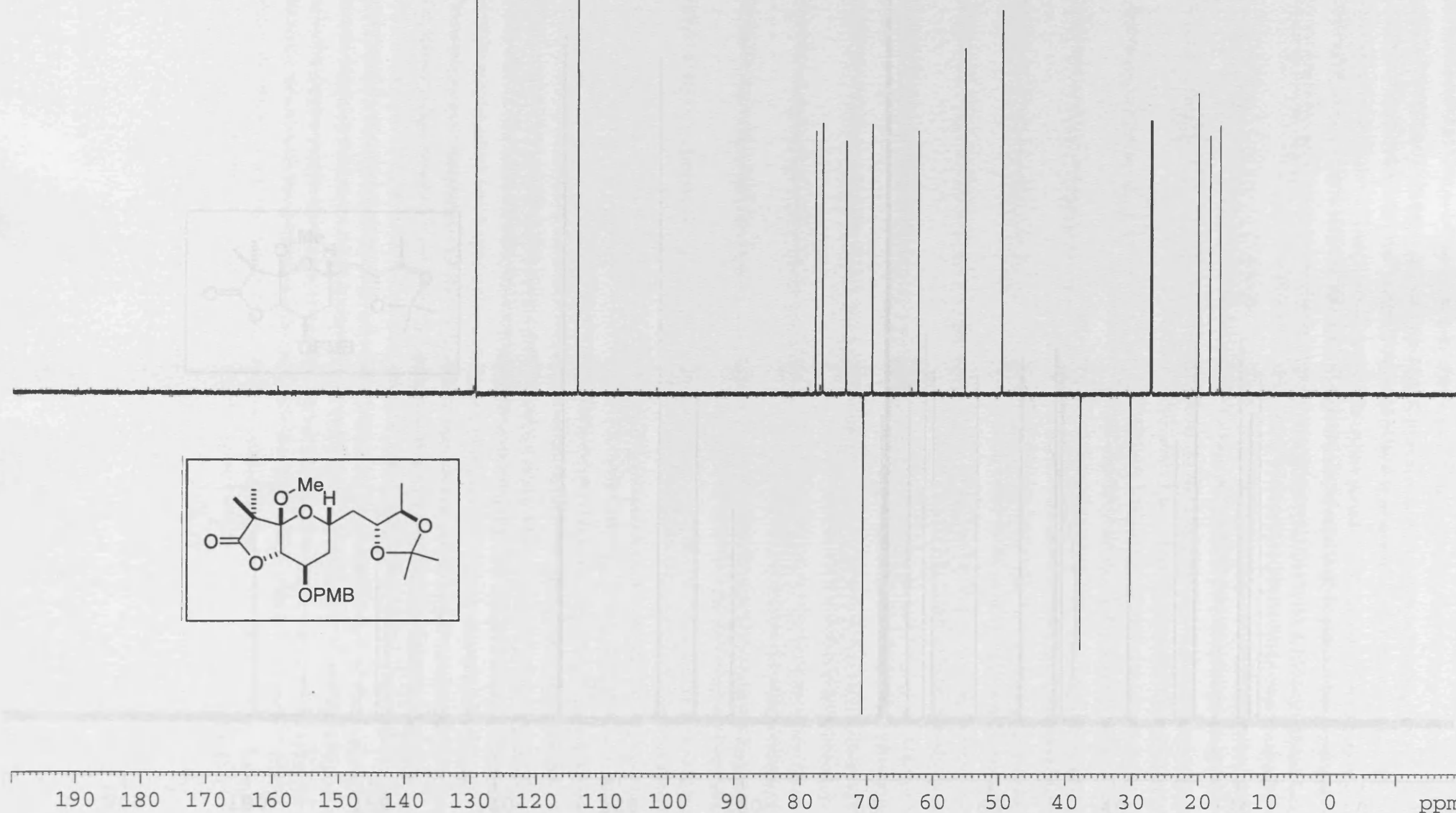
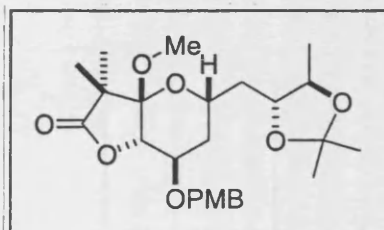
File Text:II-MF-145 FABMS MATRIX MNOBA + NA



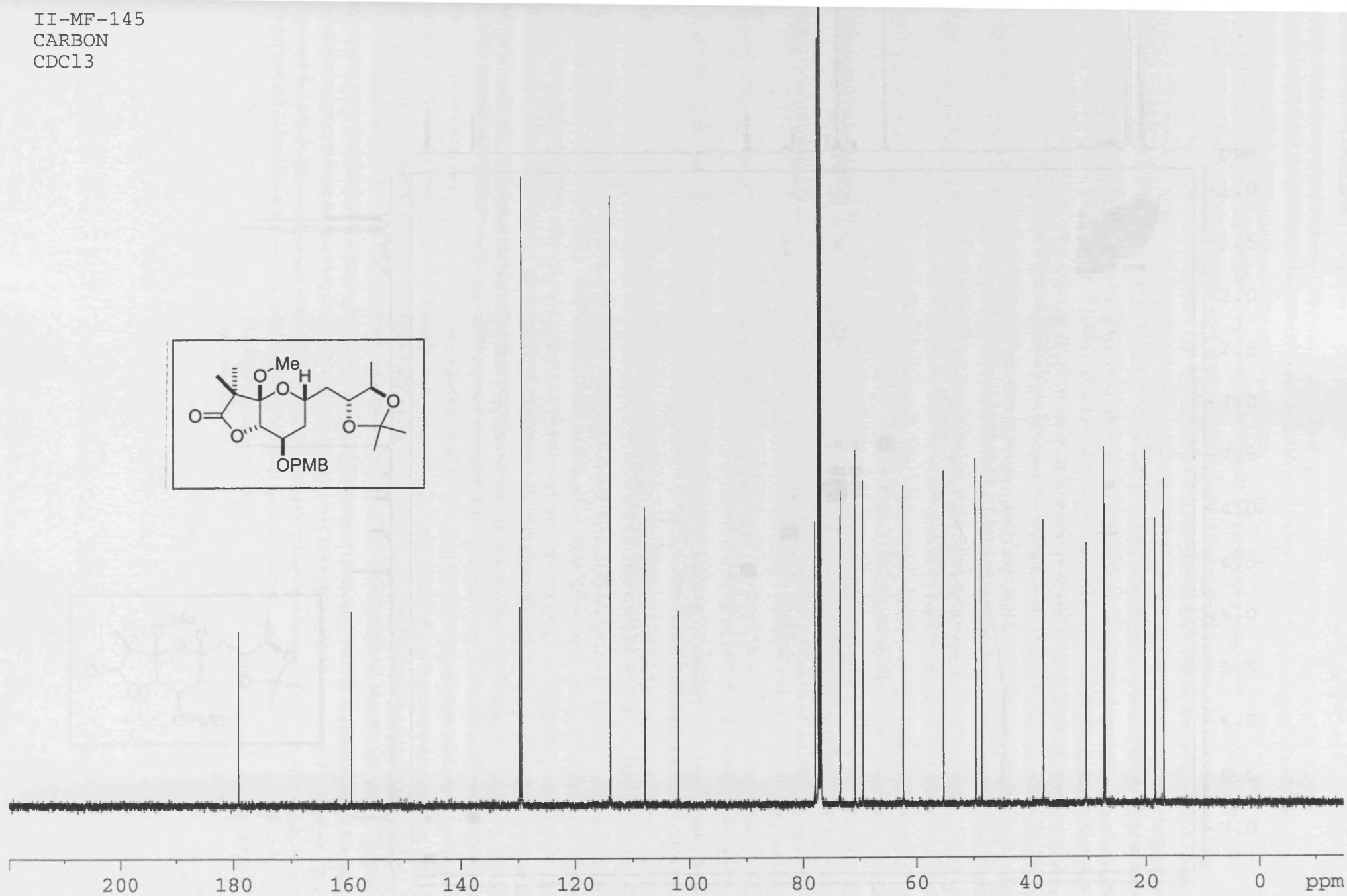
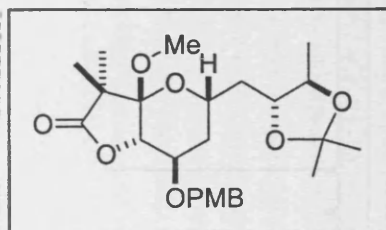
II-MF-145
HMQC
CDCl₃



II-MF-145
DEPT
CDC13



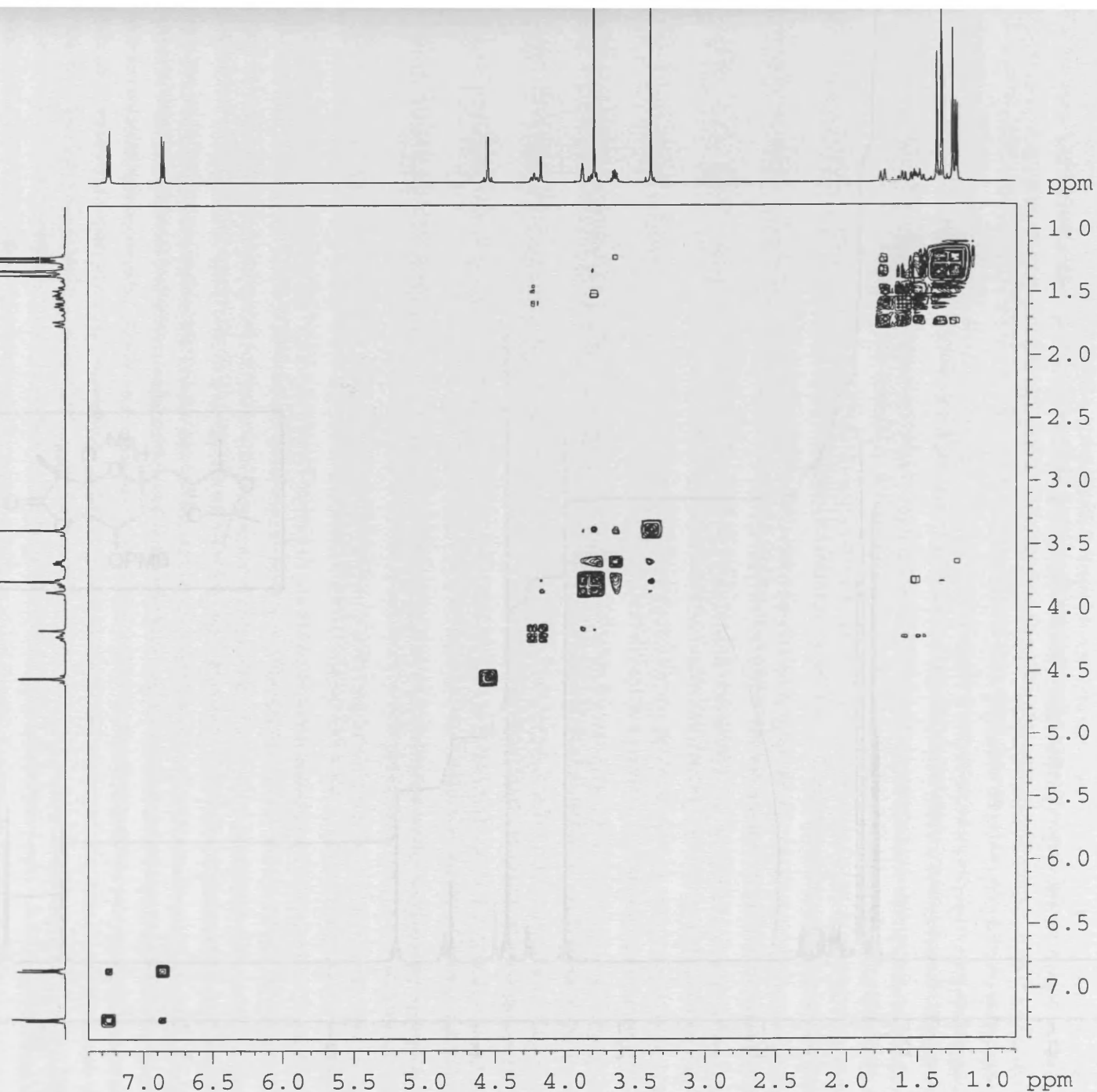
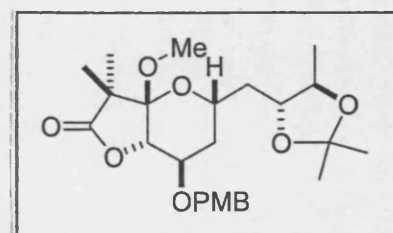
II-MF-145
CARBON
CDCl₃



II-MF-145

COSY

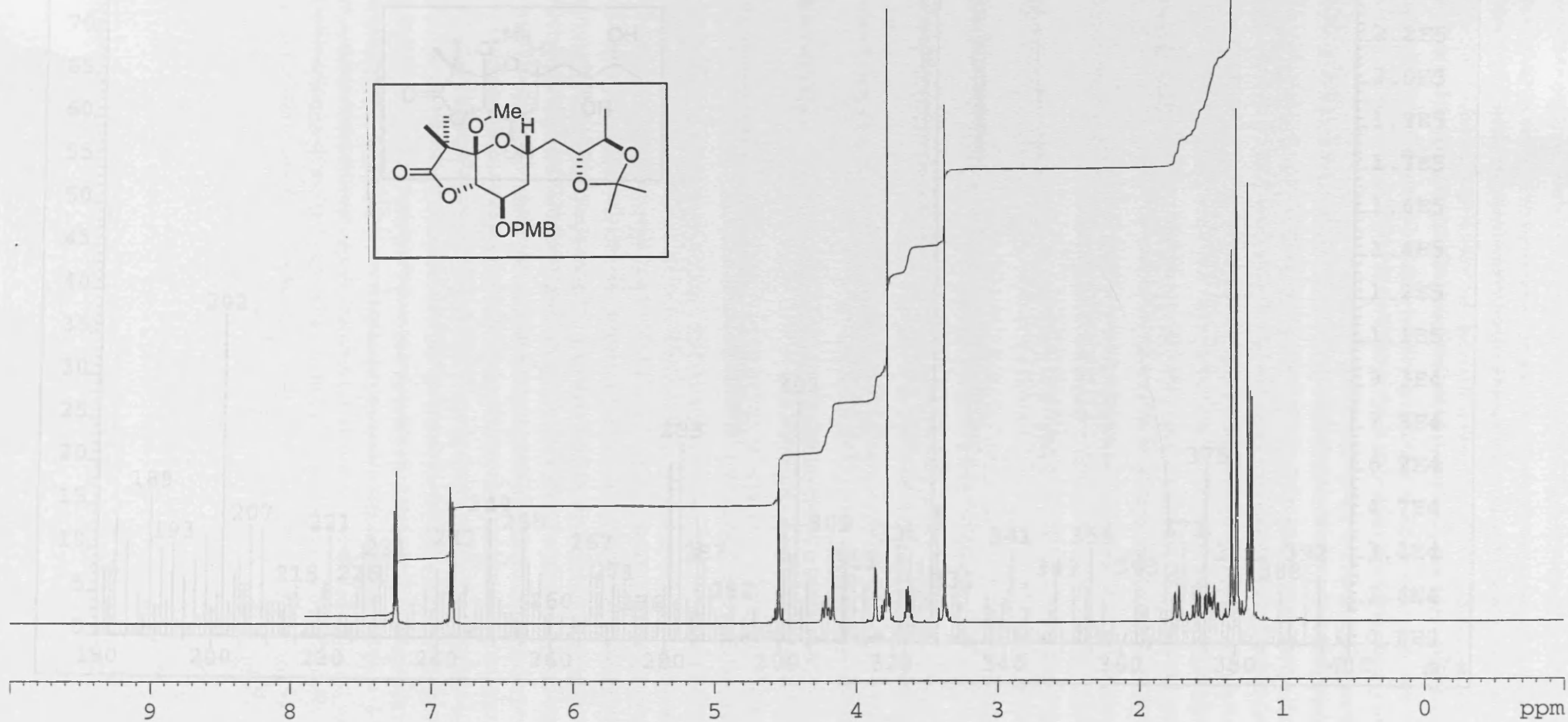
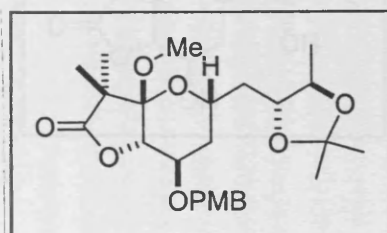
CDC13



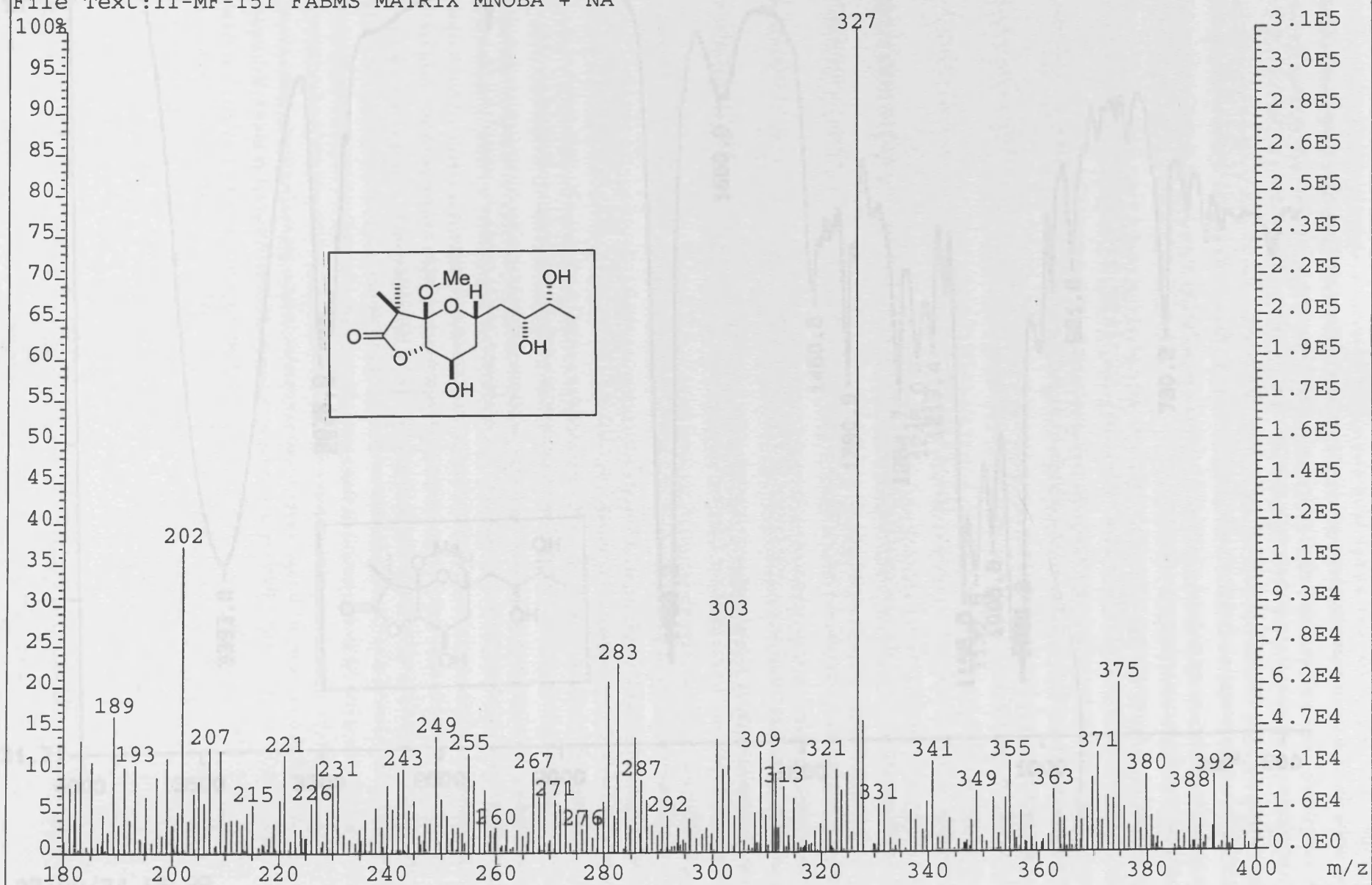
II-MF-145

PROTON

CDC13

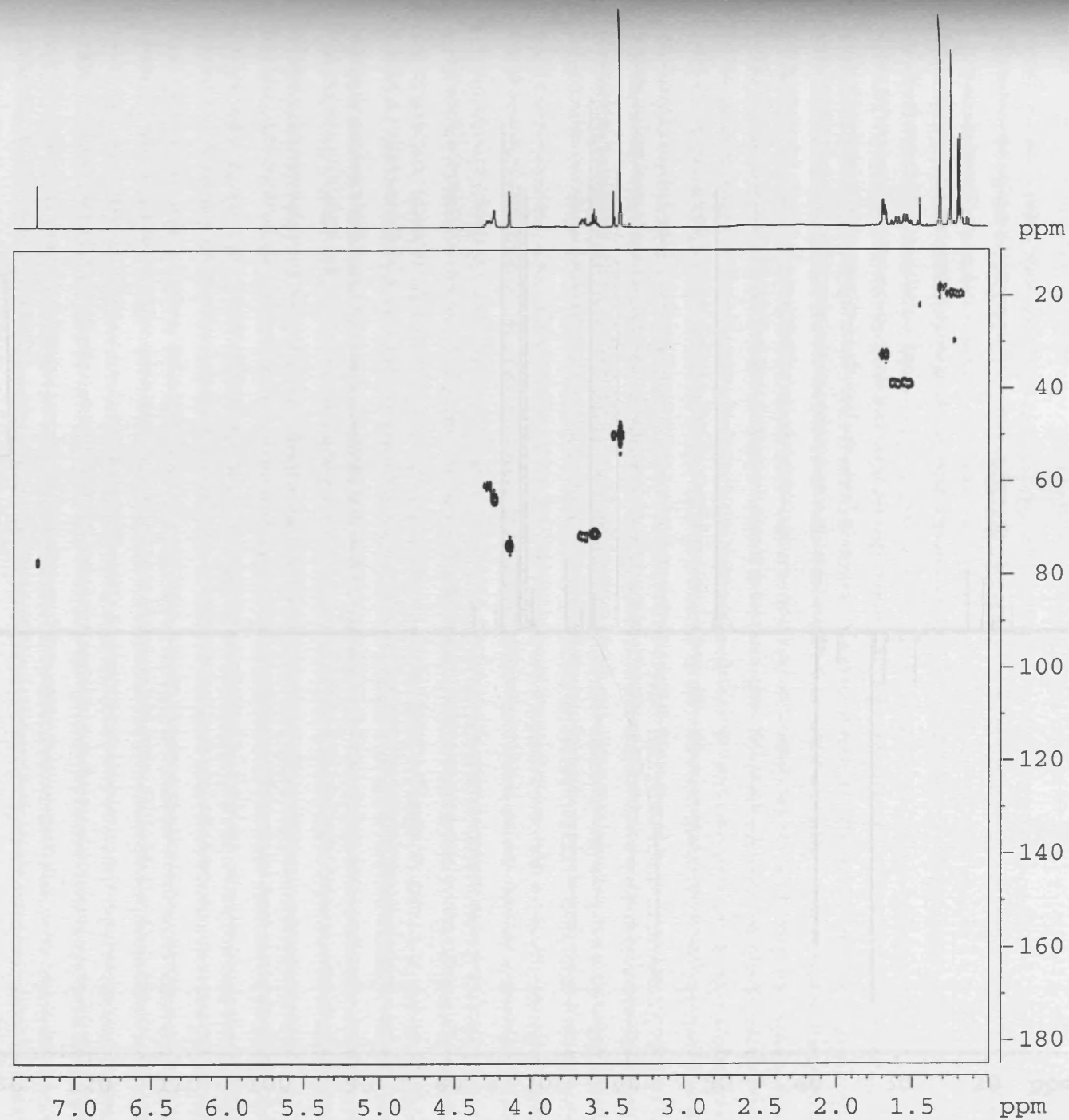
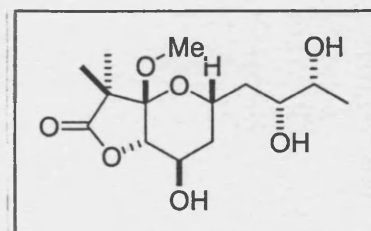


File:01SE928 Ident:44_49-15 Win 1000PPM Acq: 9-MAR-2001 11:07:50 +2:30 Cal:FABLM090301_1
ZAB-SE4F FAB+ Magnet BpM:121 BpI:5528406 TIC:23462890 Flags:HALL
File Text:II-MF-151 FABMS MATRIX MNOBA + NA

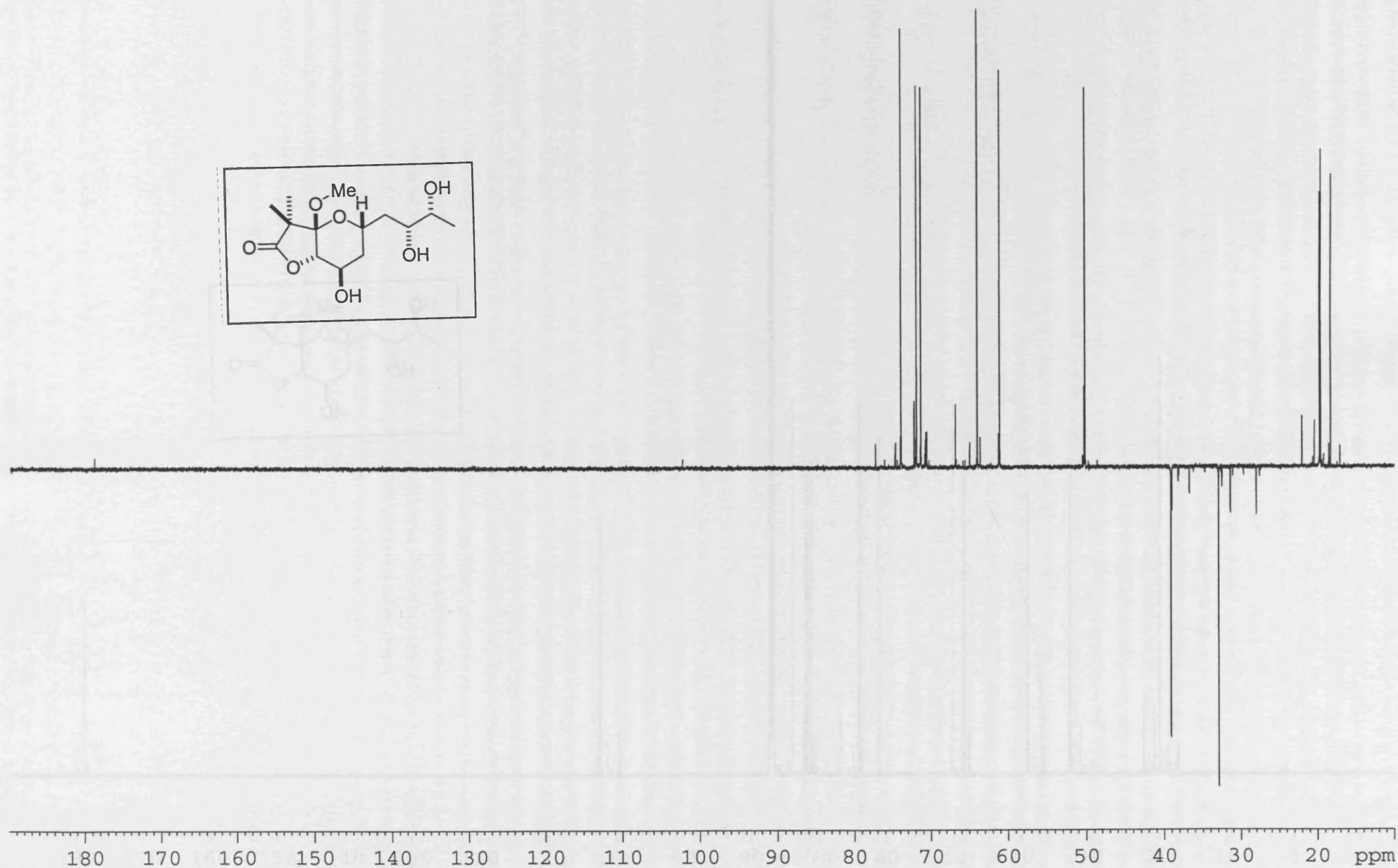
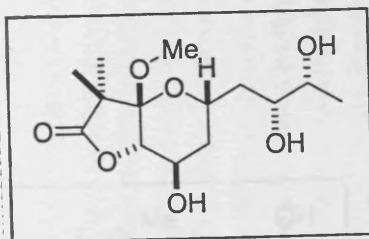


X: 64 scans, 16.0cm⁻¹, apod none, flat

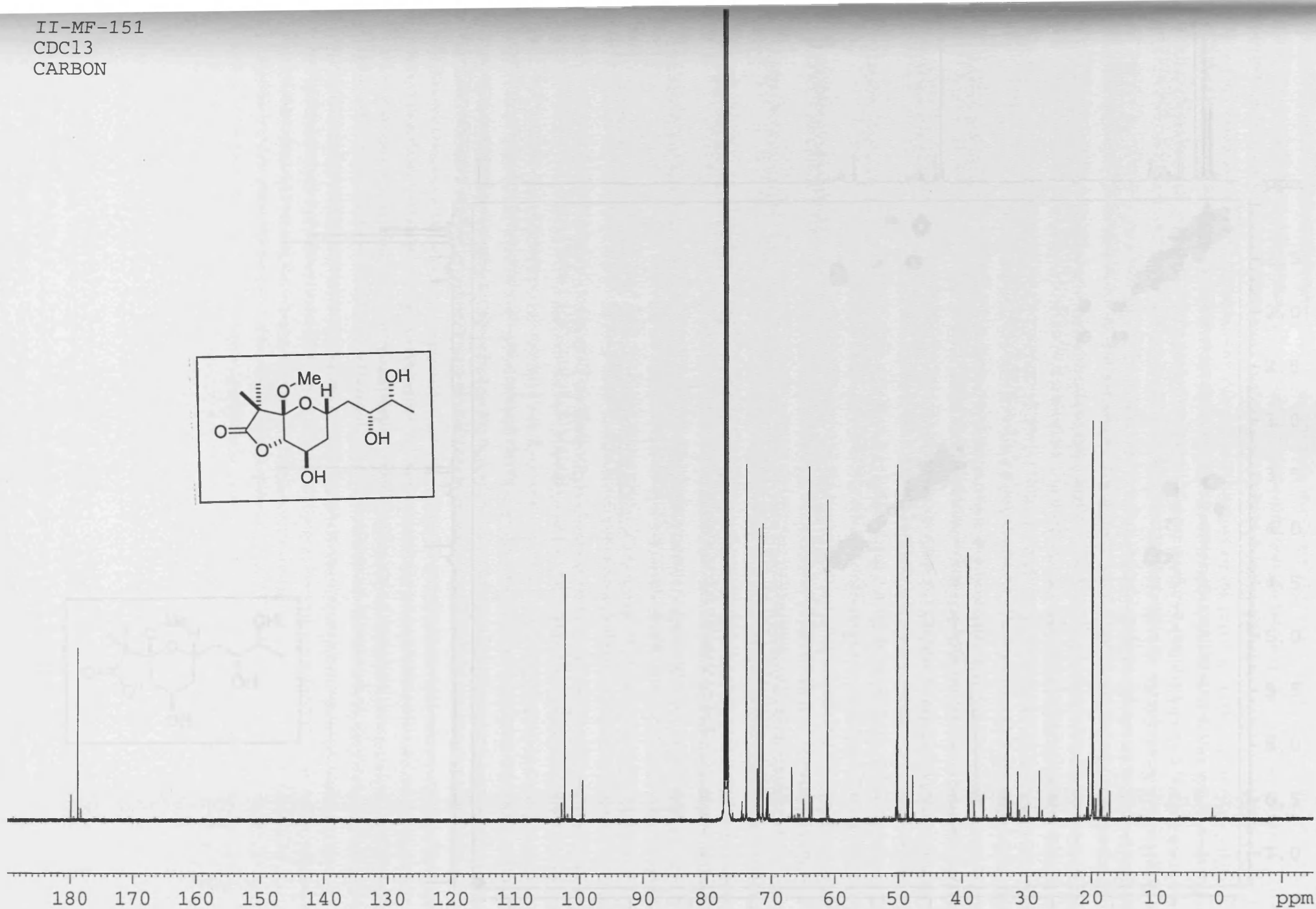
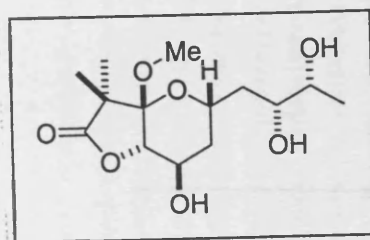
II-MF-151
CDCl₃
HMQC



II-MF-151
CDCl₃
DEPT



II-MF-151
CDCl₃
CARBON

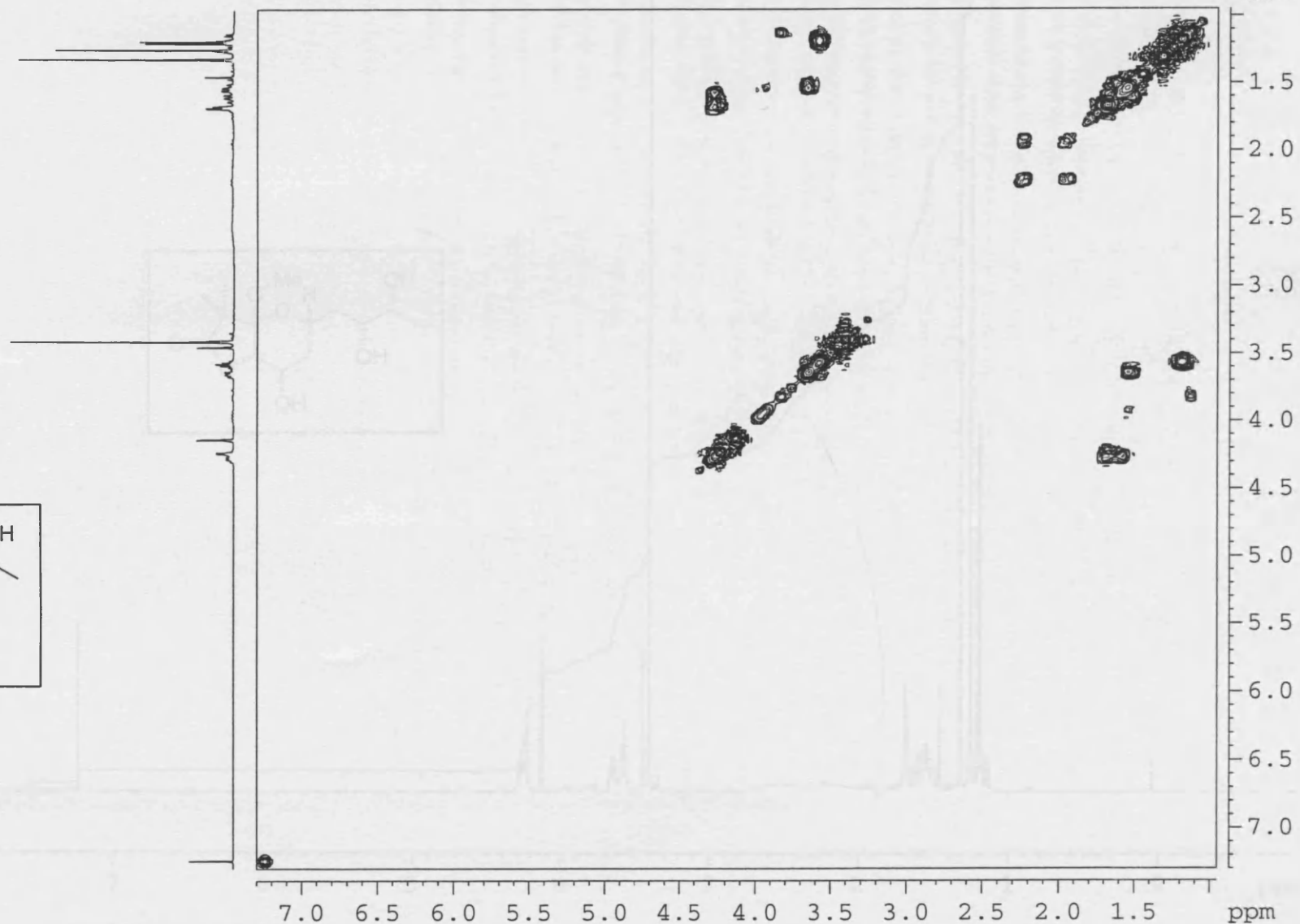
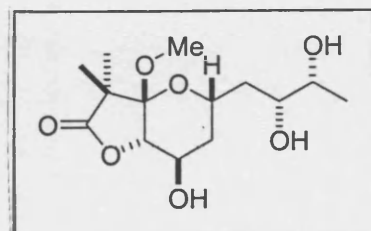


II-MF-151

CDC13

COSY

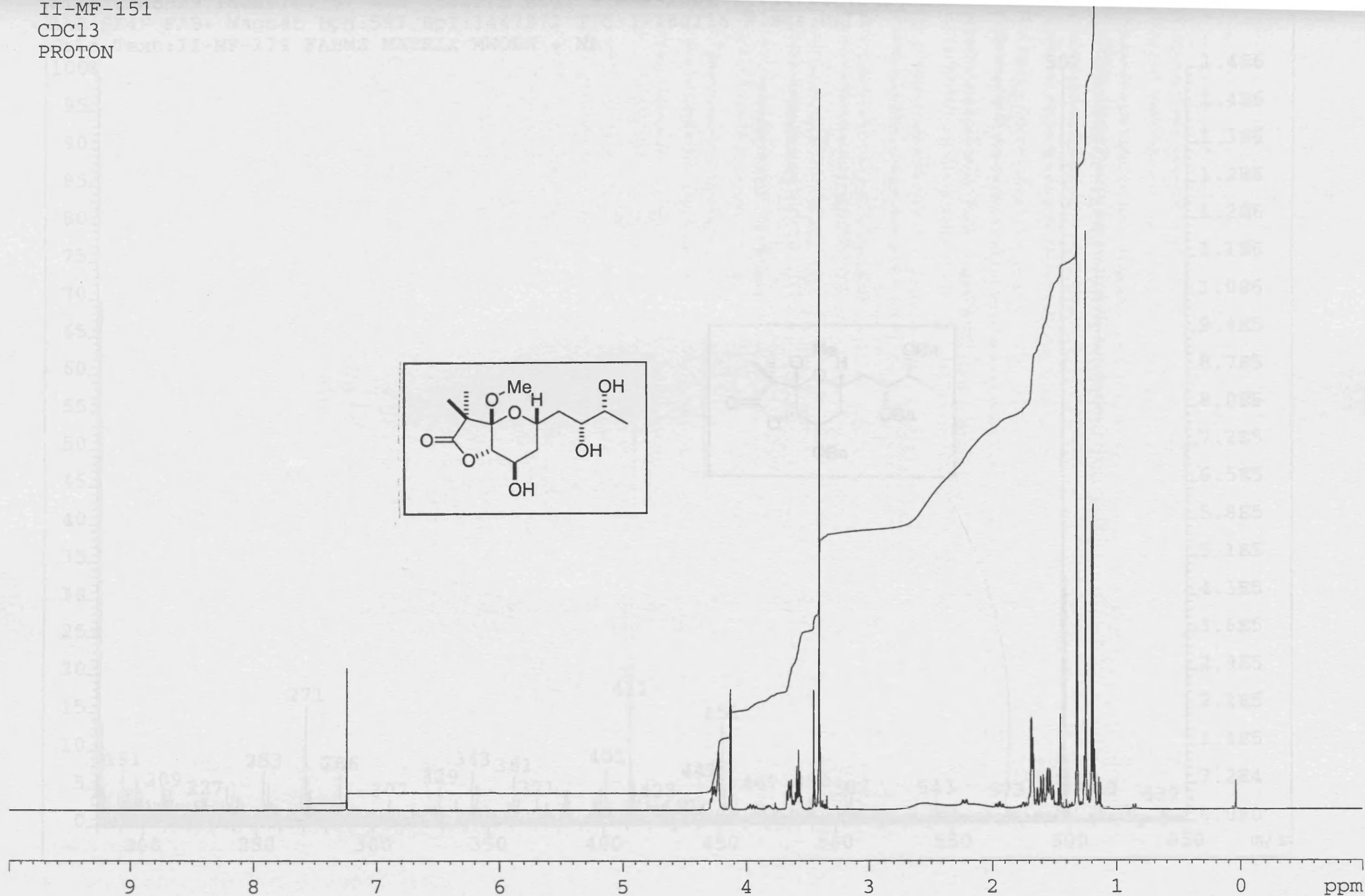
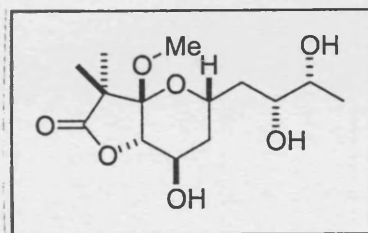
PROTON



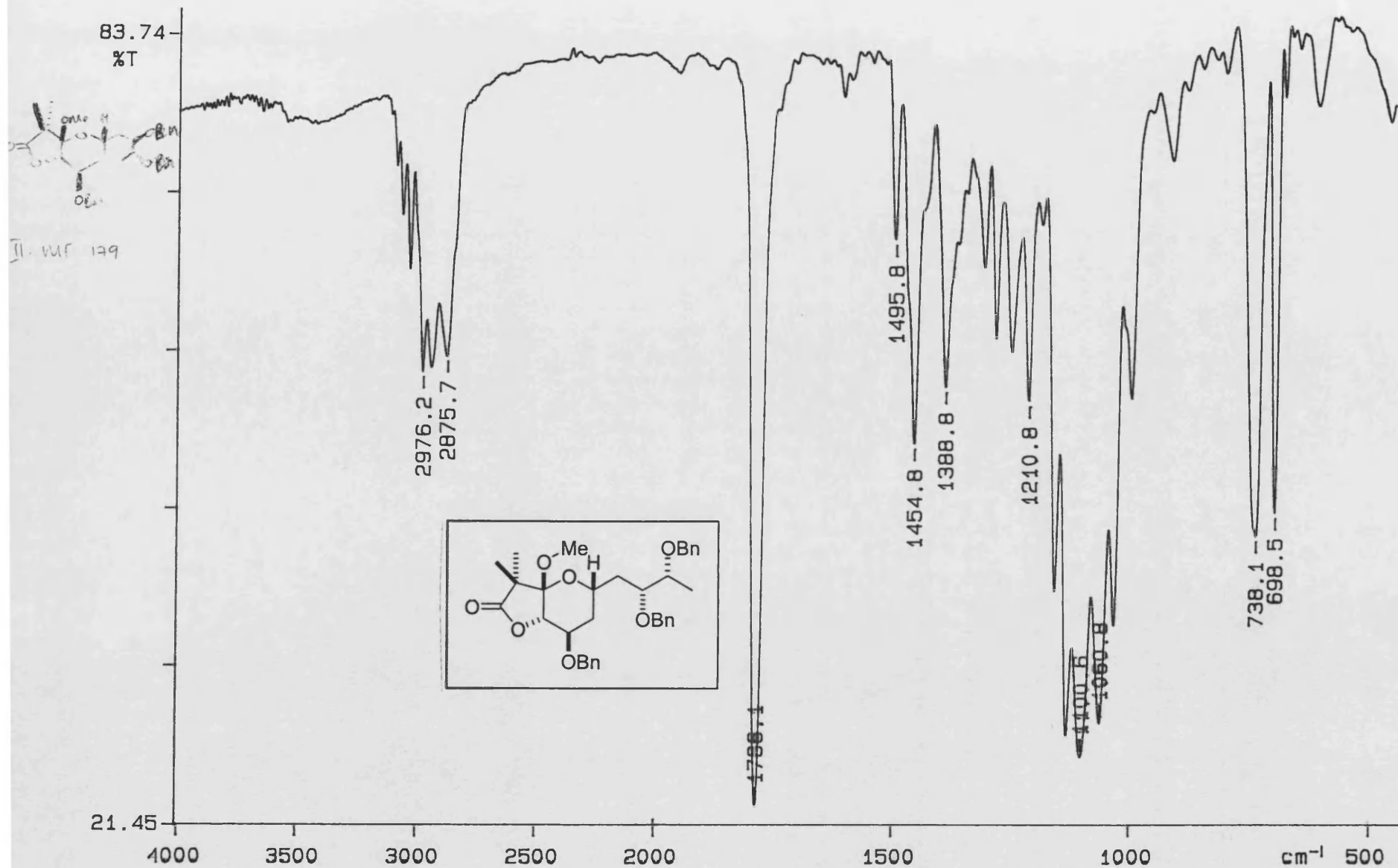
II-MF-151

CDC13

PROTON



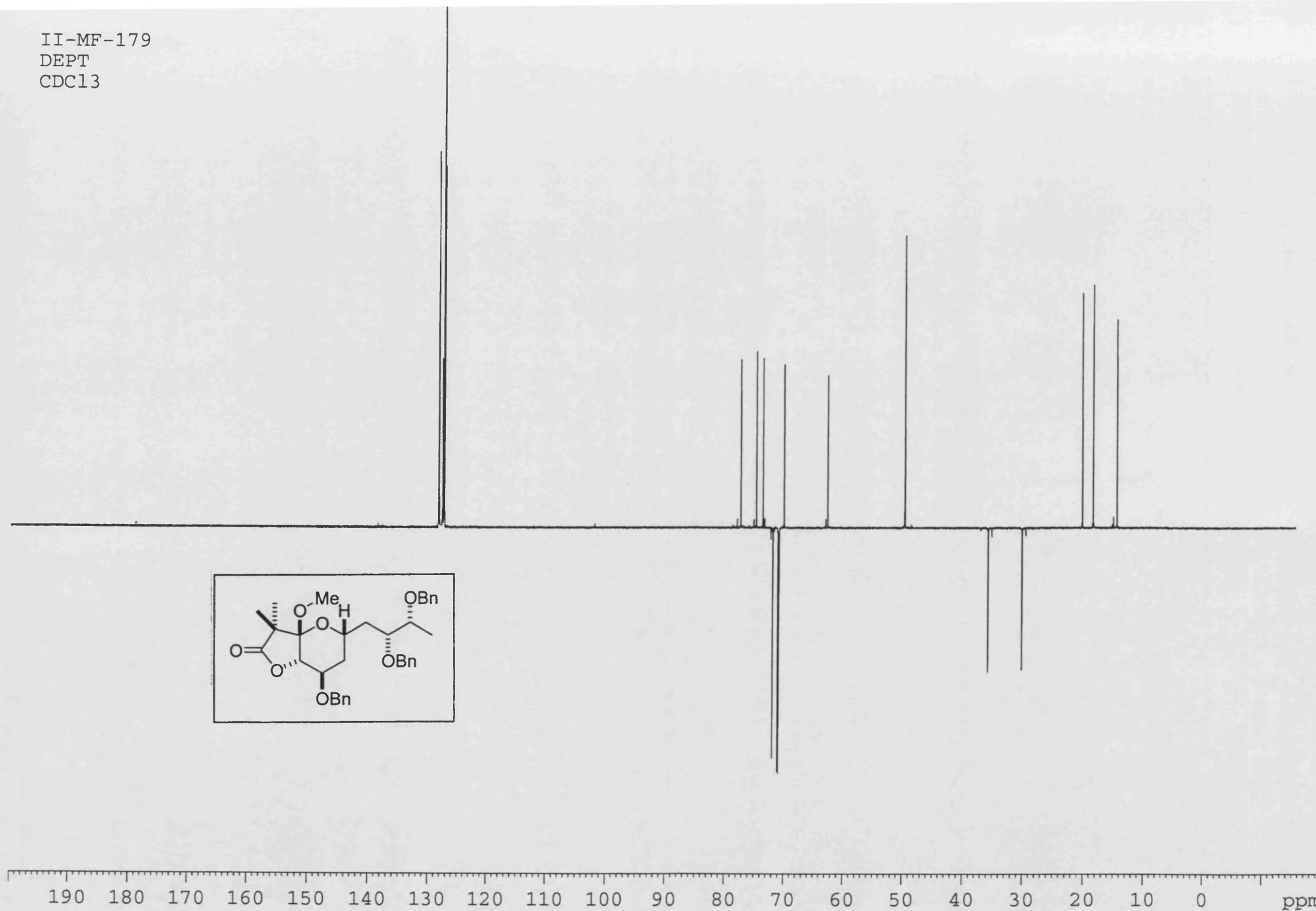
PERKIN ELMER



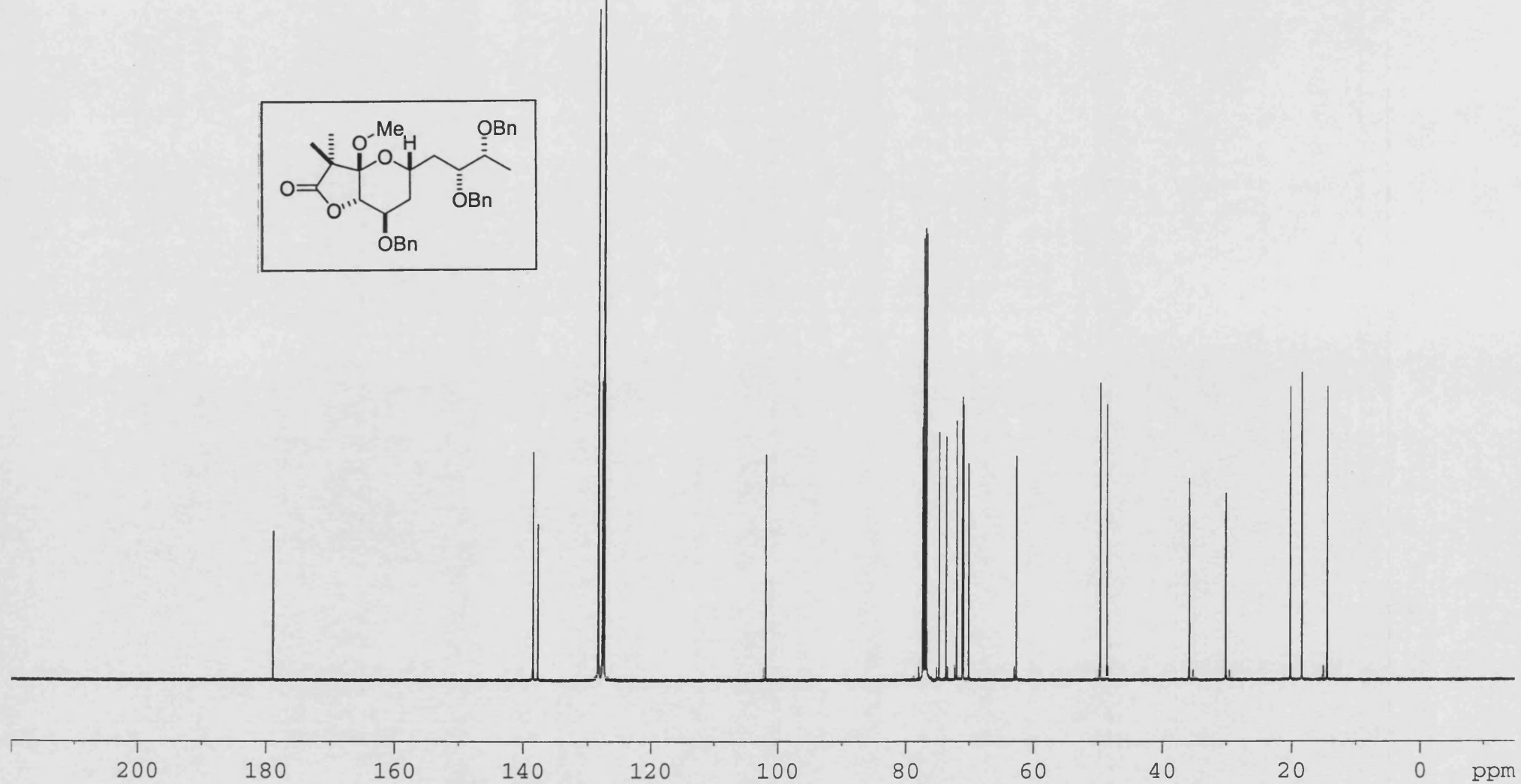
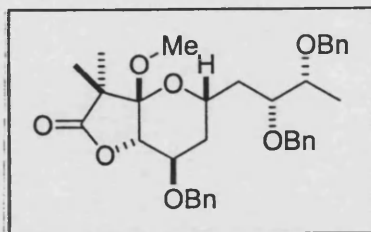
01/12/06 11:23

X: 64 scans, 16.0cm⁻¹, apod none

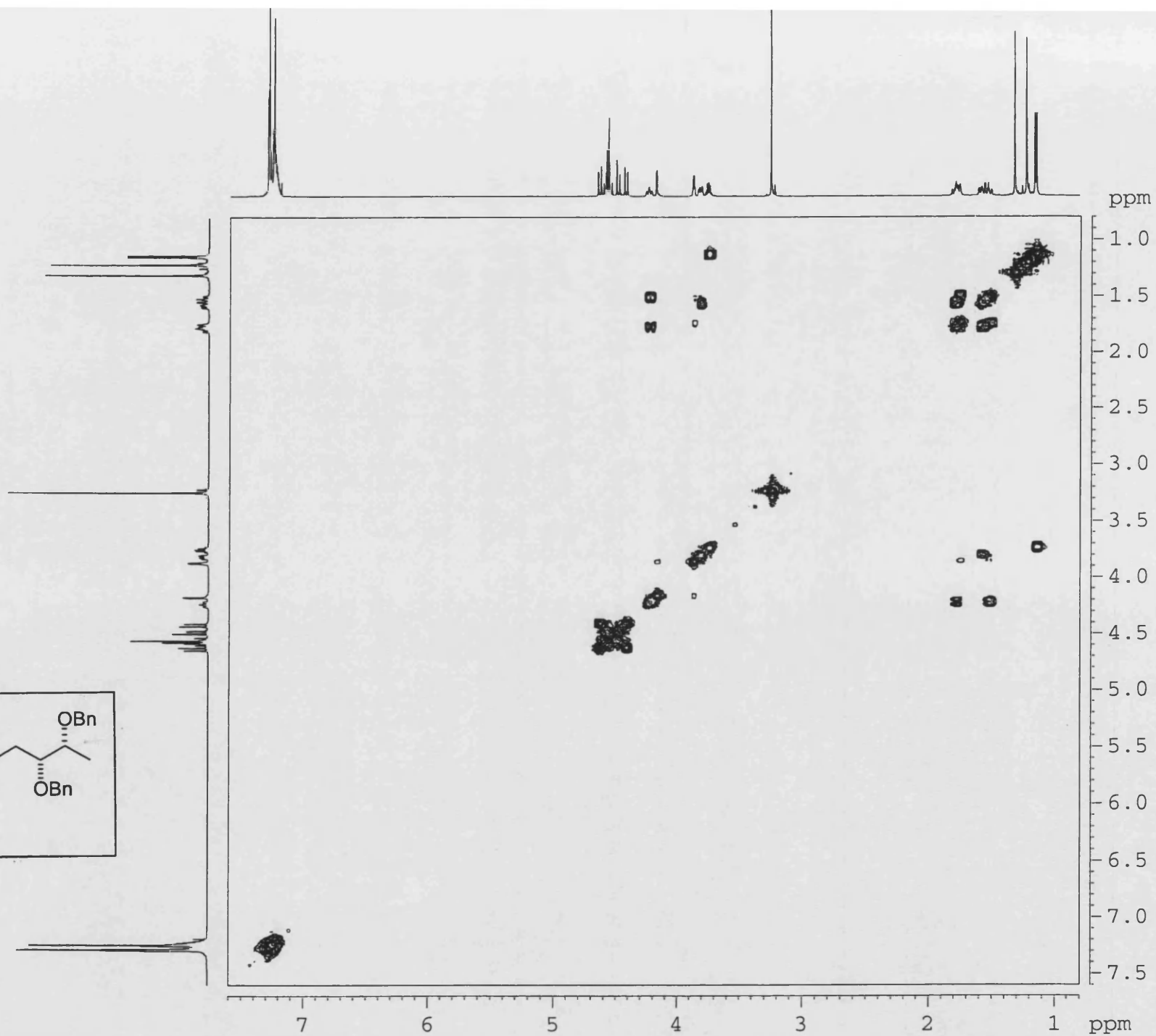
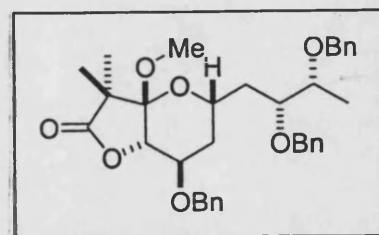
II-MF-179
DEPT
CDCl₃



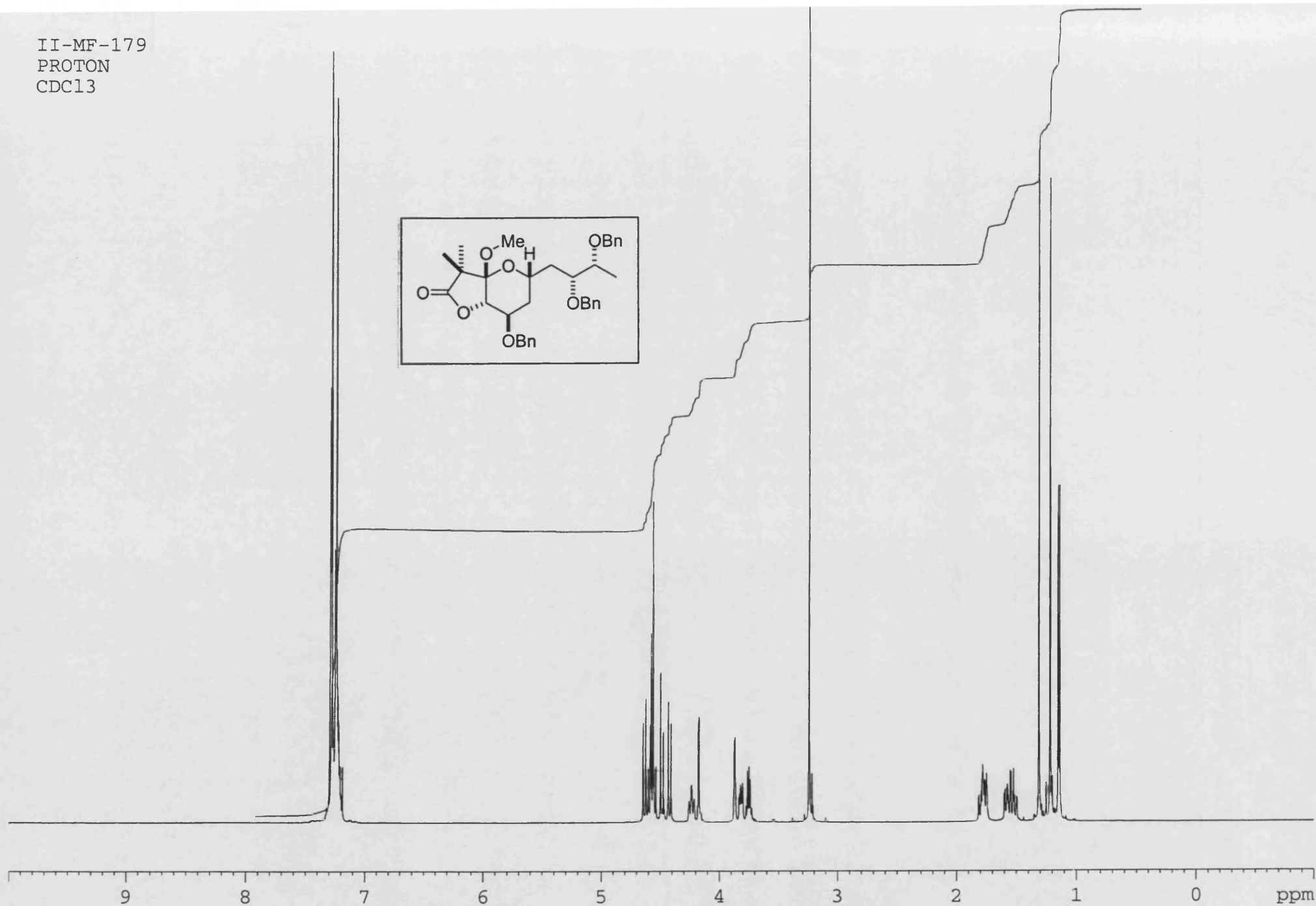
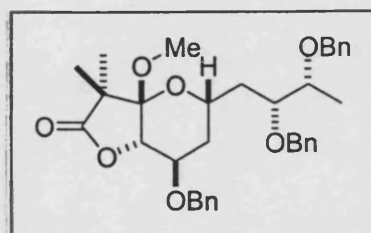
II-MF-179
CARBON
CDCl₃



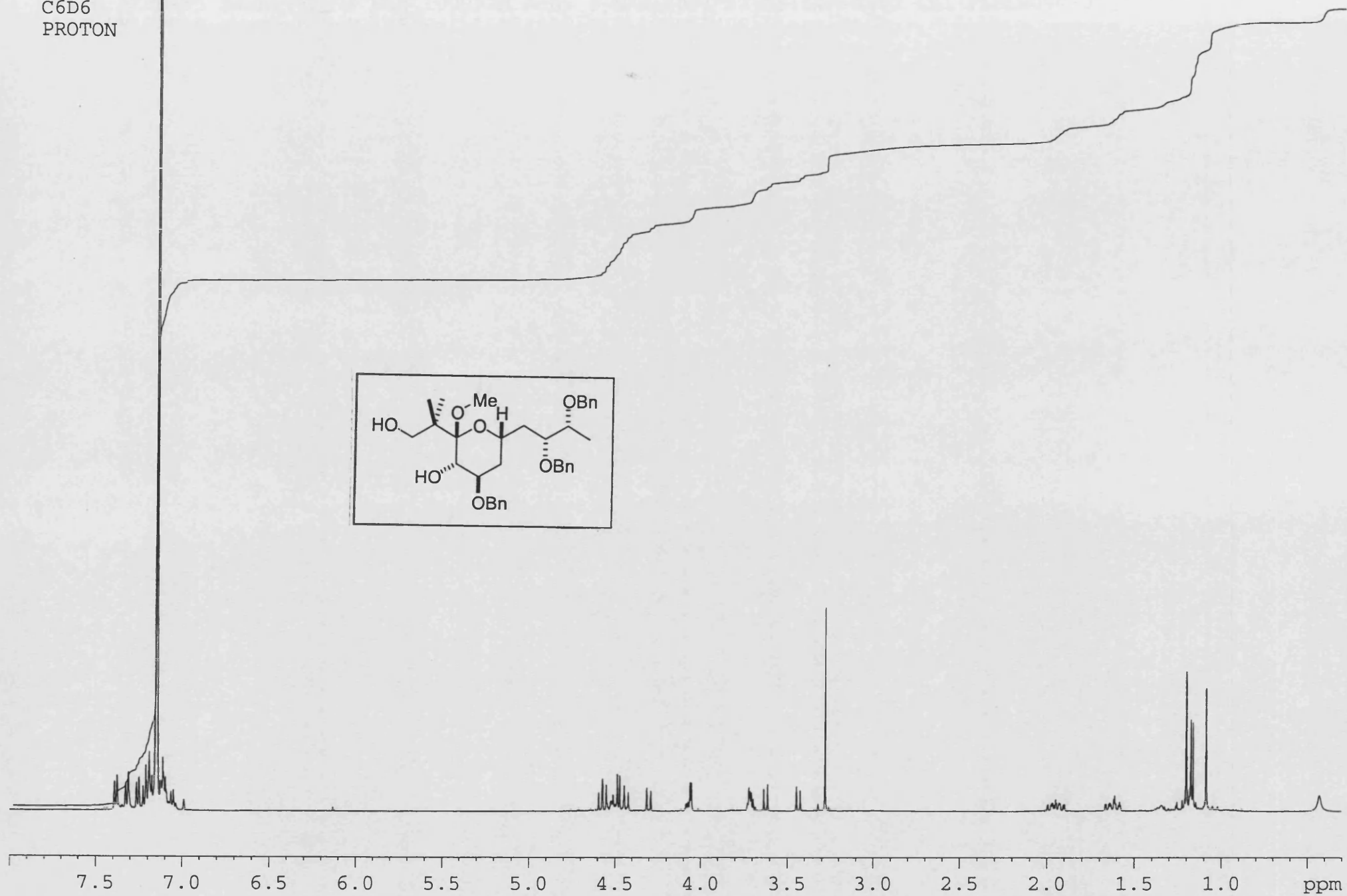
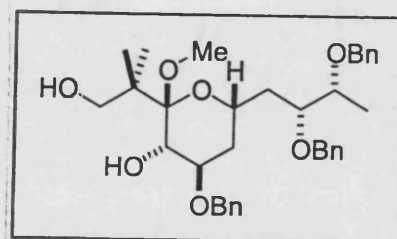
II-MF-179
COSY
CDCl₃



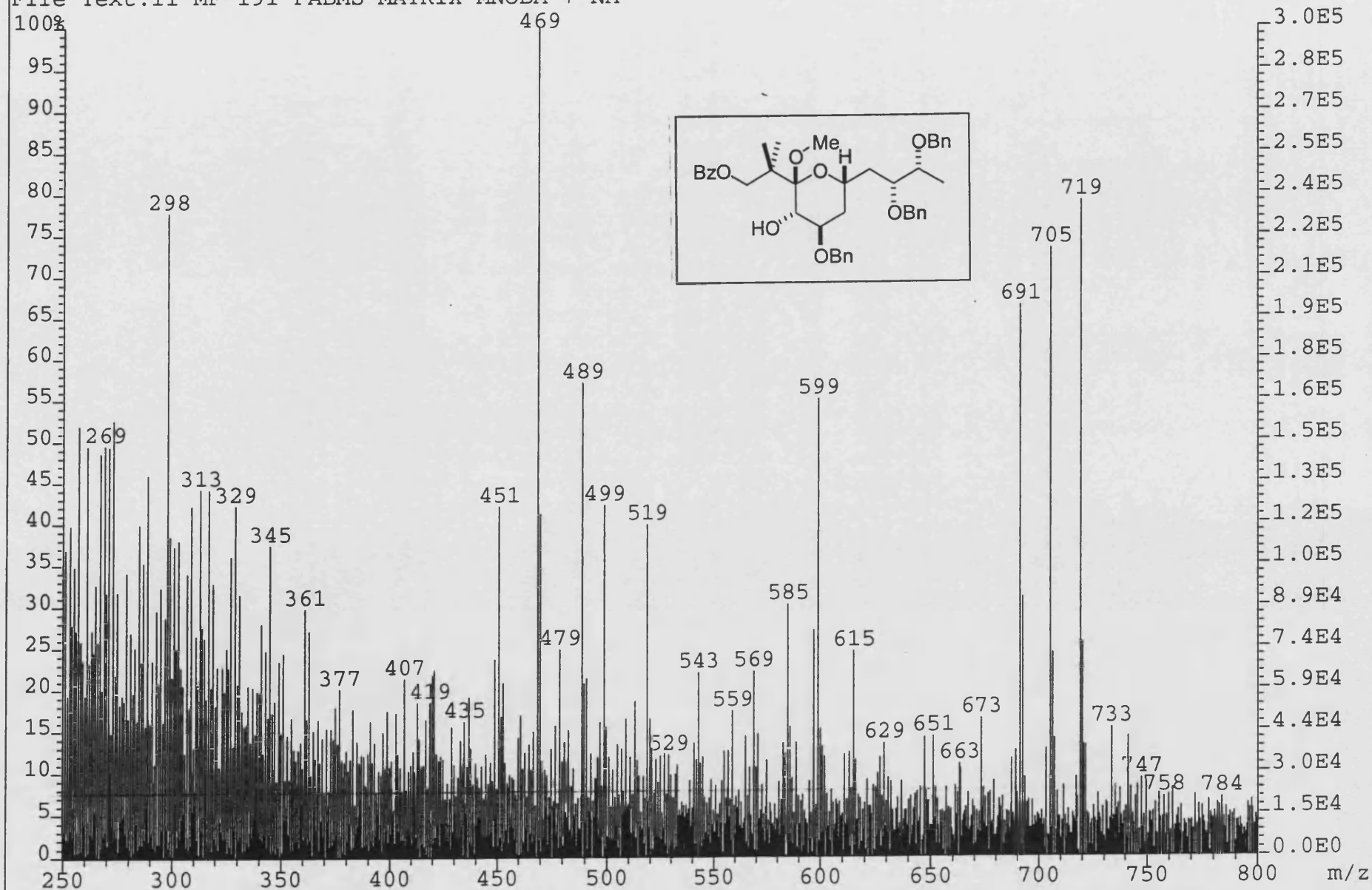
II-MF-179
PROTON
CDCl₃



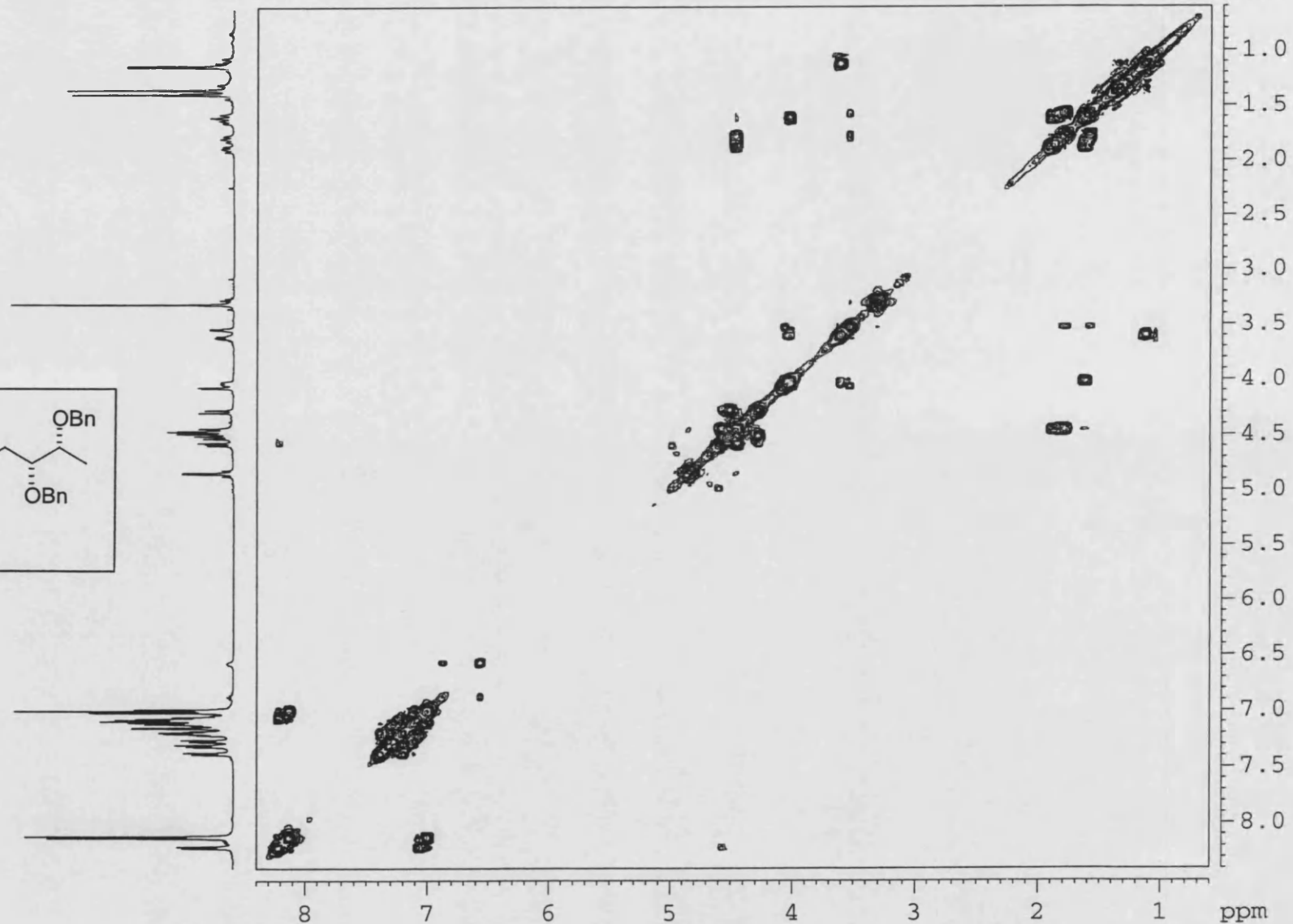
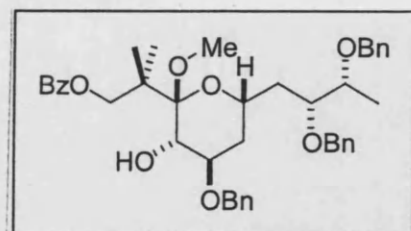
II-MF-160
C6D6
PROTON



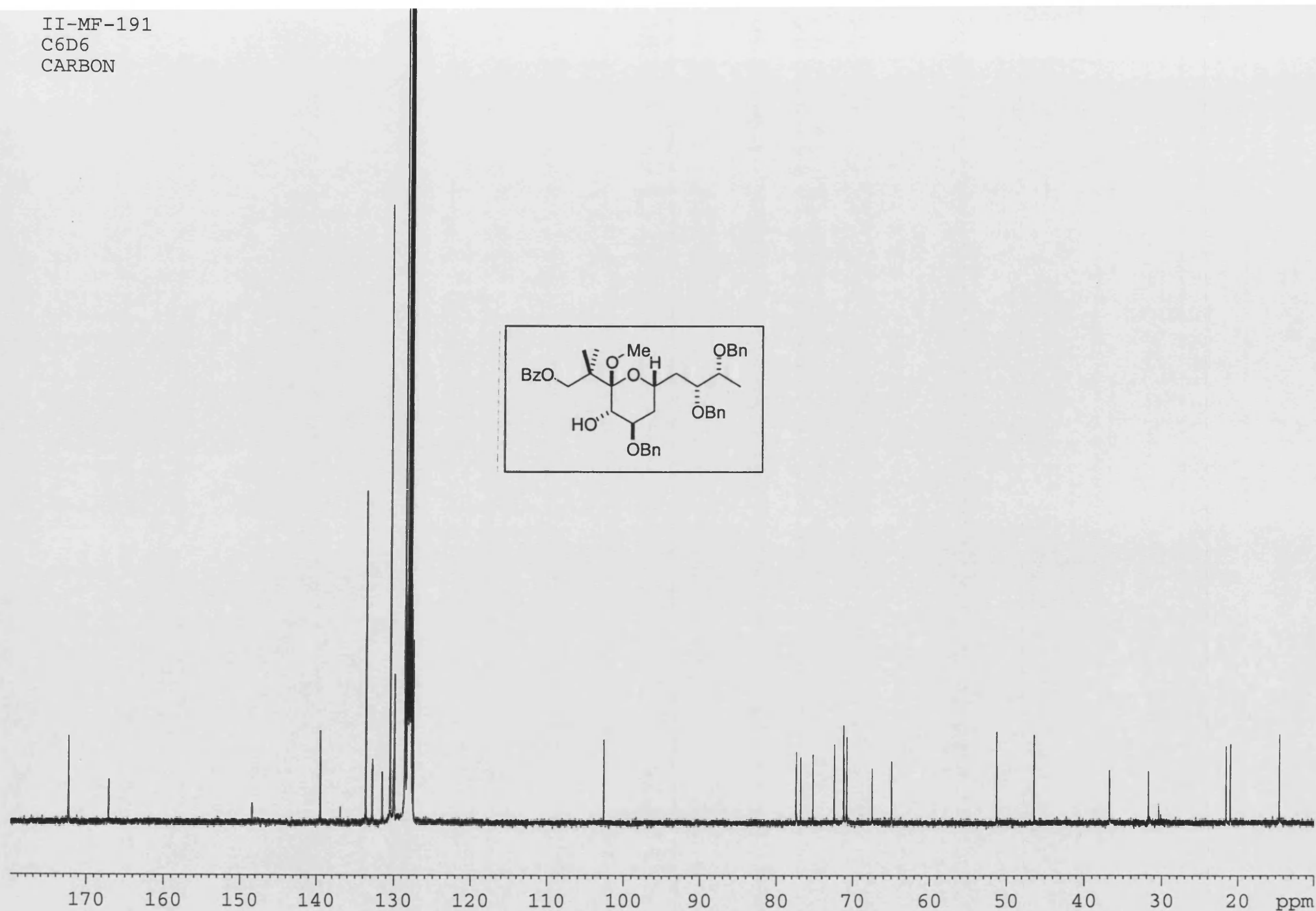
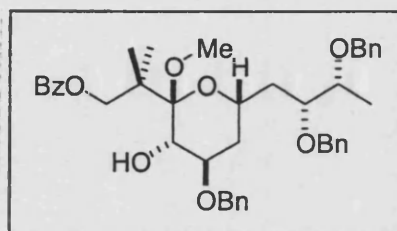
File:01SE935 Ident:72_79 Win 1000PPM Acq: 9-MAR-2001 12:19:44 +4:02 Cal:FABLM090301_1
ZAB-SE4F FAB+ Magnet BpM:105 BpI:16184320 TIC:122157408 Flags:HALL
File Text:II-MF-191 FABMS MATRIX MNOBA + NA



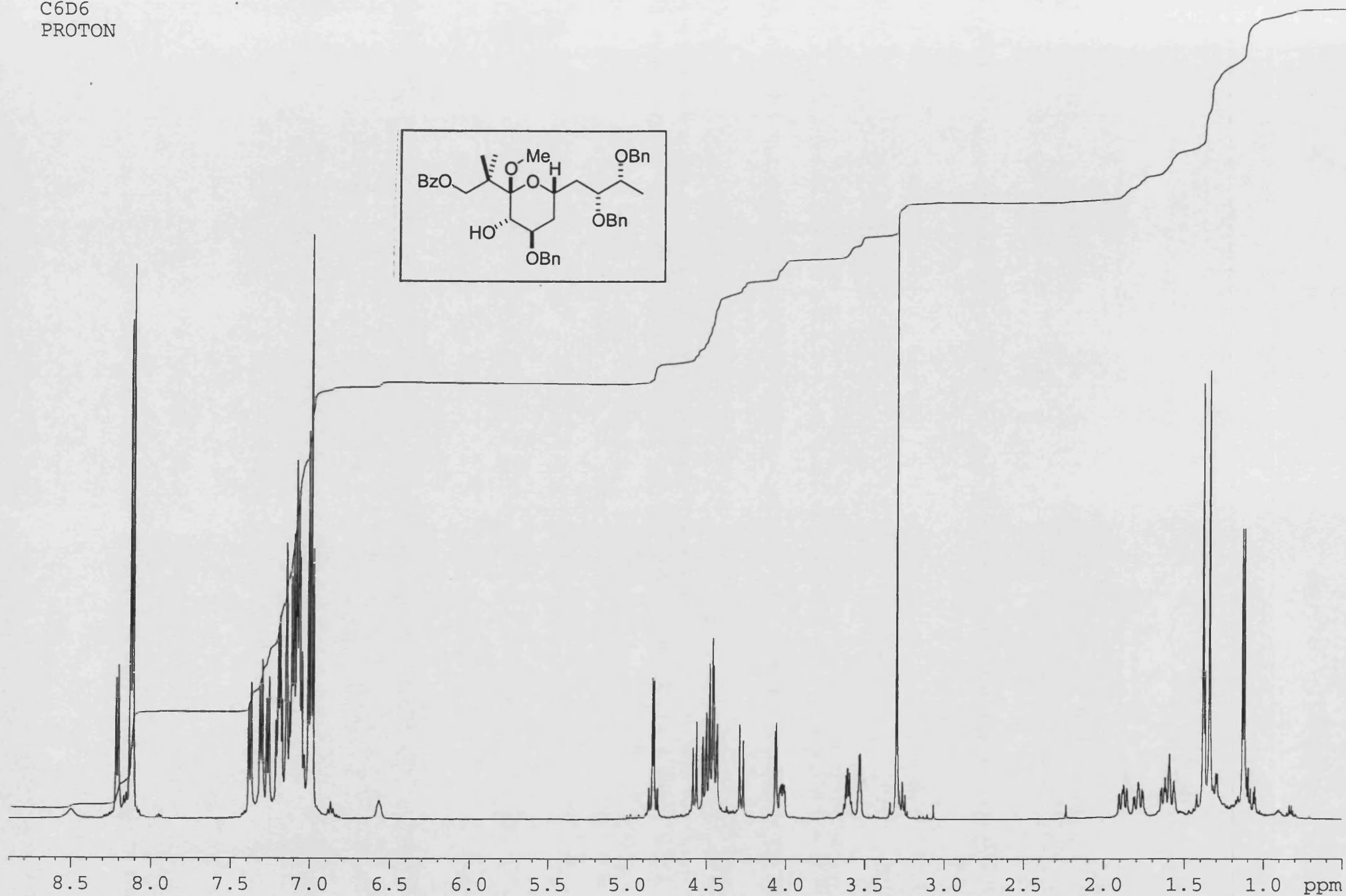
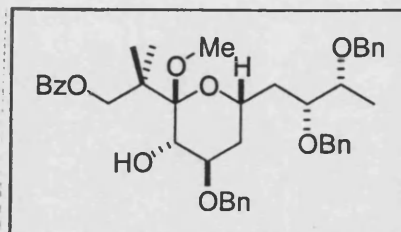
II-MF-191
C6D6
COSY

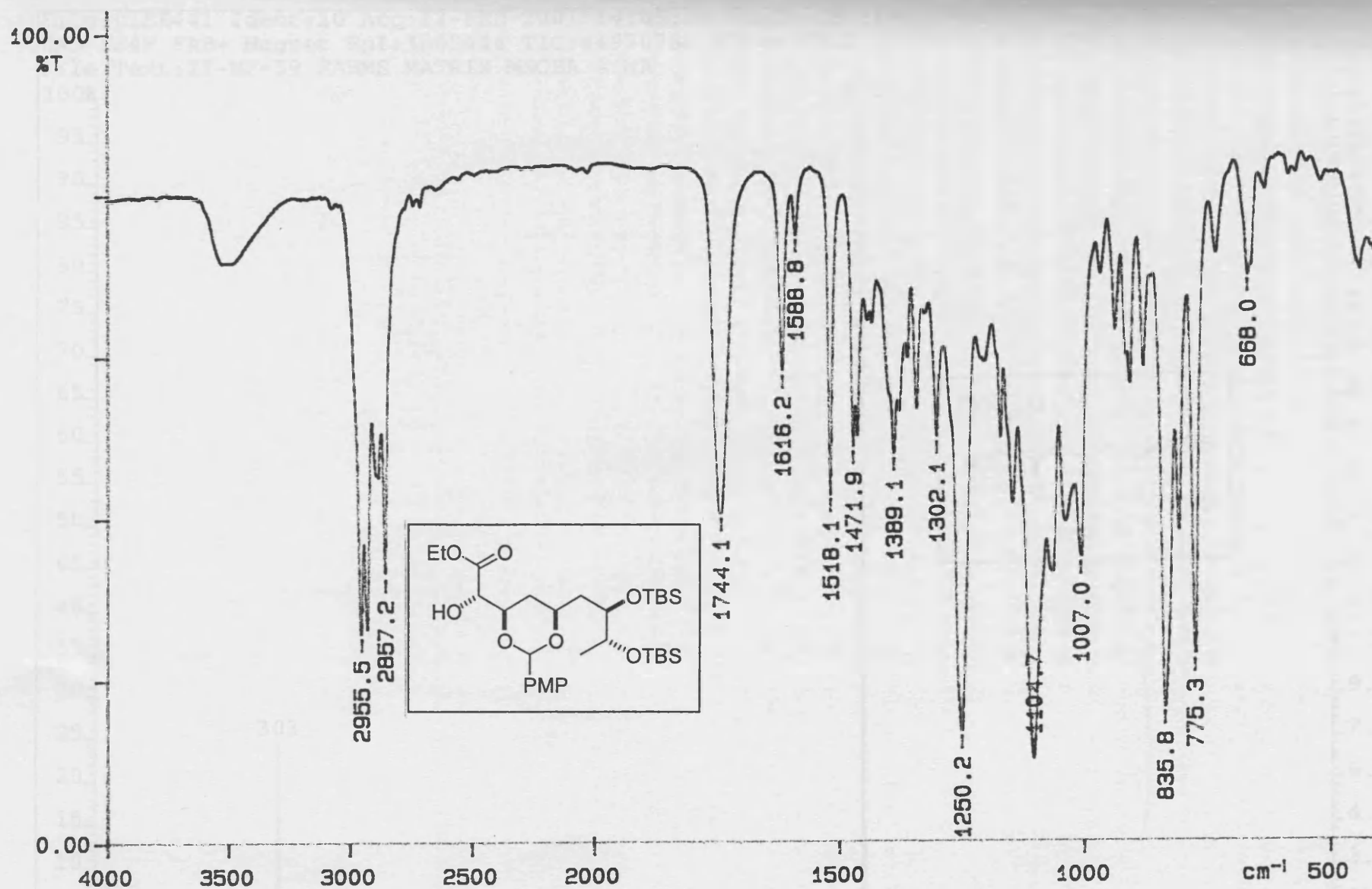


II-MF-191
C6D6
CARBON



II-MF-191
C6D6
PROTON

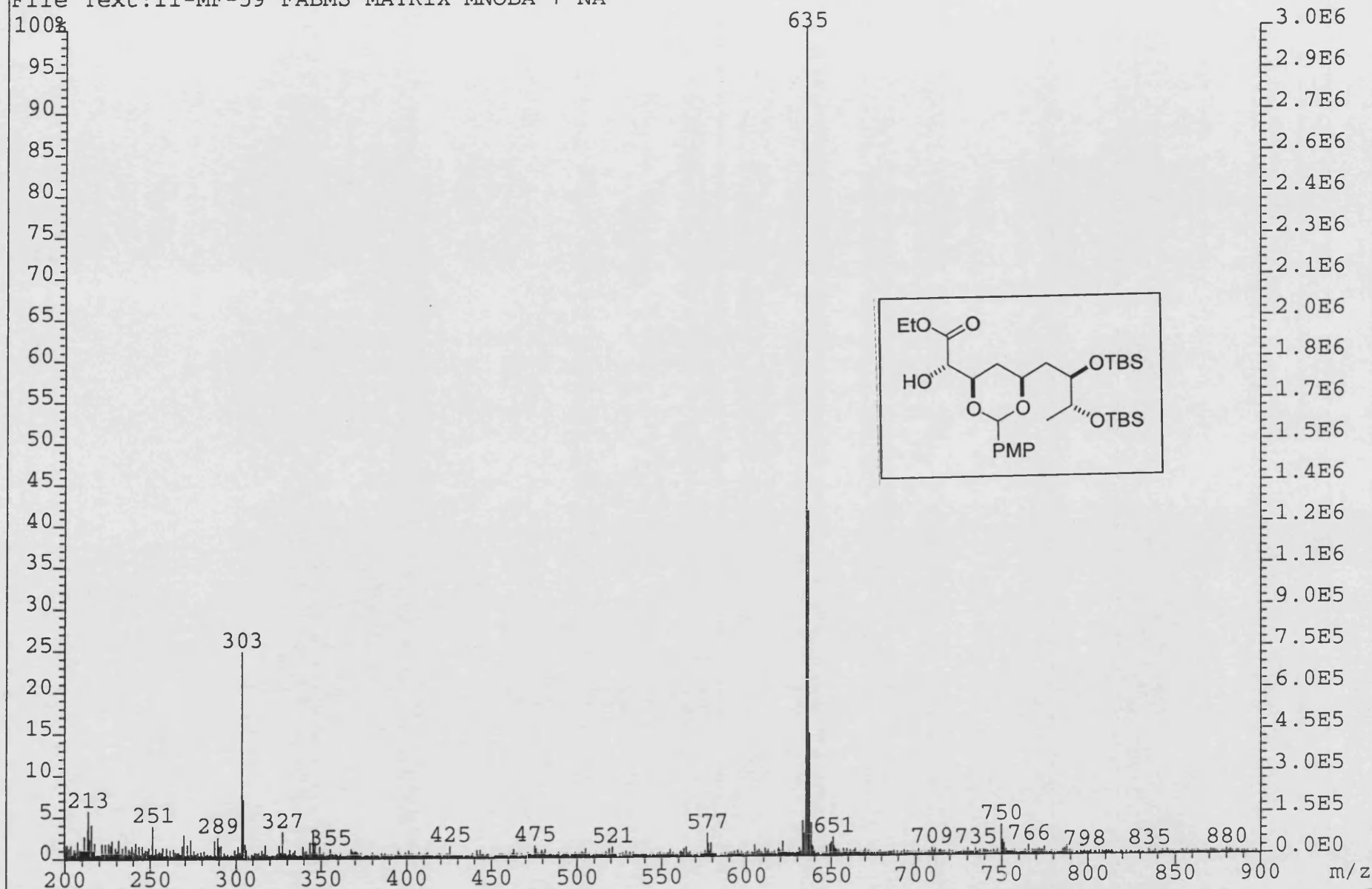




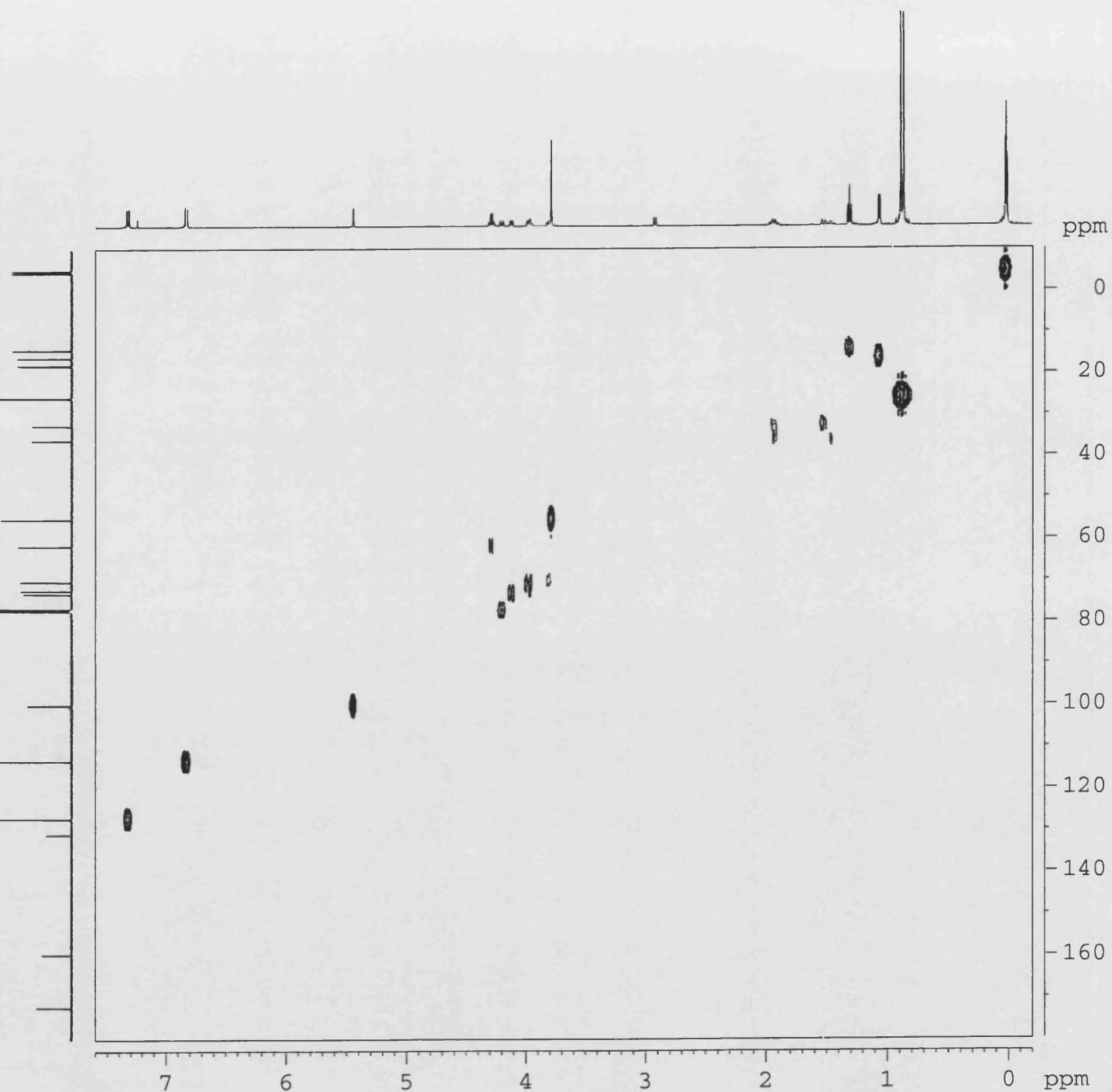
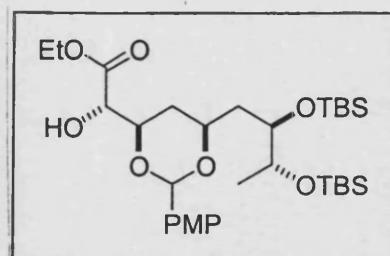
01/03/05 11:53

X: 64 scans, 4.0 cm^{-1}

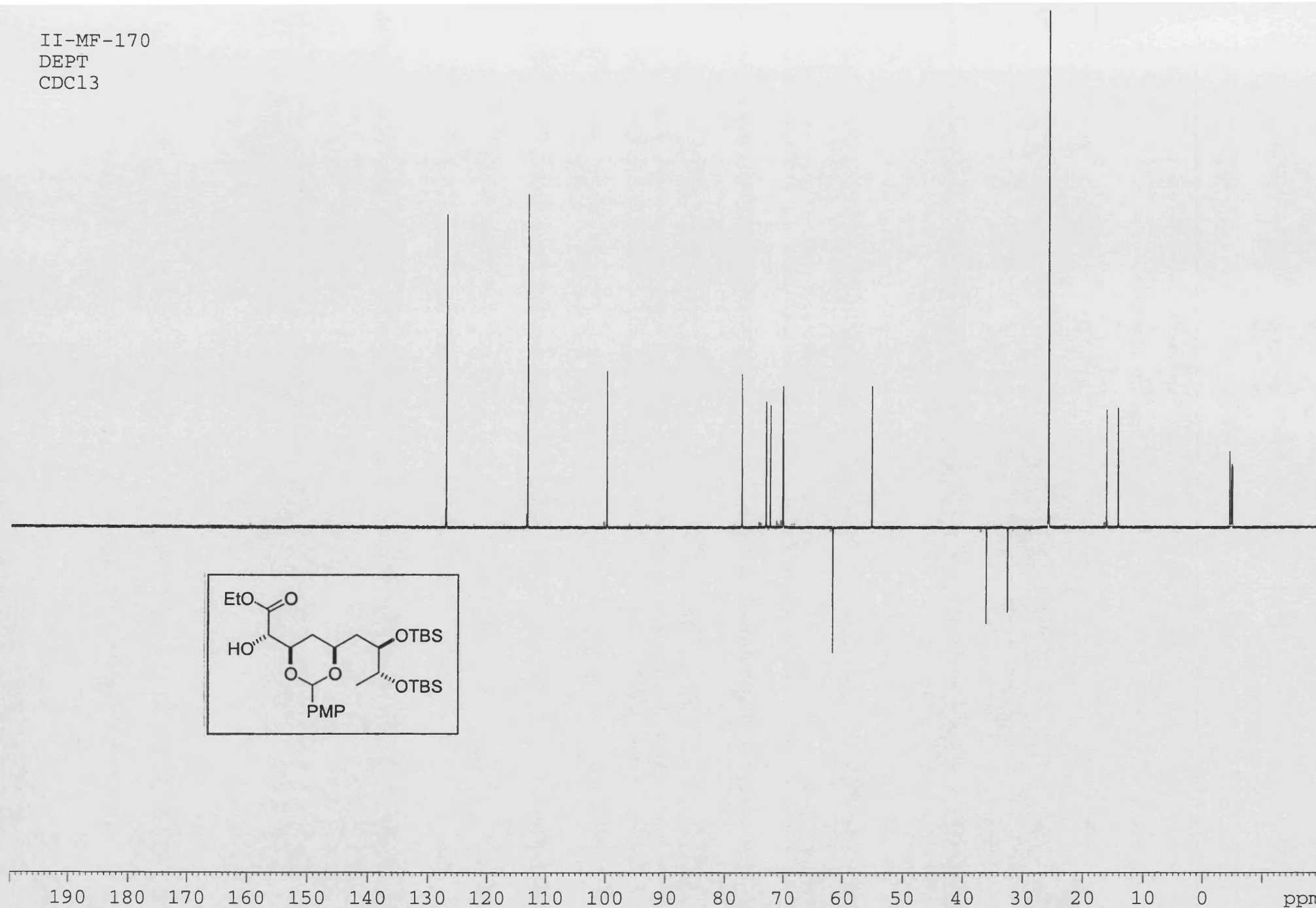
File:01SE441 Ident:10 Acq:12-FEB-2001 14:45:37 +0:35 Cal:FABLM080201_1
ZAB-SE4F FAB+ Magnet BpI:3005444 TIC:44970784 Flags:HALL
File Text:II-MF-59 FABMS MATRIX MNOBA + NA



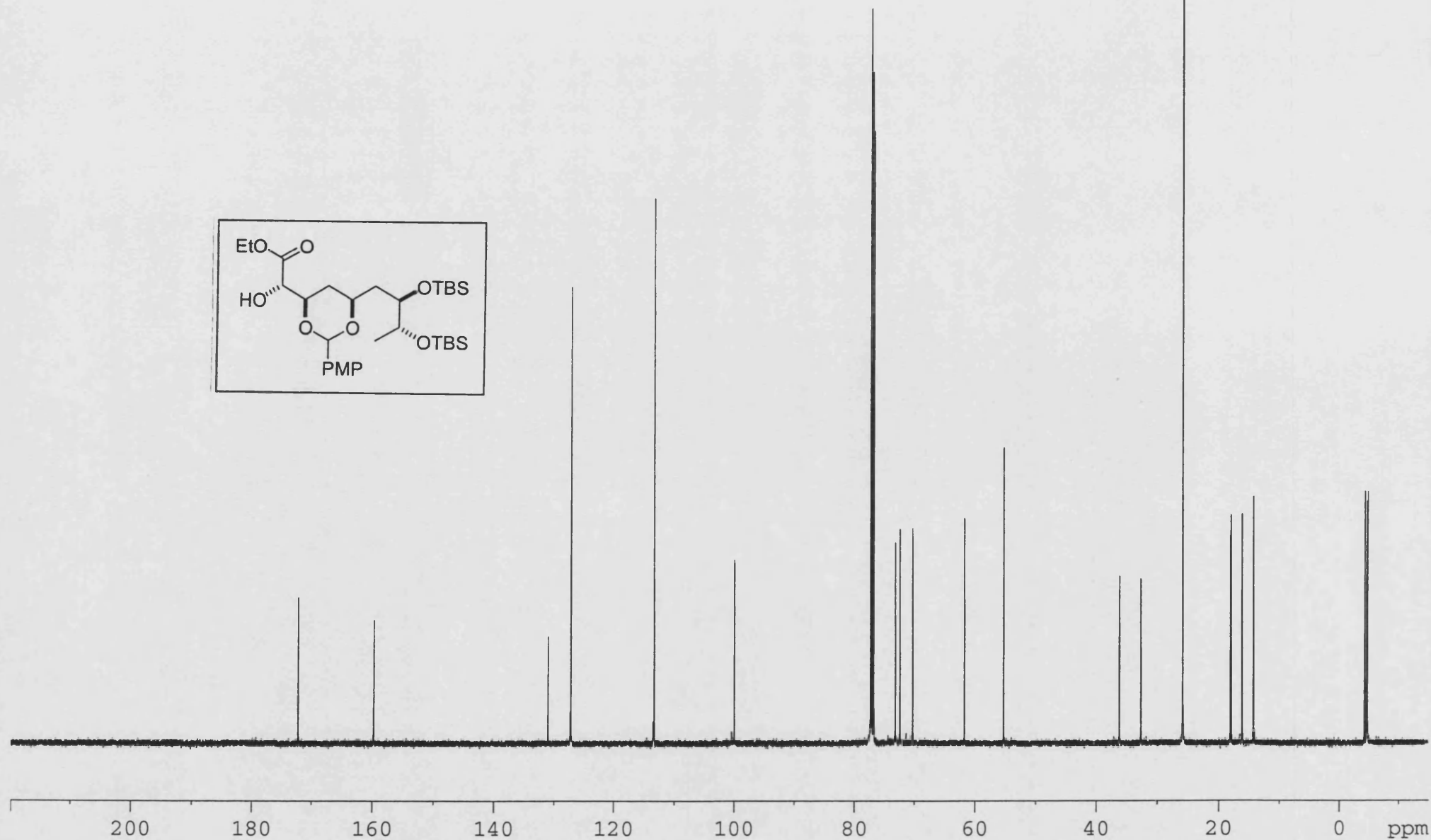
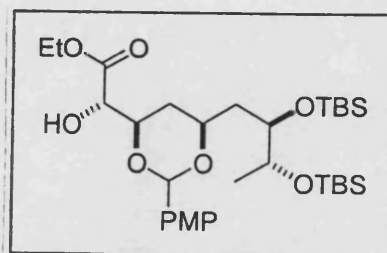
II-MF-170
HMQC
CDC13



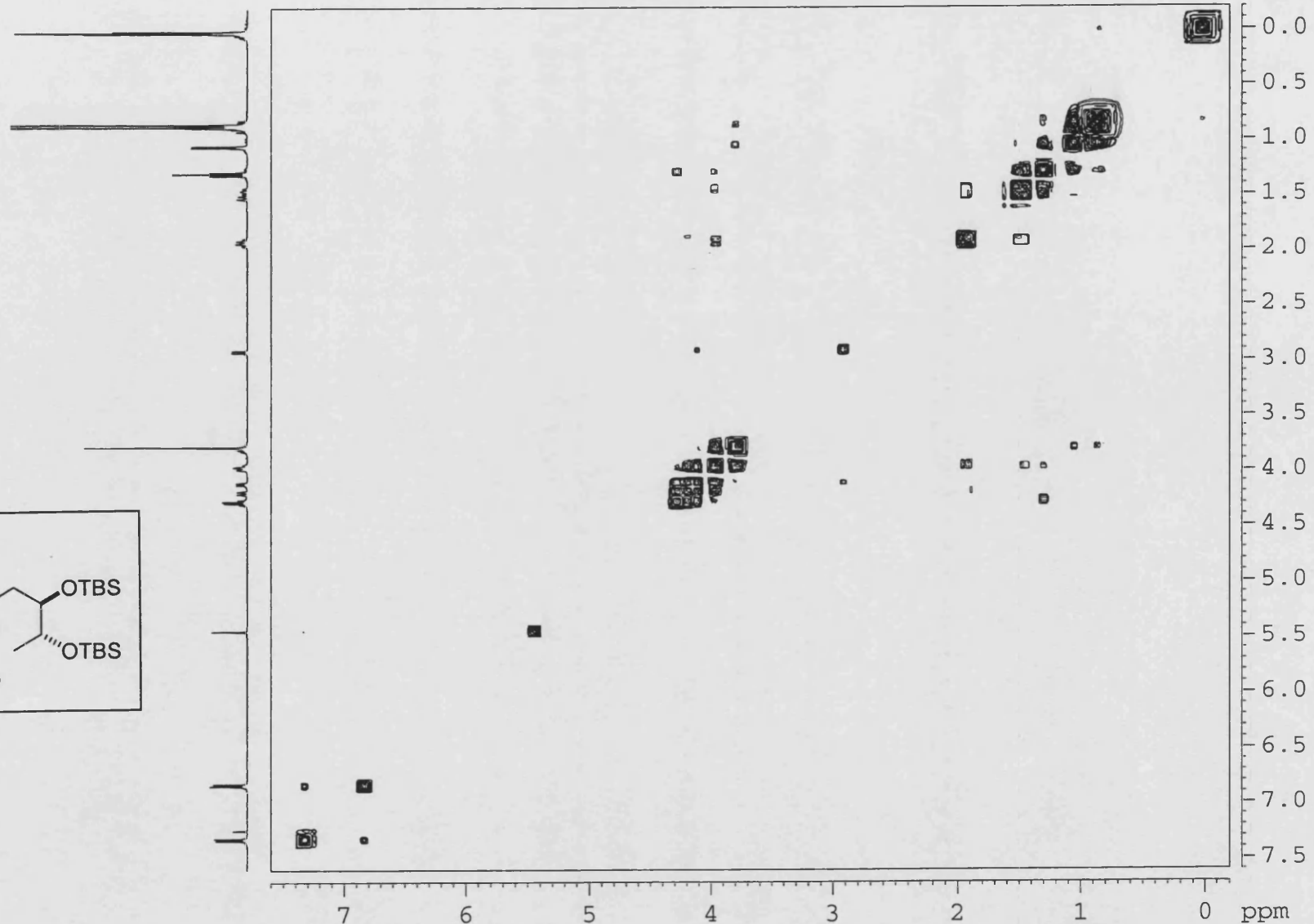
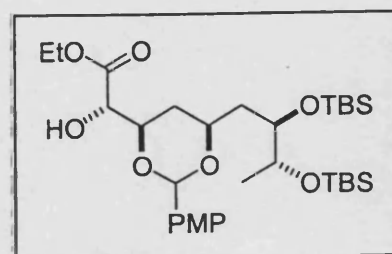
II-MF-170
DEPT
CDCl₃



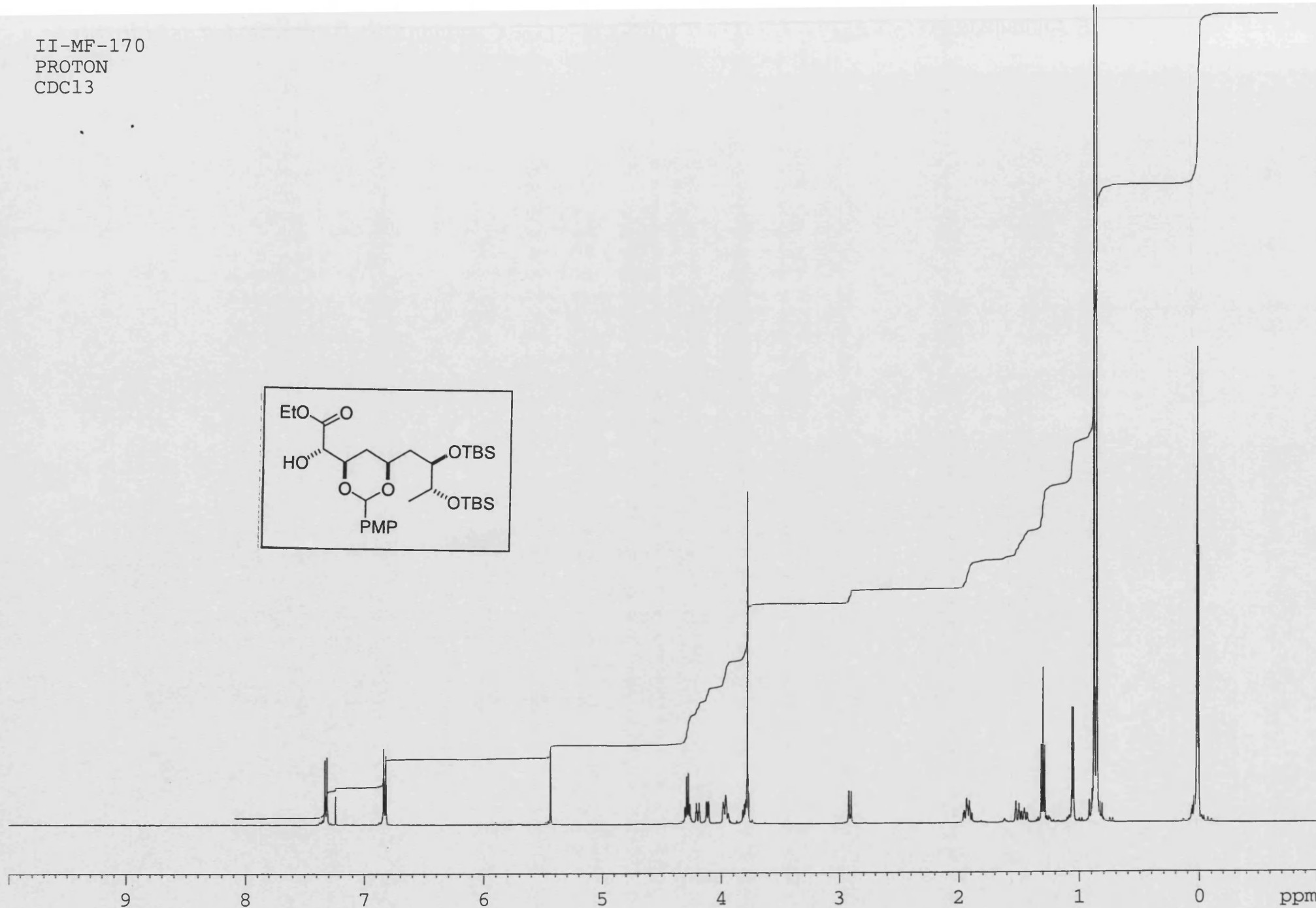
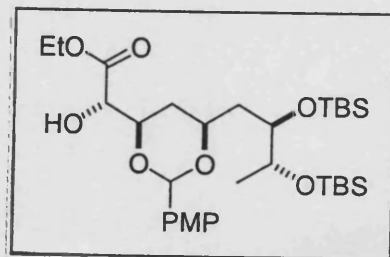
II-MF-170
CARBON
CDCl₃



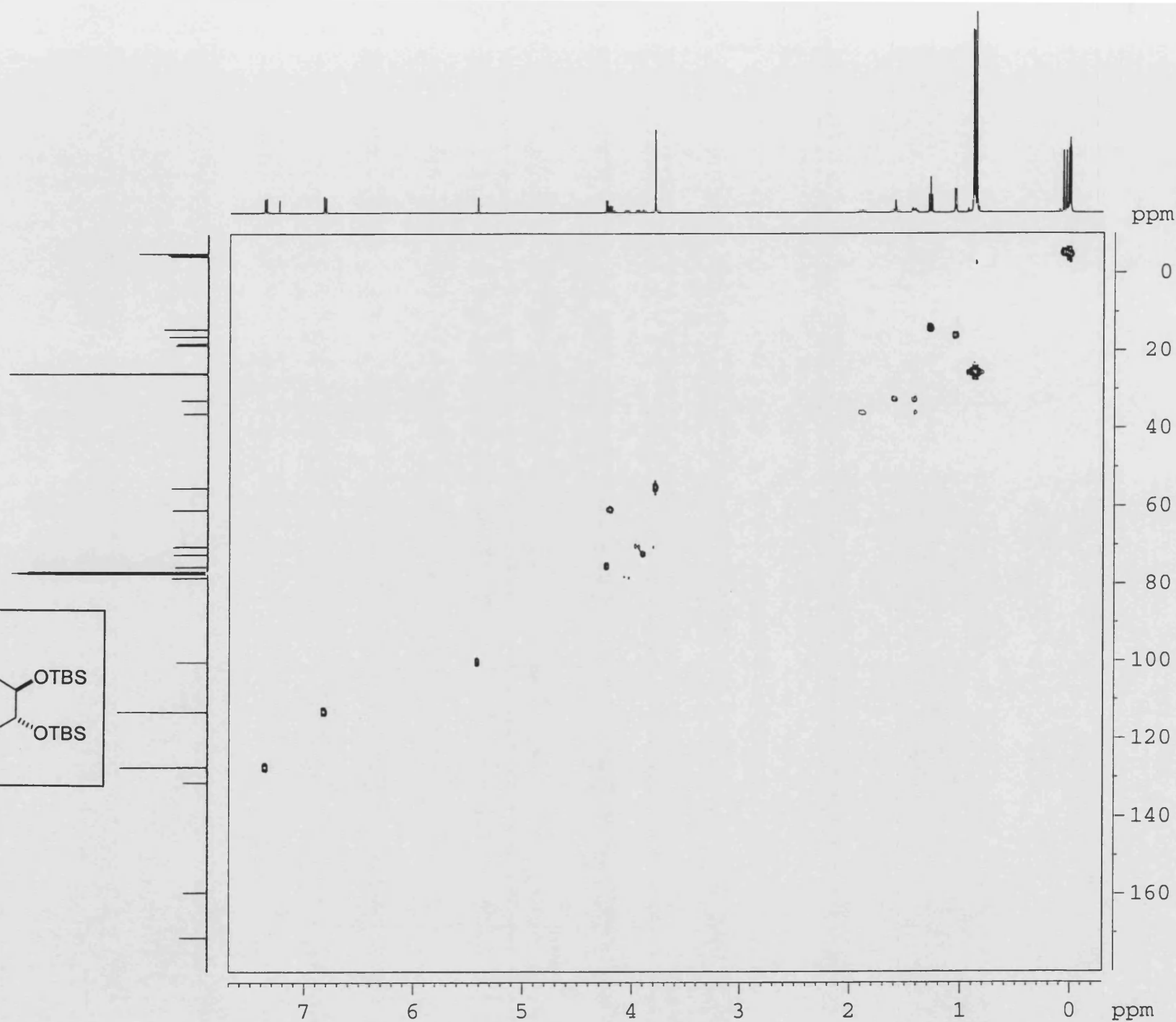
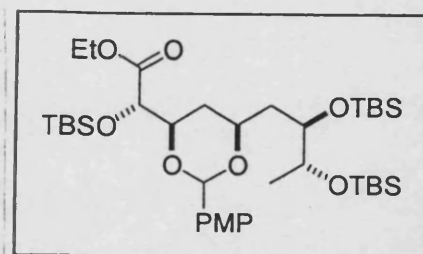
II-MF-170
COSY
CDCl₃



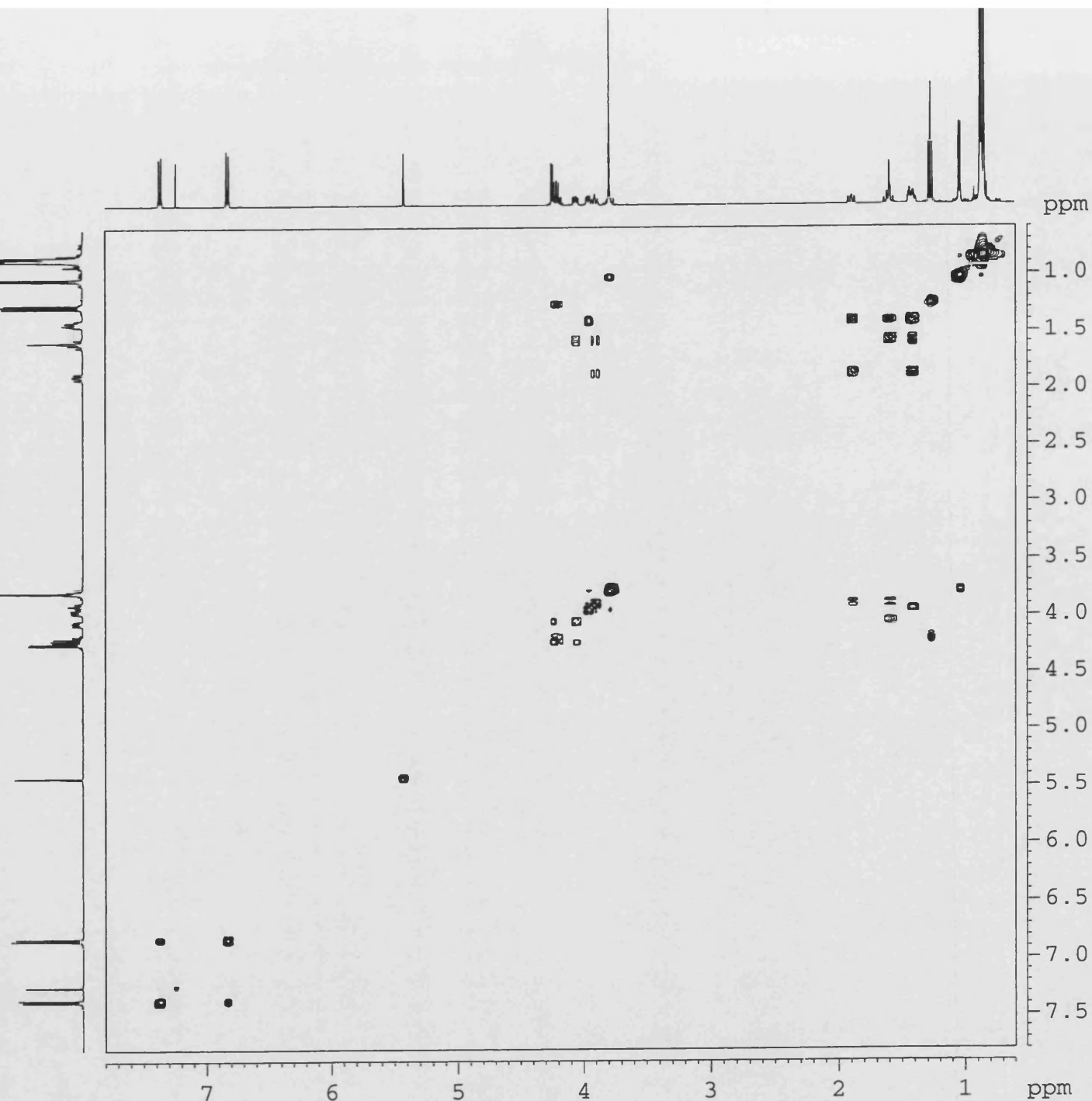
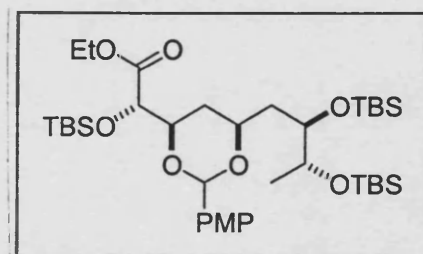
II-MF-170
PROTON
CDCl3



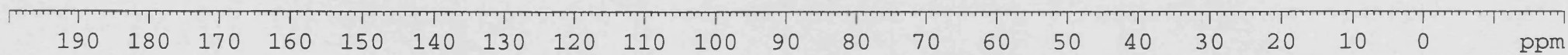
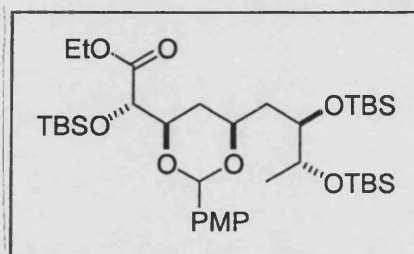
MFII
HMQC
CDCl3



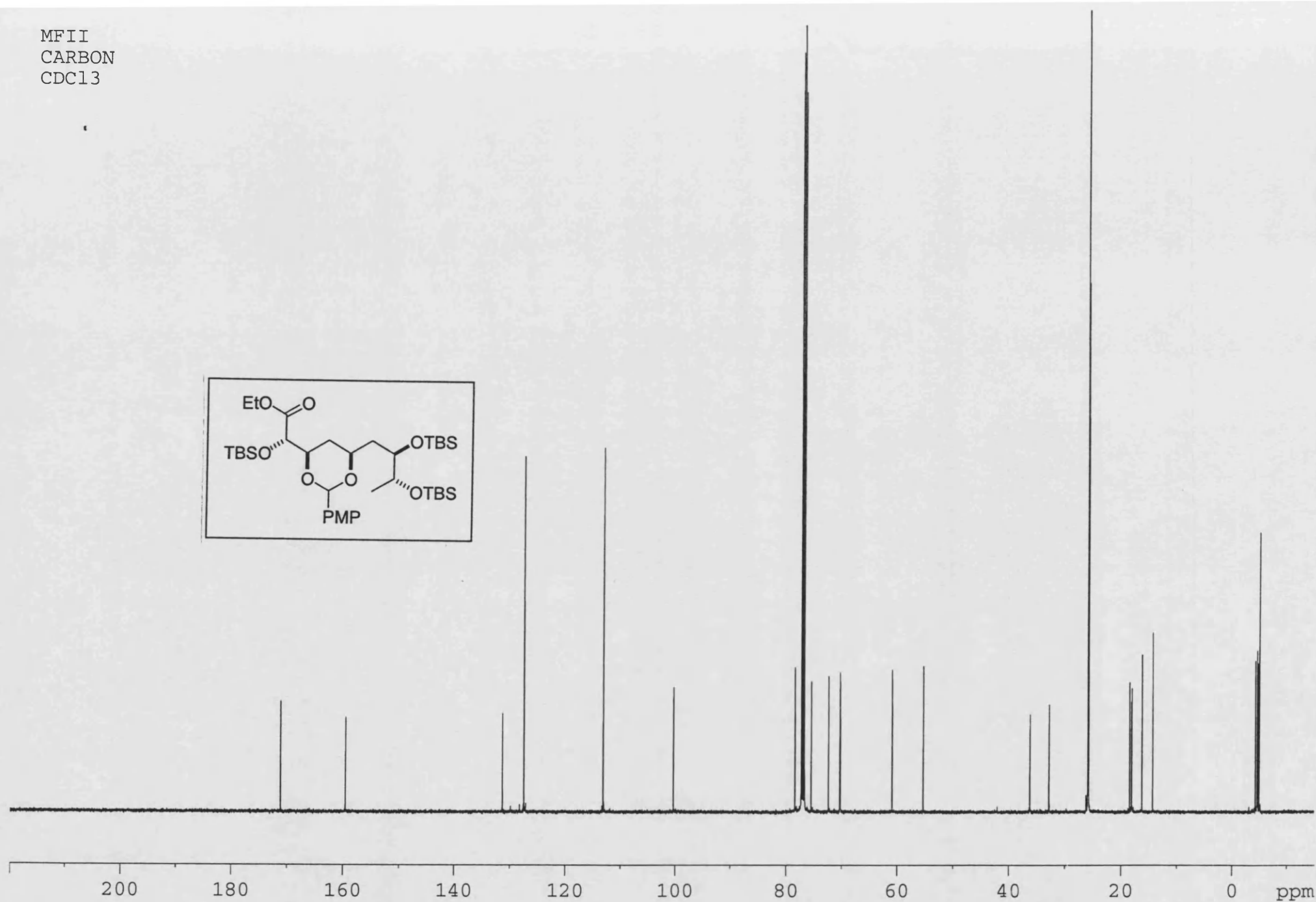
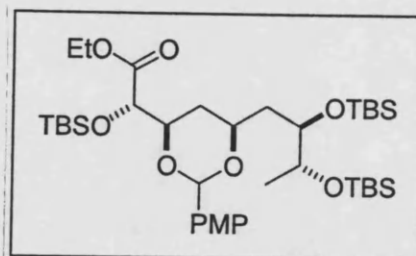
MF11
CDC13
COSY



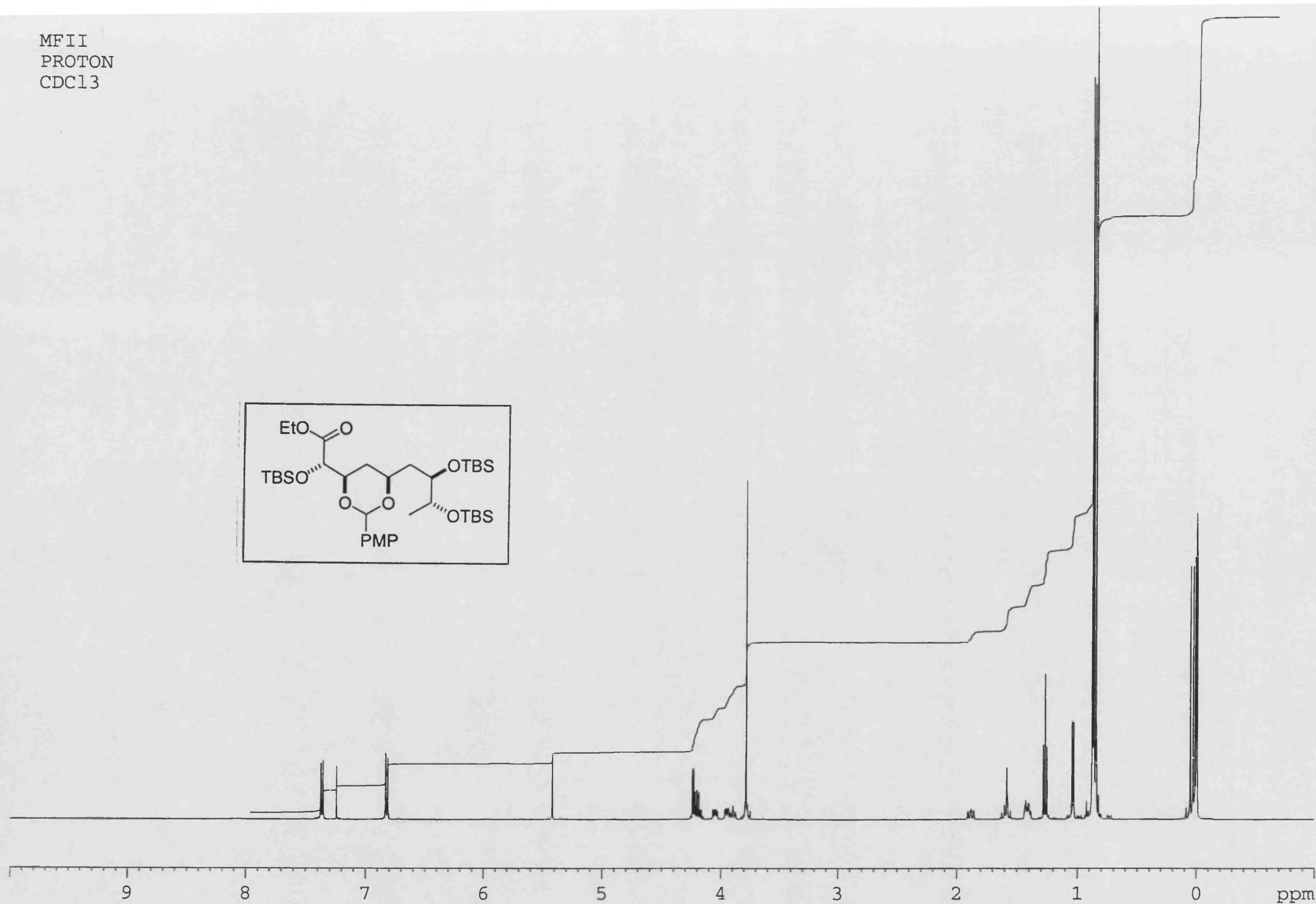
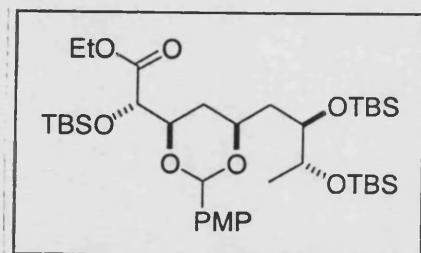
MFII
DEPT
CDCl3

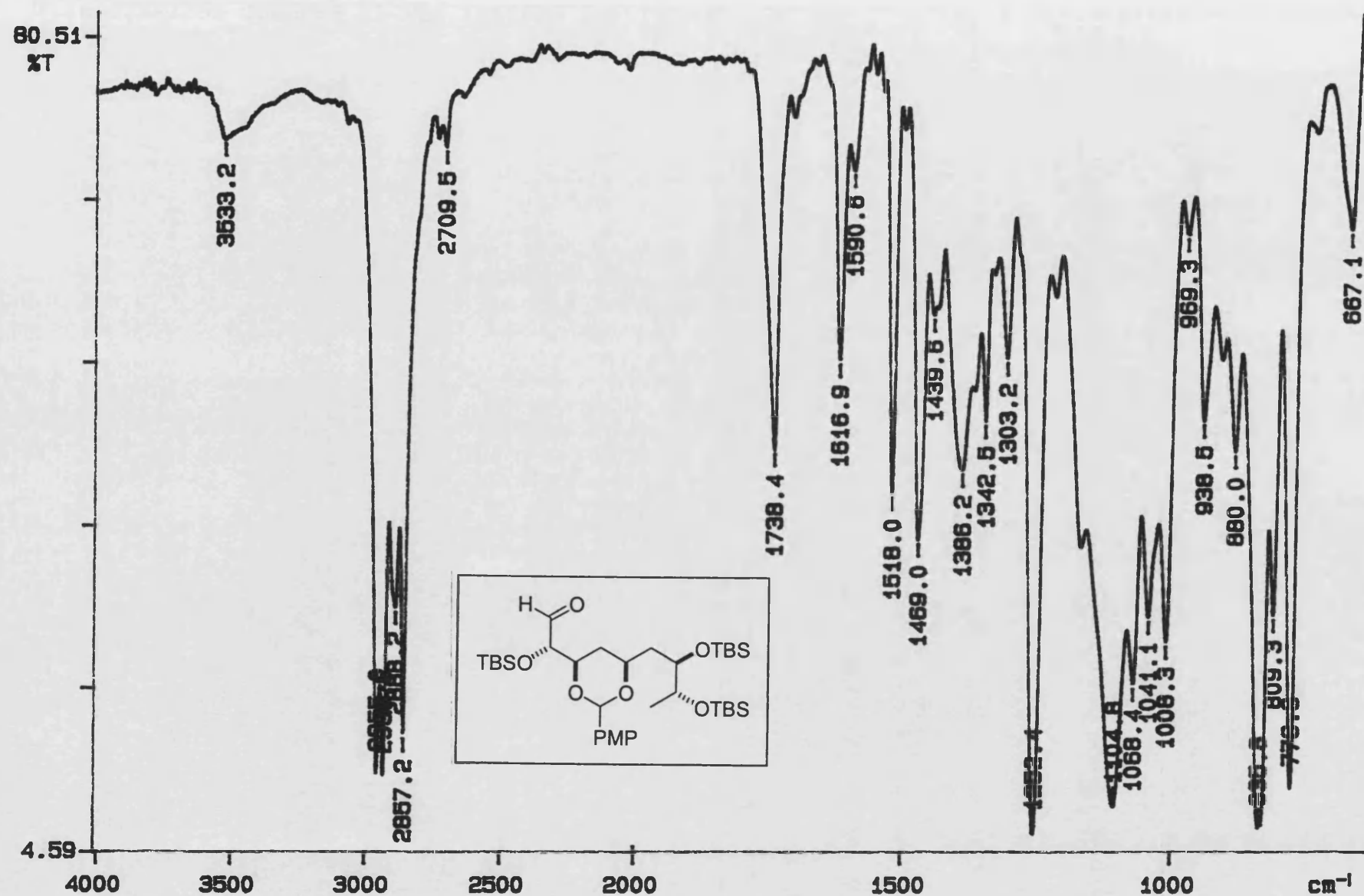


MFII
CARBON
CDCl3



MFII
PROTON
CDC13





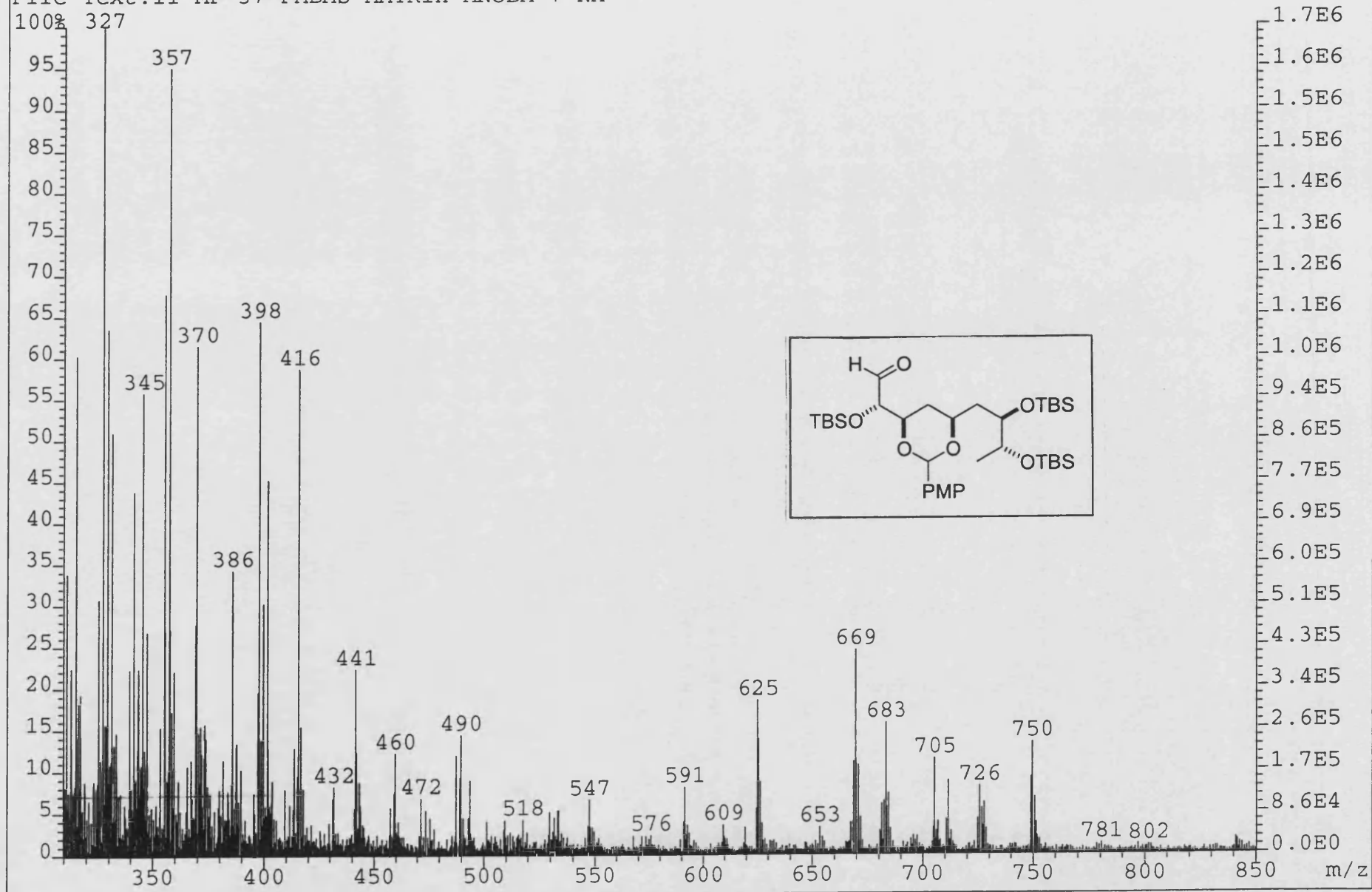
02/07/13 16:19

X: 16 scans, 16.0 cm^{-1} , apod none, flat

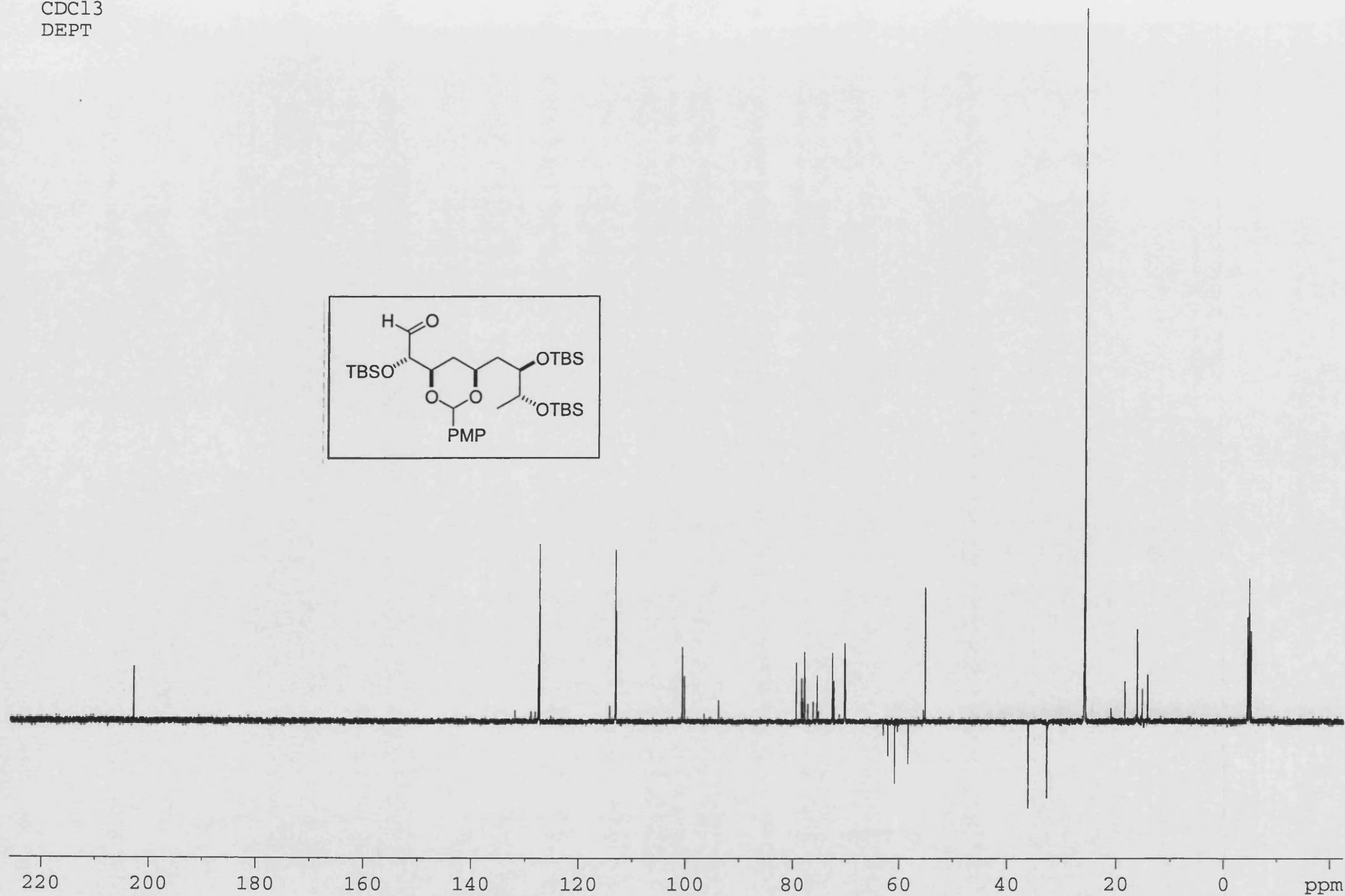
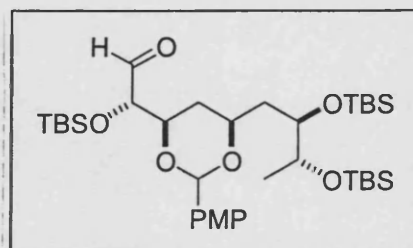
File:02SE2855 Ident:8_13 Win 1000PPM Acq:19-JUL-2002 08:32:34 +0:36 Cal:FABLM190702_1

ZAB-SE4F FAB+ Magnet BpM:137 BpI:22837932 TIC:987213632 Flags:HALL

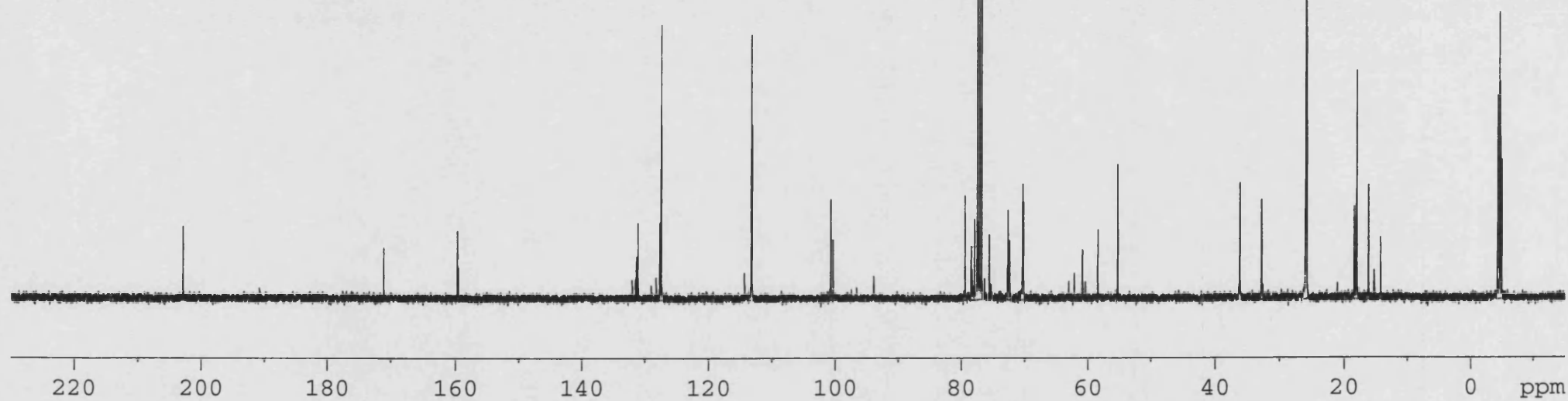
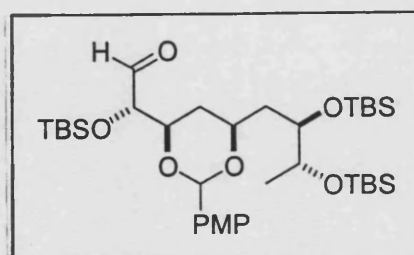
File Text:II-MF-37 FABMS MATRIX MNOBA + NA



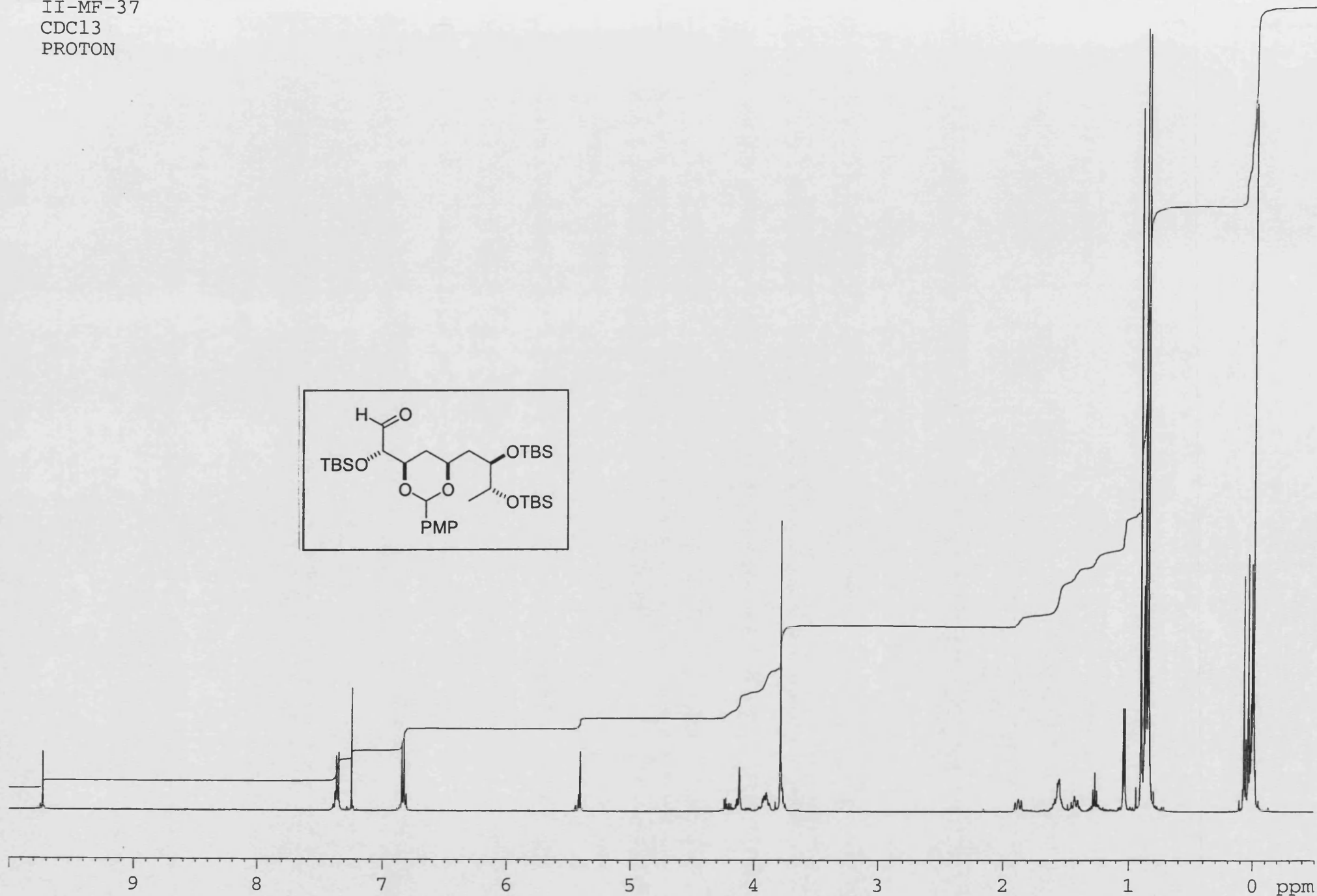
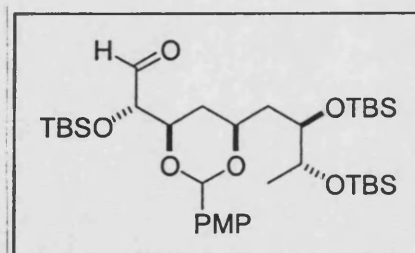
II-MF-37
CDCl₃
DEPT



II-MF-37
CDCl₃
CARBON

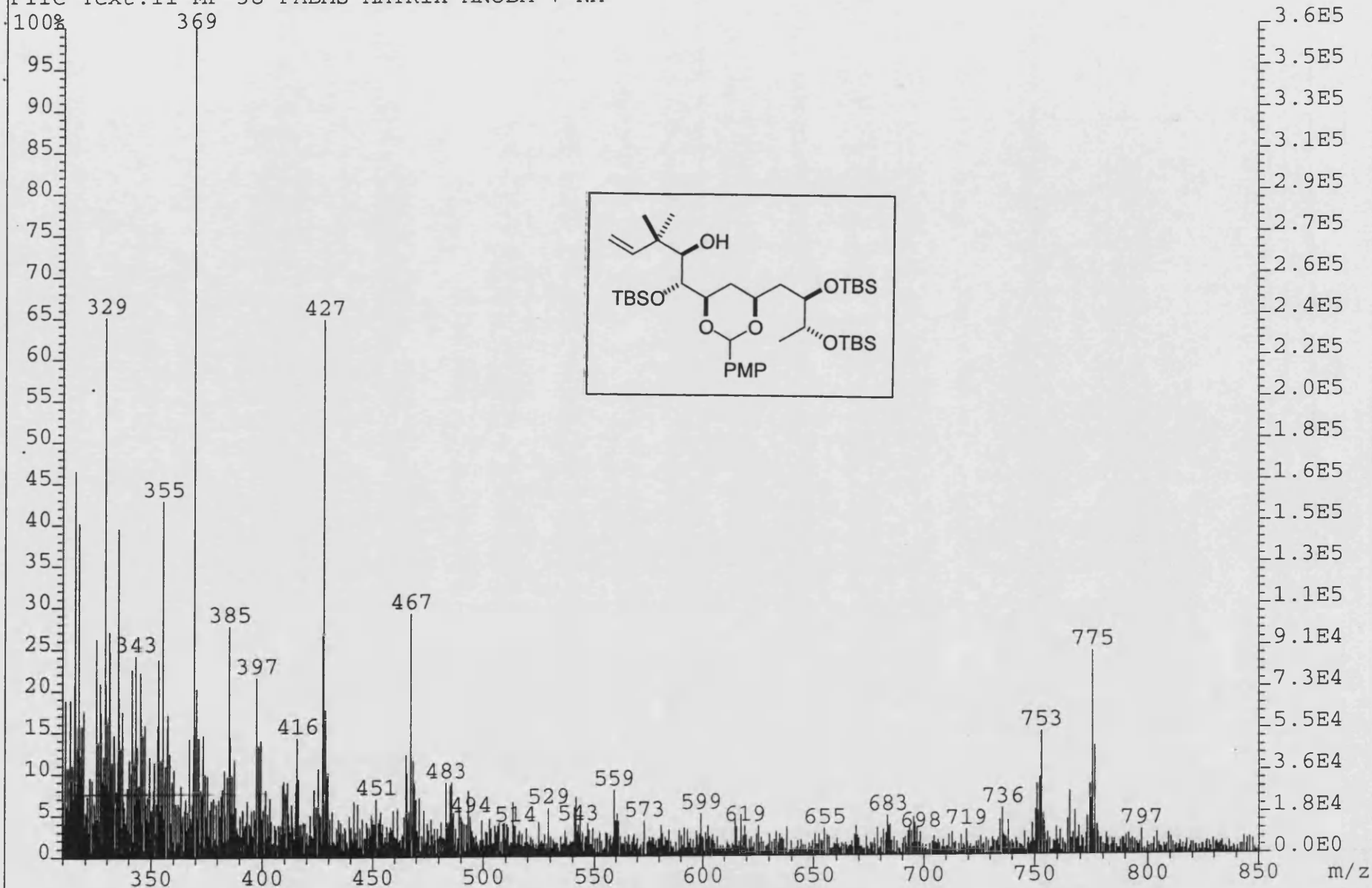


II-MF-37
CDCl₃
PROTON

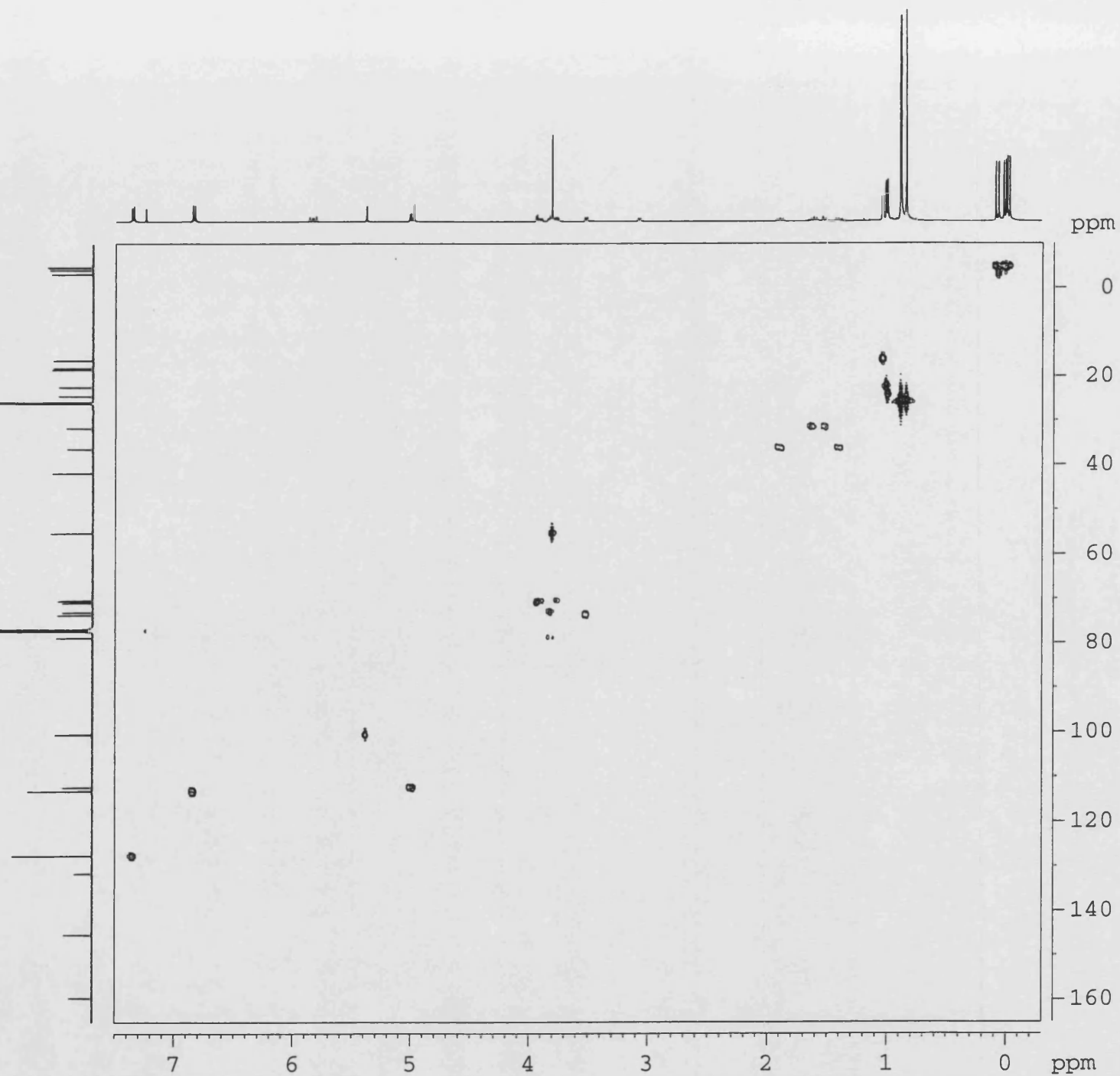
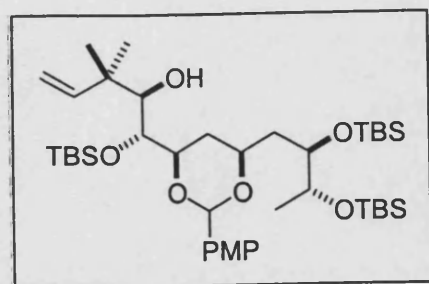


Z: 64 scans, 4.0cm-1, apod none, flat

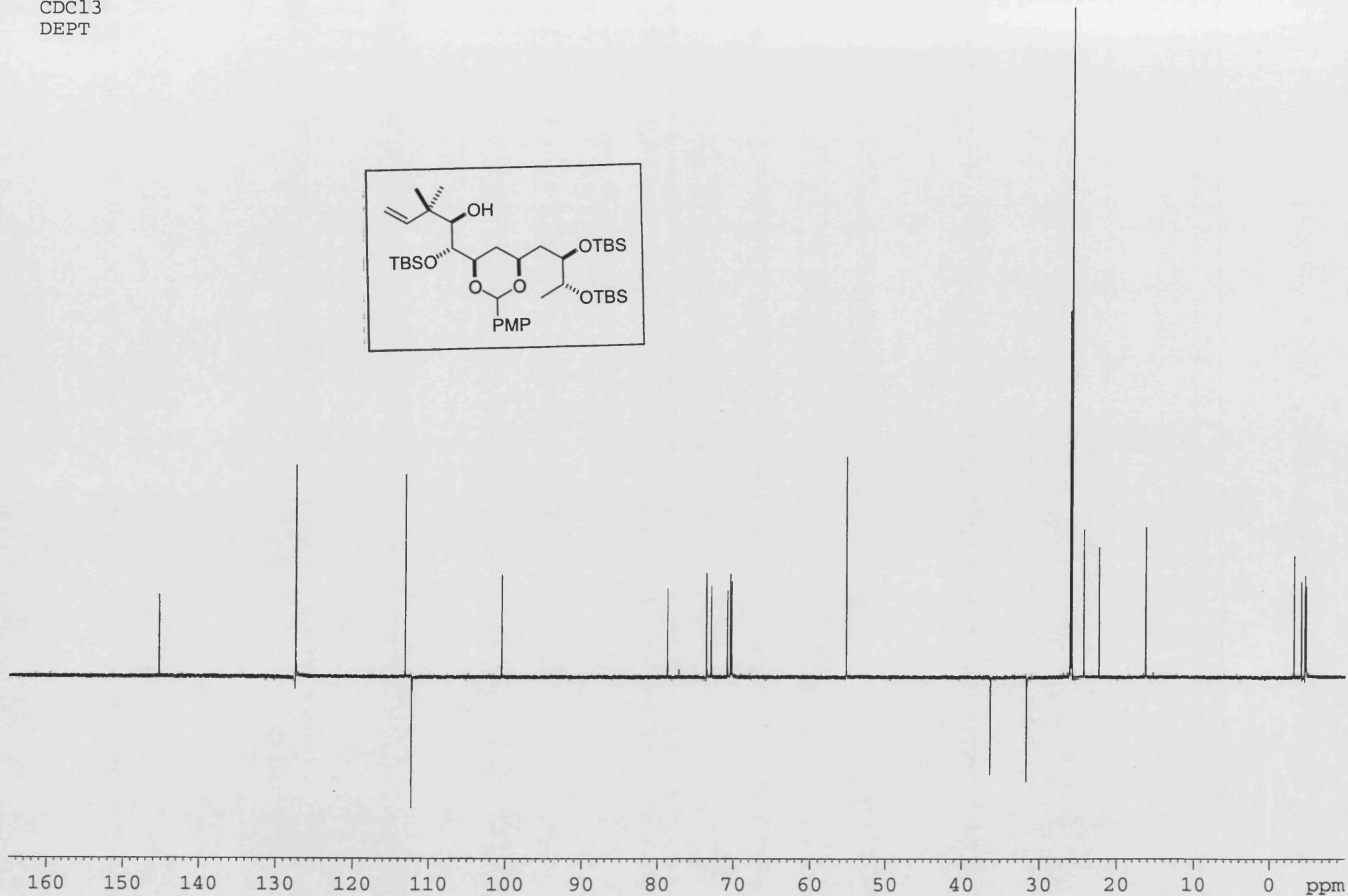
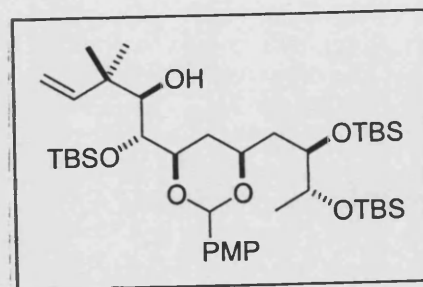
File:02SE2854 Ident:20_23 Win 1000PPM Acq:19-JUL-2002 08:27:03 +1:13 Cal:FABLM190702_1
ZAB-SE4F FAB+ Magnet BpM:115 BpI:14973952 TIC:282465568 Flags:HALL
File Text:II-MF-38 FABMS MATRIX MNOBA + NA



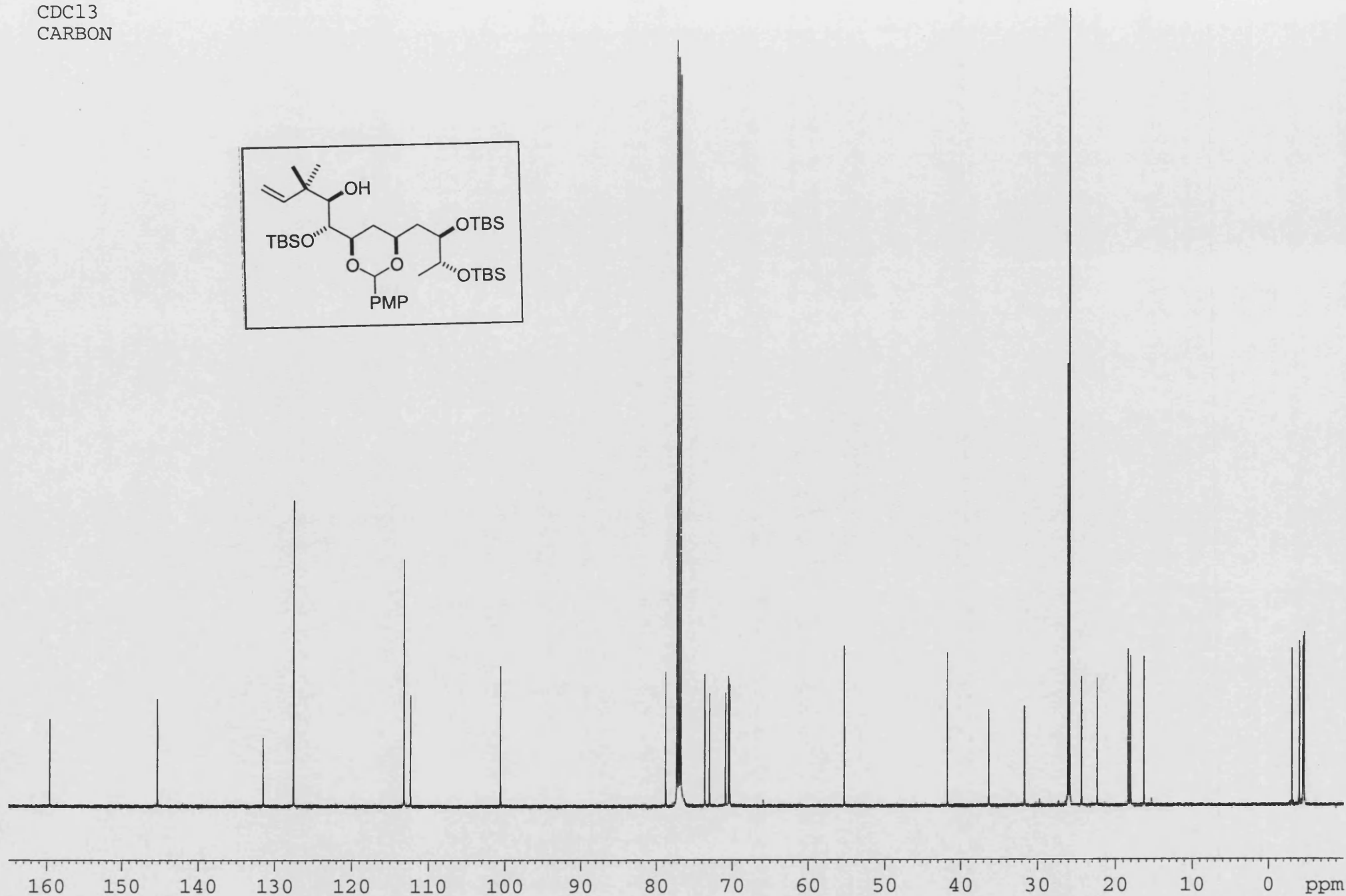
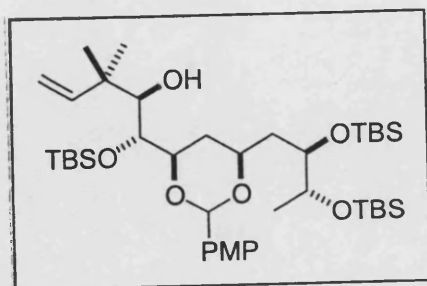
II-MF-38
CDCl₃
HMQC



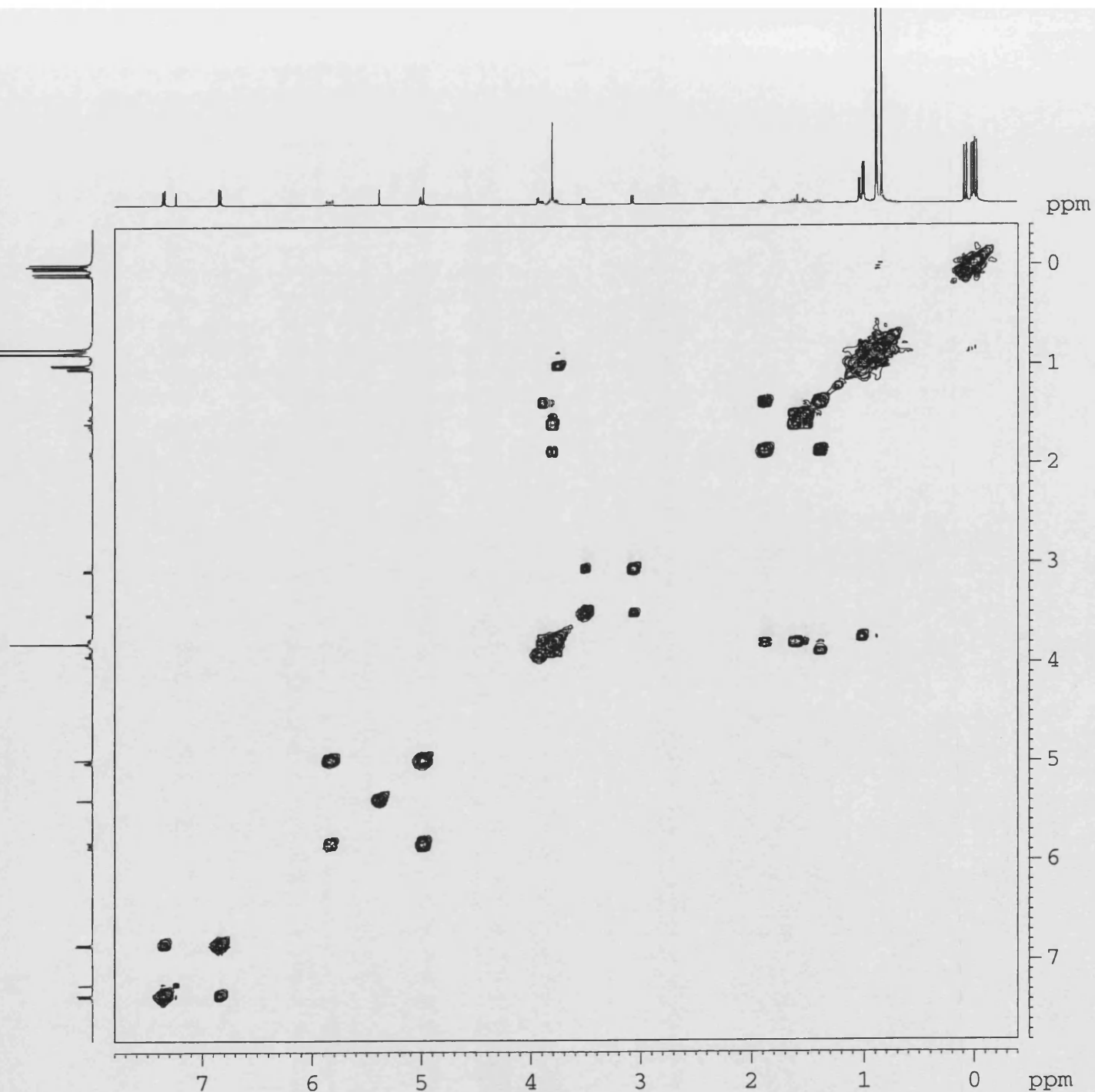
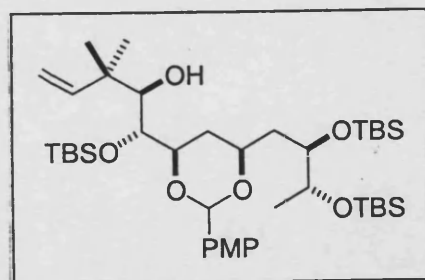
II-MF-38
CDCl₃
DEPT



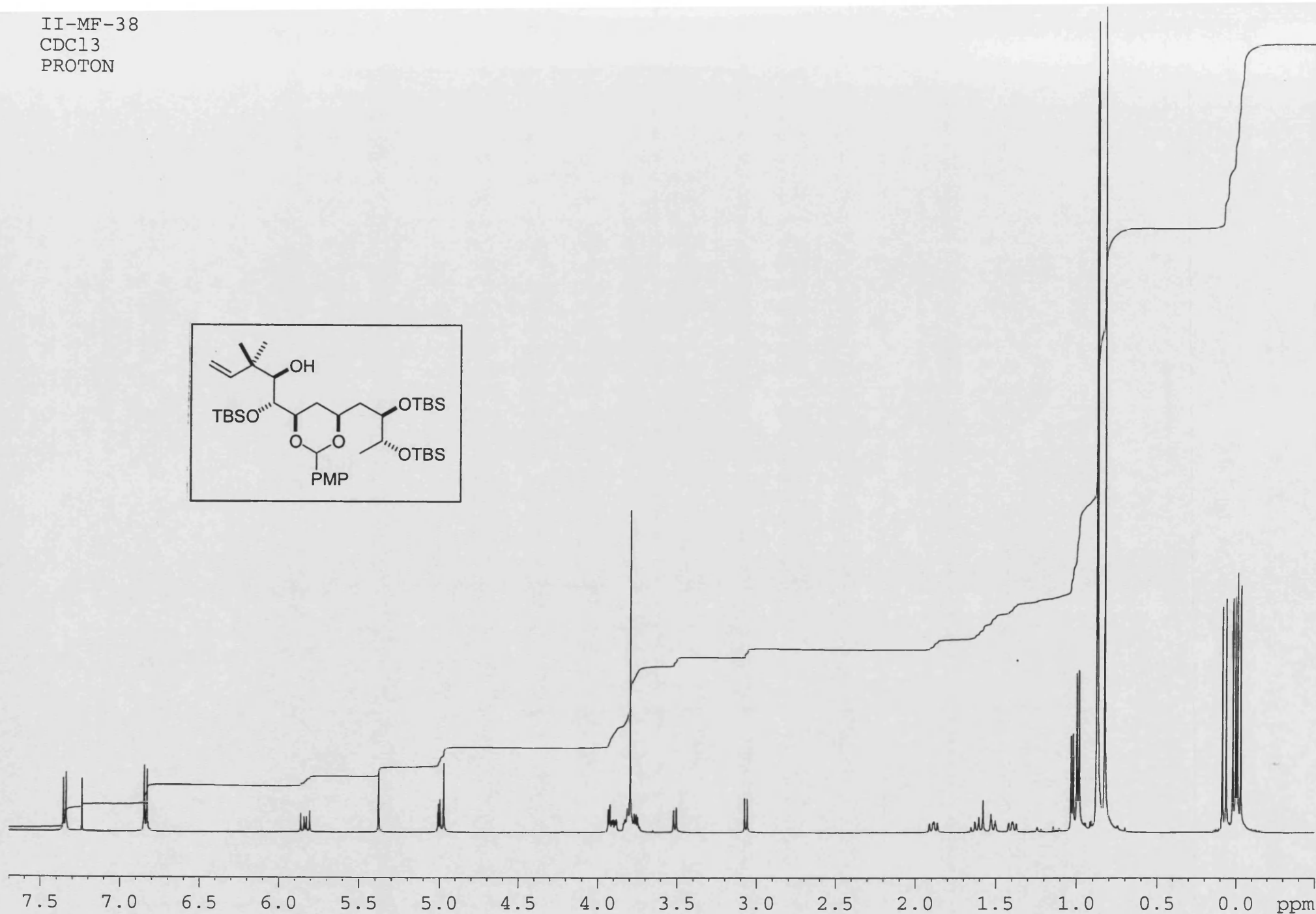
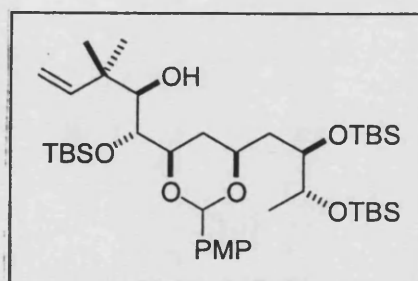
II-MF-38
CDCl₃
CARBON

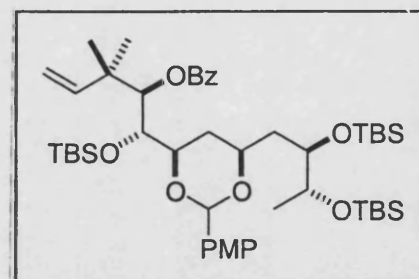


II-MF-38
CDCl₃
COSY

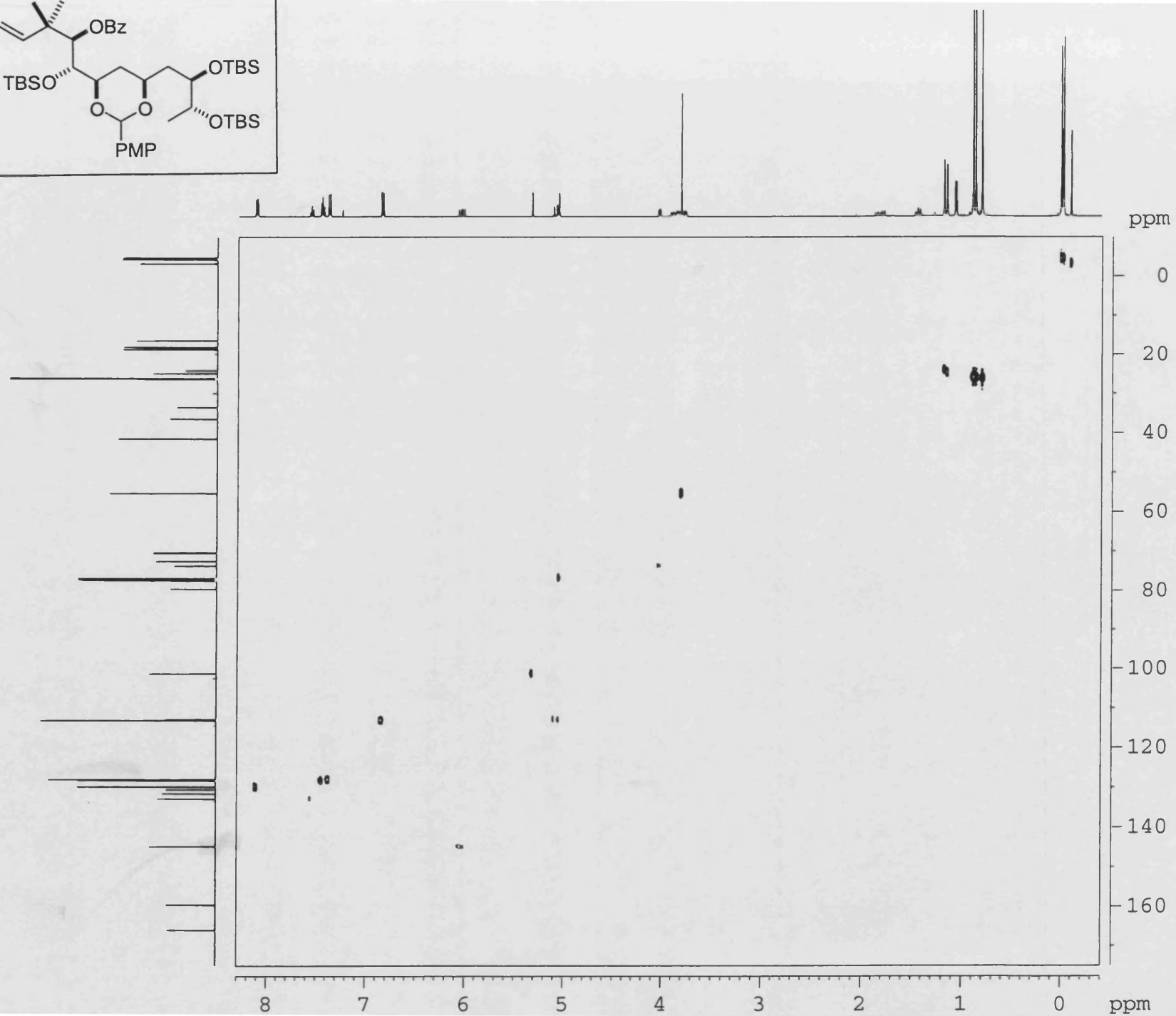
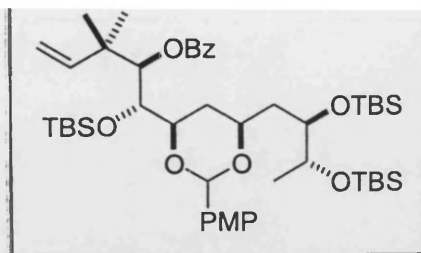


II-MF-38
CDCl₃
PROTON

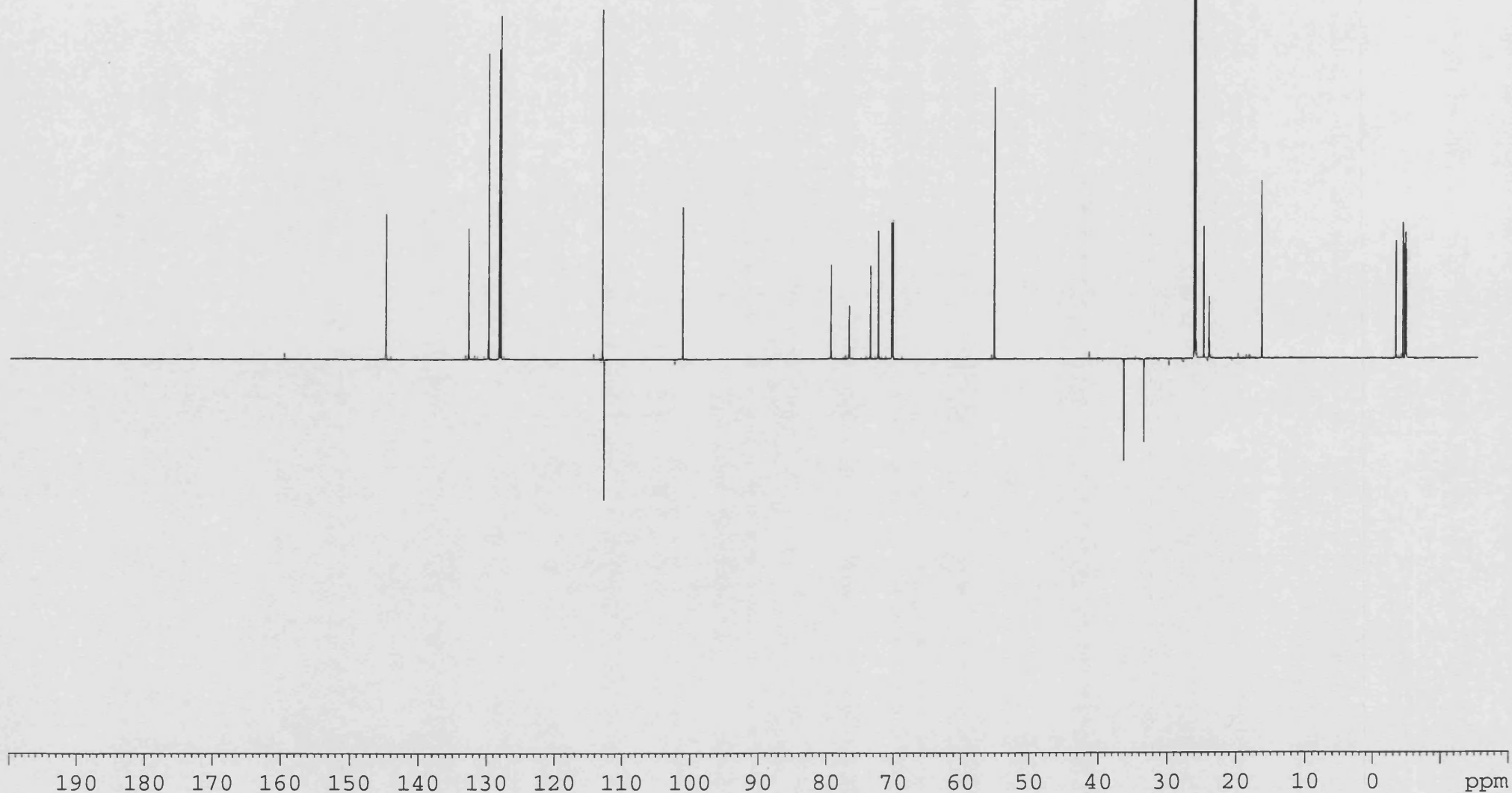
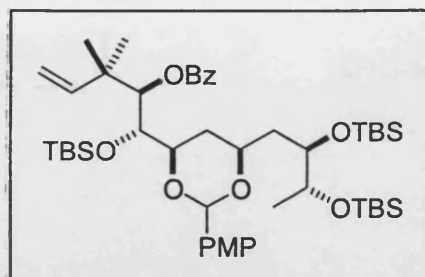


[illegible]

II-MF-73
HMQC
CDC13

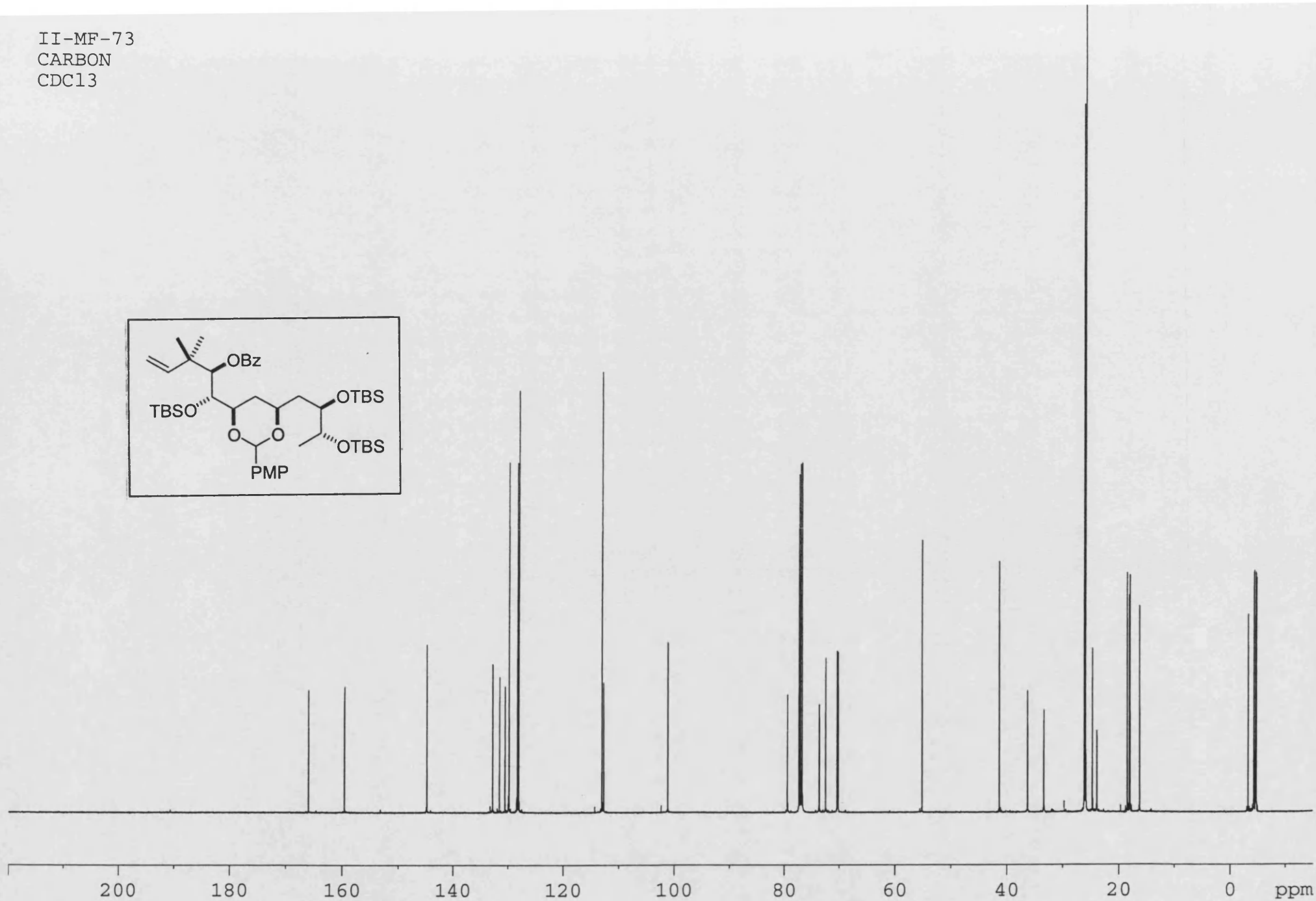
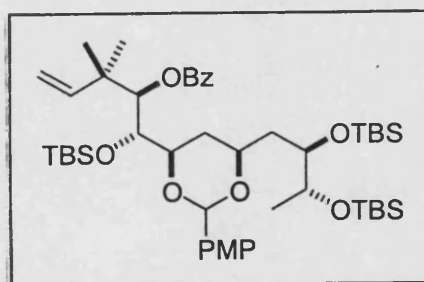


II-MF-73
DEPT
CDCl₃

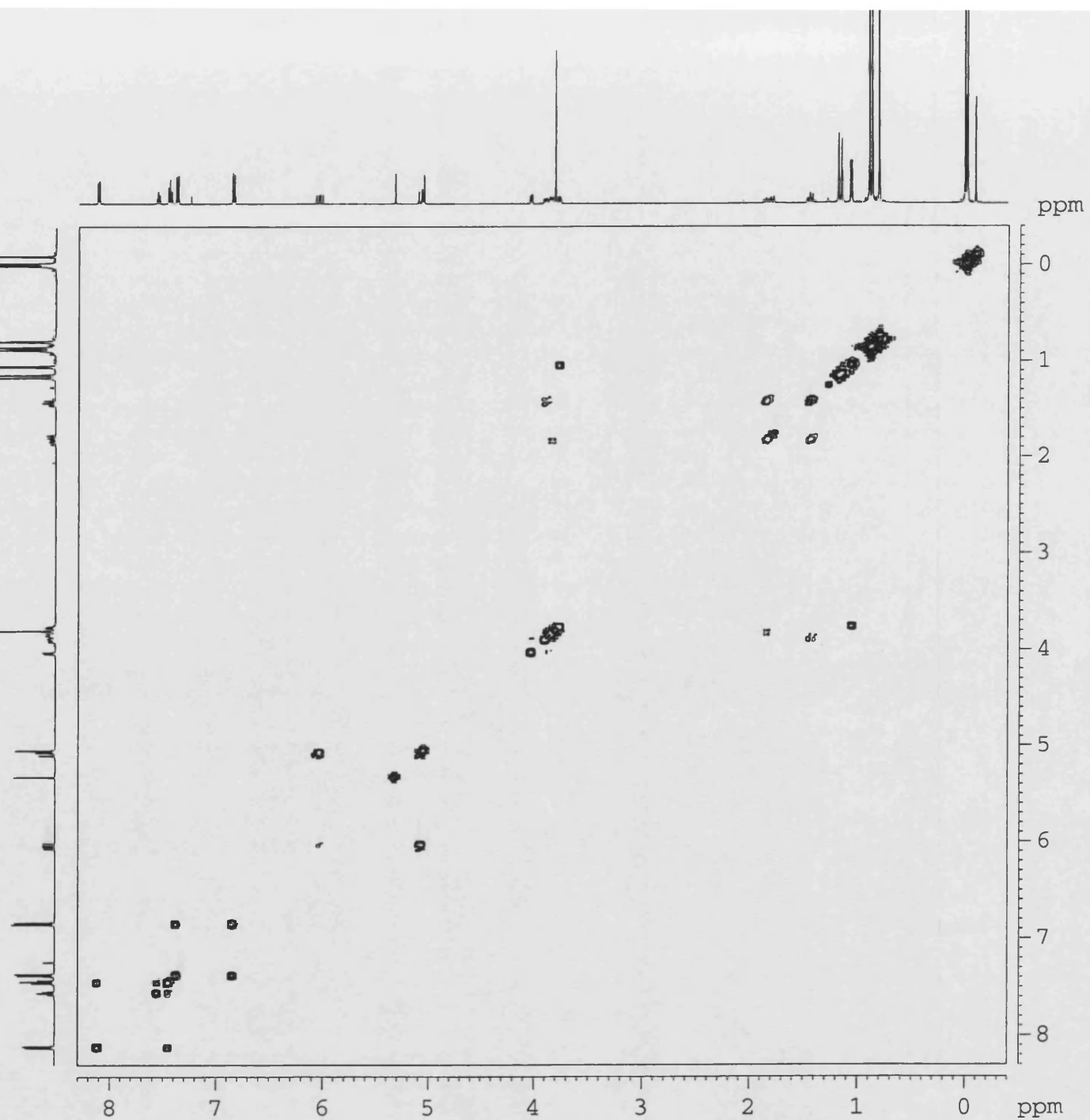
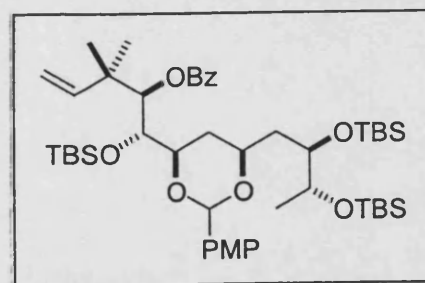


Y: 64 scans, 16.0cm-1, apod none, flat

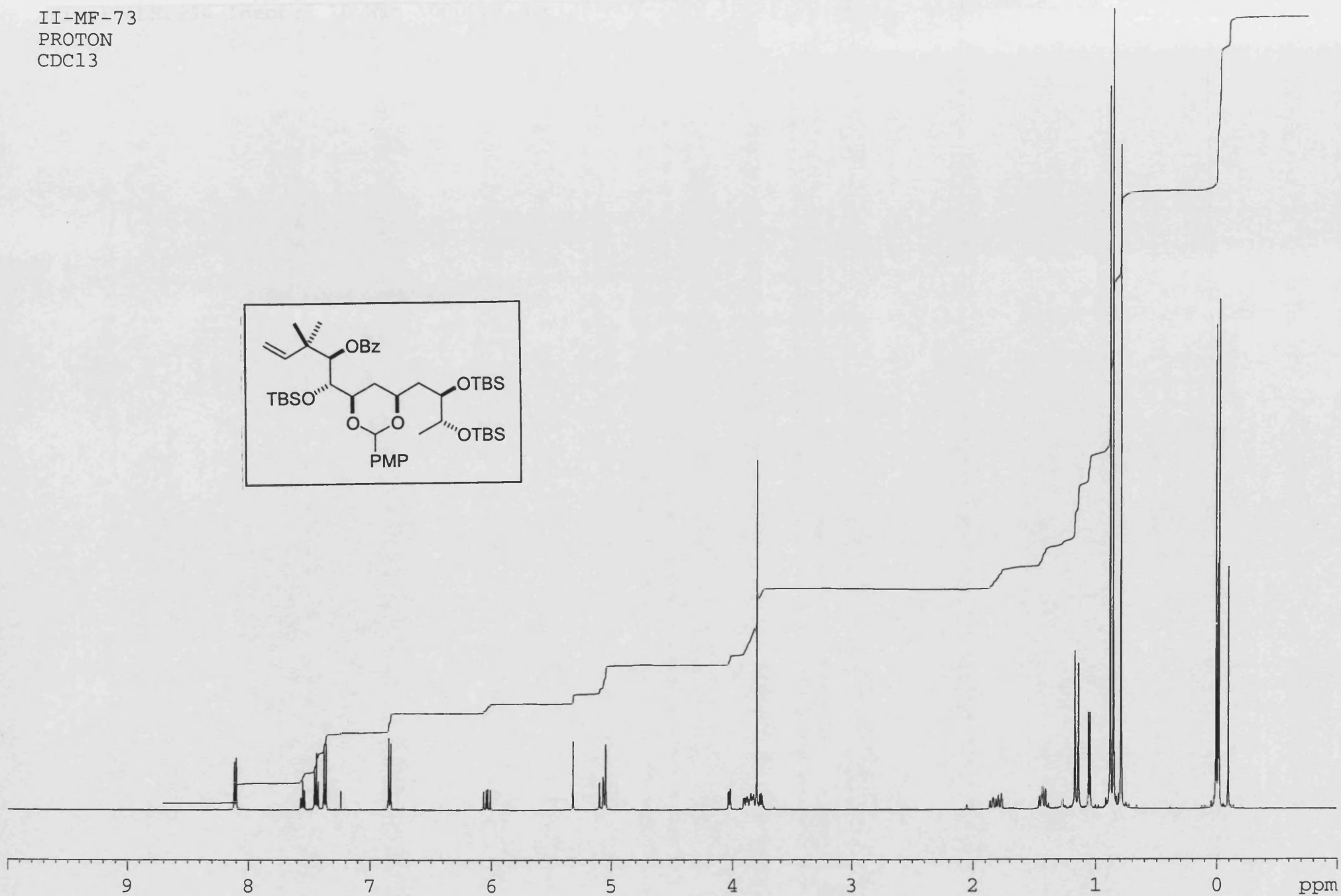
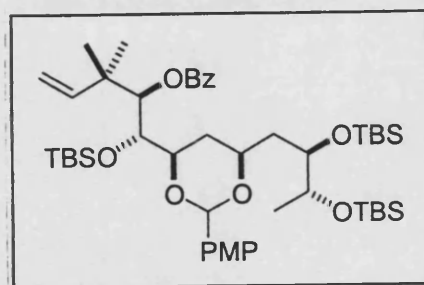
II-MF-73
CARBON
CDC13



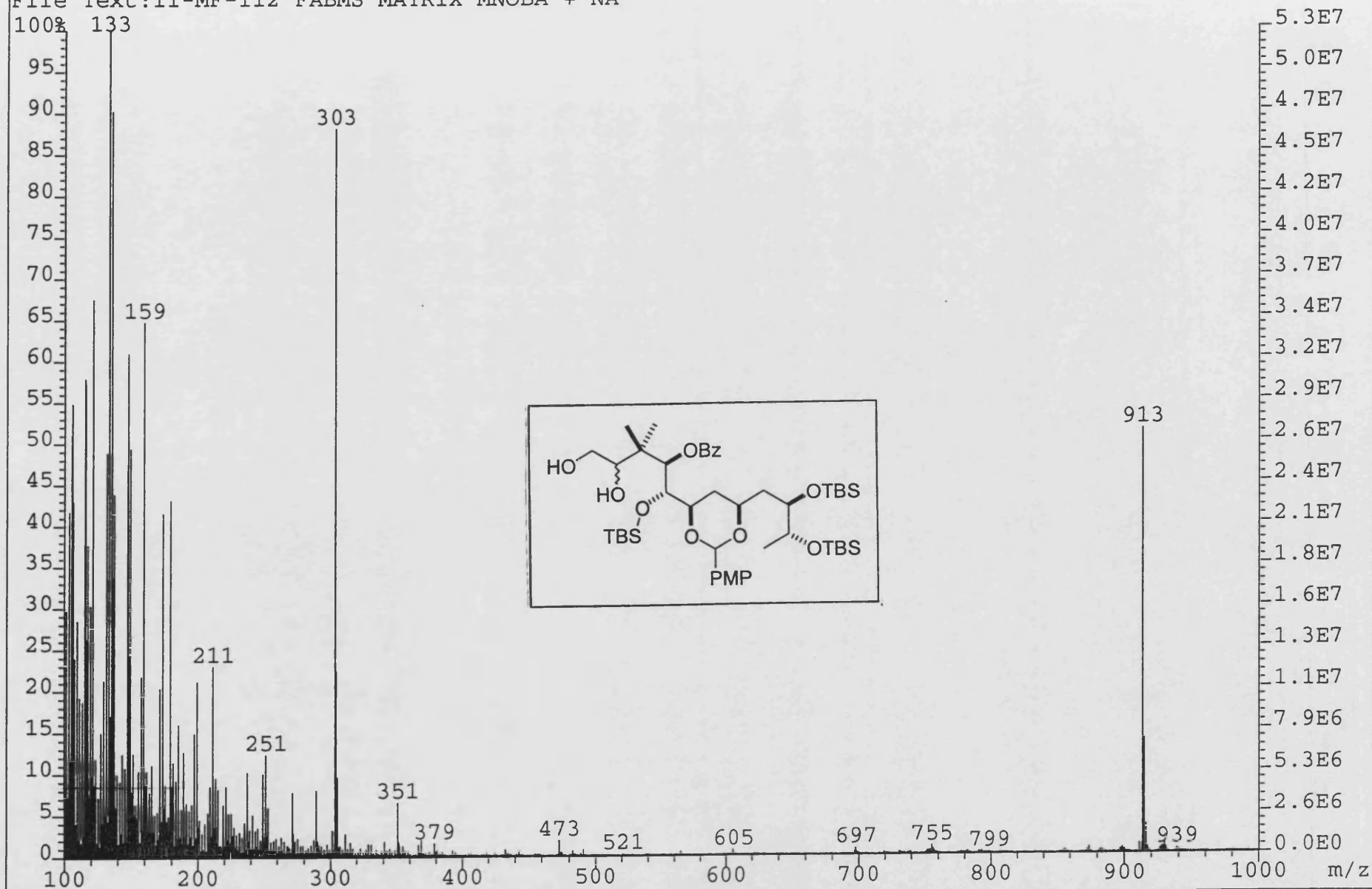
II-MF-73
COSY
CDCl₃

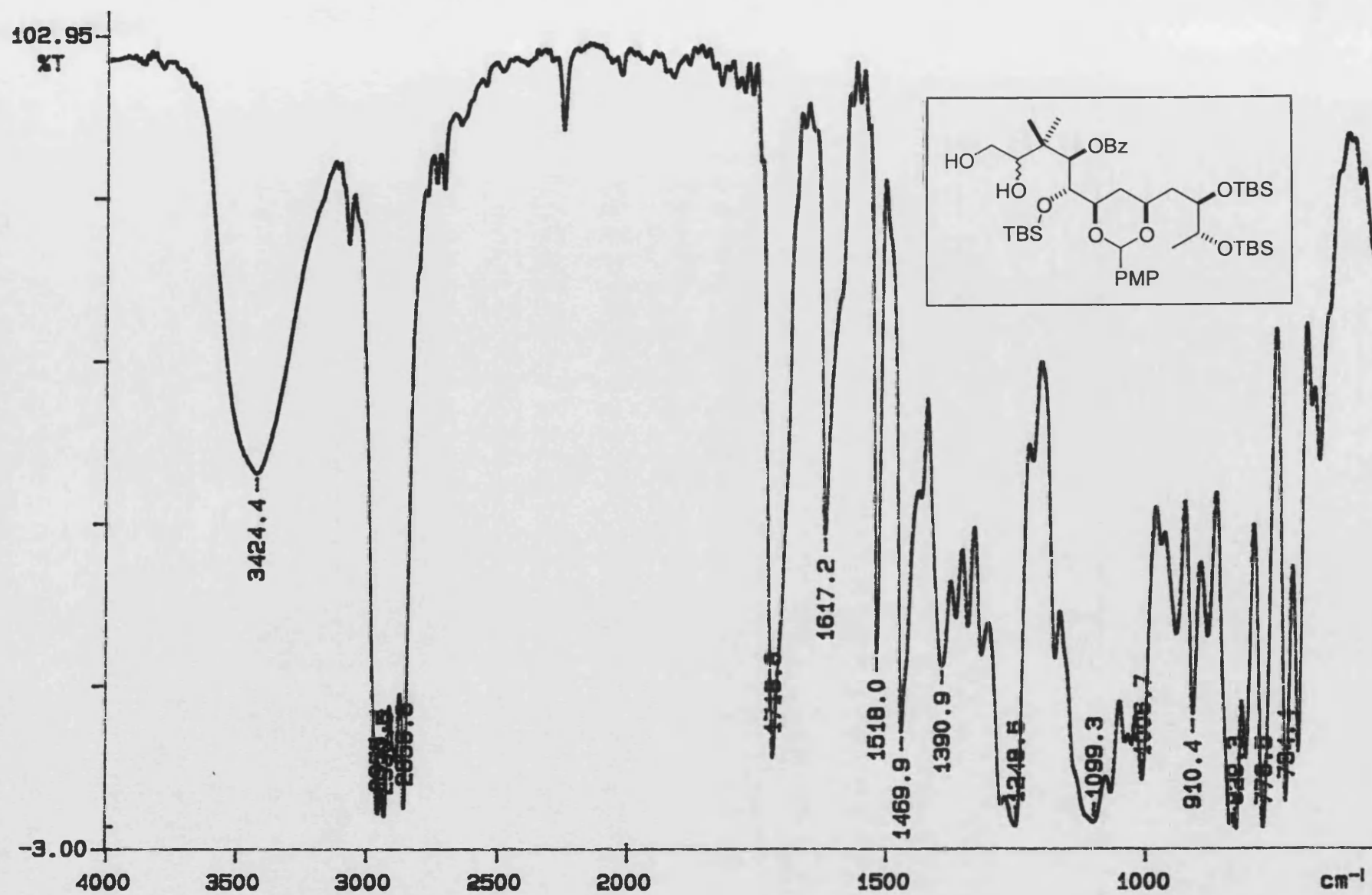


II-MF-73
PROTON
CDC13



File:00SE2994 Ident:2_10 Win 1000PPM Acq:28-NOV-2000 15:18:00 +0:42 Cal:FABMM281100_1
ZAB-SE4F FAB+ Magnet BpM:133 BpI:52712788 TIC:1518479872 Flags:HALL
File Text:II-MF-112 FABMS MATRIX MNOBA + NA

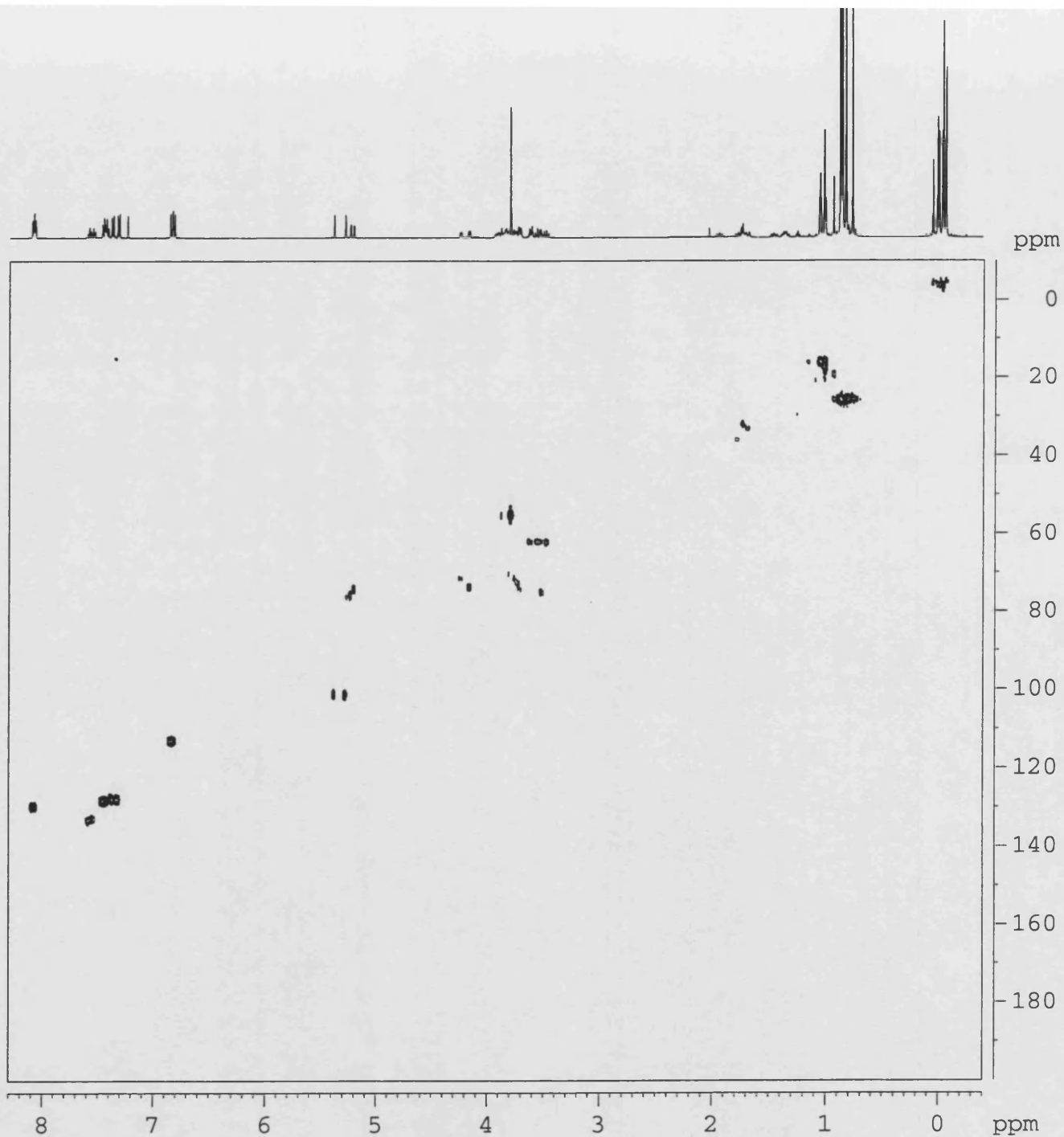
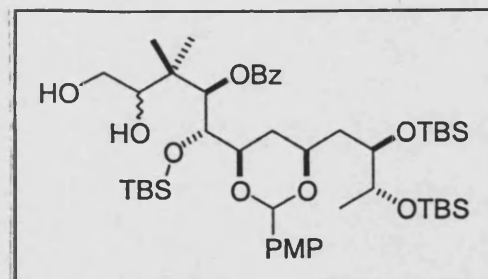




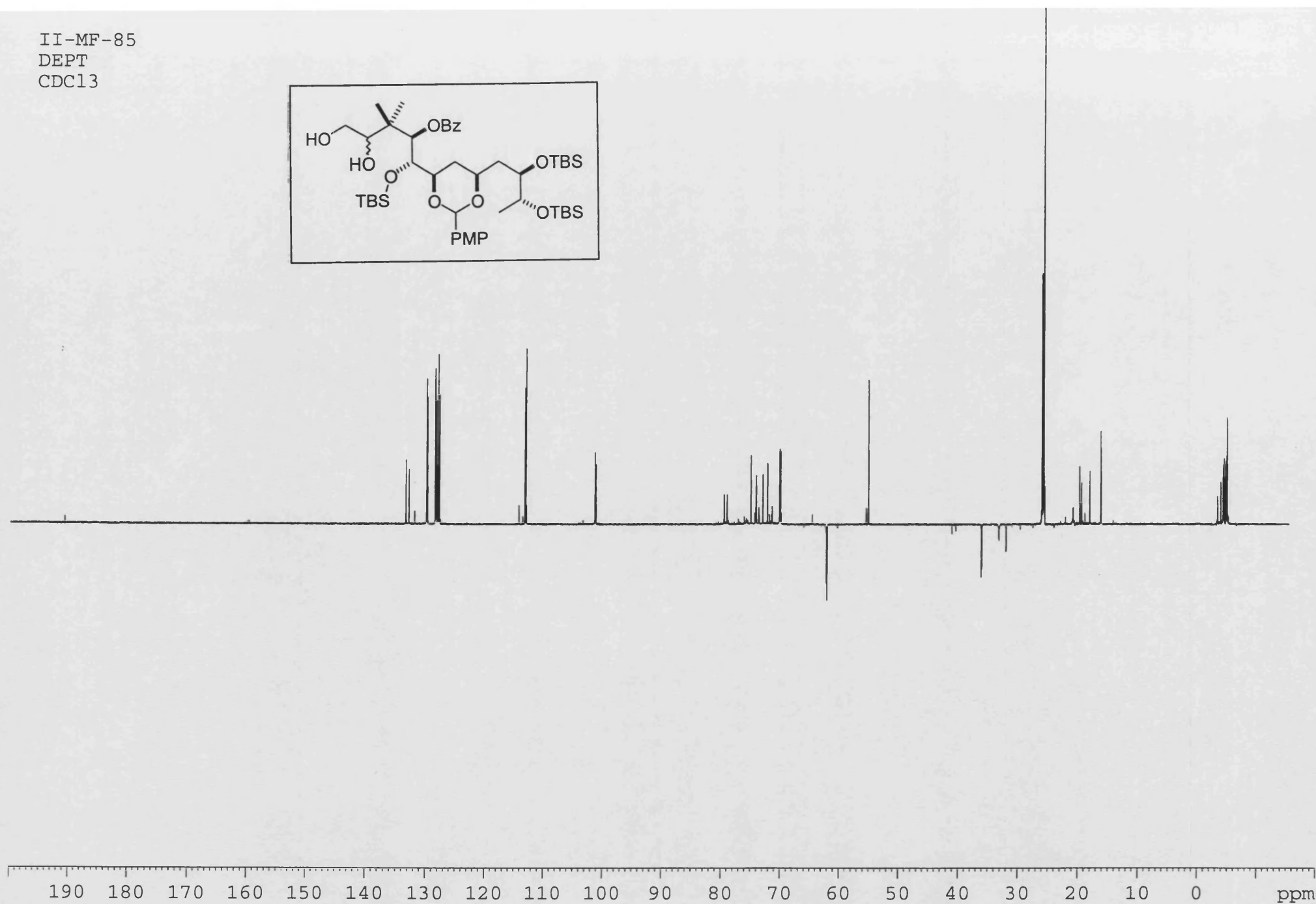
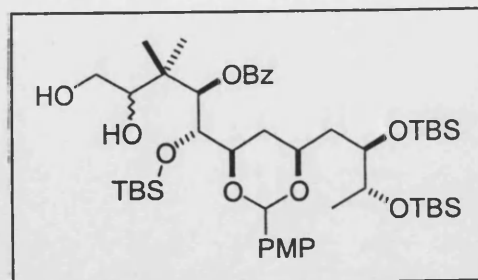
02/08/01 11:33

X: 64 scans, 16.0cm⁻¹, apod none, flat

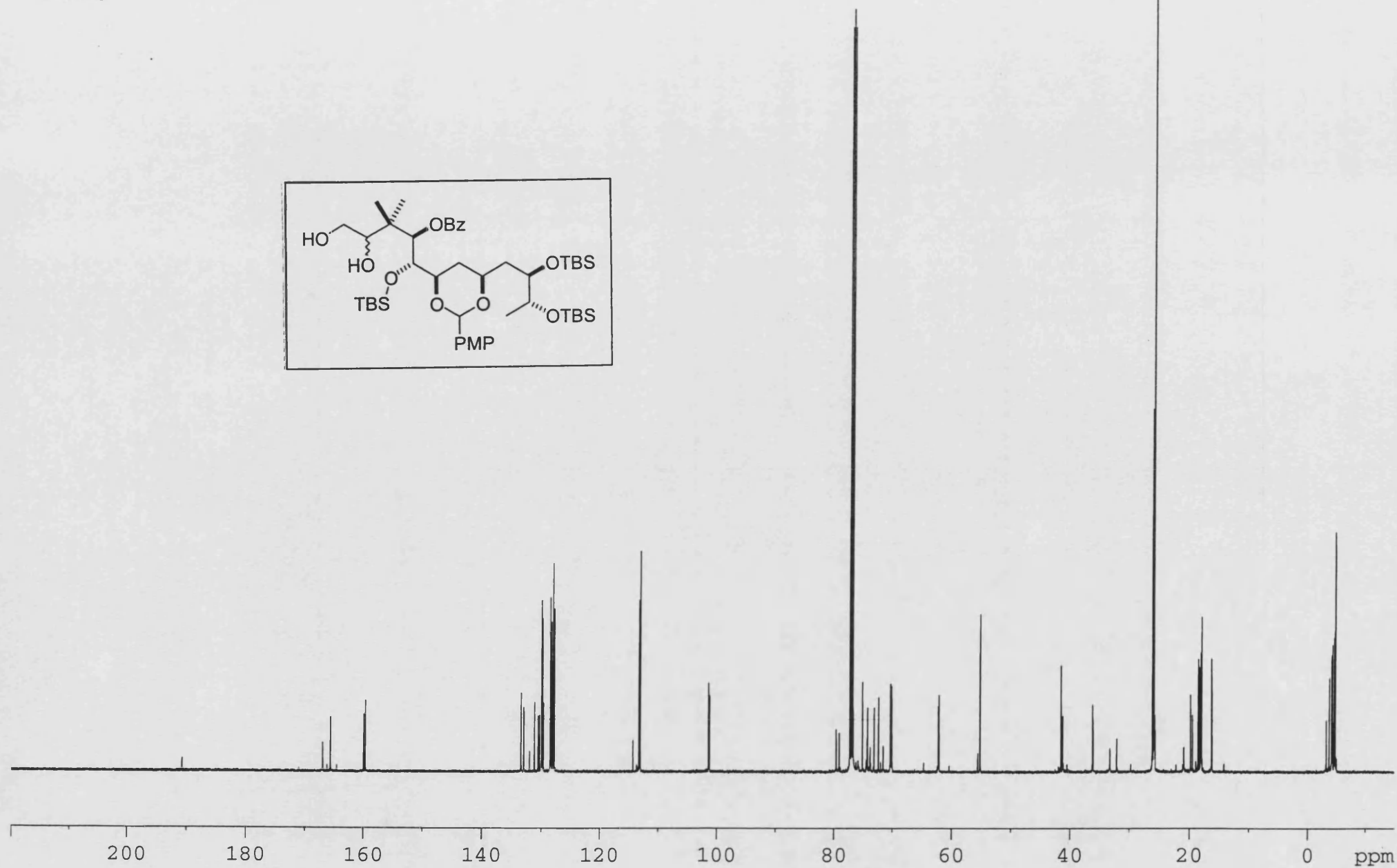
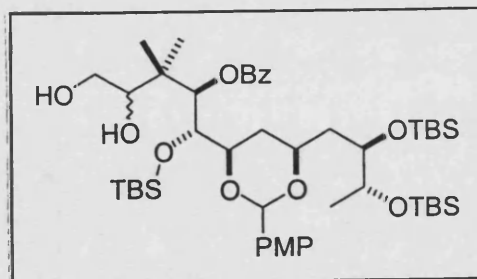
II-MF-85
HMQC
CDCl₃



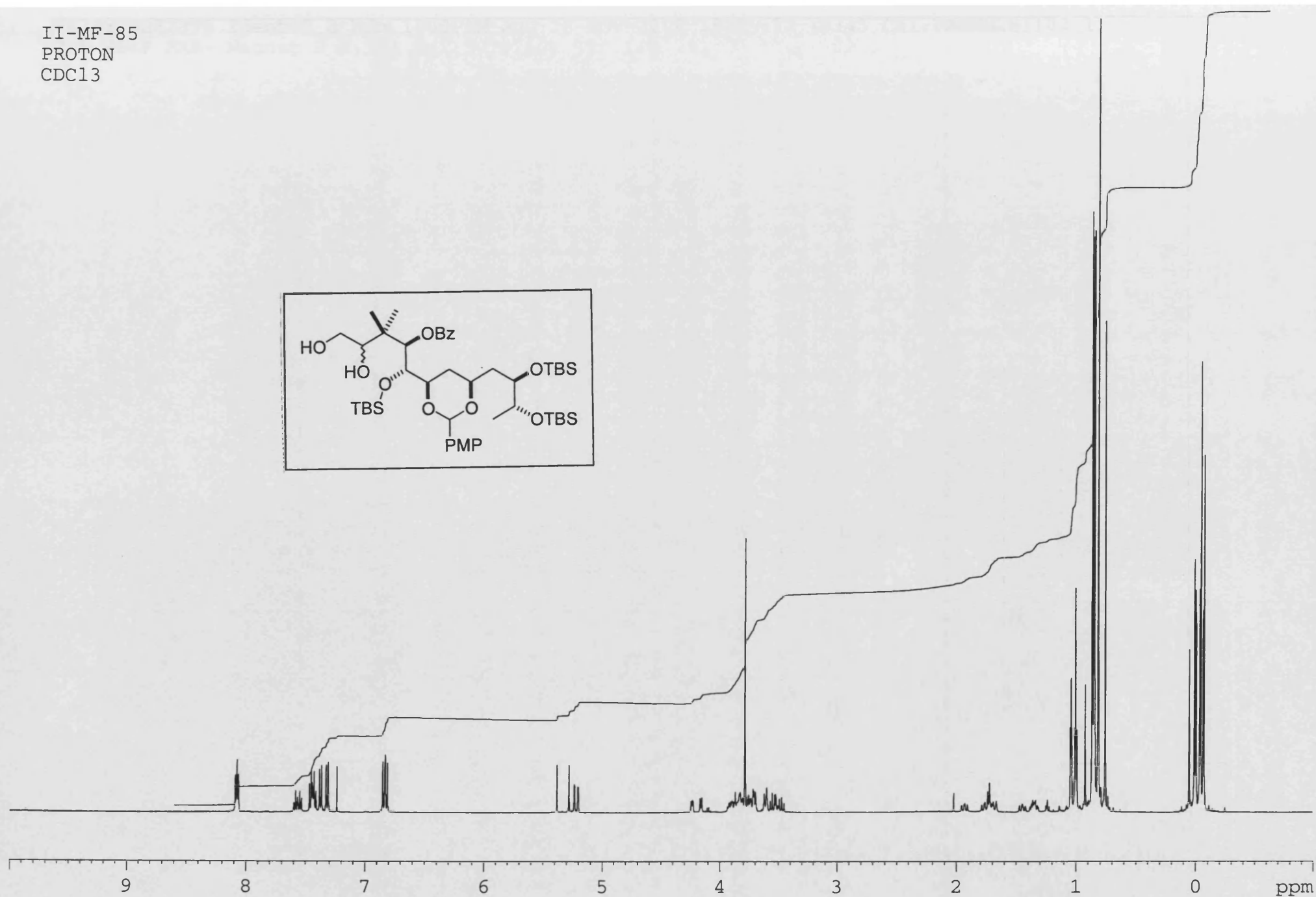
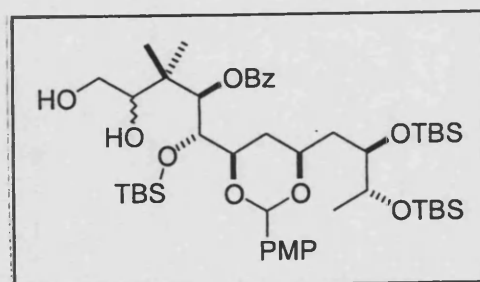
II-MF-85
DEPT
CDCl₃



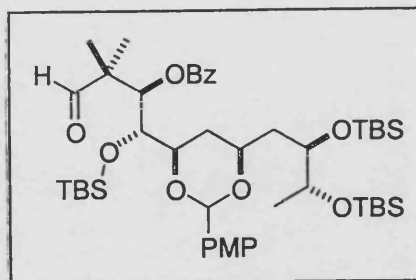
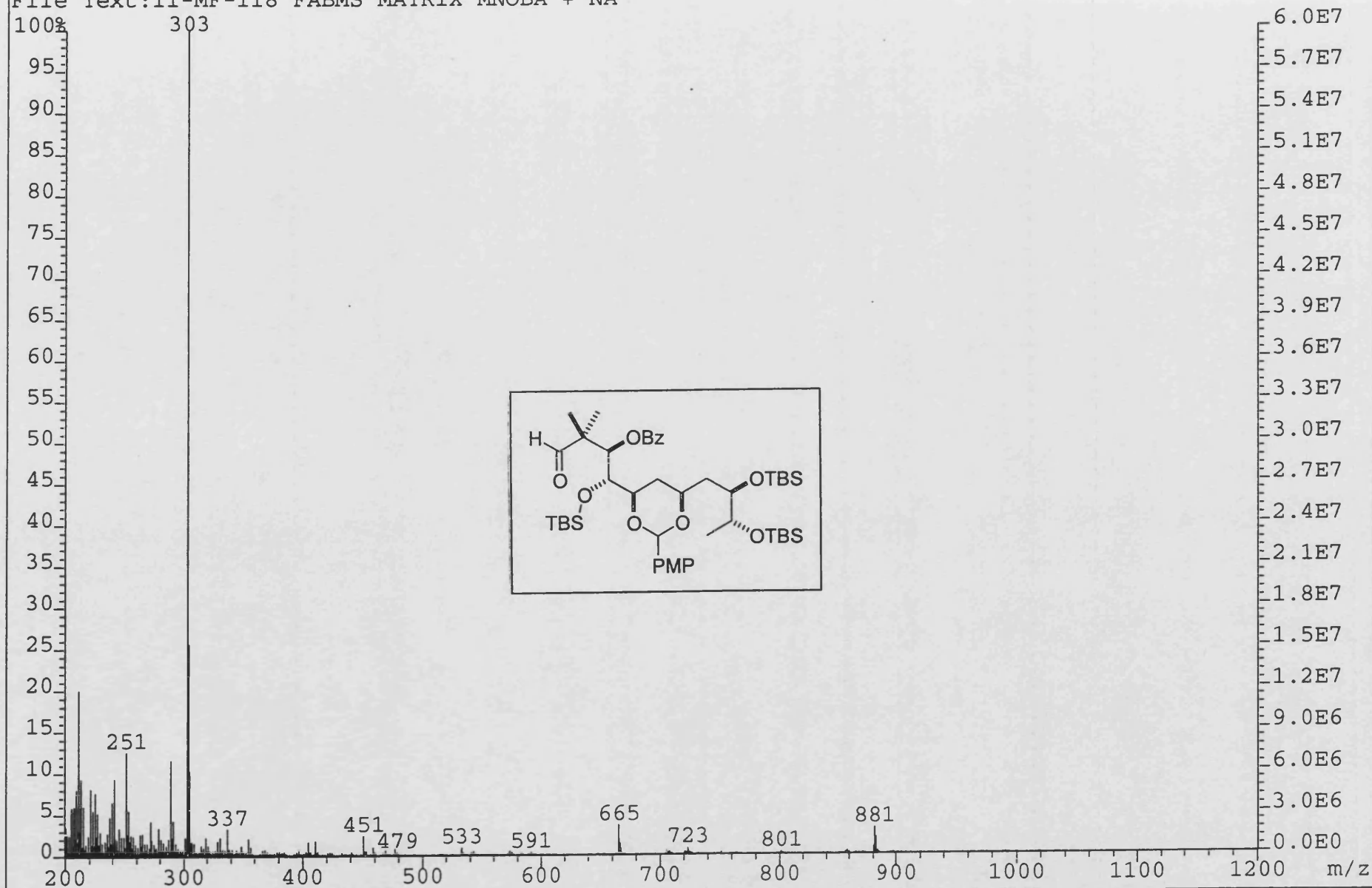
II-MF-85
CARBON
CDCl₃



II-MF-85
PROTON
CDCl₃

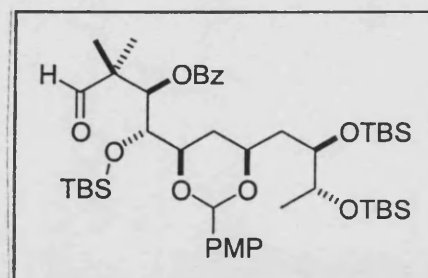
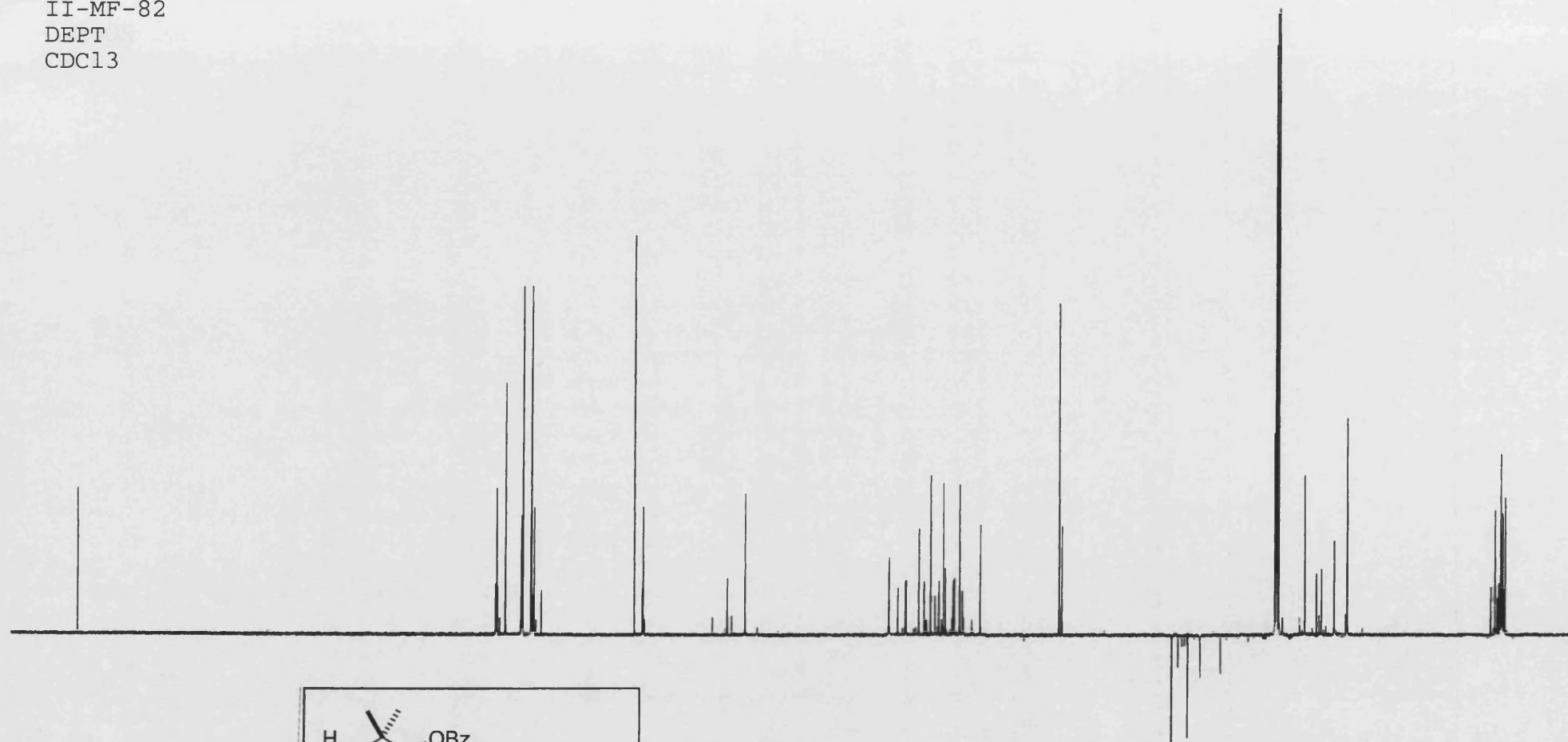


File Text:II-MF-118 FABMS MATRIX MNOBA + NA

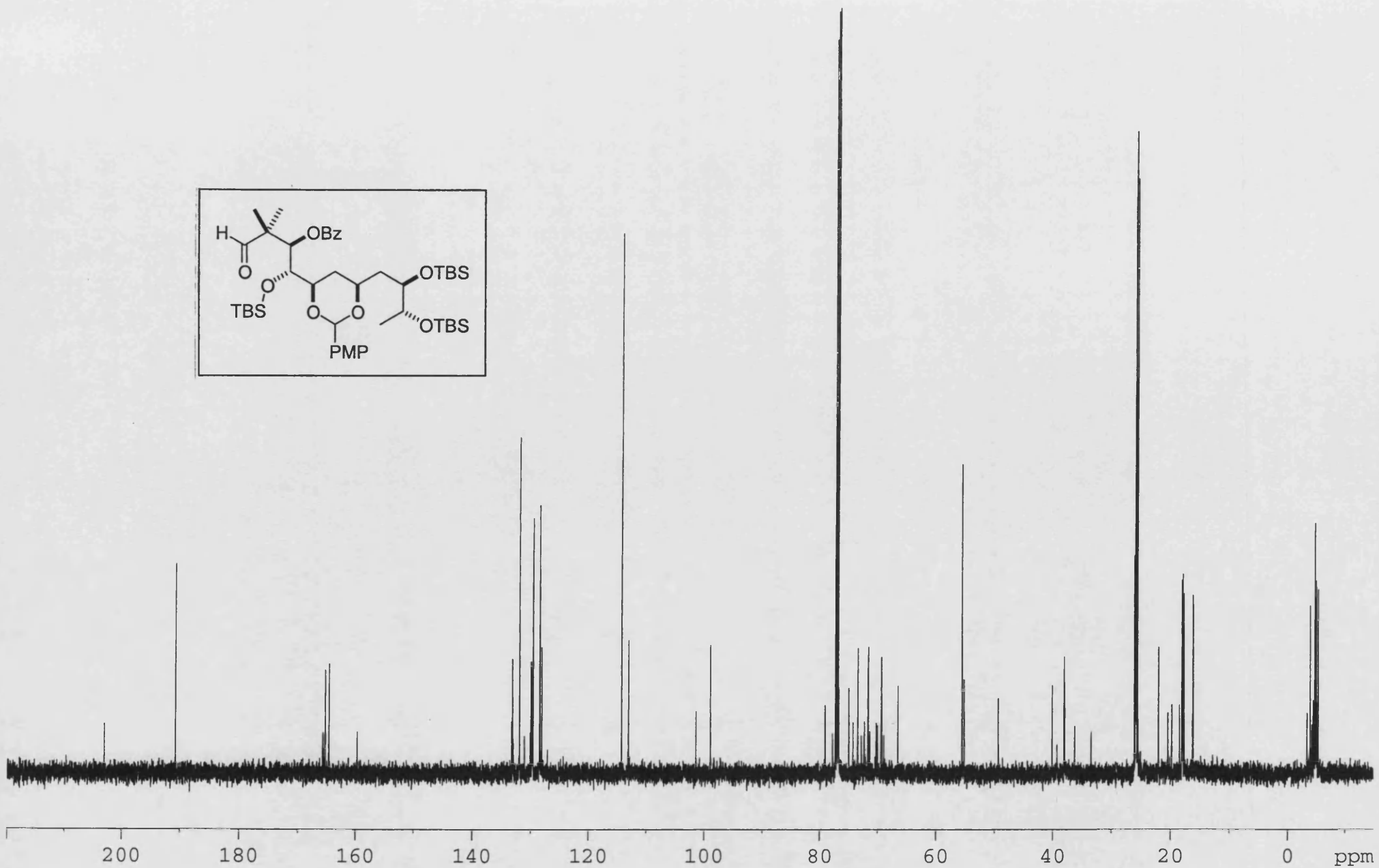
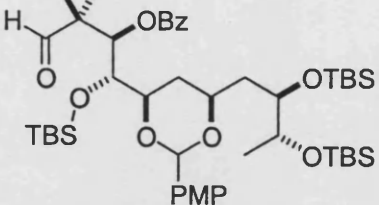


Z: 64 scans, 16.0cm⁻¹, apod none, flat

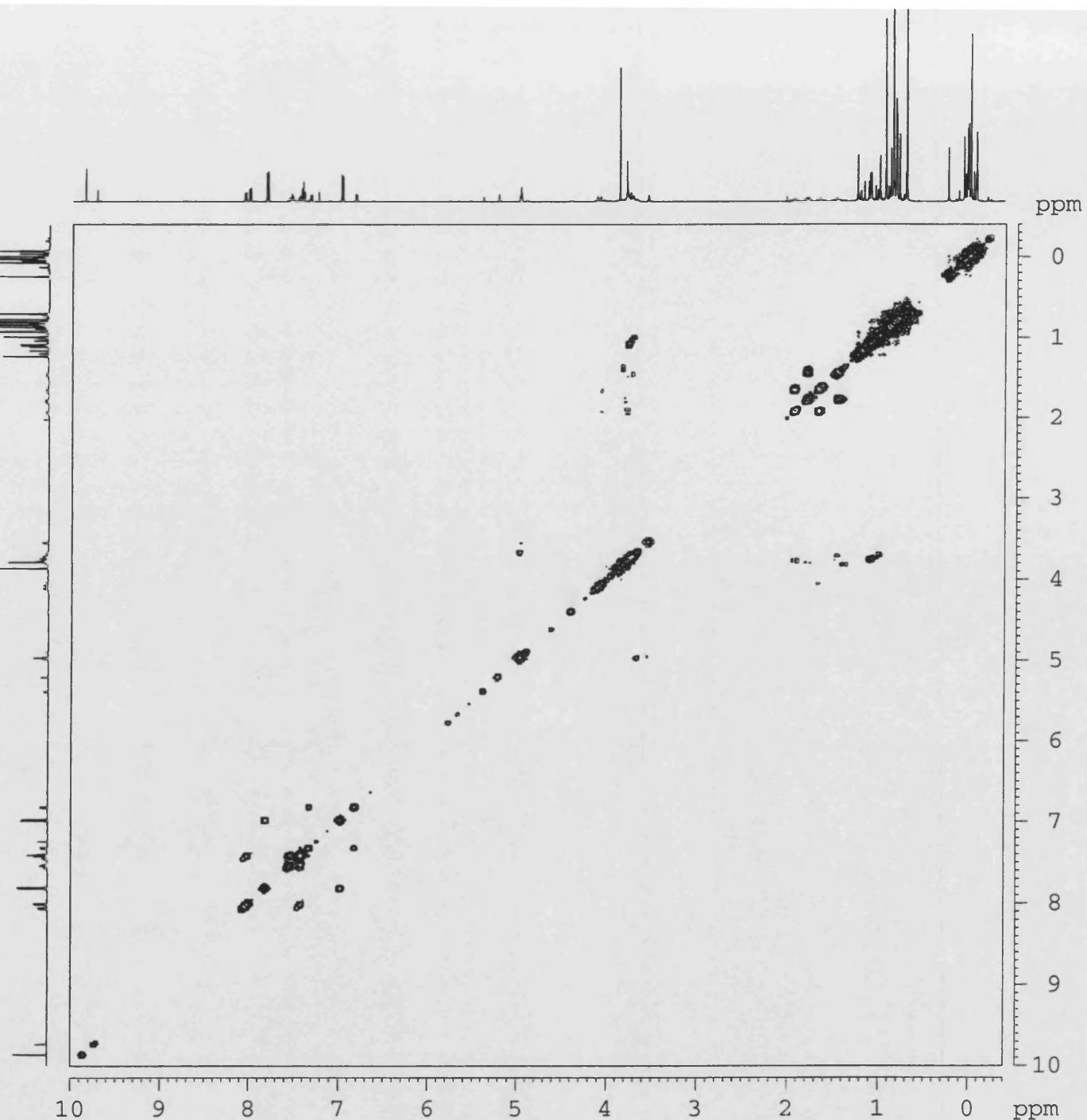
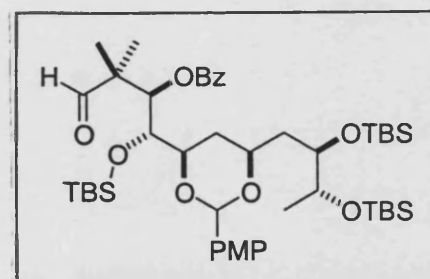
CDC13



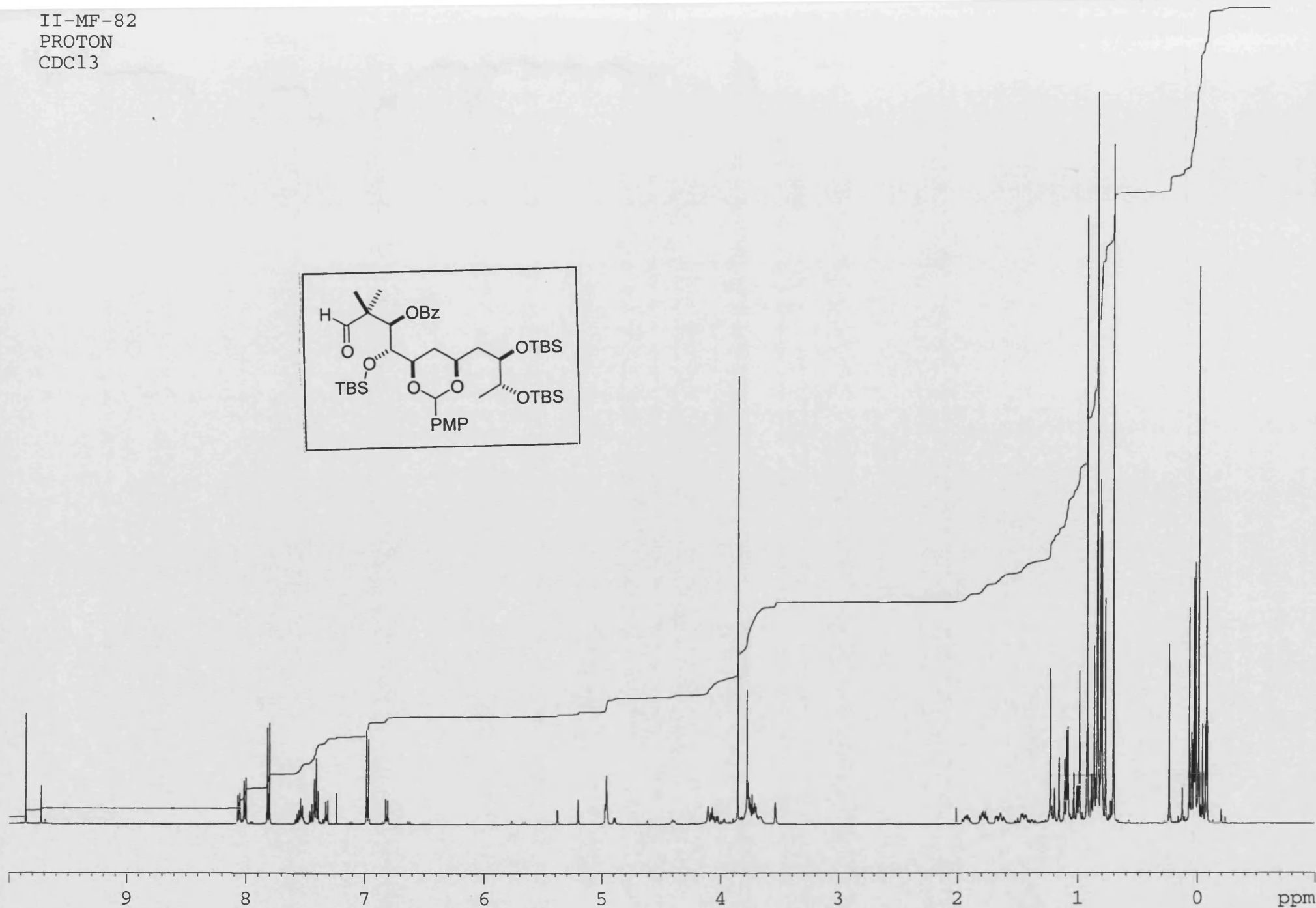
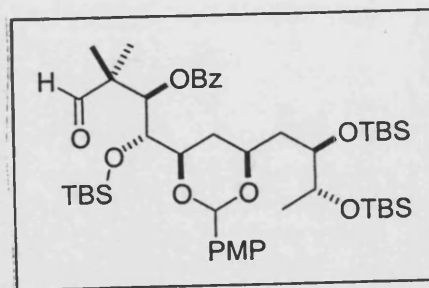
CDC13



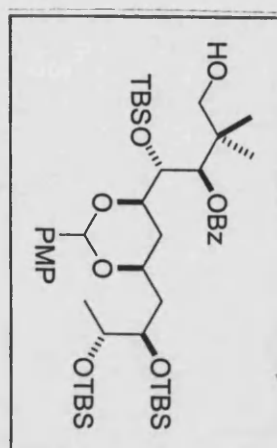
II-MF-82
COSY
CDC13



II-MF-82
PROTON
CDC13



The infrared spectrum shows a single, very sharp and intense absorption peak at a wavenumber of 16.58 cm⁻¹. The x-axis is labeled with wavenumbers in cm⁻¹, ranging from 4000 to 1000. The y-axis represents transmittance. The peak is located at the top of the scale, corresponding to the 16.58 cm⁻¹ mark.



2955.3 2857.1 2887.5

1719.6

1617.3

1518.4

1470.3

1389.3 -

1281.3

~~\$100.2~~

1064.8

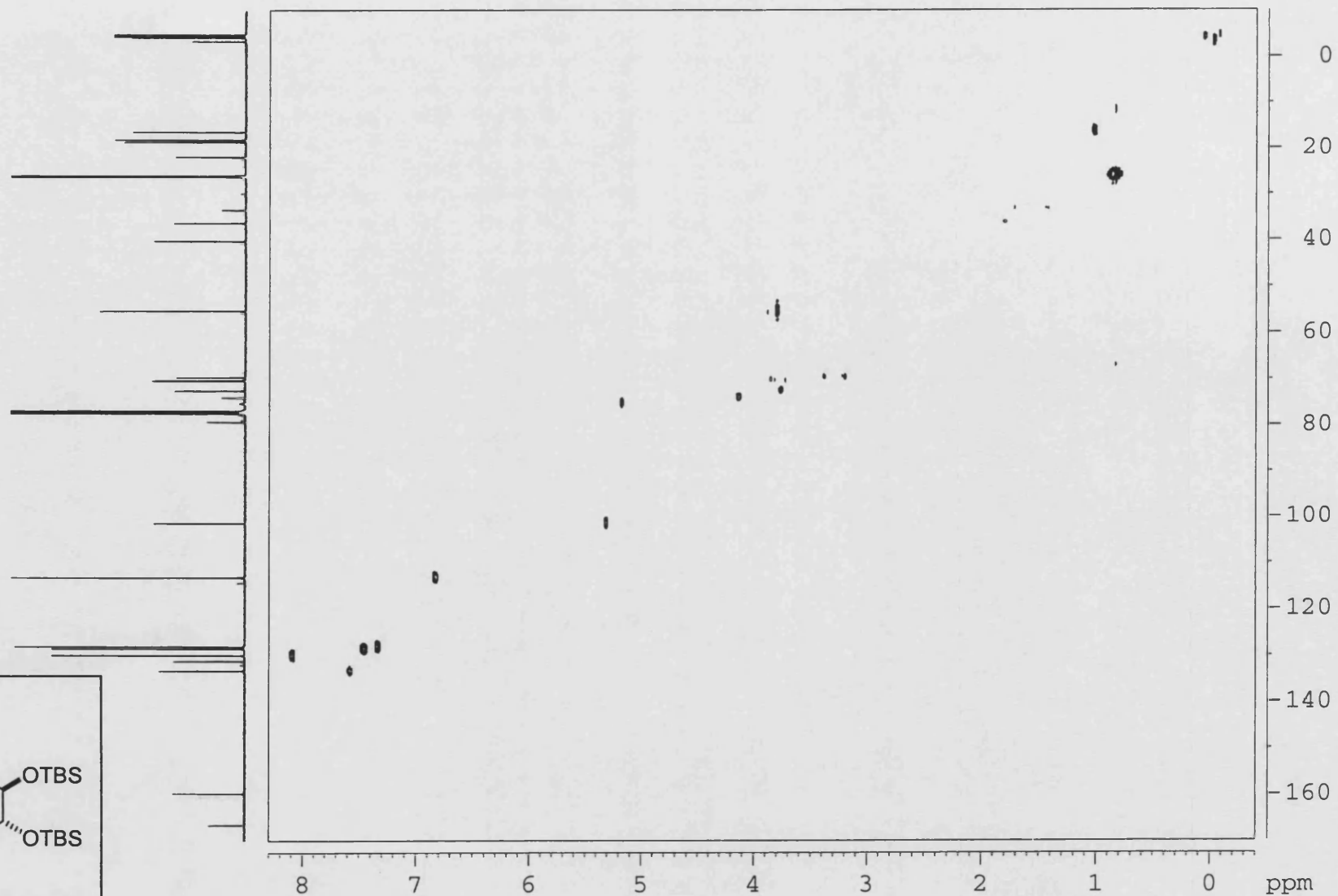
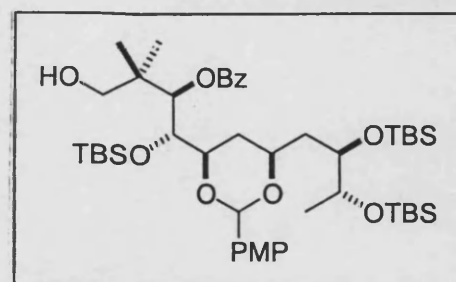
1008.0

832-3

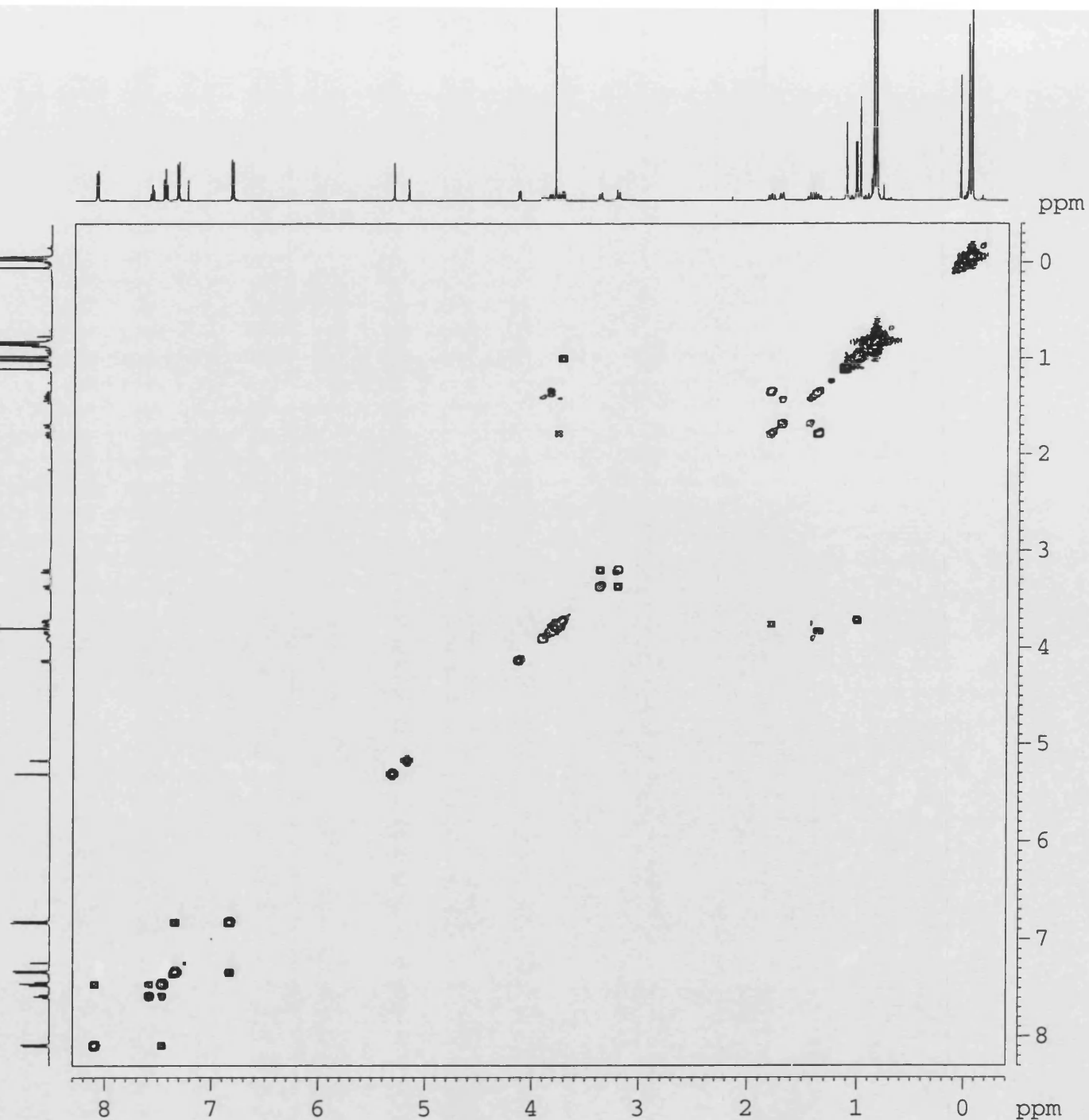
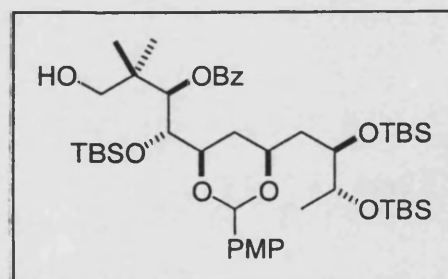
776.3 -

710.6

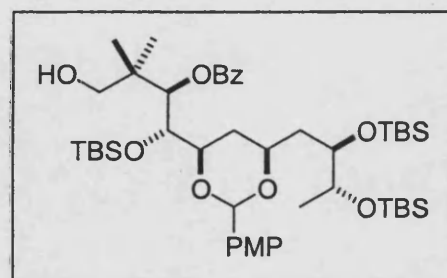
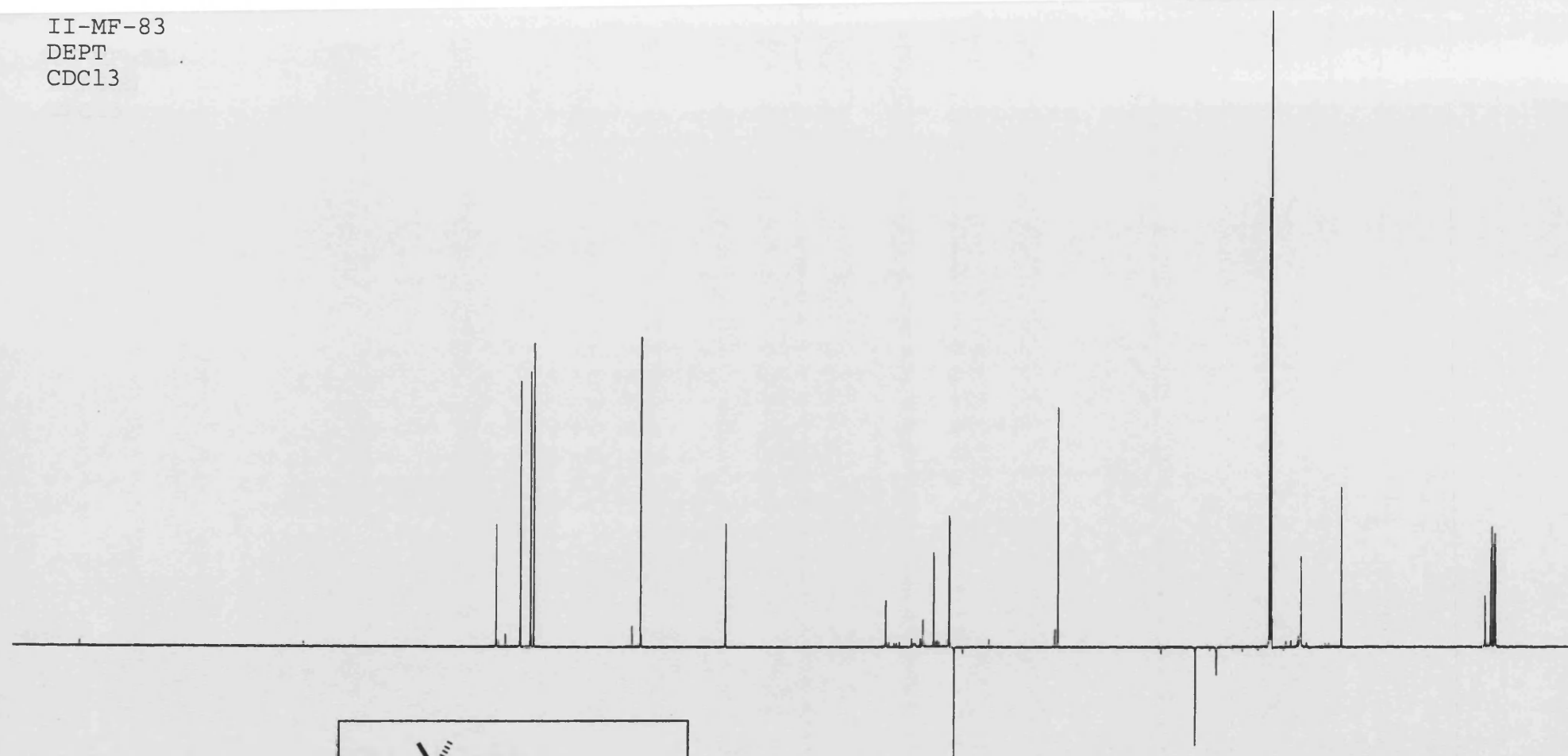
II-MF-83
HMQC
CDC13



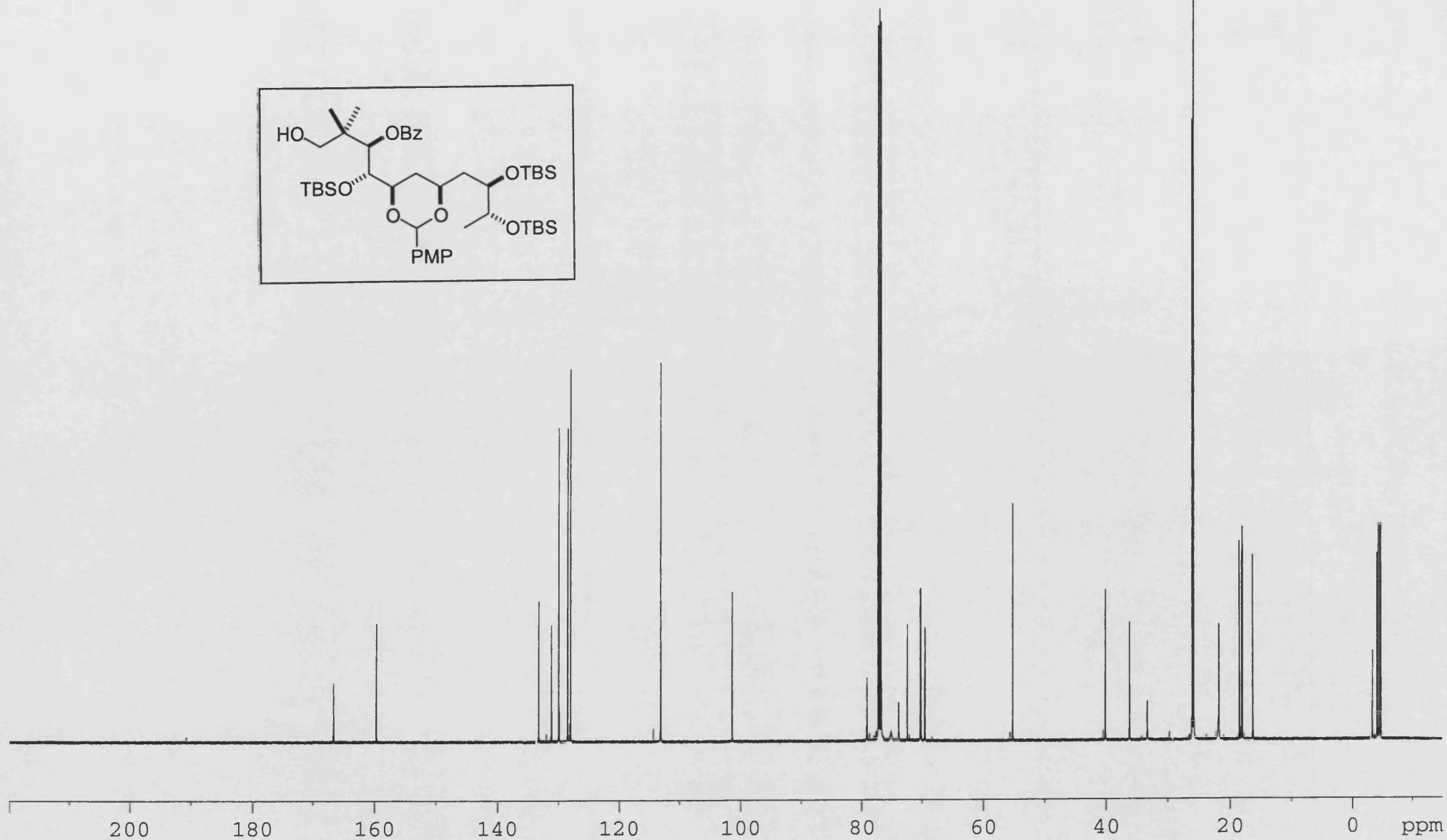
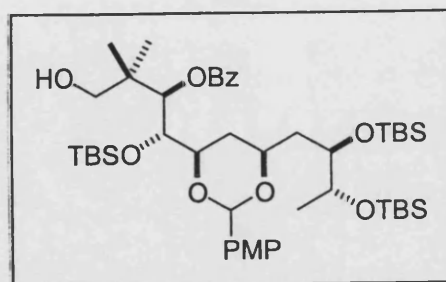
II-MF-83
COSY
CDCl₃



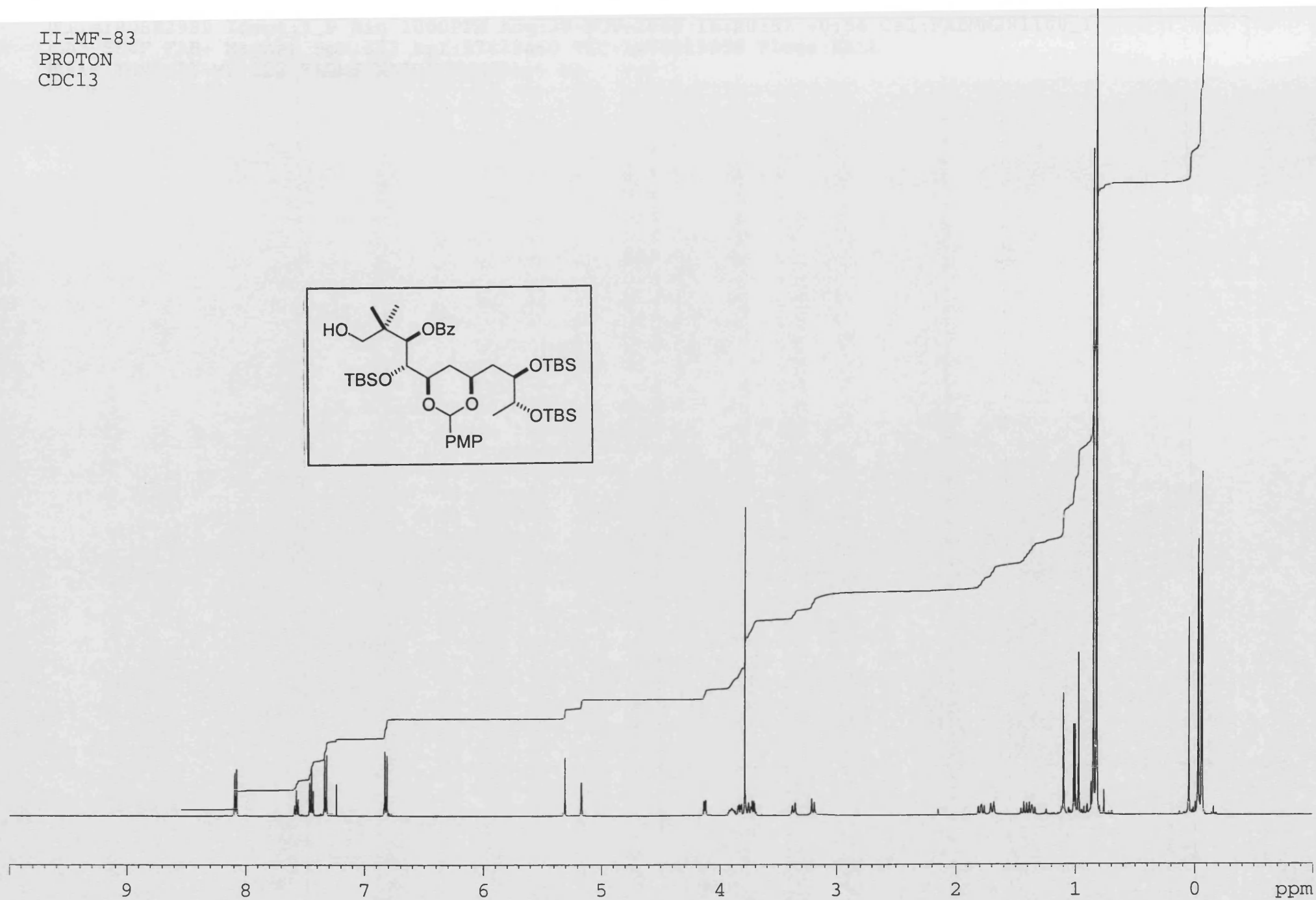
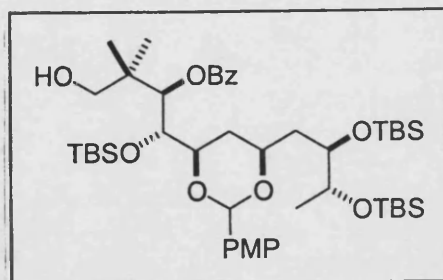
CDC13



II-MF-83
CARBON
CDCl₃



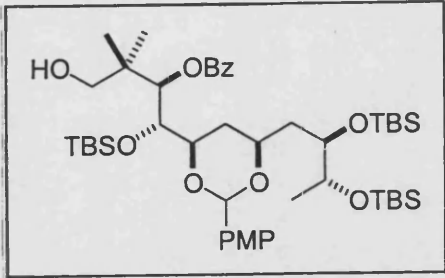
II-MF-83
PROTON
CDC13



File:00SE2999 Ident:7 9 Win 1000PPM Acq:28-NOV-2000 16:20:57 +0:54 Cal:FABMM281100_1

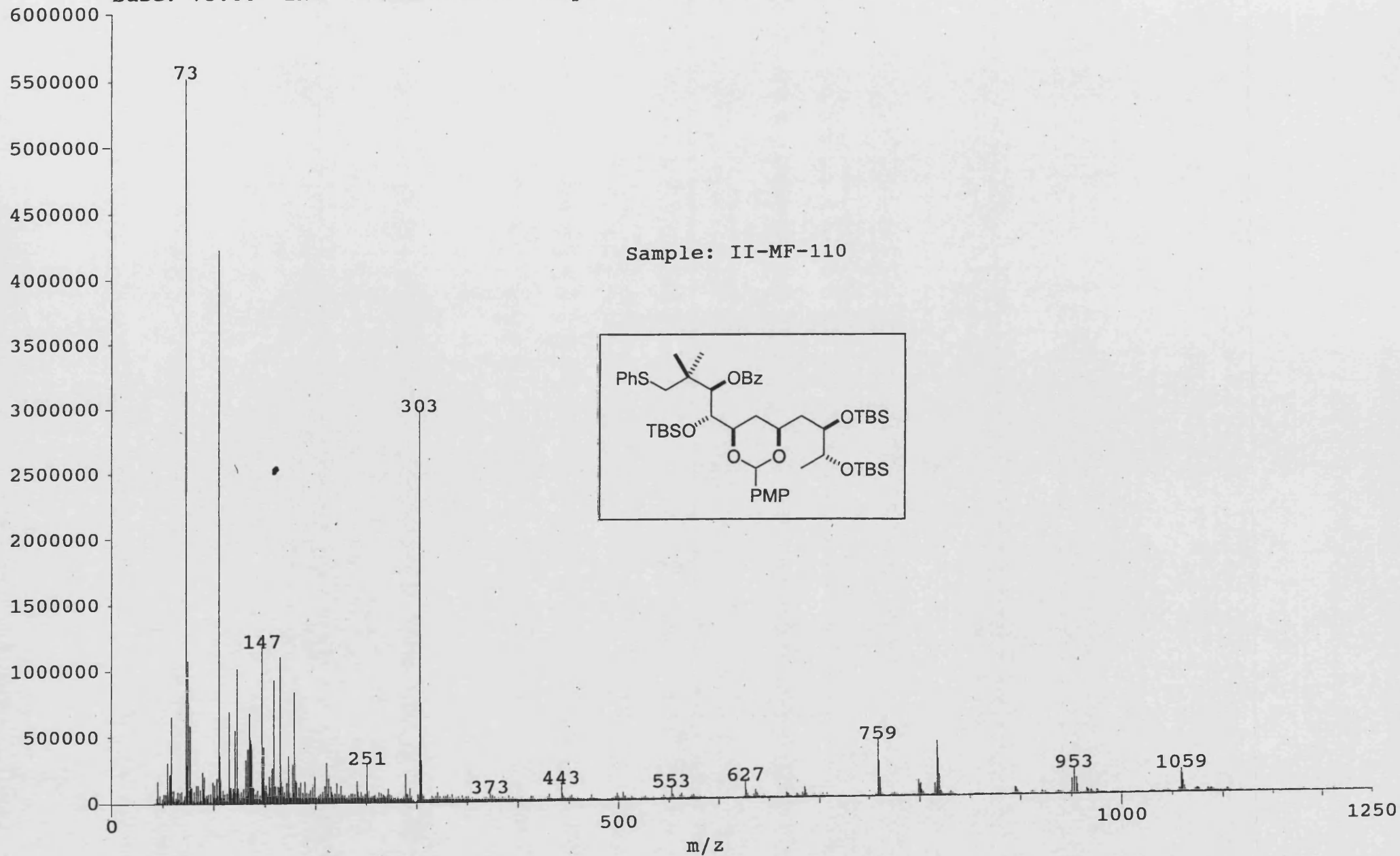
ZAB-SE4F FAB+ Magnet BpM:303 BpI:57420460 TIC:1478313856 Flags:HALL

File Text:II-MF-122 FABMS MATRIX MNOBA + NA

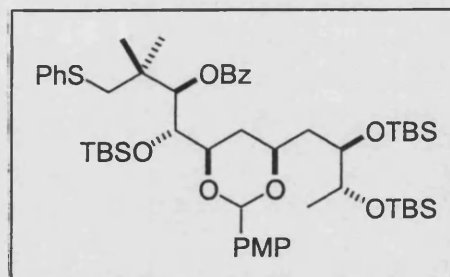


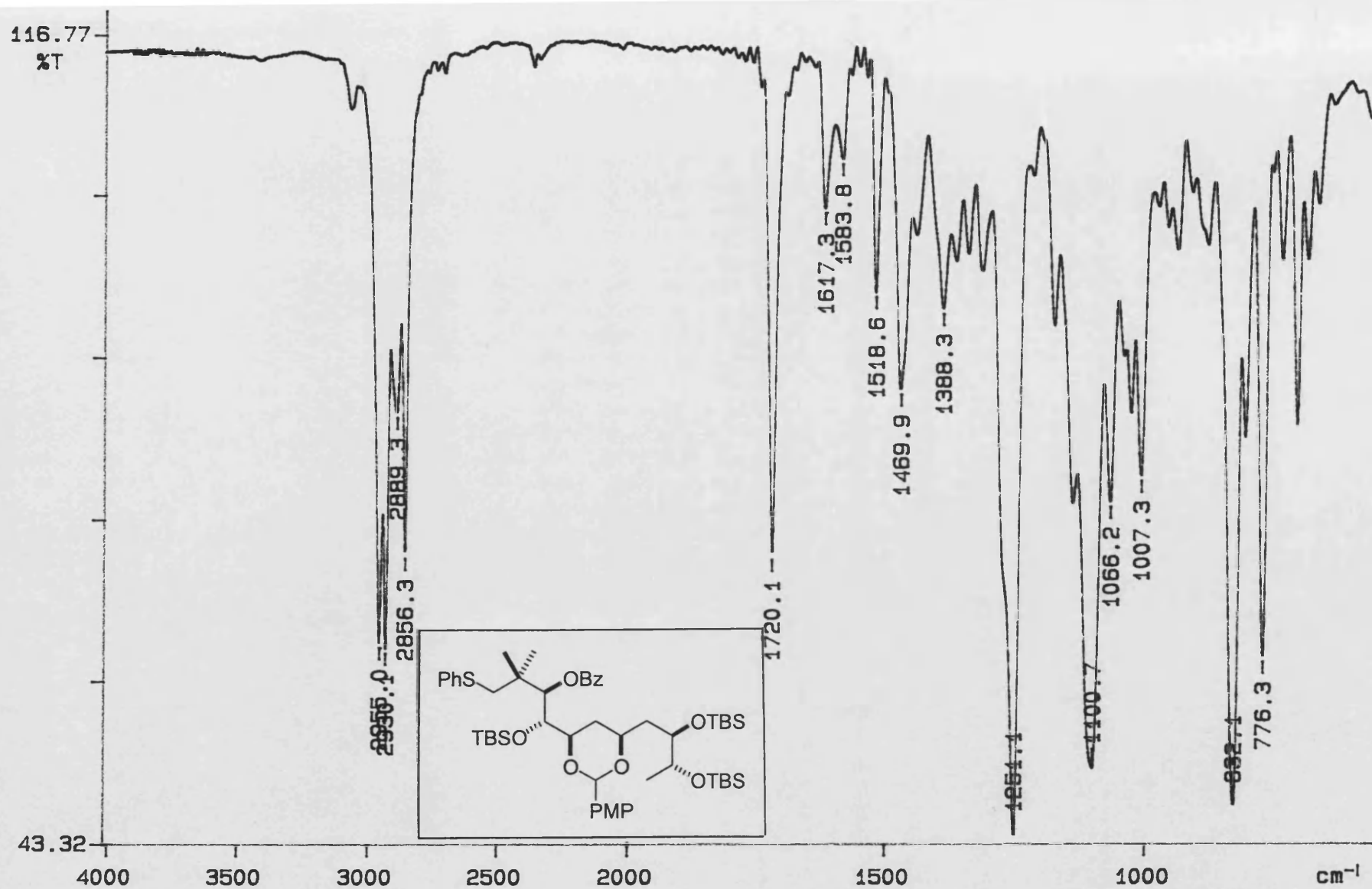
04081002: Scan 139 (32.23 min)

Base: 73.00 Int: 5.51684e+006 Sample: VG70-SE Positive Ion FAB



Sample: II-MF-110

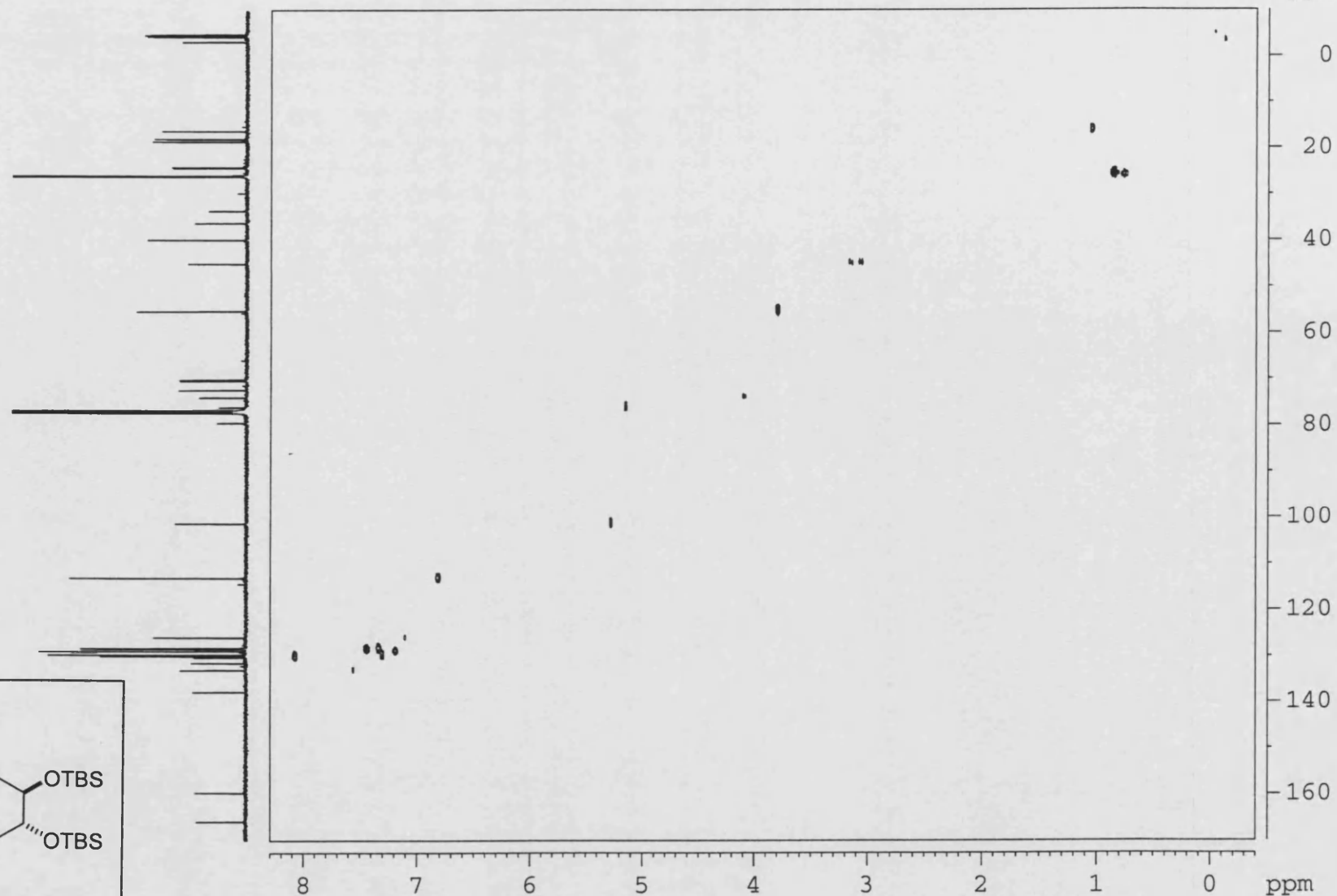
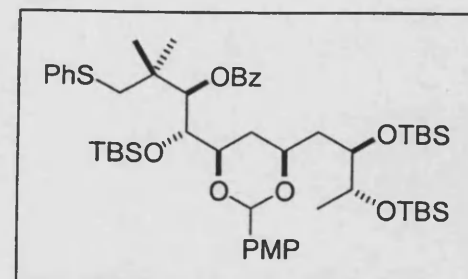




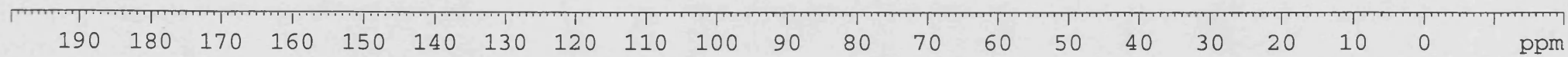
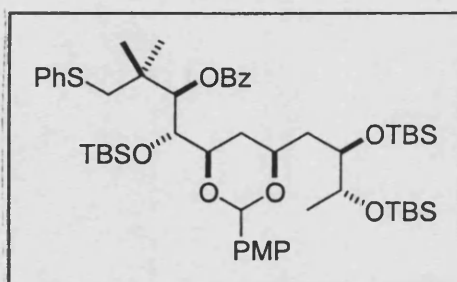
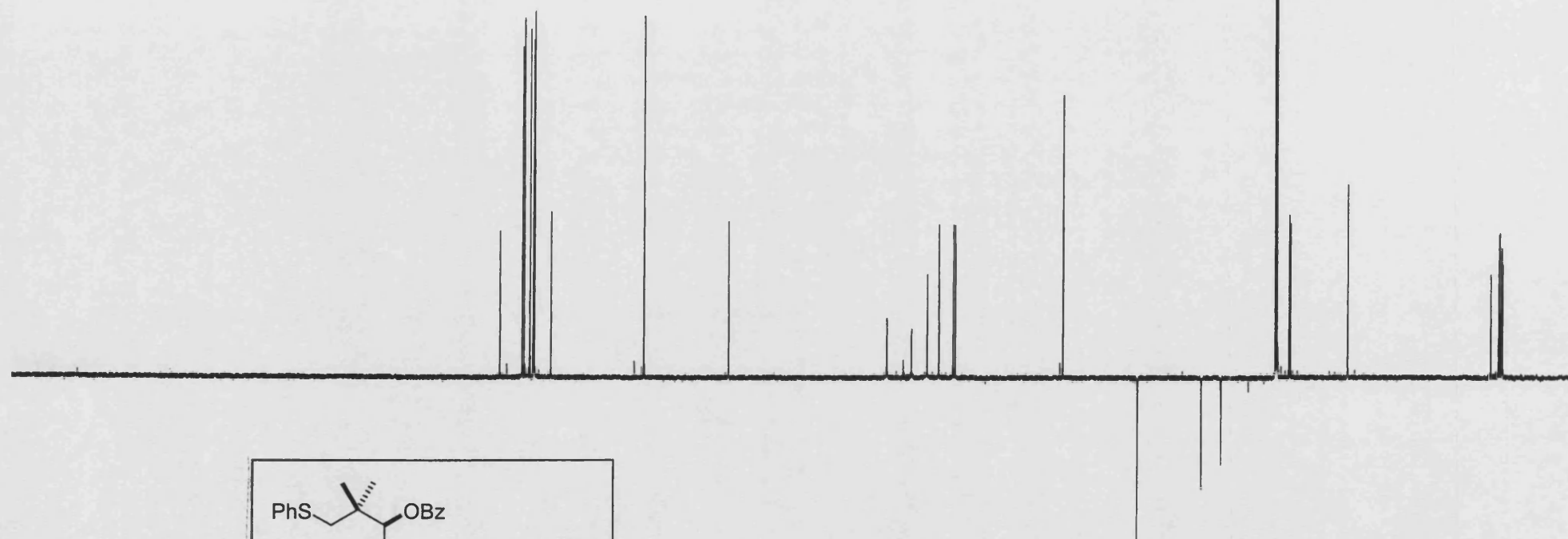
02/08/22 08:29

Y: 64 scans, 16.0cm⁻¹, apod none, flat

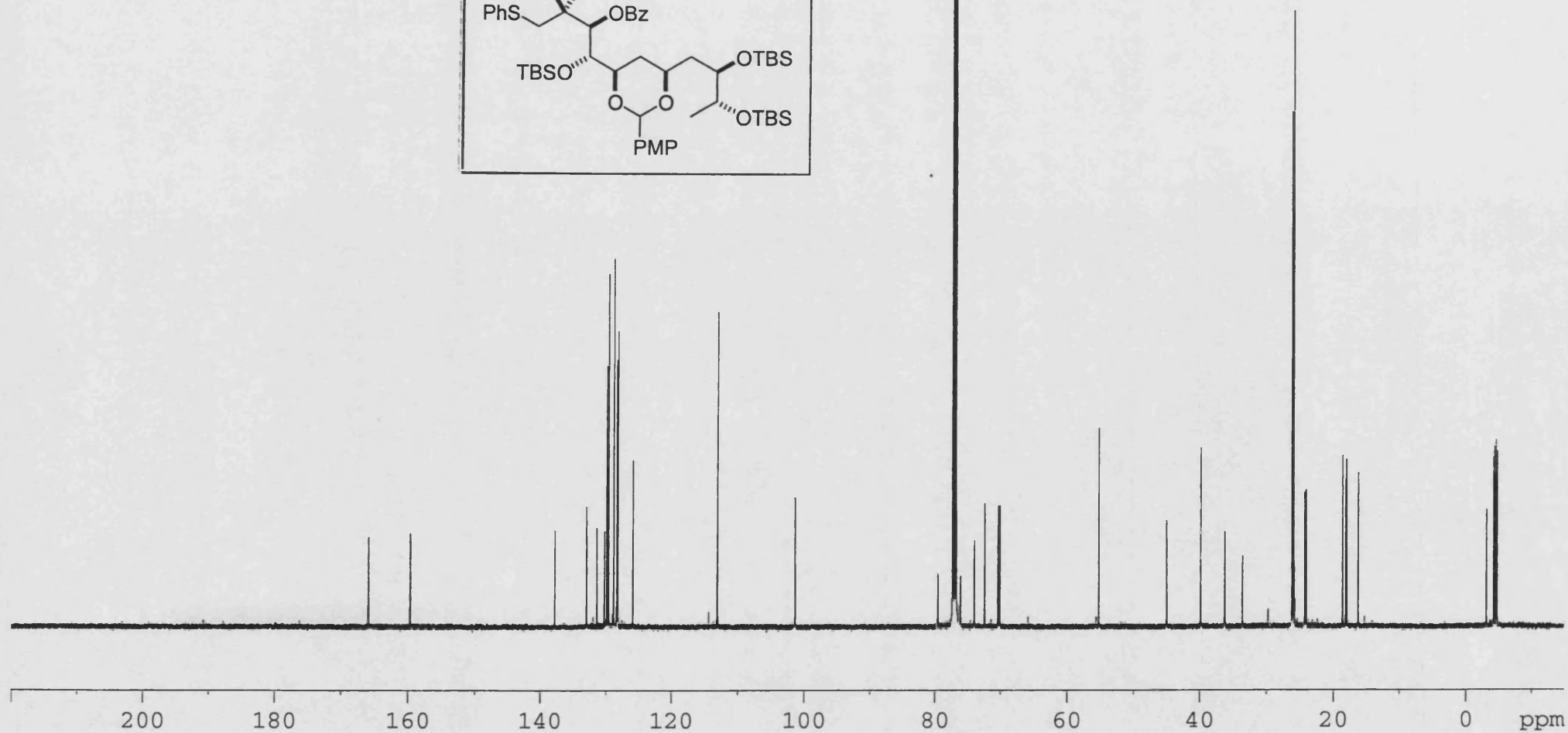
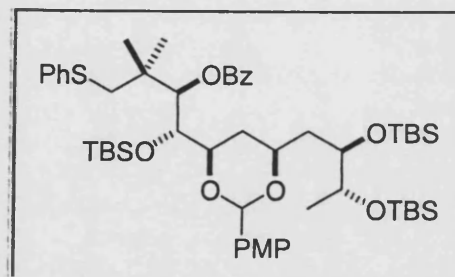
II-MF-110
HMQC
CDCl₃



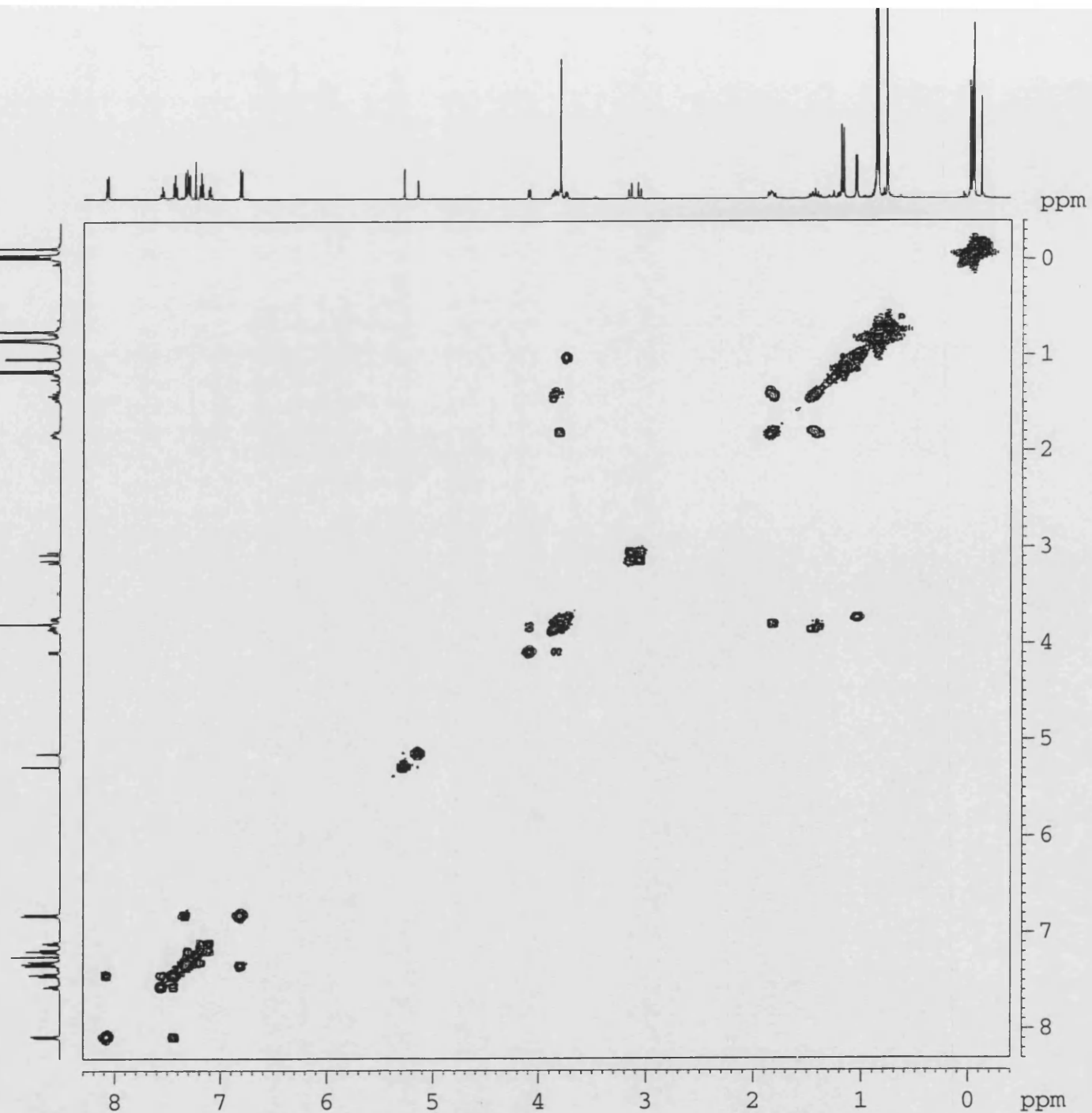
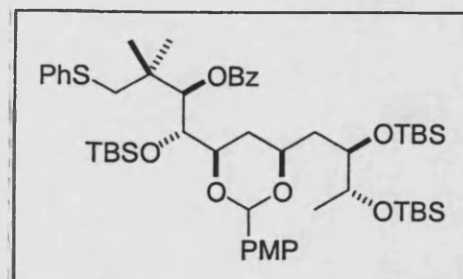
II-MF-110
DEPT
CDCl₃



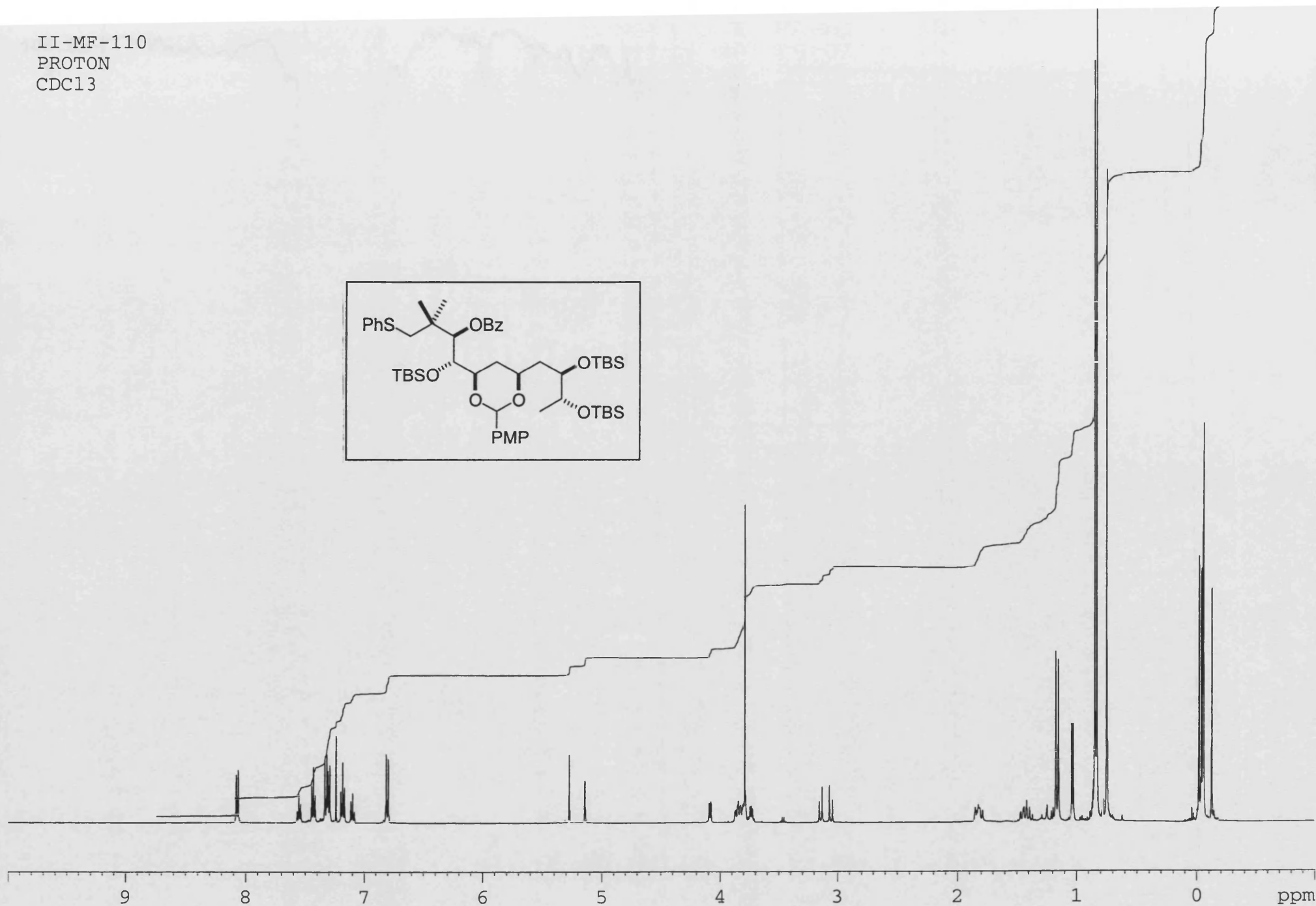
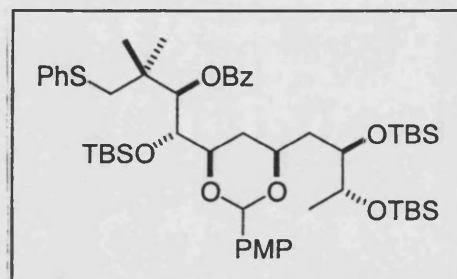
II-MF-110
CARBON
CDCl₃

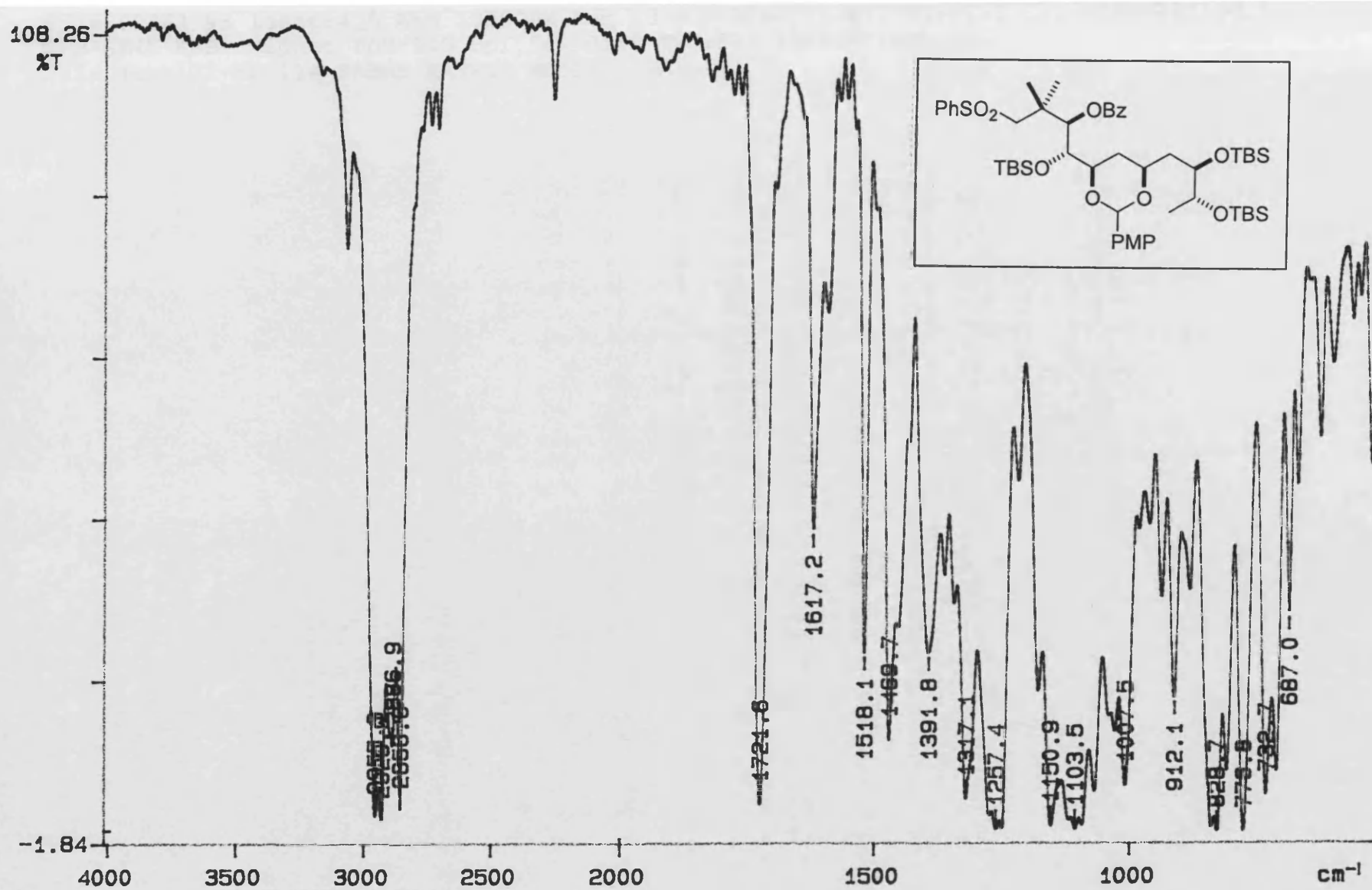


II-MF-110
COSY
CDCl₃



II-MF-110
PROTON
CDC13

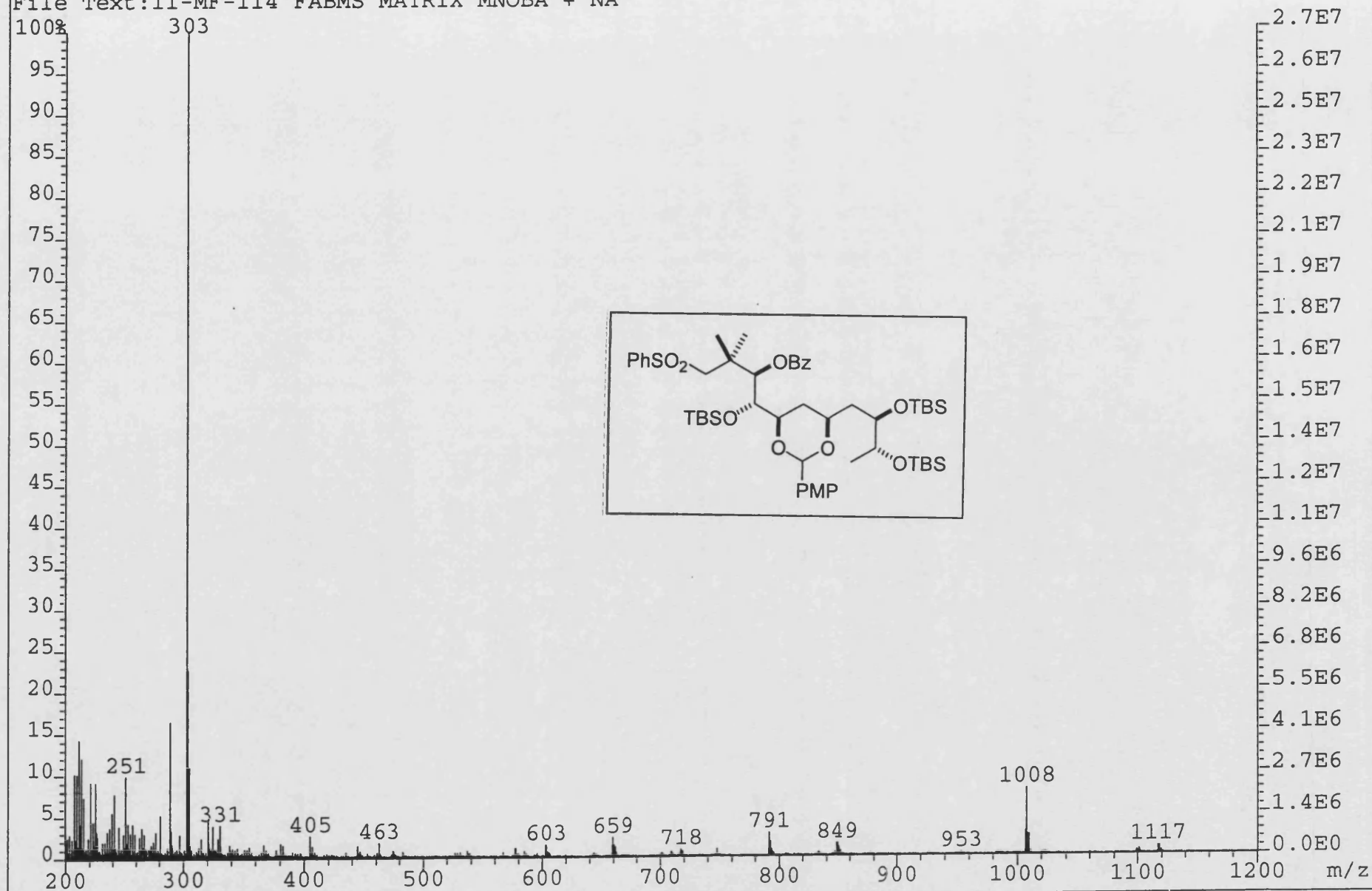




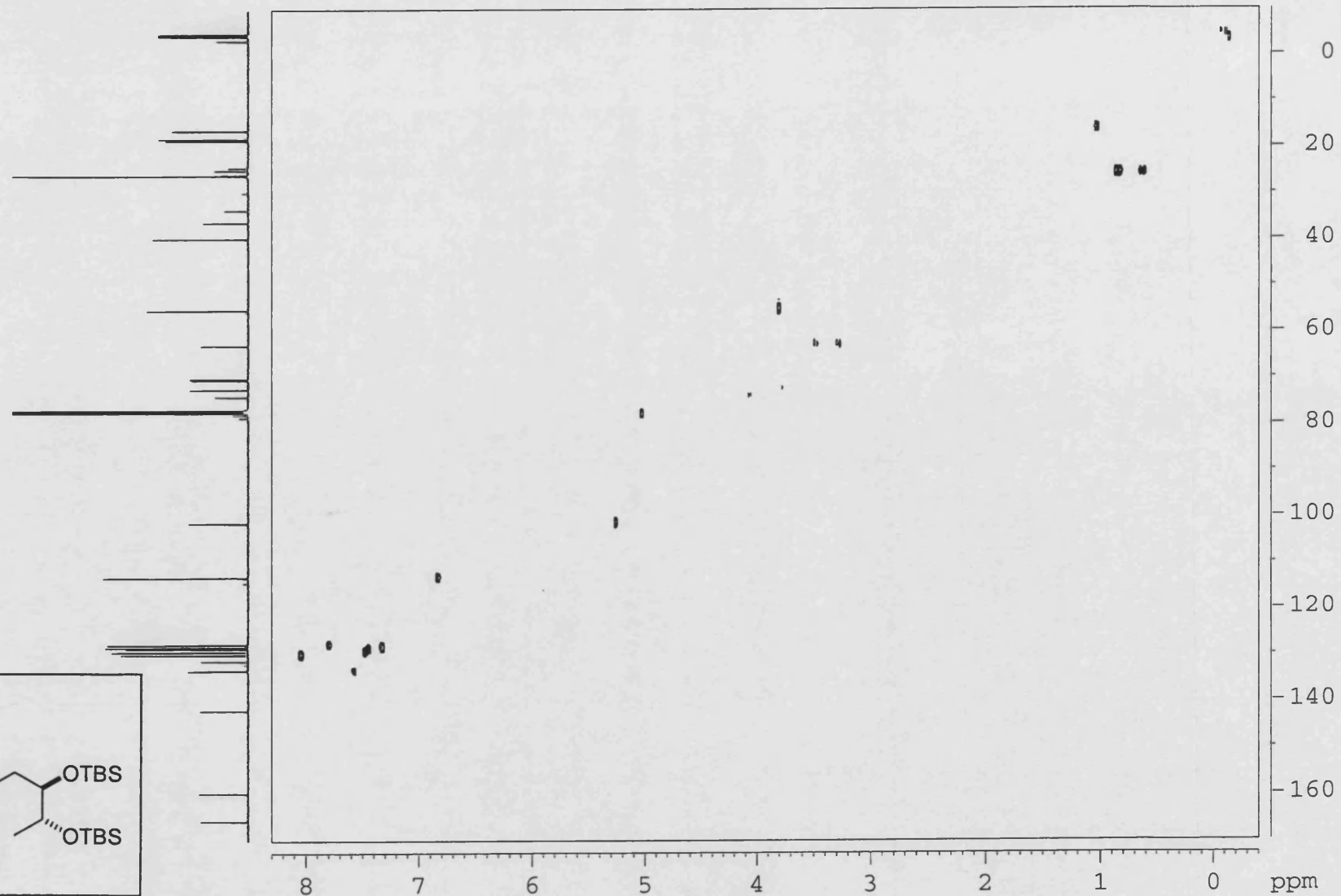
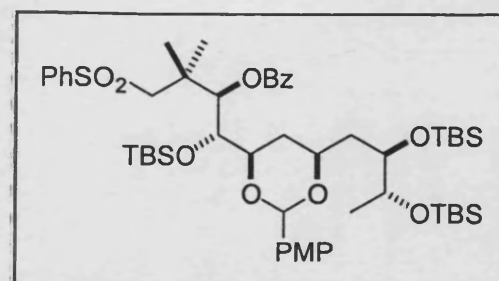
02/08/28 09:14

Y: 64 scans, 16.0cm⁻¹, apod none, flat

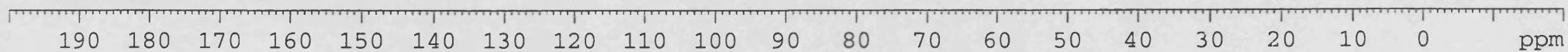
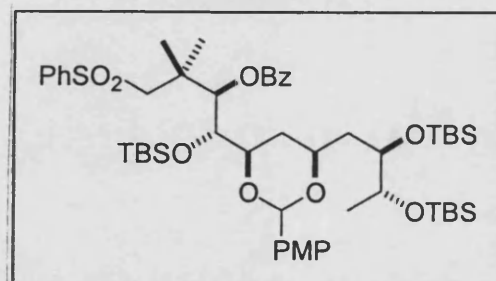
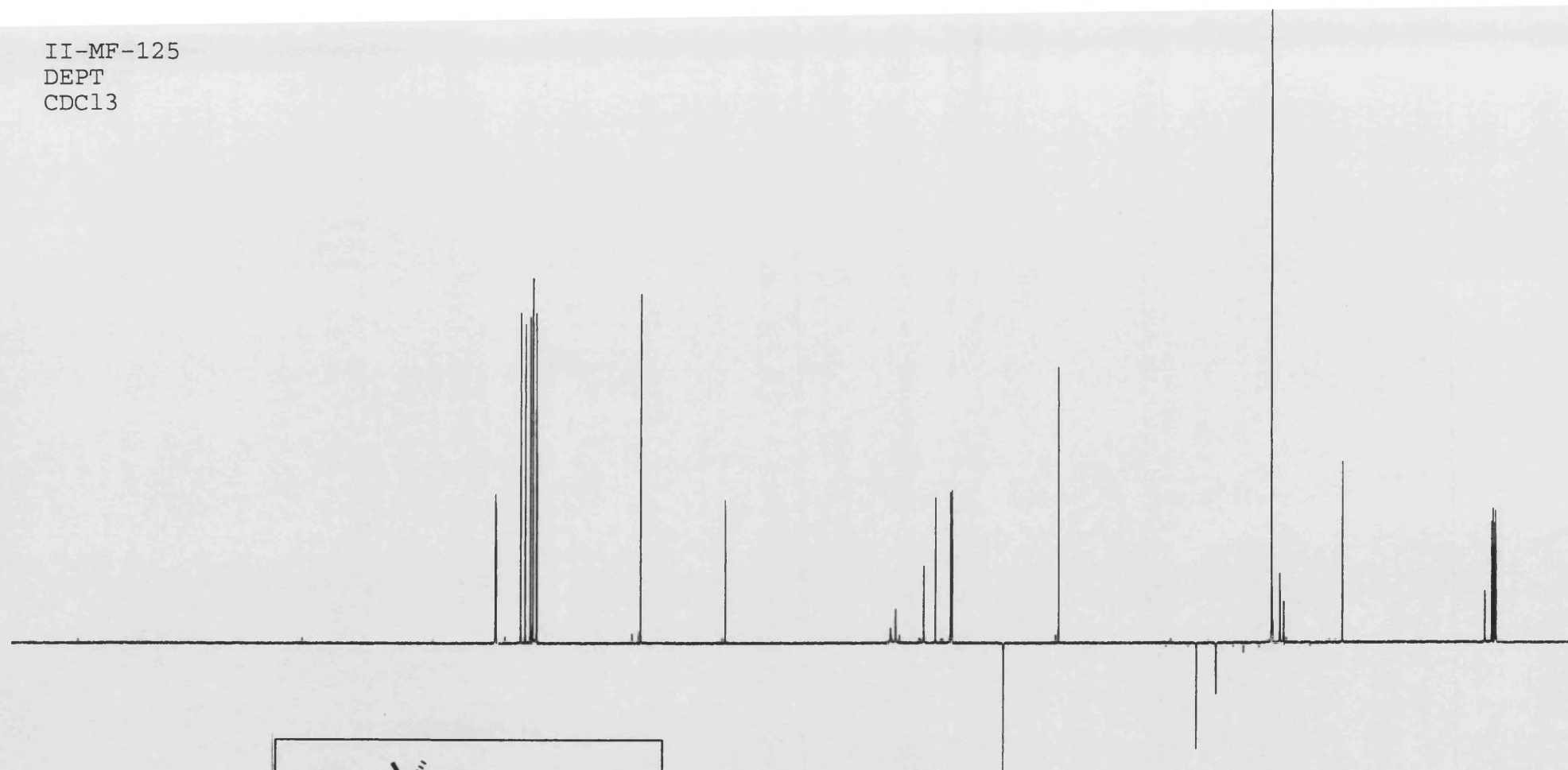
File:00SE2995 Ident:4_6 Win 1000PPM Acq:28-NOV-2000 15:43:38 +0:36 Cal:FABMM281100_1
ZAB-SE4F FAB+ Magnet BpM:115 BpI:54990168 TIC:890109888 Flags:HALL
File Text:II-MF-114 FABMS MATRIX MNOBA + NA



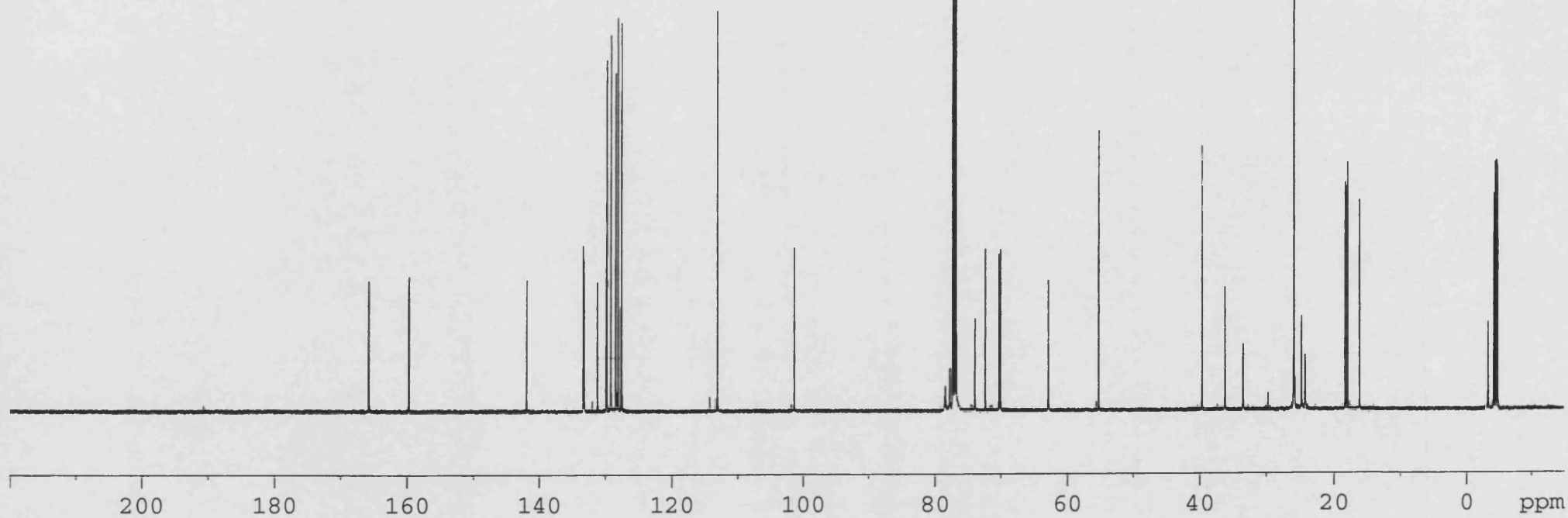
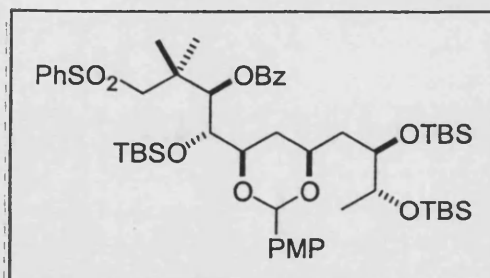
II-MF-125
HMQC
CDCl₃



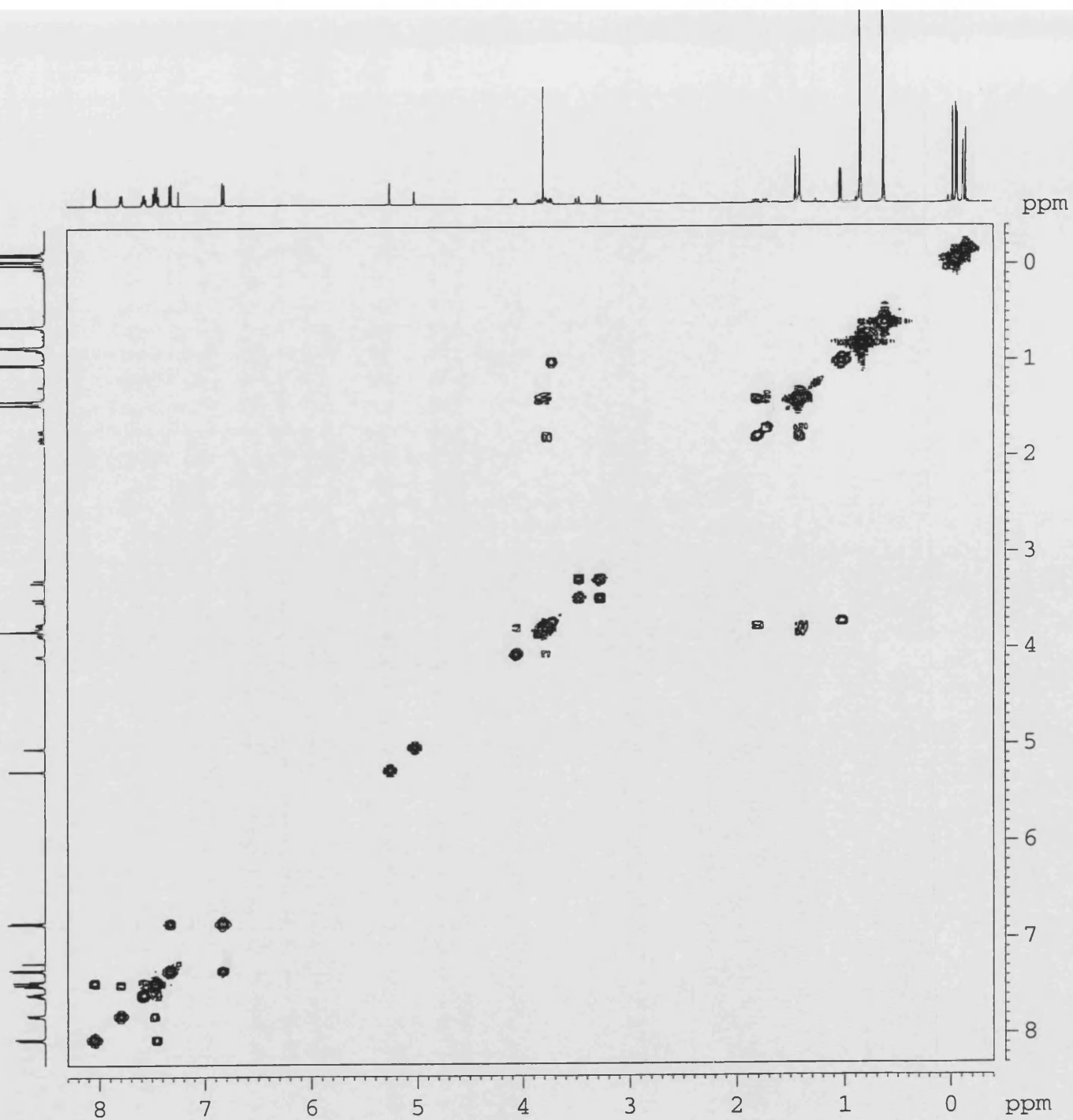
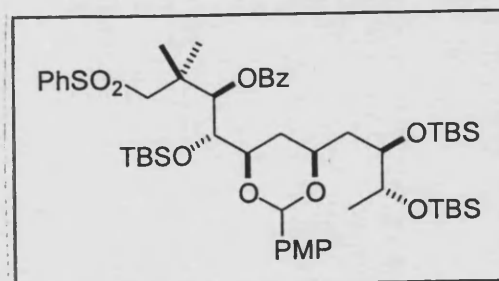
II-MF-125
DEPT
CDC13



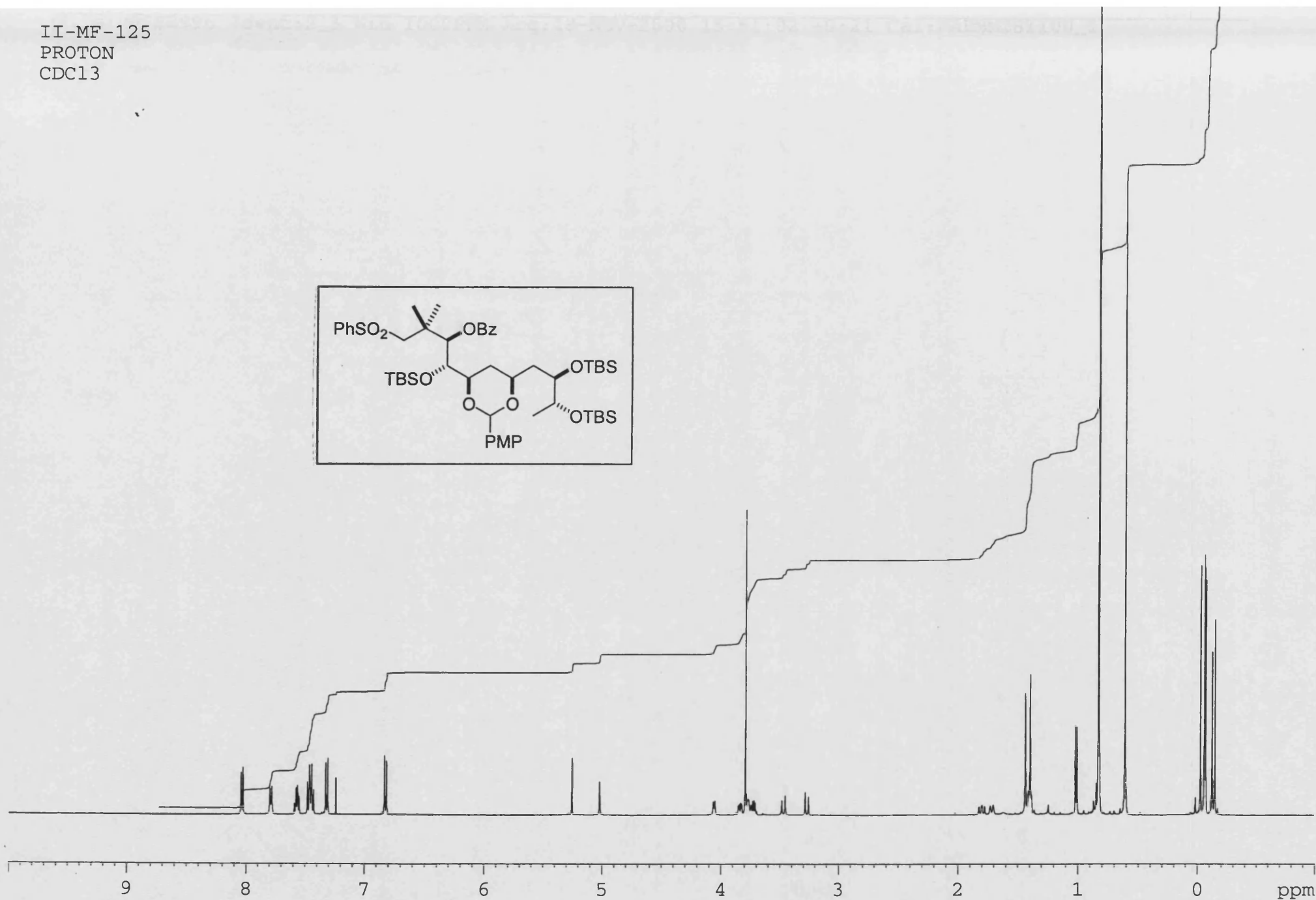
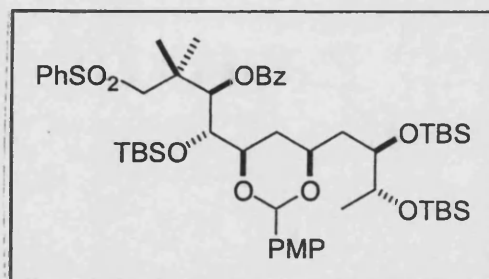
II-MF-125
CARBON
CDC13

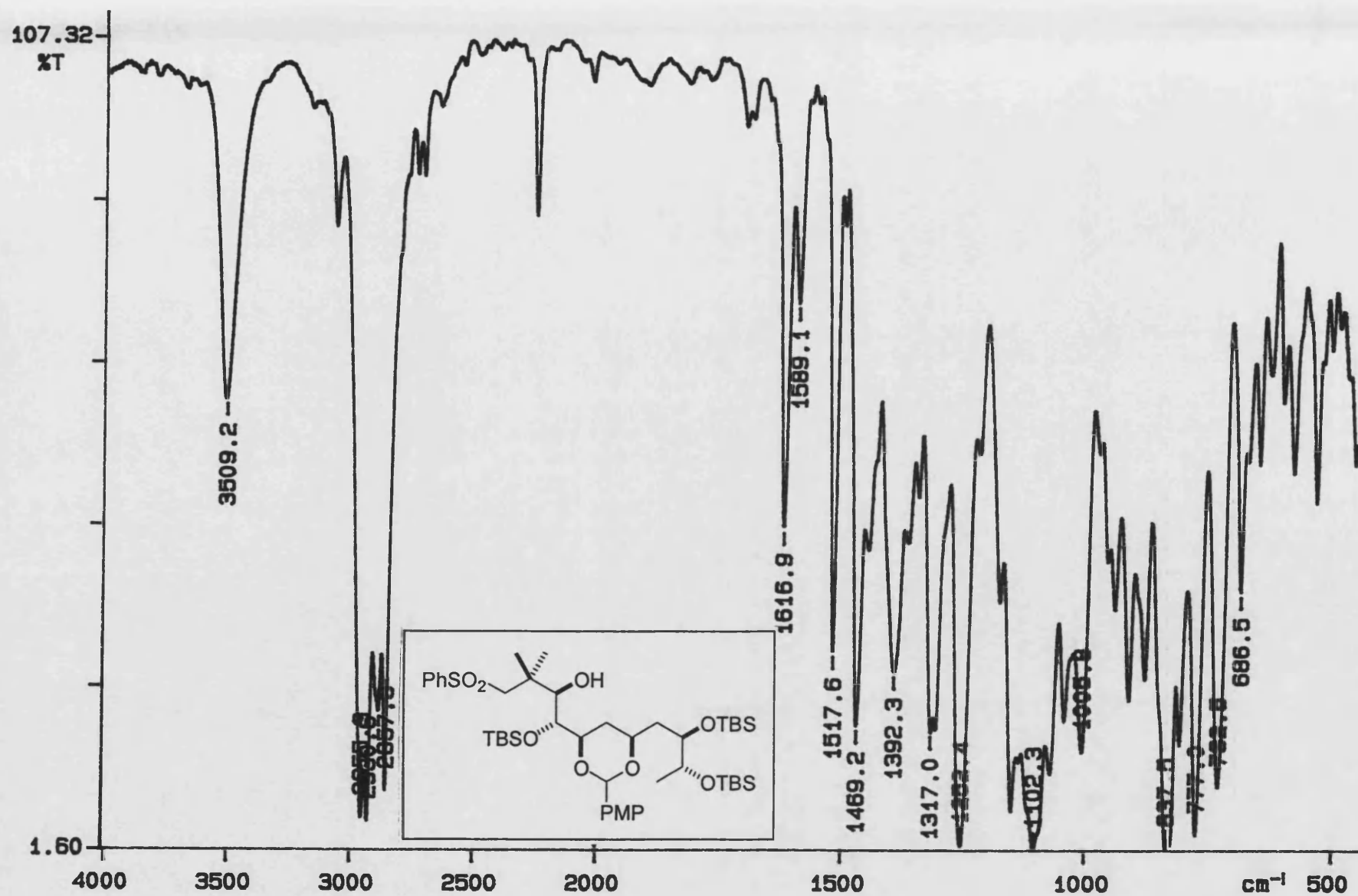


II-MF-125
COSY
CDCl₃



II-MF-125
PROTON
CDCl₃

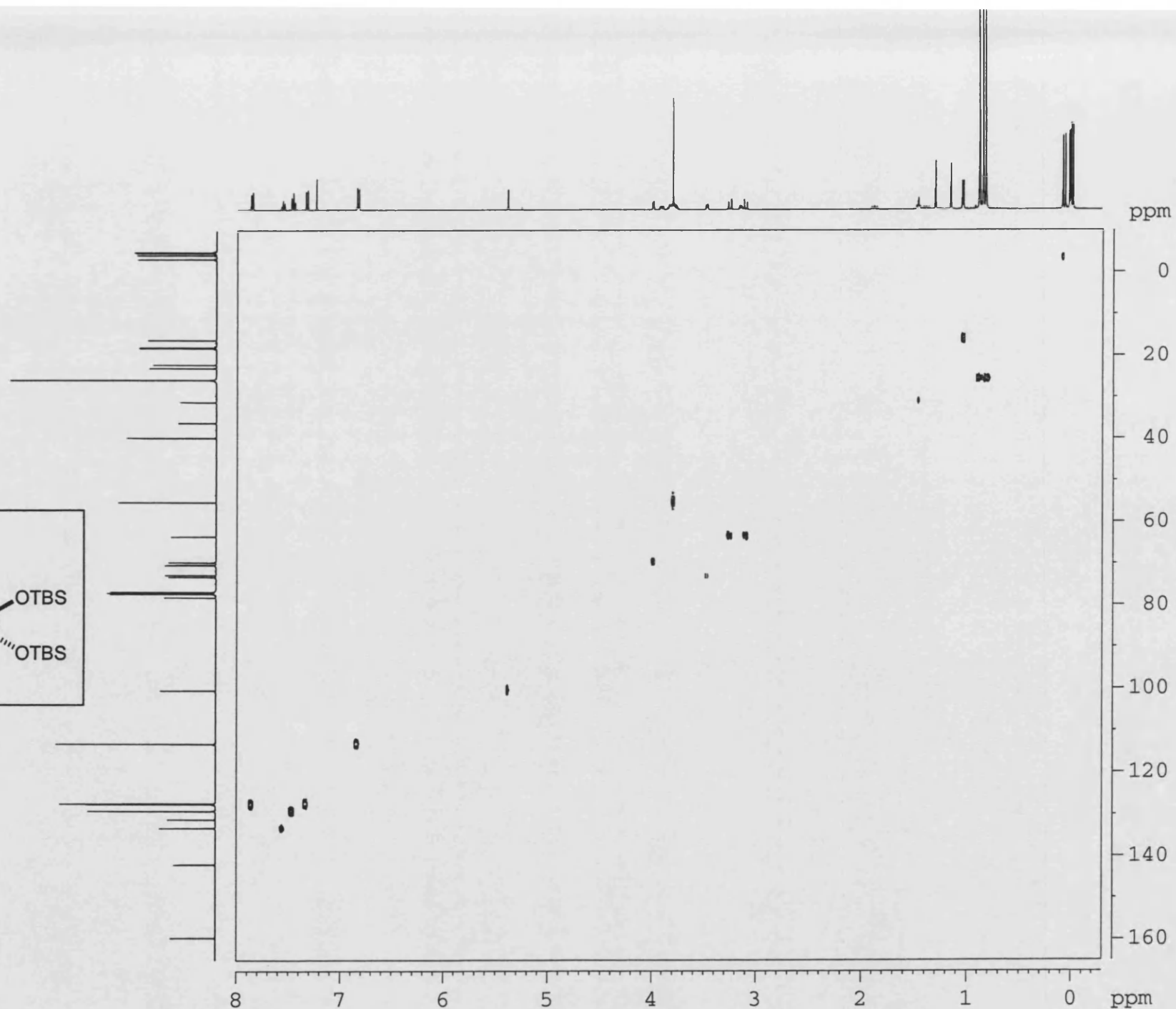
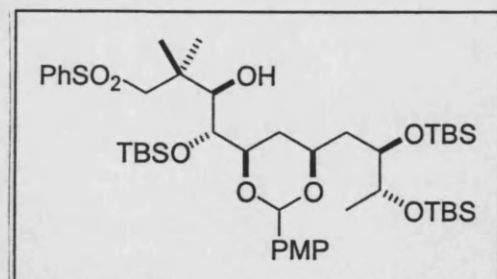




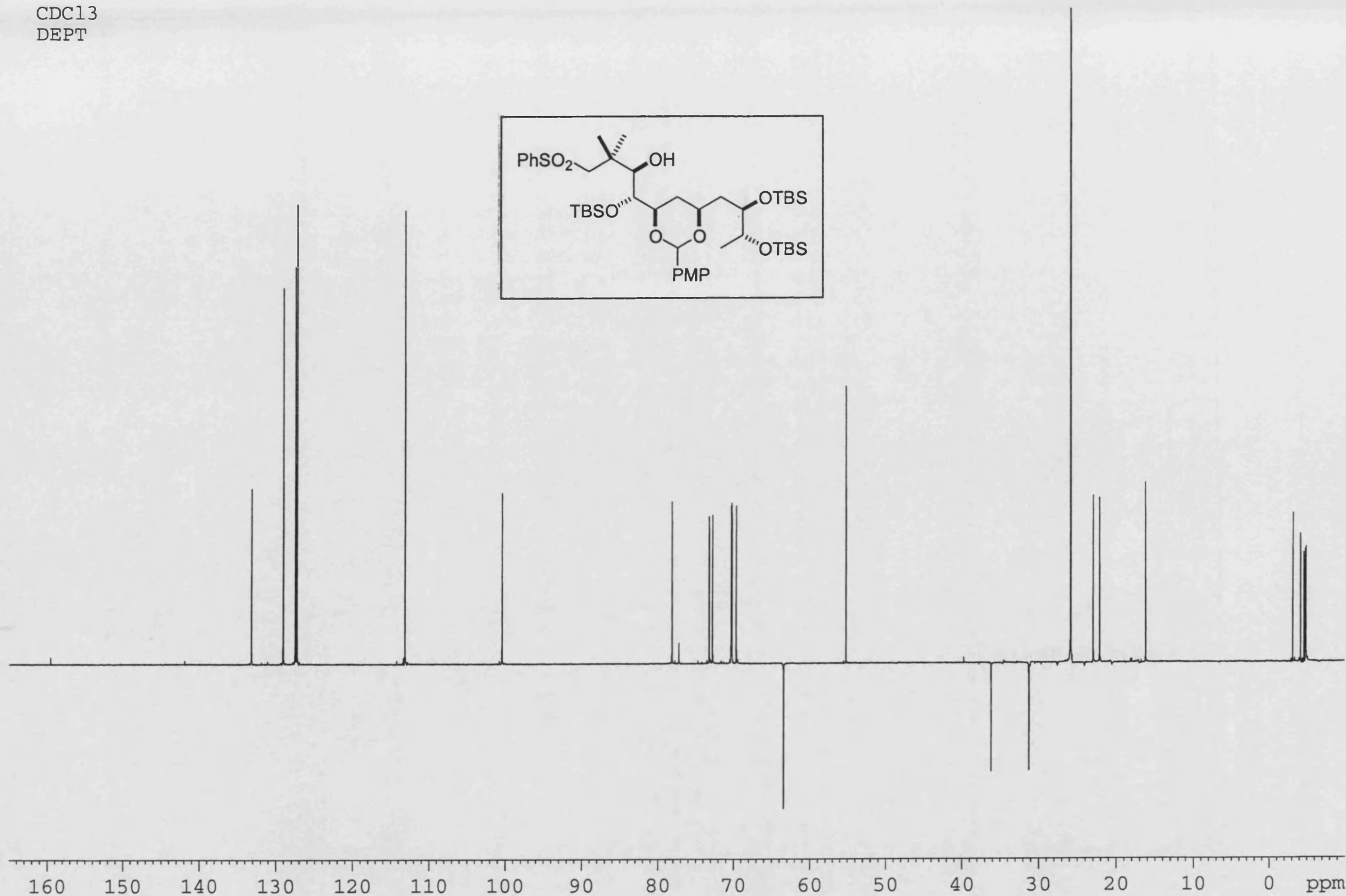
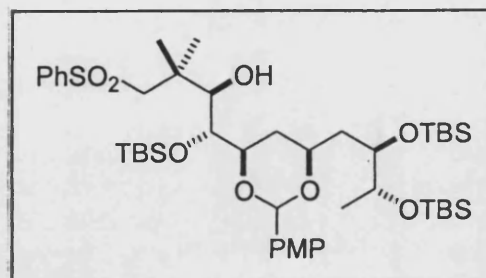
02/09/27 10:33

X: 64 scans, 16.0cm⁻¹, apod none, flat

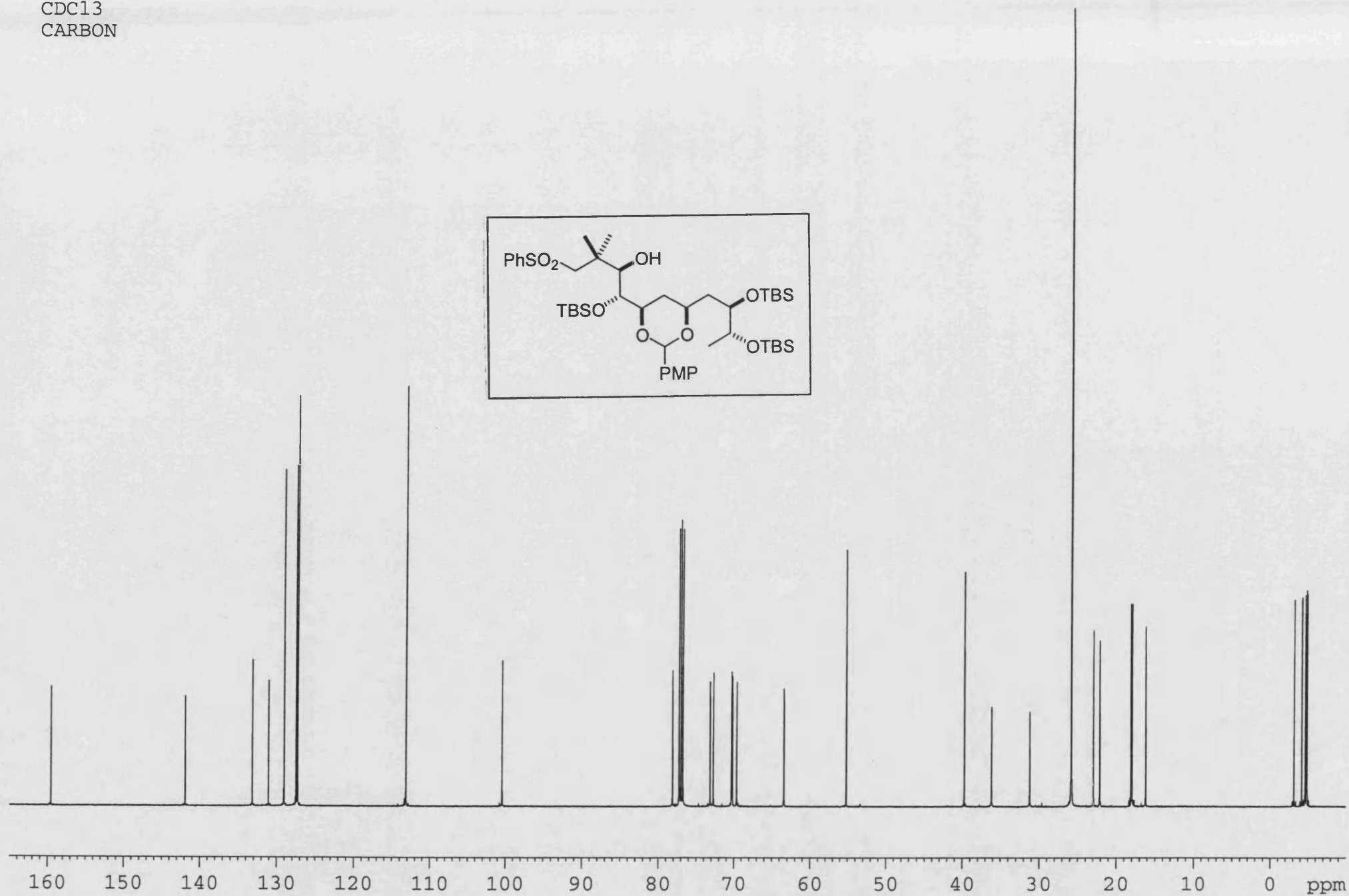
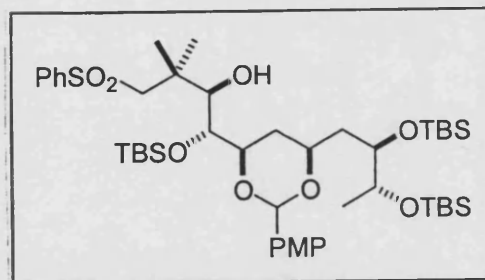
II-MF-115
CDCl₃
HMQC



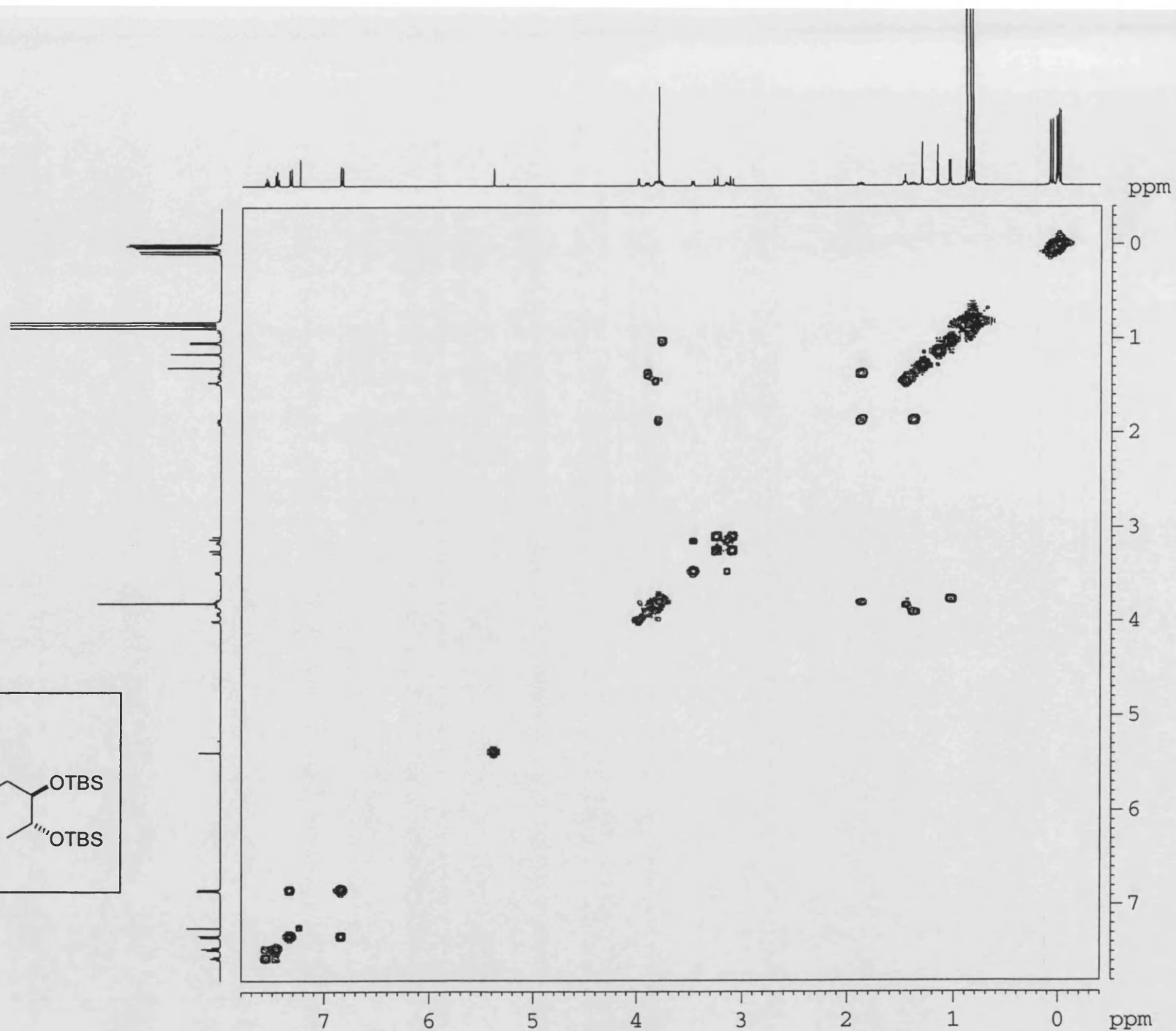
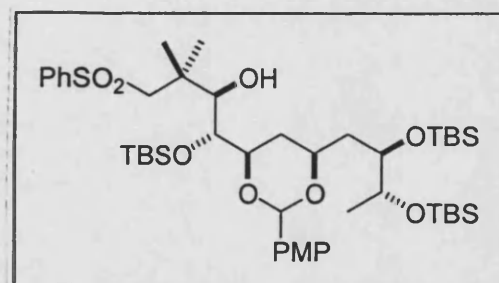
II-MF-115
CDCl₃
DEPT



II-MF-115
CDC13
CARBON



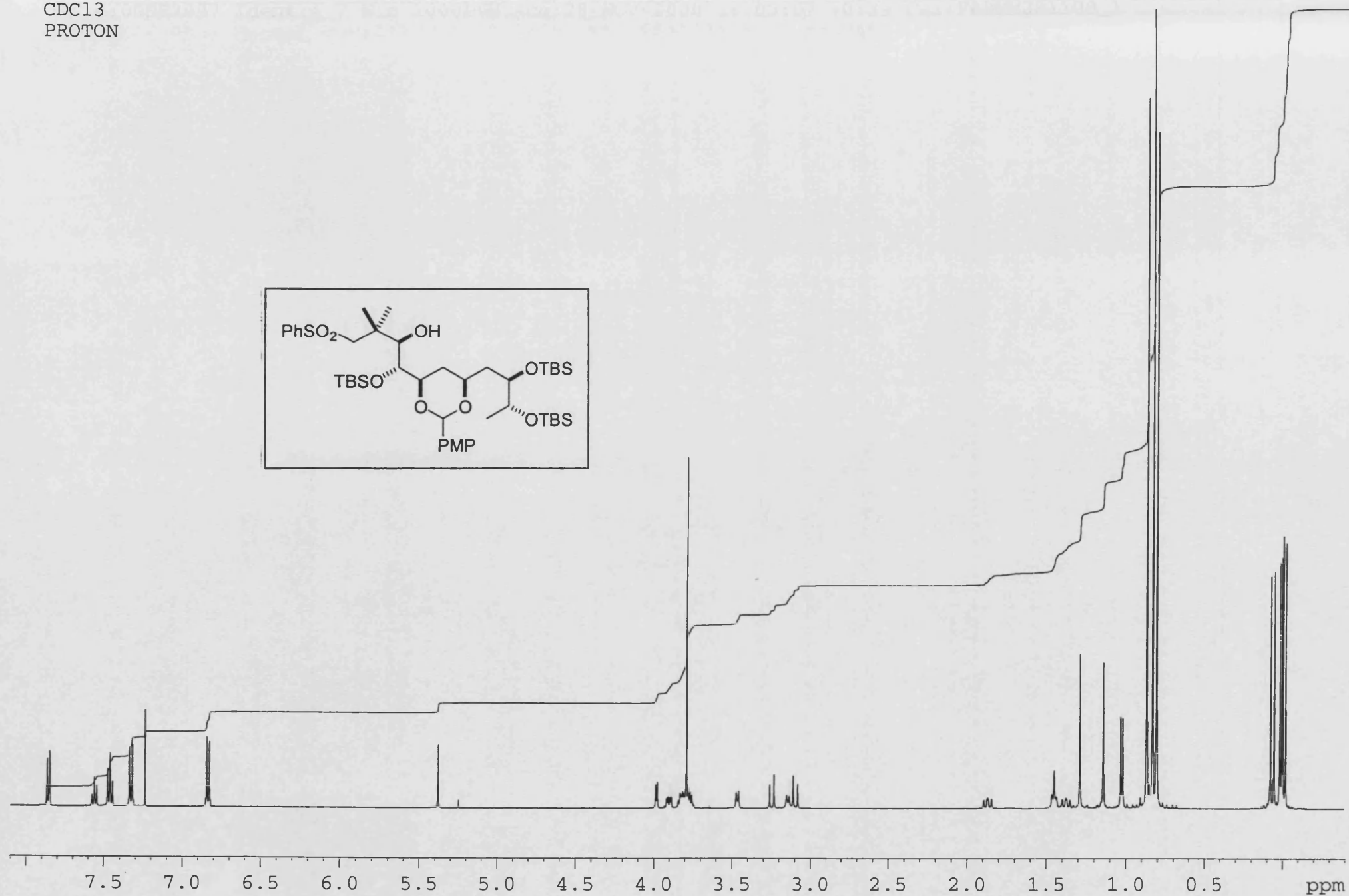
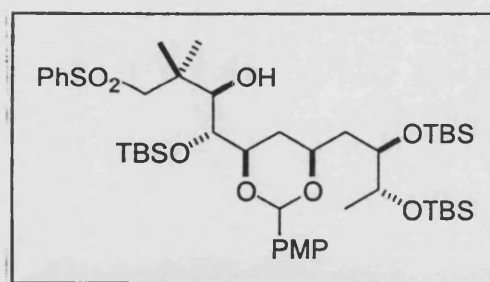
II-MF-115
CDCl₃
COSY



II-MF-115

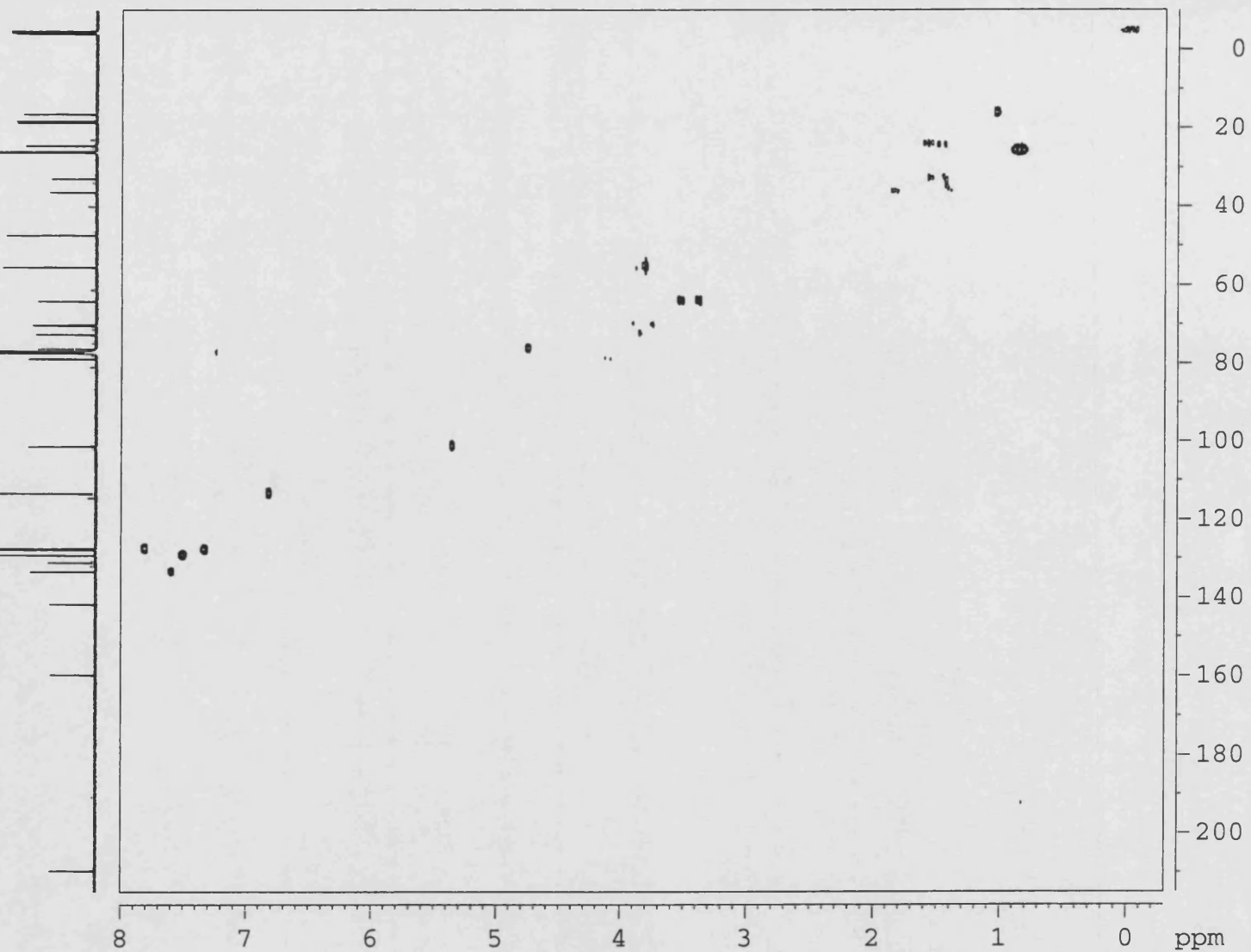
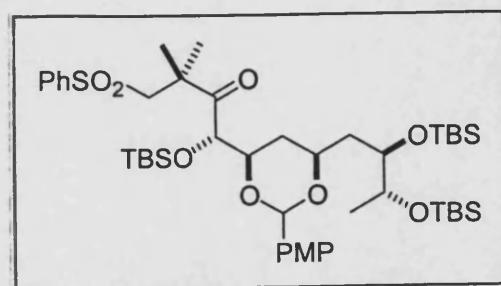
CDCl₃

PROTON

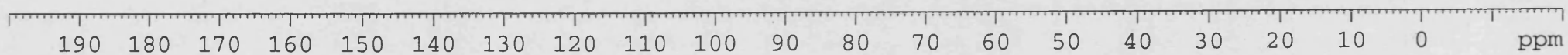
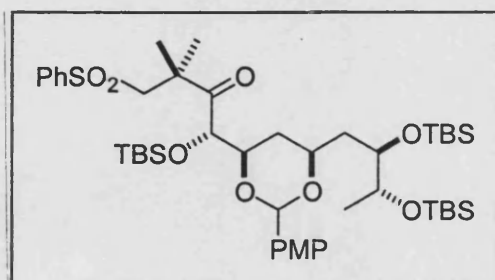
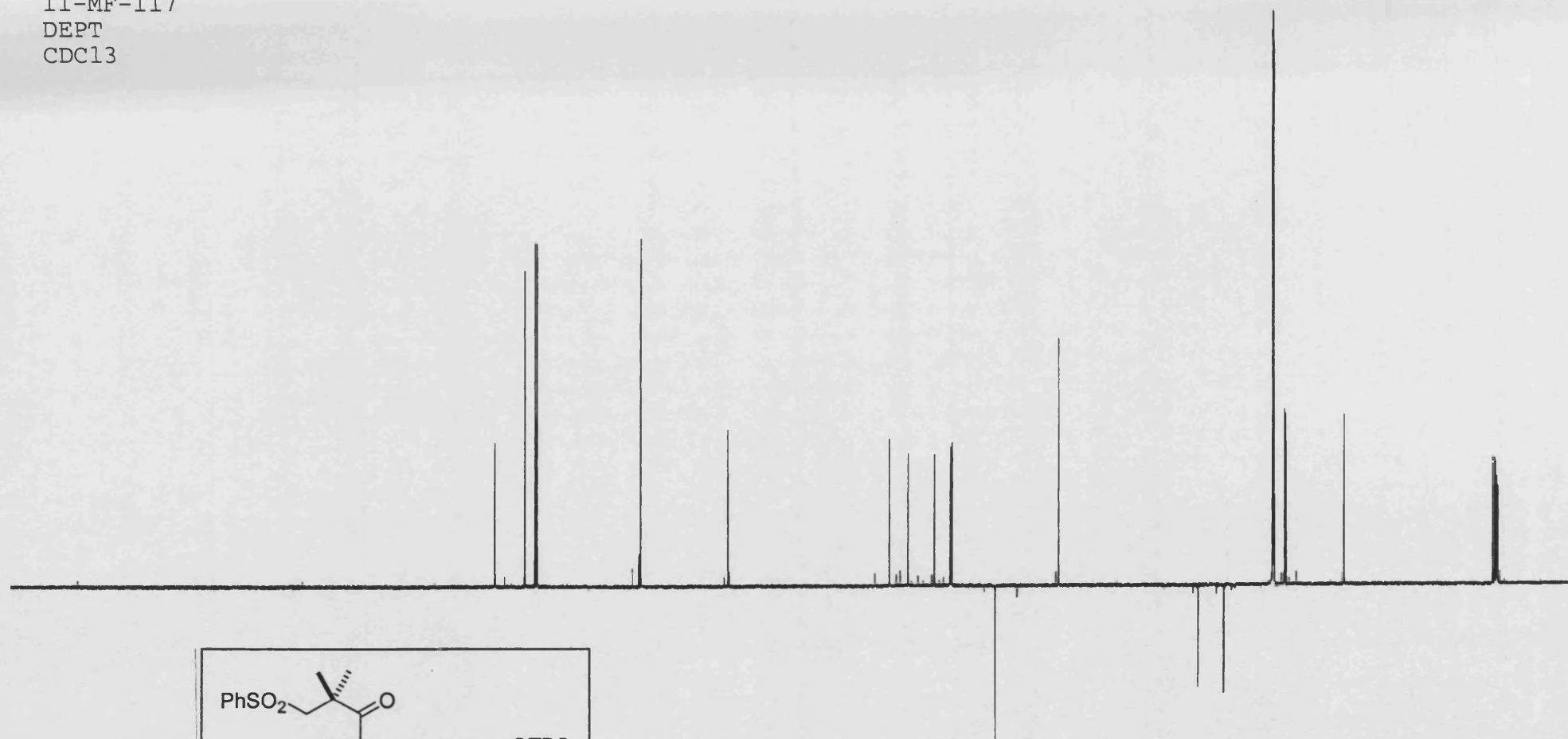


X: 64 scans, 16.0cm⁻¹, apod none, flat

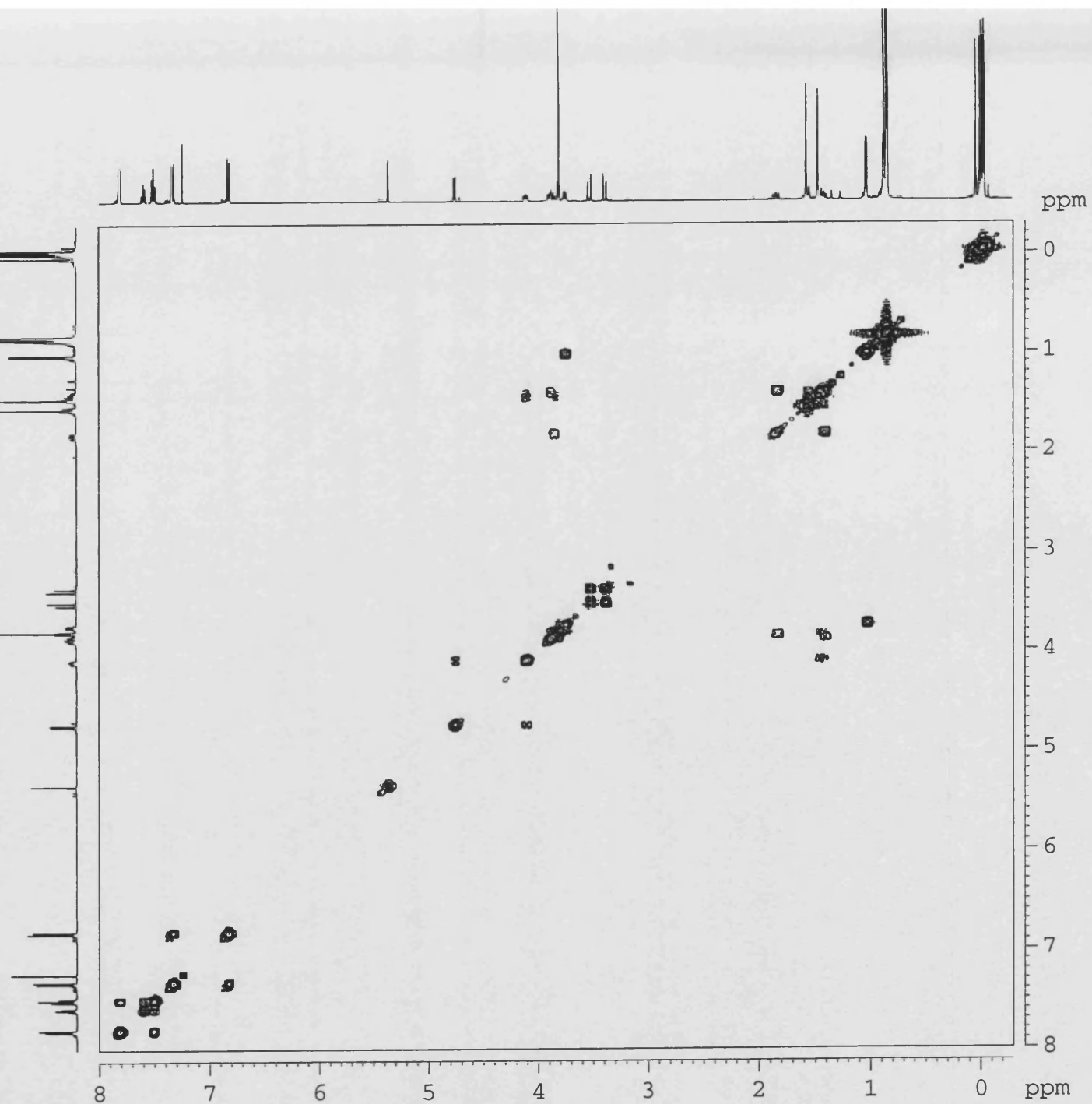
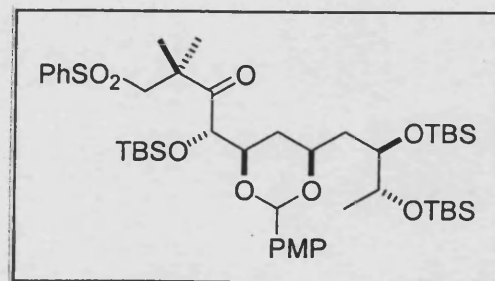
II-MF-117
HMQC
CDCl₃



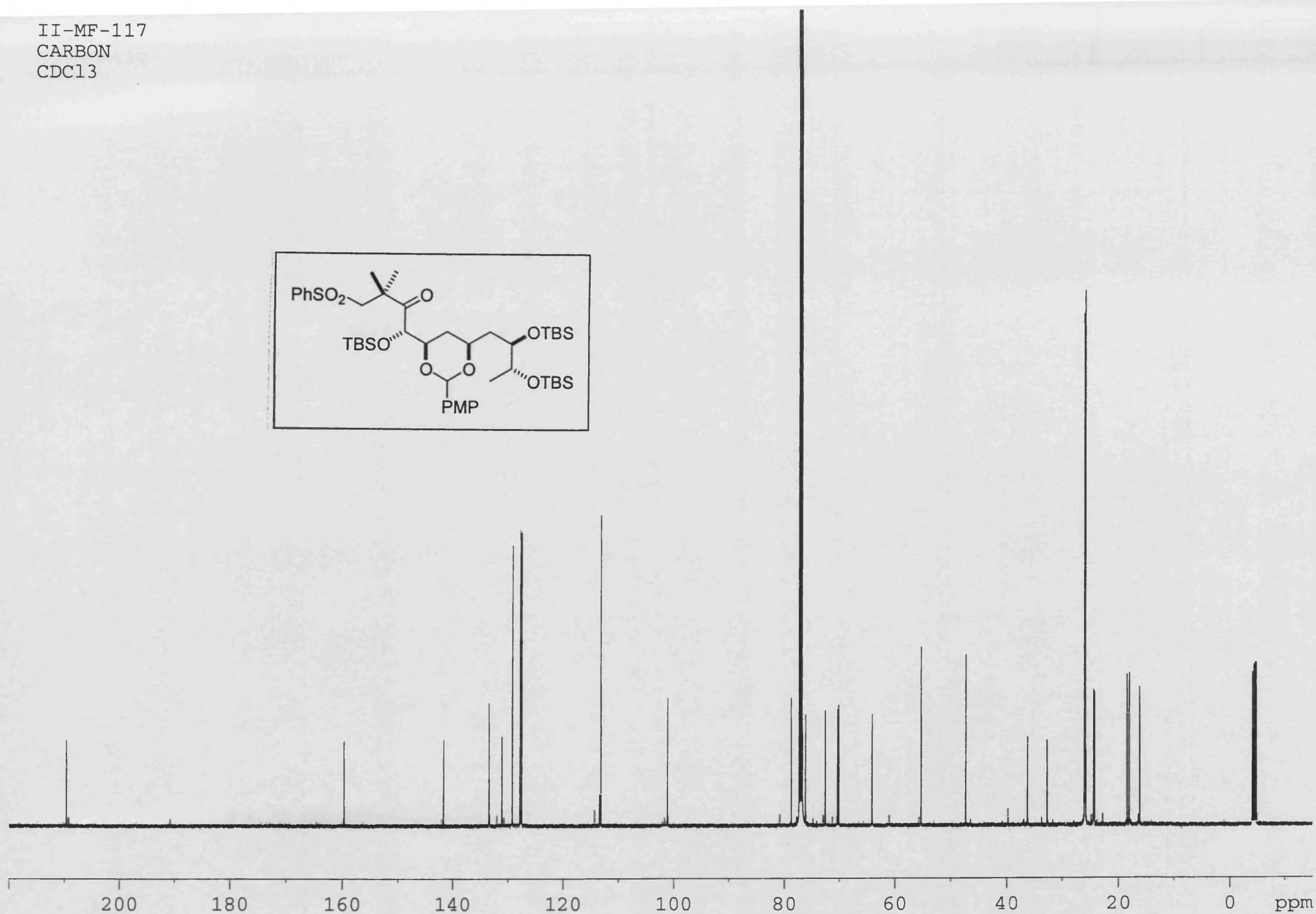
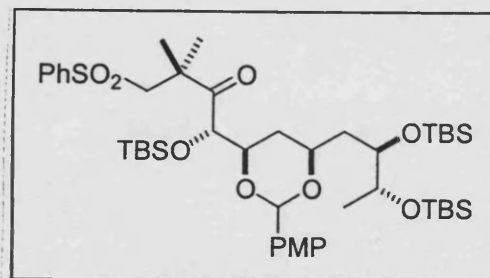
II-MF-117
DEPT
CDCl₃



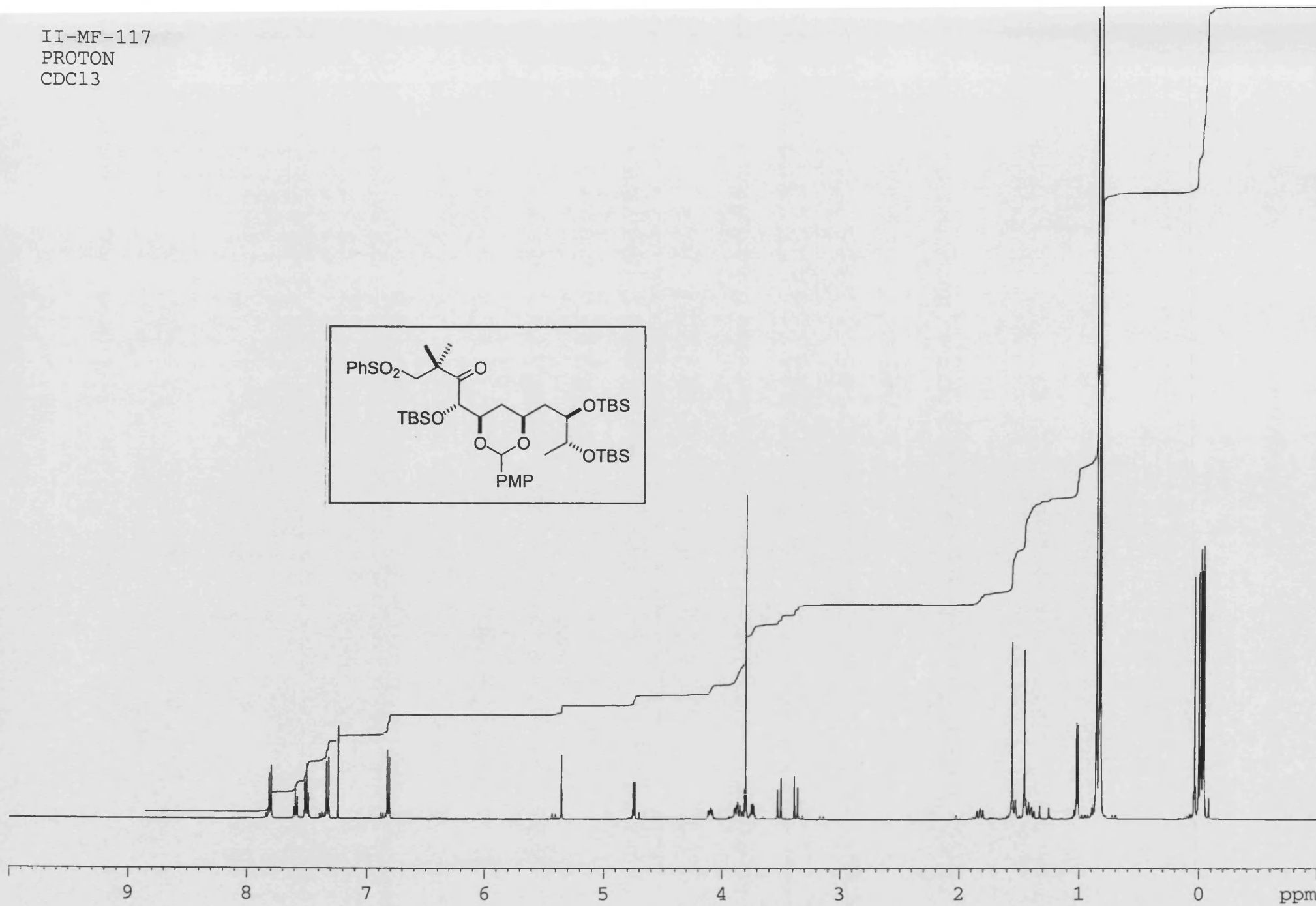
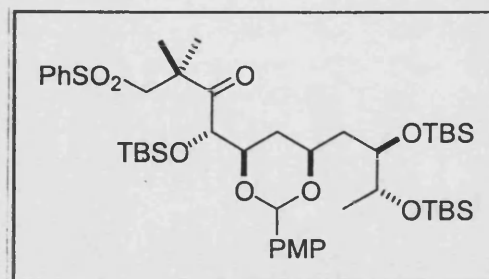
II-MF-117
COSY
CDCl₃



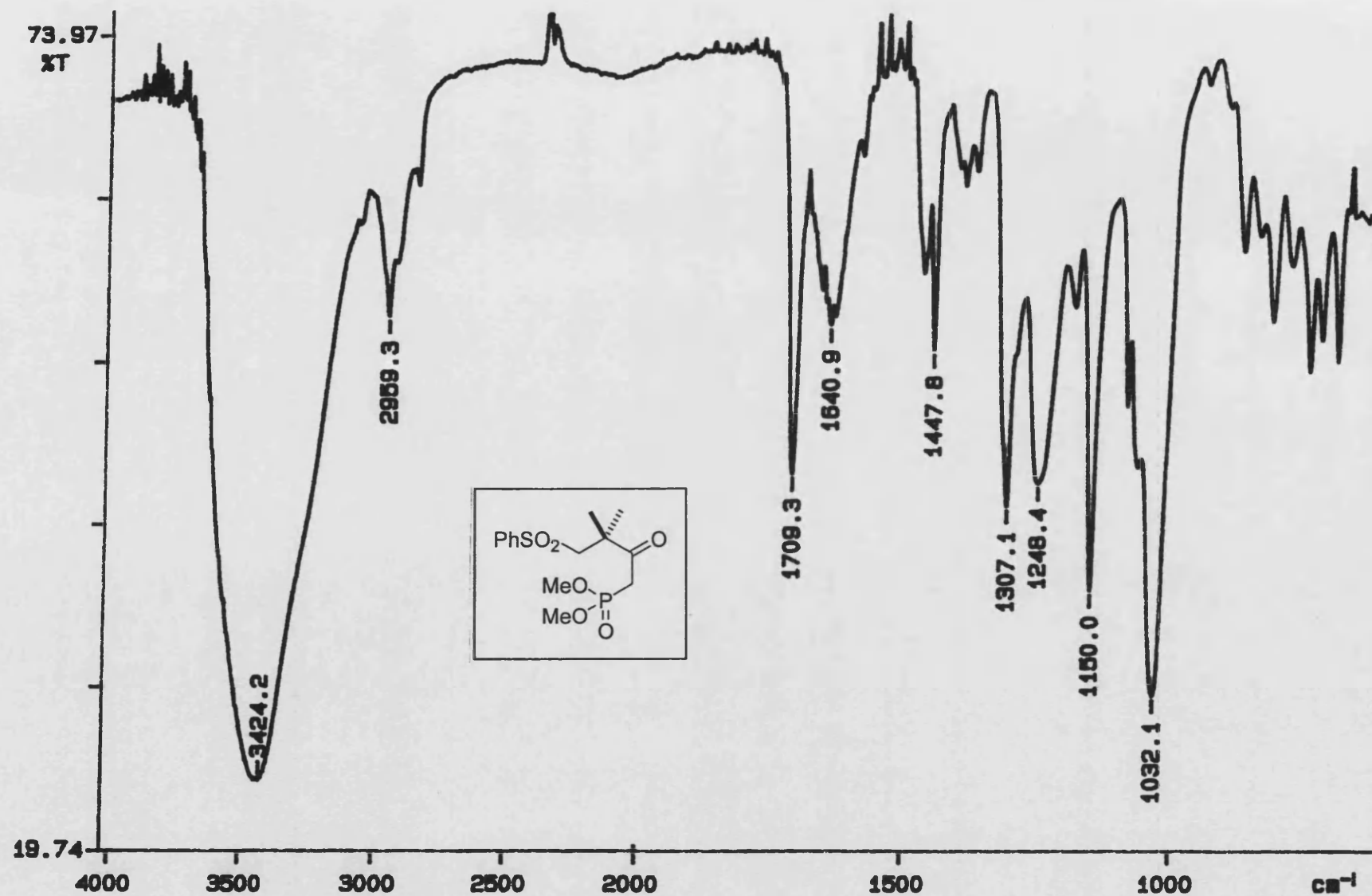
II-MF-117
CARBON
CDCl₃



II-MF-117
PROTON
CDCl₃



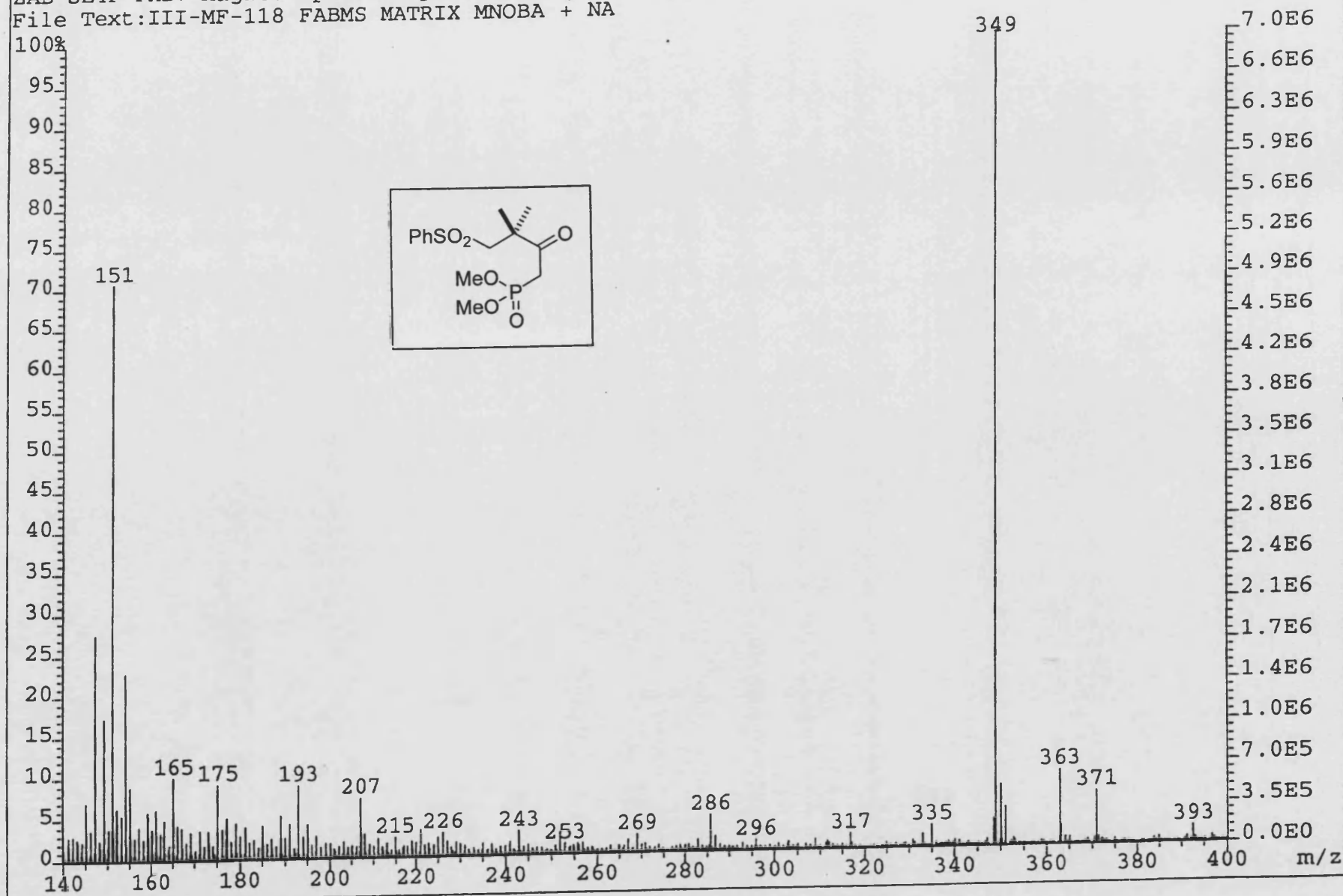
PERKIN ELMER



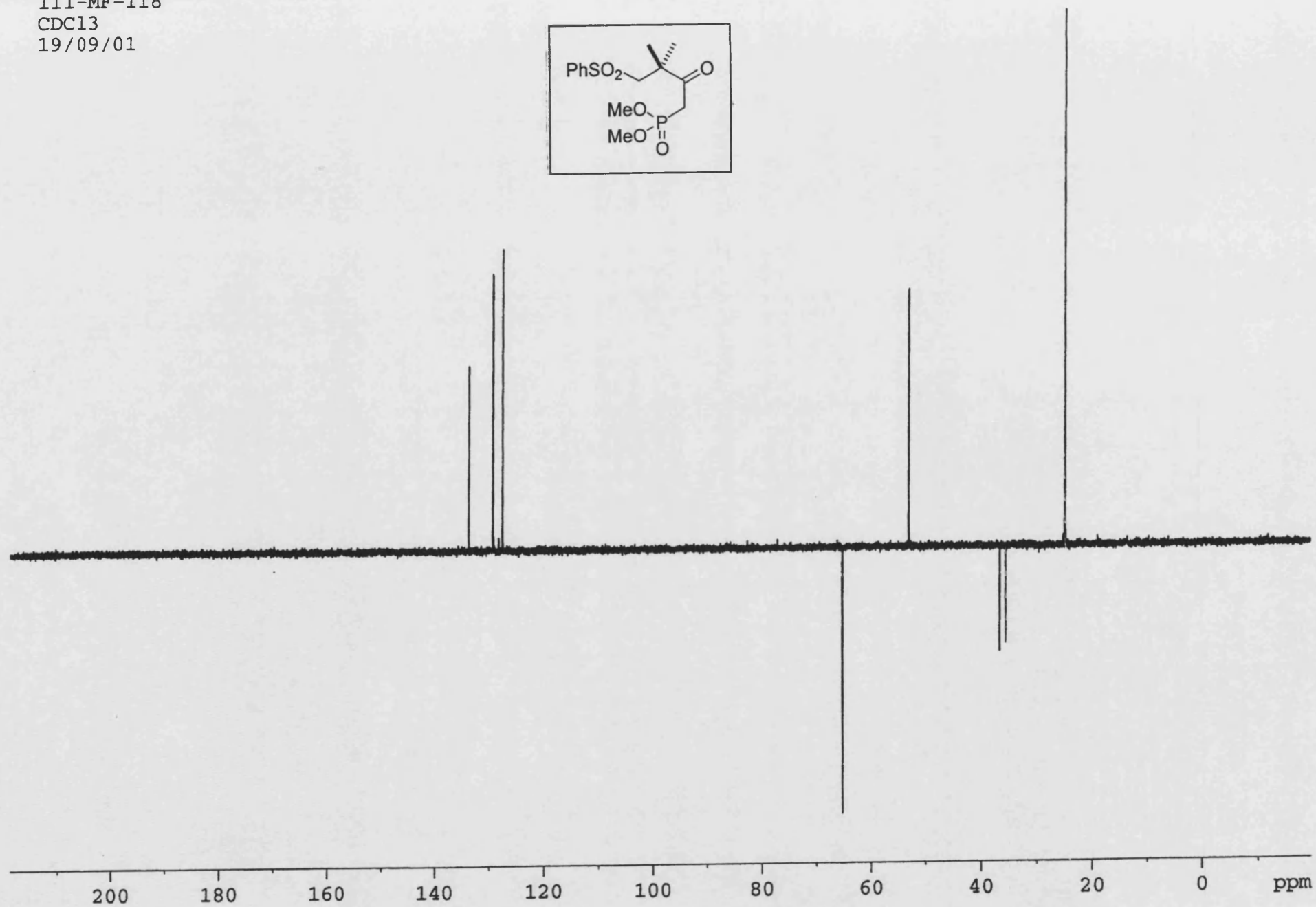
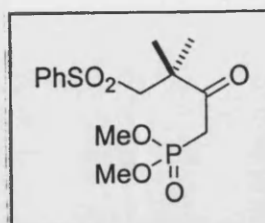
01/09/19 16:50

Y: 1 scan, 4.0cm⁻¹, flat

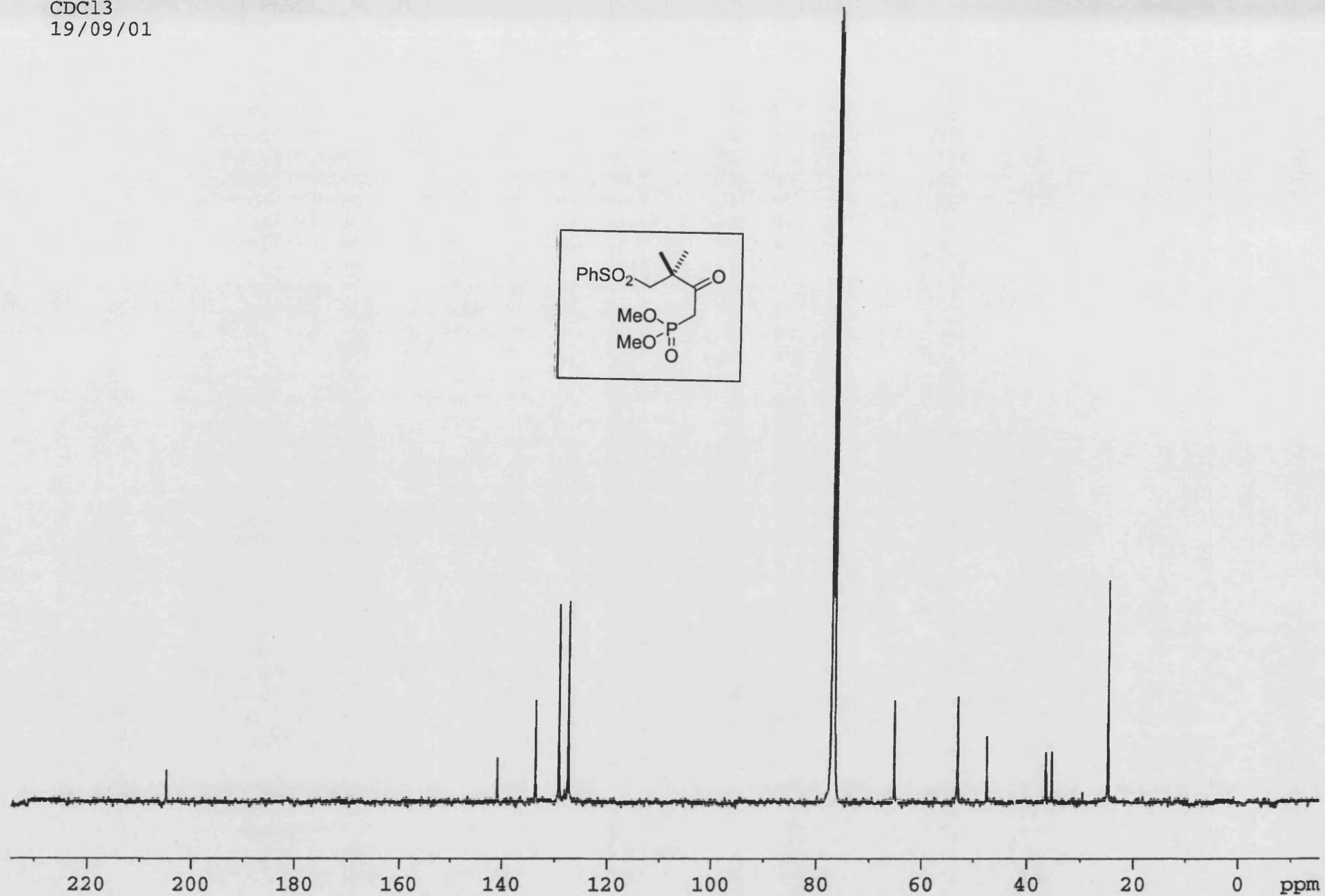
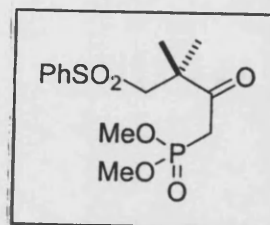
File:01SE3345 Ident:61_67 Win 1000PPM Acq: 3-SEP-2001 15:52:25 +3:26 Cal:FABLM0320901_1
ZAB-SE4F FAB+ Magnet BpM:133 BpI:13436636 TIC:145824480 Flags:HALL
File Text:III-MF-118 FABMS MATRIX MNOBA + NA



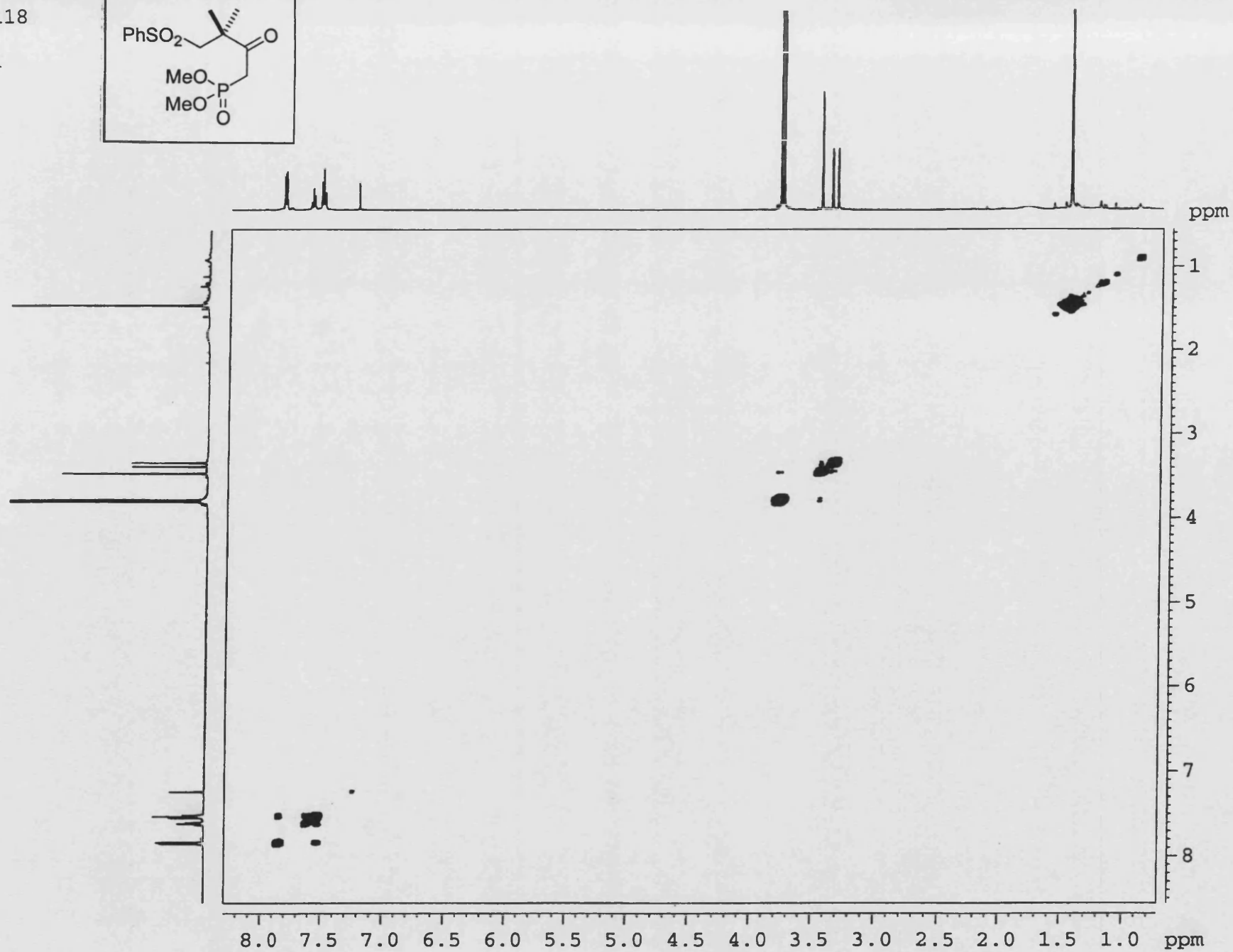
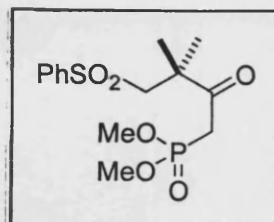
III-MF-118
CDC13
19/09/01



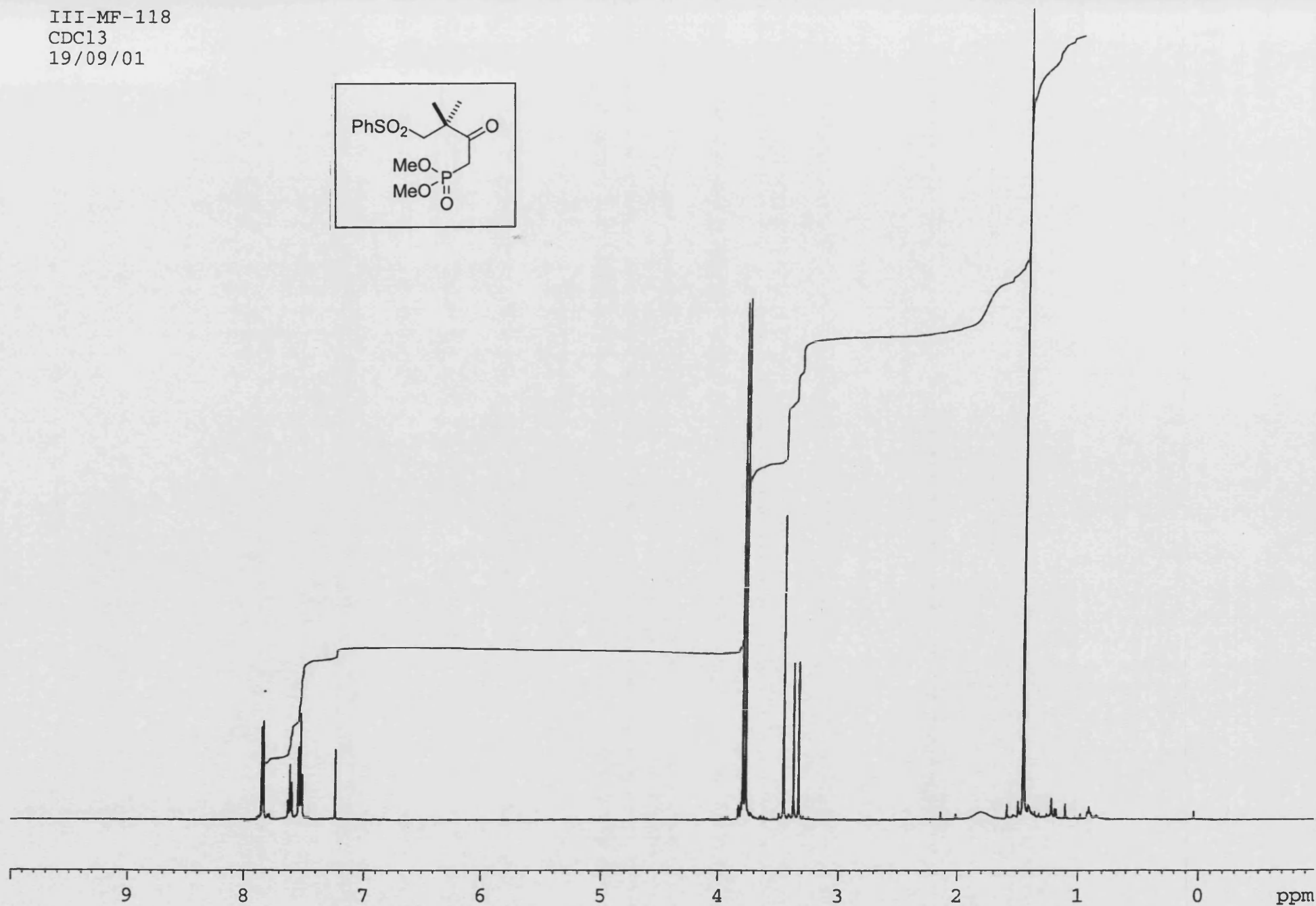
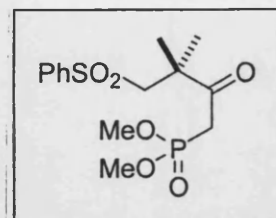
III-MF-118
CDC13
19/09/01



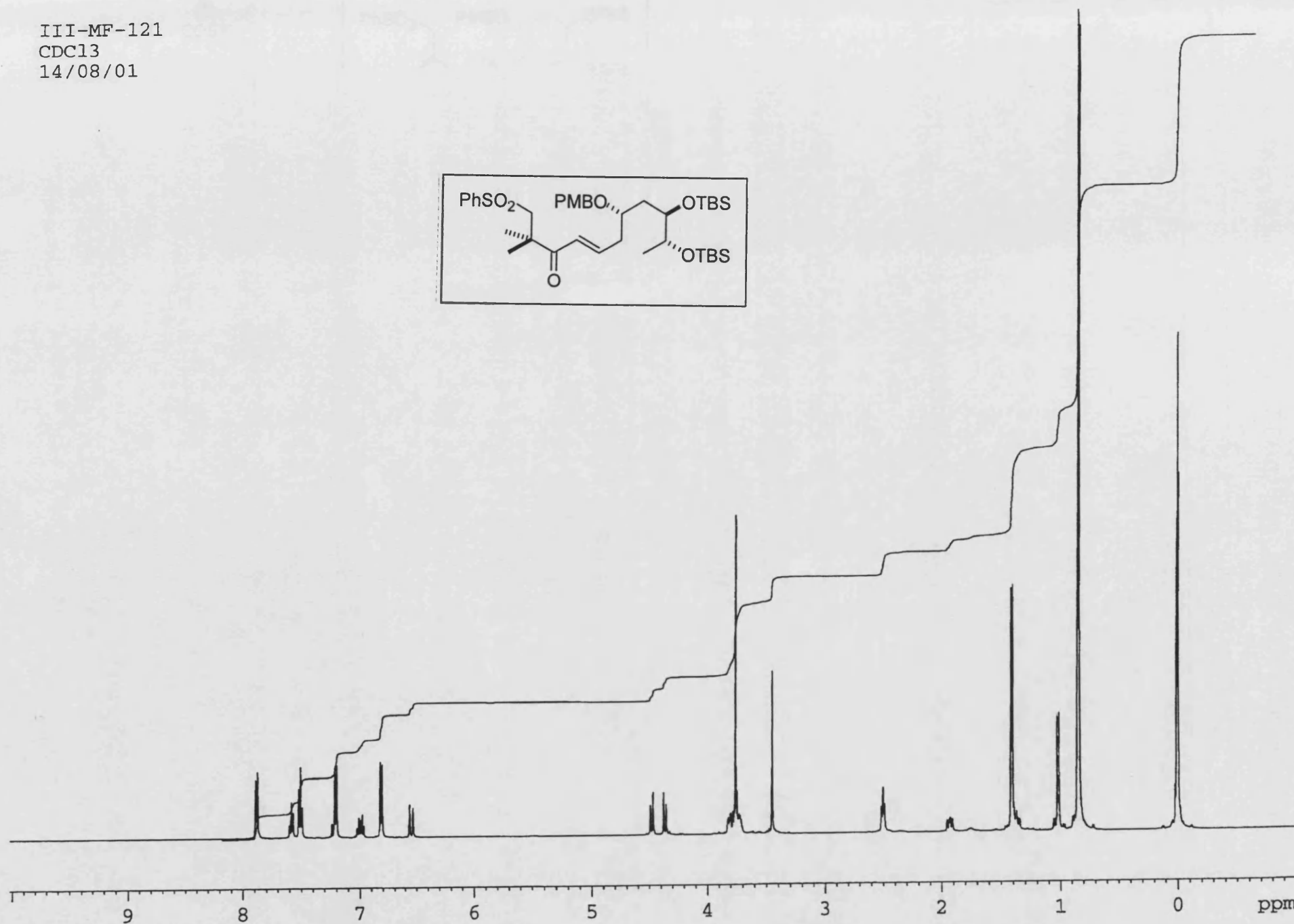
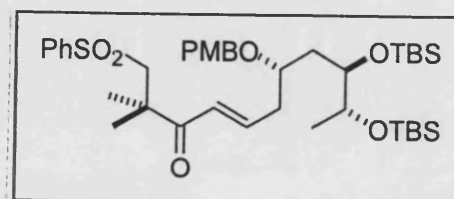
III-MF-118
CDCl₃
19/09/01



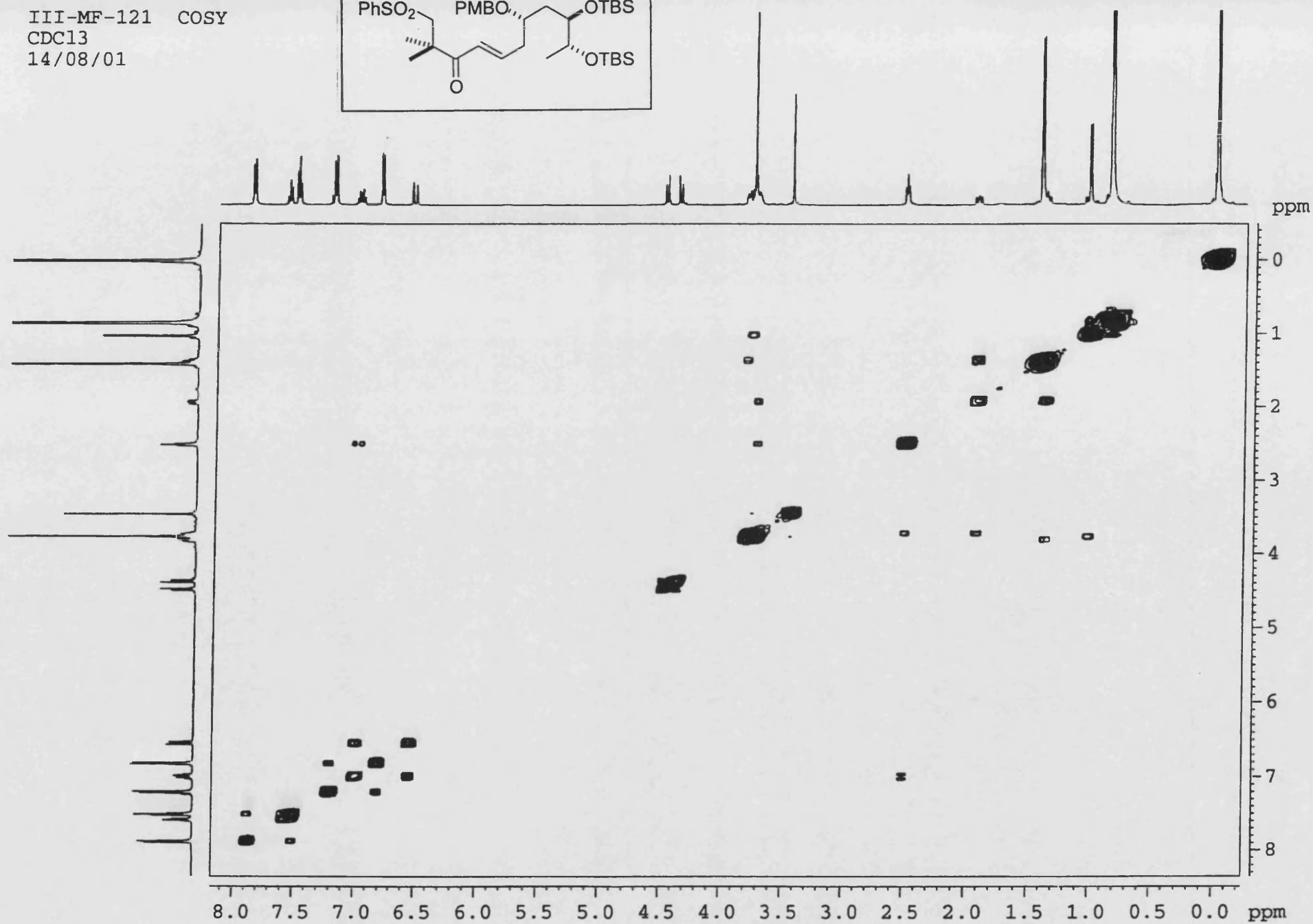
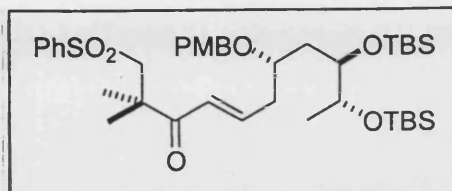
III-MF-118
CDC13
19/09/01



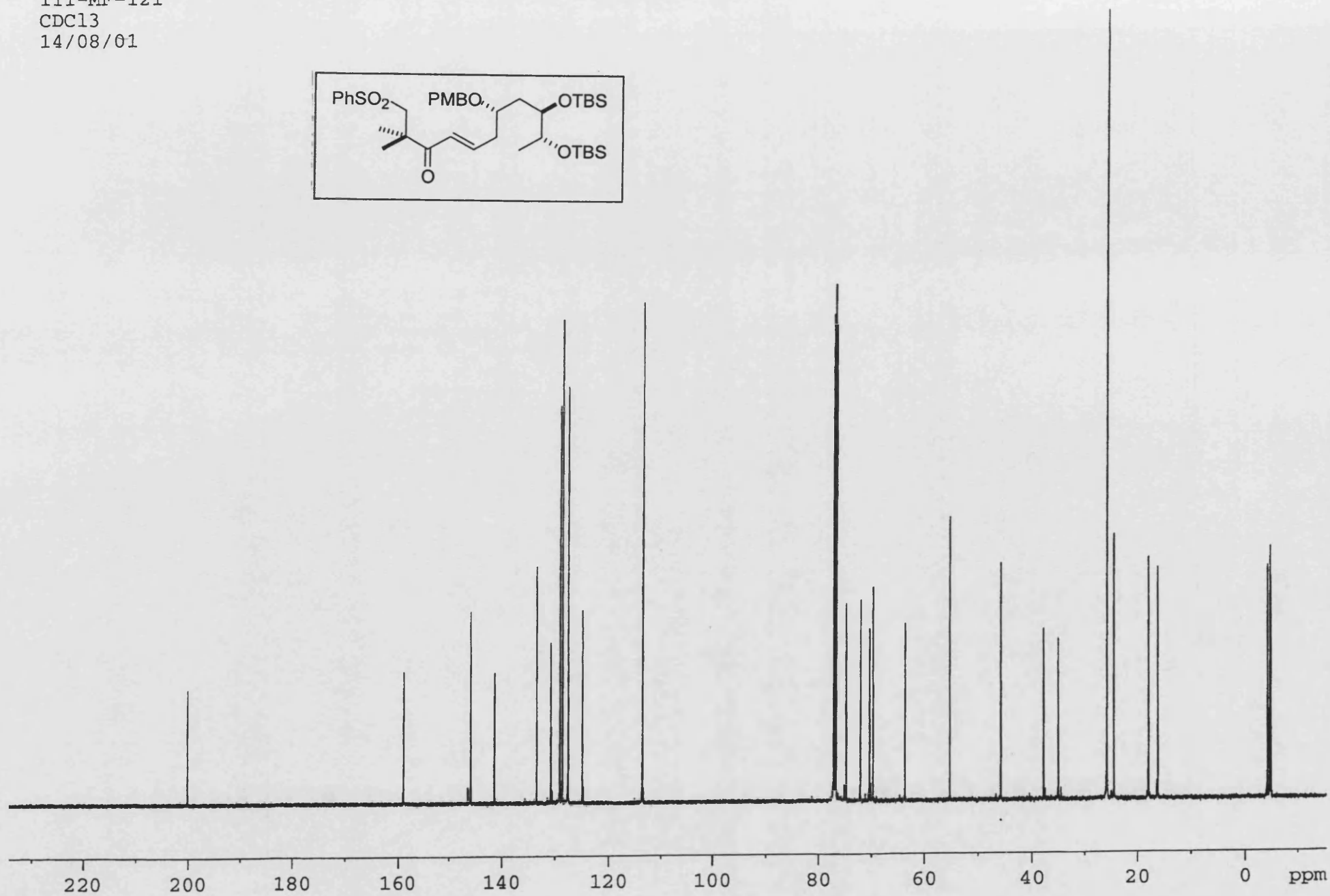
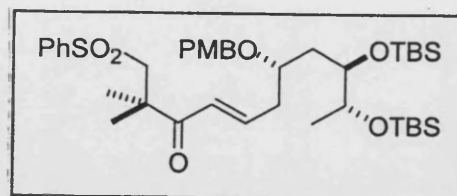
III-MF-121
CDC13
14/08/01



III-MF-121 COSY
CDC13
14/08/01



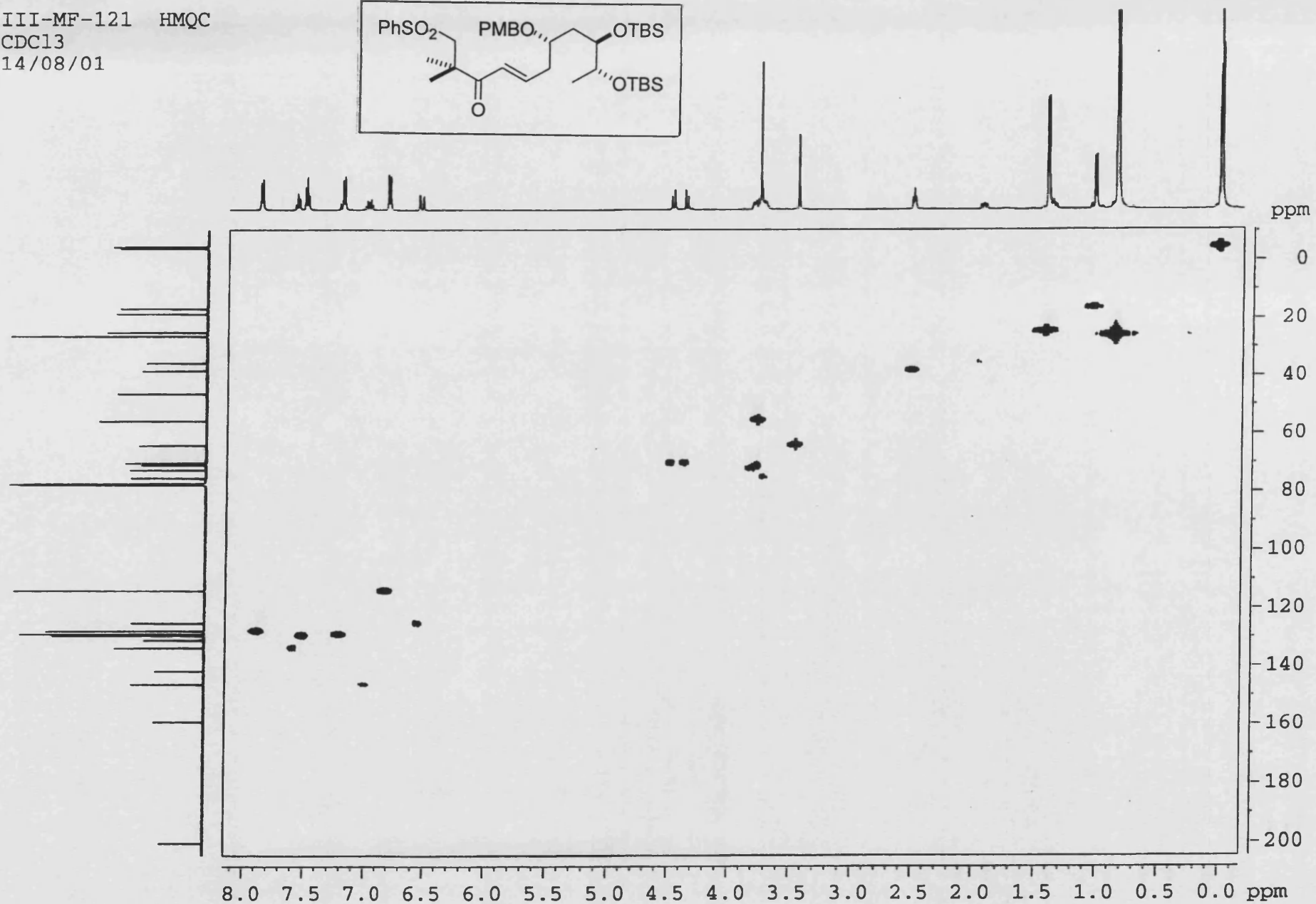
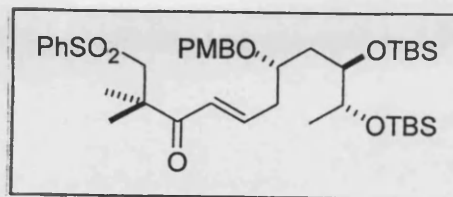
III-MF-121
CDCl₃
14/08/01



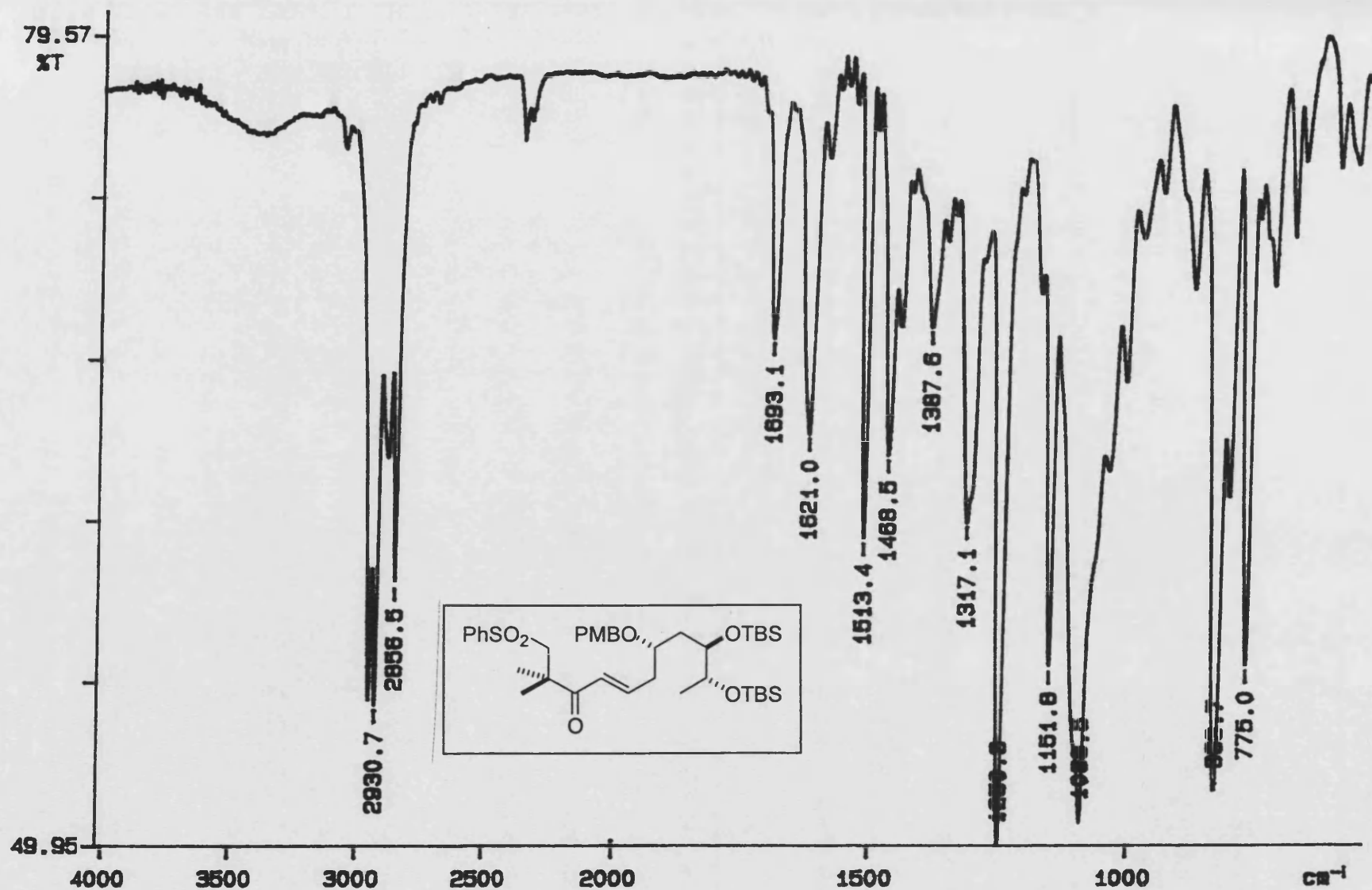
14/08/01



III-MF-121 HMQC
CDCl₃
14/08/01



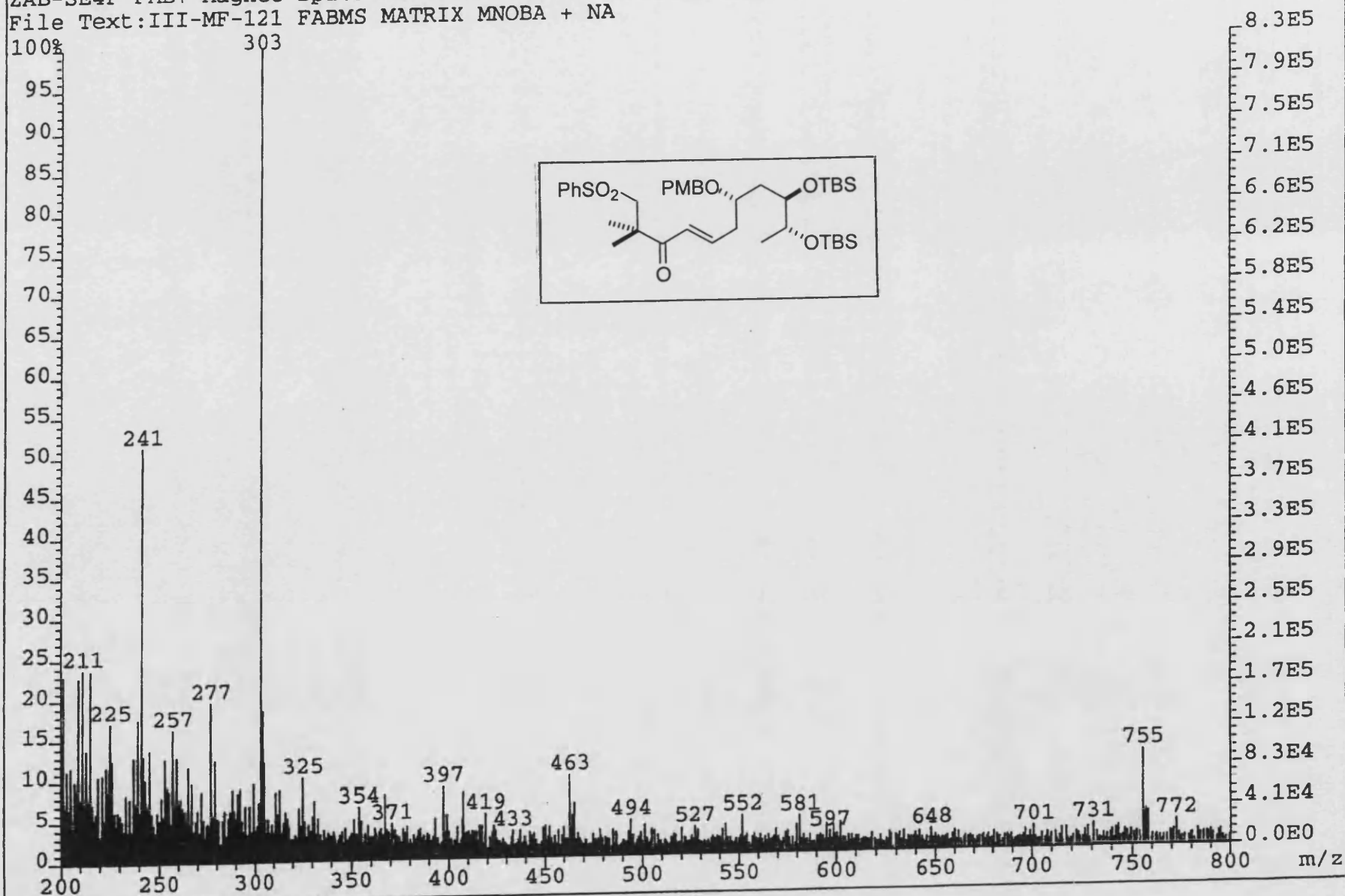
PERKIN ELMER



01/08/14 10:21

X: 64 scans, 16.0cm⁻¹, apod none, flat

File:01SE3349A Ident:13 Acq: 3-SEP-2001 16:27:25 +0:44 Cal:FABLM0320901_1
ZAB-SE4F FAB+ Magnet BpI:9488360 TIC:94920304 Flags:HALL
File Text:III-MF-121 FABMS MATRIX MNOBA + NA



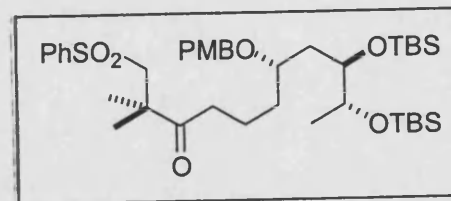
File Text: III-MF-124 FAB/MS MATRIX MNOBA + NA

Chemical structure of compound 124:

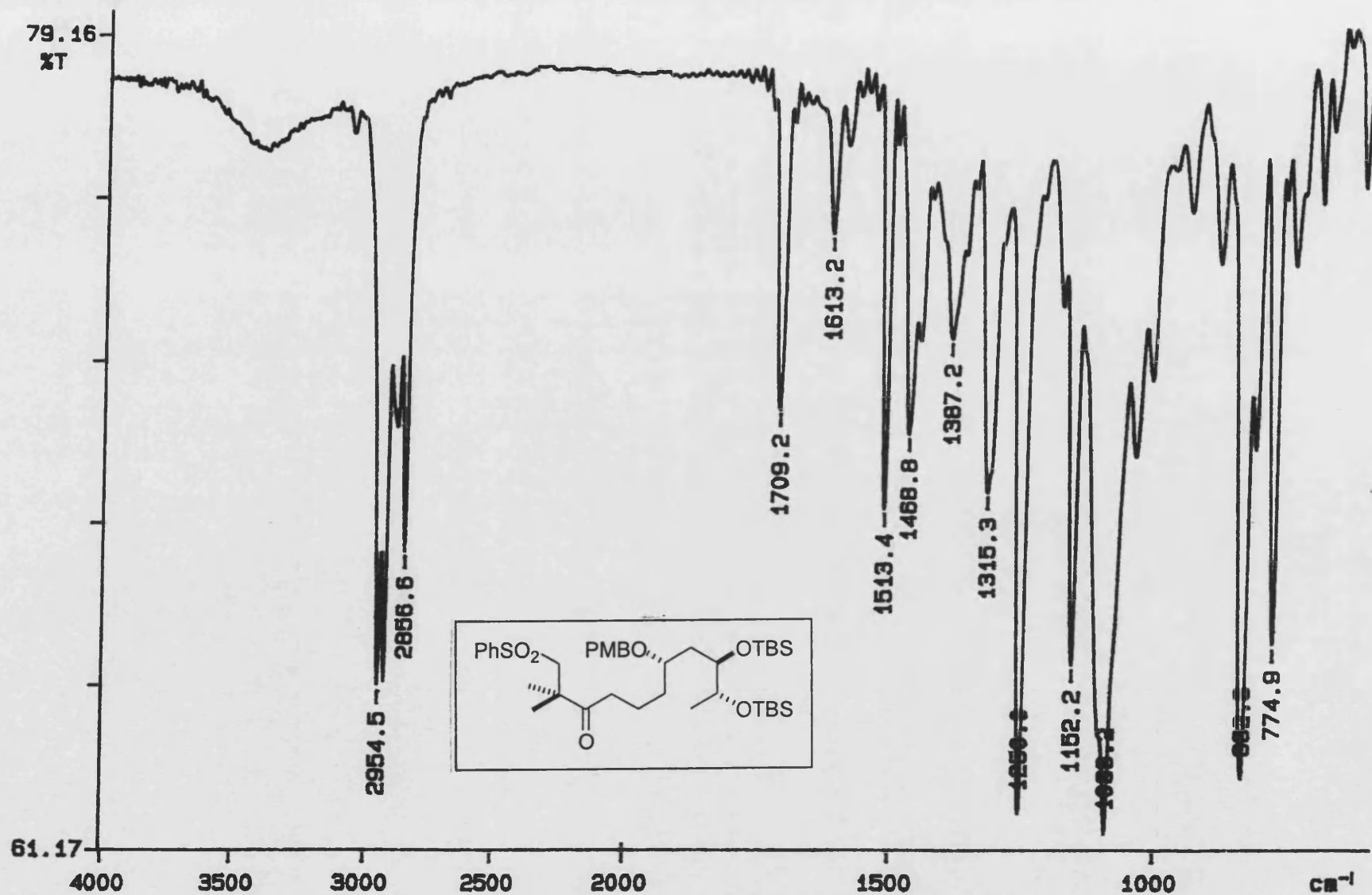
CC(C)(C(=O)CC(C)OP(=O)(OC)OC)CC(C)OP(=O)(OC)OC

Mass spectrum data (approximate relative intensity):

m/z	Relative Intensity (%)
211	15
225	25
241	65
257	25
279	20
303	95
315	10
327	8
349	10
367	5
409	40
423	8
439	12
451	5
465	100
481	8
493	5
539	5
597	10
615	5
637	5
675	5
699	5
741	5
757	75
771	5



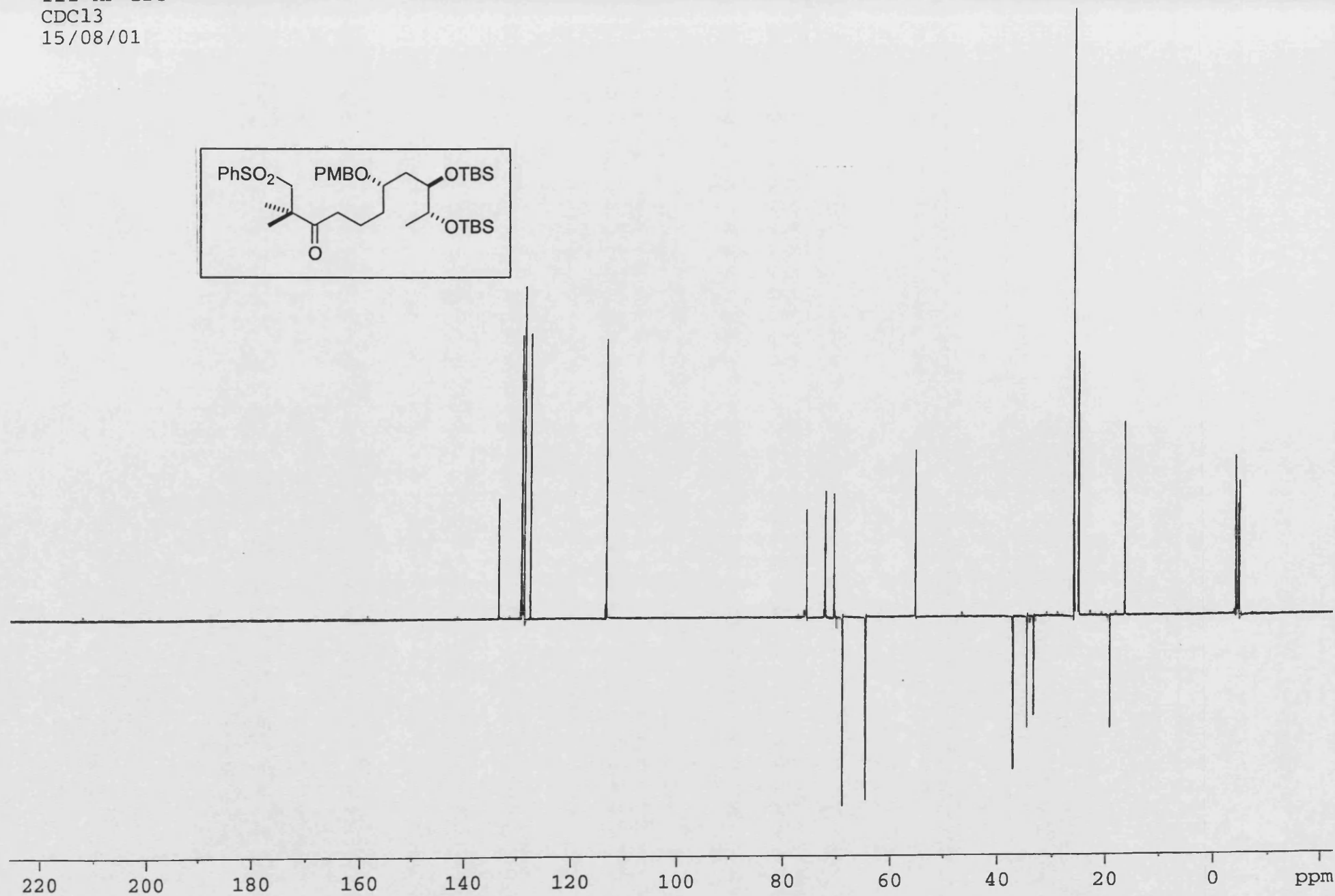
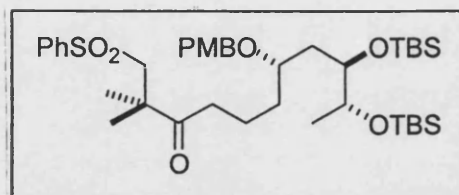
PERKIN ELMER



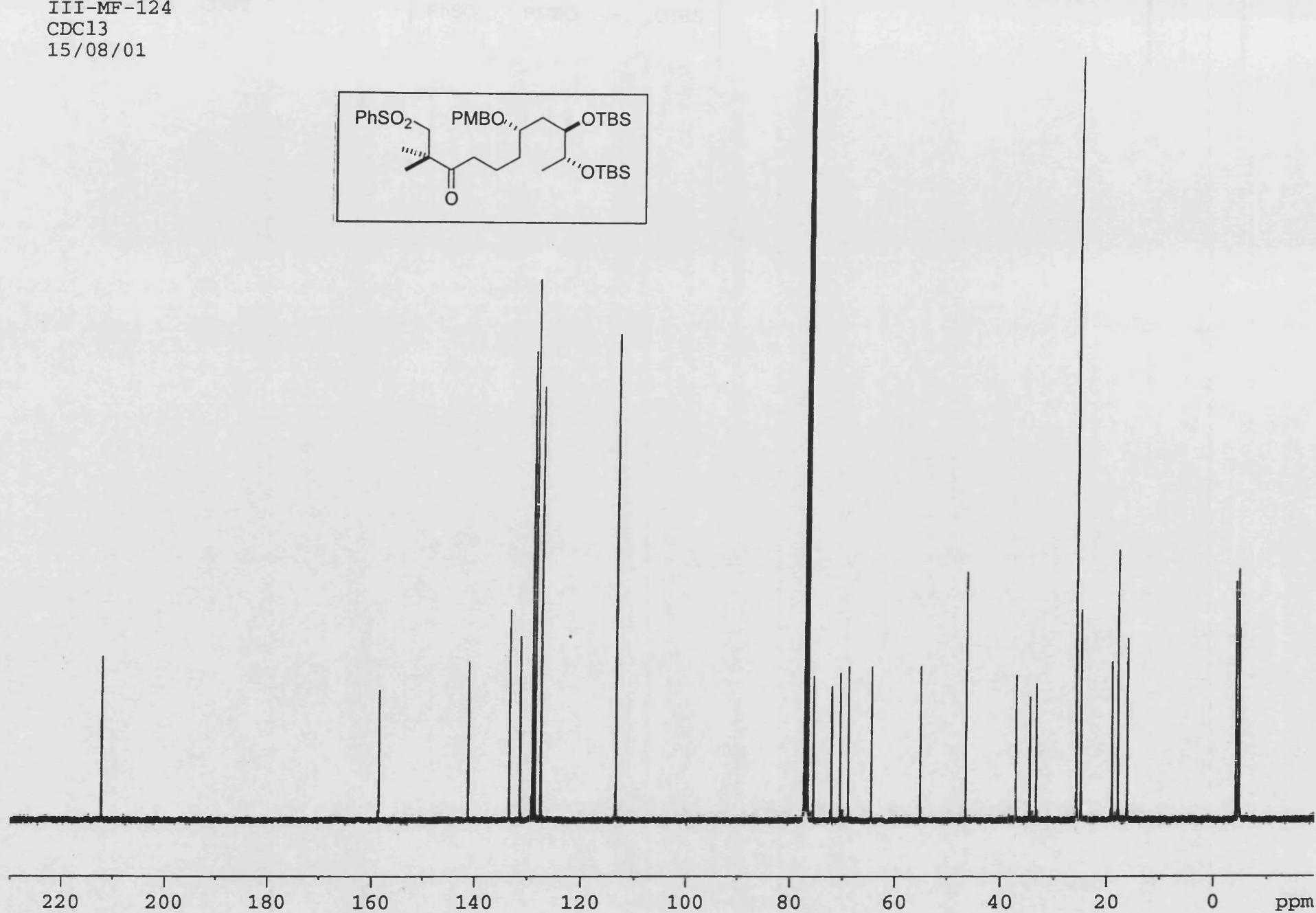
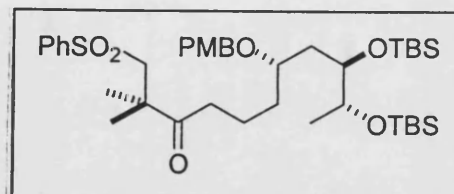
01/08/16 14:00

Y: 64 scans, 16.0cm⁻¹, apod none, flat

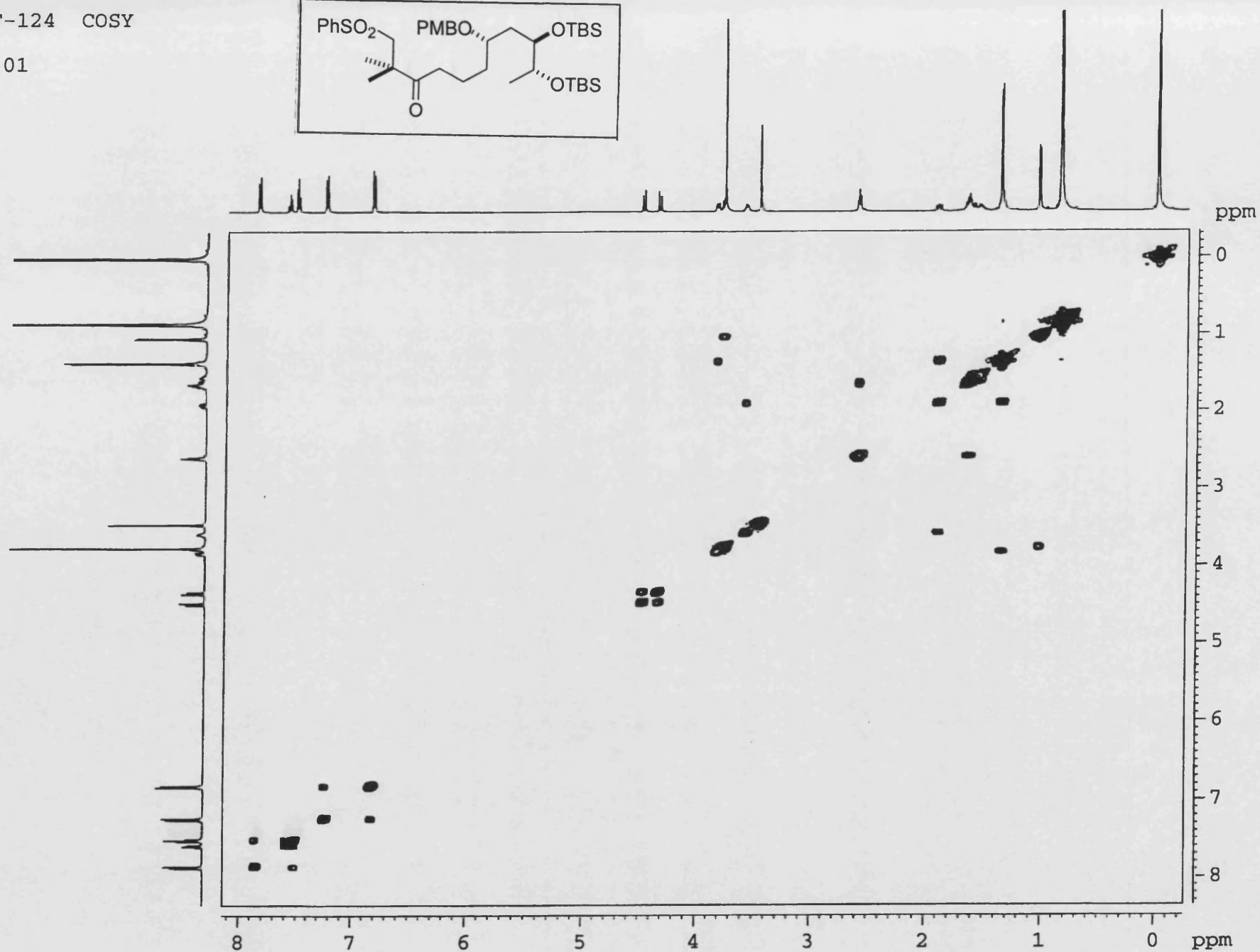
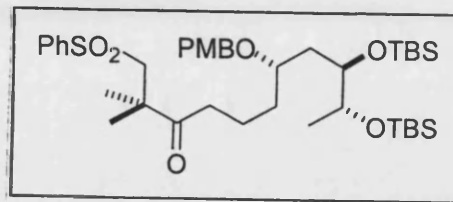
III-MF-124
CDC13
15/08/01



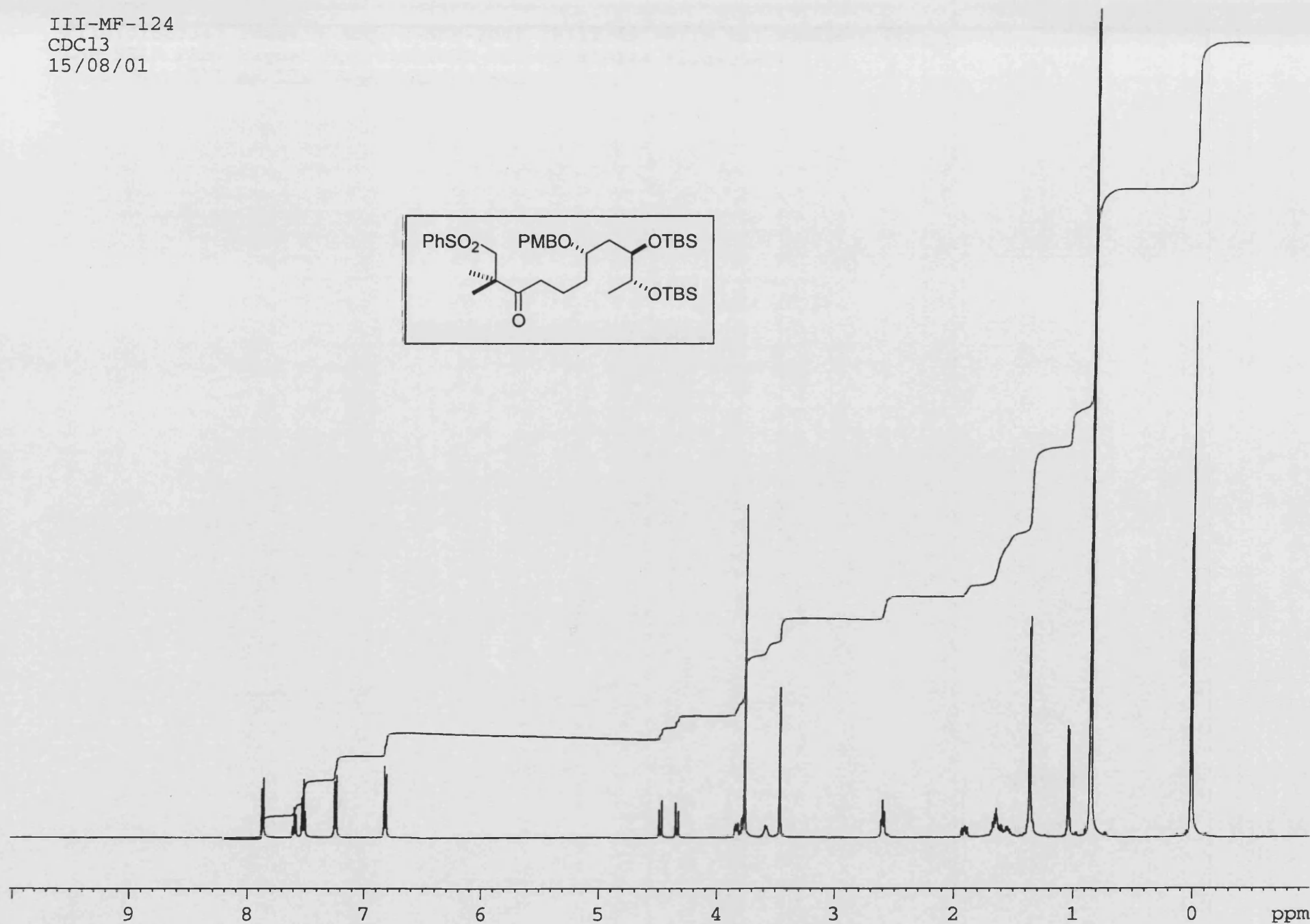
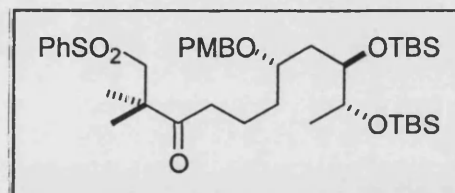
III-MF-124
CDC13
15/08/01



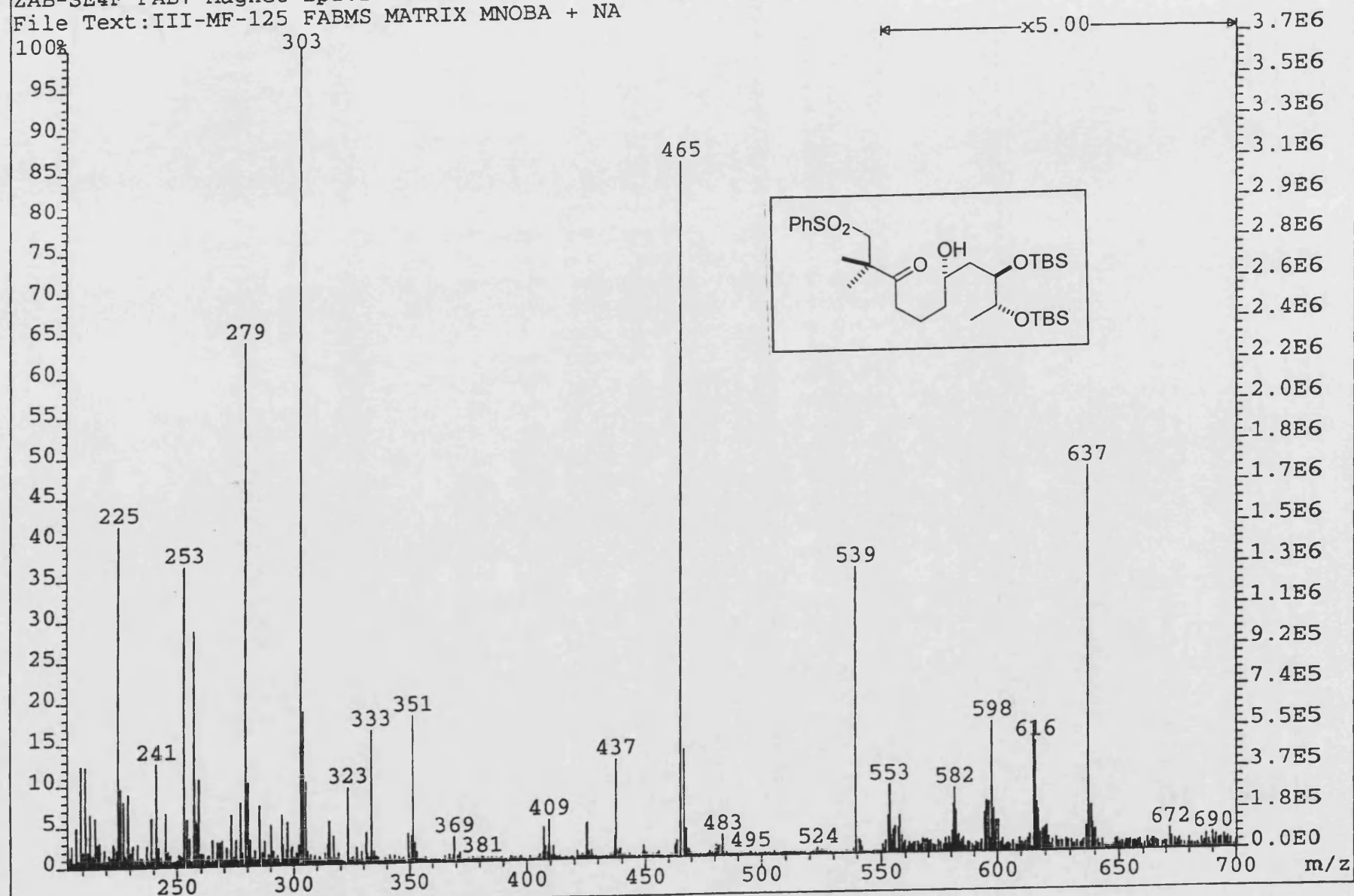
III-MF-124 COSY
CDCl₃
15/08/01



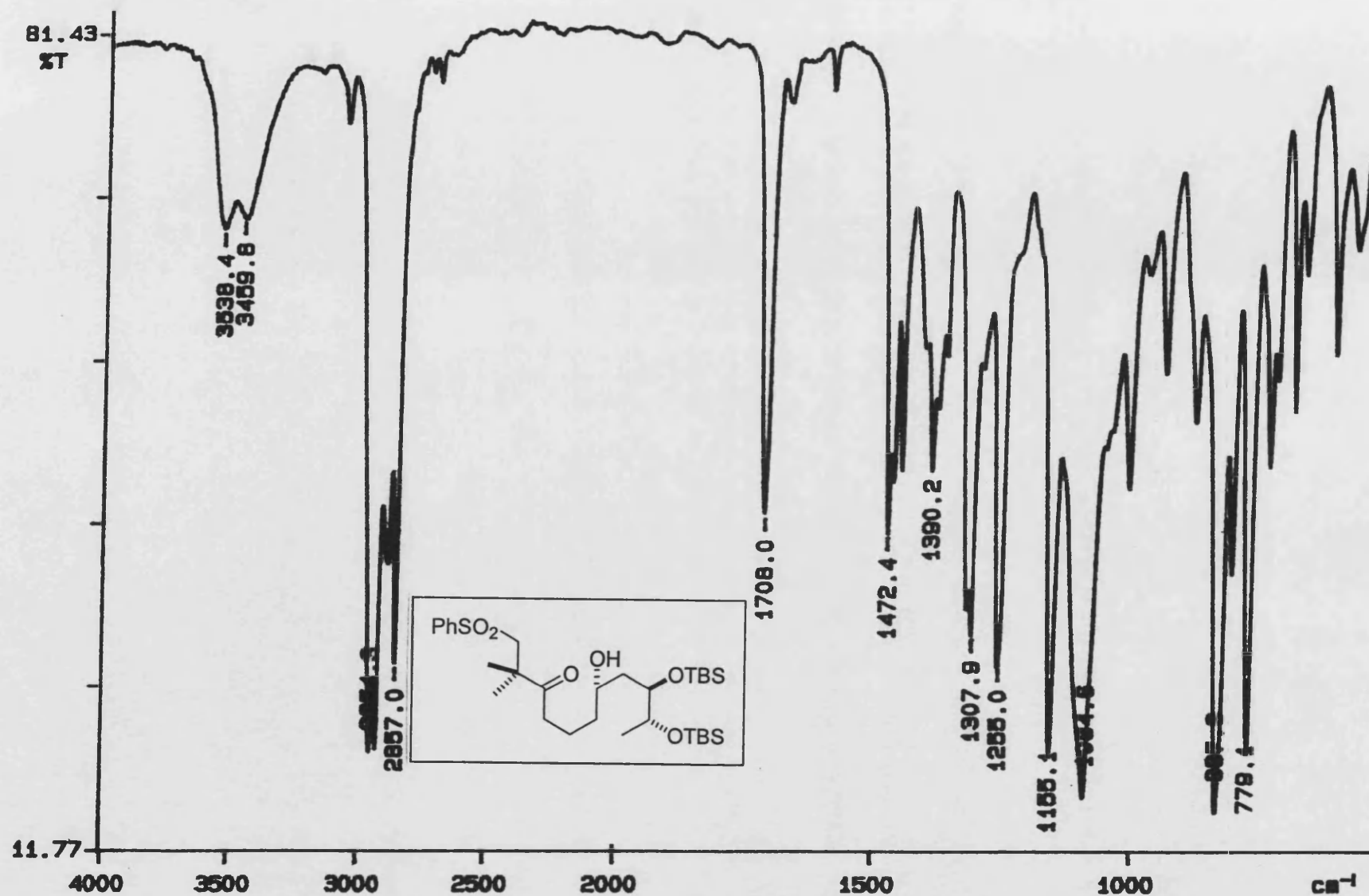
III-MF-124
CDC13
15/08/01



File:01SE3347 Ident:5 Acq: 3-SEP-2001 16:12:45 +0:19 Cal:FABLM0320901_1
ZAB-SE4F FAB+ Magnet BpI:11525136 TIC:167546144 Flags:HALL
File Text:III-MF-125 FABMS MATRIX MNOBA + NA



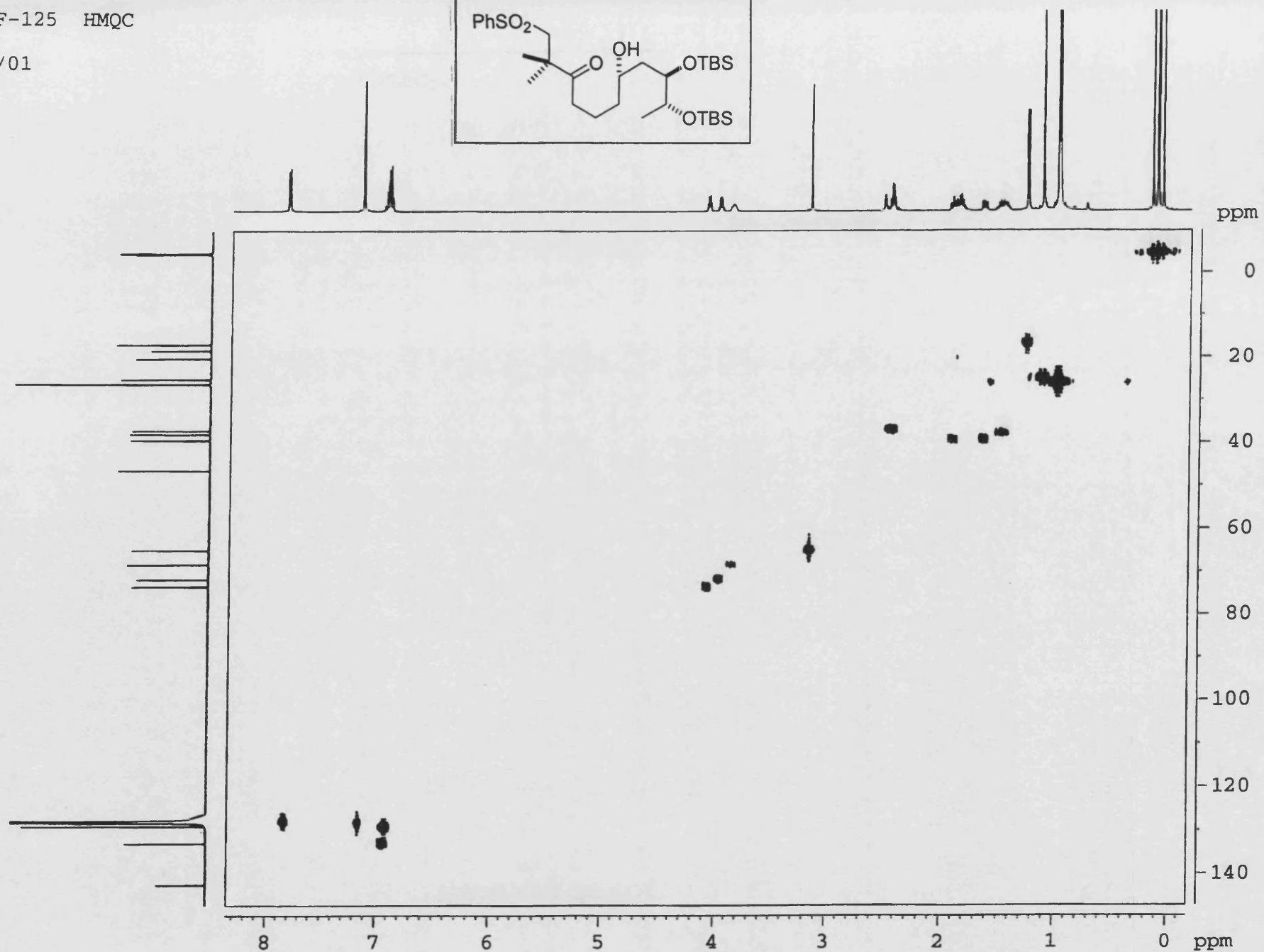
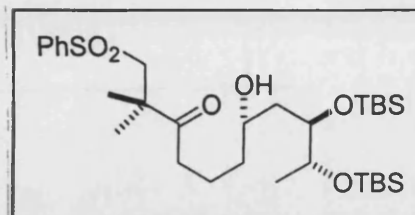
PERKIN ELMER



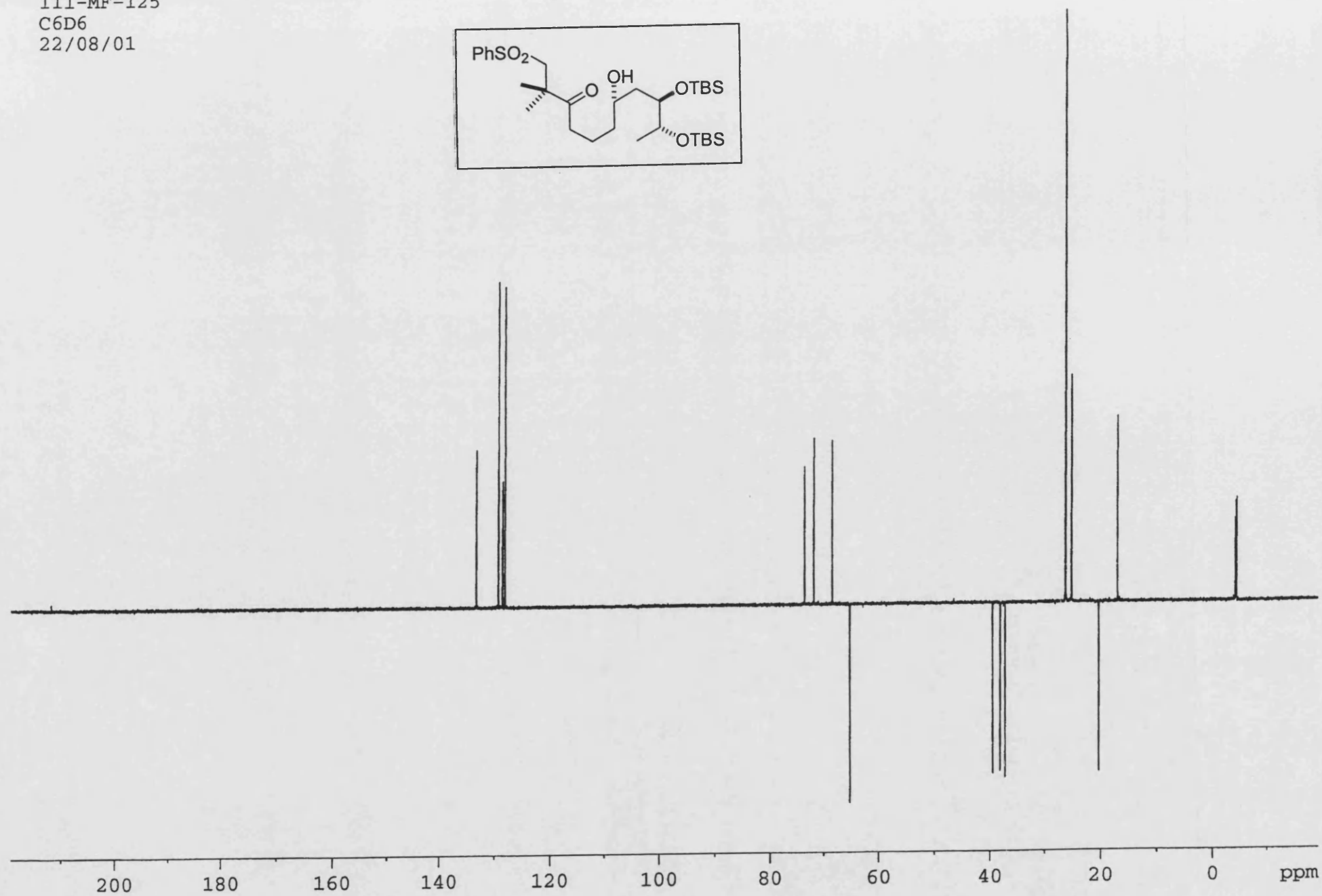
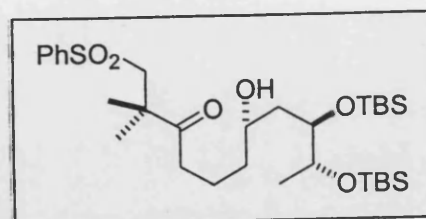
01/08/21 18:53

X: 64 scans, 4.0 cm^{-1} , flat

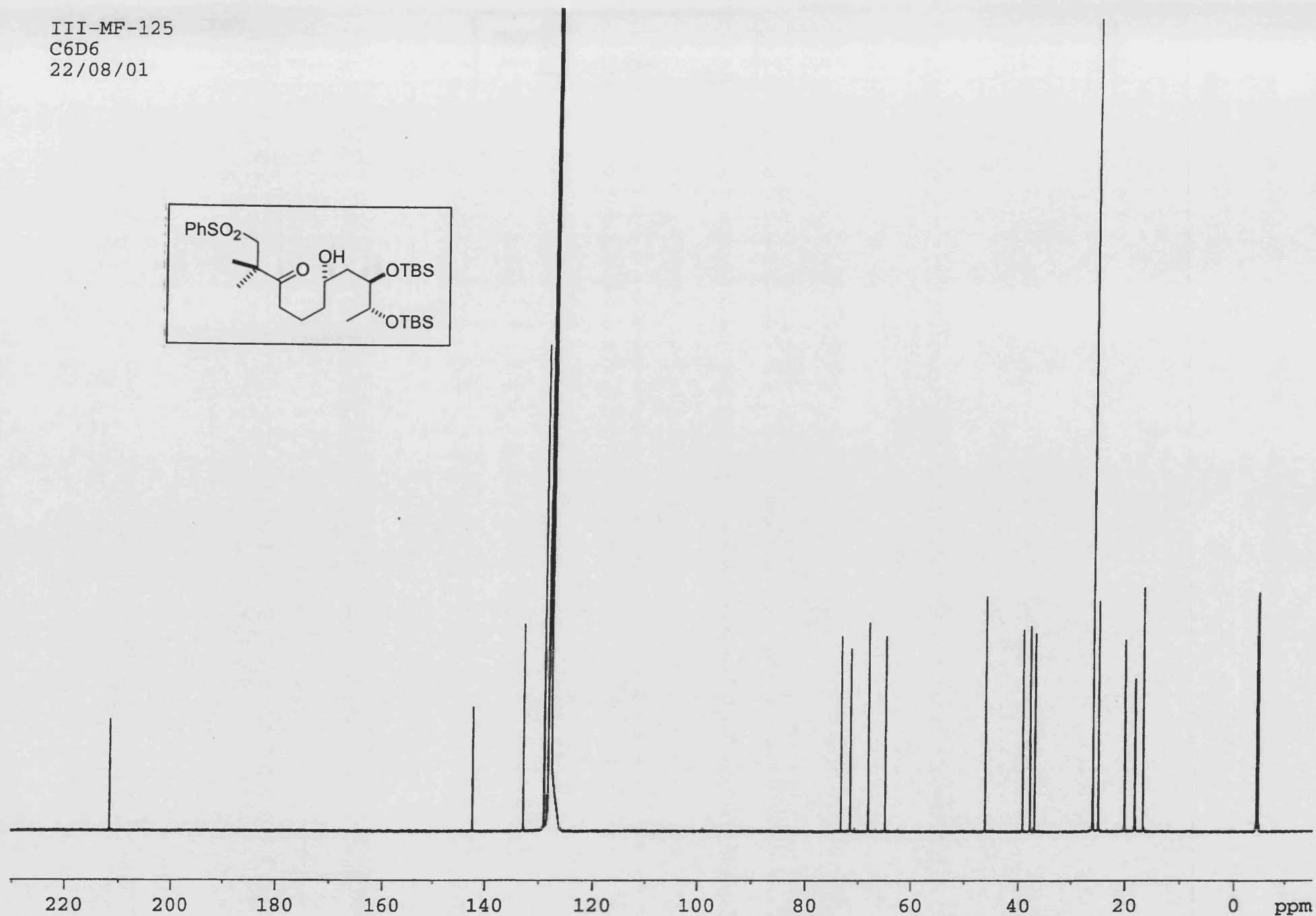
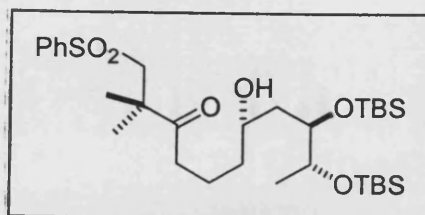
III-MF-125 HMQC
C6D6
22/08/01



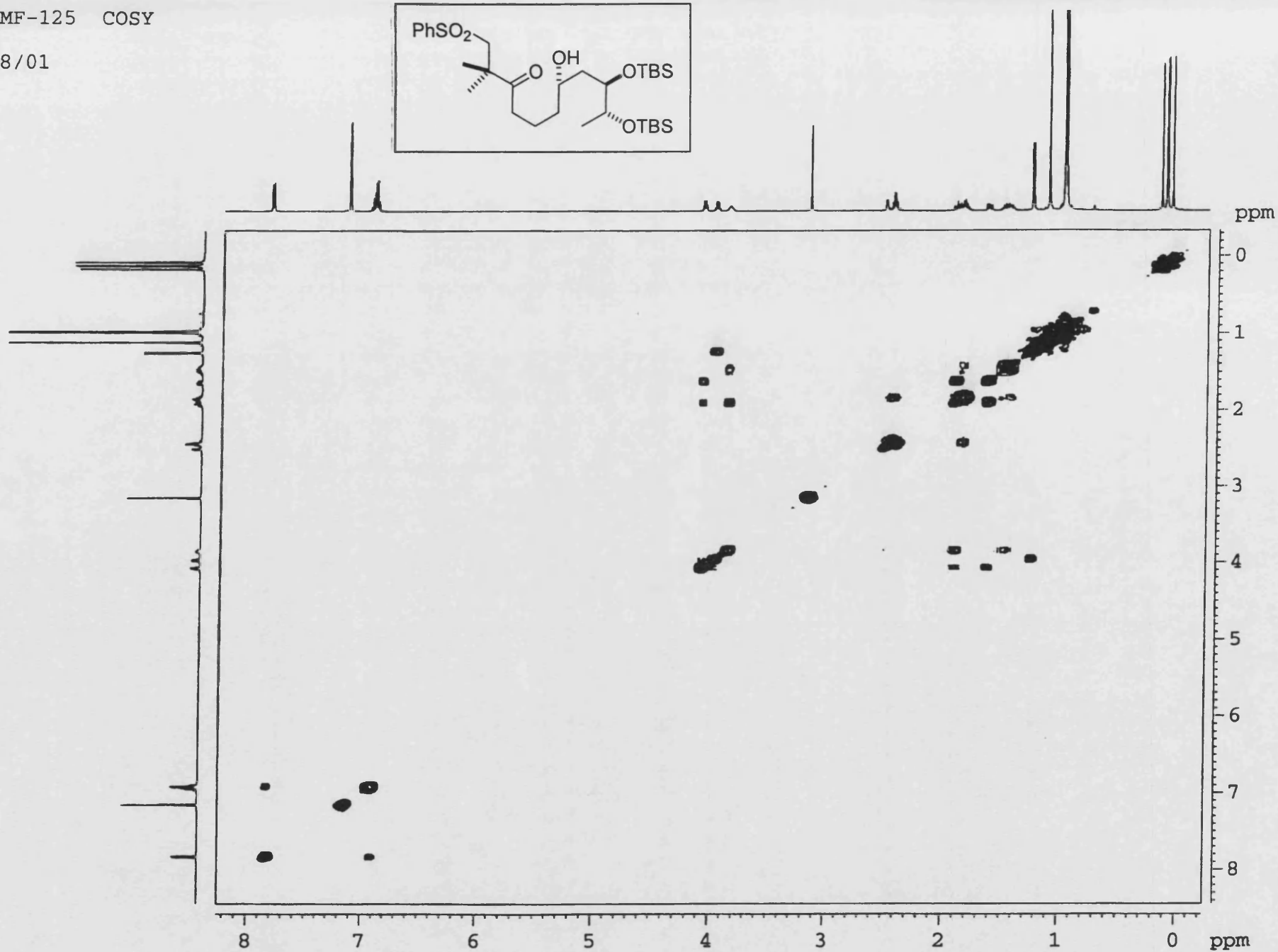
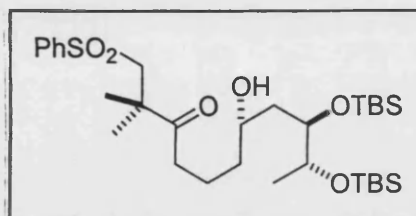
III-MF-125
C6D6
22/08/01



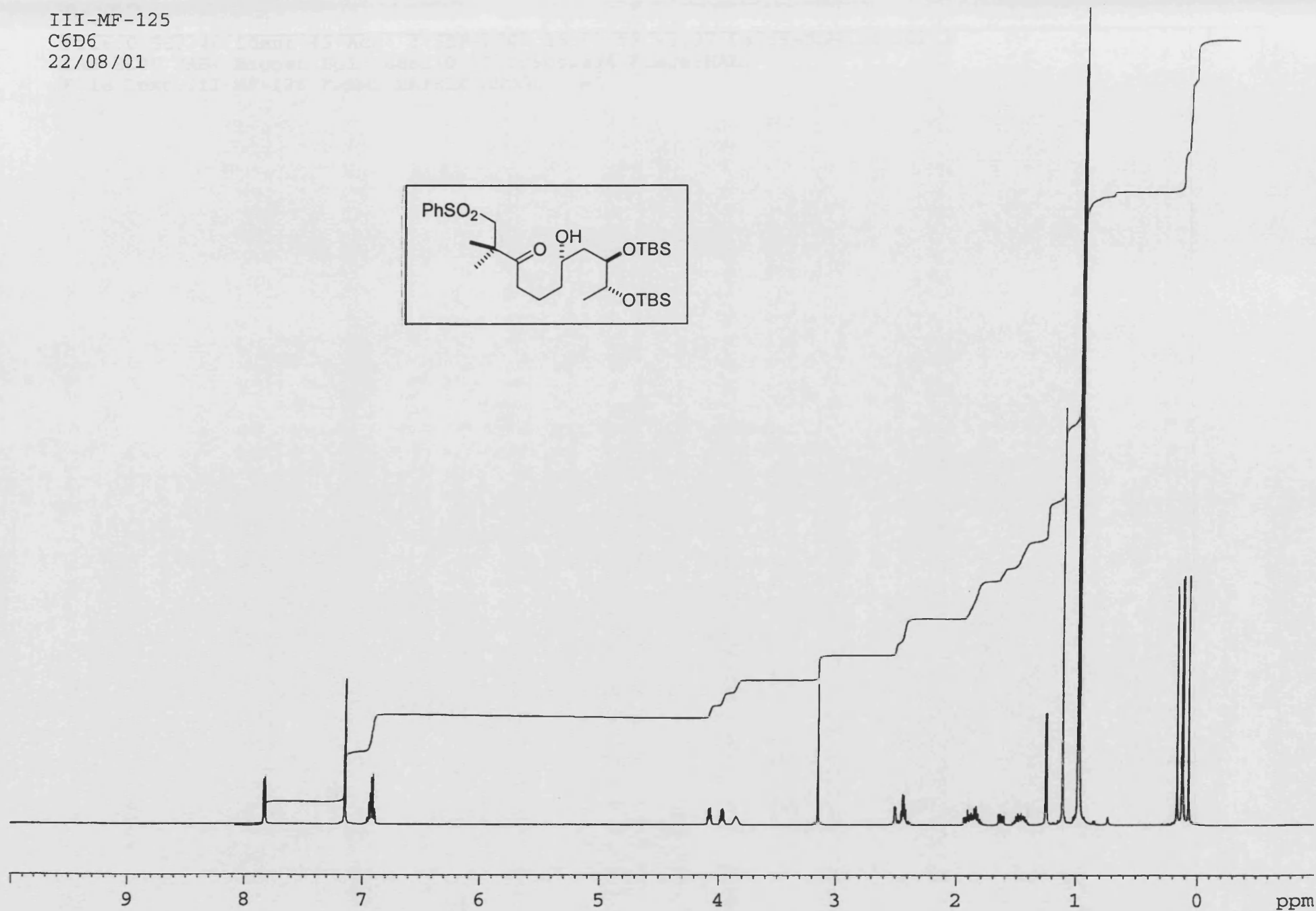
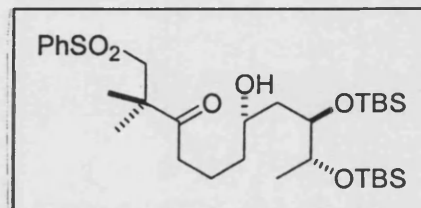
III-MF-125
C6D6
22/08/01



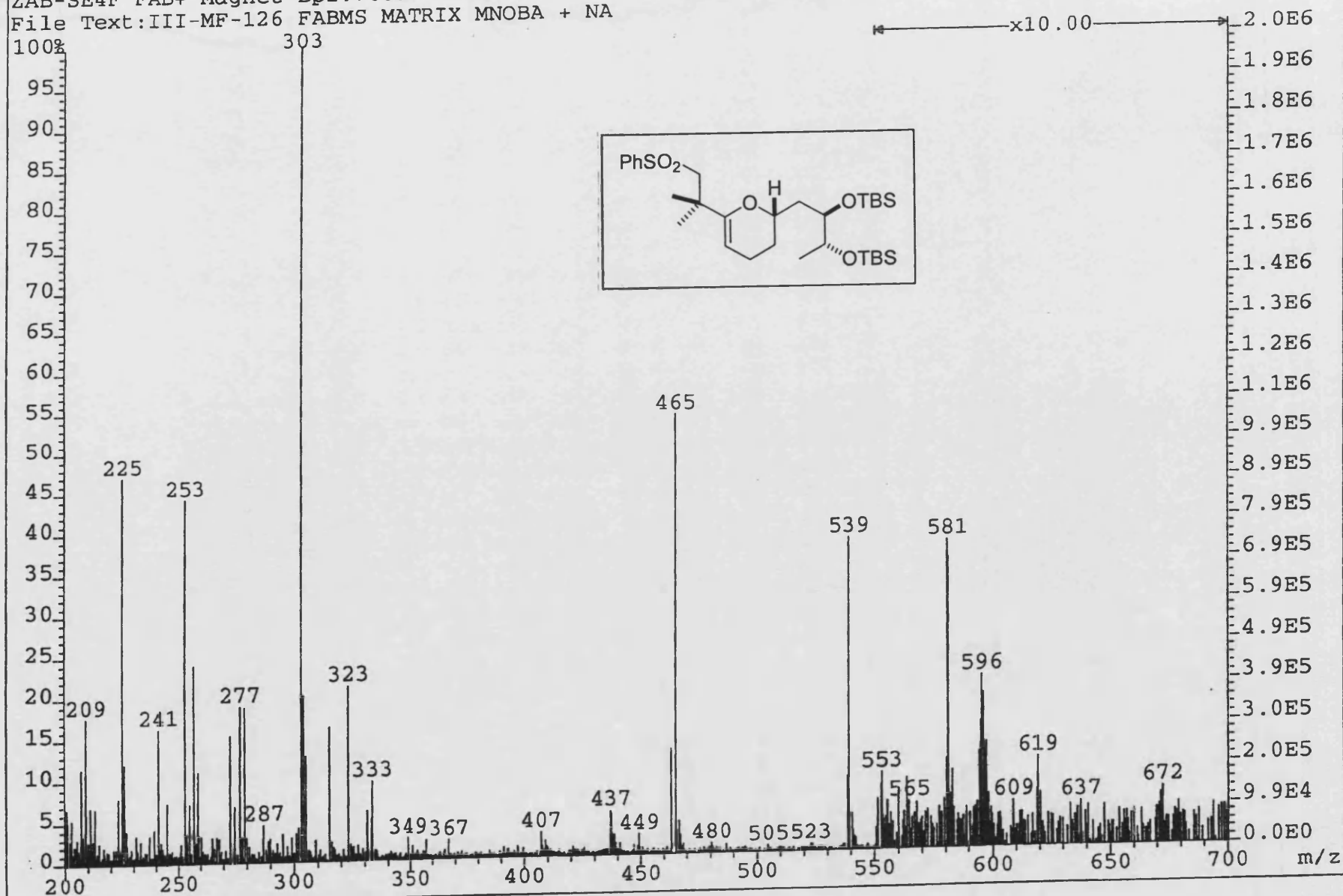
III-MF-125 COSY
C6D6
22/08/01



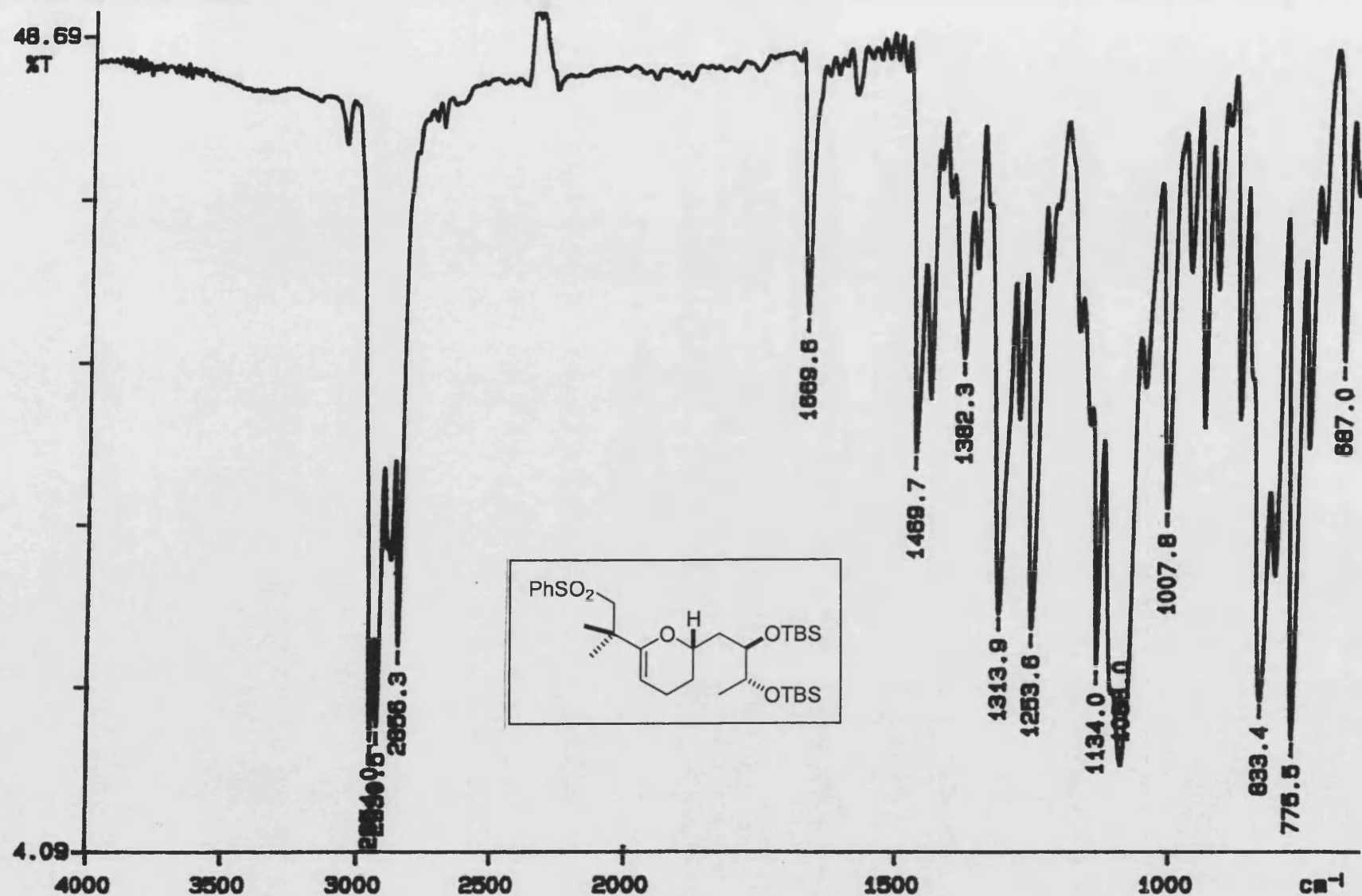
III-MF-125
C6D6
22/08/01



File:01SE3346 Ident:49 Acq: 3-SEP-2001 16:00:59 +2:37 Cal:FABLM0320901-1
ZAB-SE4F FAB+ Magnet BpI:7688270 TIC:99062696 Flags:HALL
File Text:III-MF-126 FABMS MATRIX MNOBA + NA



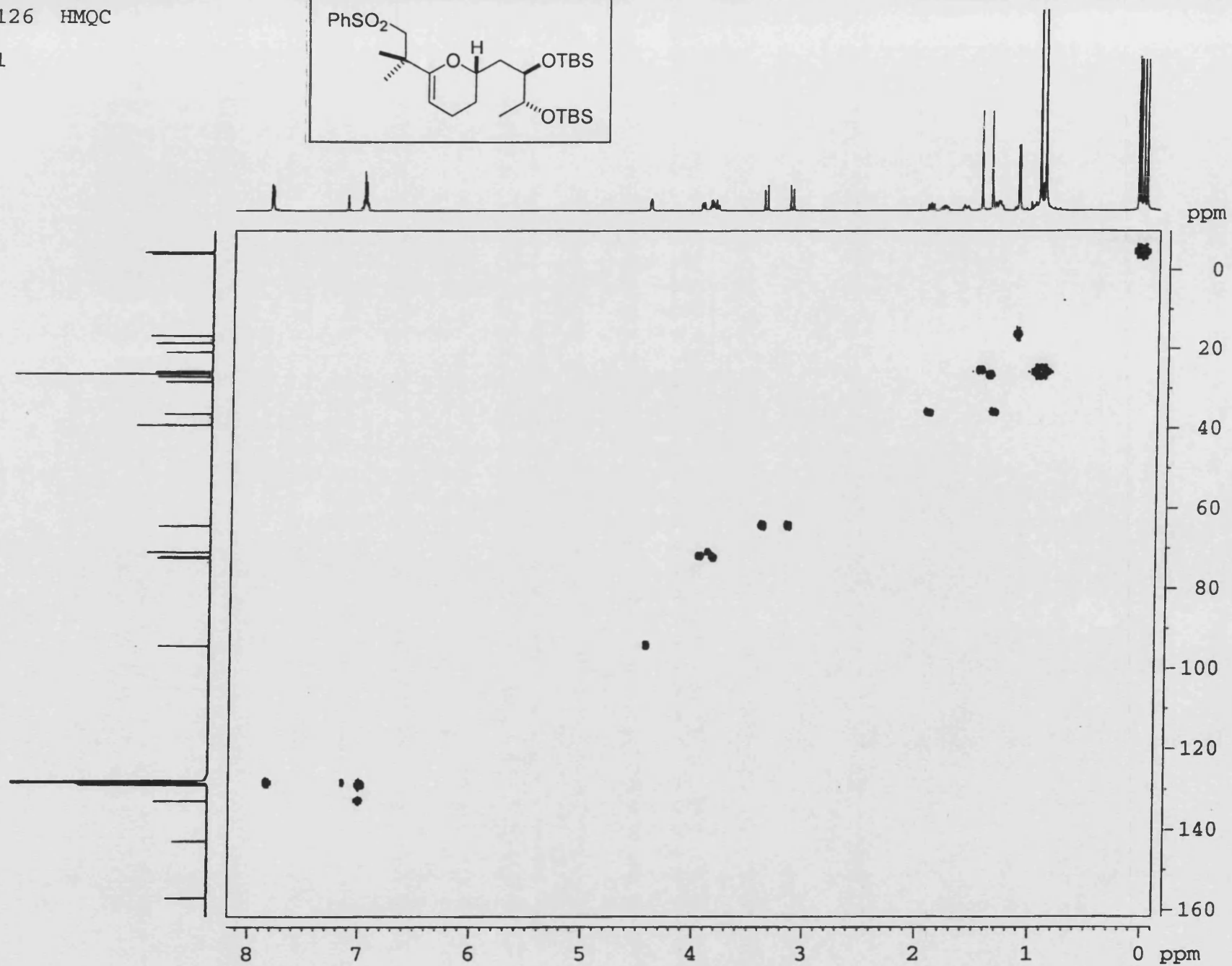
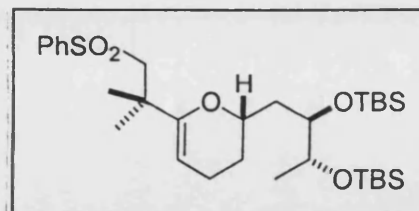
PERKIN ELMER



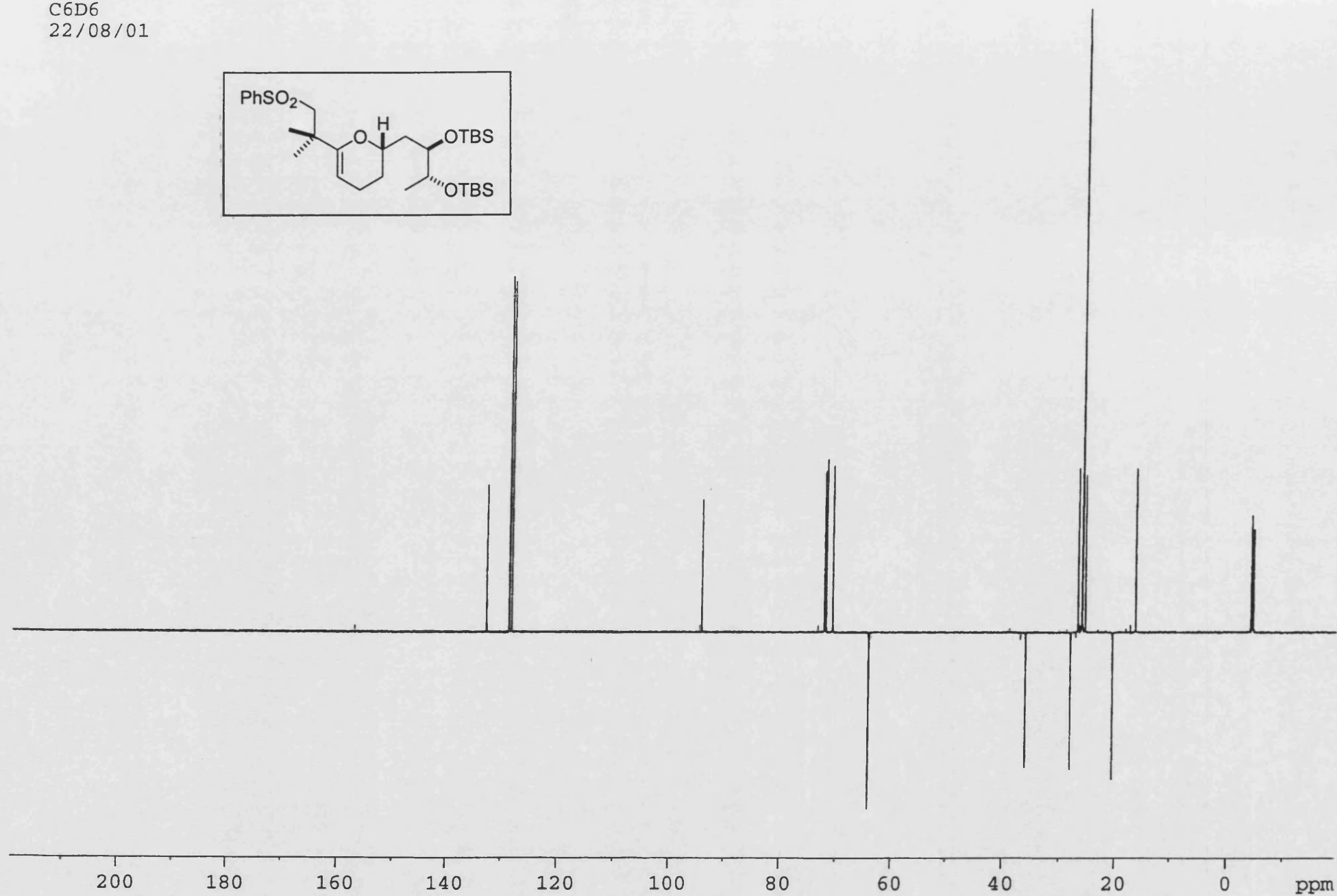
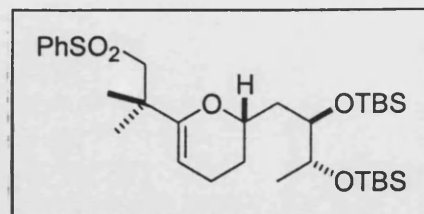
01/08/22 16:12

X: 64 scans, 16.0 cm^{-1} , apod none, flat

III-MF-126 HMQC
C6D6
22/08/01



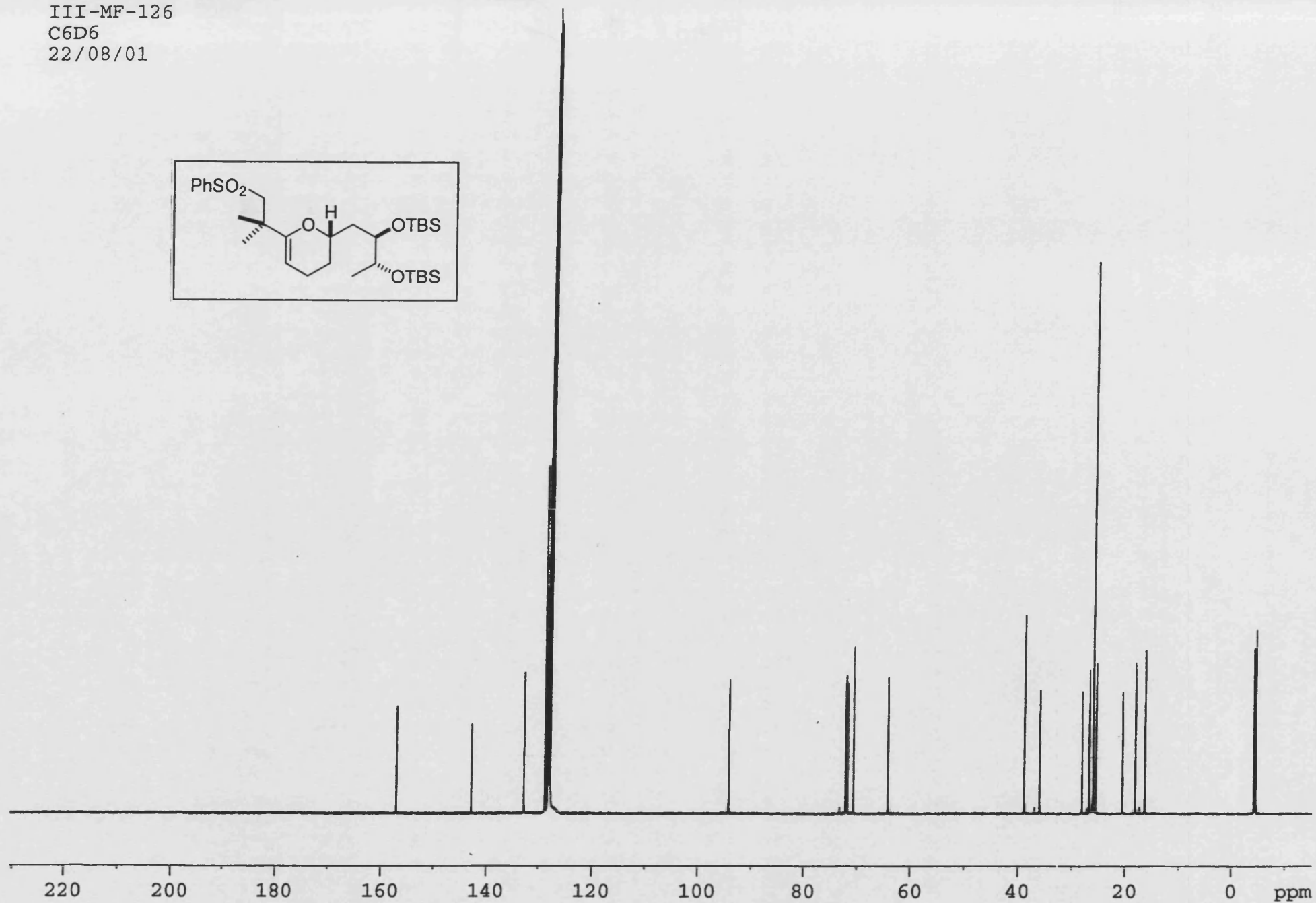
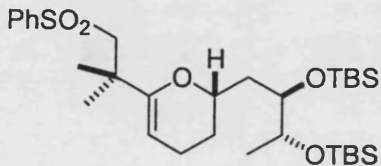
III-MF-126
C6D6
22/08/01



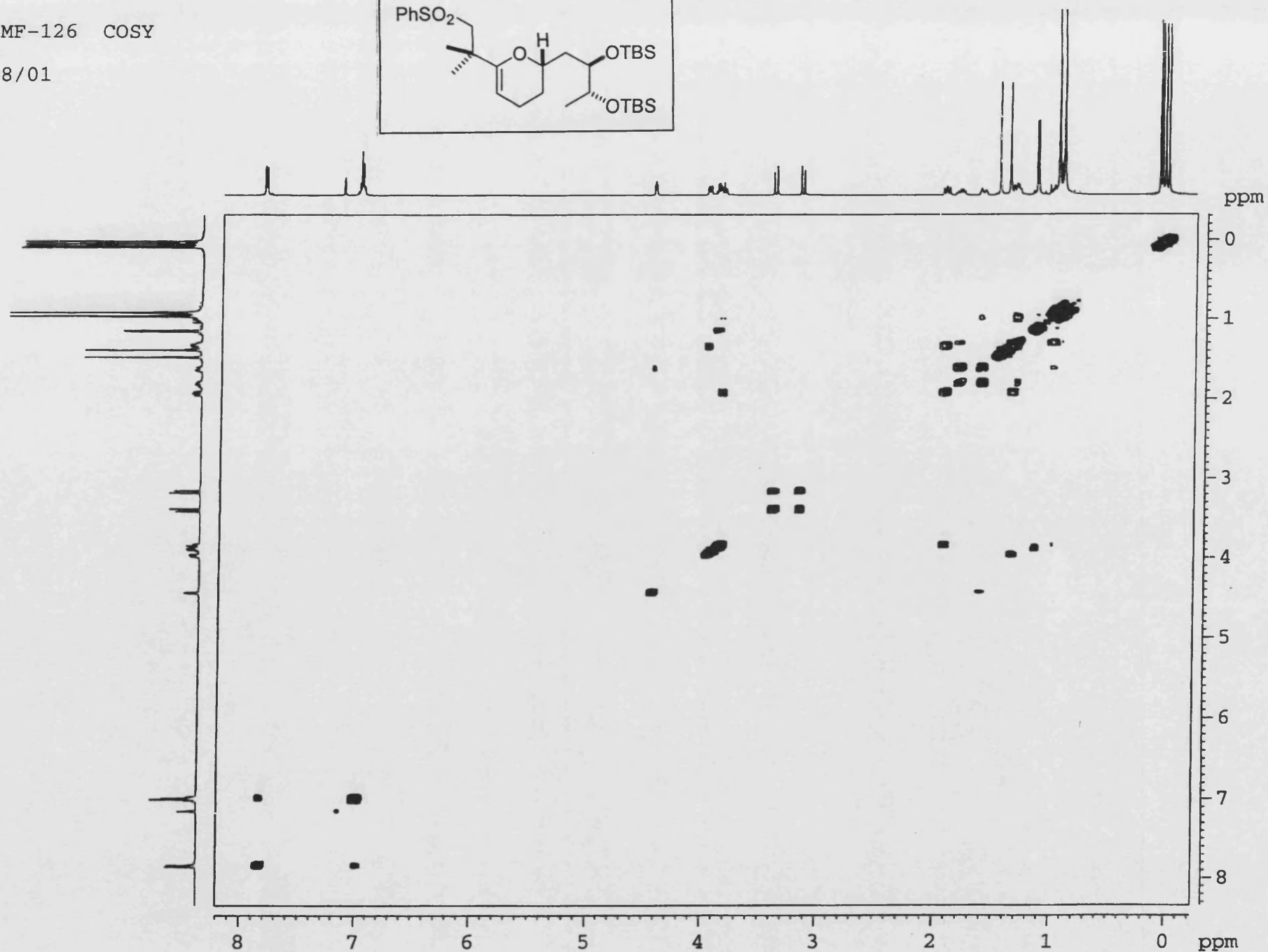
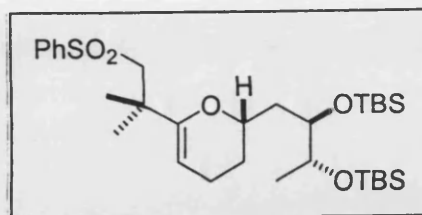
III-MF-126

C6D6

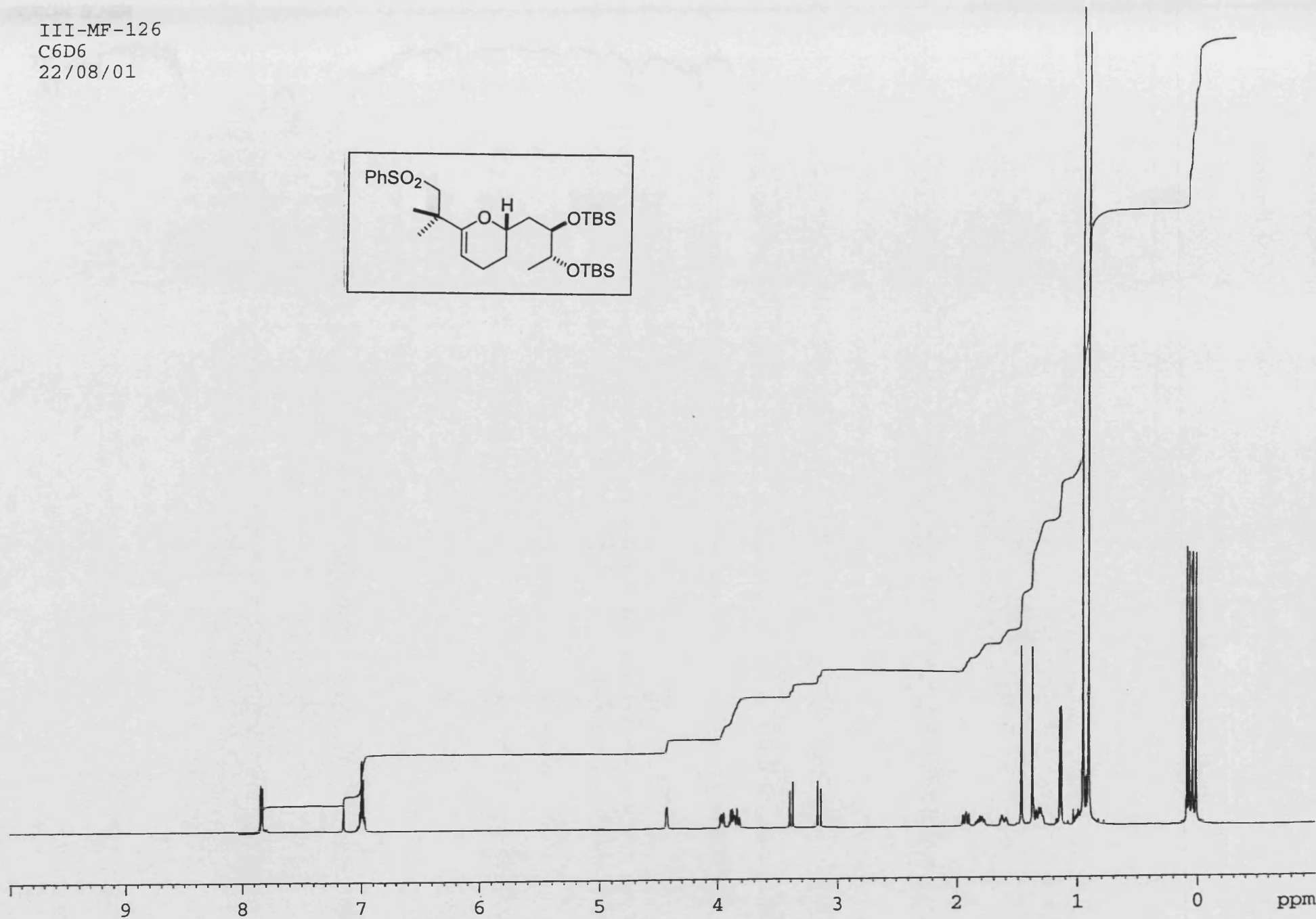
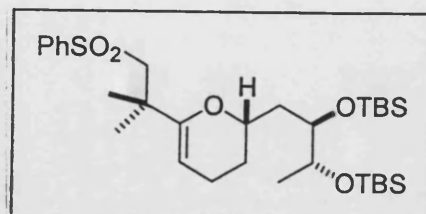
22/08/01



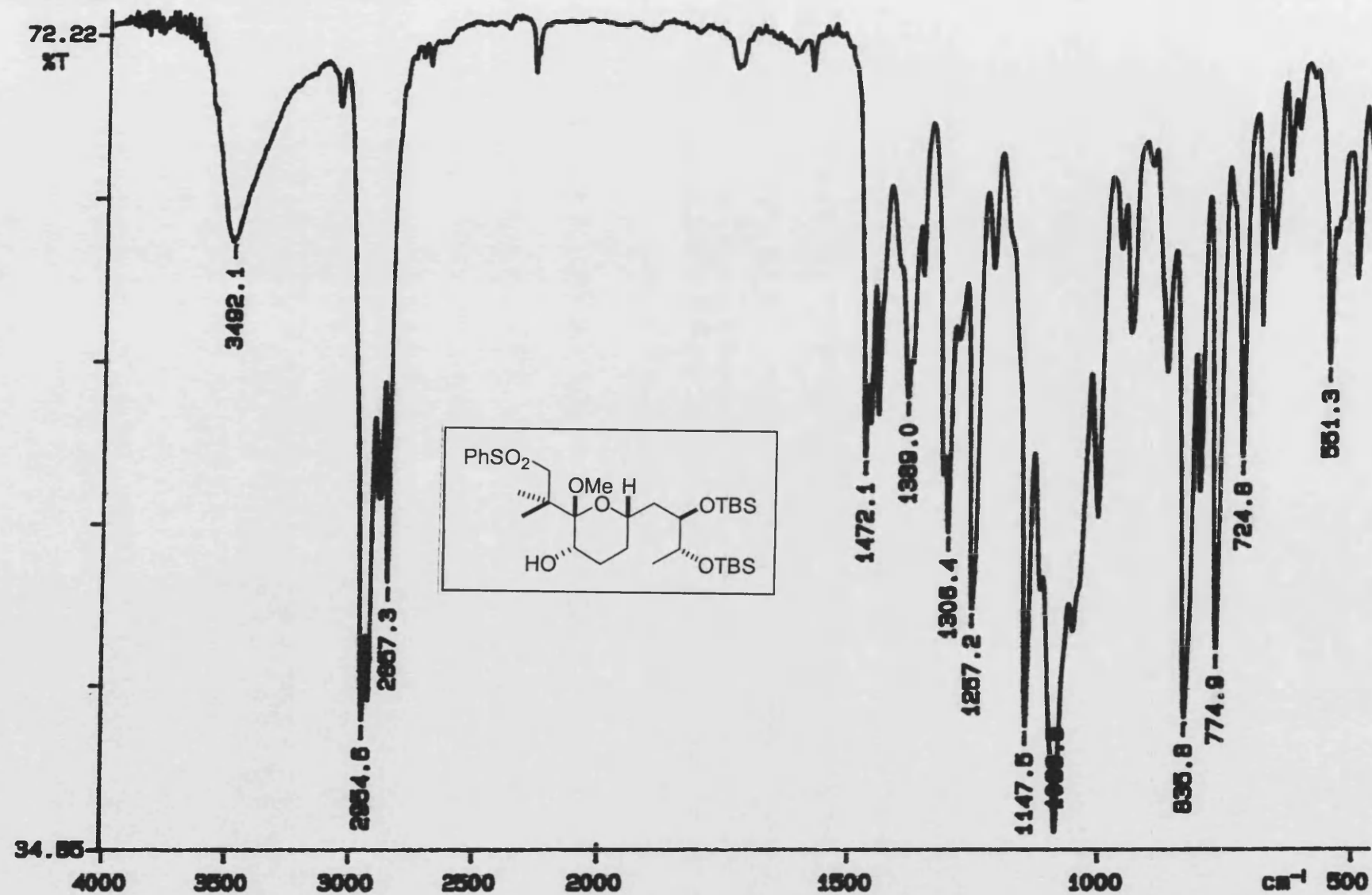
III-MF-126 COSY
C6D6
22/08/01



III-MF-126
C6D6
22/08/01



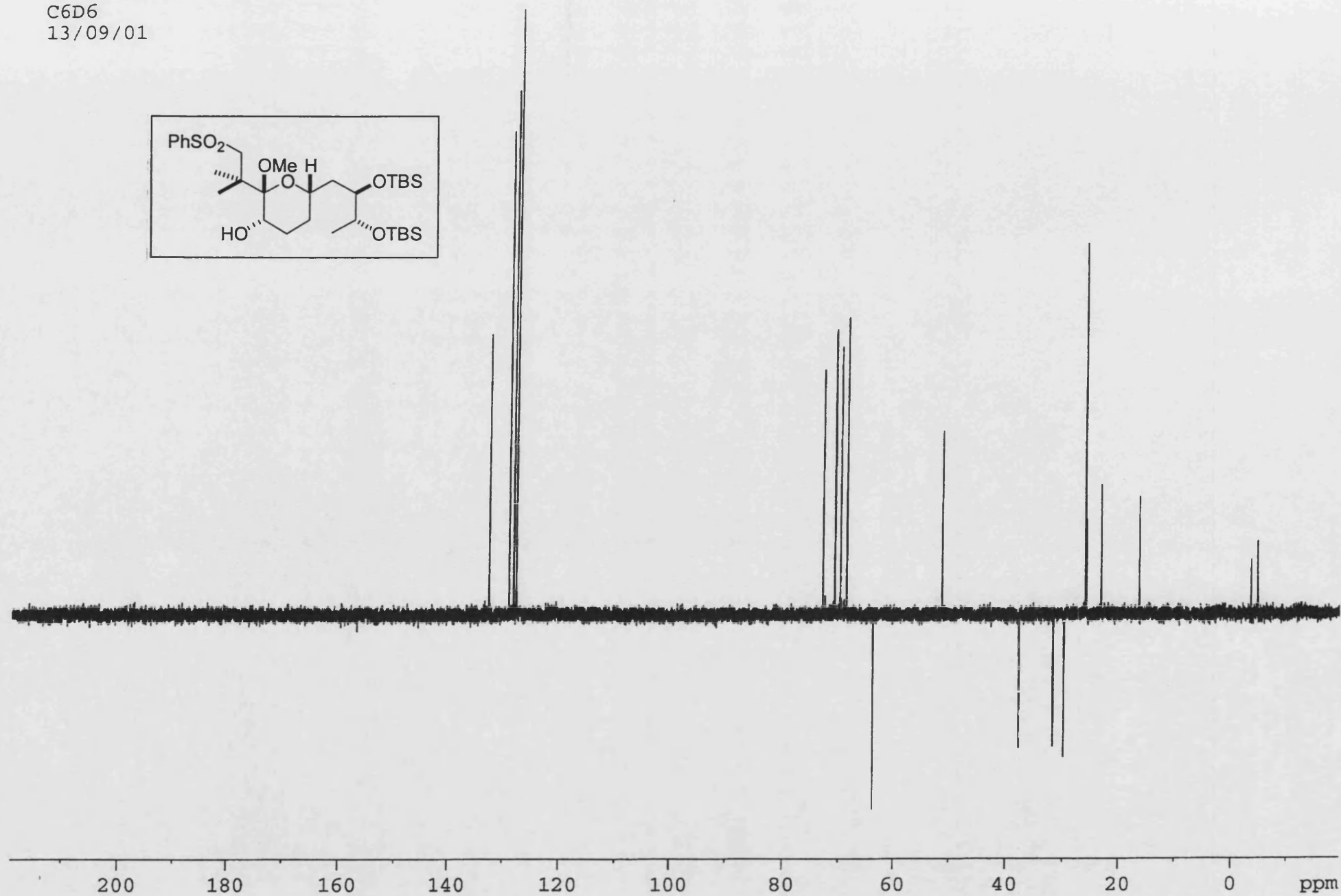
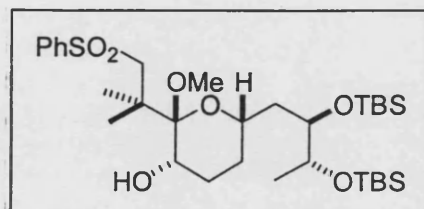
PERKIN ELMER



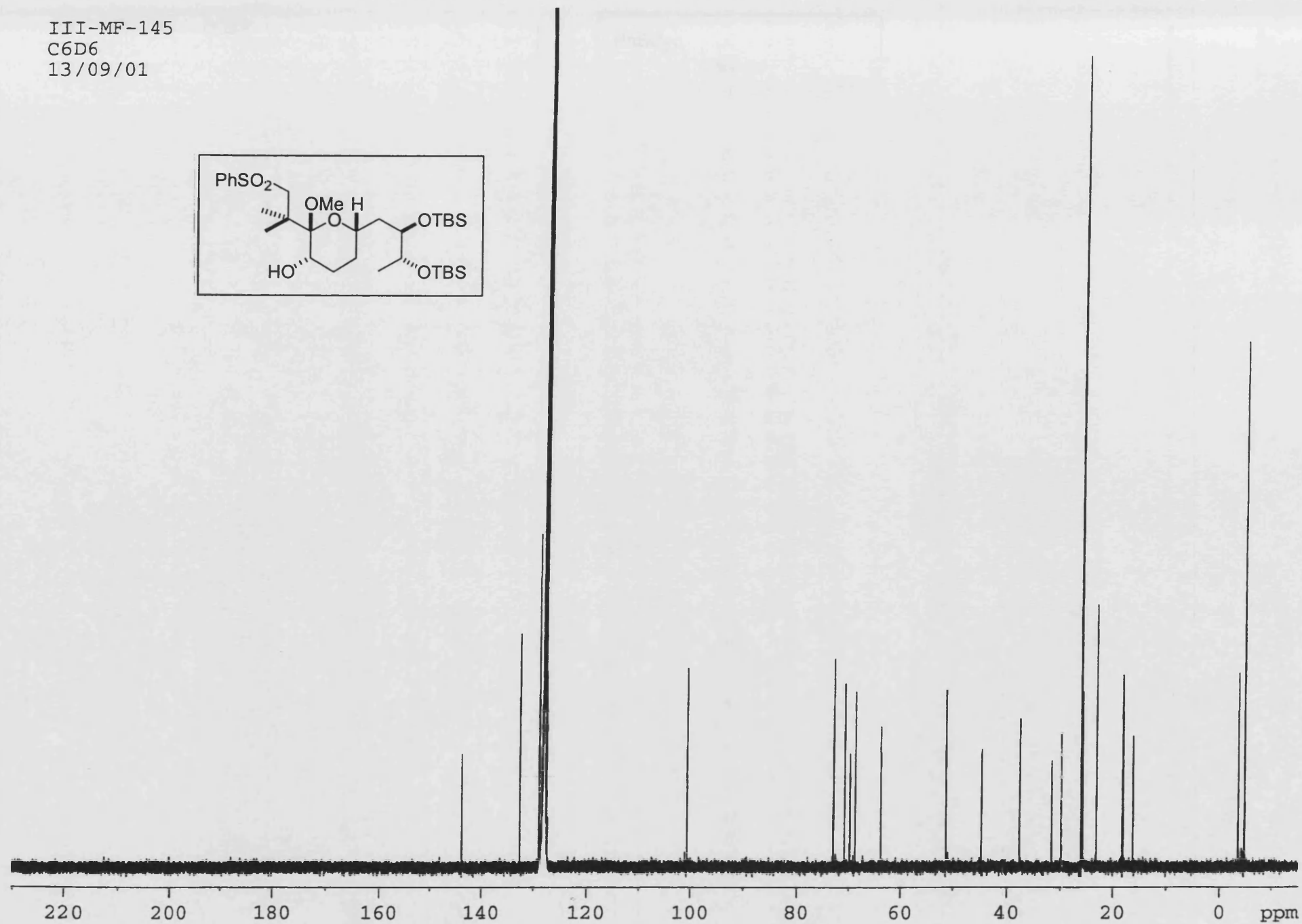
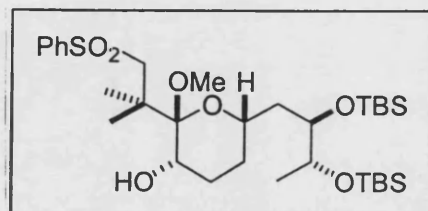
01/09/06 19:48

X: 64 scans, 4.0cm⁻¹, flat

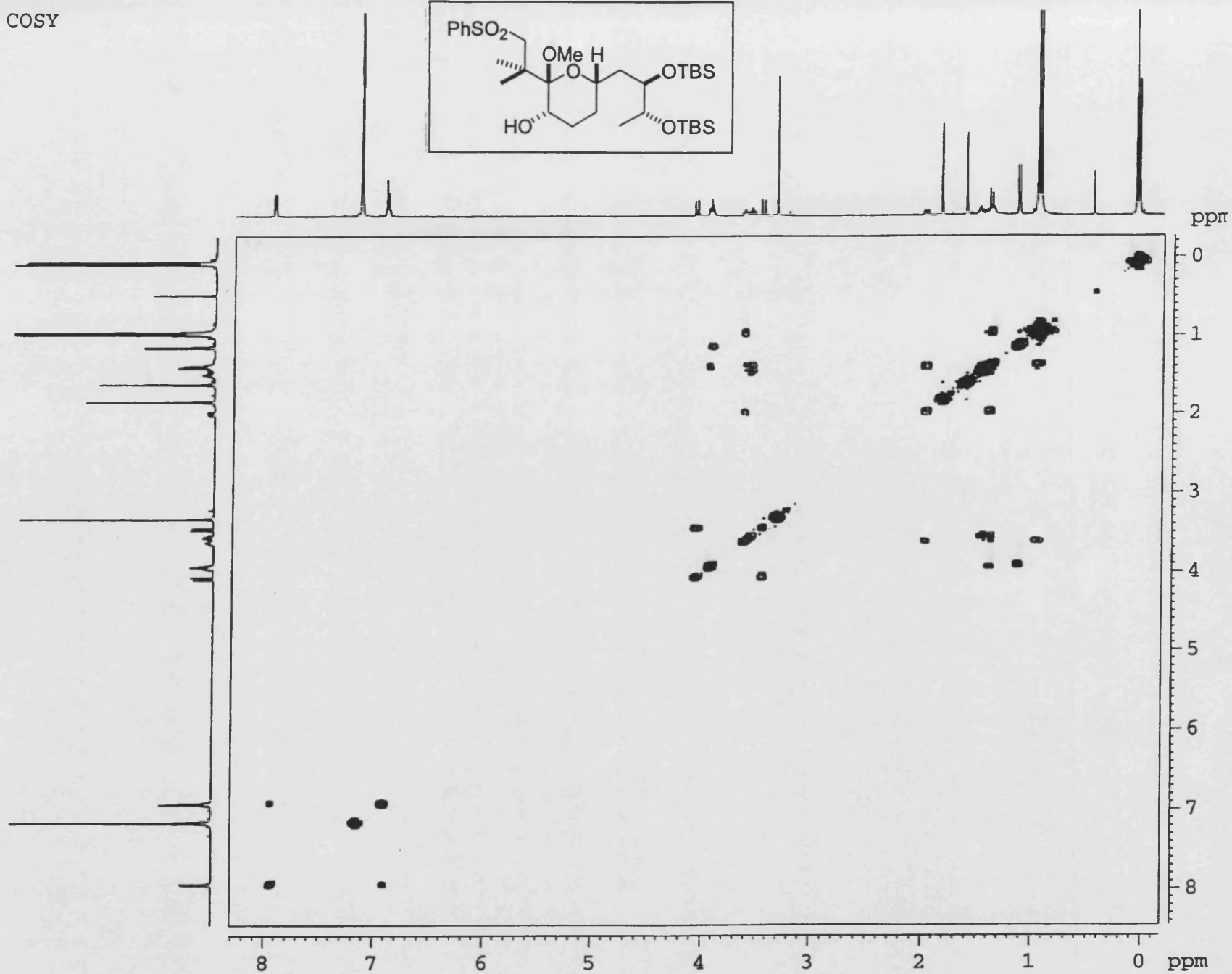
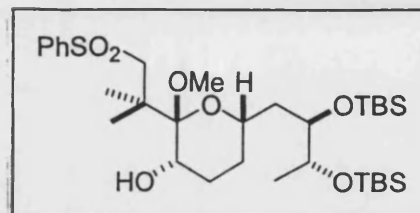
III-MF-145
C6D6
13/09/01



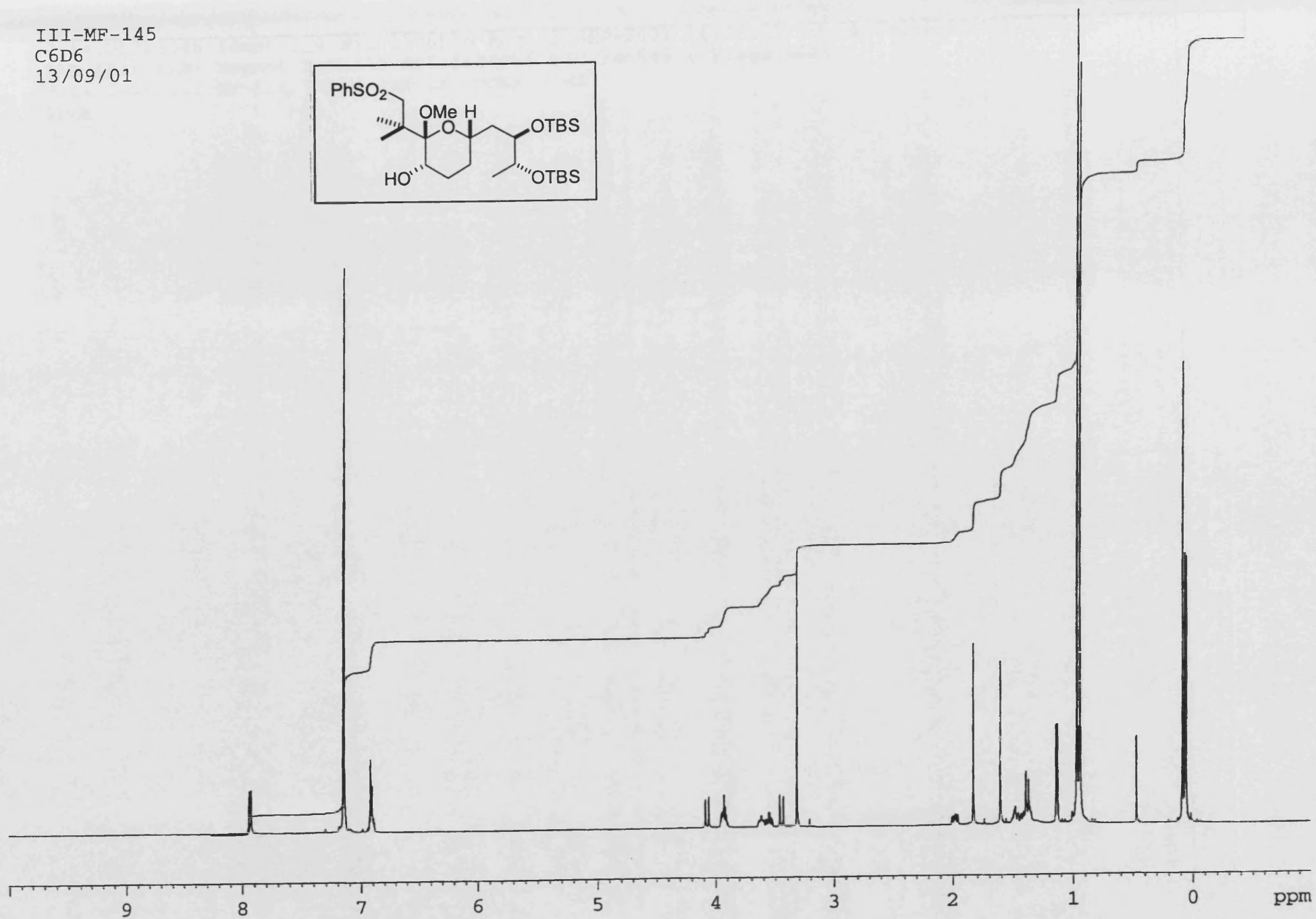
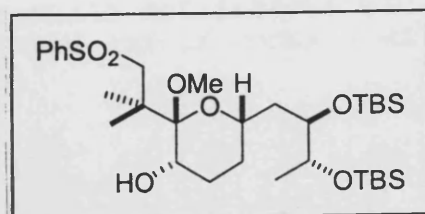
III-MF-145
C6D6
13/09/01



III-MF-145 COSY
C6D6
13/09/01

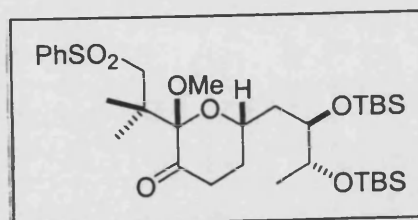


III-MF-145
C6D6
13/09/01



FAB-SEI FAB+ Magnet Spin...
File Text:III-MF-104 FABMS MATRIX MNOBA + NA

Chemical structure inset:

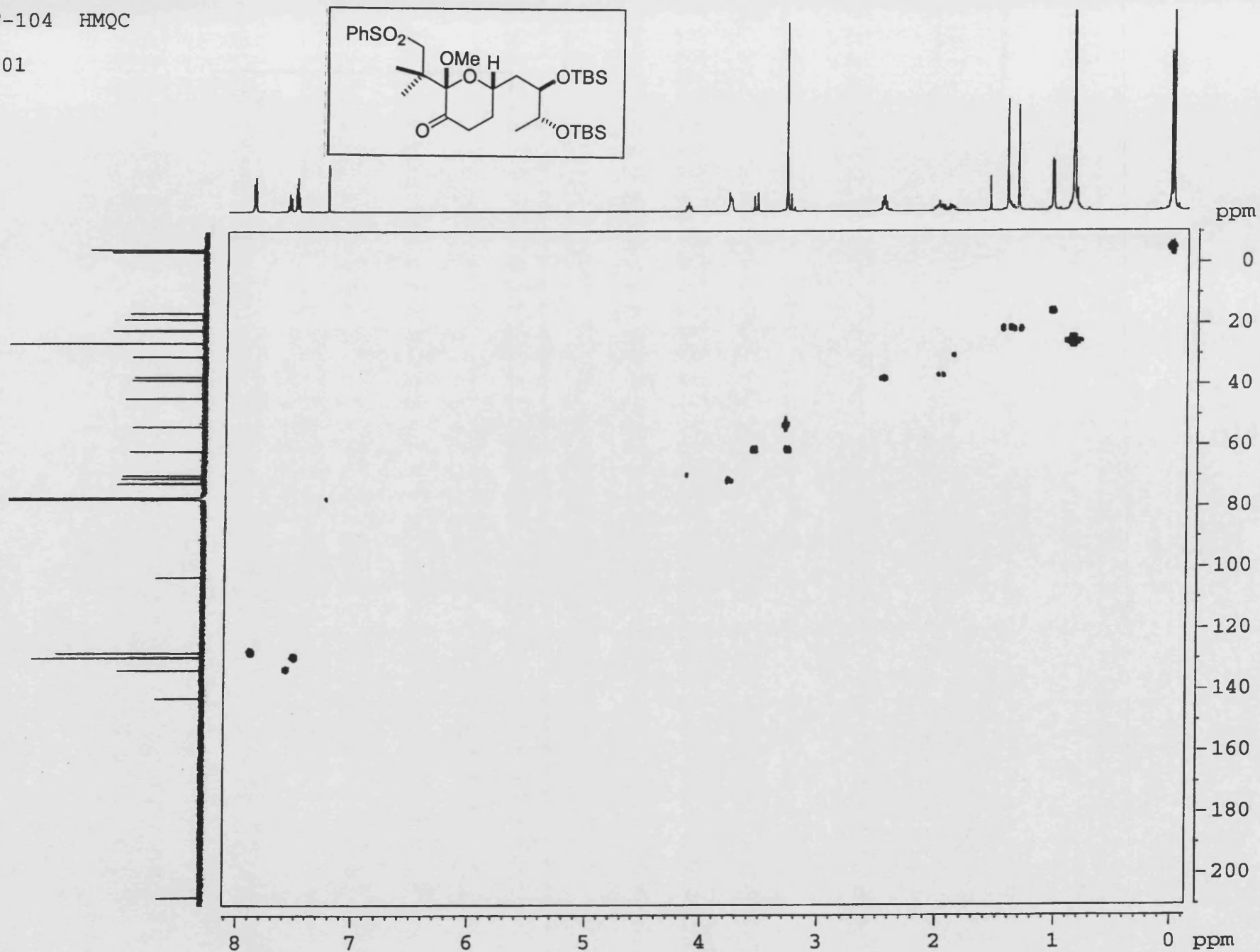
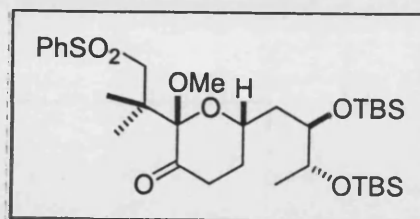
C[C@H](C)[C@@H](CS(=O)(=O)c1ccccc1)C(=O)OC[C@H]1CC[C@@H](C)[C@H](OSi(C)(C)C)O1

IR spectrum of compound **10**. The x-axis represents wavenumber in cm^{-1} (4000 to 1000), and the y-axis represents transmittance (%T). The spectrum shows characteristic absorption bands for the compound, including a strong peak at 1723.8 cm^{-1} (C=O stretch) and a broad peak at 3400 cm^{-1} (O-H stretch). The chemical structure of compound **10** is shown in the inset.

CC(C)(C)OSi(C)(C)C(C)C1OC(C(OC)C1C(C)C(C)OSi(C)(C)C(C)C)C(=O)C(C)C(S(=O)(=O)C2=CC=CC=C2)C

X: 64 scans, 16.0cm⁻¹, apod none, flat

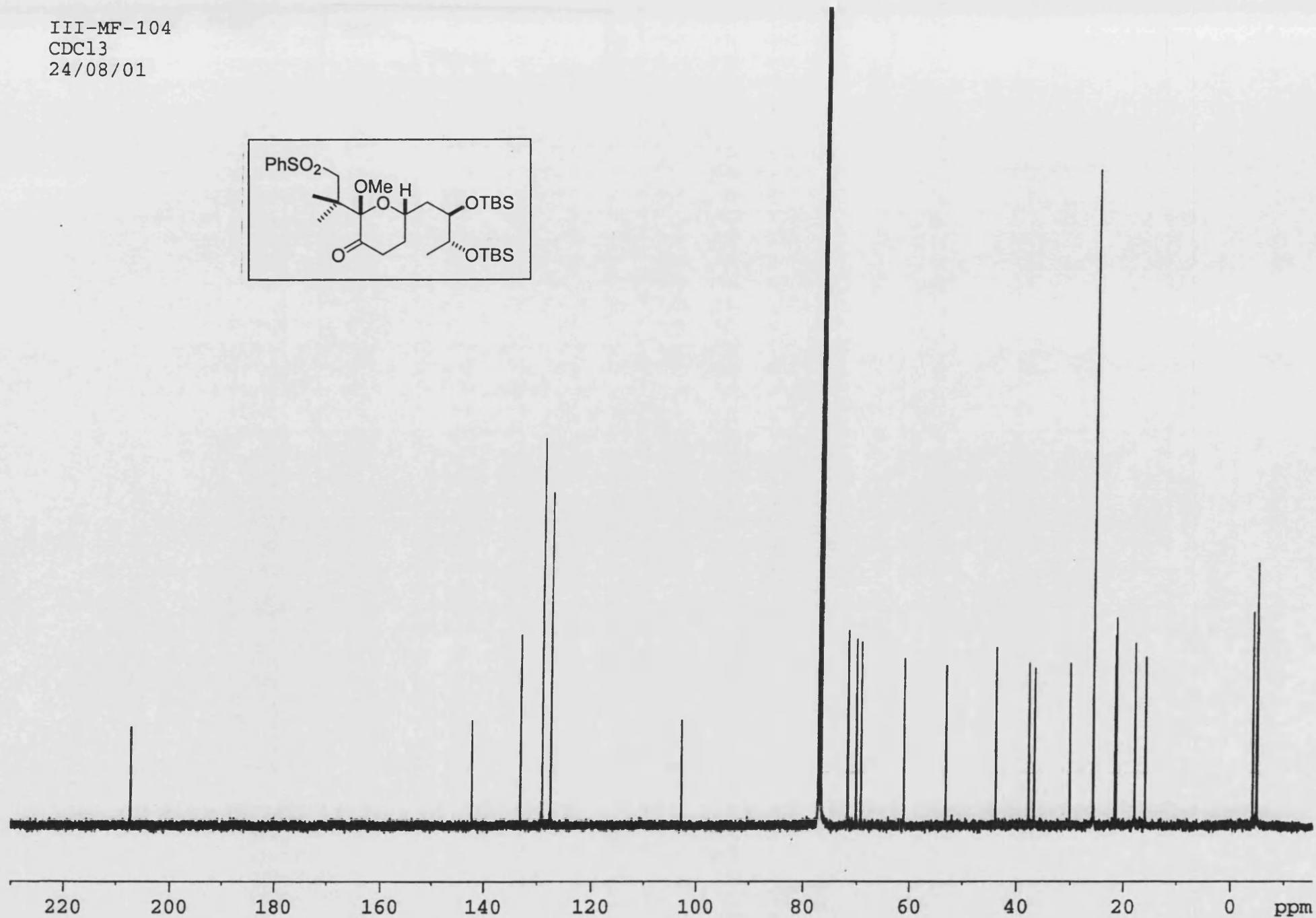
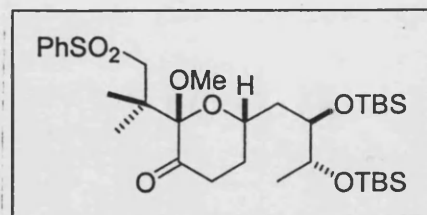
III-MF-104 HMQC
CDCl₃
24/08/01



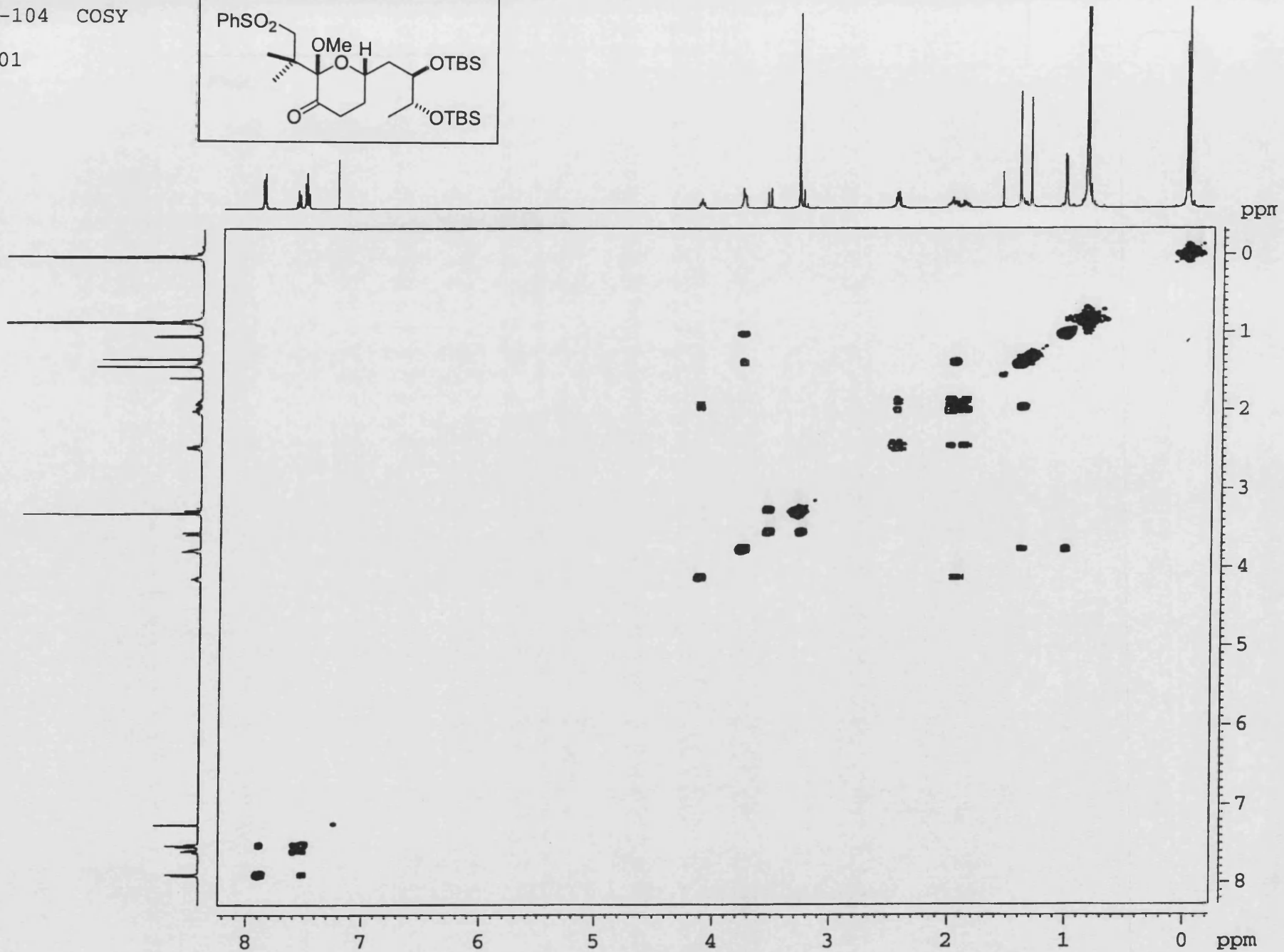
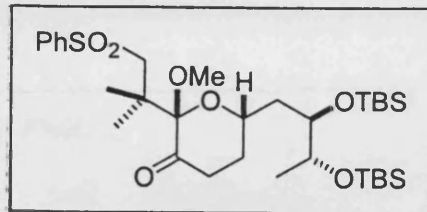
24/08/01



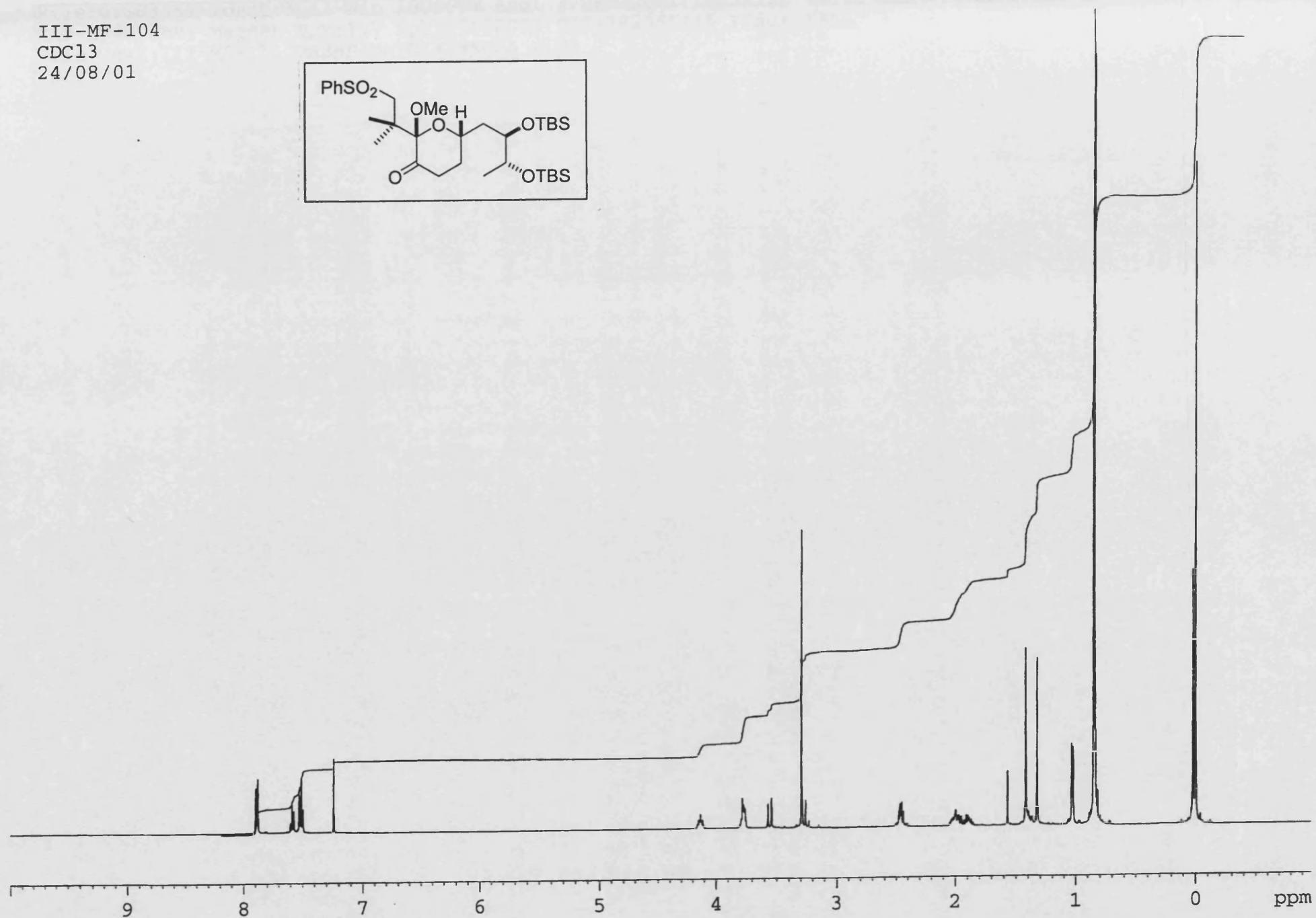
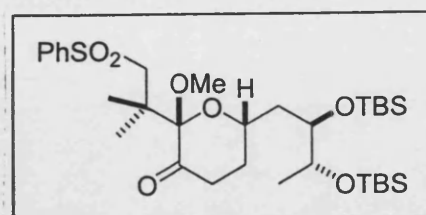
III-MF-104
CDC13
24/08/01

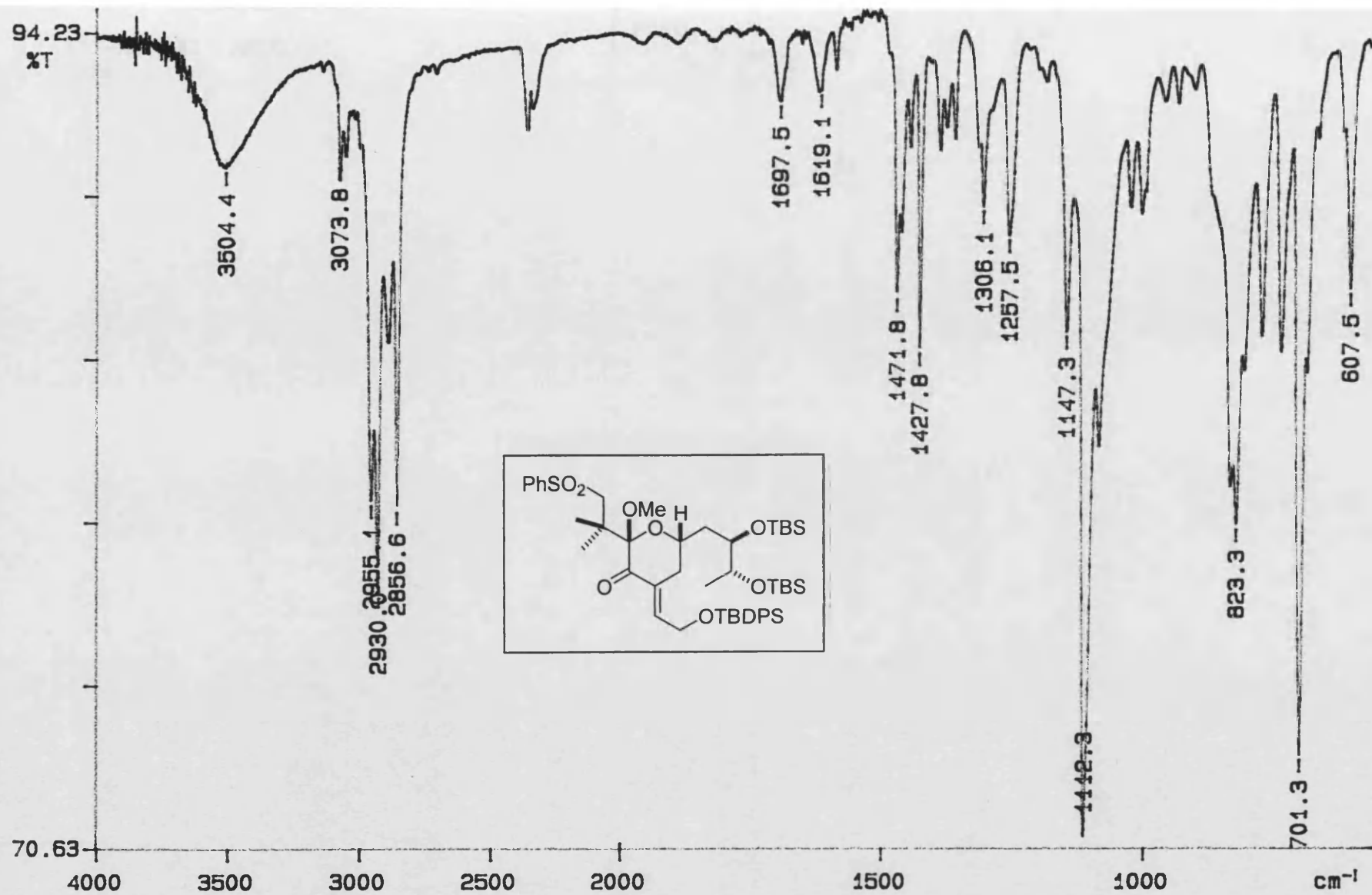


III-MF-104 COSY
CDC13
24/08/01



III-MF-104
CDC13
24/08/01

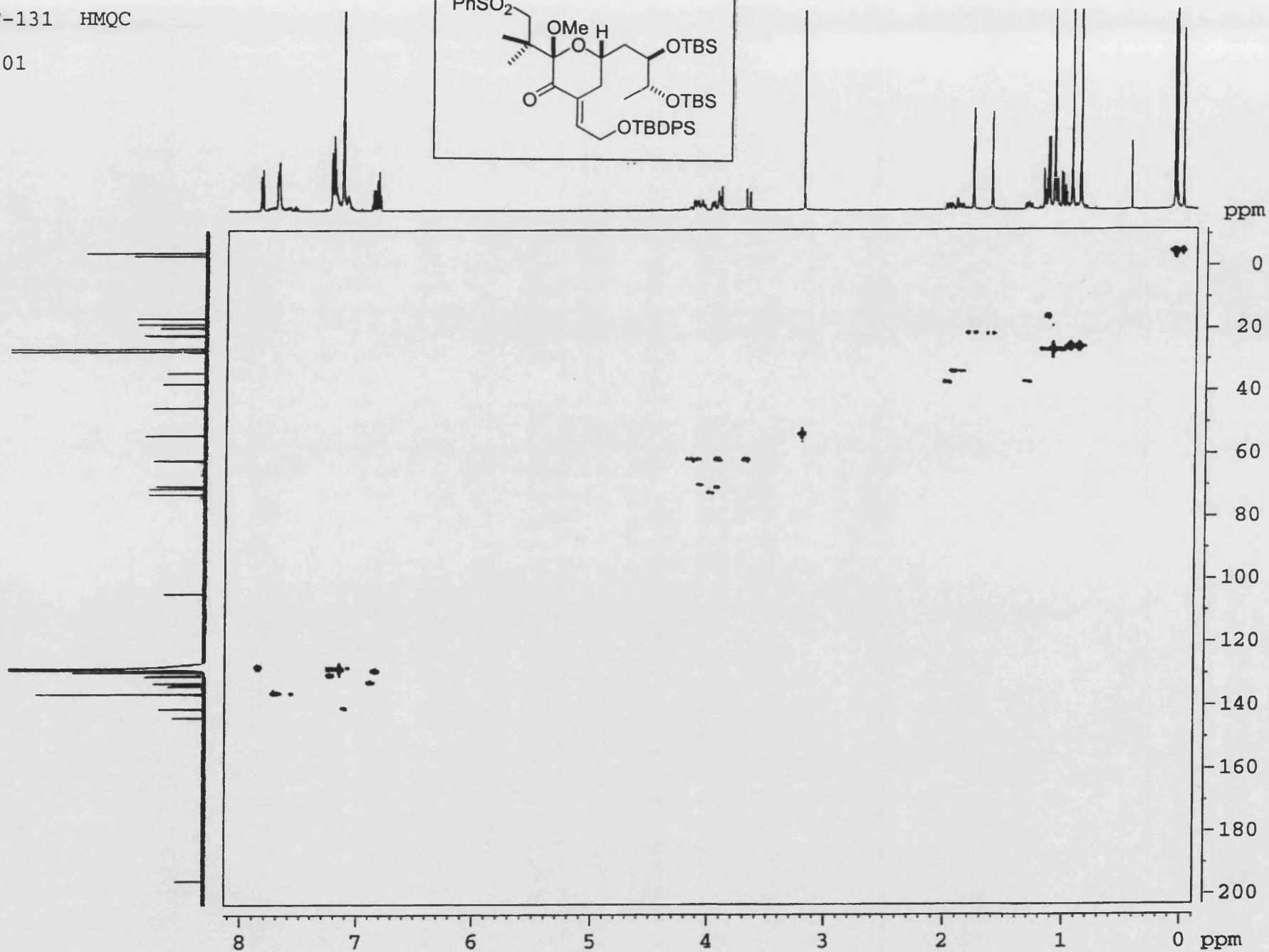
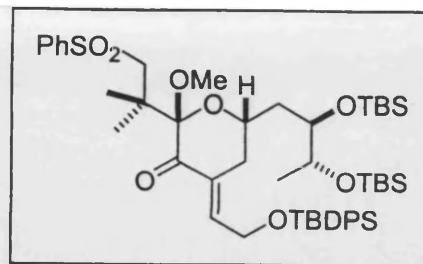




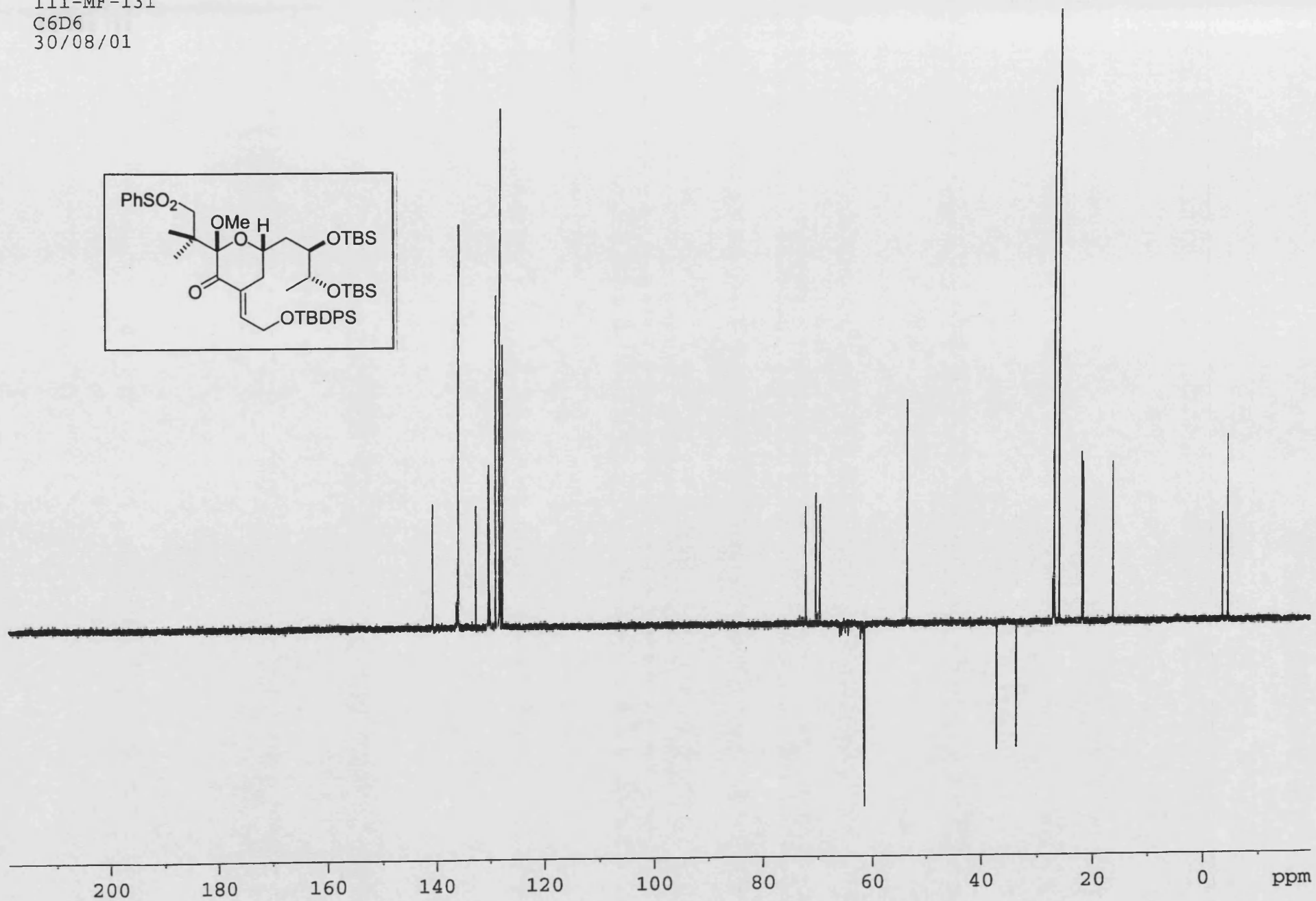
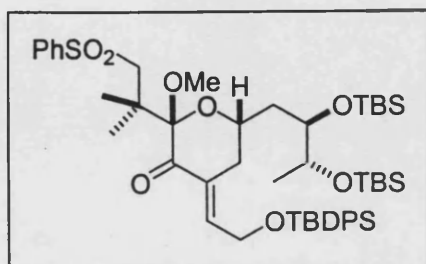
02/04/23 16: 47

Y: 64 scans, 4.0cm⁻¹, flat

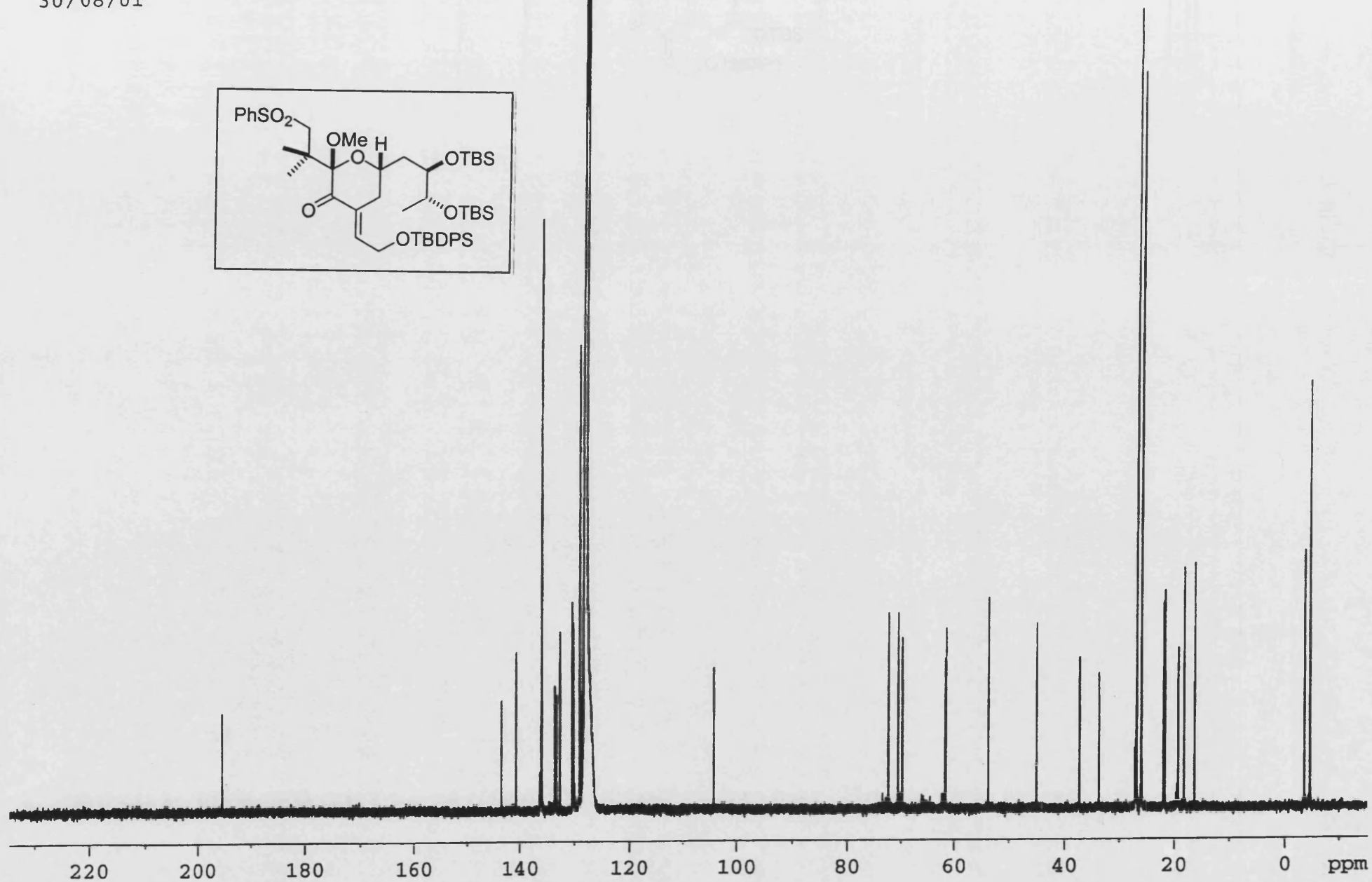
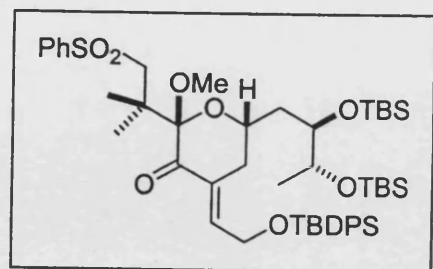
III-MF-131 HMQC
C6D6
30/08/01



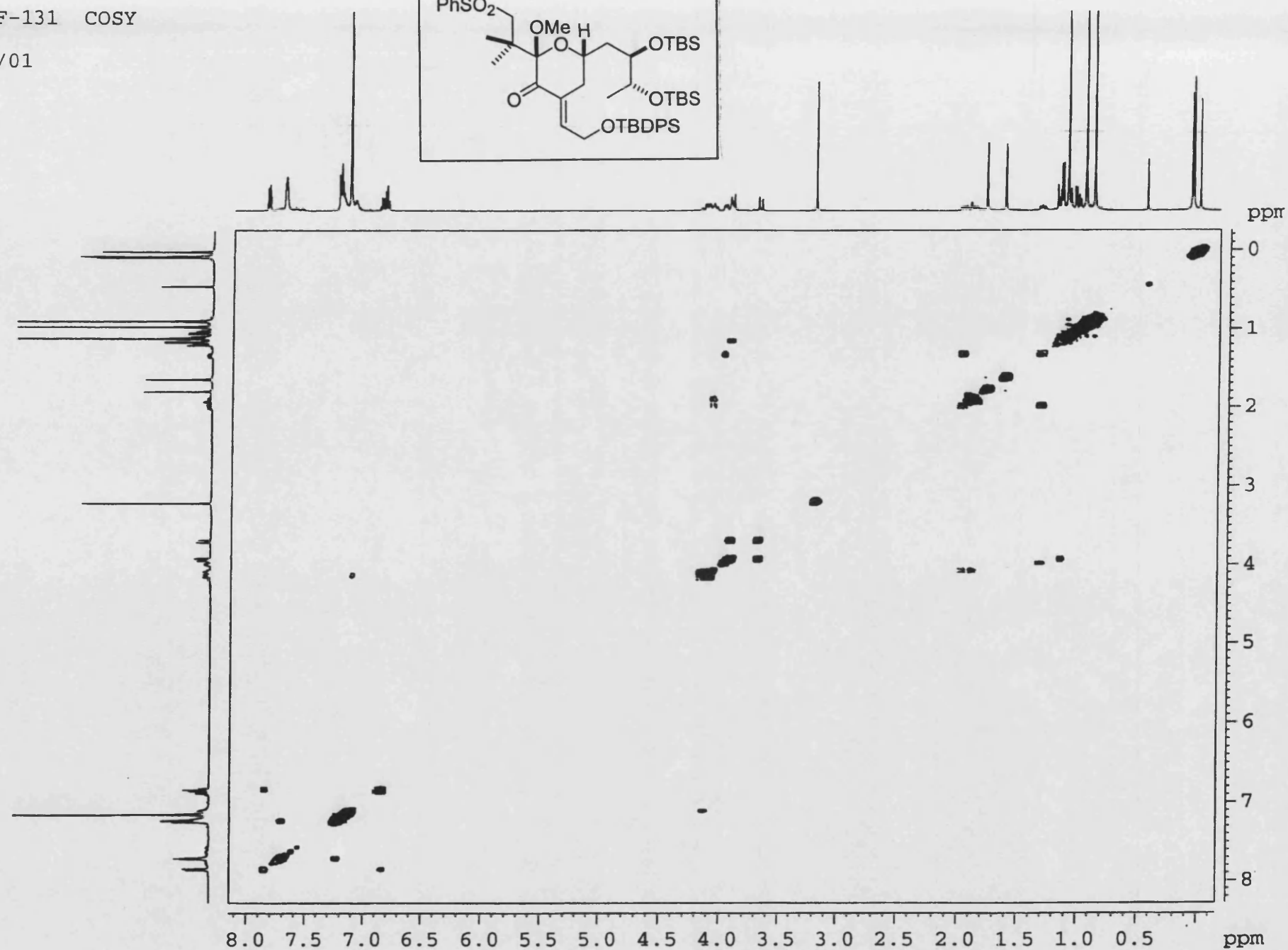
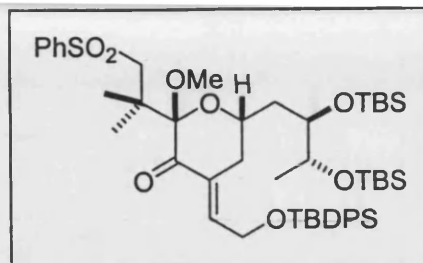
III-MF-131
C6D6
30/08/01



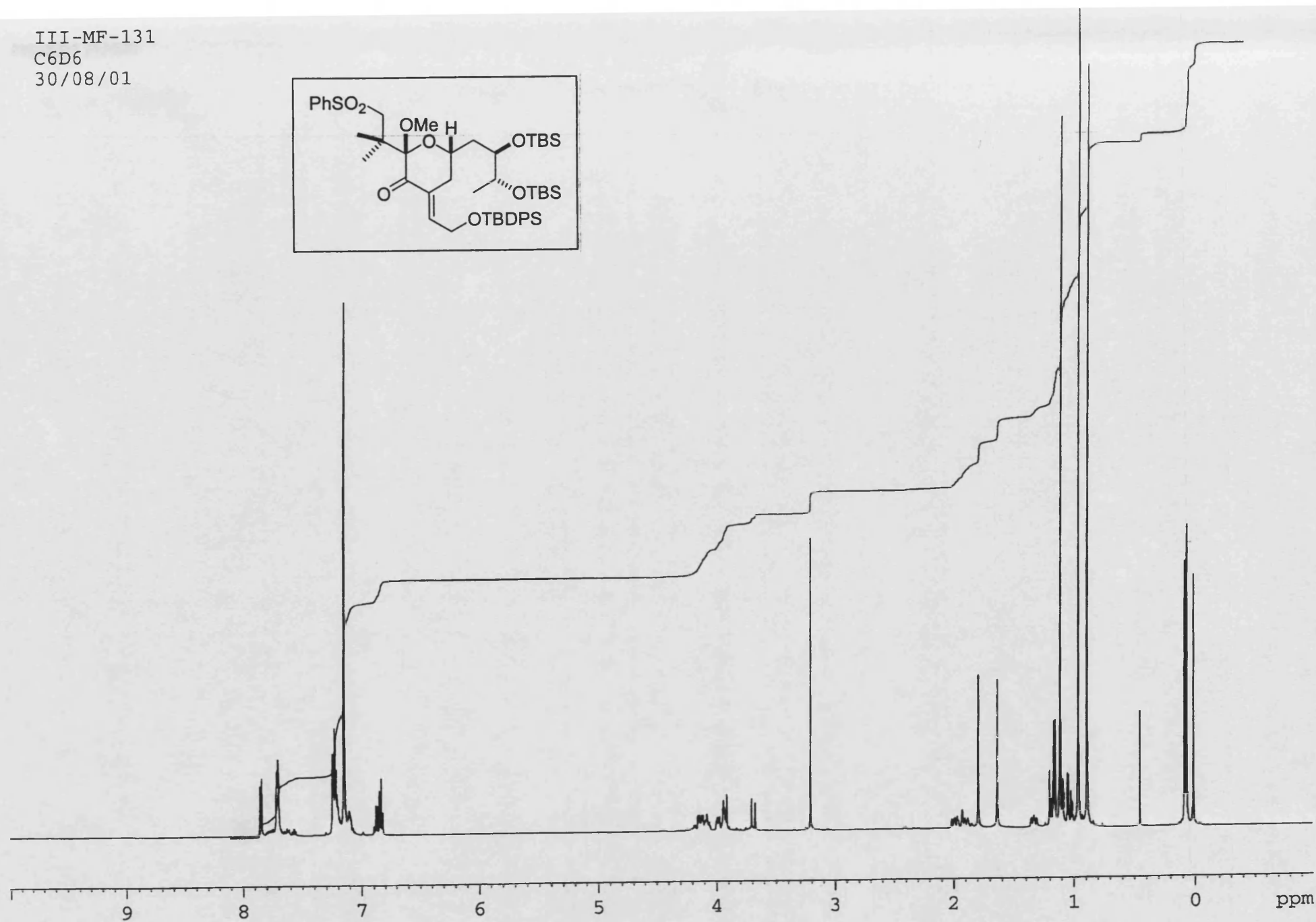
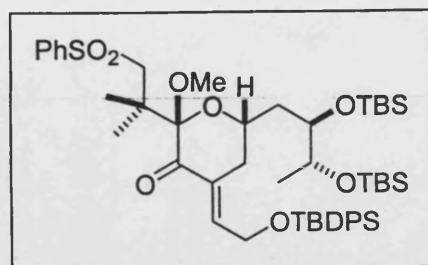
III-MF-131
C6D6
30/08/01



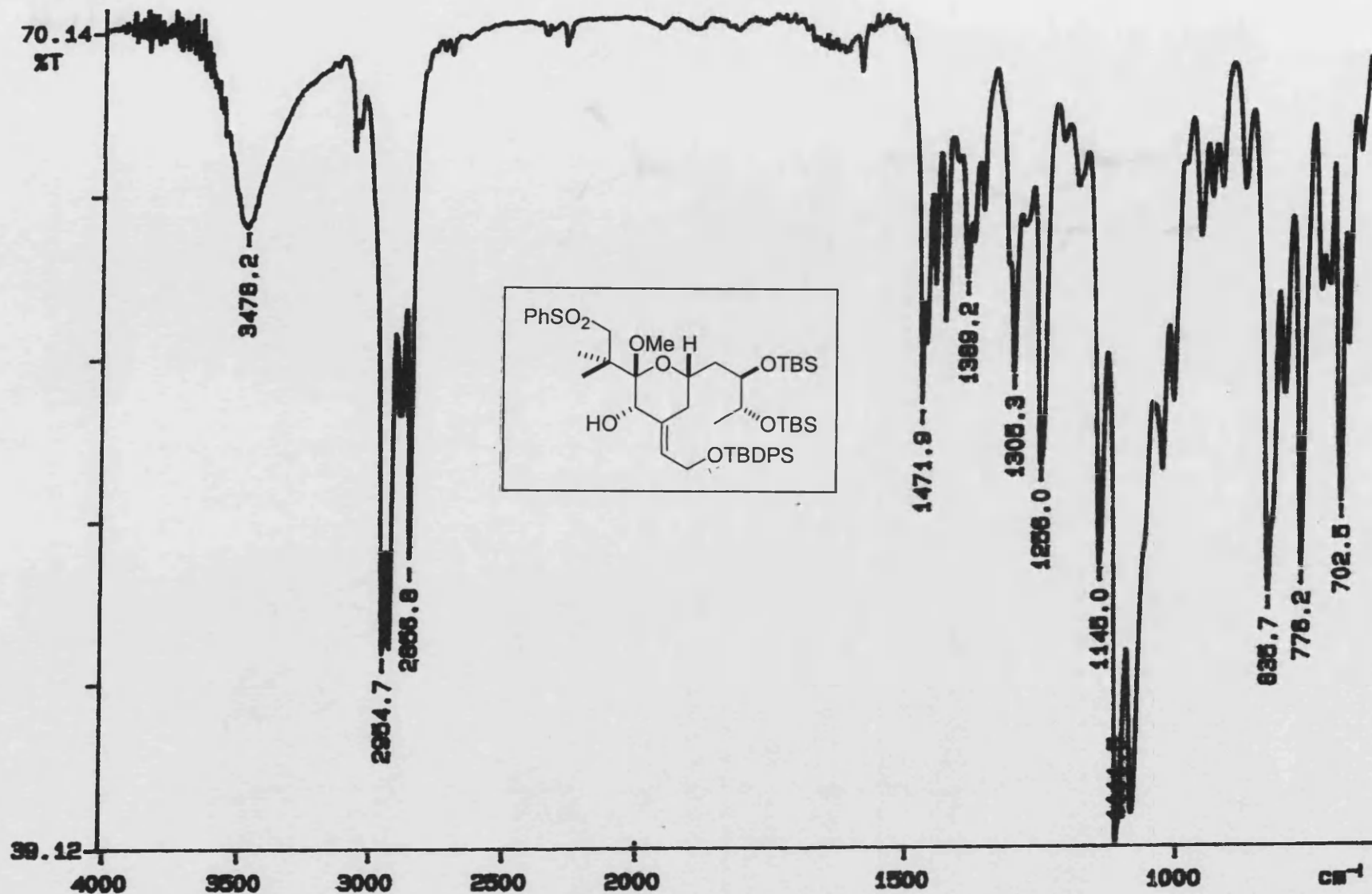
III-MF-131 COSY
C6D6
30/08/01



III-MF-131
C6D6
30/08/01



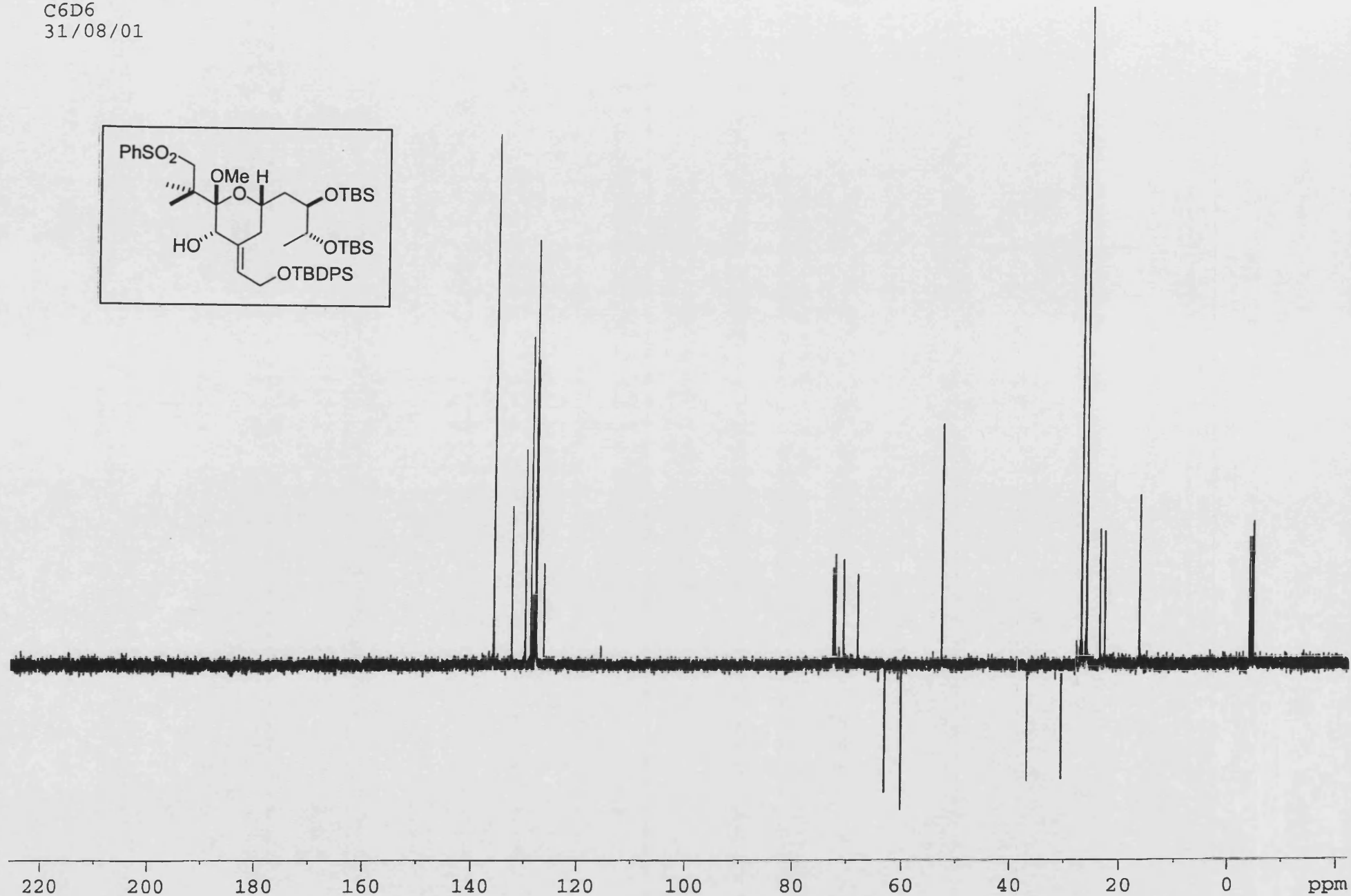
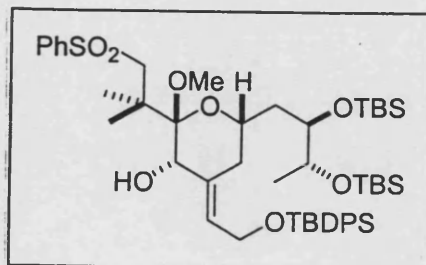
PERKIN ELMER



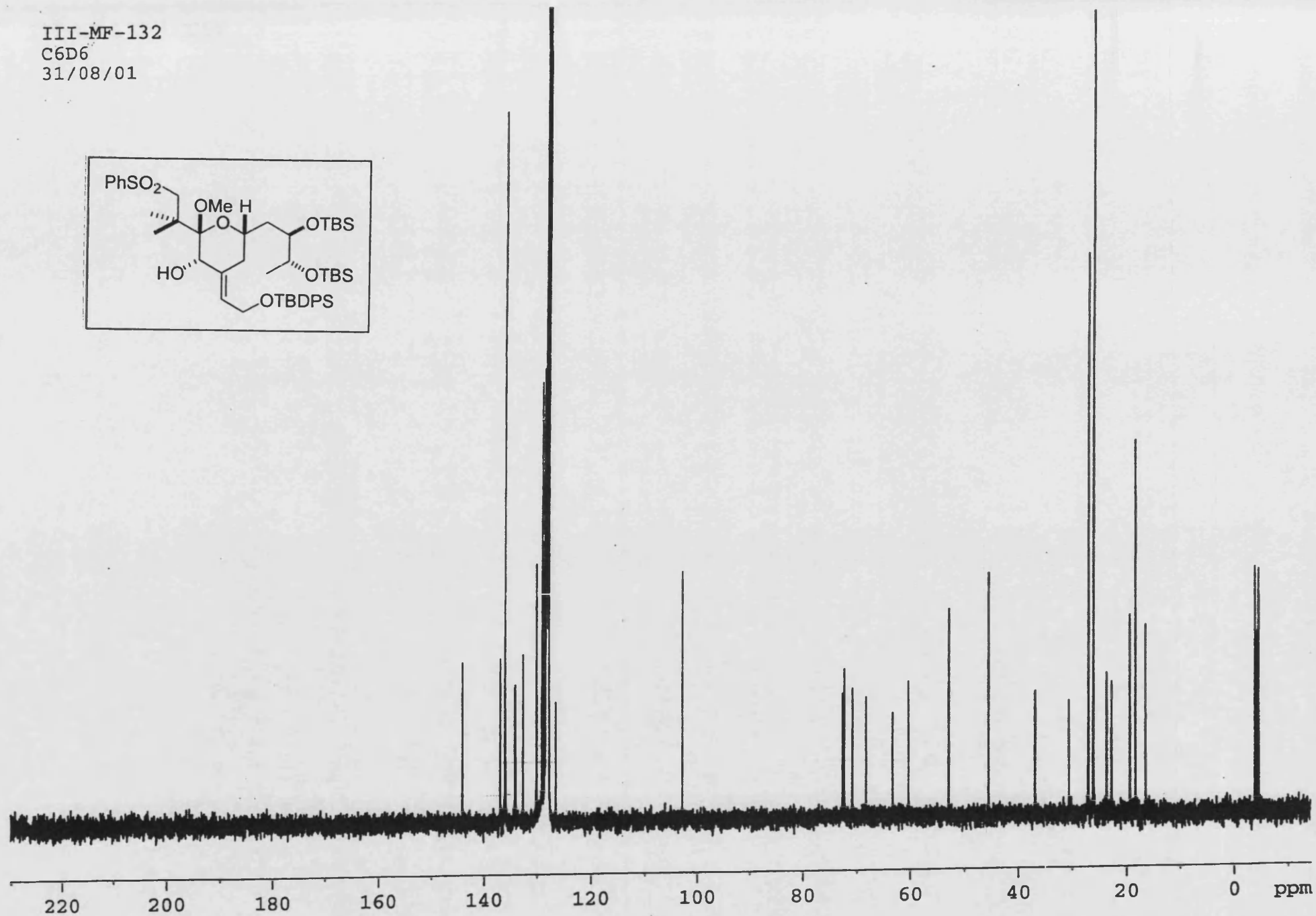
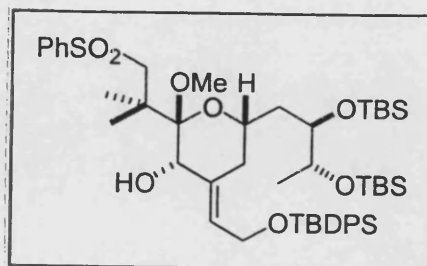
01/08/31 15:49

X: 64 scans, 4.0cm⁻¹, flat

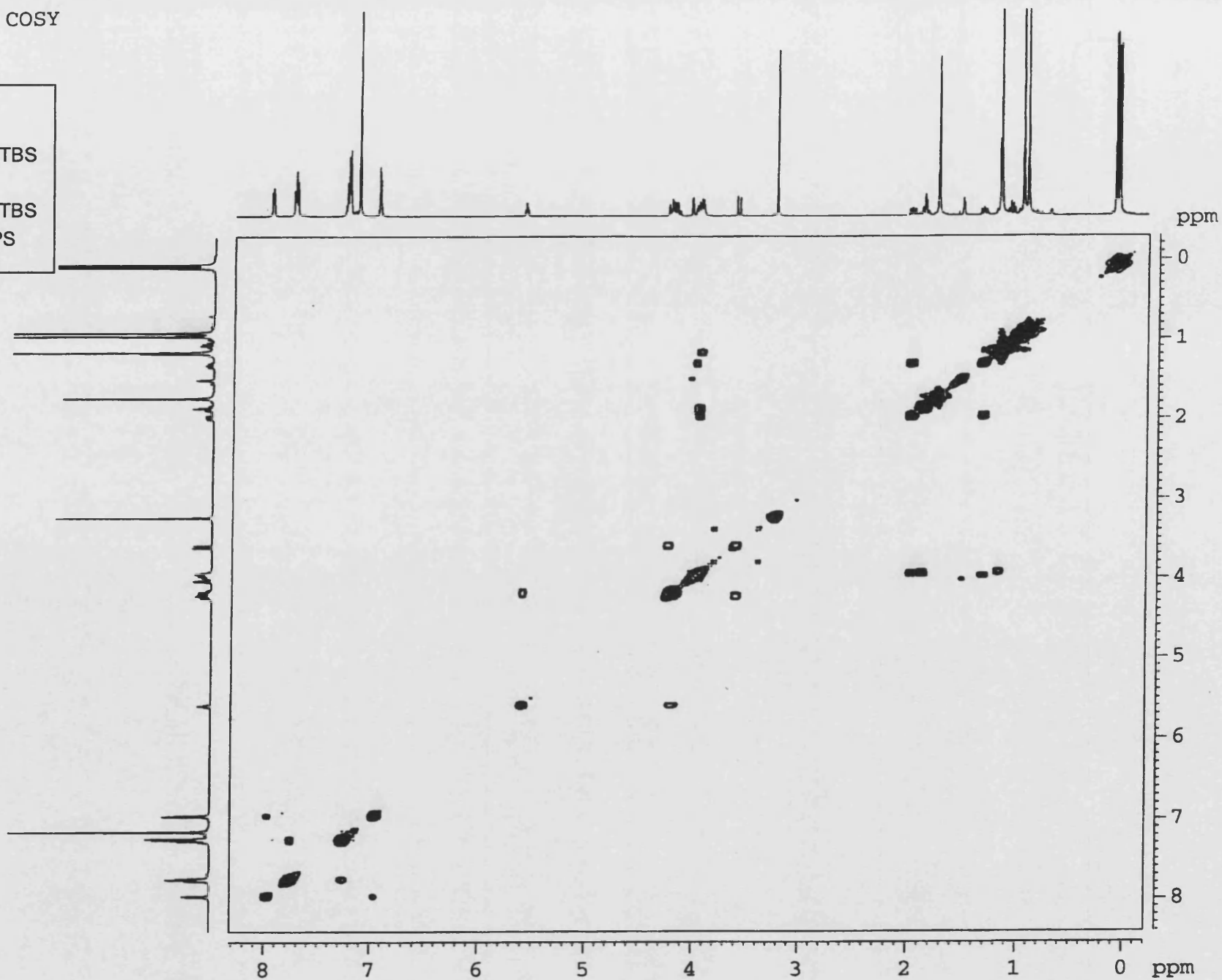
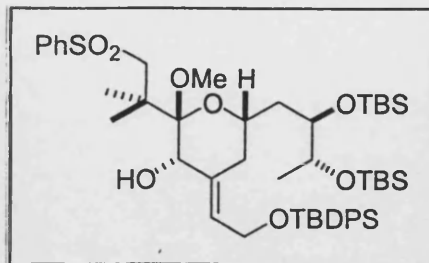
III-MF-132
C6D6
31/08/01



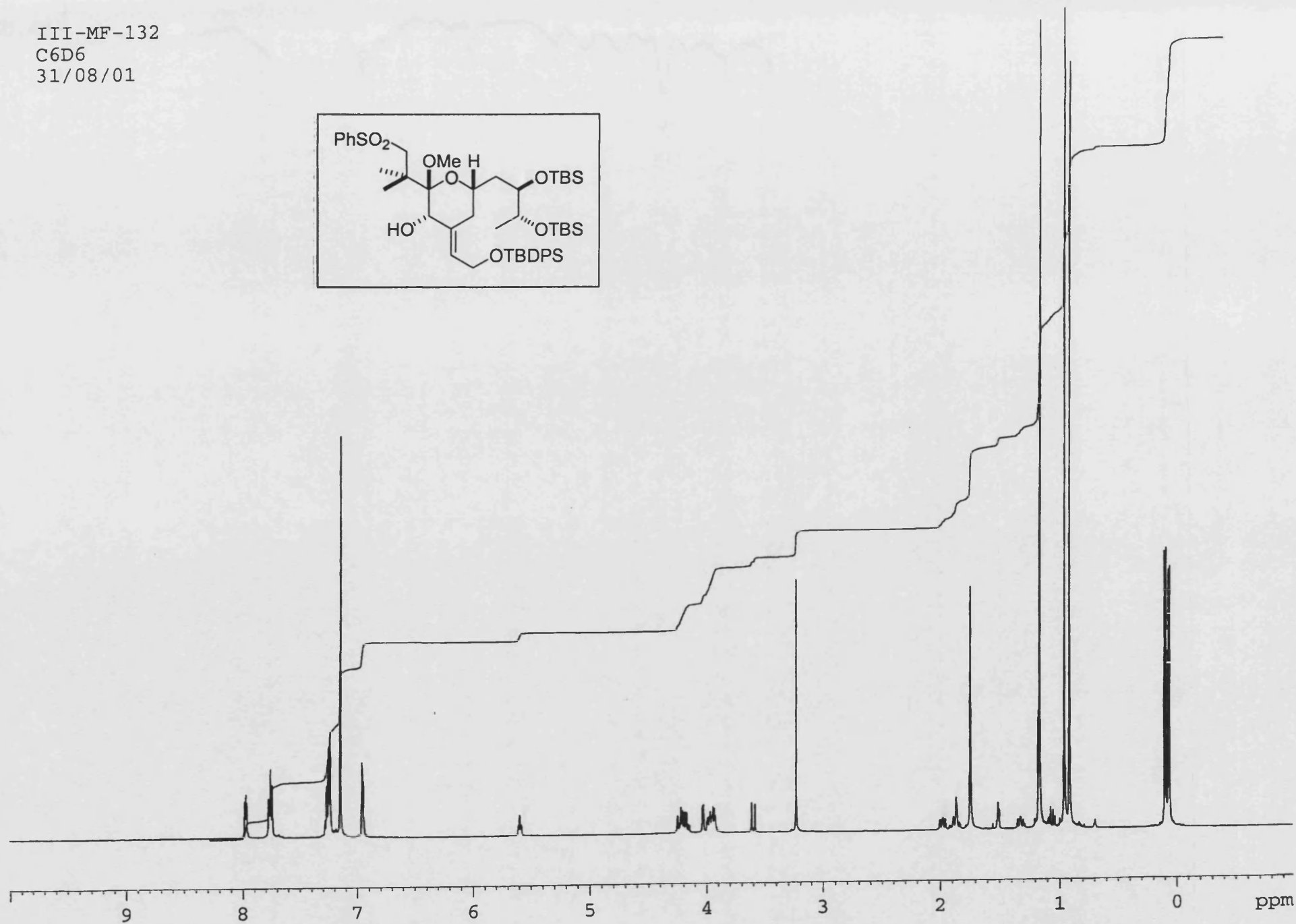
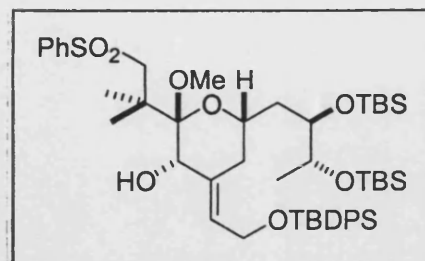
III-MF-132
C6D6
31/08/01

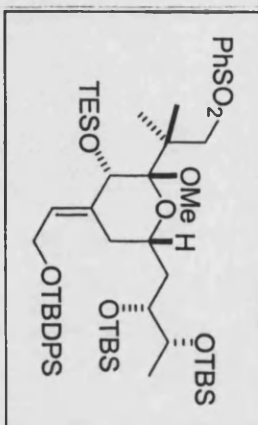


III-MF-132 COSY
C6D6
31/08/01



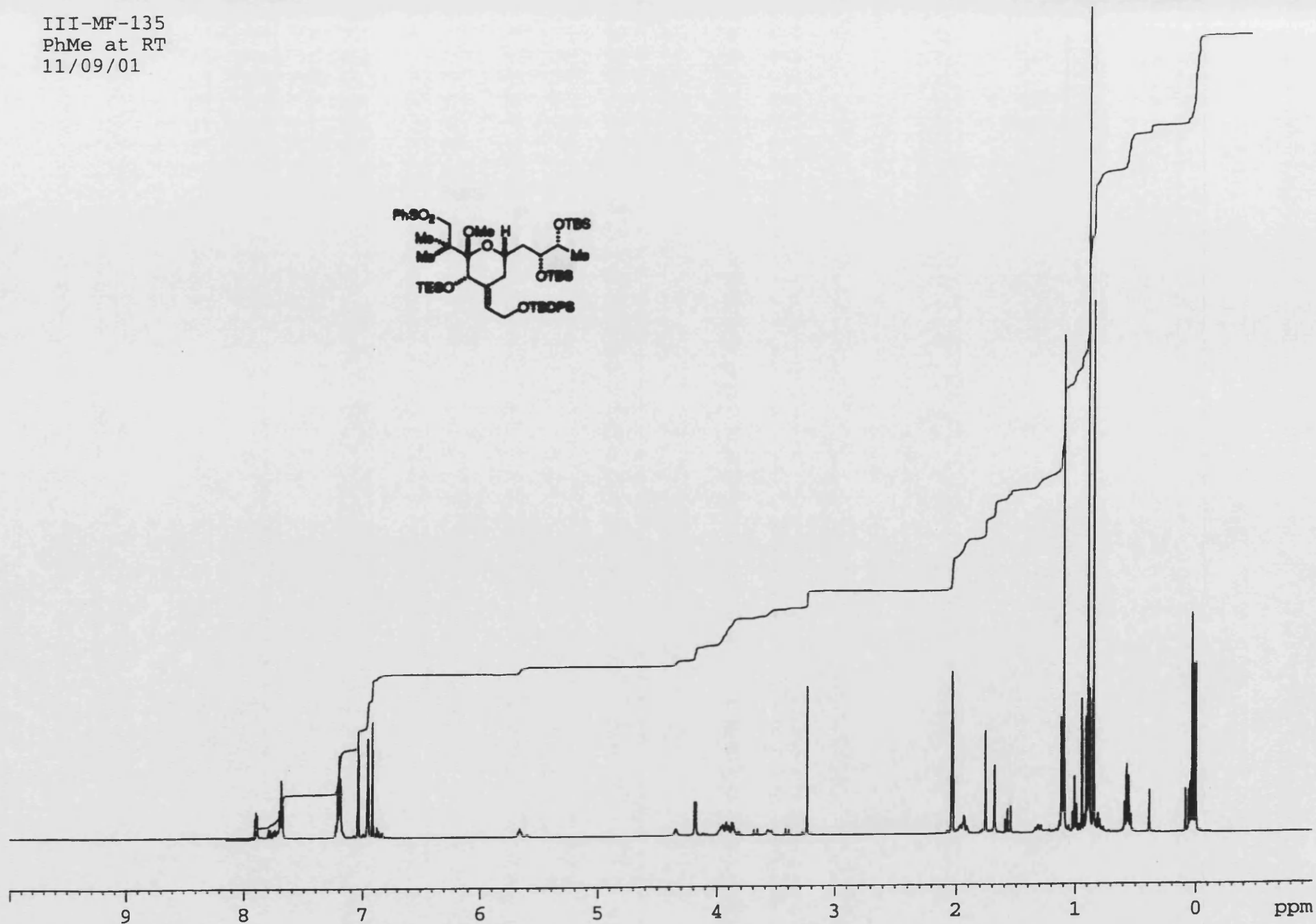
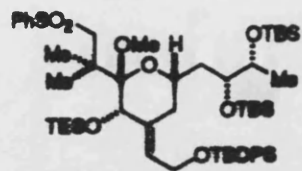
III-MF-132
C6D6
31/08/01



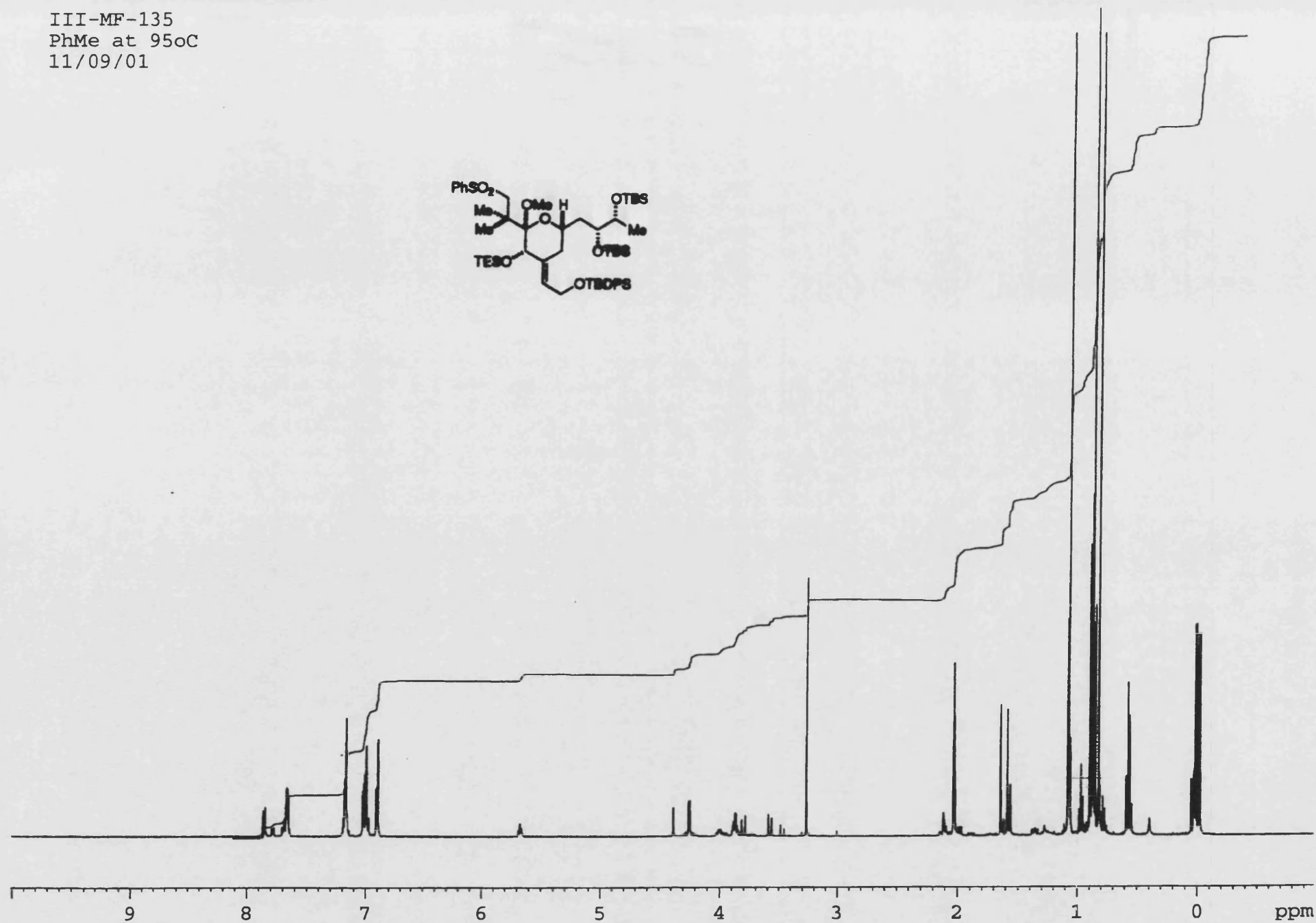
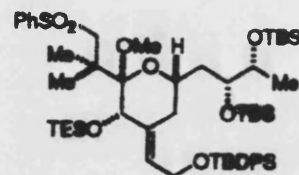


7.35

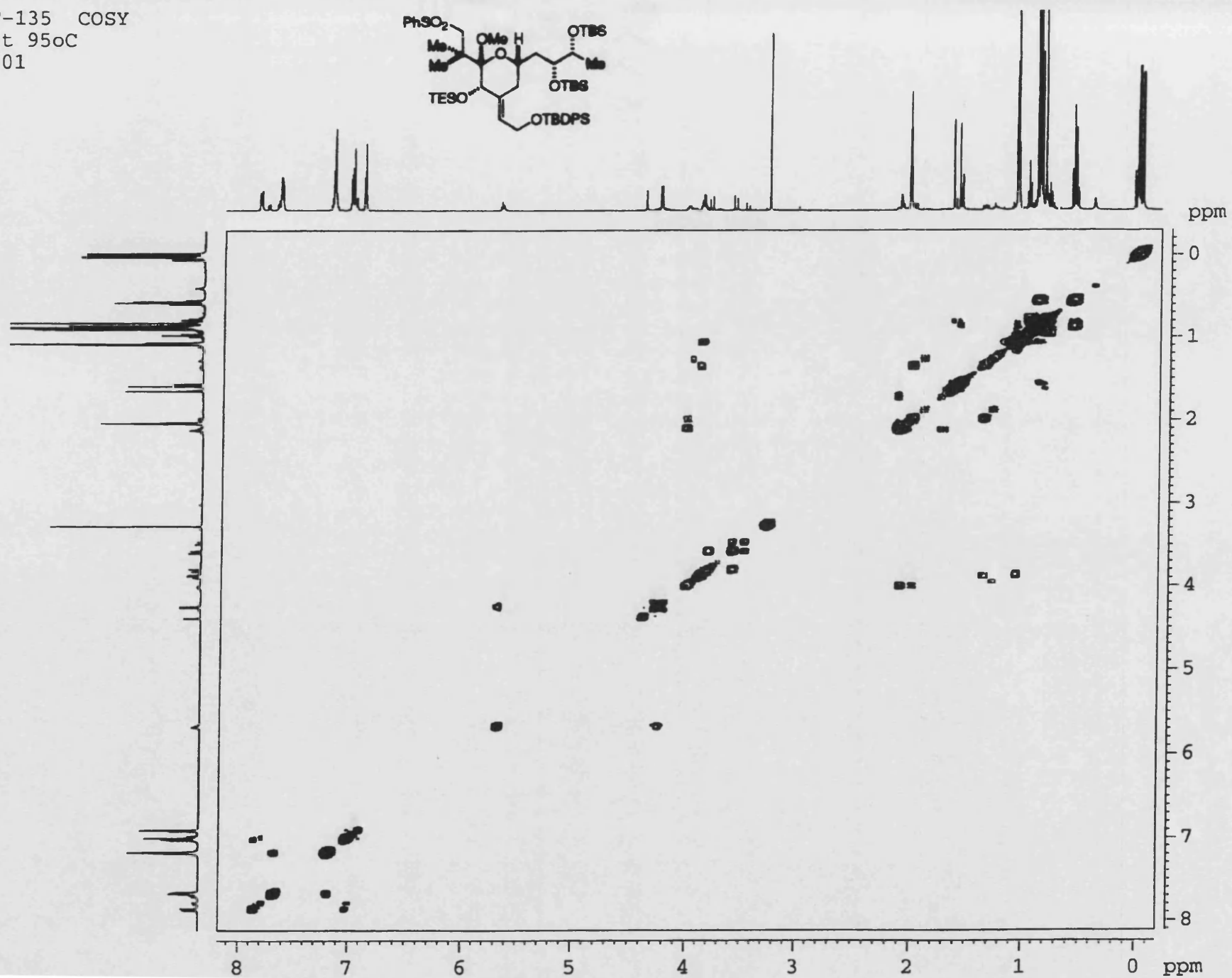
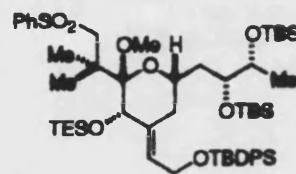
III-MF-135
PhMe at RT
11/09/01



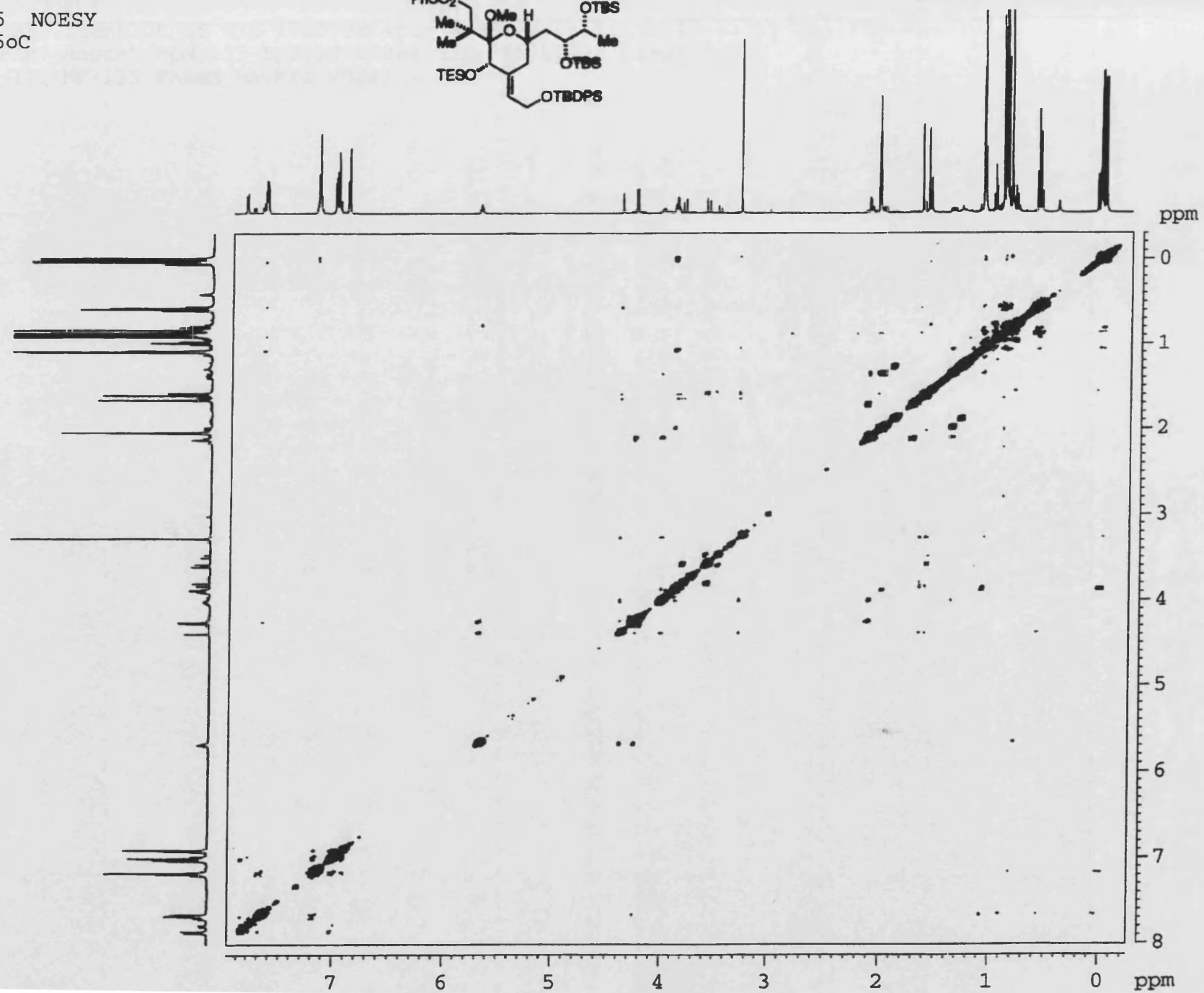
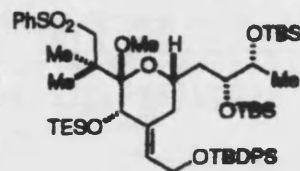
III-MF-135
PhMe at 95oC
11/09/01



III-MF-135 COSY
PhMe at 95oC
11/09/01



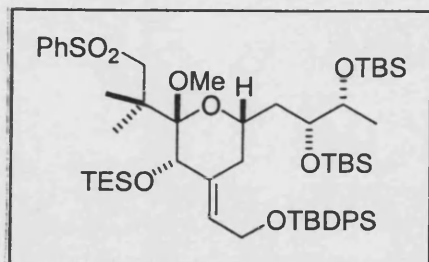
III-MF-135 NOESY
PhMe at 95oC
11/09/01



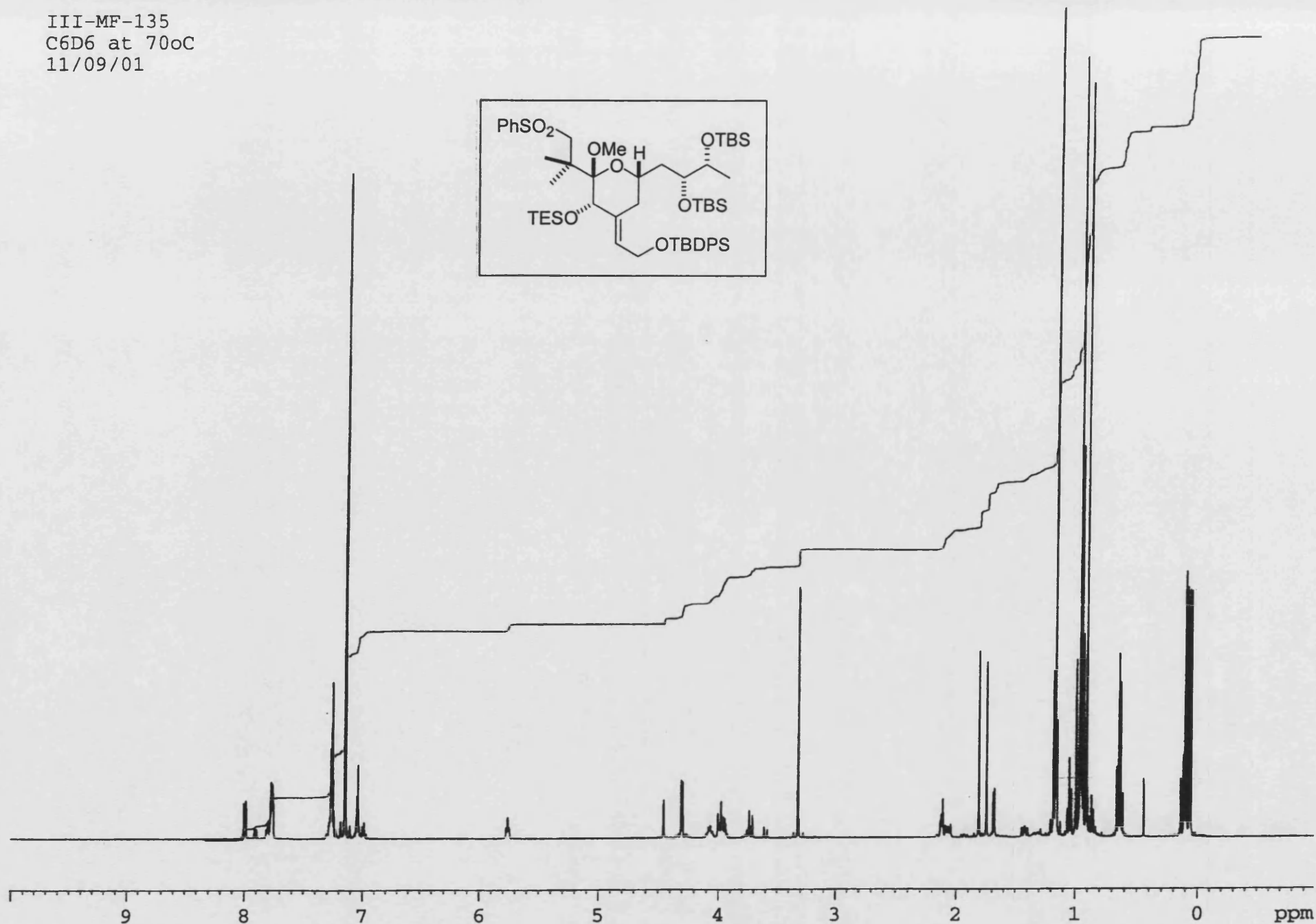
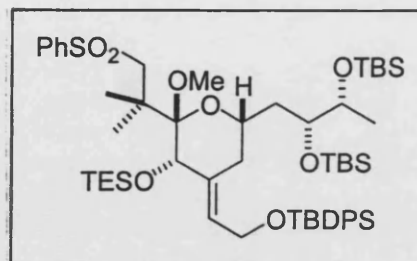
File Text:III-MF-135 FAB/MS MATRIX MNOBA + NA

Chemical structure of compound 11b is shown in the inset. The structure is a complex polycyclic molecule, likely a steroid derivative, featuring several functional groups and protecting groups: a phenylsulfonyl (PhSO₂) group, a methoxy (OMe) group, a tert-butyldimethylsilyl (TBS) ether (OTBS), a triethylsilyl (TES) ether (TESO), and a tert-butyldiphenylsilyl (OTBDPS) ether.

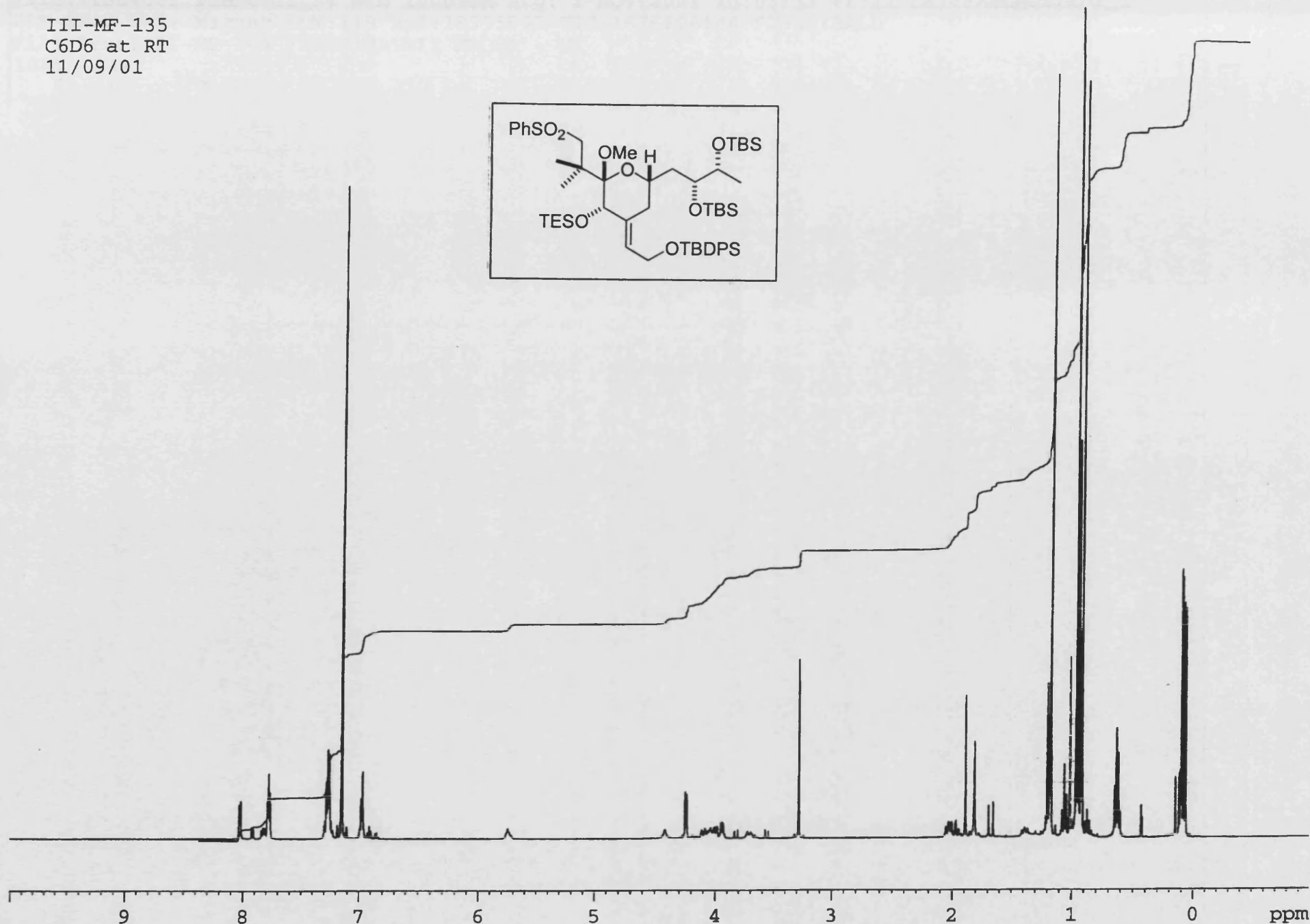
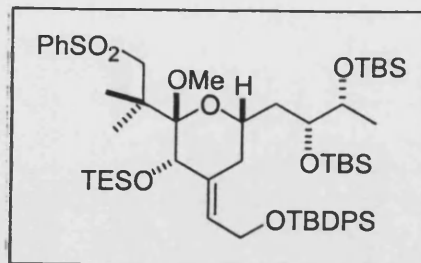
m/z	Relative Intensity (%)
419	25
453	12
473	8
523	6
571	4
619	5
652	12
693	4
752	10
783	45
810	2
876	3
949	2
1005	32
1039	2
1061	1
1138	38
1171	100
1195	2
1260	1



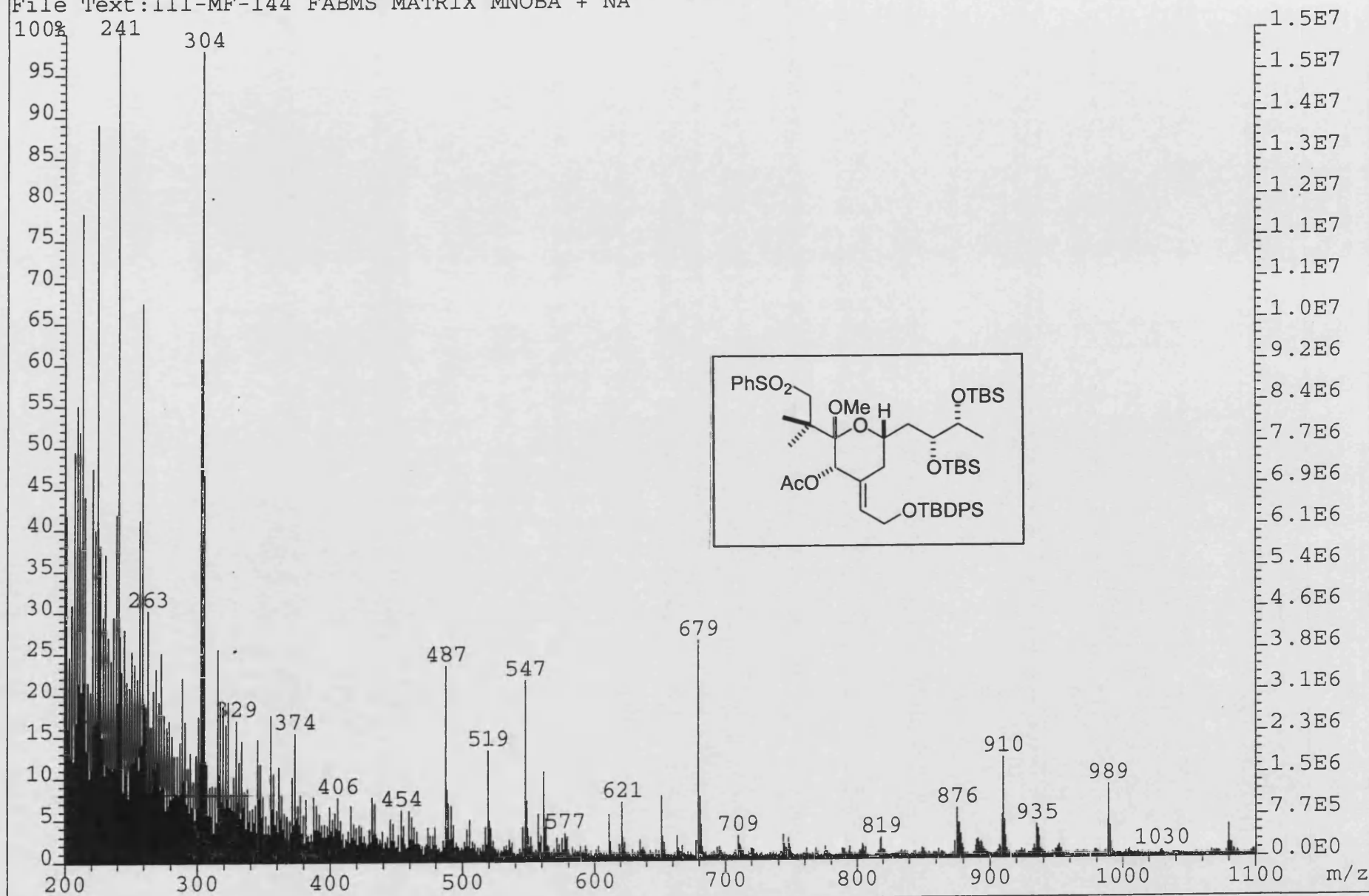
III-MF-135
C6D6 at 70oC
11/09/01

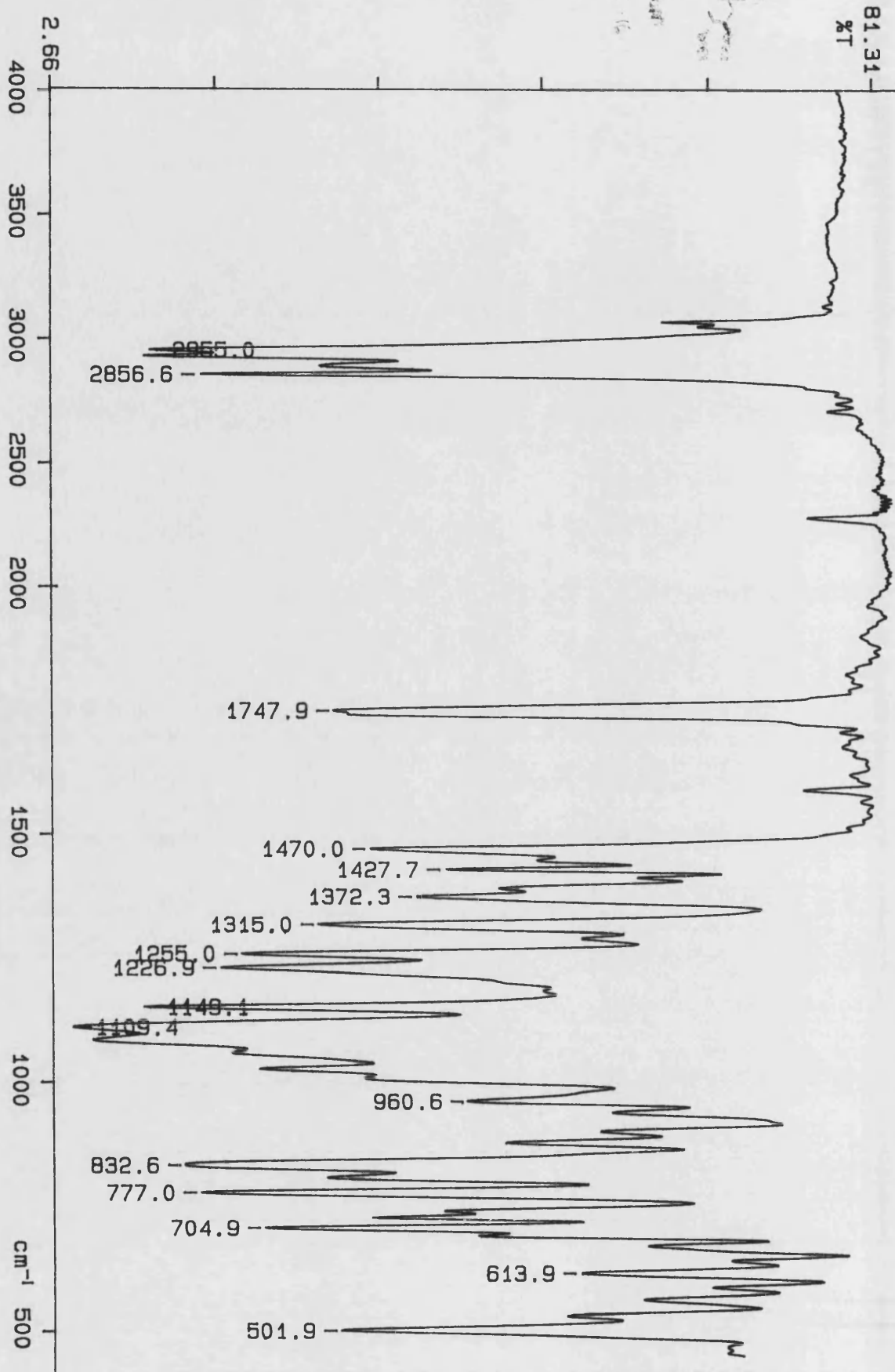


III-MF-135
C6D6 at RT
11/09/01

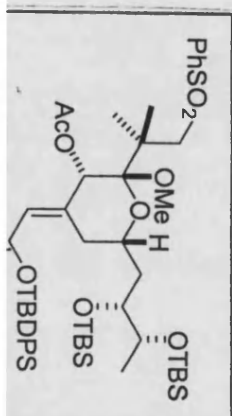


File:01SE4061 Ident:11_34 Win 1000PPM Acq: 1-NOV-2001 10:03:33 +1:11 Cal:FABLM011101_1
ZAB-SE4F FAB+ Magnet BpM:119 BpI:18995542 TIC:1675206144 Flags:HALL
File Text:III-MF-144 FABMS MATRIX MNOBA + NA

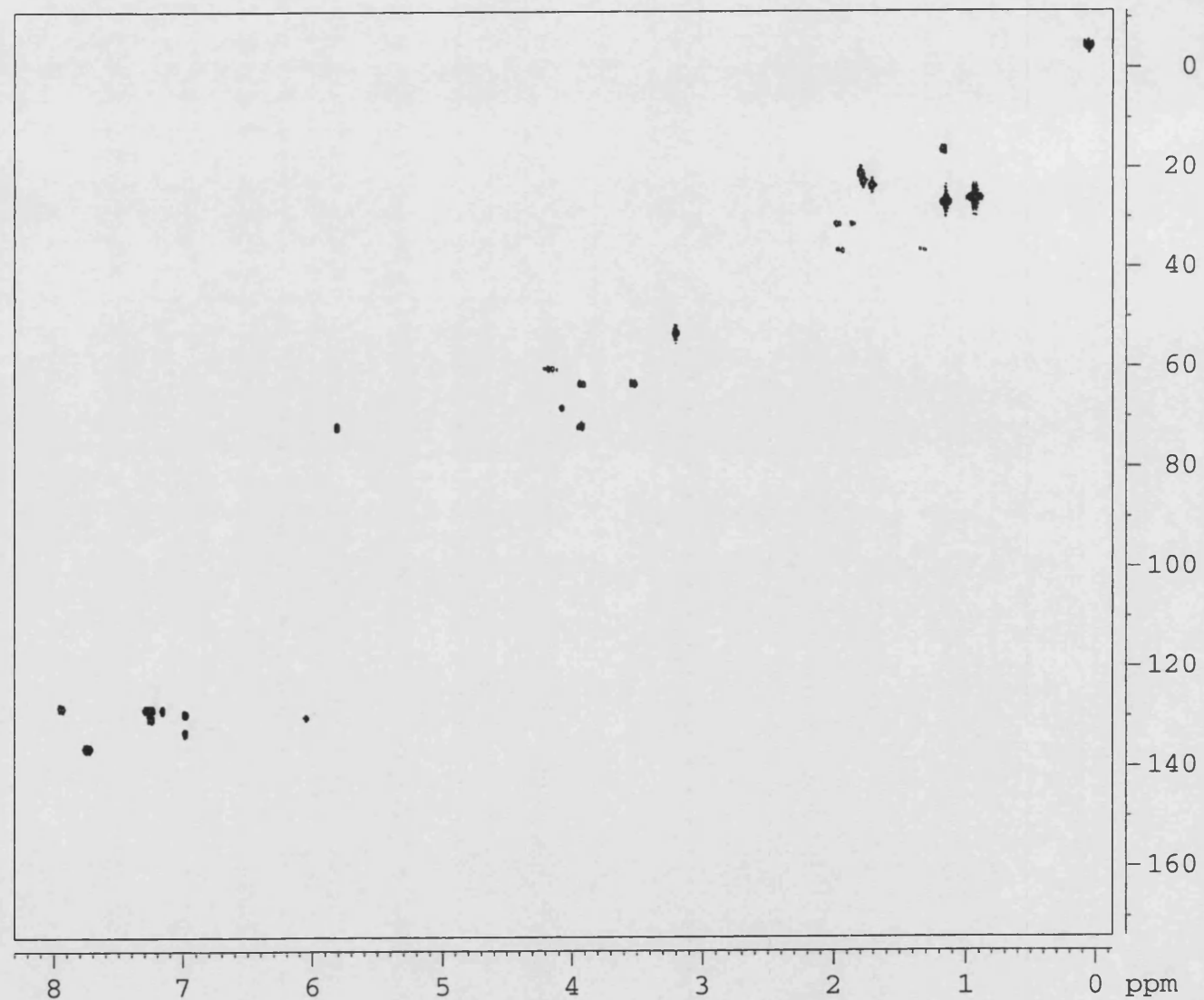
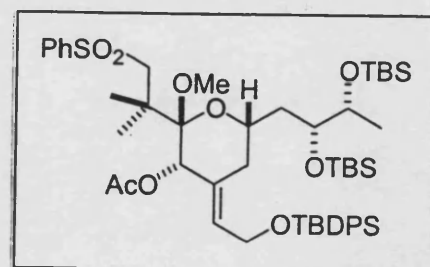




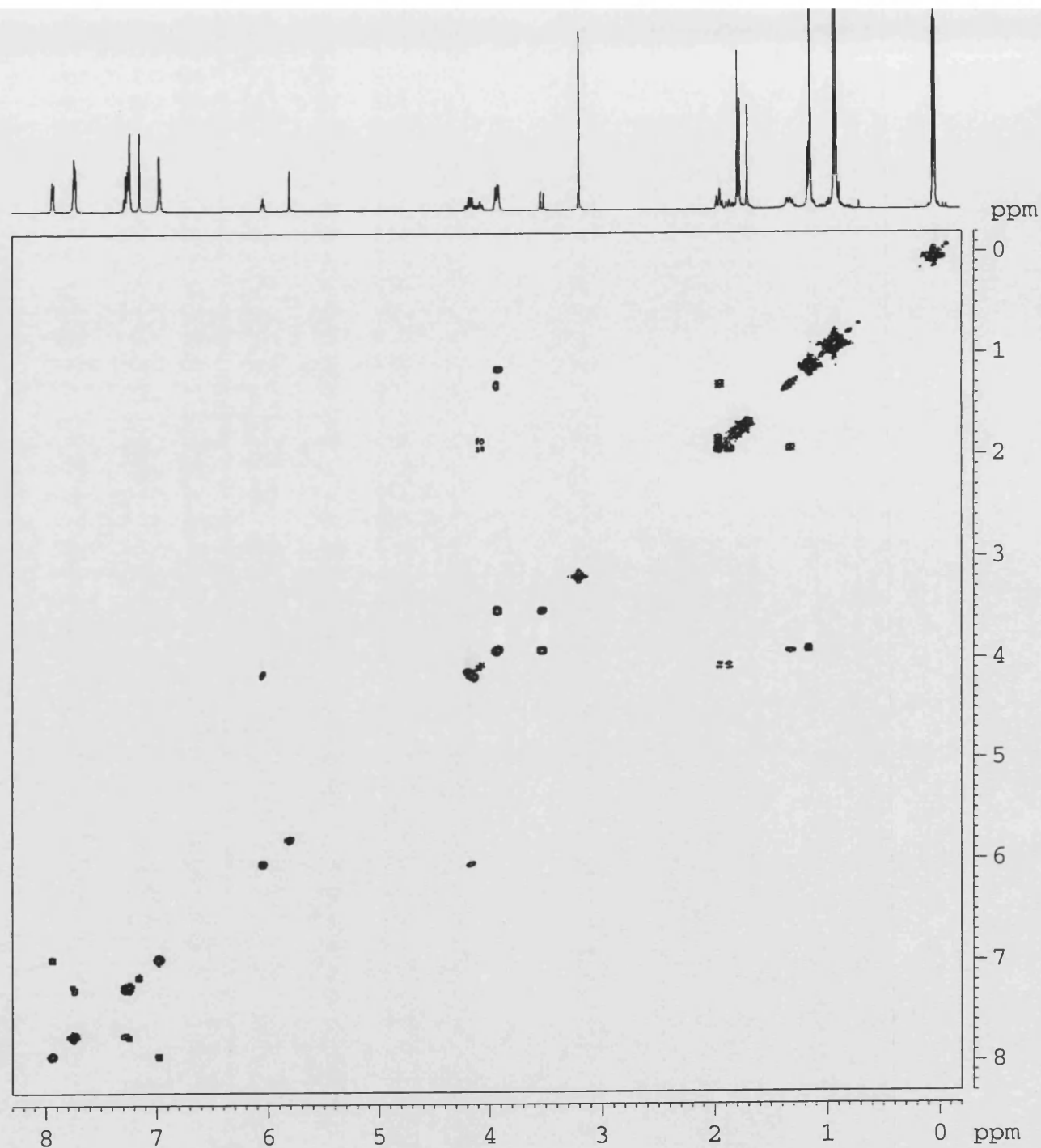
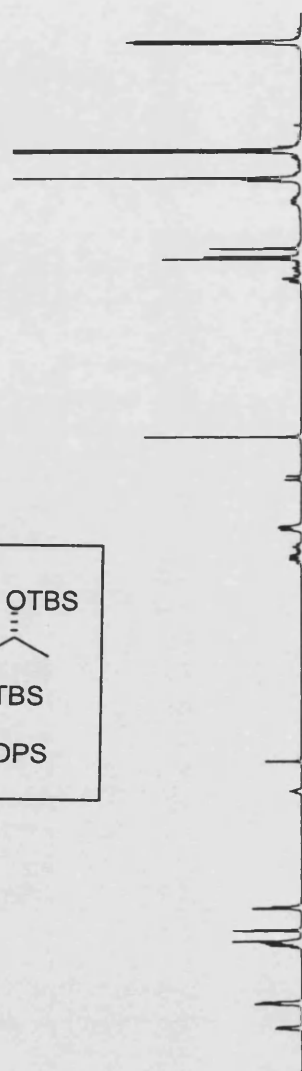
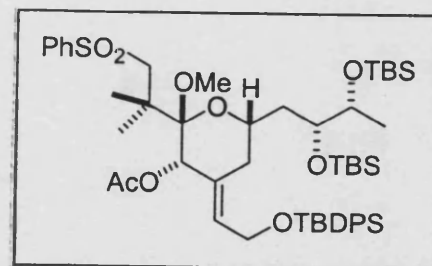
01/12/06 11:07
Y: 64 scans, 16.0cm⁻¹, apod none



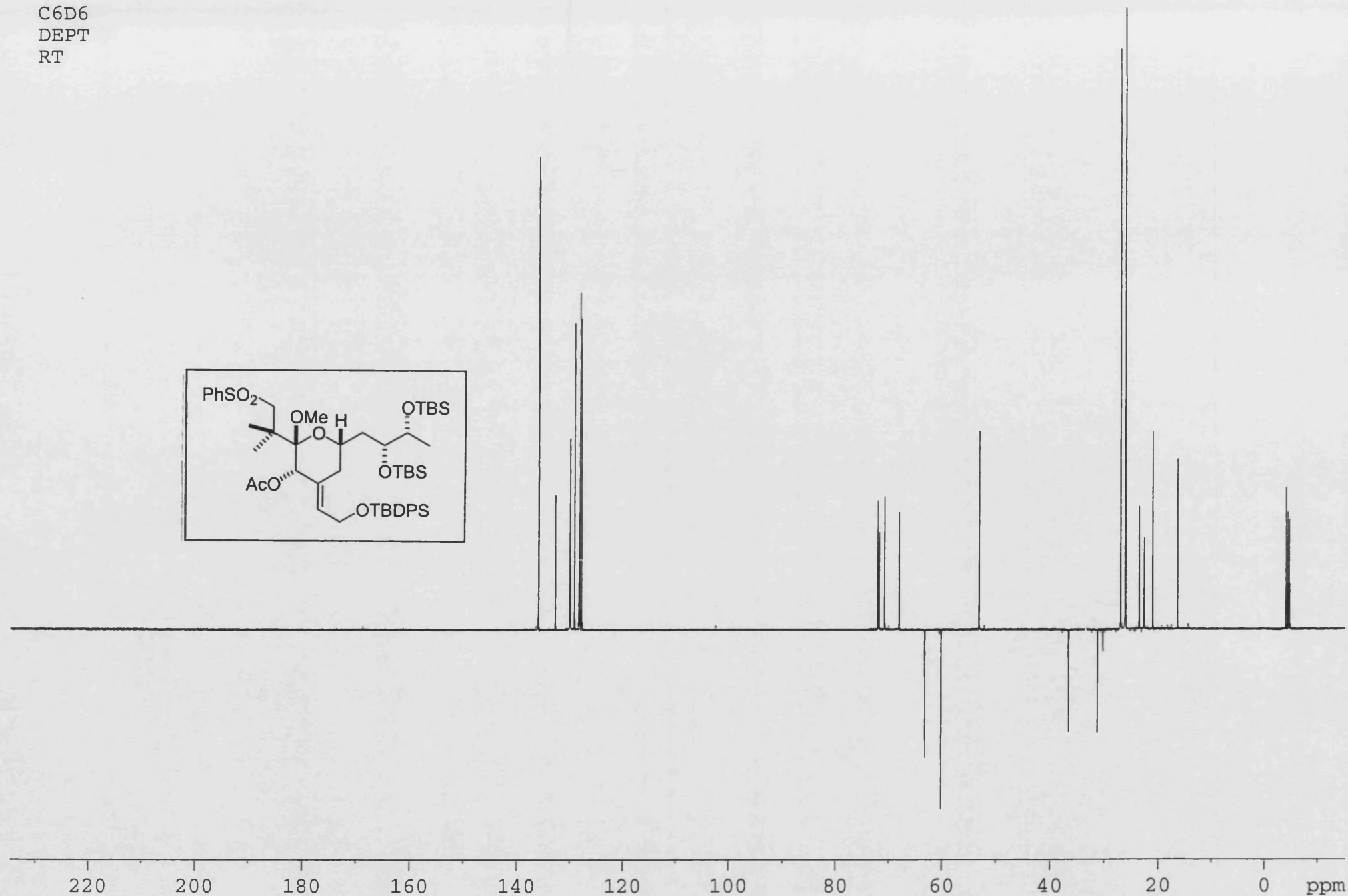
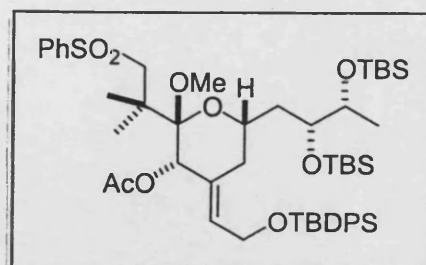
III-MF-144
C6D6
HMQC
RT



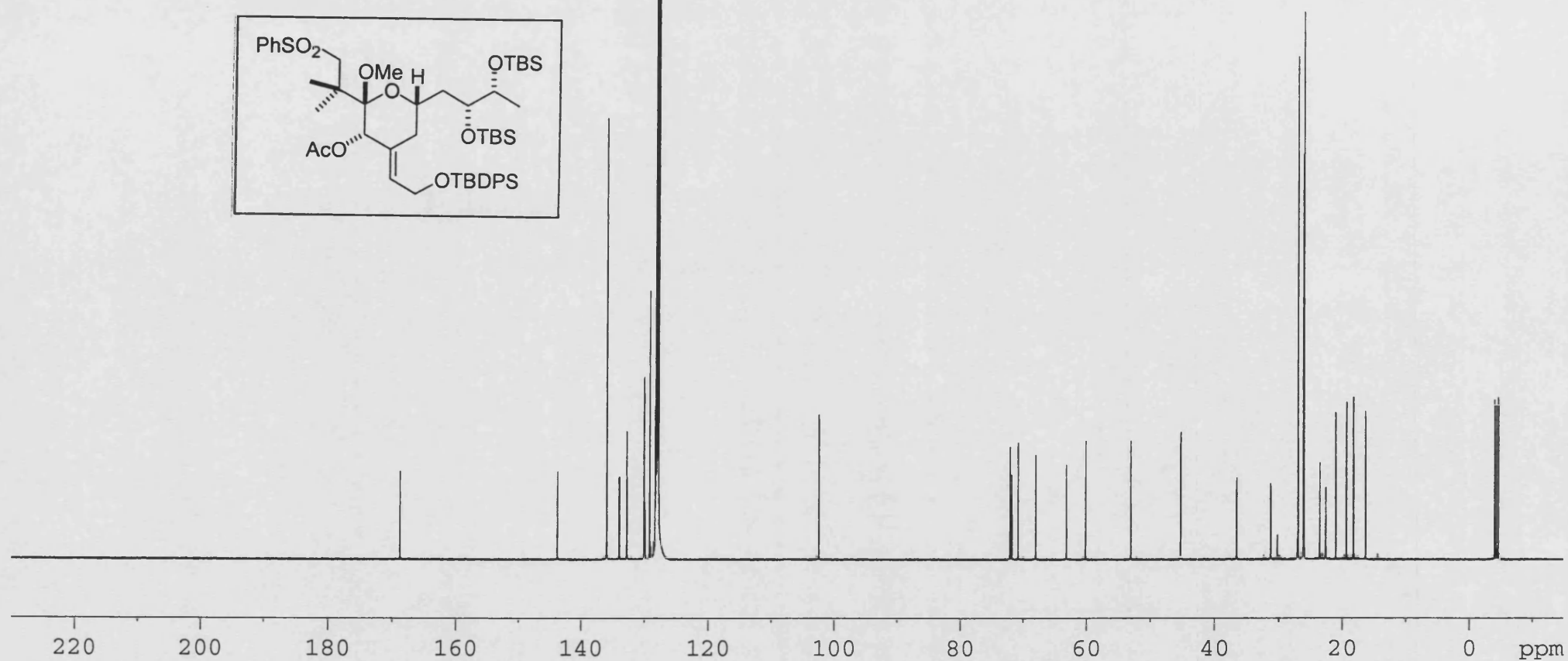
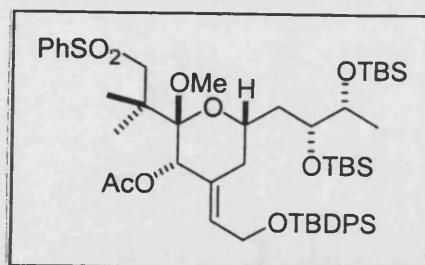
III-MF-144
C6D6
COSY
RT



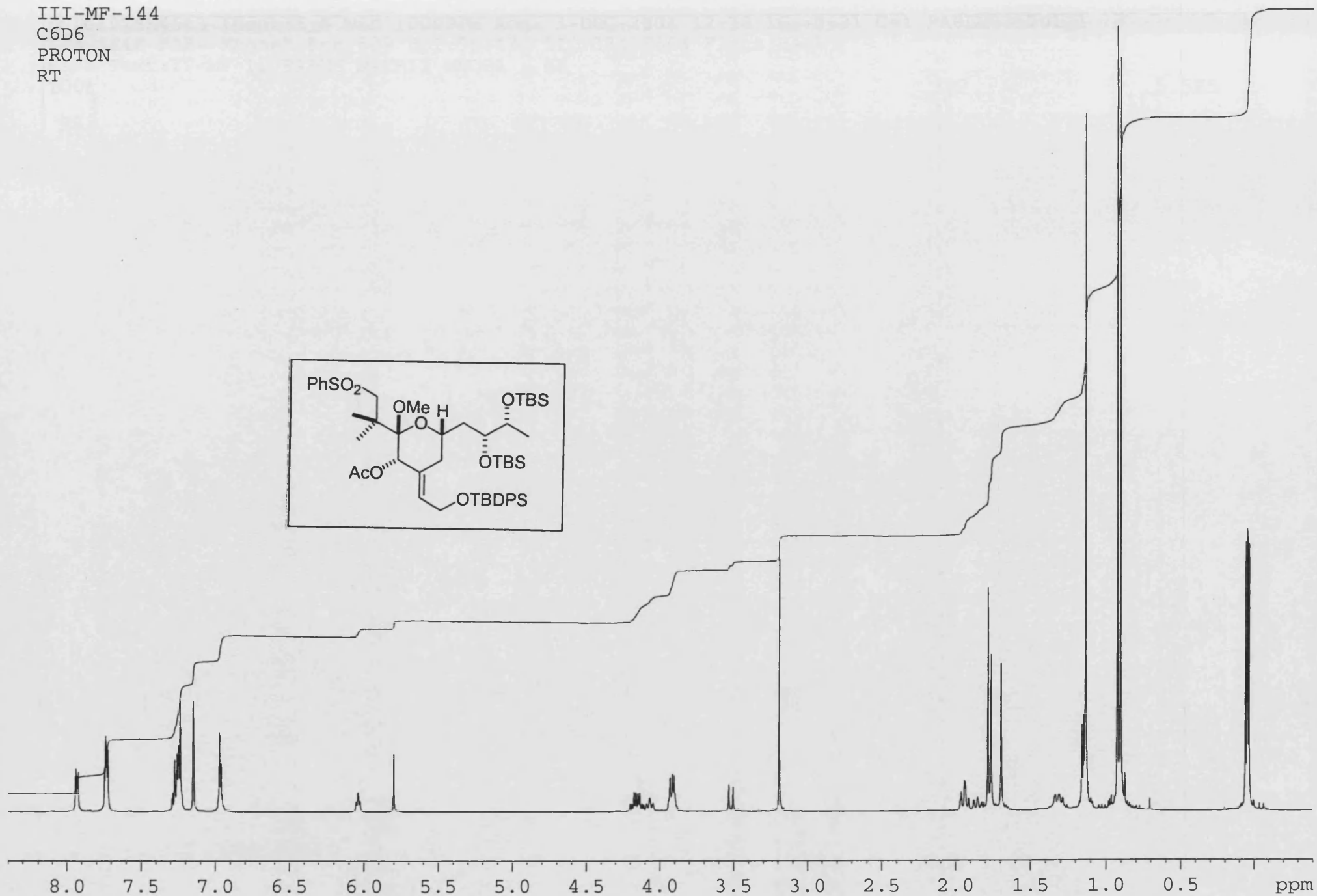
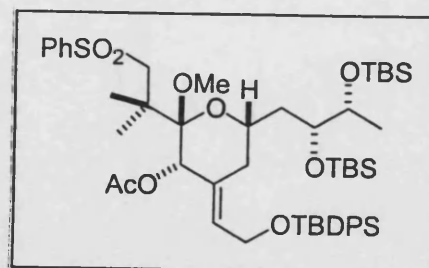
III-MF-144
C6D6
DEPT
RT



III-MF-144
C6D6
CARBON
RT



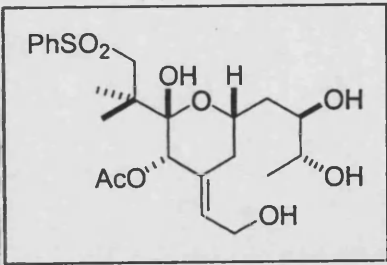
III-MF-144
C6D6
PROTON
RT



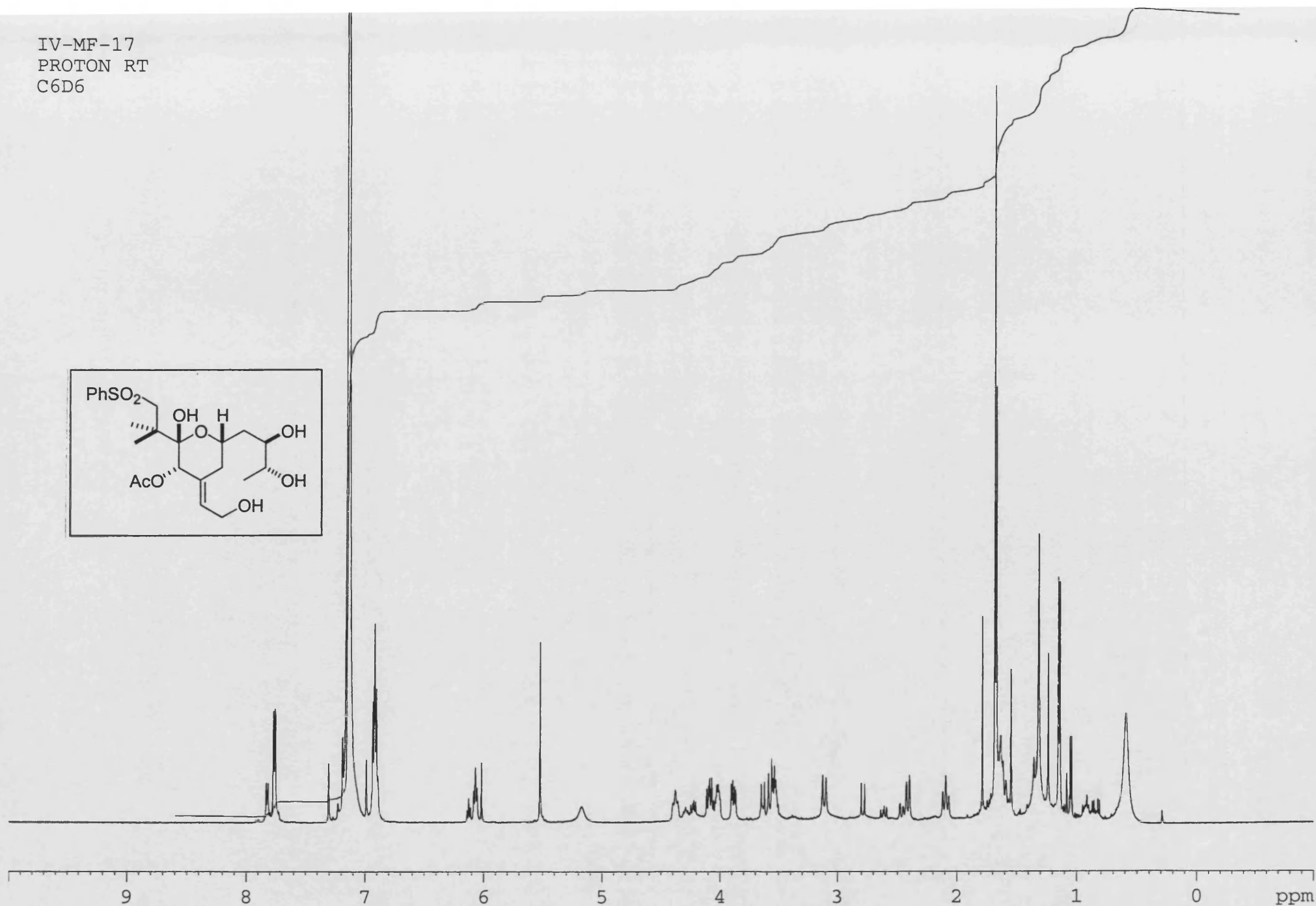
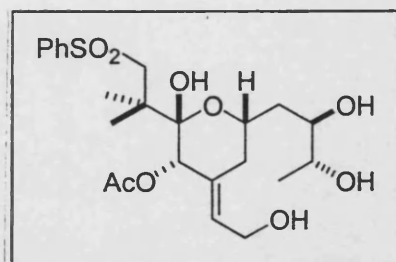
File:01SE4543 Ident:3 8 Win 1000PPM Acq: 3-DEC-2001 12:18:15 +0:21 Cal:FABLM031201_1

ZAB-SE4F FAB+ Magnet BpM:509 BpI:553472 TIC:32406504 Flags:HALL

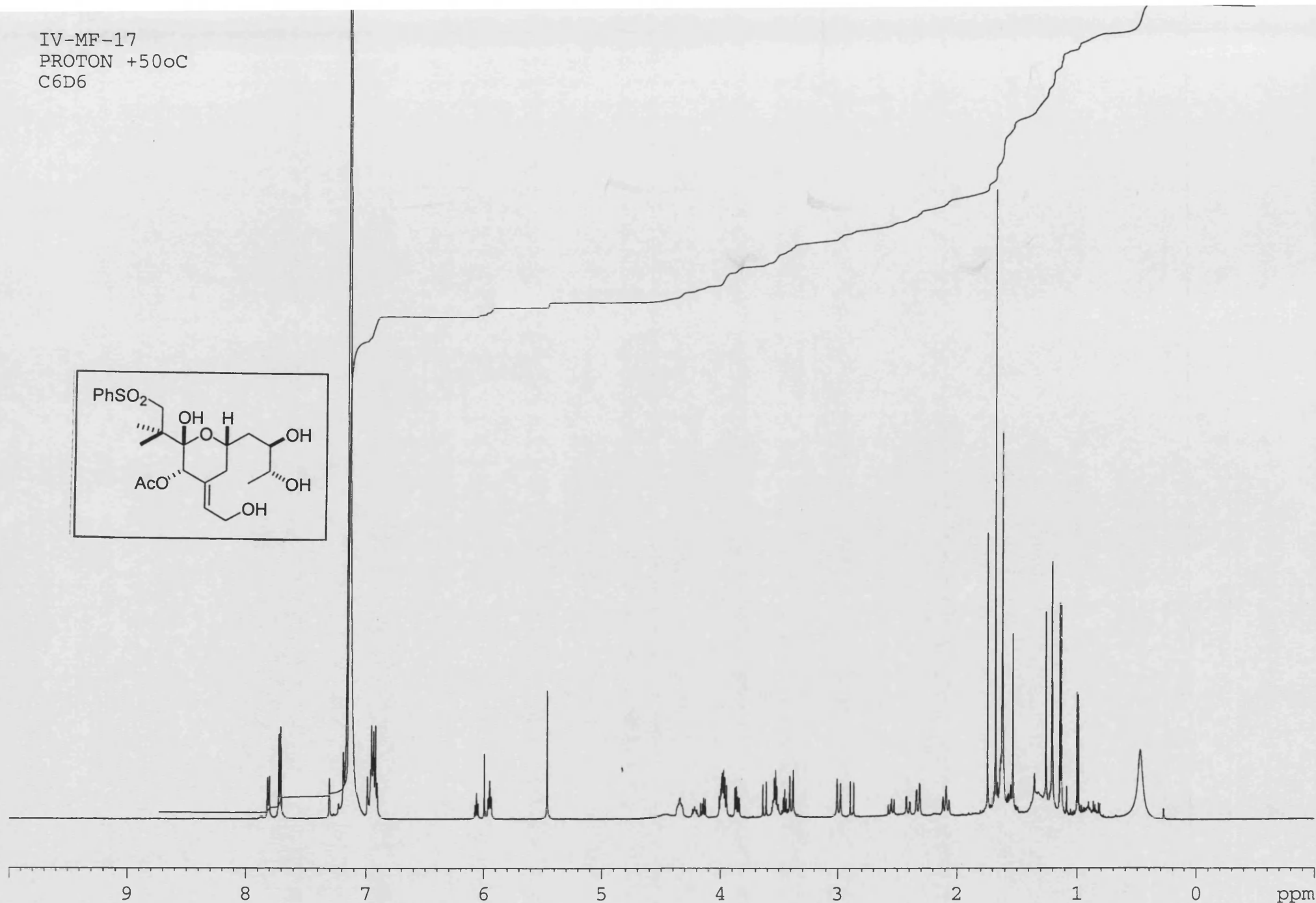
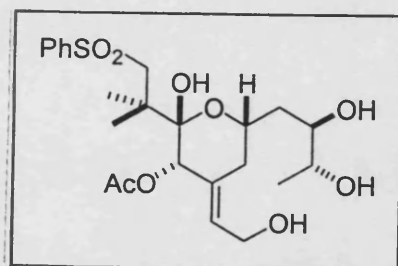
File Text:IV-MF-11 FABMS MATRIX MNOBA + NA



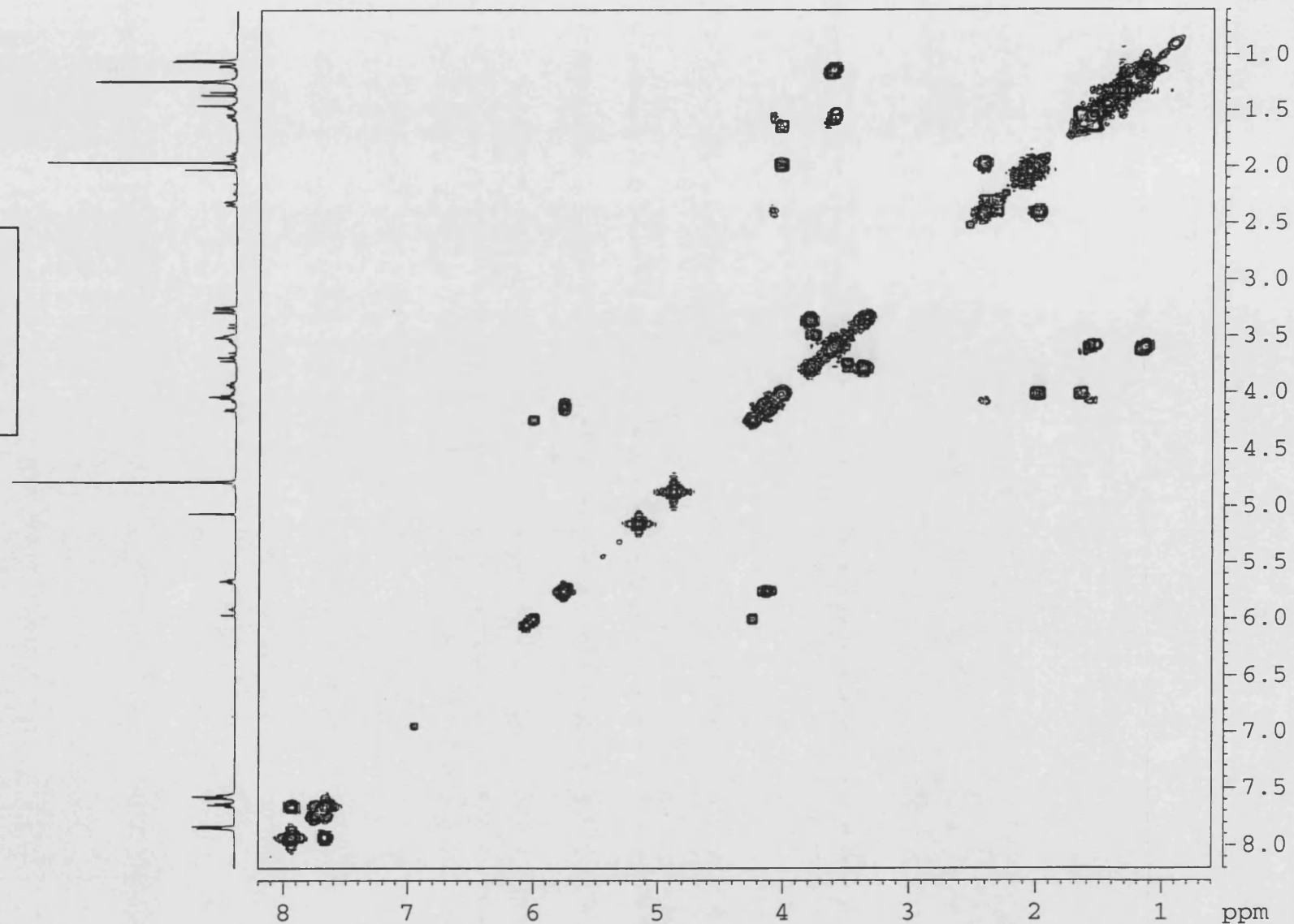
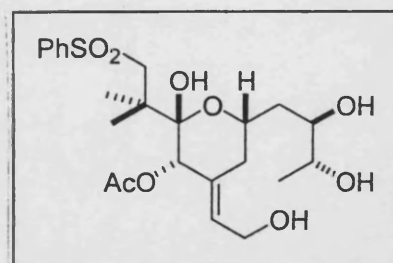
IV-MF-17
PROTON RT
C6D6



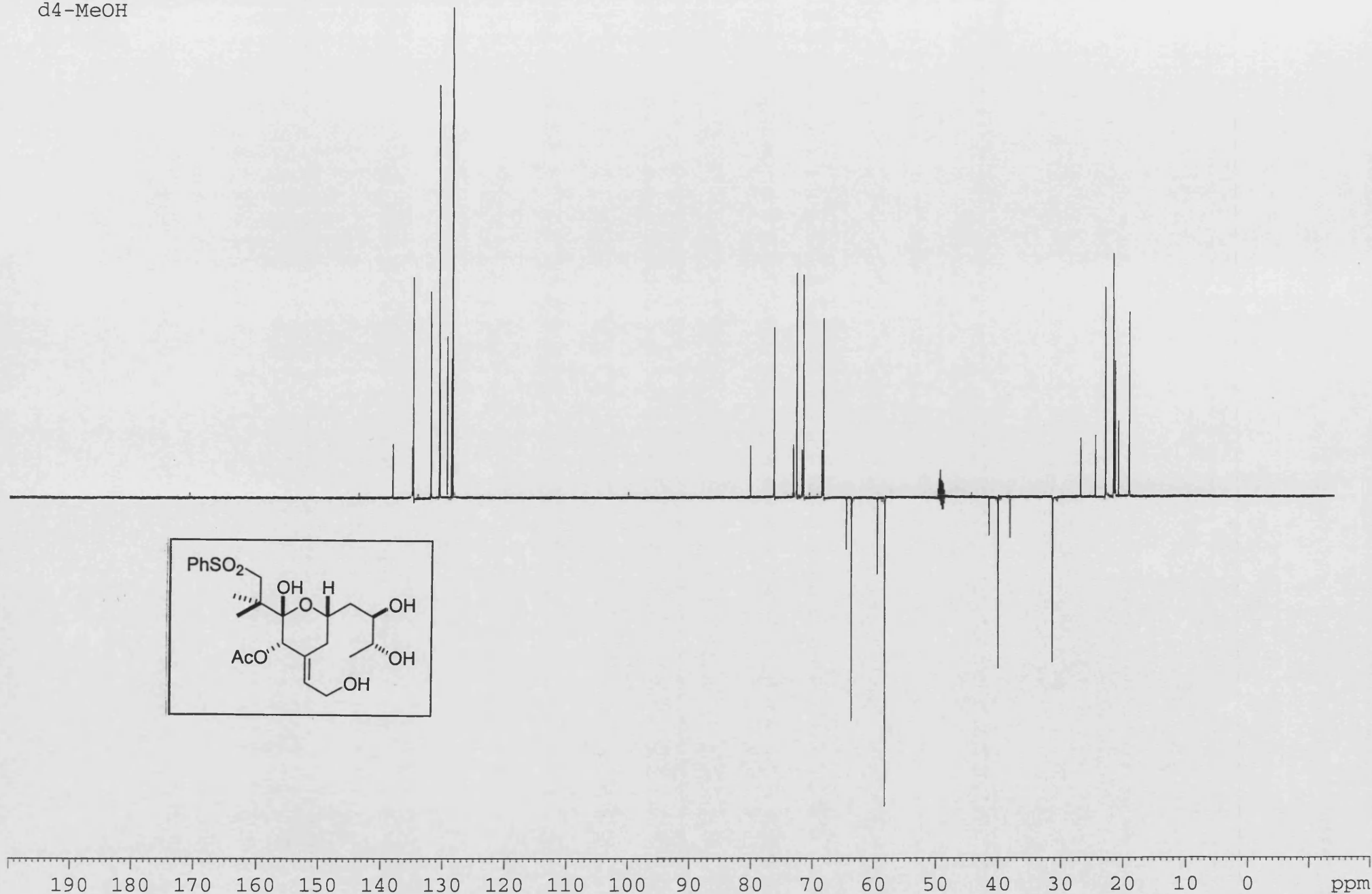
IV-MF-17
PROTON +50oC
C6D6



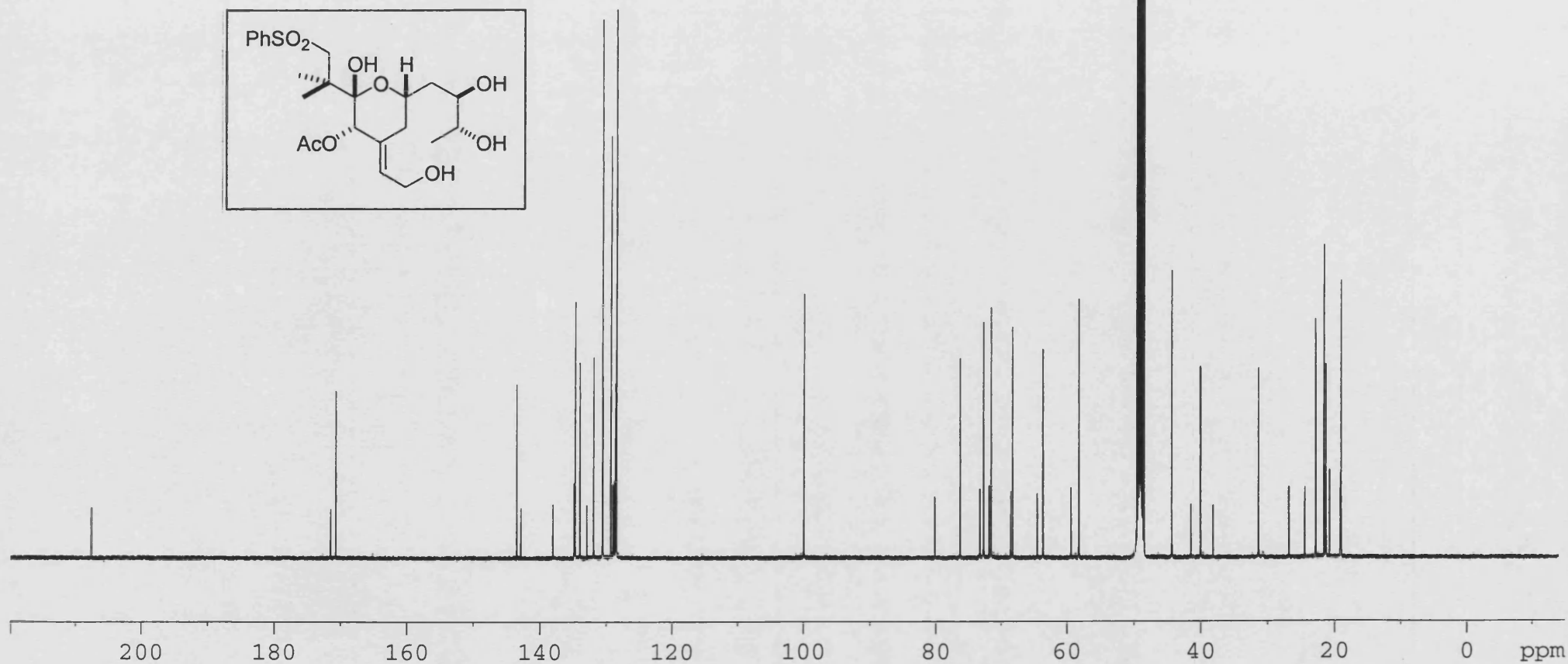
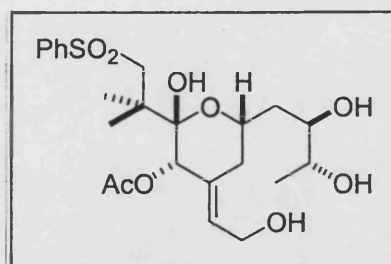
IV-MF-11
d4-MeOH
COSY



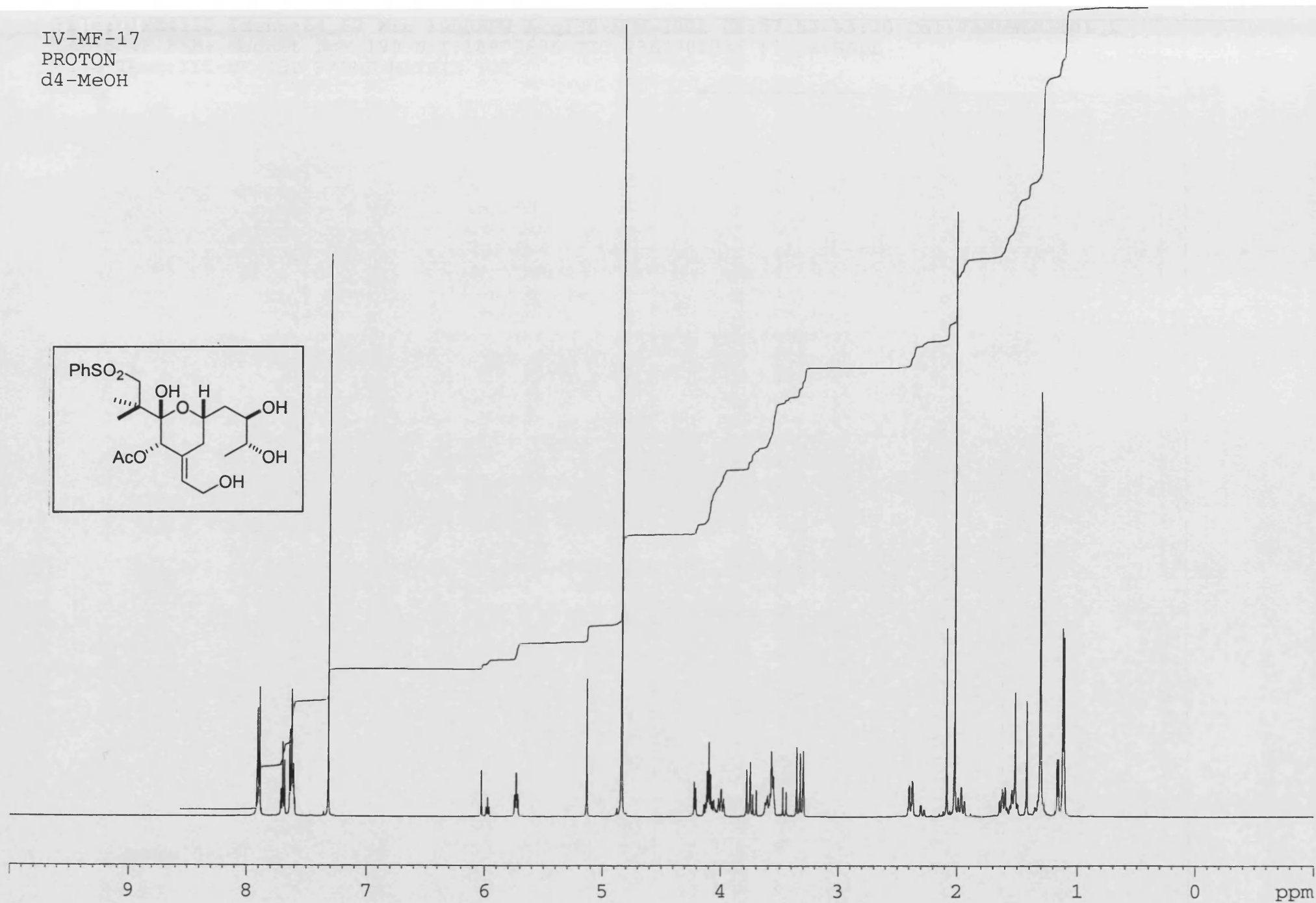
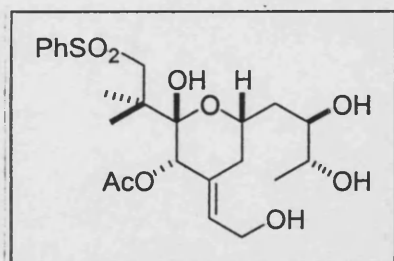
IV-MF-17
DEPT
d4-MeOH



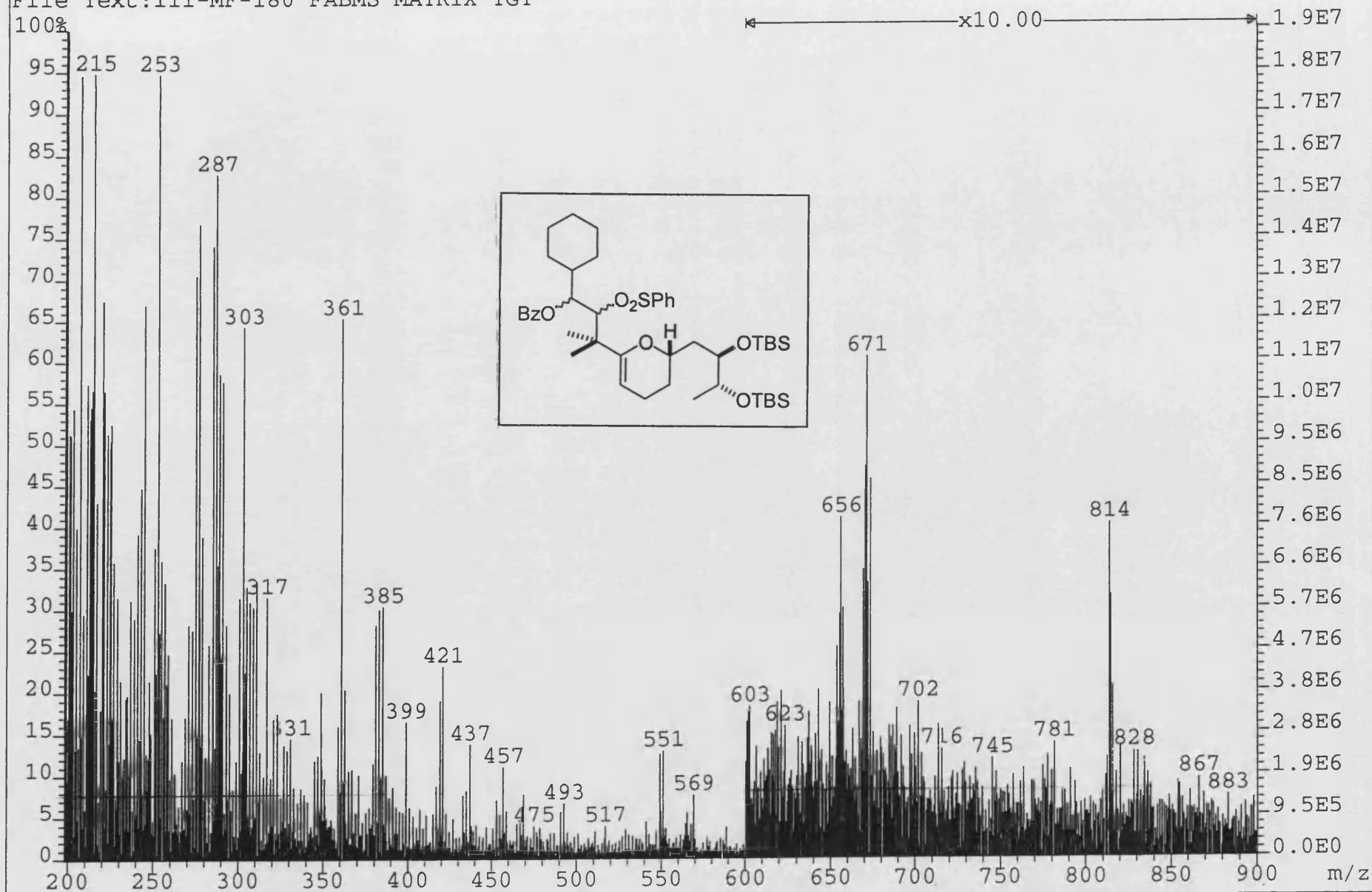
IV-MF-17
CARBON
d4-MeOH



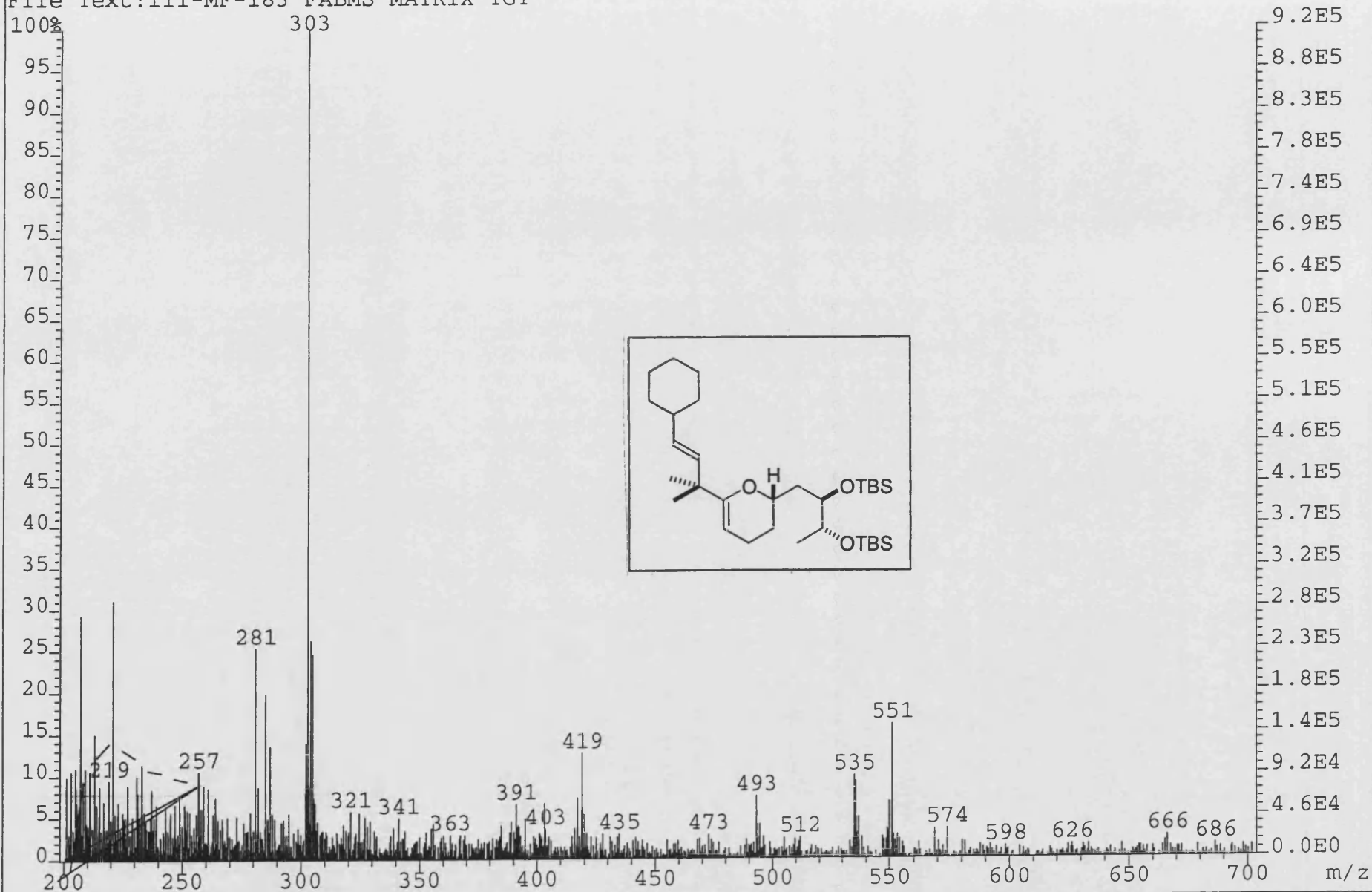
IV-MF-17
PROTON
d4-MeOH



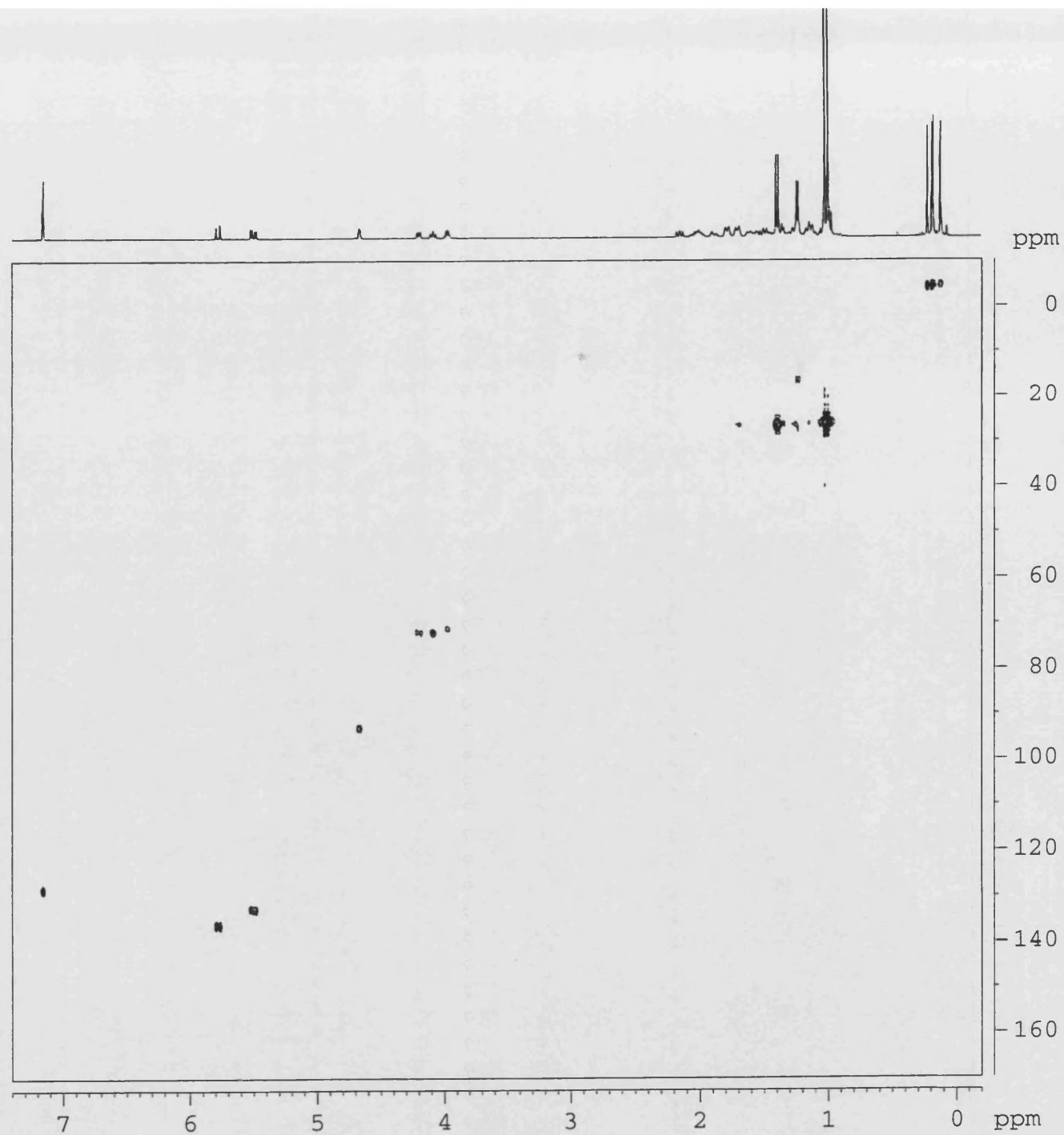
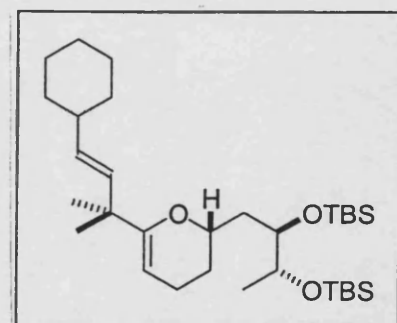
File:01SE4520 Ident:64_67 Win 1000PPM Acq:30-NOV-2001 08:57:53 +3:30 Cal:FABLM301101_1
ZAB-SE4F FAB+ Magnet BpM:199 BpI:18973696 TIC:2367700736 Flags:HALL
File Text:III-MF-180 FABMS MATRIX TGT



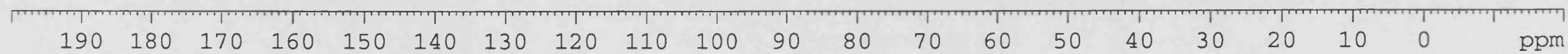
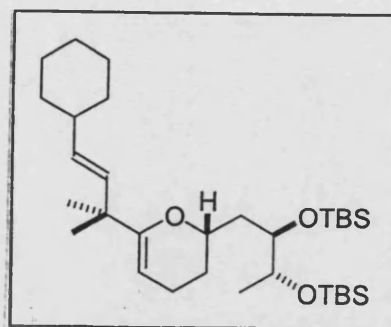
File:01SE4519 Ident:10_12 Win 1000PPM Acq:30-NOV-2001 08:48:37 +0:38 Cal:FABLM301101_1
ZAB-SE4F FAB+ Magnet BpM:147 BpI:6099968 TIC:76917584 Flags:HALL
File Text:III-MF-183 FABMS MATRIX TGT



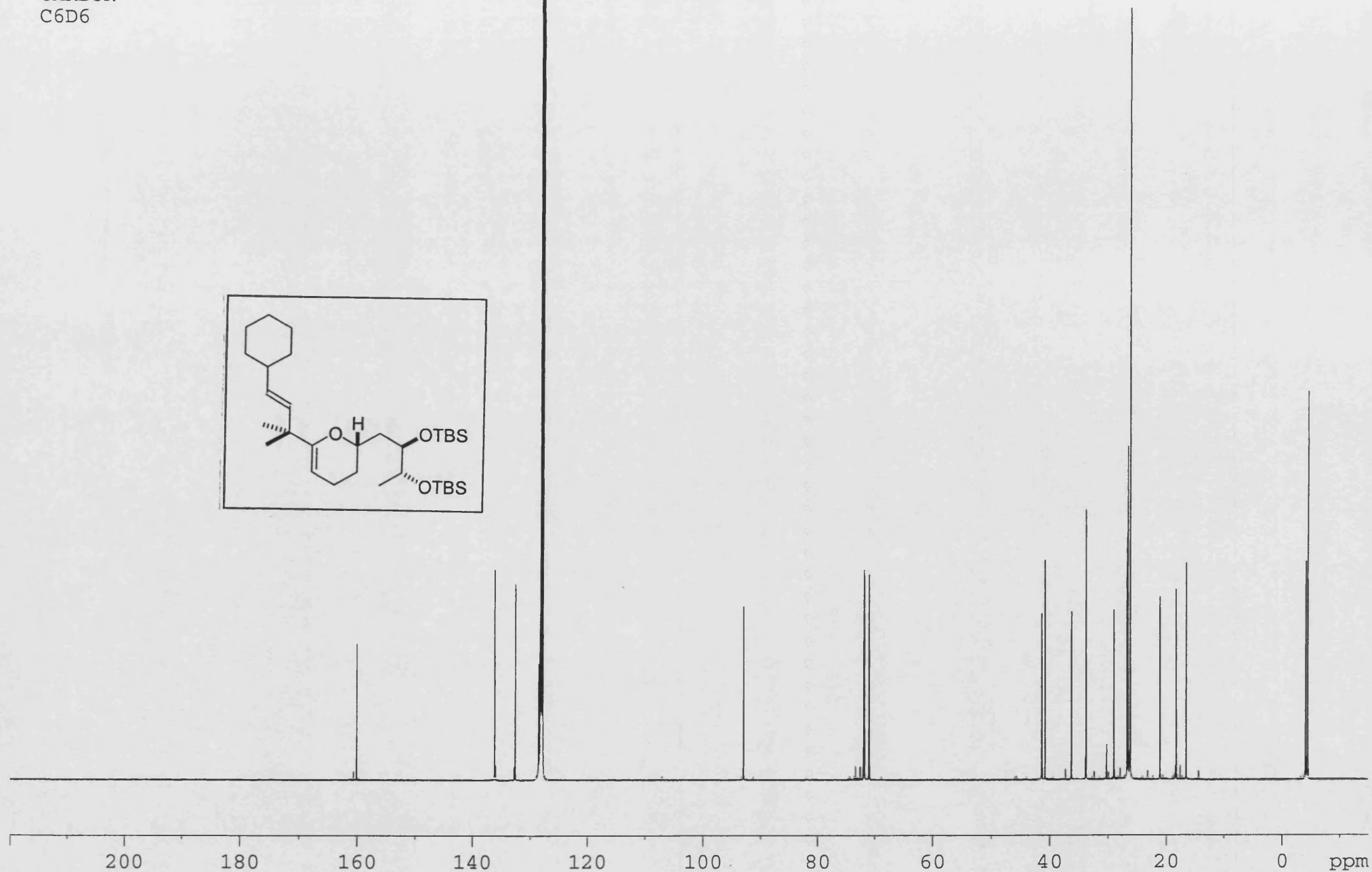
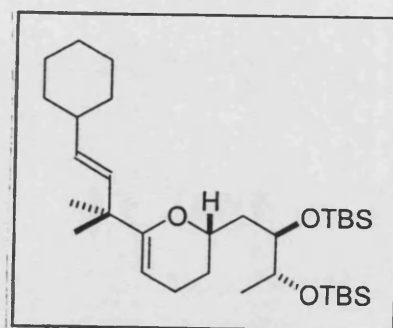
IV-MF-06
HMQC
C6D6



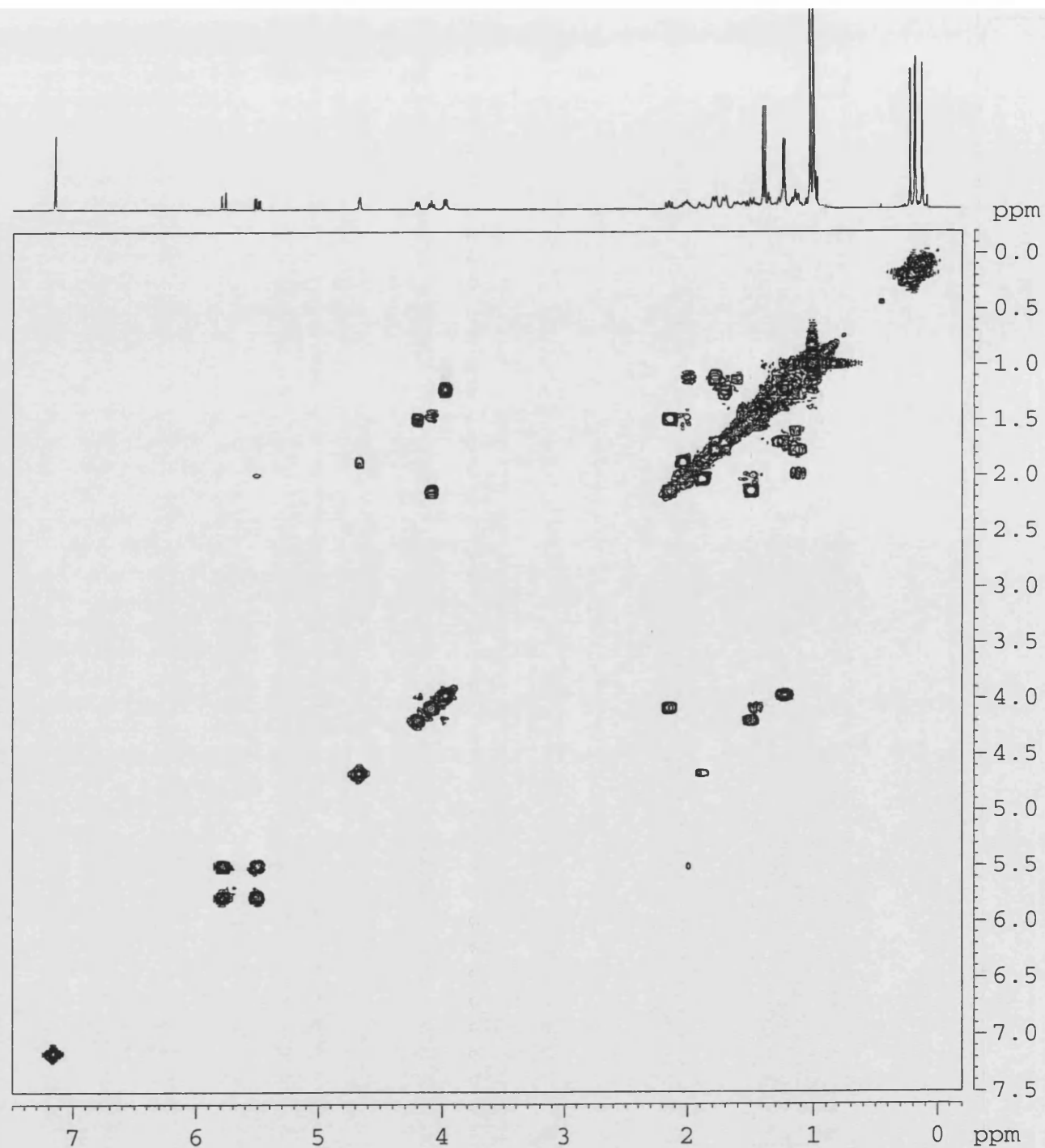
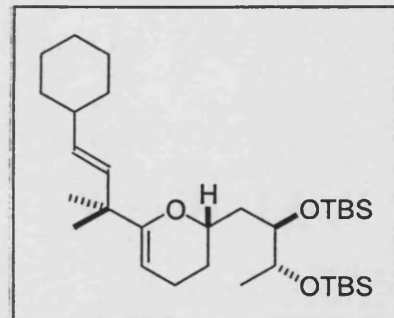
IV-MF-06
DEPT
C6D6



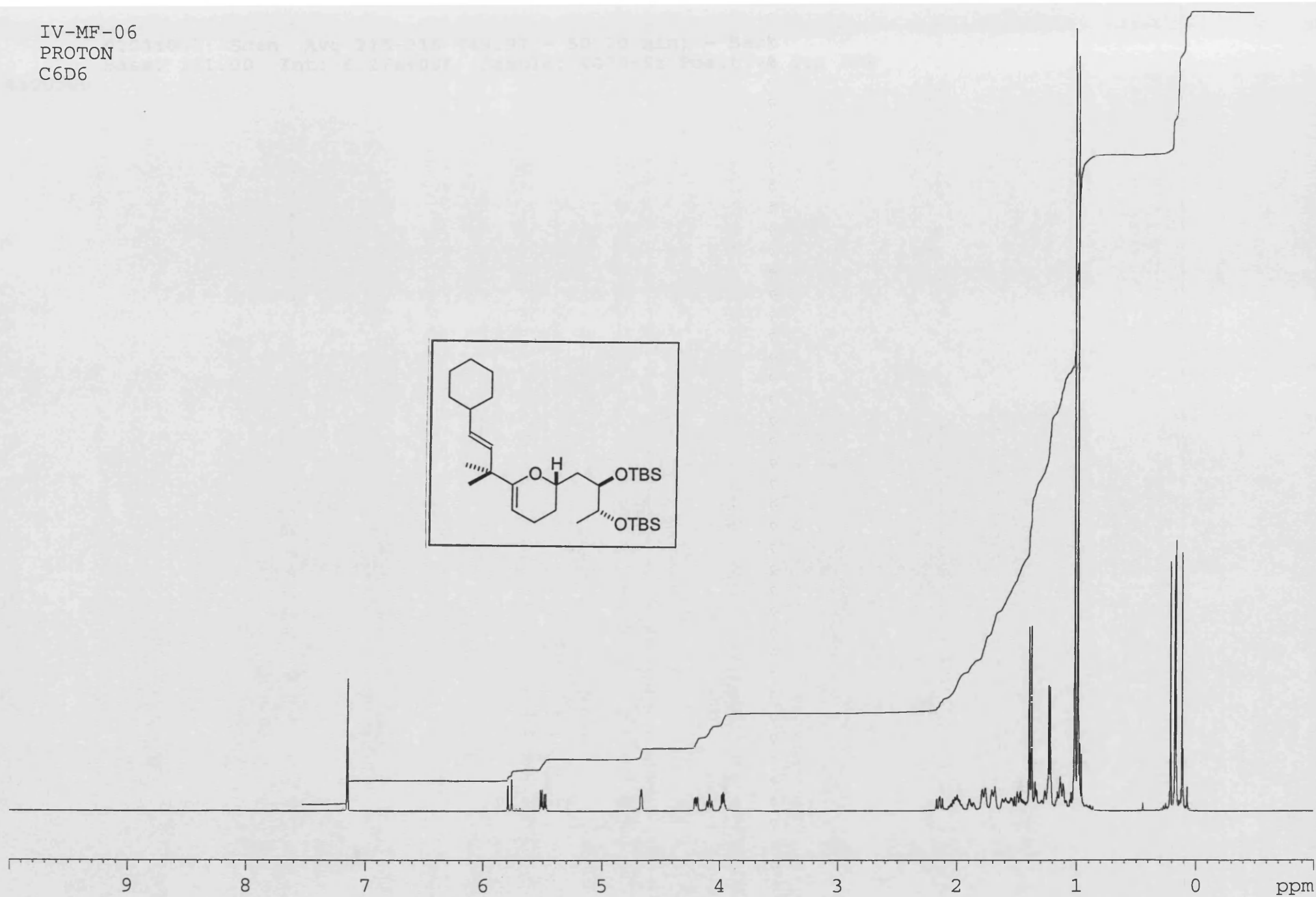
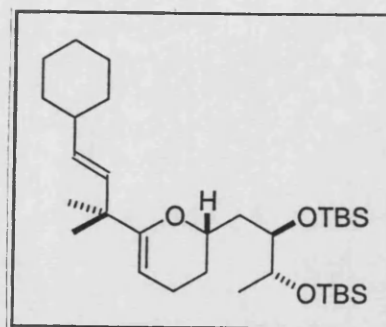
IV-MF-06
CARBON
C6D6



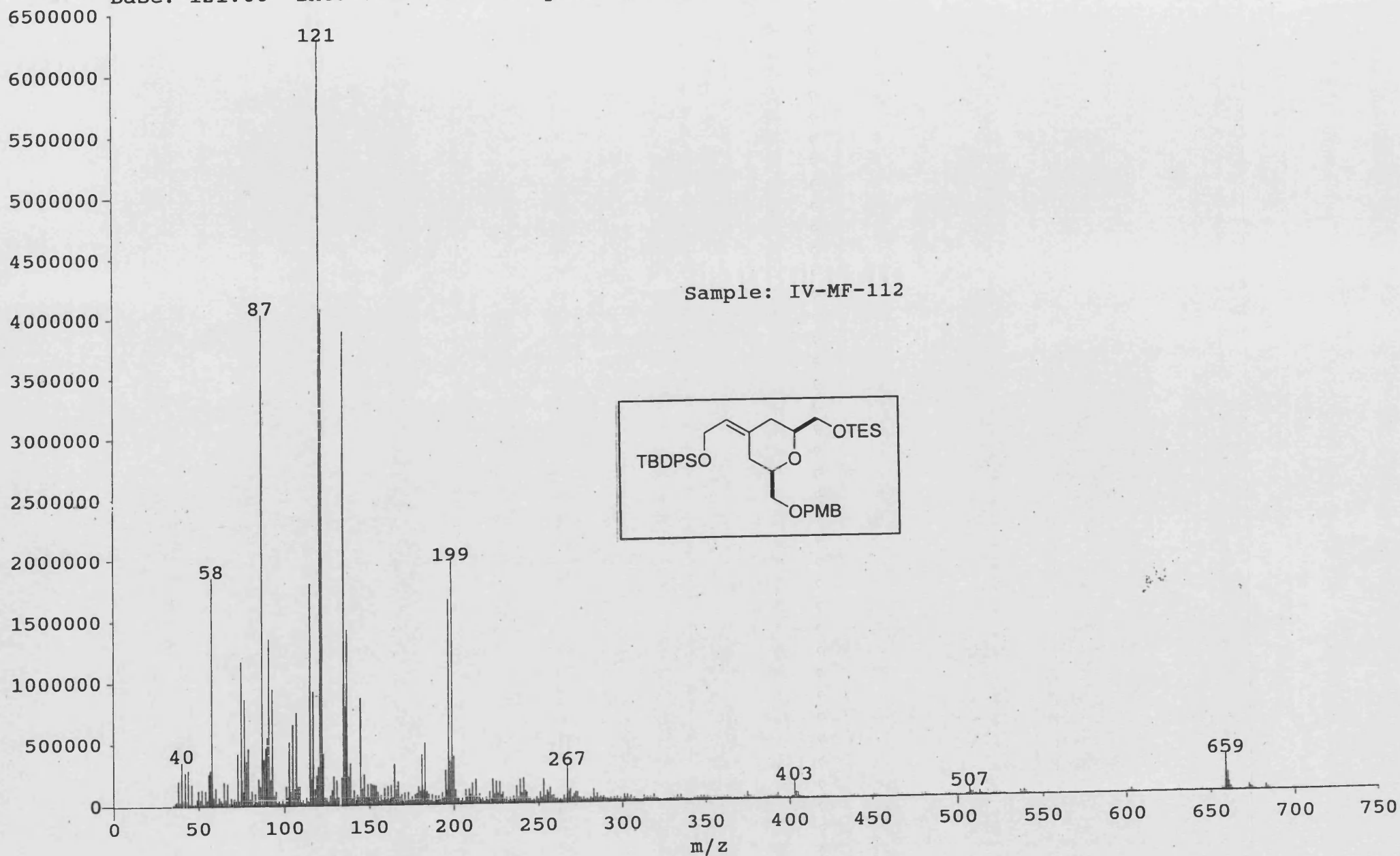
IV-MF-06
COSY
C6D6



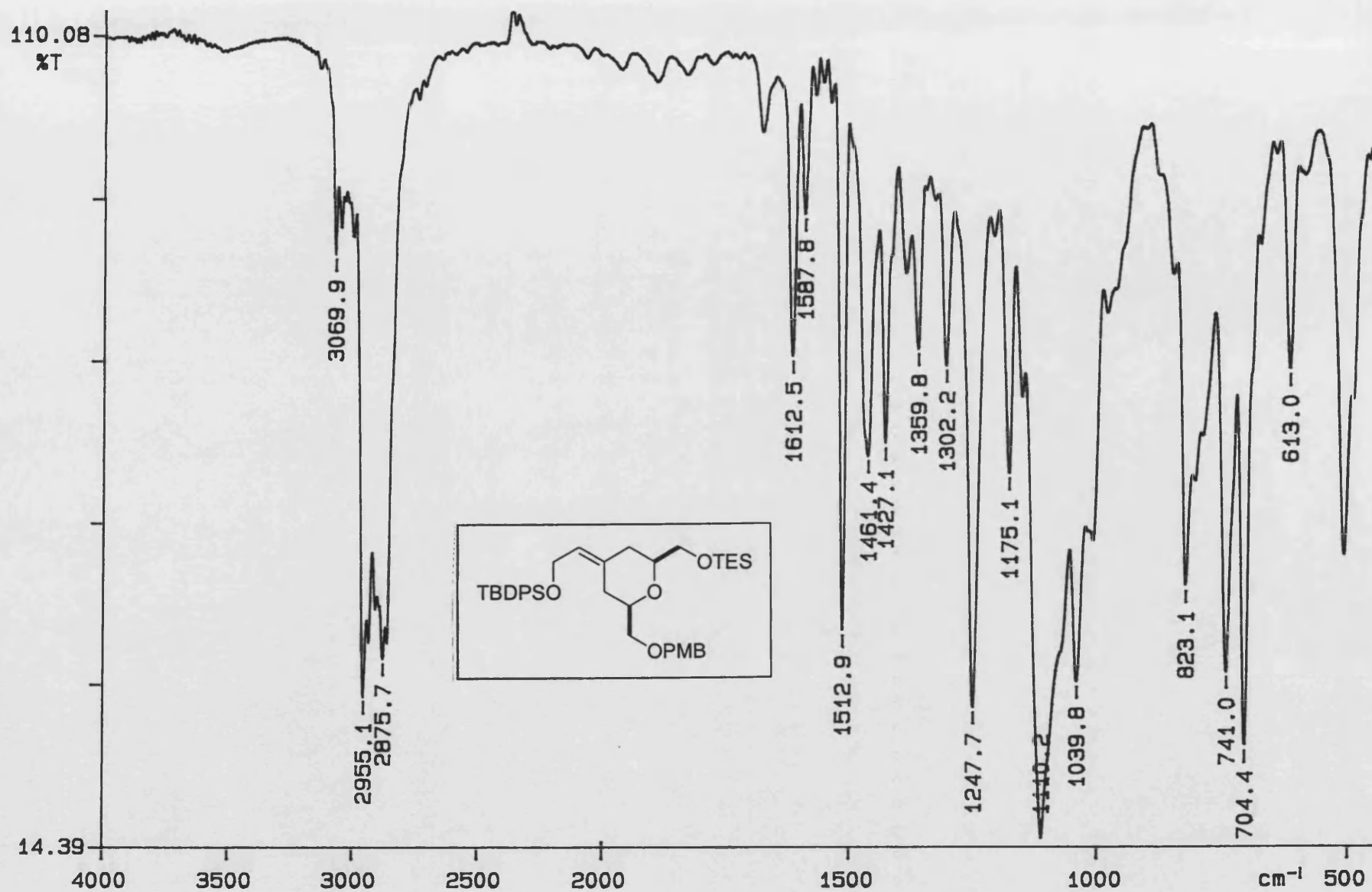
IV-MF-06
PROTON
C6D6



01031002: Scan Avg 215-216 (49.97 - 50.20 min) - Back
Base: 121.00 Int: 6.27e+006 Sample: VG70-SE Positive Ion FAB



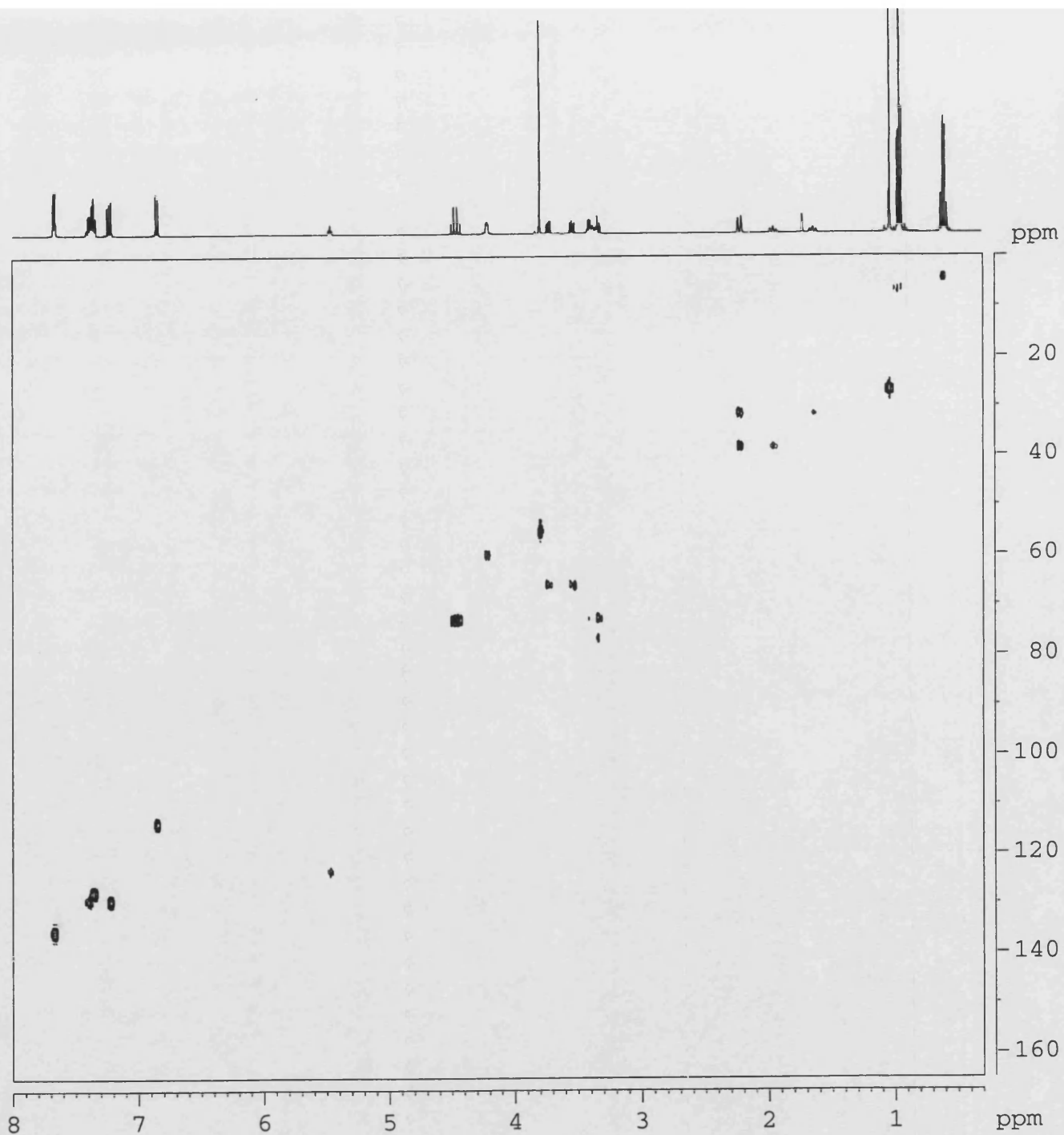
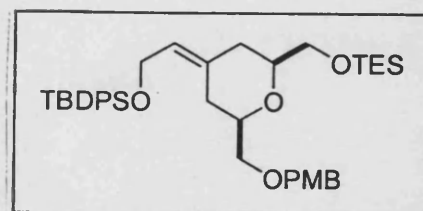
PERKIN ELMER



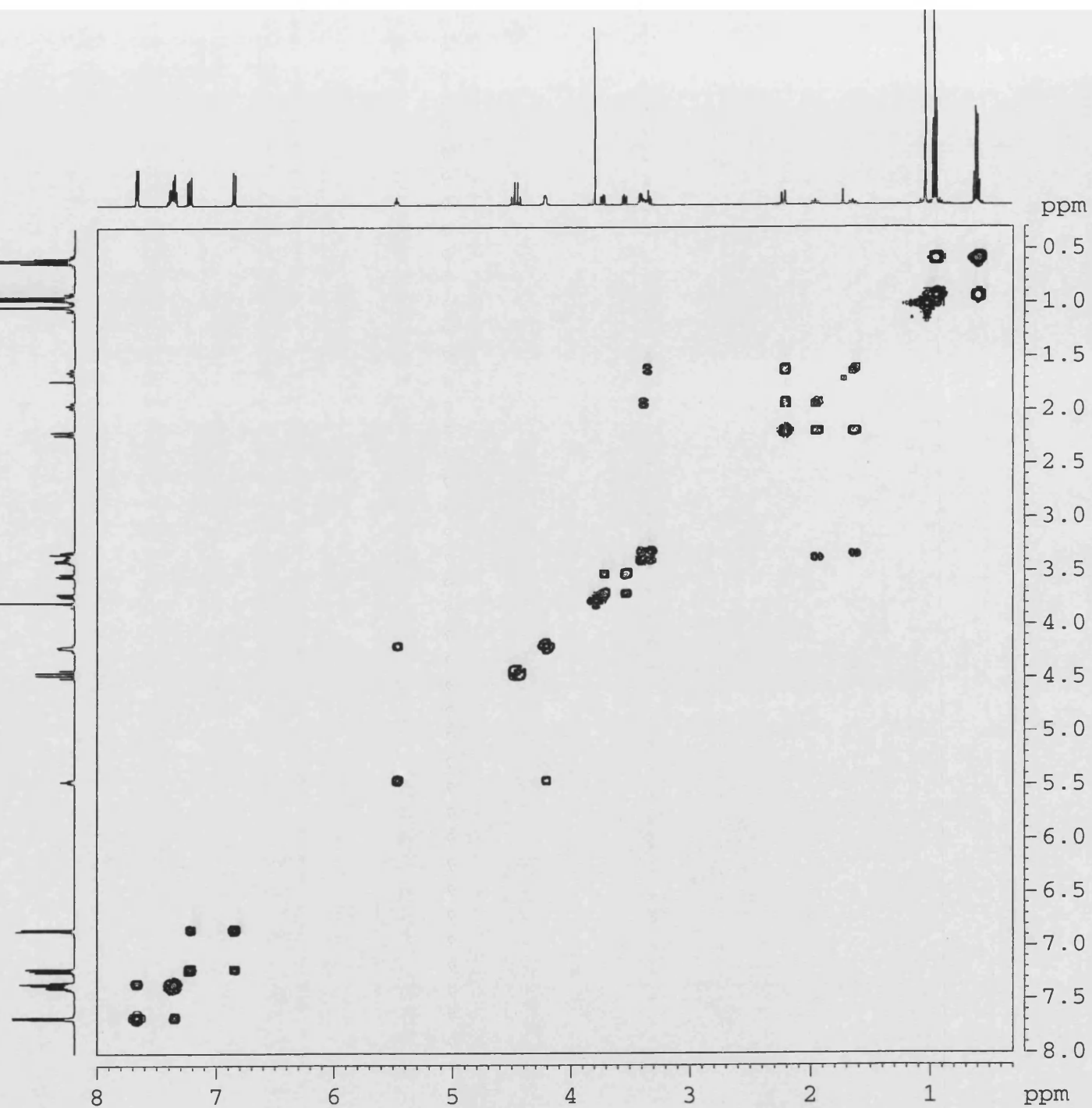
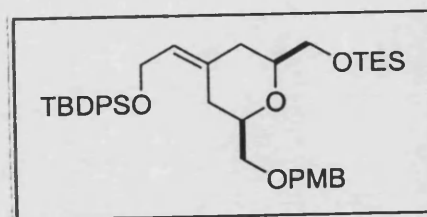
02/09/16 09:40

X: 64 scans, 16.0cm⁻¹, apod none, flat

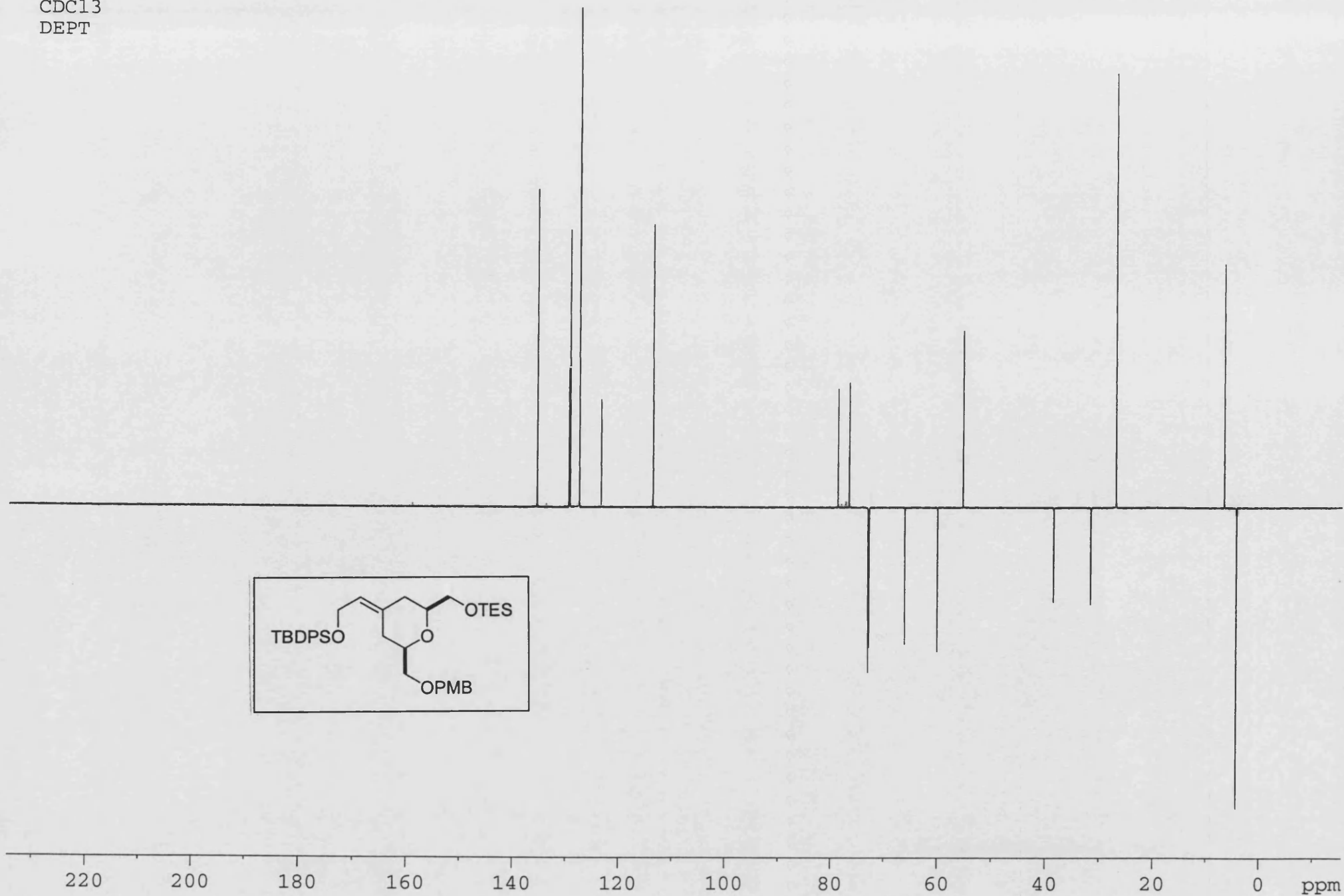
IV-MF-112
CDC13
HMQC



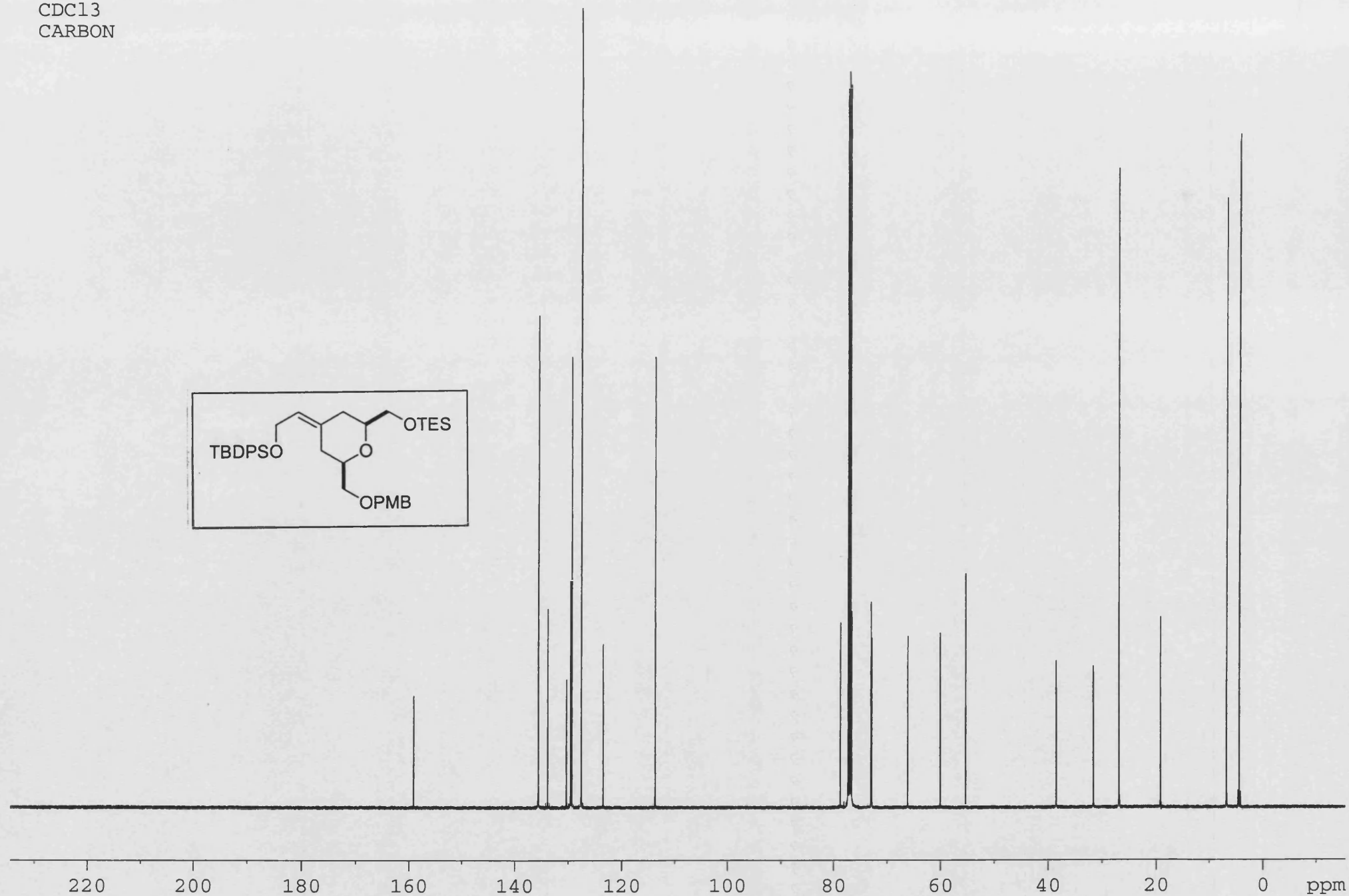
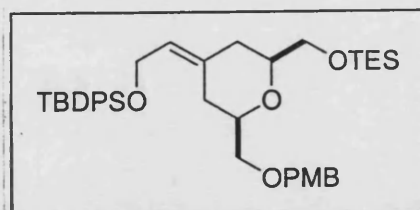
IV-MF-112
CDCl₃
COSY



IV-MF-112
CDCl₃
DEPT



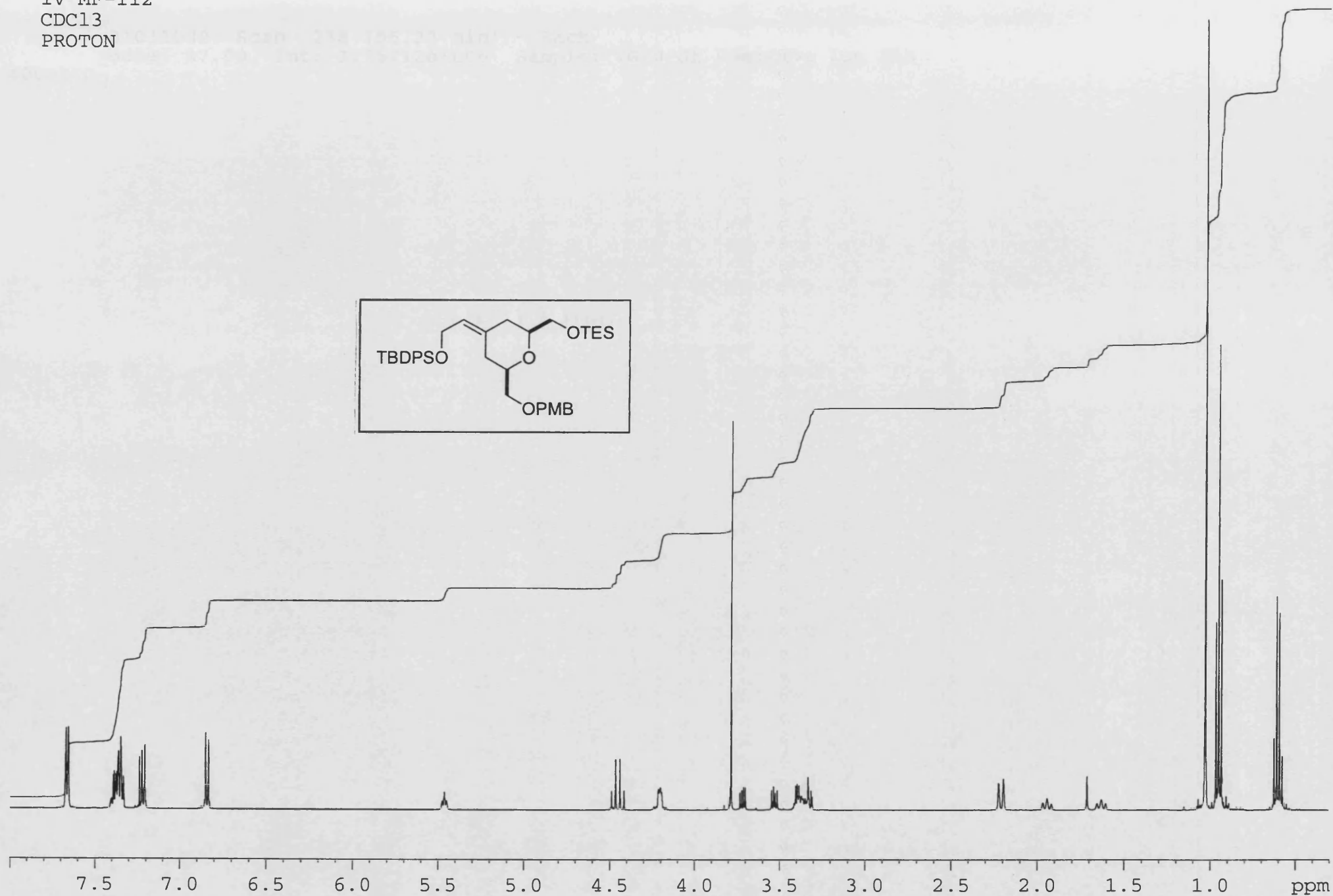
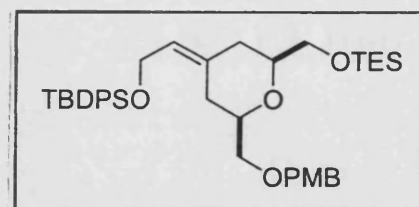
IV-MF-112
CDCl₃
CARBON



IV-MF-112

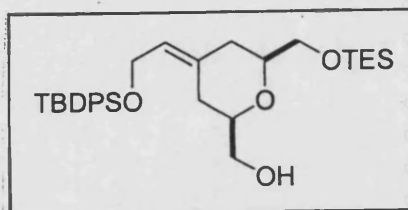
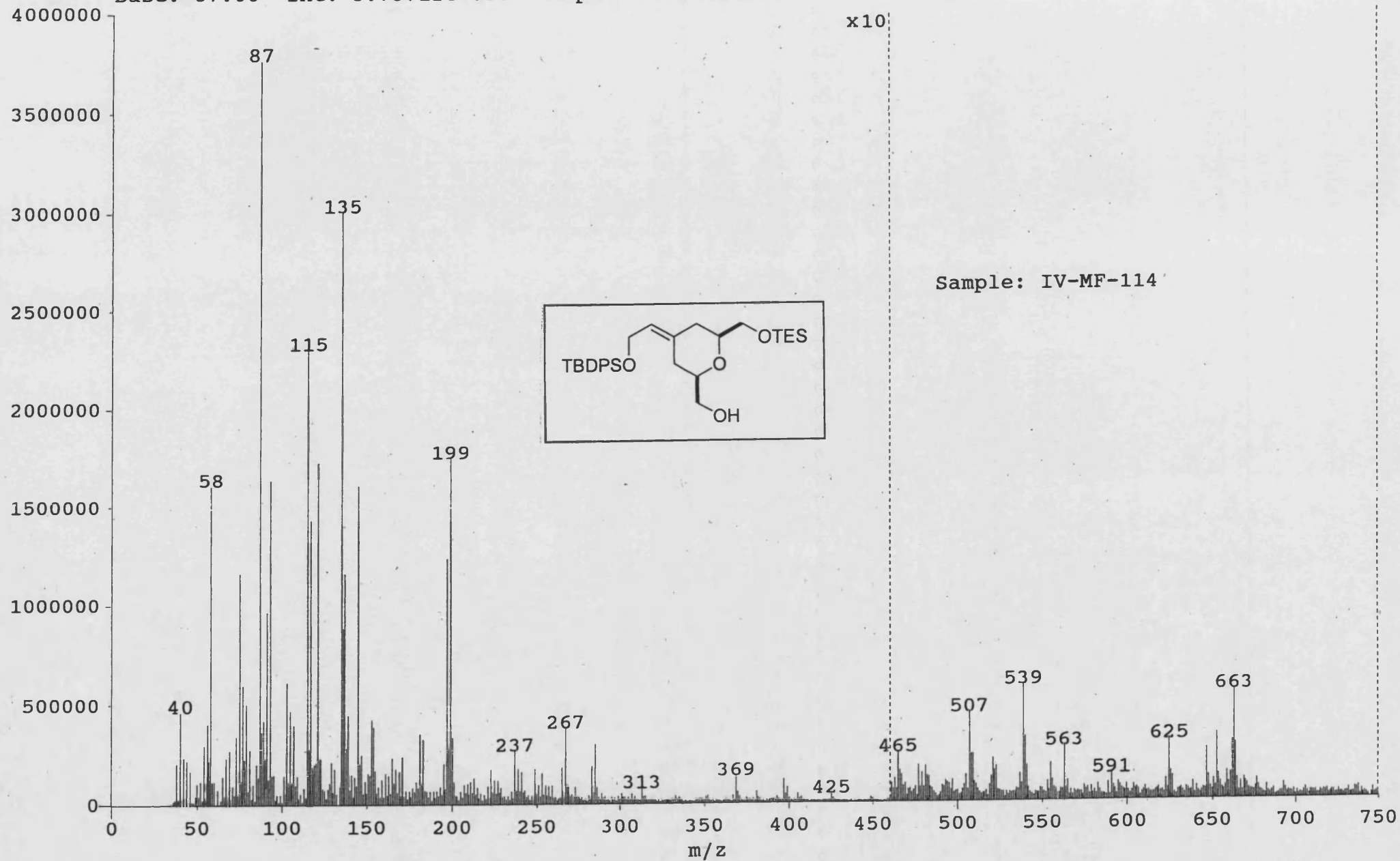
CDC13

PROTON



Base: 87.00 Int: 3.75712e+006 Sample: VG70-SE Positive Ion FAB

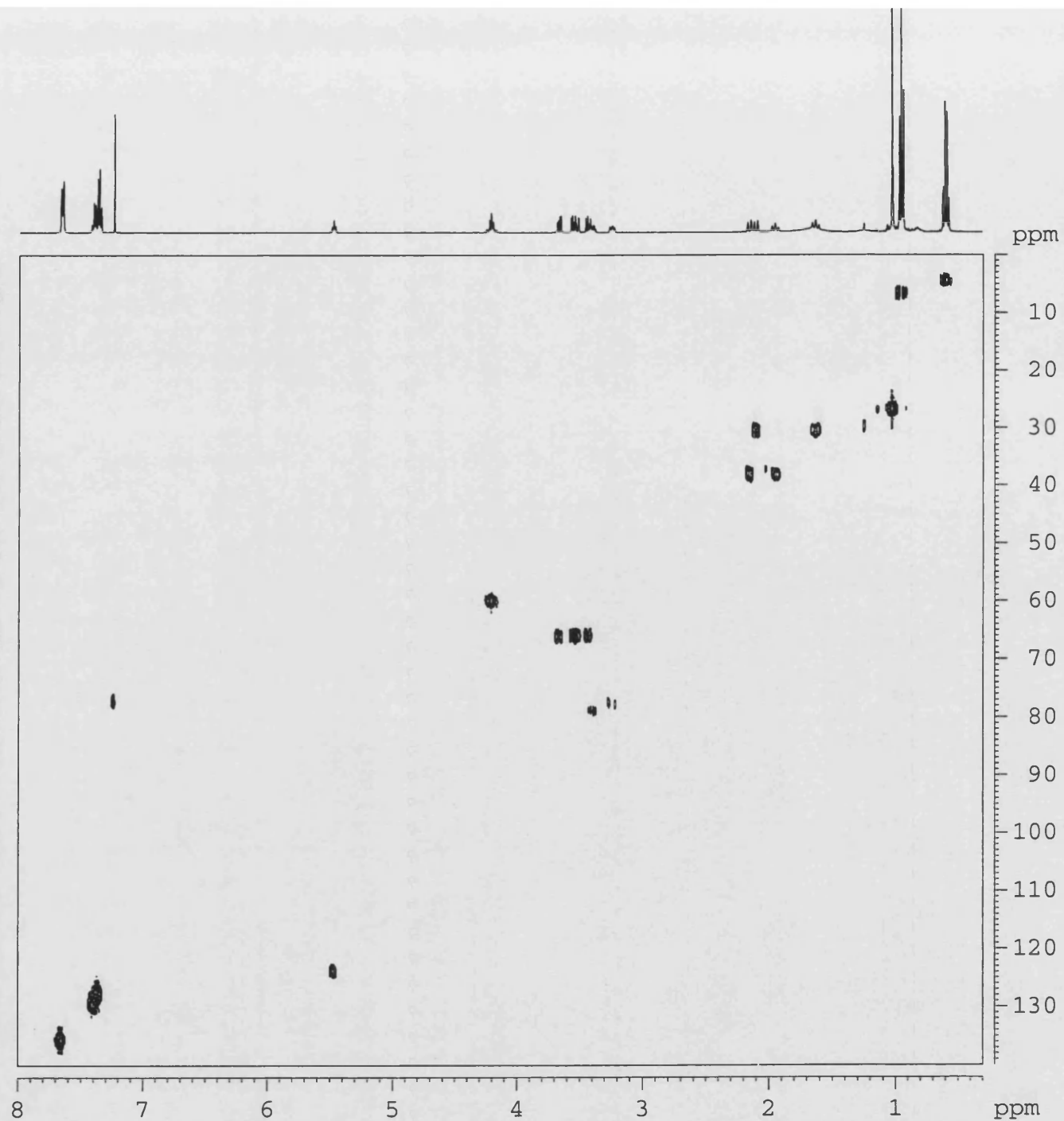
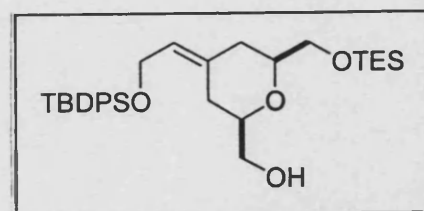
Base: 87.00 Int: 3.75712e+006 Sample: VG70-SE Positive Ion FAB



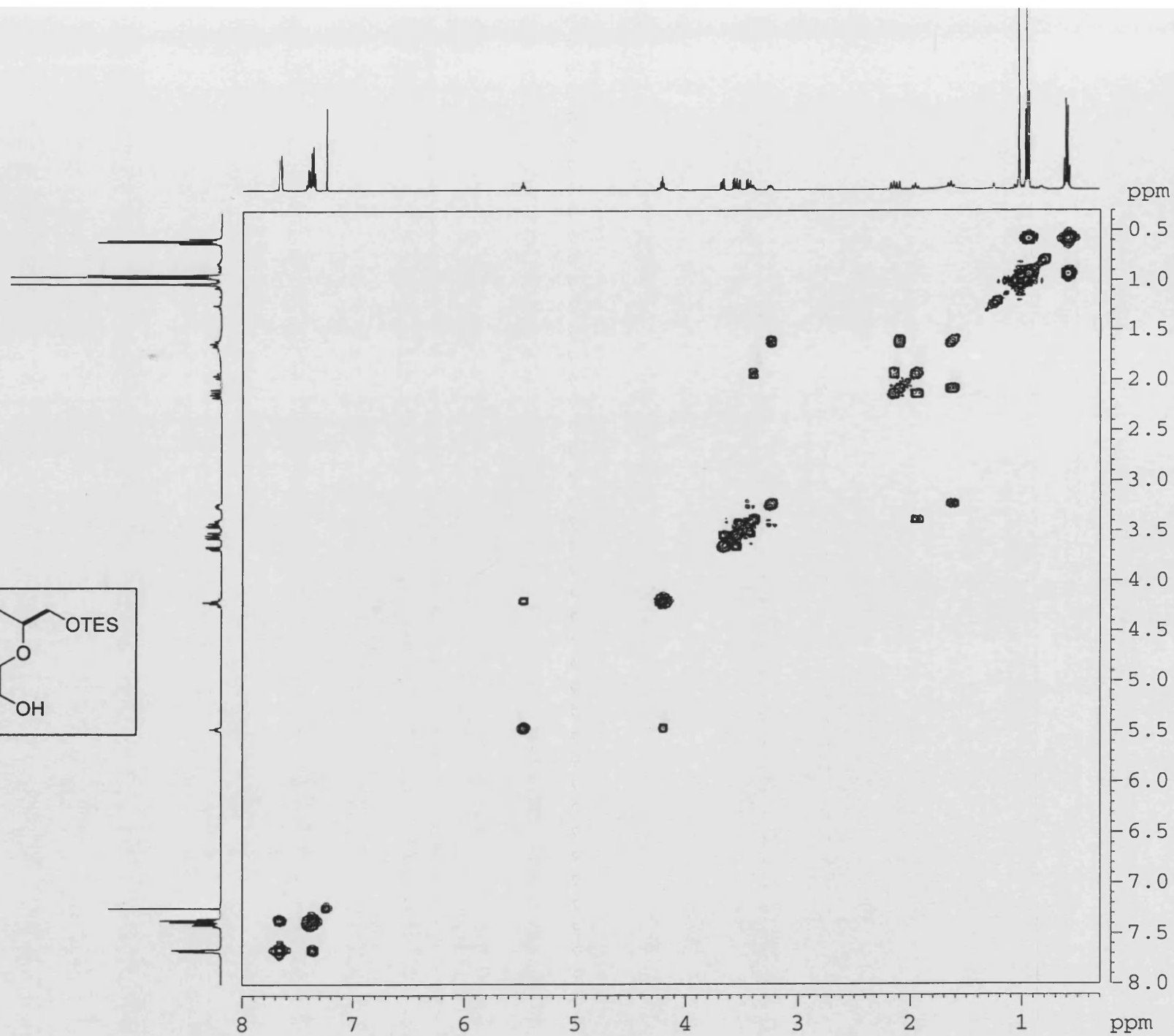
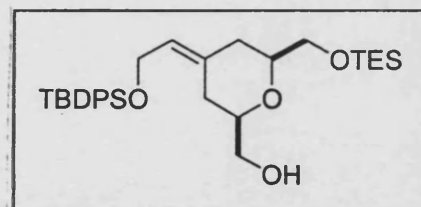
Sample: IV-MF-114

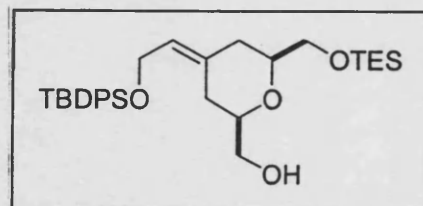
X: 64 scans, 16.0cm⁻¹, apod none, flat

IV-MF-114
CDCl₃
HMQC

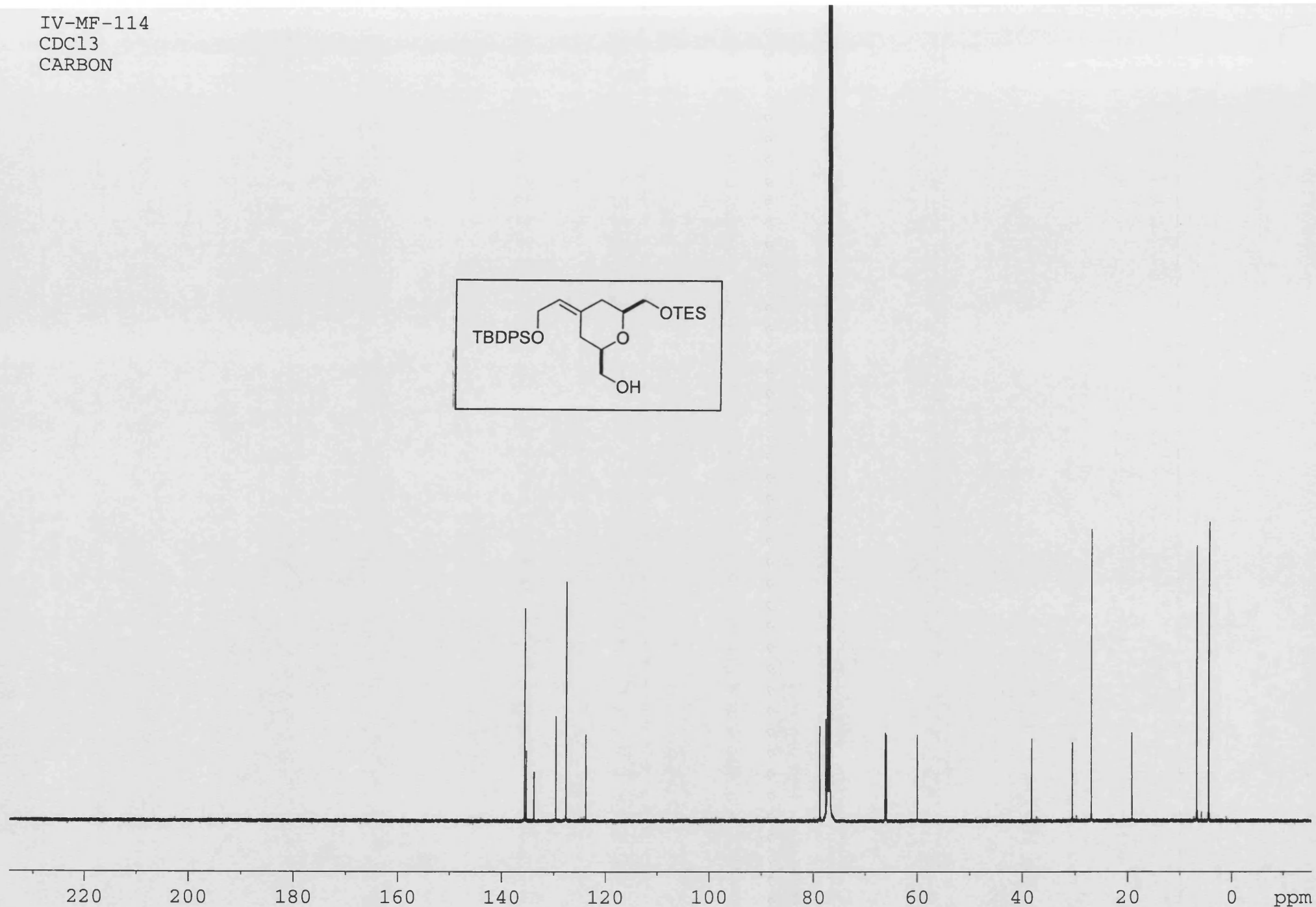
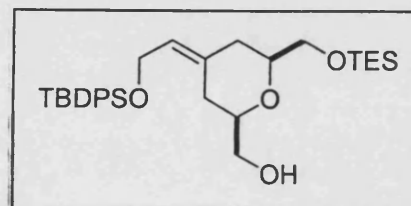


IV-MF-114
CDCl₃
COSY

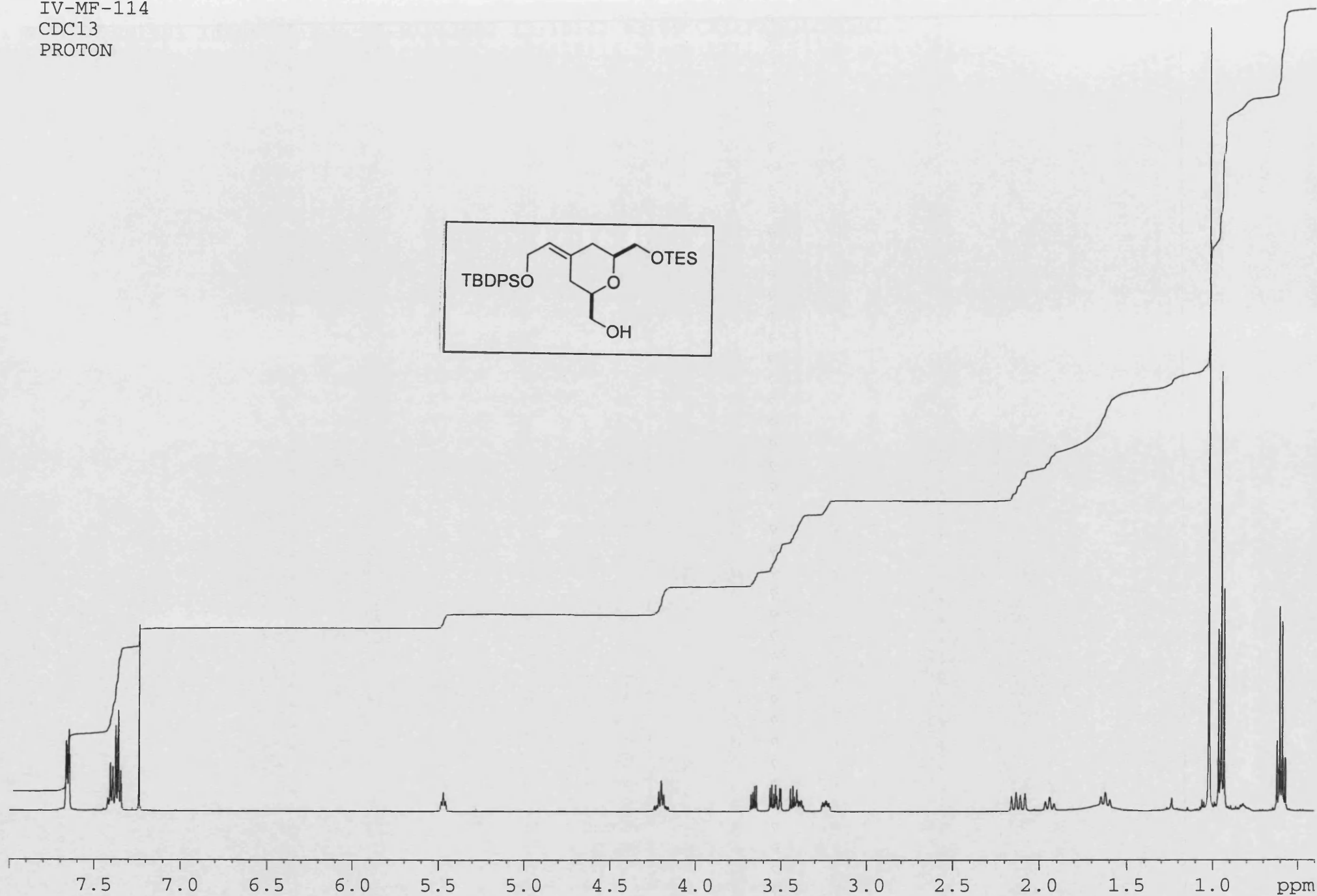
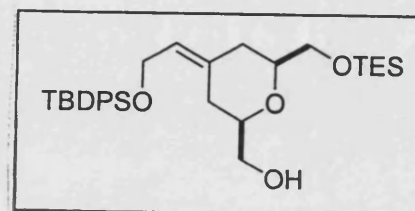


[illegible]

IV-MF-114
CDCl₃
CARBON



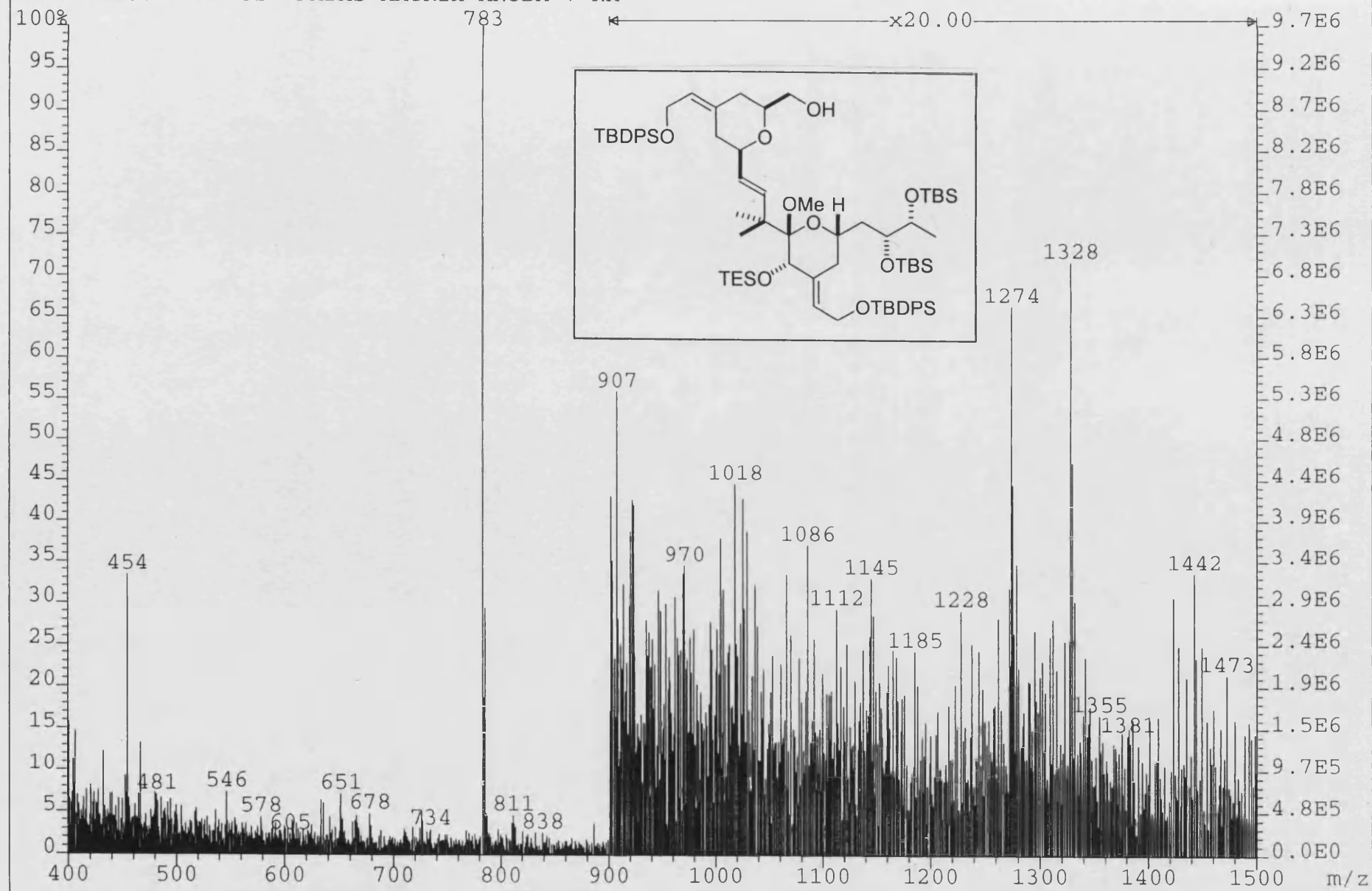
IV-MF-114
CDCl₃
PROTON

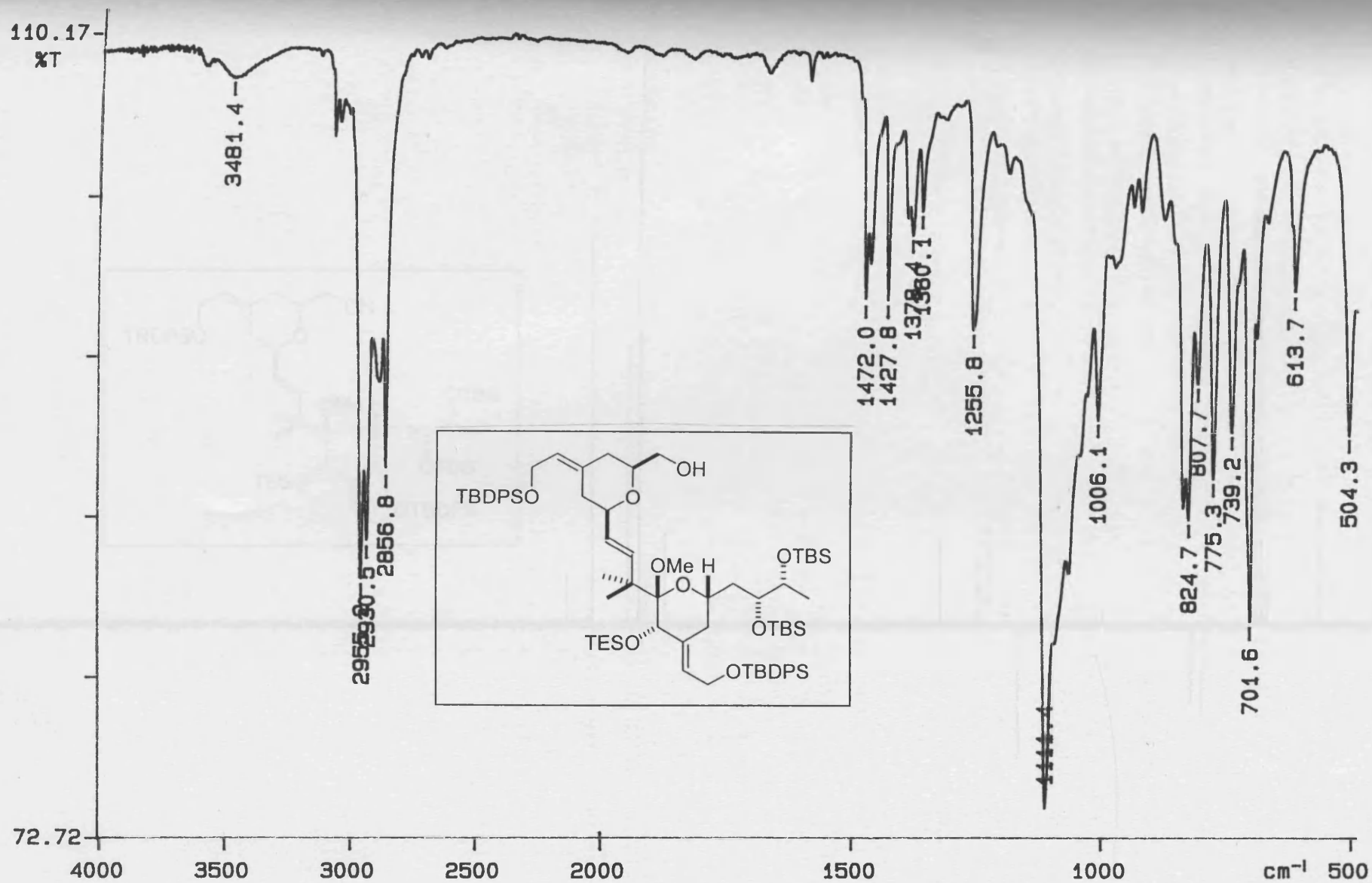


File:02SE1993 Ident:70 Acq:29-MAY-2002 13:10:42 +3:59 Cal:FABLM290502_1

ZAB-SE4F FAB+ Magnet BpI:23371080 TIC:2486428416 Flags:HALL

File Text:IV-MF-117 FABMS MATRIX MNOBA + NA





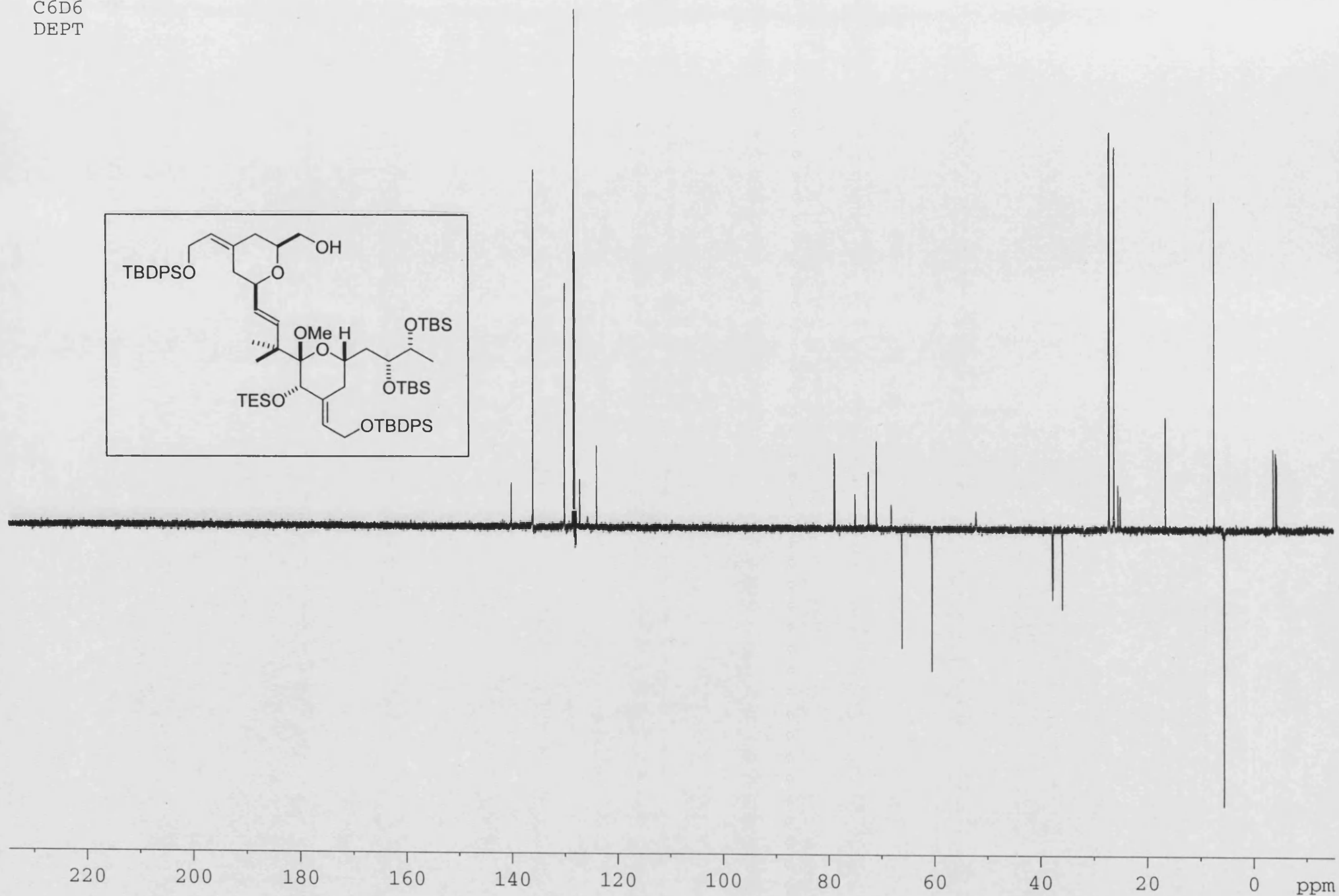
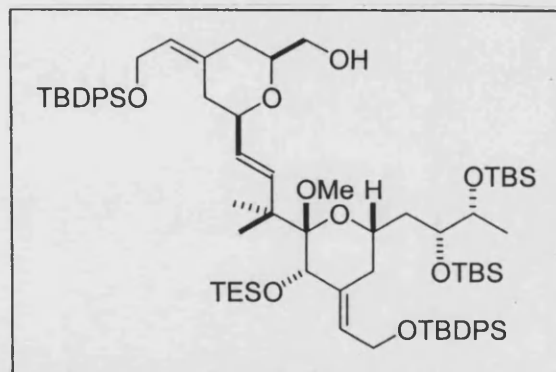
Y: 64 scans, 4.0cm⁻¹, flat

Year	2000	2001	2002	2003	2004	2005	2006	2007	2008	2009	2010	2011	2012	2013	2014	2015	2016	2017	2018	2019	2020	2021	2022	2023	2024	2025	2026	2027	2028	2029	2030	2031	2032	2033	2034	2035	2036	2037	2038	2039	2040	2041	2042	2043	2044	2045	2046	2047	2048	2049	2050	2051	2052	2053	2054	2055	2056	2057	2058	2059	2060	2061	2062	2063	2064	2065	2066	2067	2068	2069	2070	2071	2072	2073	2074	2075	2076	2077	2078	2079	2080	2081	2082	2083	2084	2085	2086	2087	2088	2089	2090	2091	2092	2093	2094	2095	2096	2097	2098	2099	2100																																																																																																																																																																																																																																														
Population	238	240	242	244	246	248	250	252	254	256	258	260	262	264	266	268	270	272	274	276	278	280	282	284	286	288	290	292	294	296	298	300	302	304	306	308	310	312	314	316	318	320	322	324	326	328	330	332	334	336	338	340	342	344	346	348	350	352	354	356	358	360	362	364	366	368	370	372	374	376	378	380	382	384	386	388	390	392	394	396	398	400	402	404	406	408	410	412	414	416	418	420	422	424	426	428	430	432	434	436	438	440	442	444	446	448	450	452	454	456	458	460	462	464	466	468	470	472	474	476	478	480	482	484	486	488	490	492	494	496	498	500	502	504	506	508	510	512	514	516	518	520	522	524	526	528	530	532	534	536	538	540	542	544	546	548	550	552	554	556	558	560	562	564	566	568	570	572	574	576	578	580	582	584	586	588	590	592	594	596	598	600	602	604	606	608	610	612	614	616	618	620	622	624	626	628	630	632	634	636	638	640	642	644	646	648	650	652	654	656	658	660	662	664	666	668	670	672	674	676	678	680	682	684	686	688	690	692	694	696	698	700	702	704	706	708	710	712	714	716	718	720	722	724	726	728	730	732	734	736	738	740	742	744	746	748	750	752	754	756	758	760	762	764	766	768	770	772	774	776	778	780	782	784	786	788	790	792	794	796	798	800	802	804	806	808	810	812	814	816	818	820	822	824	826	828	830	832	834	836	838	840	842	844	846	848	850	852	854	856	858	860	862	864	866	868	870	872	874	876	878	880	882	884	886	888	890	892	894	896	898	900	902	904	906	908	910	912	91

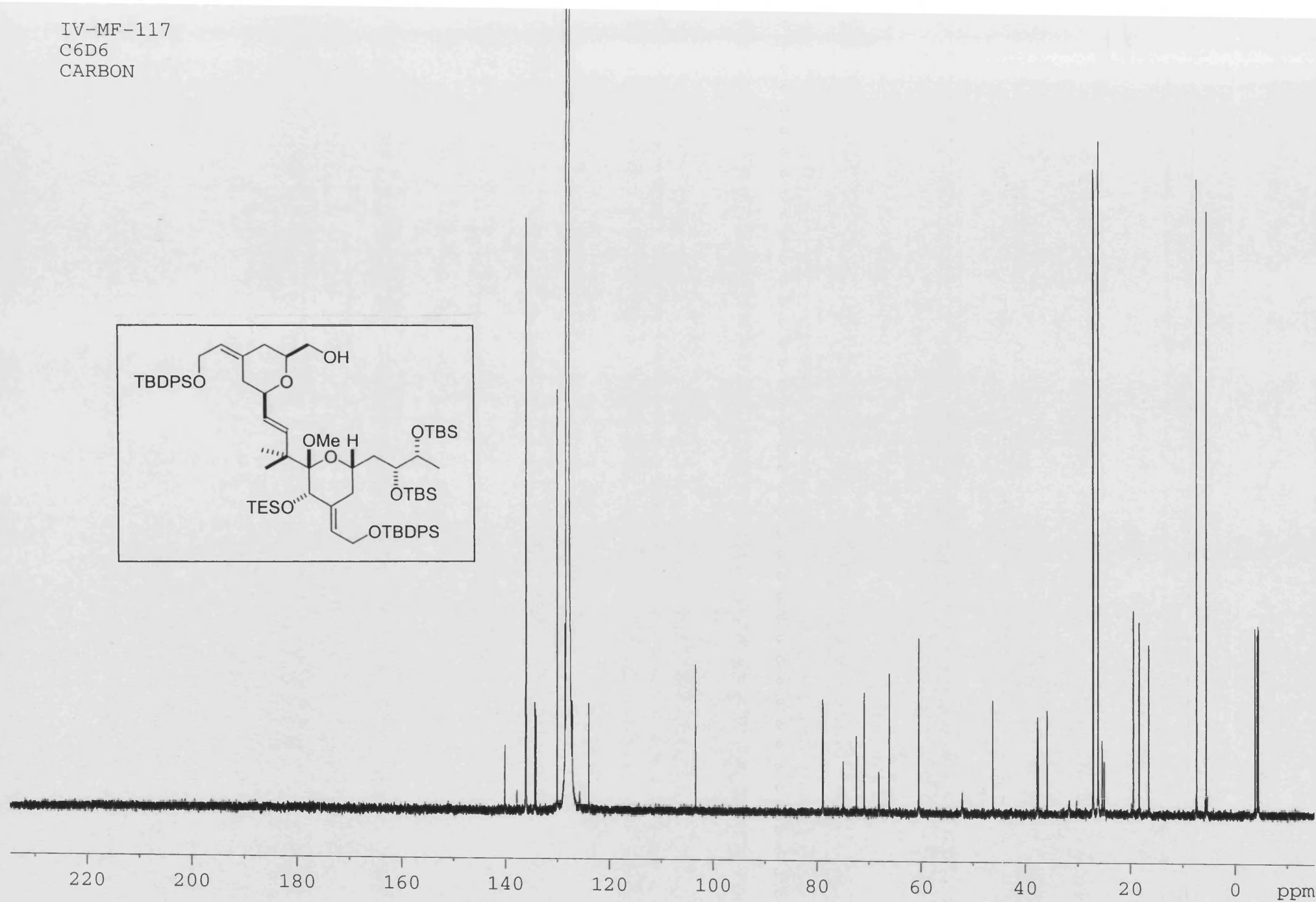
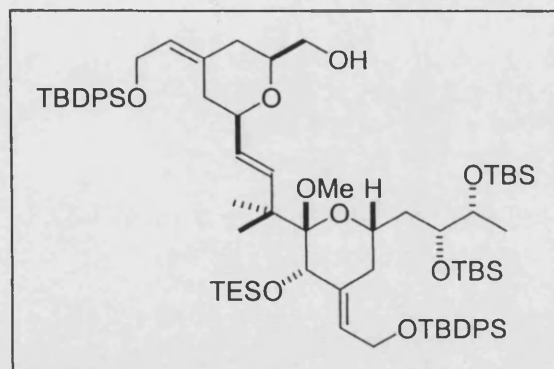
IV-MF-117

C6D6

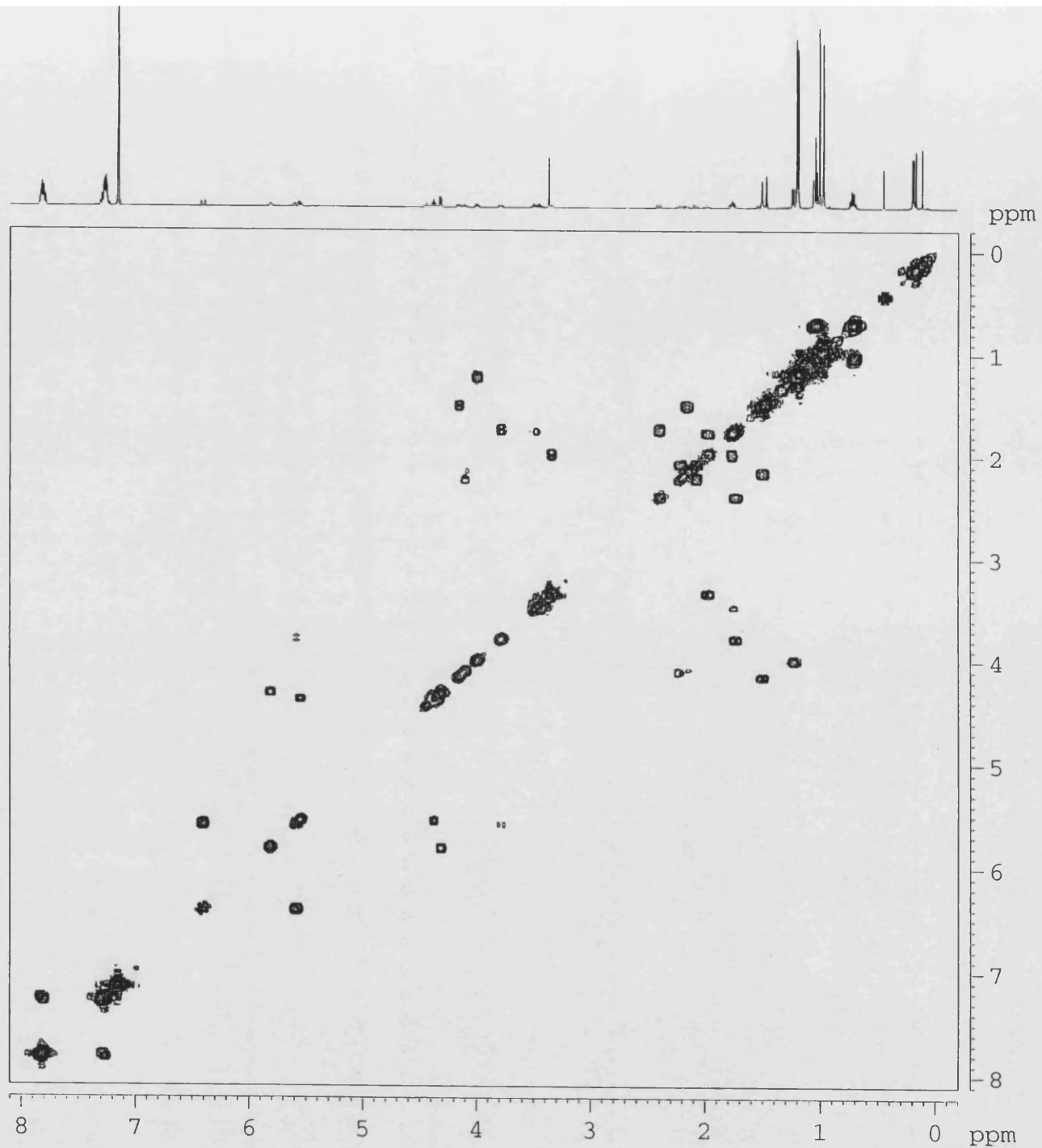
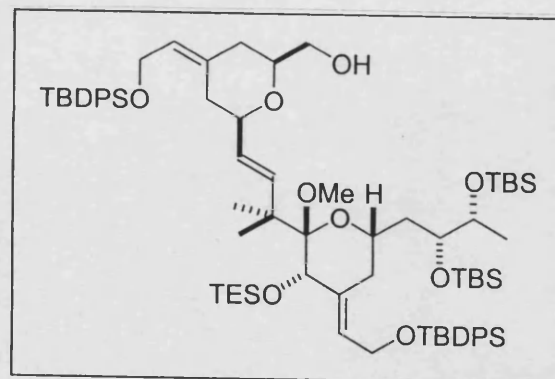
DEPT



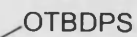
IV-MF-117
C6D6
CARBON



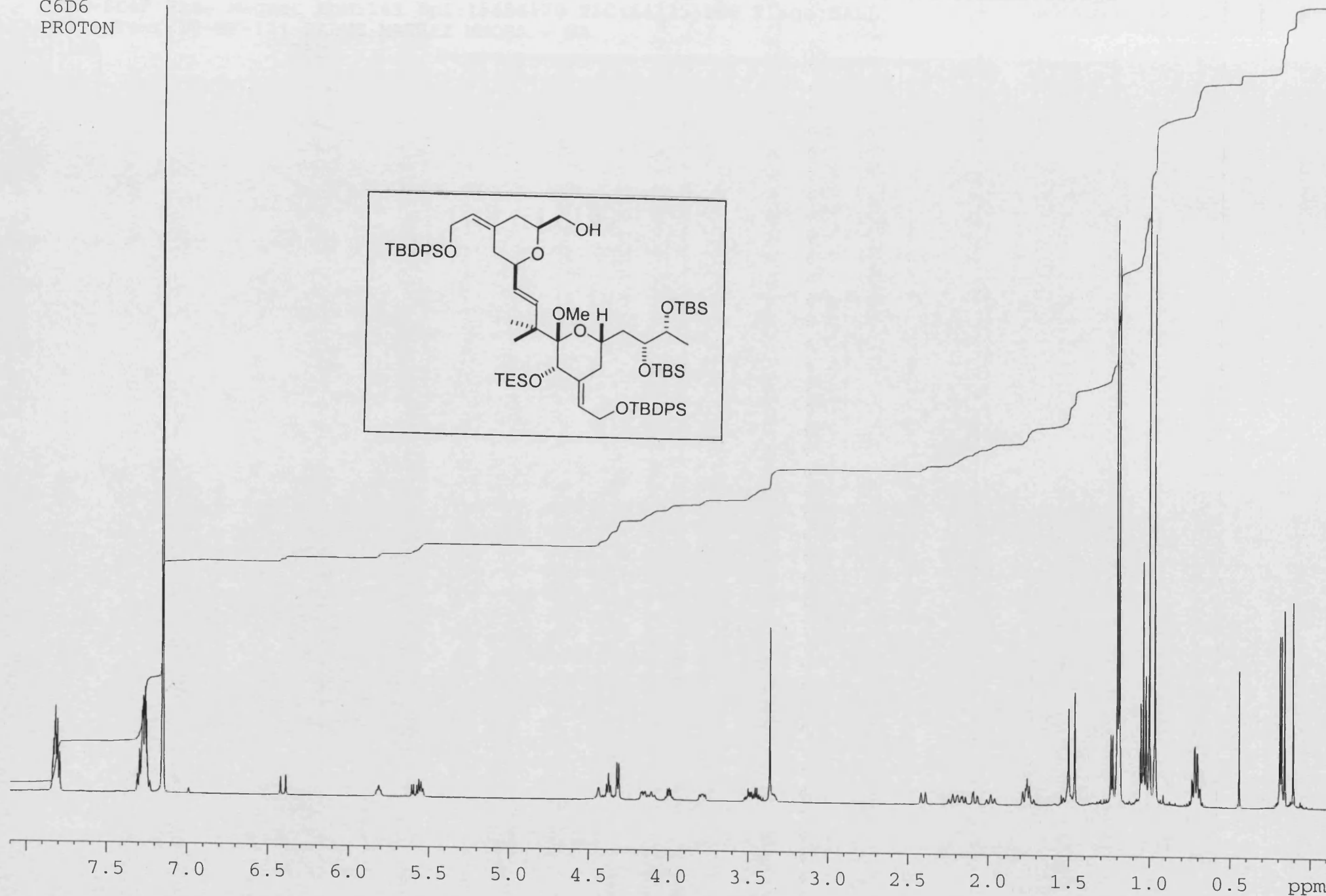
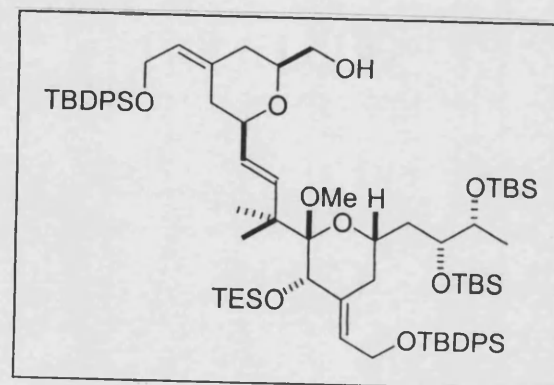
IV-MF-117
C6D6
COSY



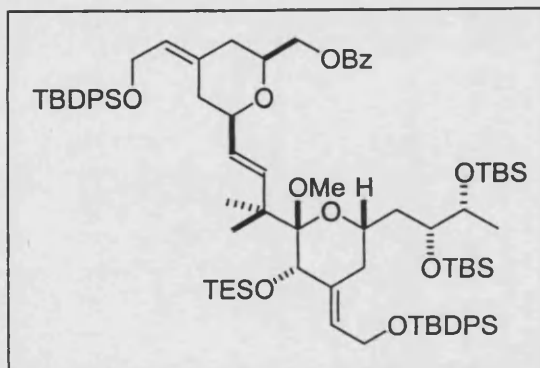
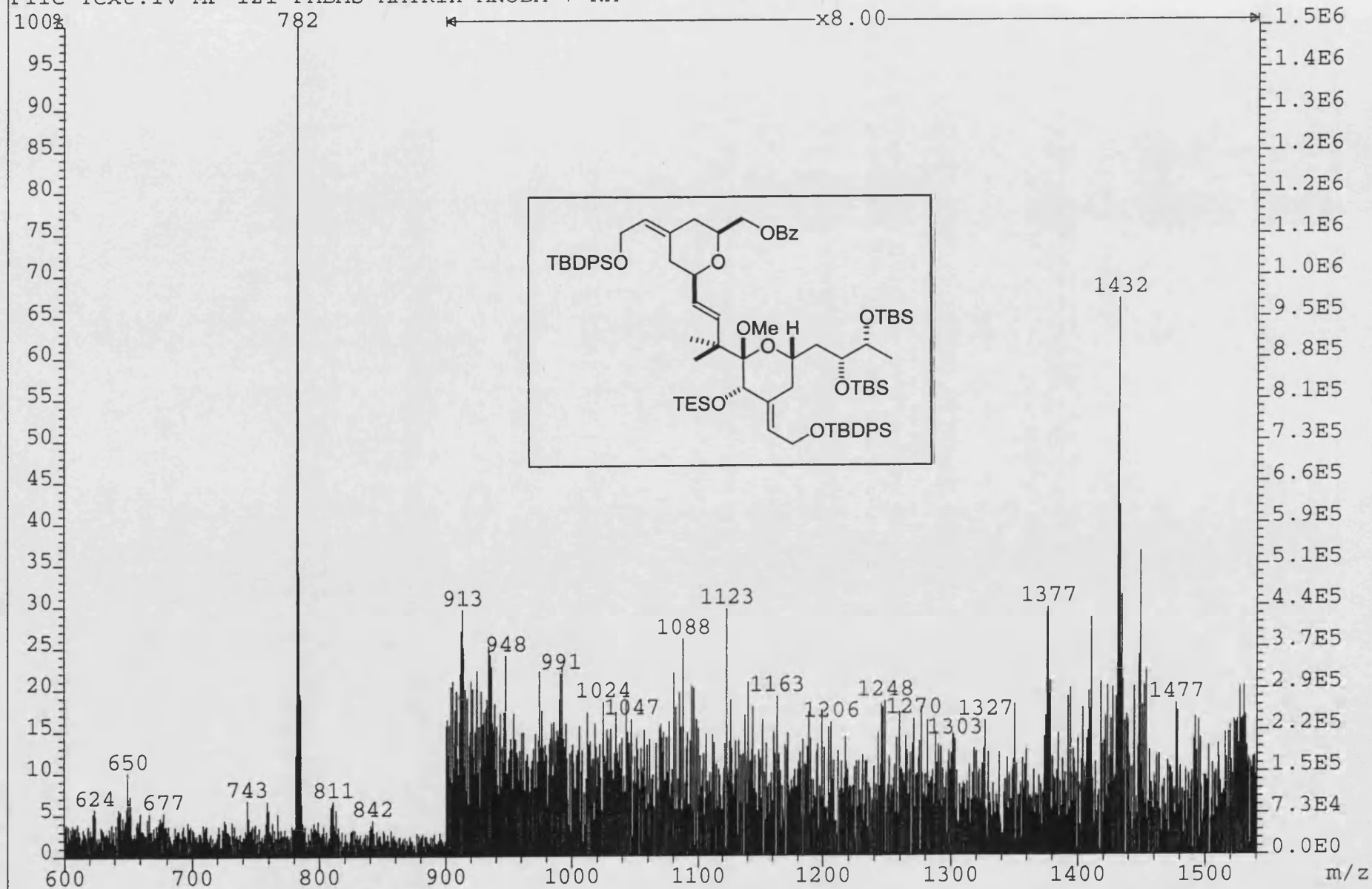
NOESY

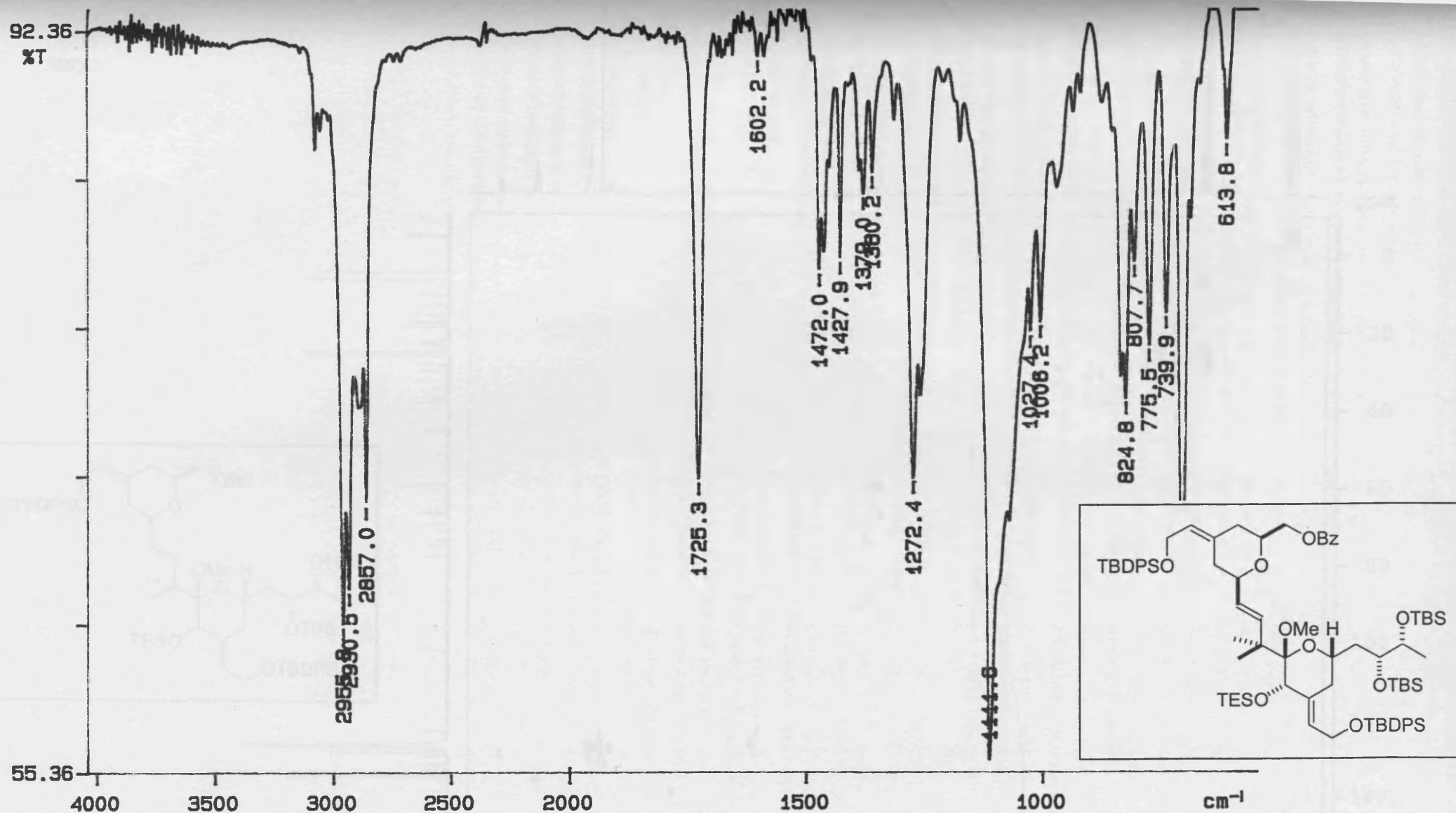


IV-MF-117
C6D6
PROTON



File Text:IV-MF-121 FABMS MATRIX MNOBA + NA

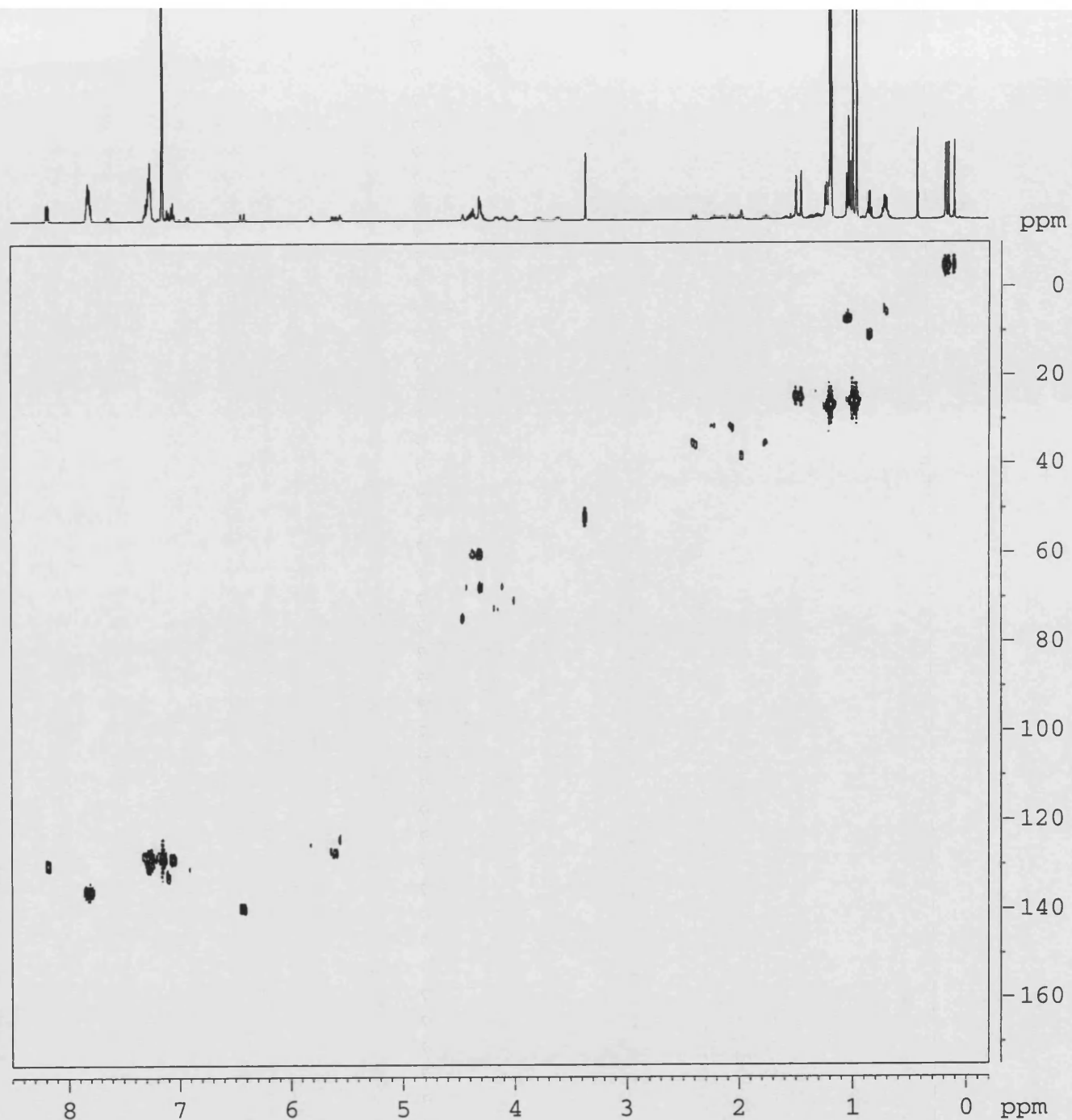
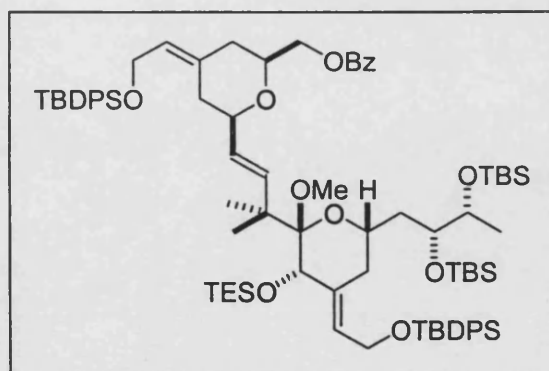




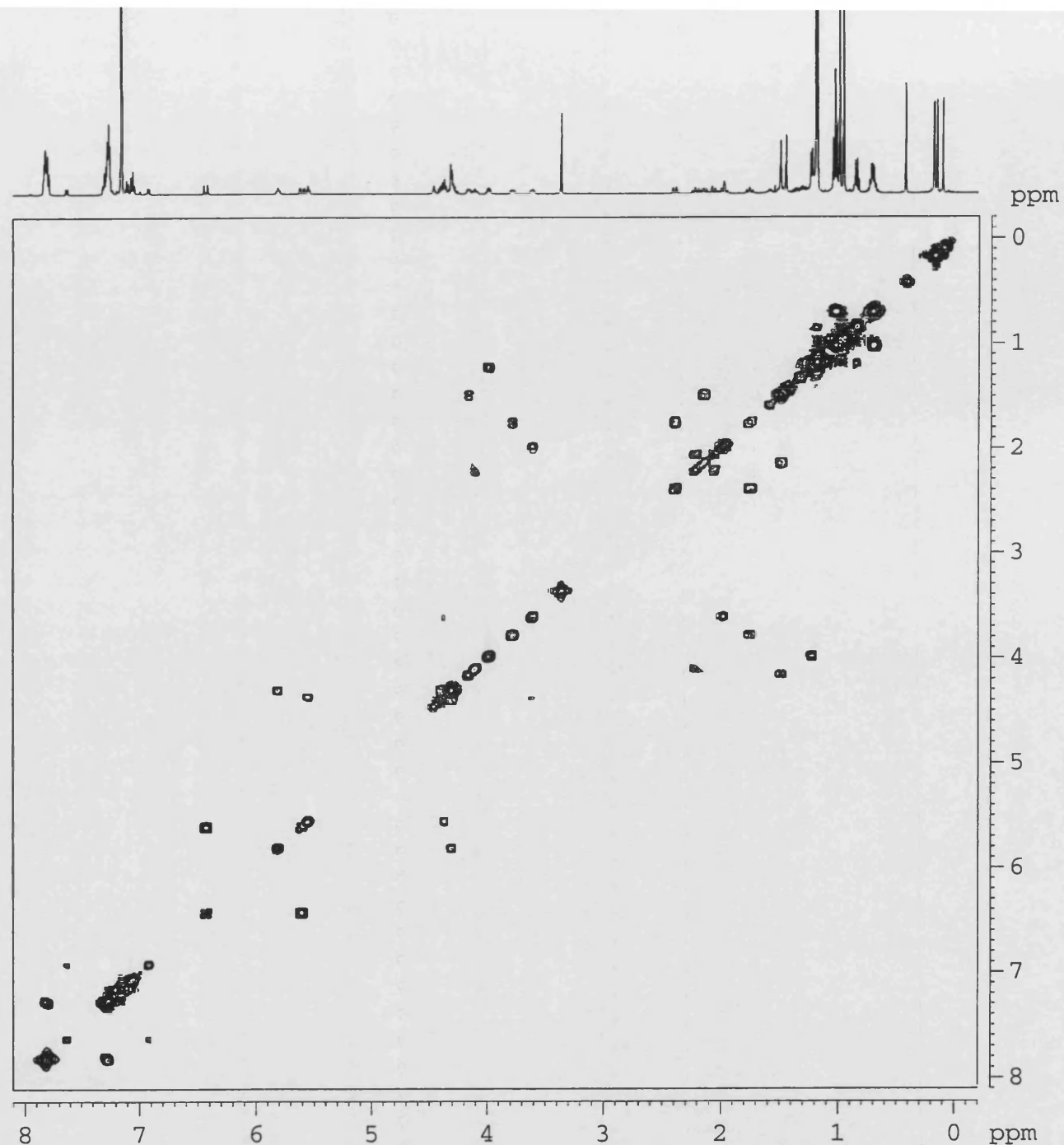
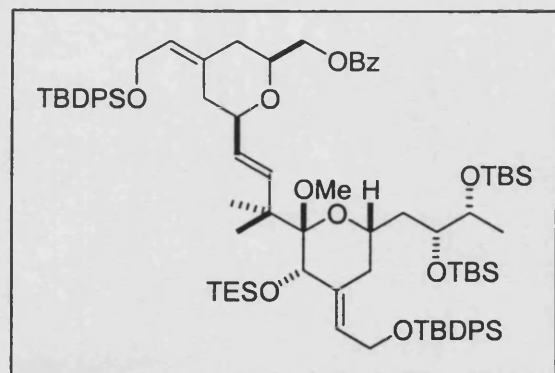
02/06/07 09:13

Y: 64 scans, 4.0cm⁻¹

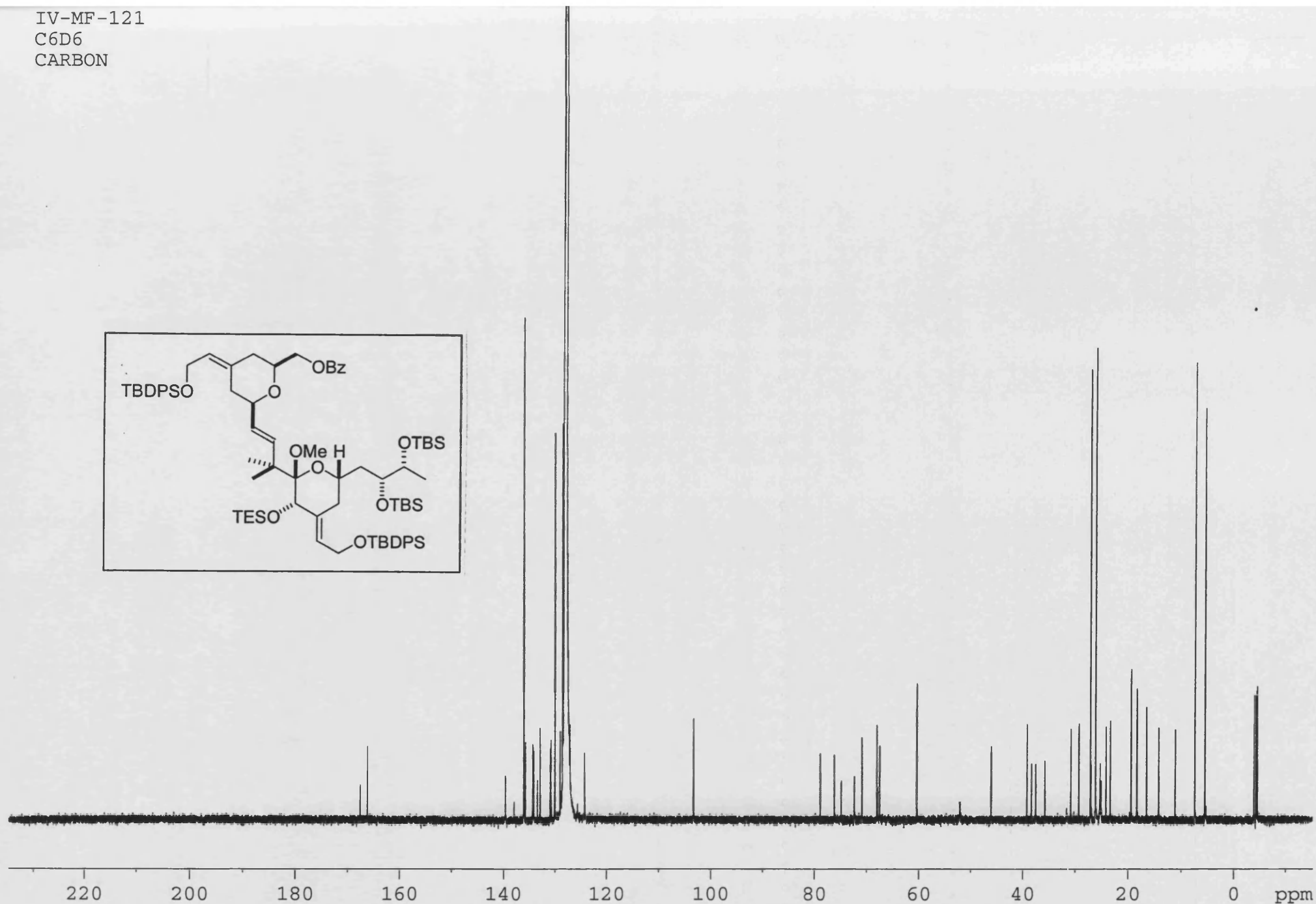
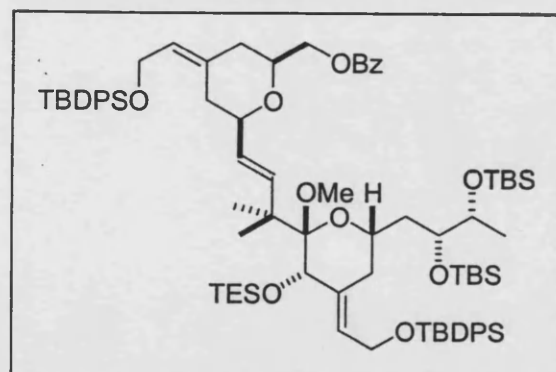
IV-MF-121
C6D6
HMQC



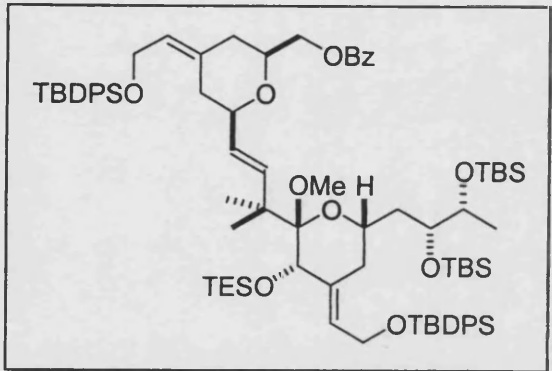
IV-MF-121
C6D6
COSY



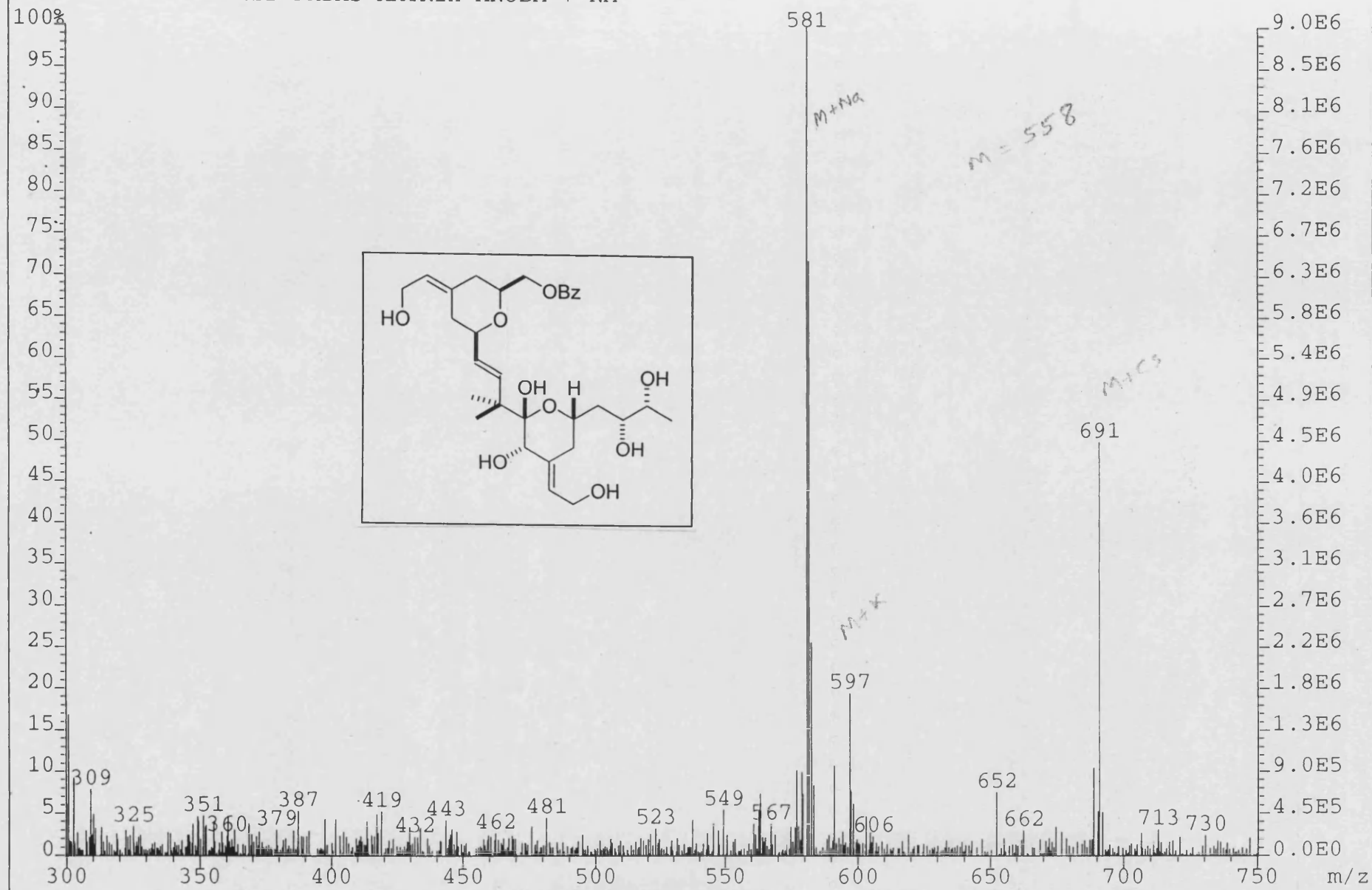
IV-MF-121
C6D6
CARBON



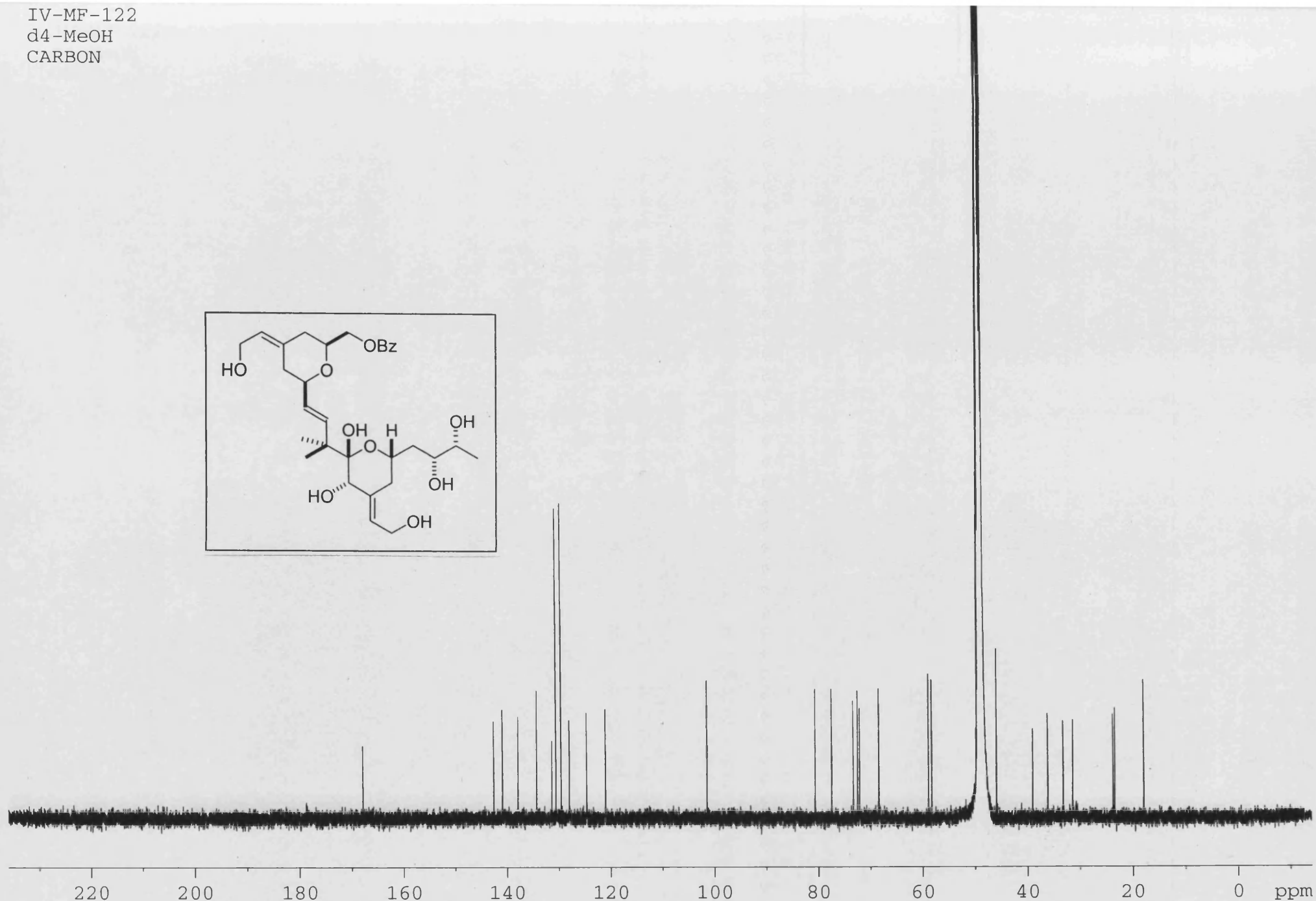
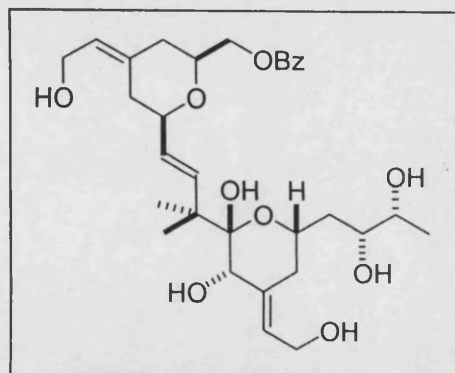
PROTON



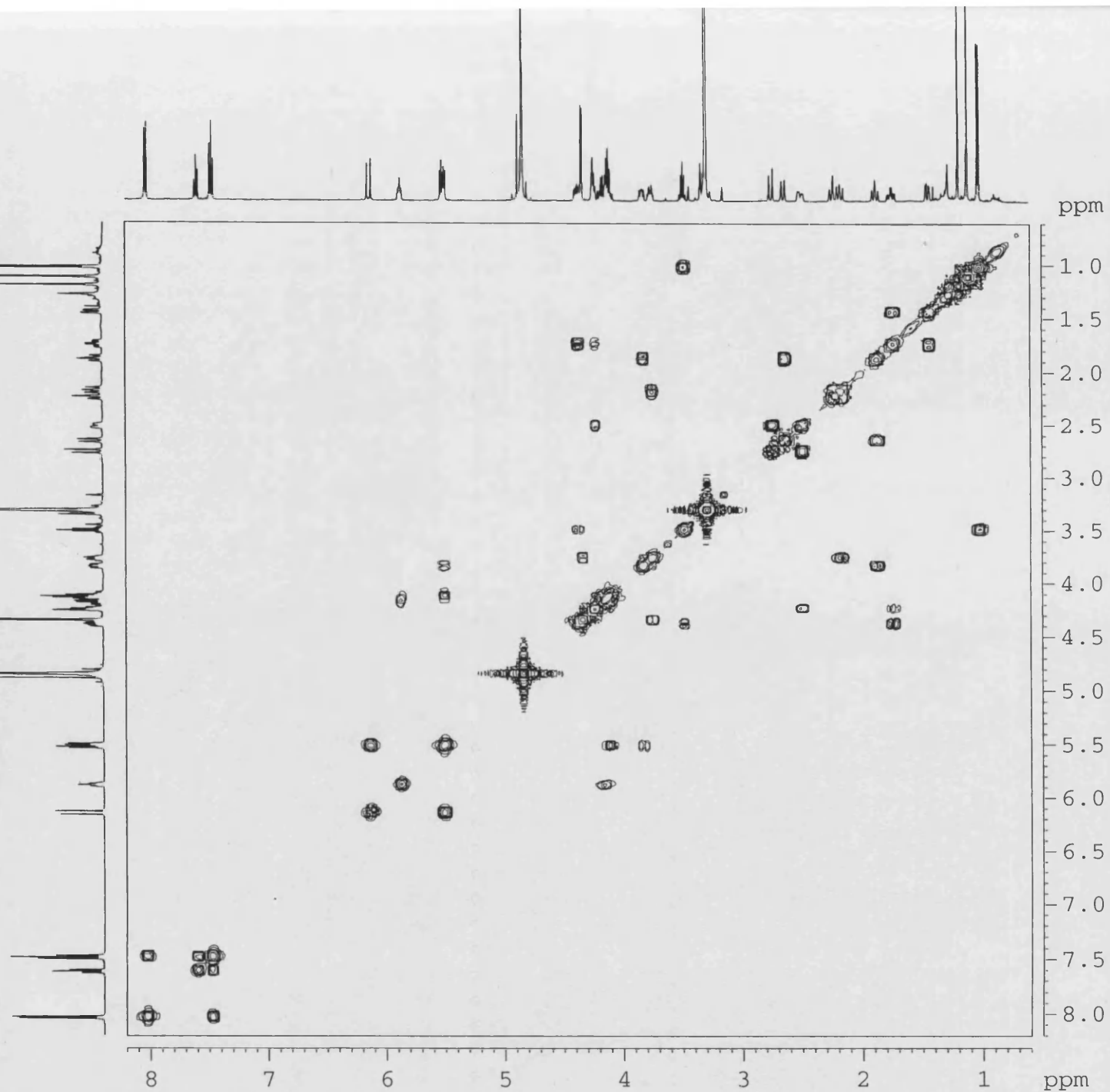
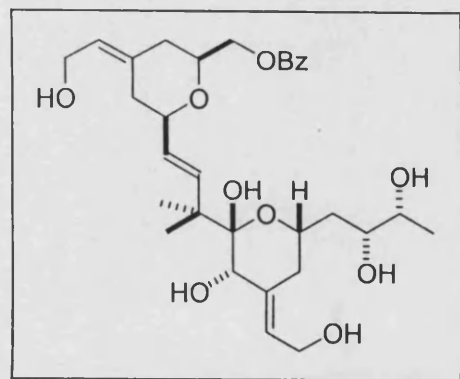
File Text:IV-MF-122 FABMS MATRIX MNOBA + NA



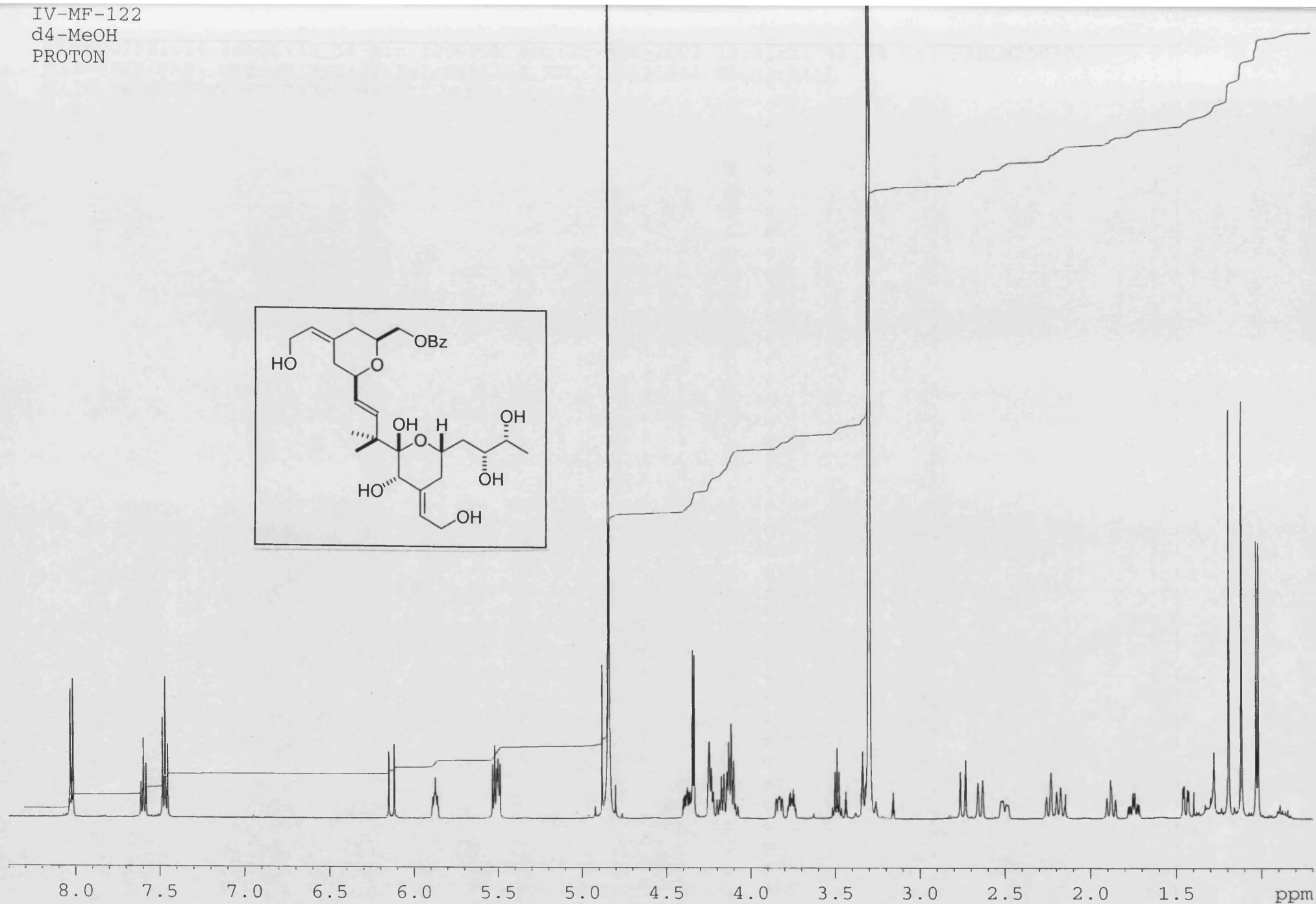
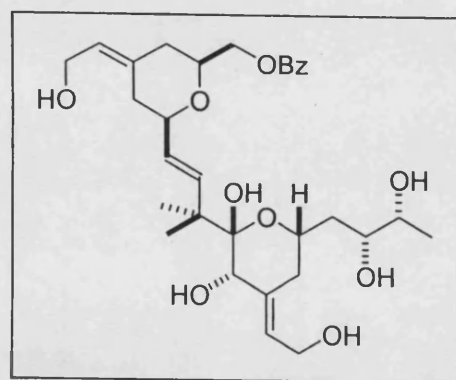
IV-MF-122
d4-MeOH
CARBON



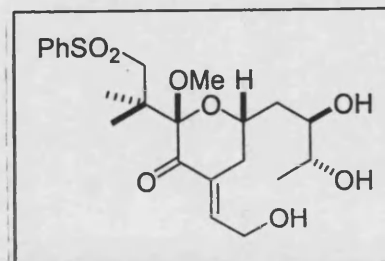
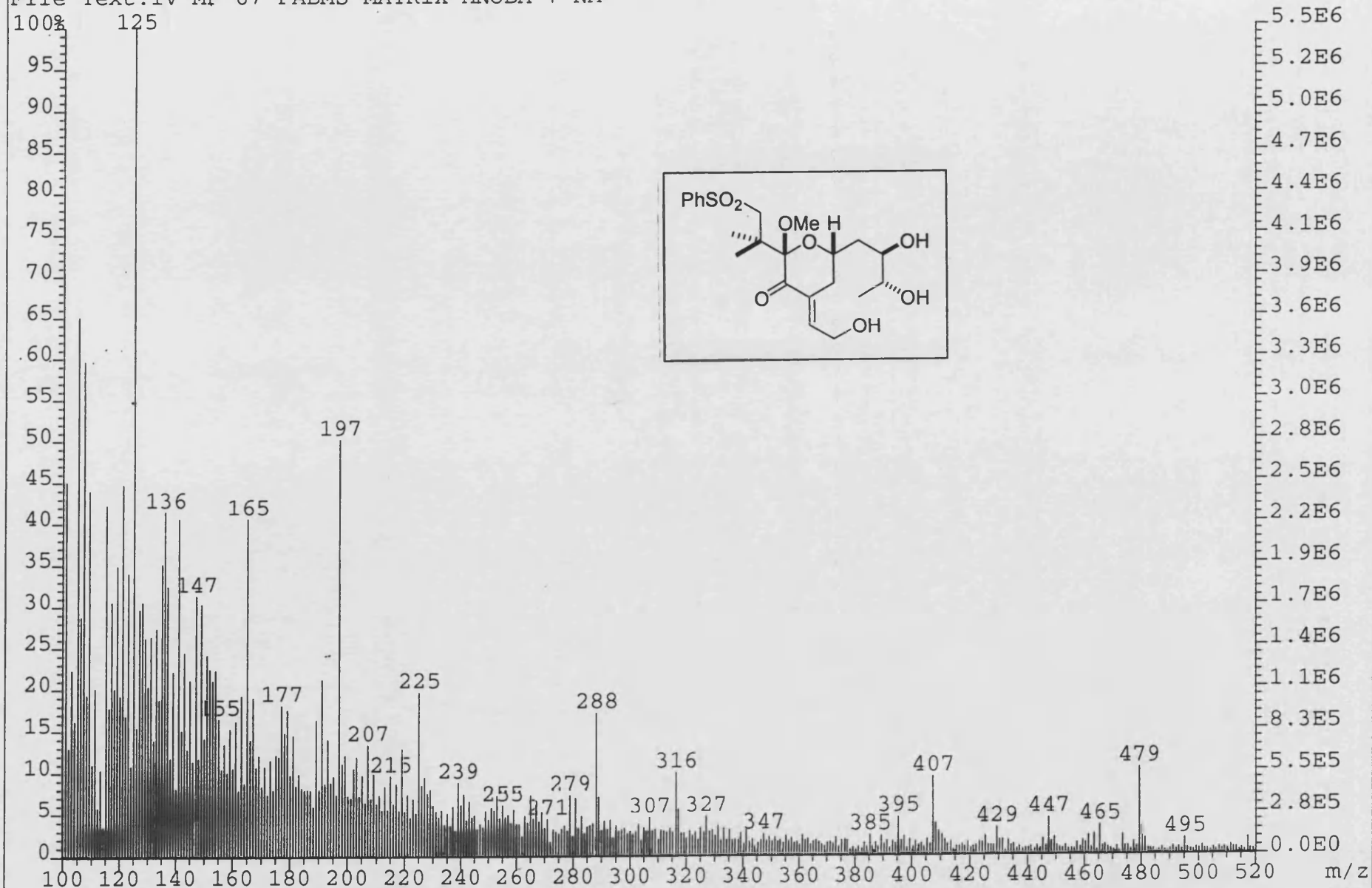
IV-MF-122
d4-MeOH
COSY



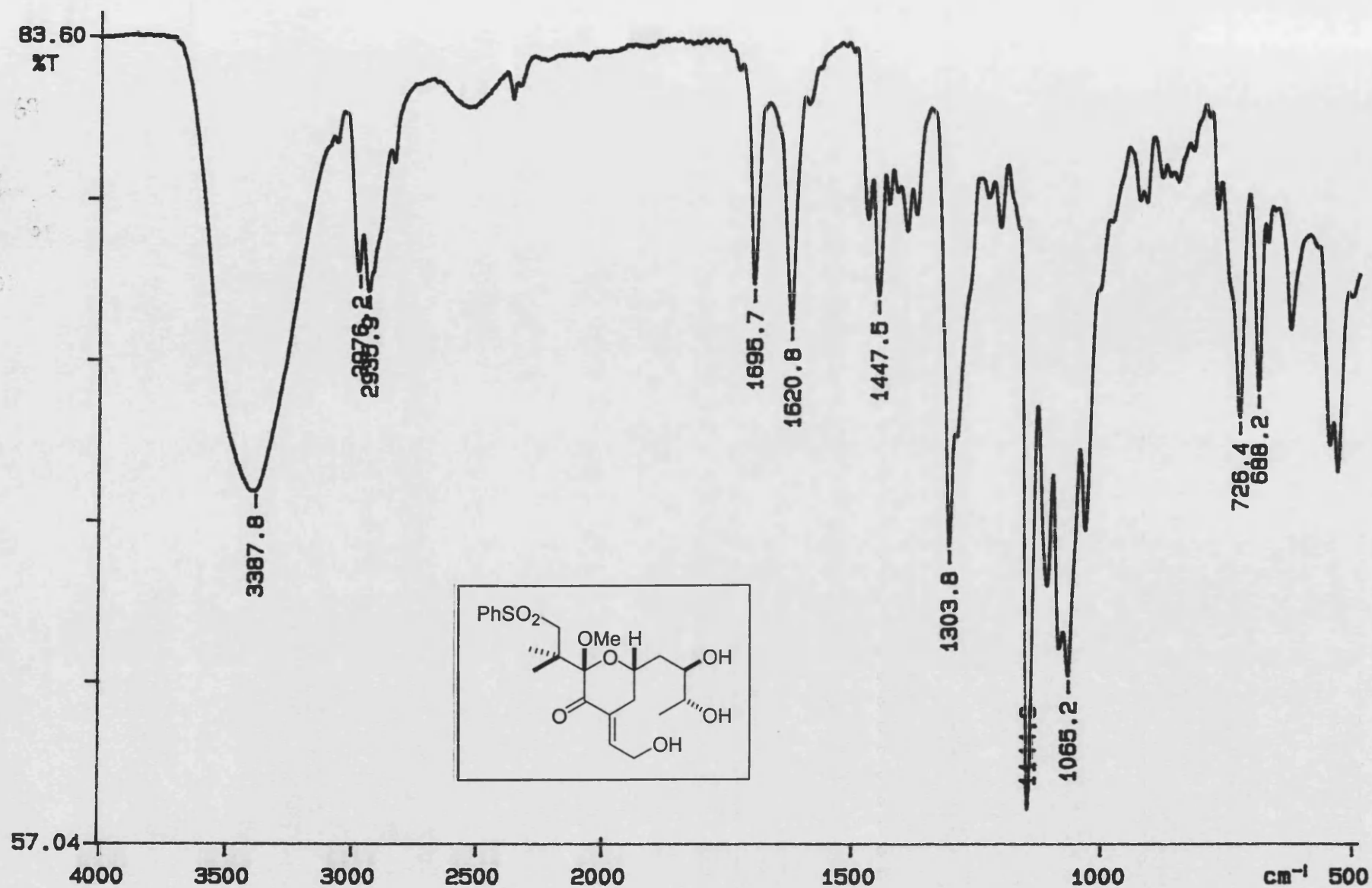
IV-MF-122
d4-MeOH
PROTON



File Text:IV-MF-67 FABMS MATRIX MNOBA + NA



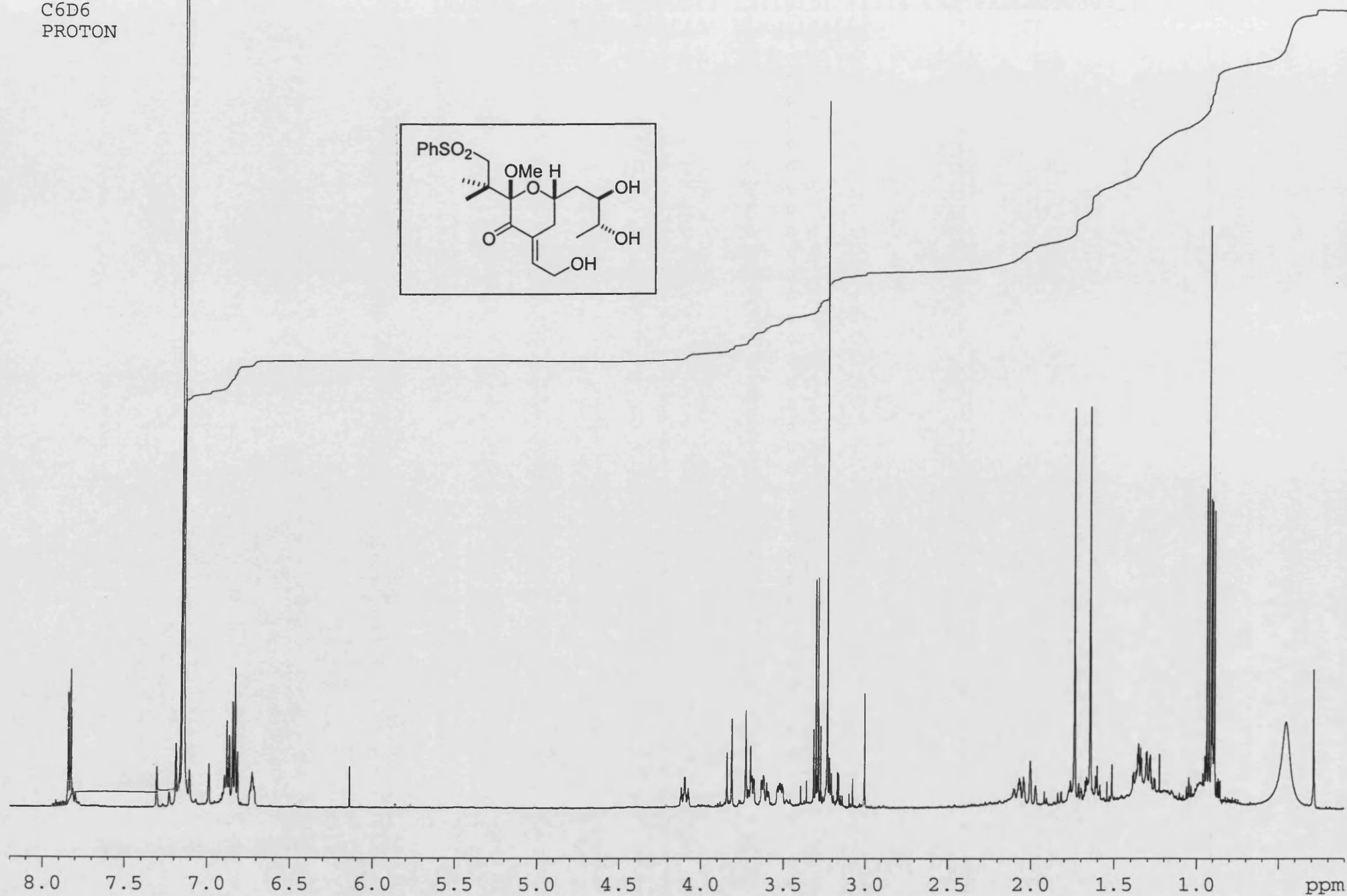
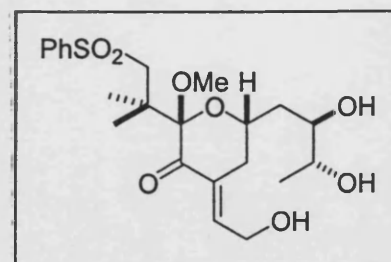
PERKIN ELMER



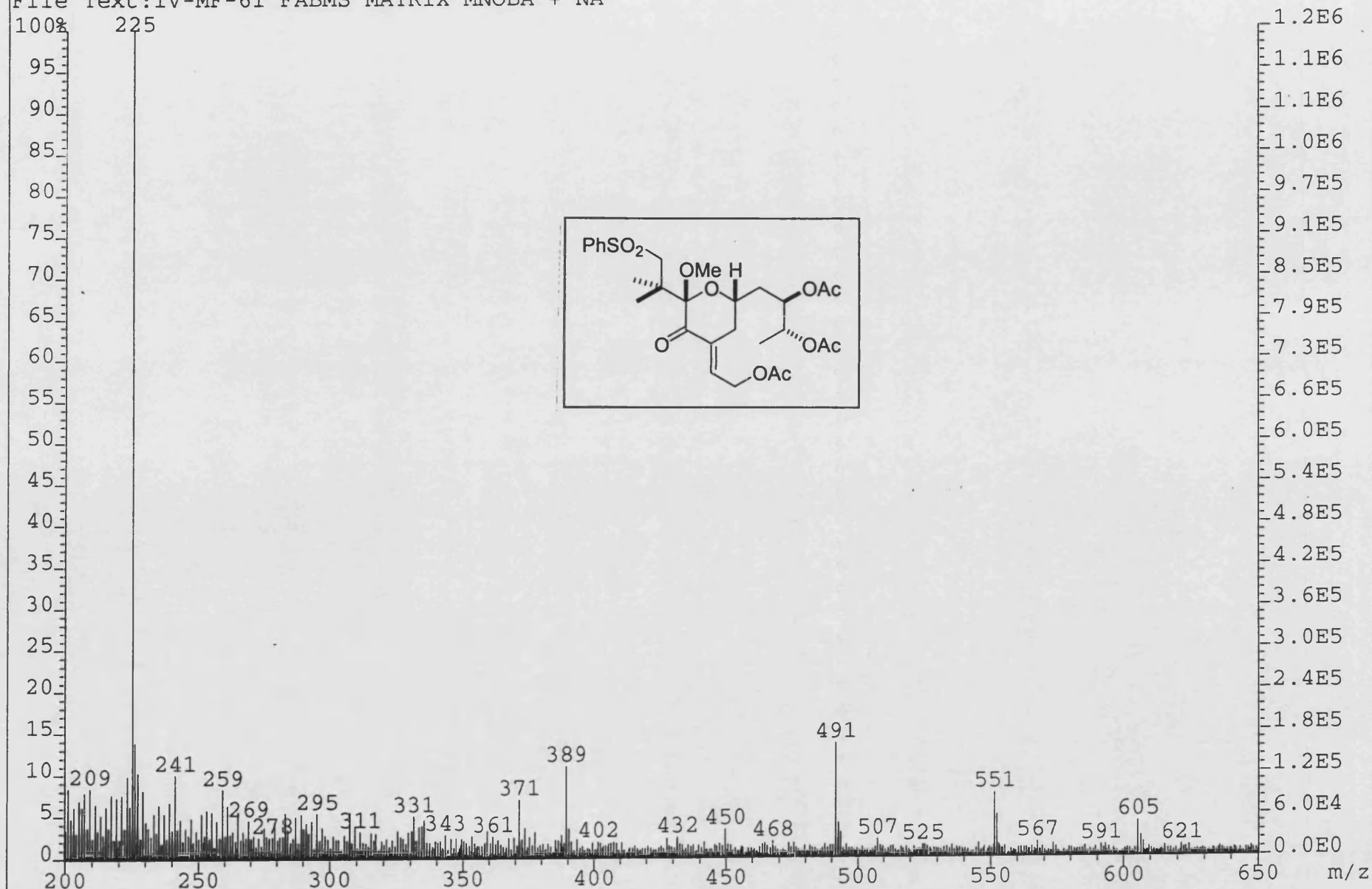
02/03/04 17:33

Y: 16 scans, 16.0 cm^{-1} , apod none, flat

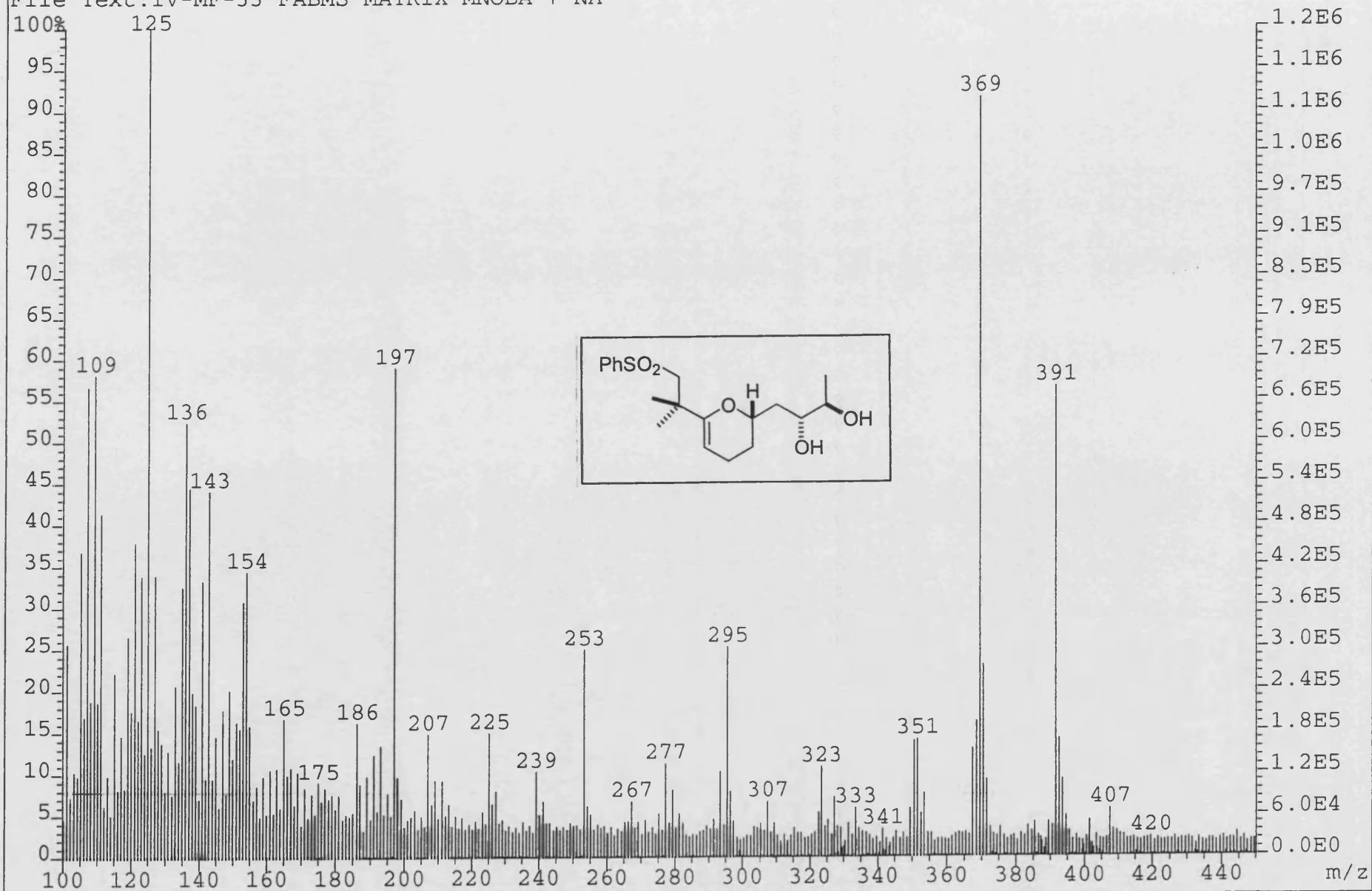
IV-MF-67
C6D6
PROTON



File:02SE1025 Ident:17_24 Win 1000PPM Acq:25-MAR-2002 12:10:51 +1:14 Cal:FABLM250302_1
ZAB-SE4F FAB+ Magnet BpM:225 BpI:1208704 TIC:46230404 Flags:HALL
File Text:IV-MF-61 FABMS MATRIX MNOBA + NA



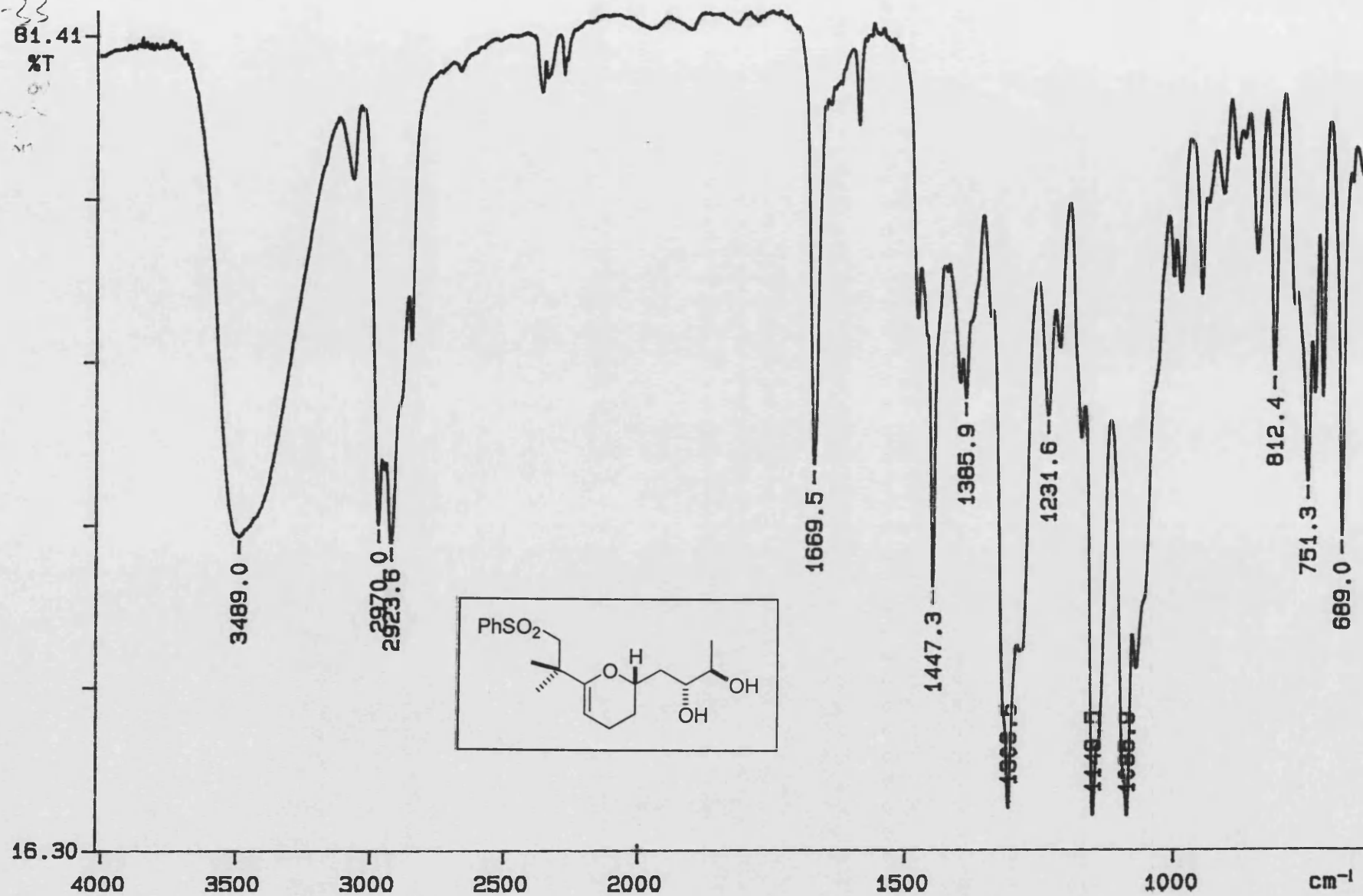
File:02SE280 Ident:6_10 Win 1000PPM Acq:29-JAN-2002 16:10:45 +0:29 Cal:FABLM280102_1
ZAB-SE4F FAB+ Magnet BpM:125 BpI:1208320 TIC:50721232 Flags:HALL
File Text:IV-MF-33 FABMS MATRIX MNOBA + NA



PERKIN ELMER

IV-MF-23

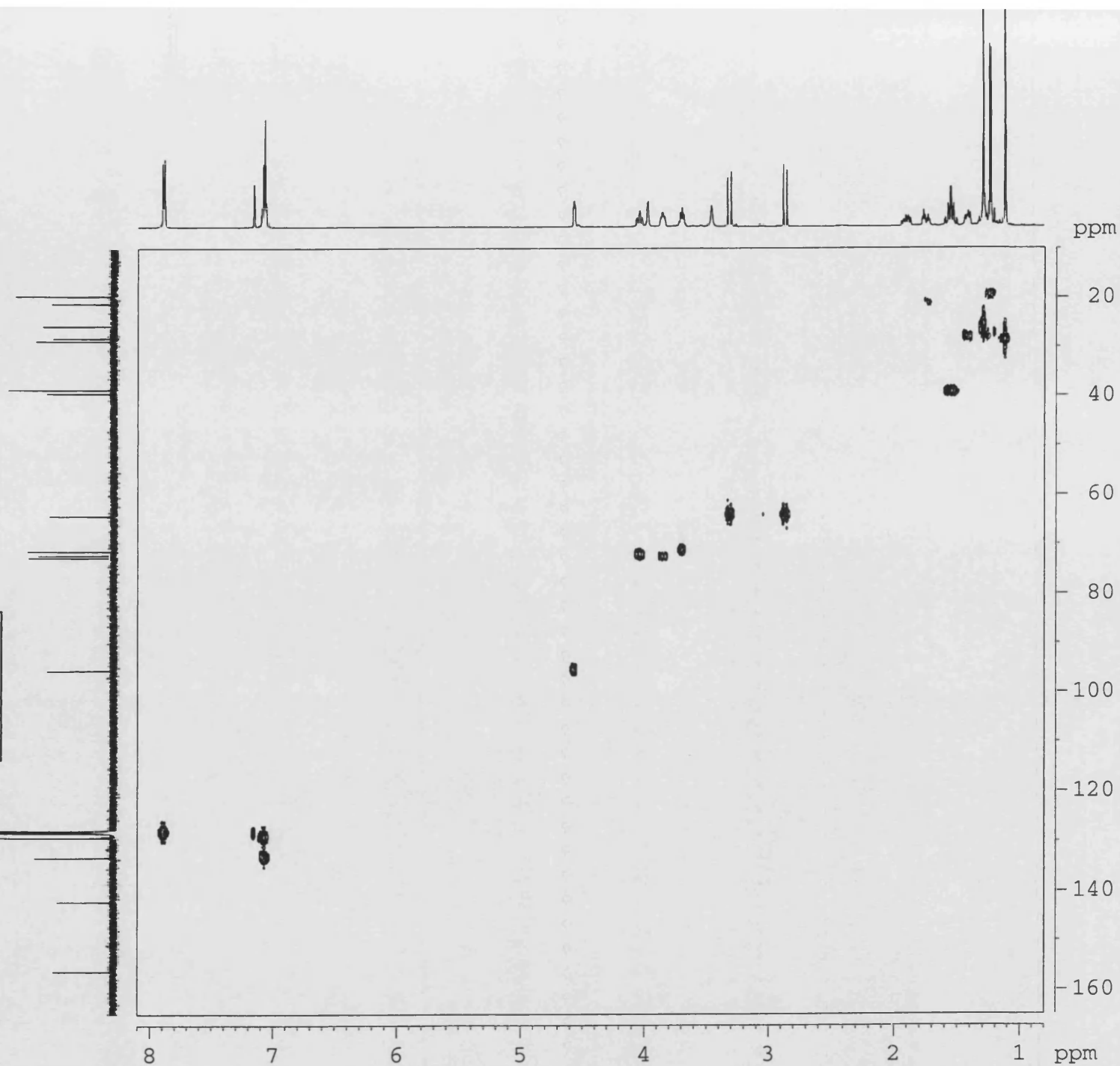
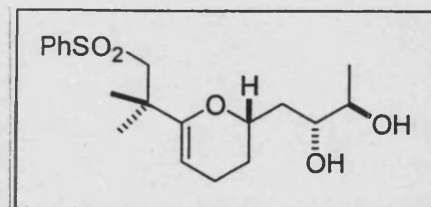
81.41
%T



02/01/23 09:28

Y: 64 scans, 4.0cm⁻¹

IV-MF-33
HMQC
C6D6

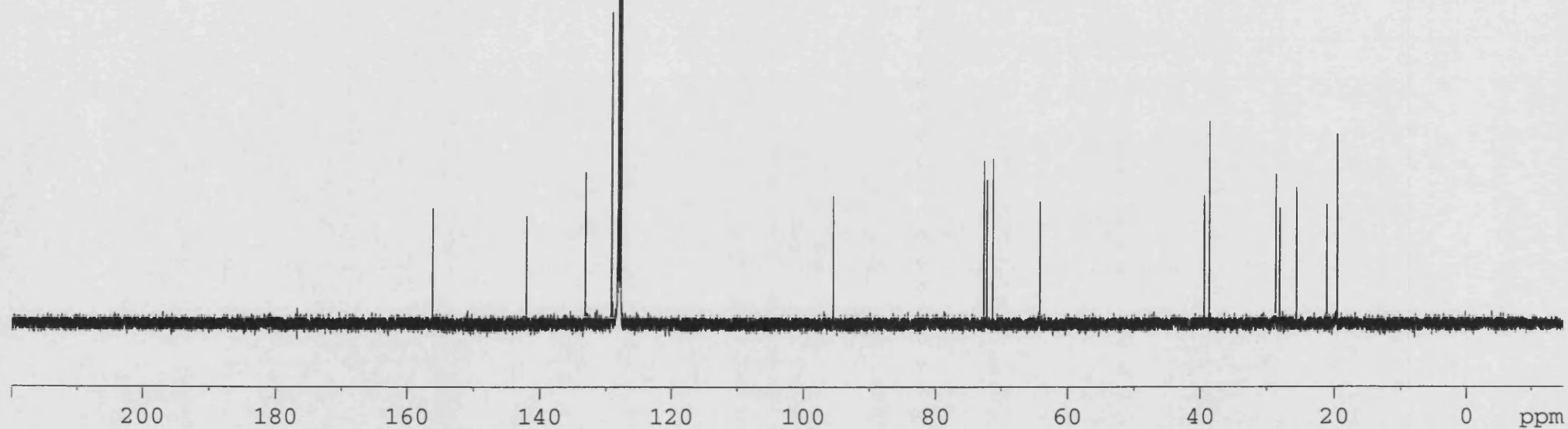
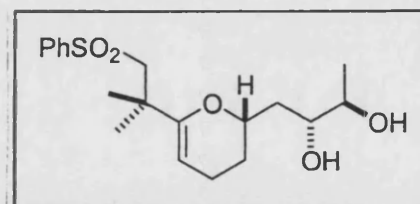


IV-MF-33
DEPT
C6D6

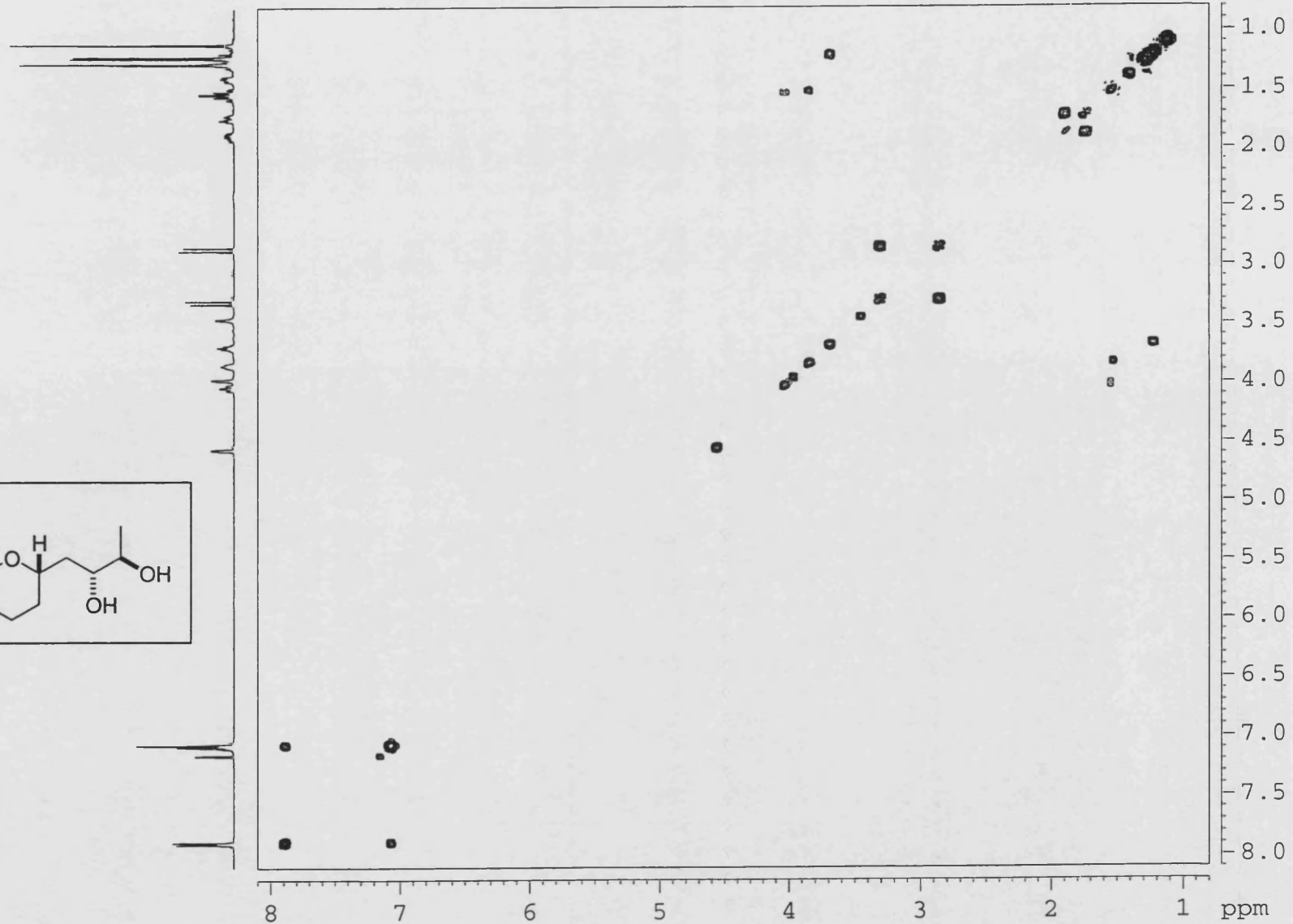
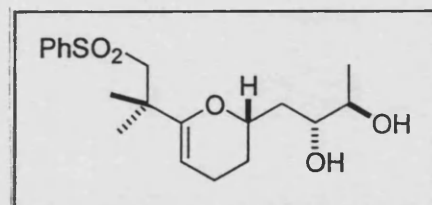


190 180 170 160 150 140 130 120 110 100 90 80 70 60 50 40 30 20 10 0 ppm

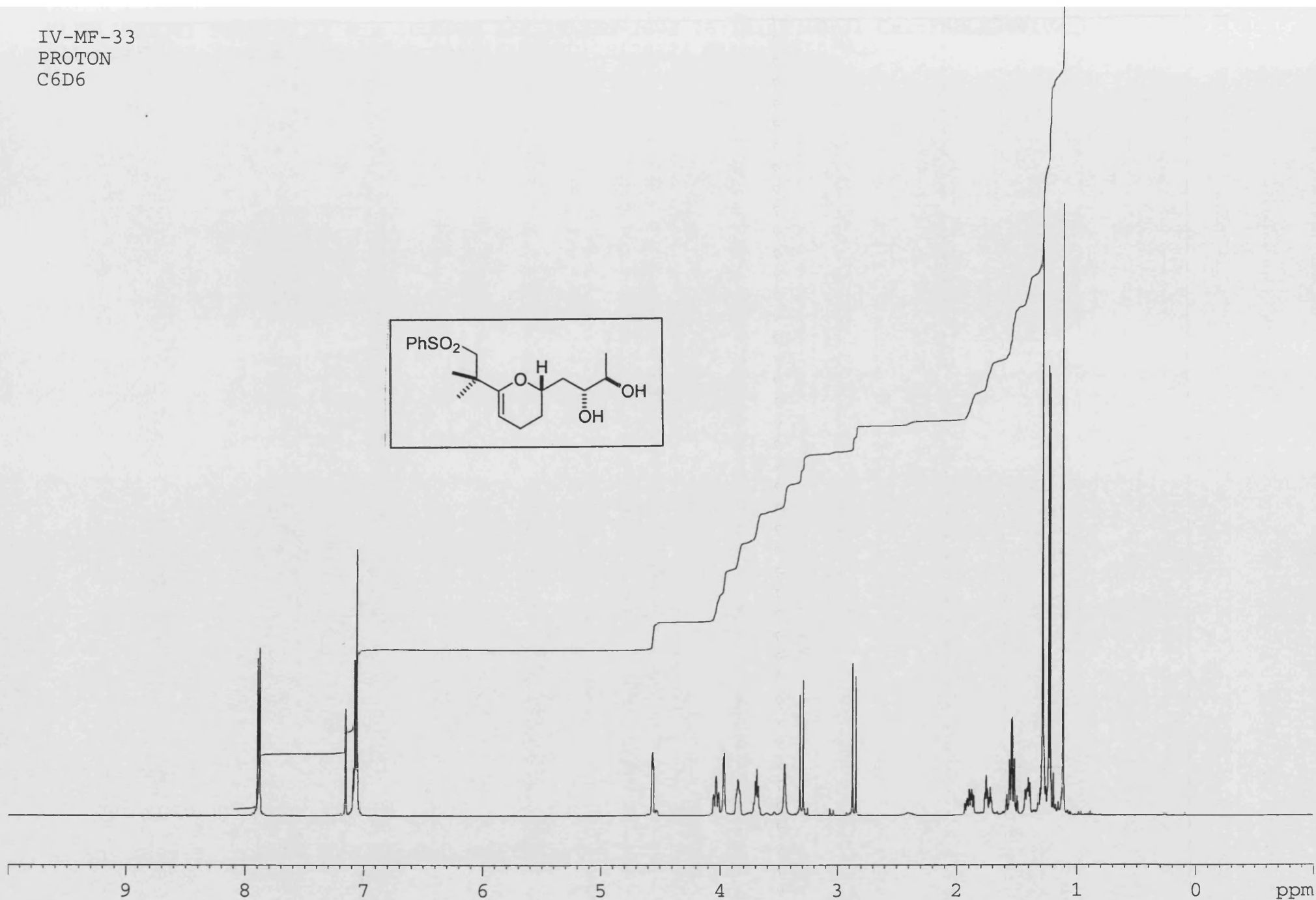
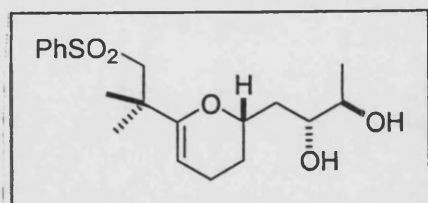
IV-MF-33
CARBON
C6D6



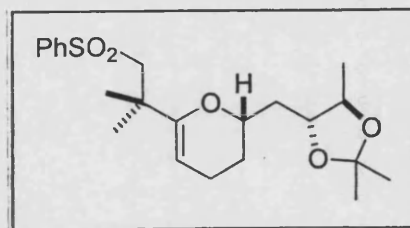
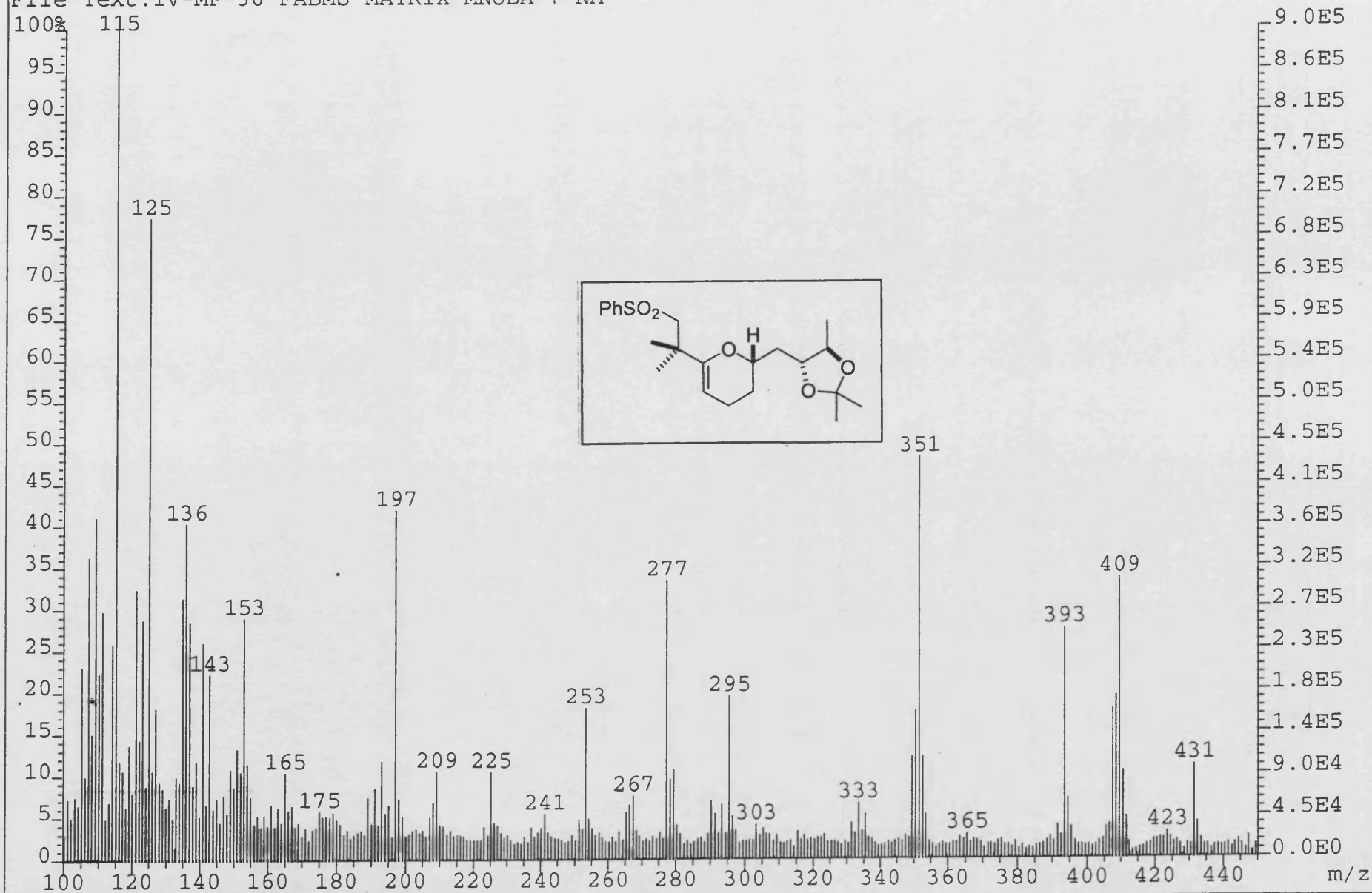
IV-MF-33
COSY
C6D6



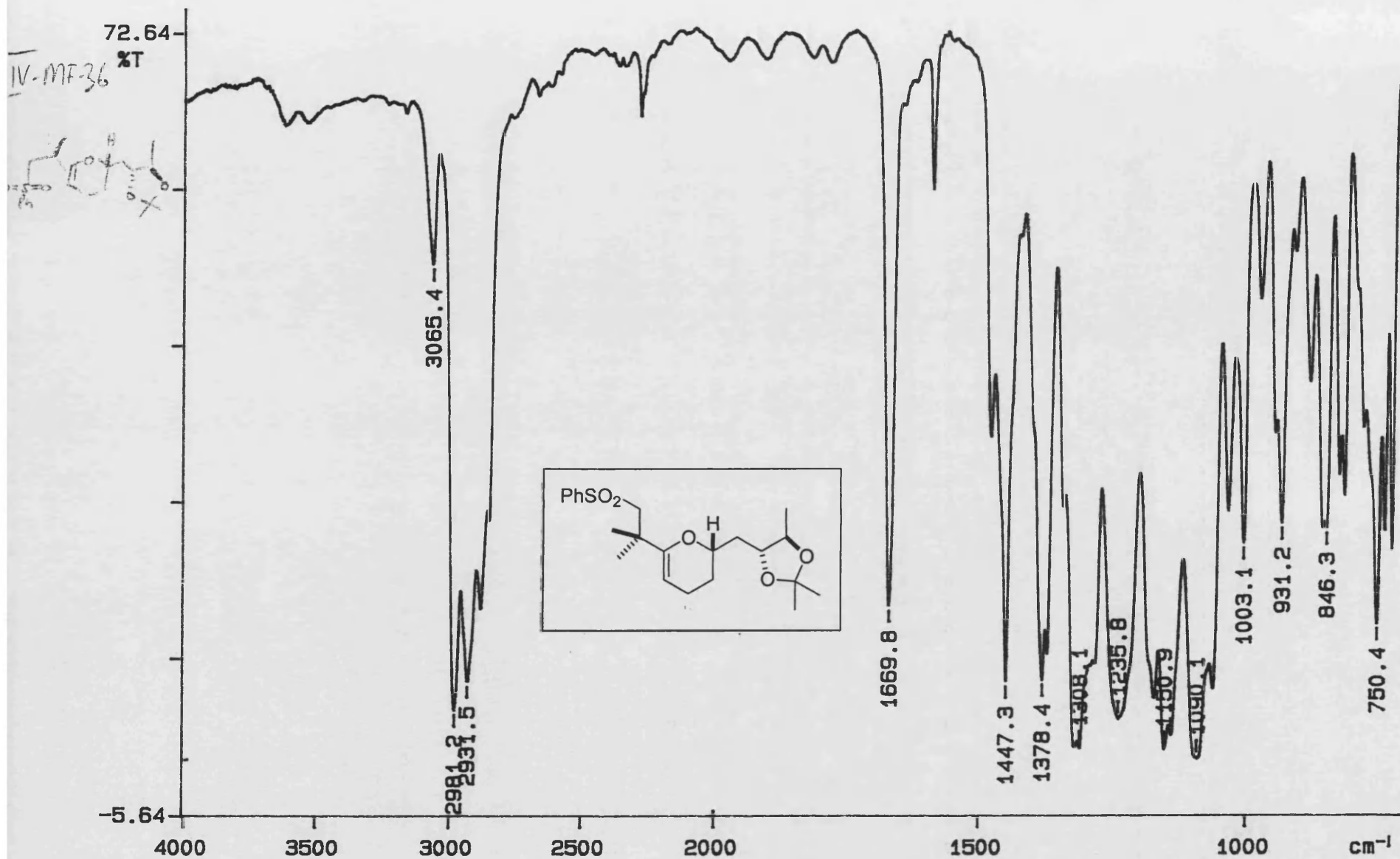
IV-MF-33
PROTON
C6D6



File Text:IV-MF-36 FABMS MATRIX MNOBA + NA



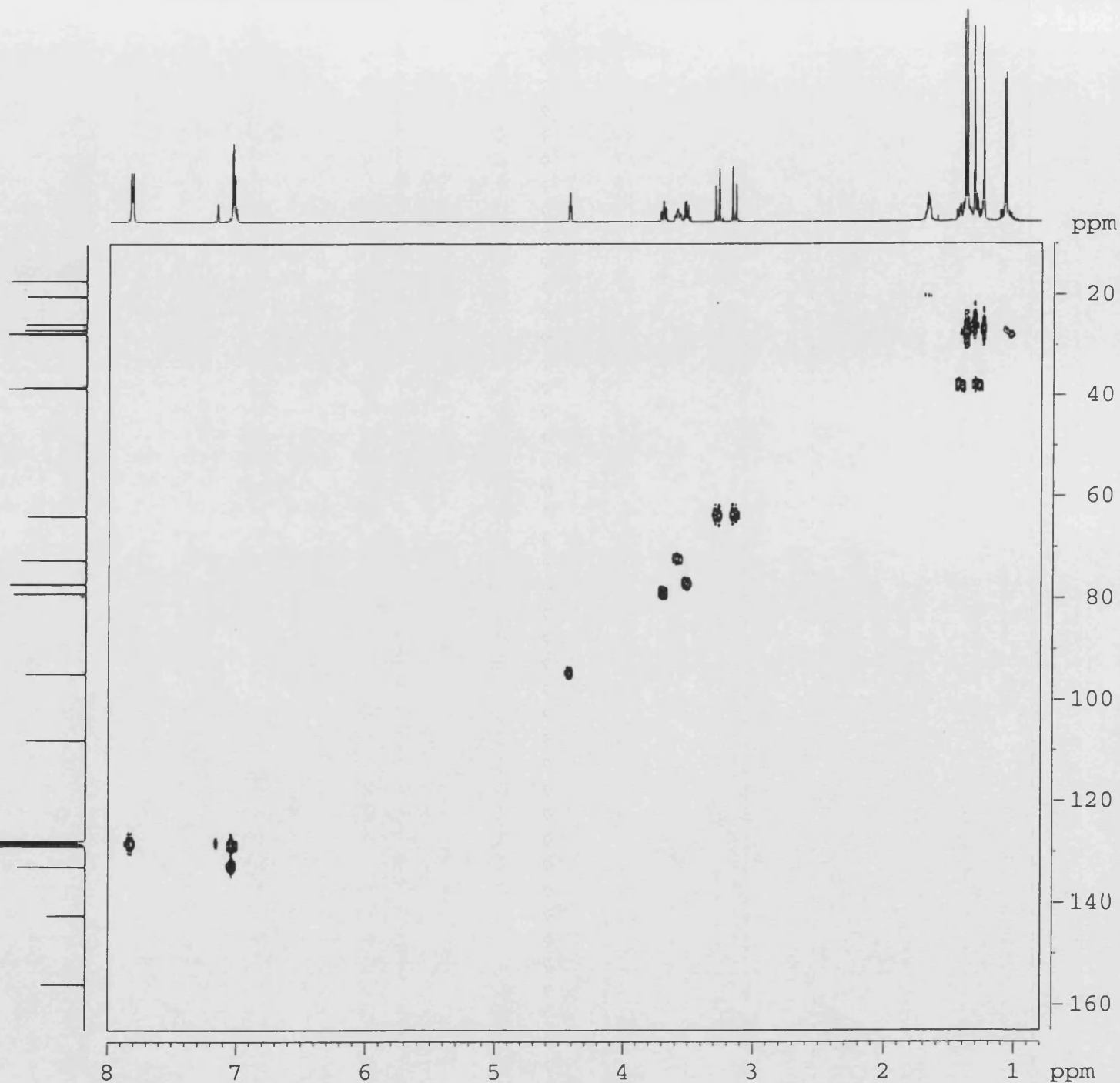
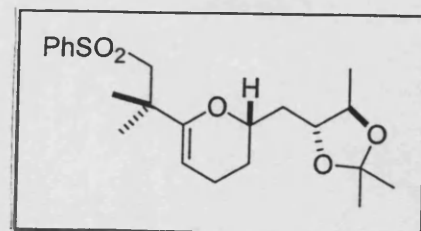
PERKIN ELMER



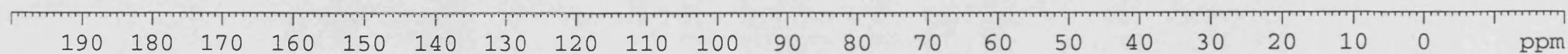
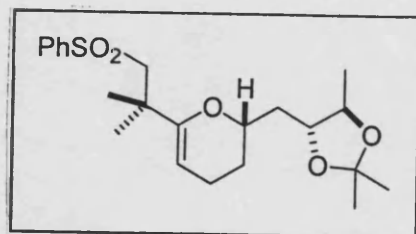
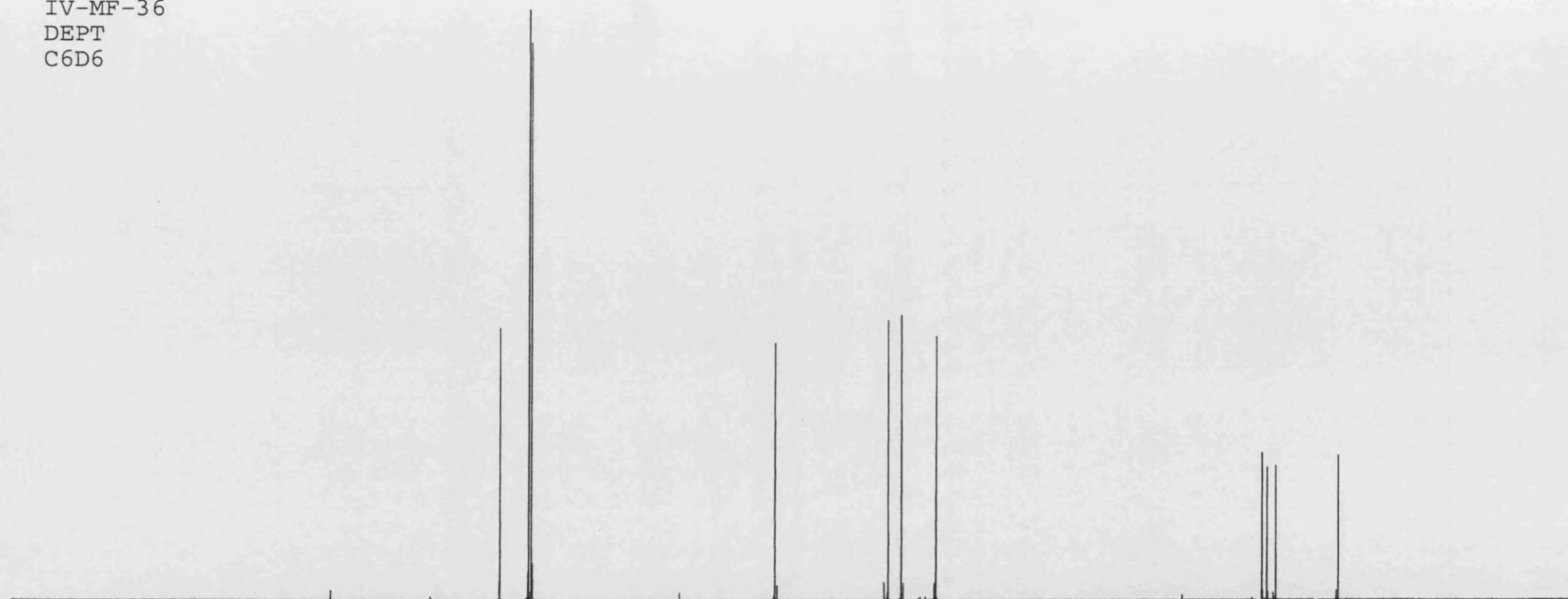
02/01/24 14:33

Y: 64 scans, 4.0cm⁻¹

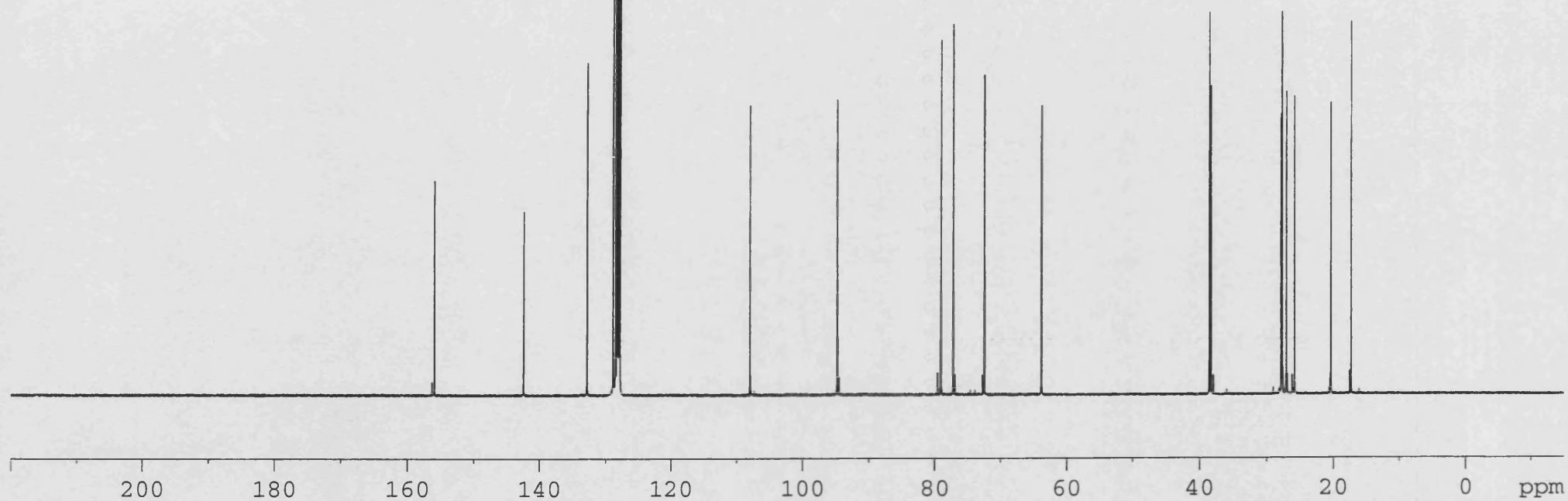
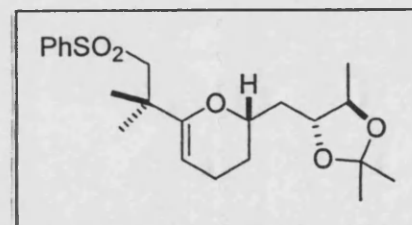
IV-MF-36
HMQC
C6D6



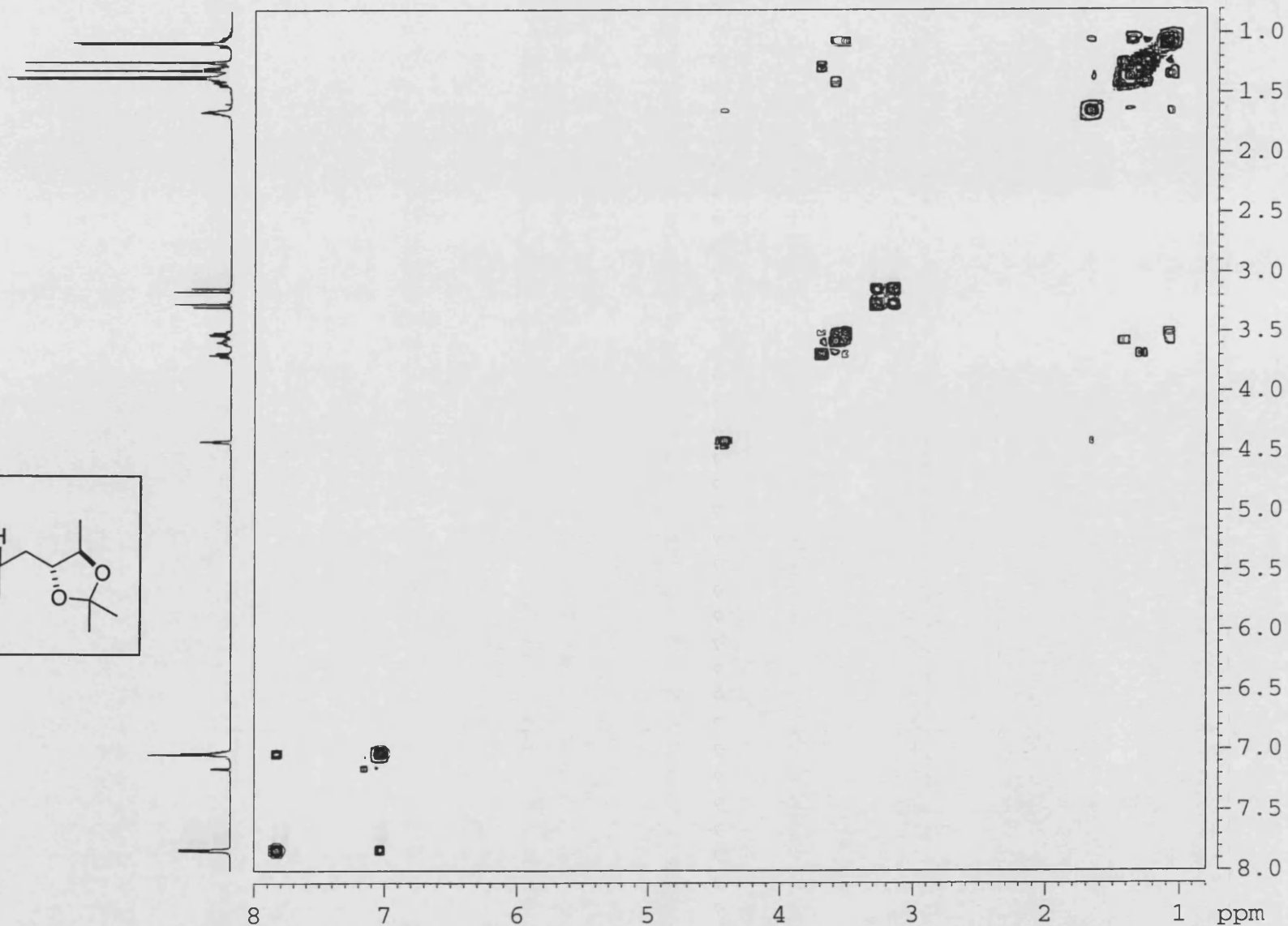
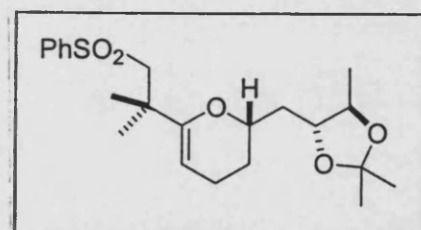
IV-MF-36
DEPT
C6D6



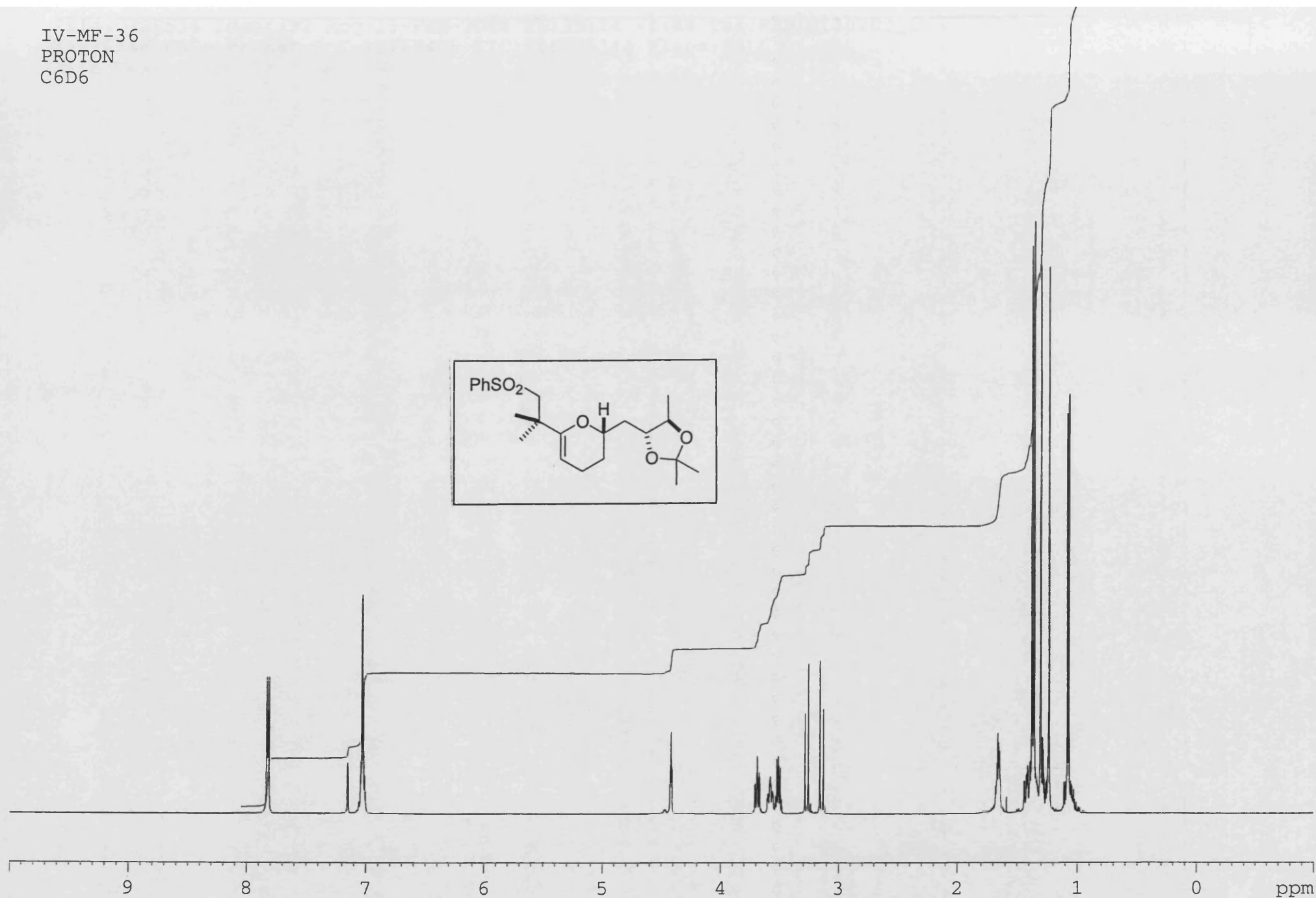
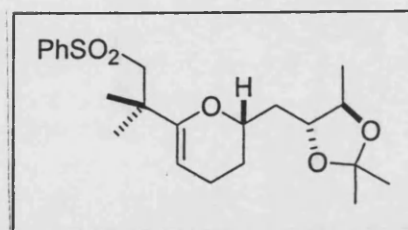
IV-MF-36
CARBON
C6D6



IV-MF-36
COSY
C6D6



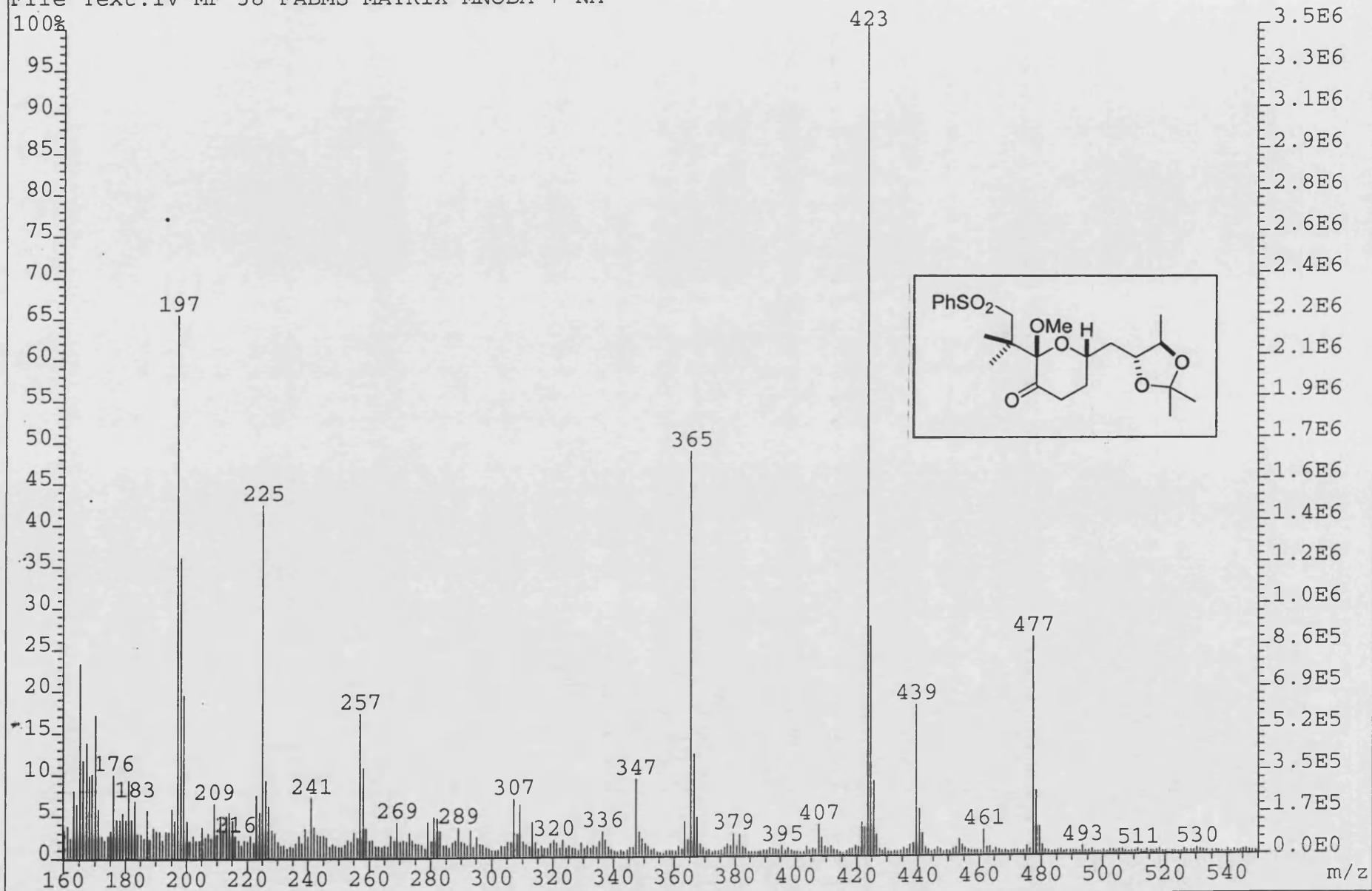
IV-MF-36
PROTON
C6D6



File:02SE536 Ident:32 Acq:13-FEB-2002 15:35:24 +1:48 Cal:FABLM130202_1

ZAB-SE4F FAB+ Magnet BpI:11769408 TIC:146205344 Flags:HALL

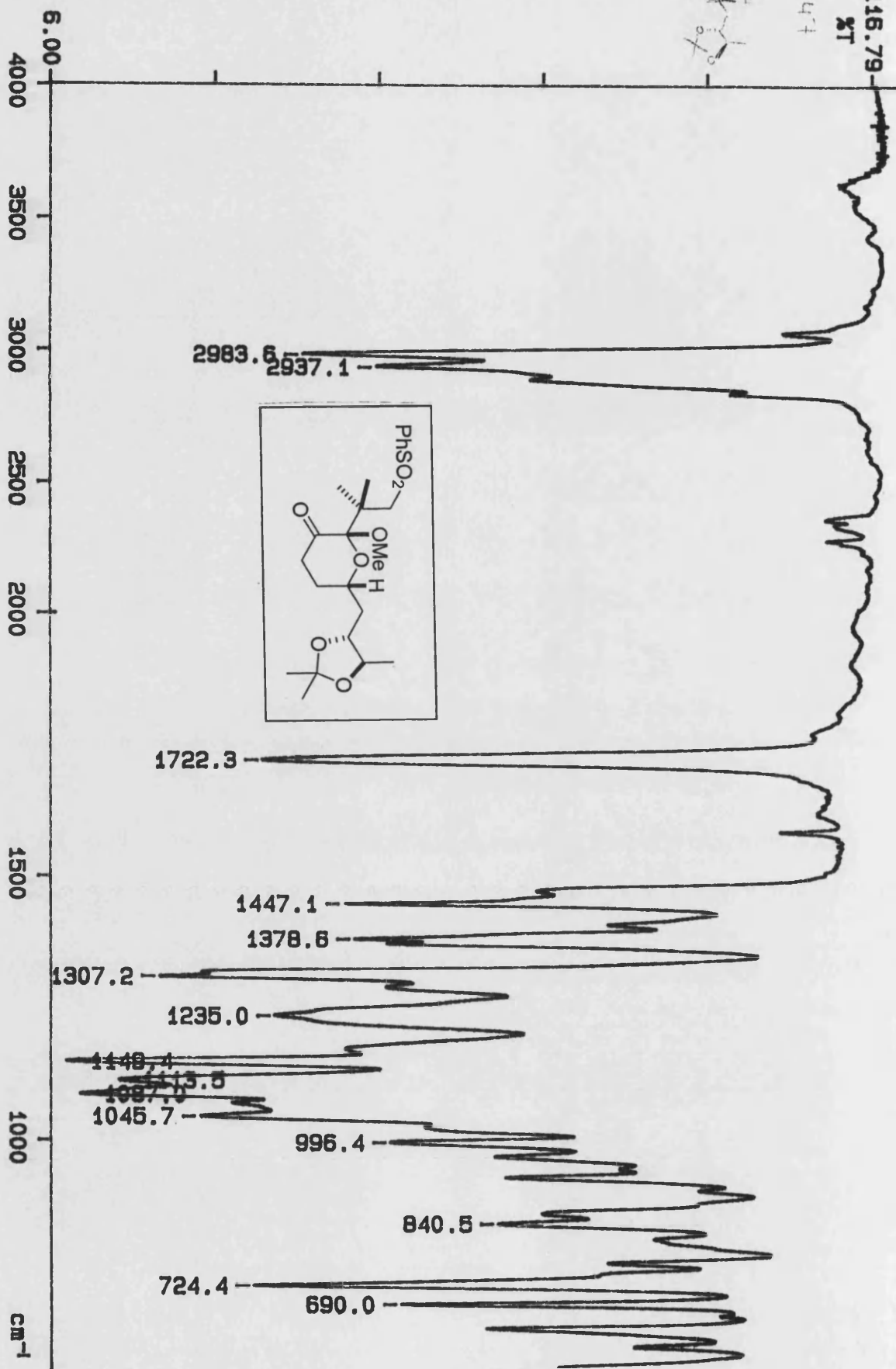
File Text:IV-MF-38 FABMS MATRIX MNOBA + NA



116.79

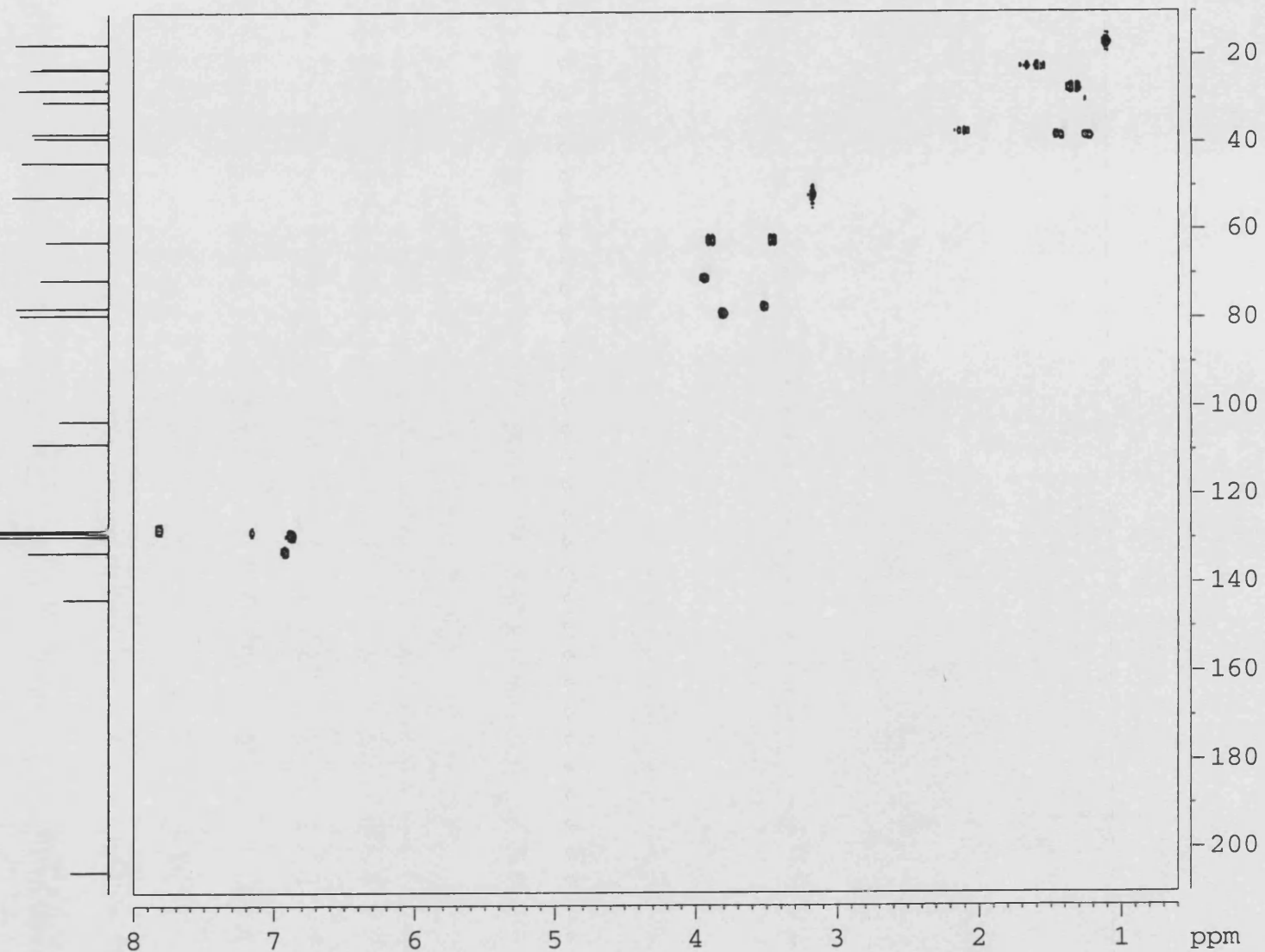
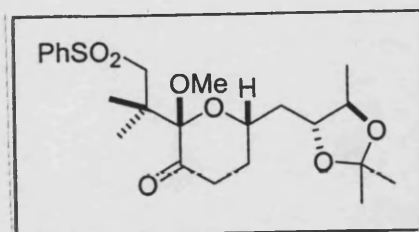
XT

M-MP-474

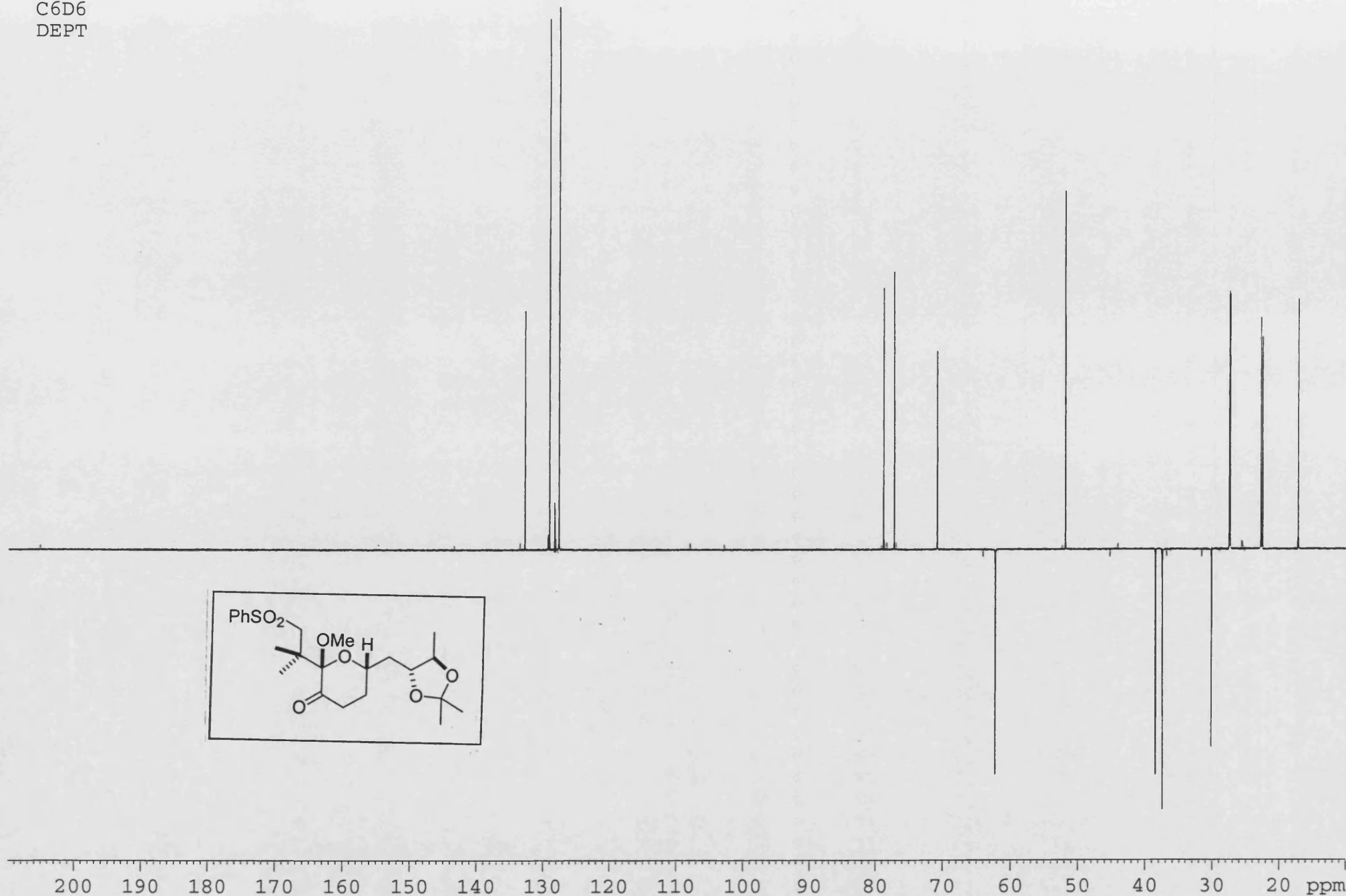


02/02/11 09:40
Y: 64 scans, 4.0cm-1, flat

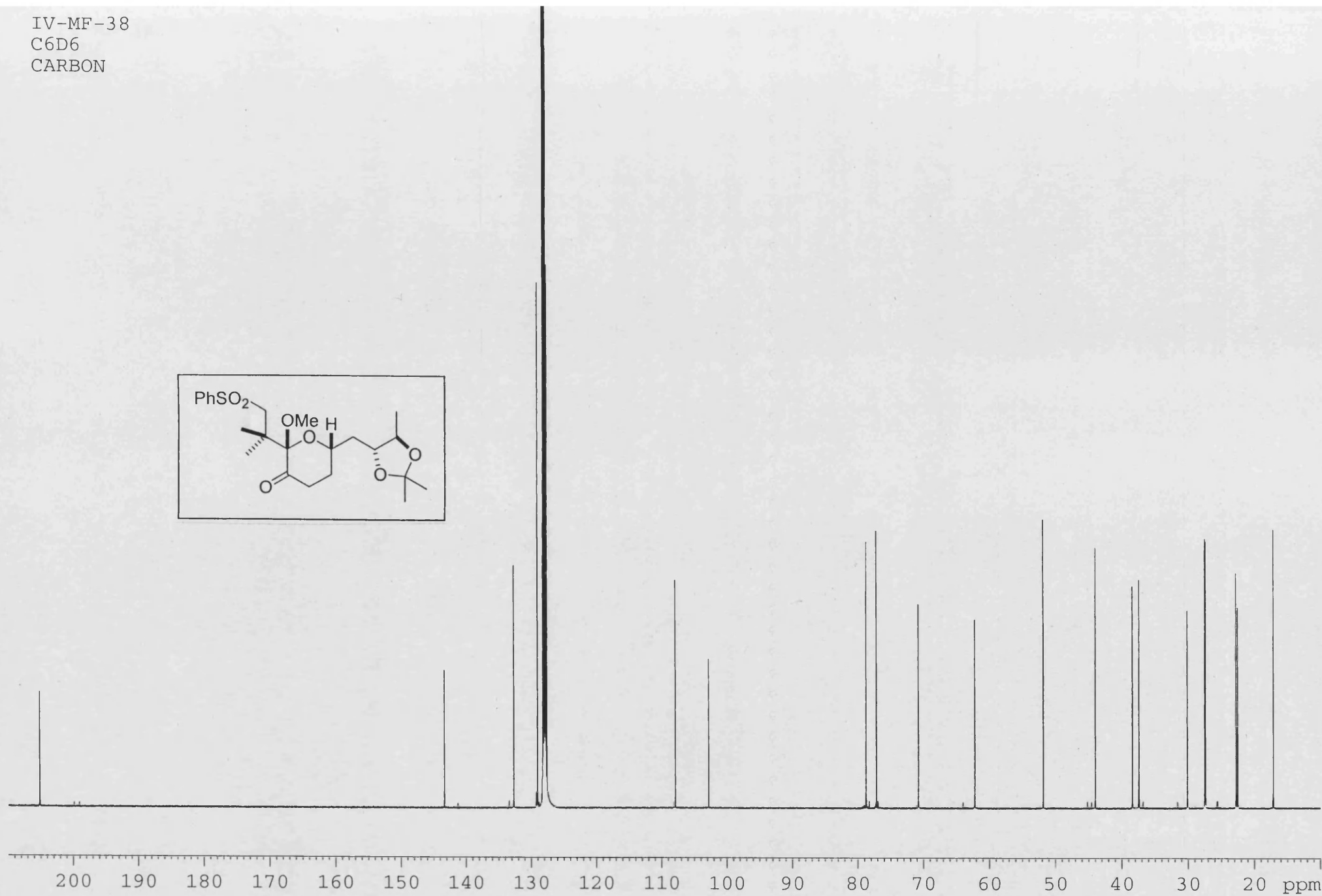
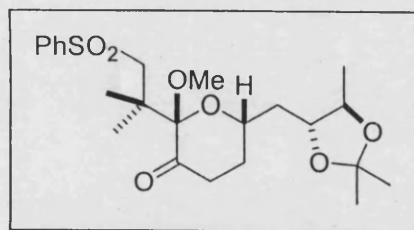
IV-MF-38
C6D6
HMQC



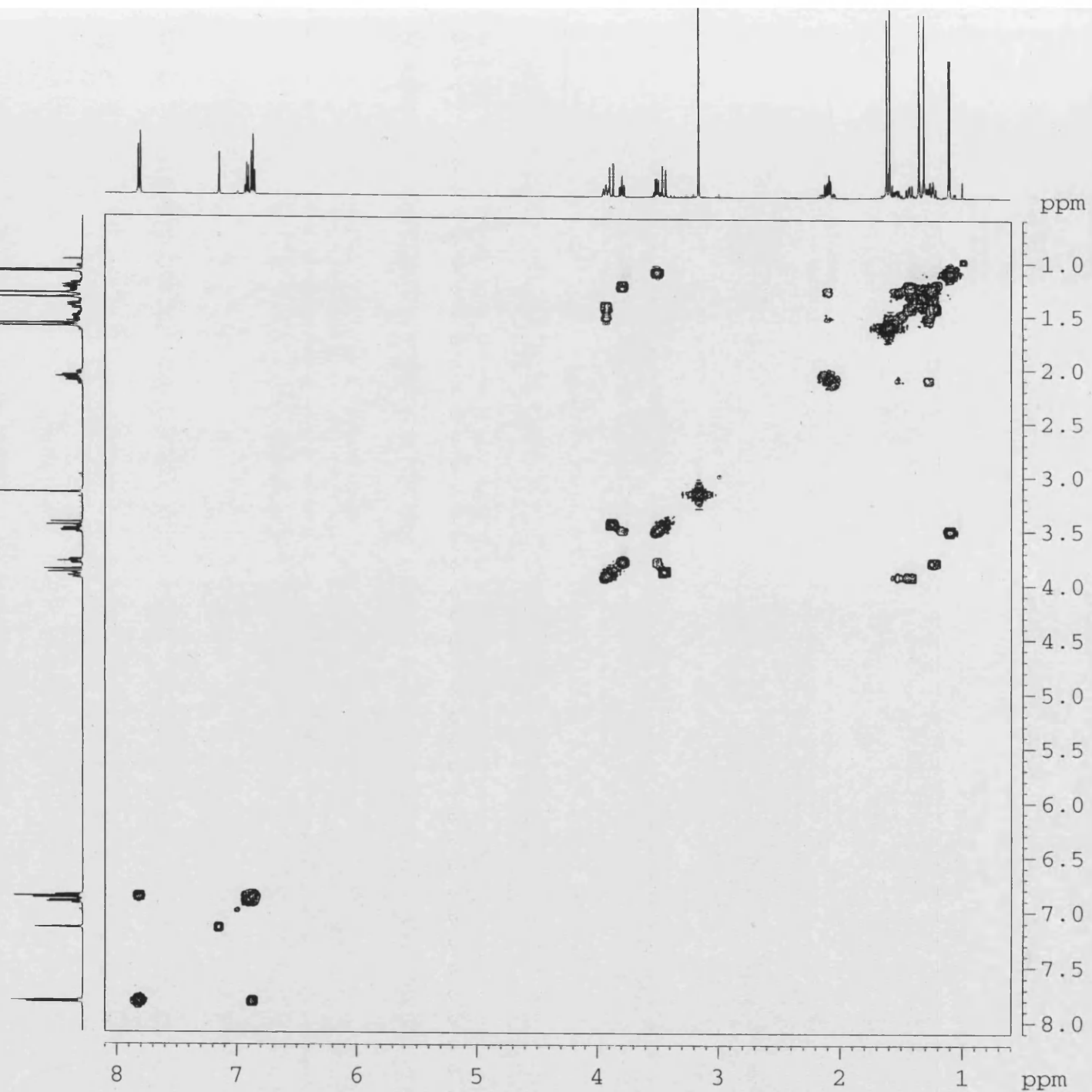
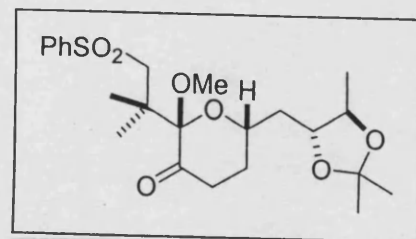
IV-MF-38
C6D6
DEPT



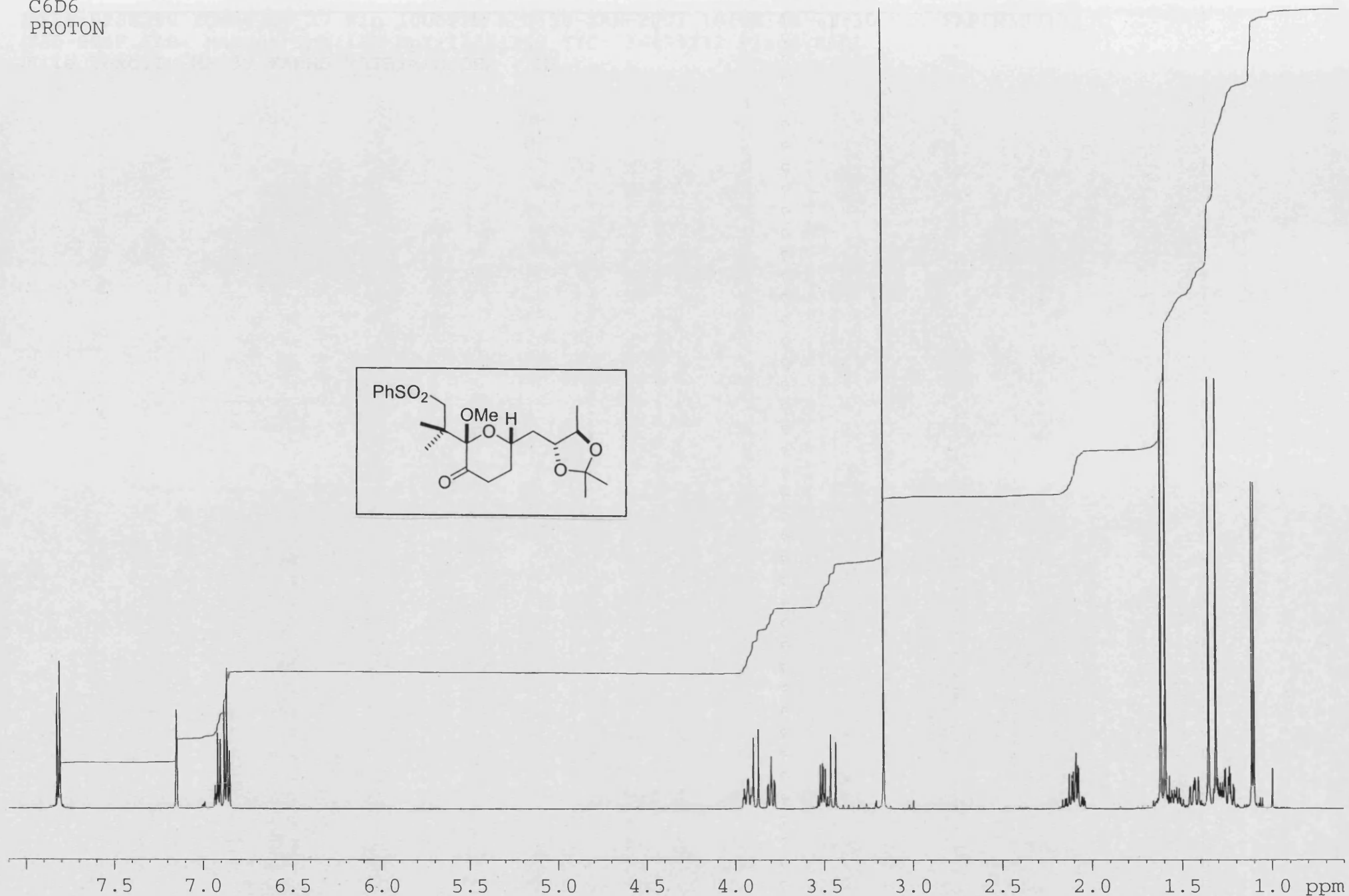
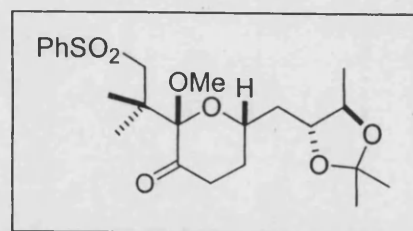
IV-MF-38
C6D6
CARBON



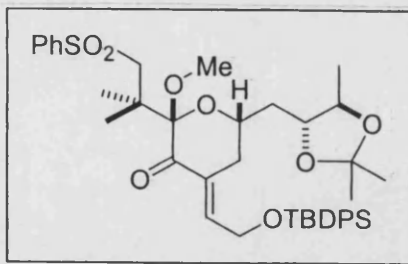
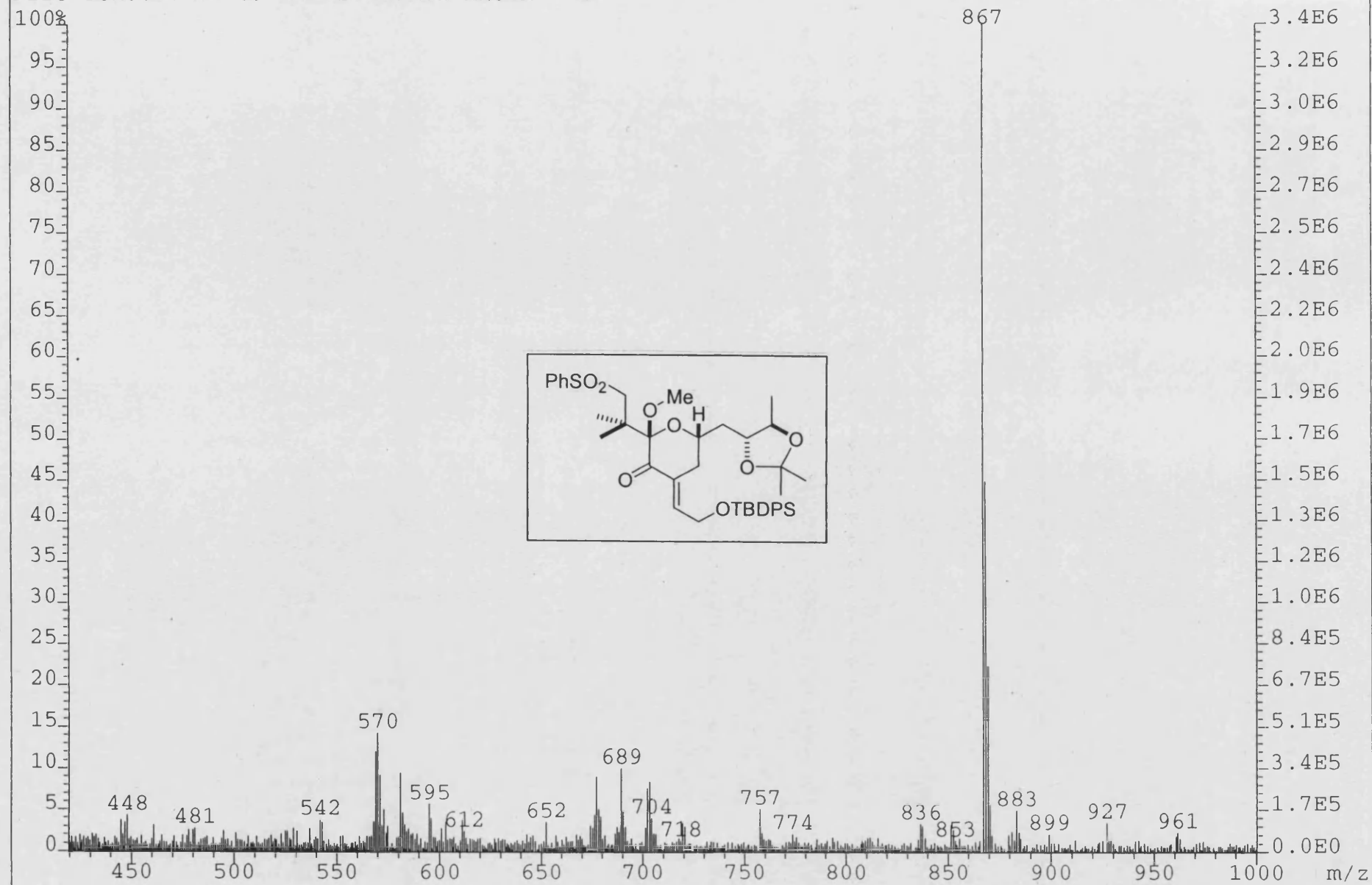
IV-MF-38
C6D6
COSY

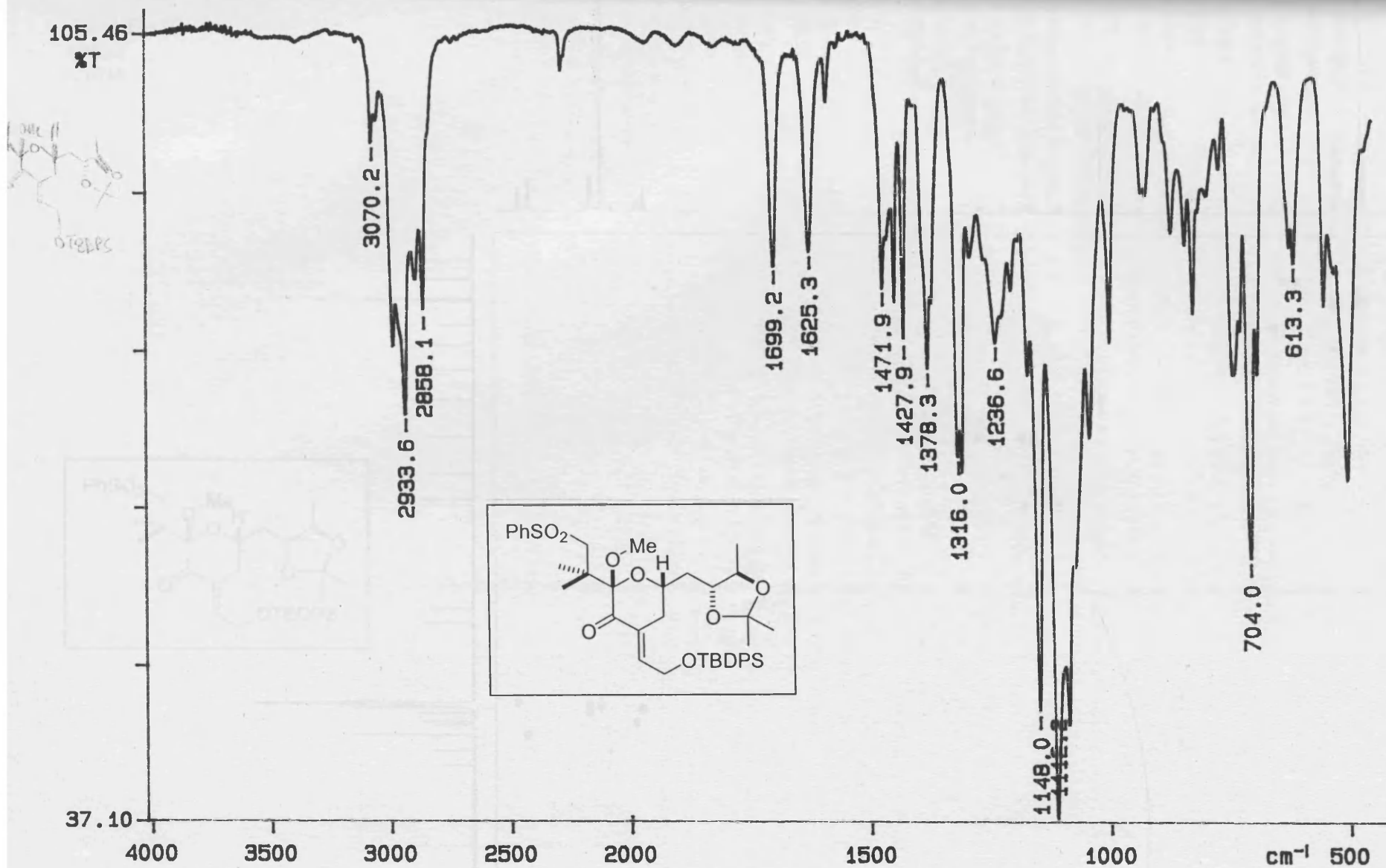


IV-MF-38
C6D6
PROTON



File Text:Iv-MF-39 FABMS MATRIX MNOBA + NA

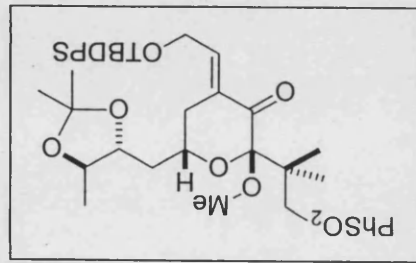
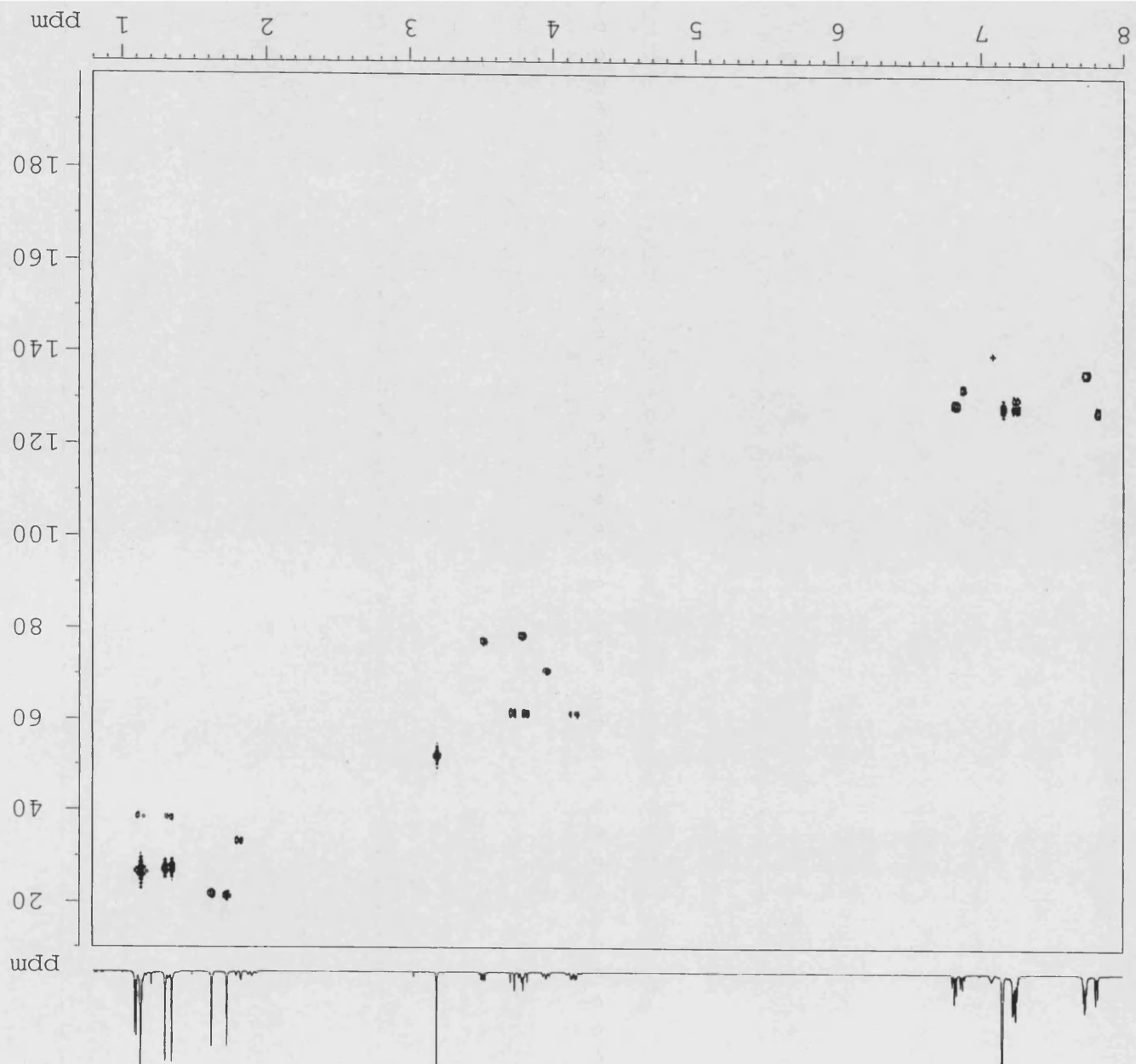




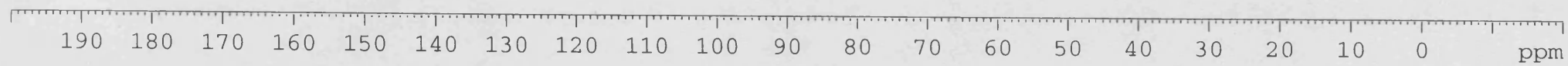
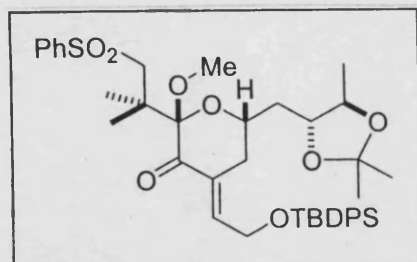
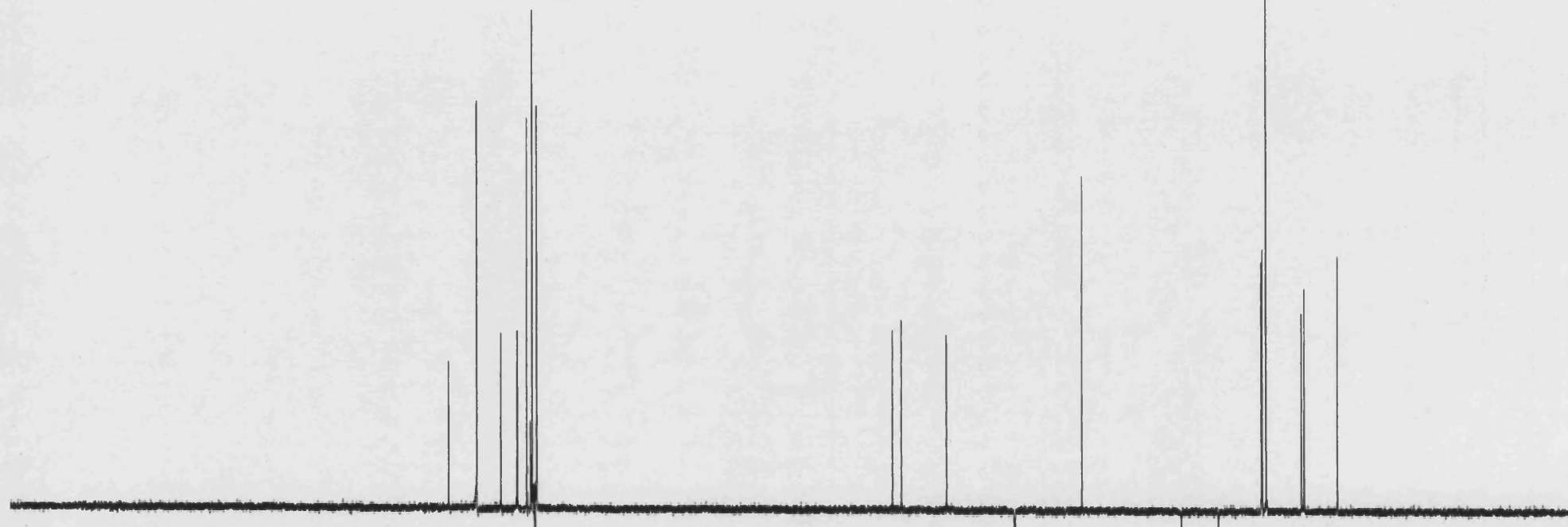
02/01/29 11:28

Y: 64 scans, 4.0cm⁻¹, flat

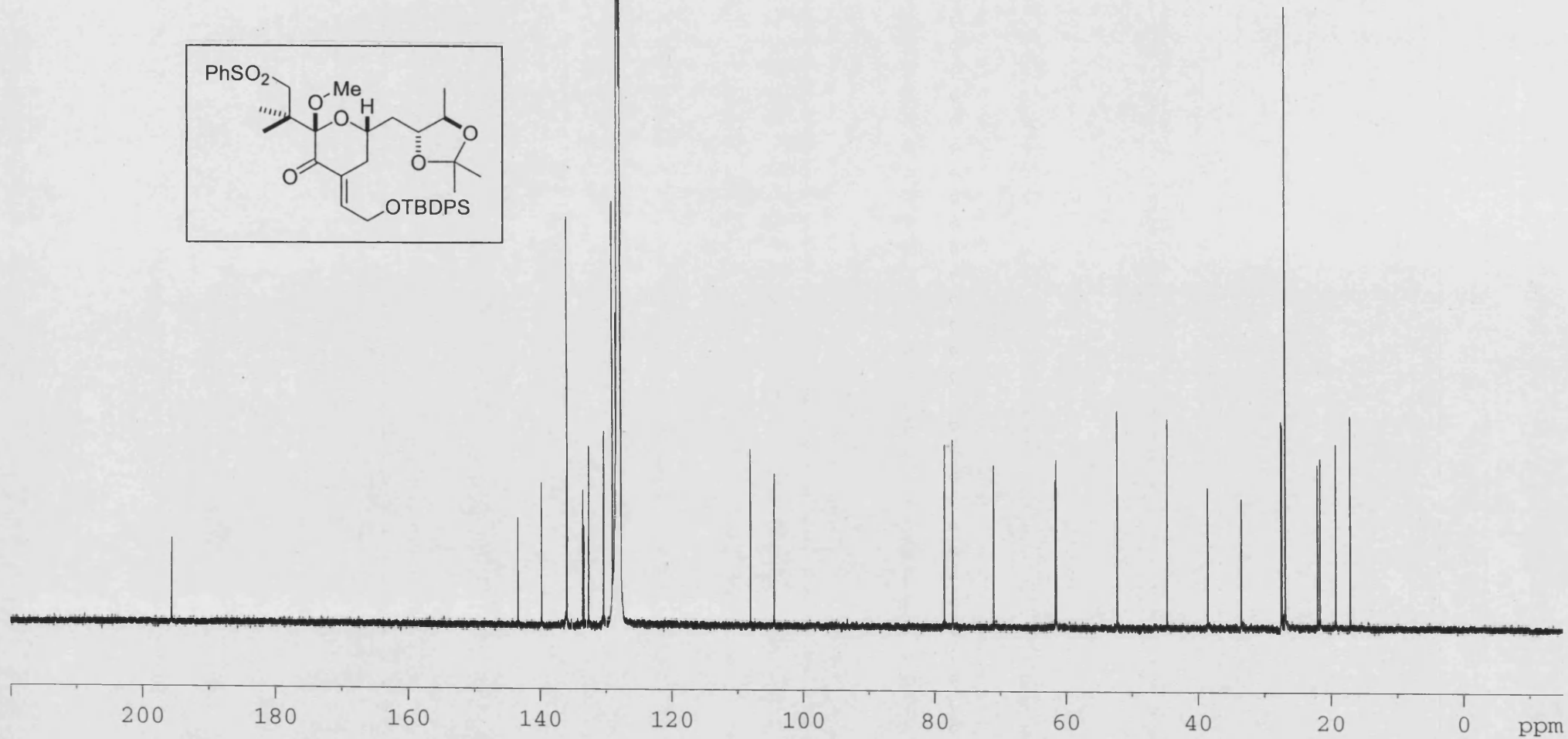
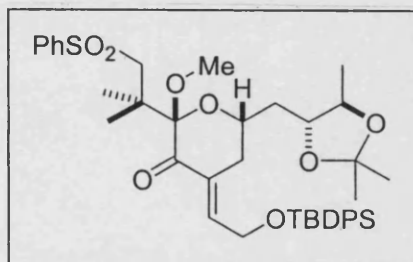
IV-MF-39
HMC
C6D6



IV-MF-39
DEPT
C6D6



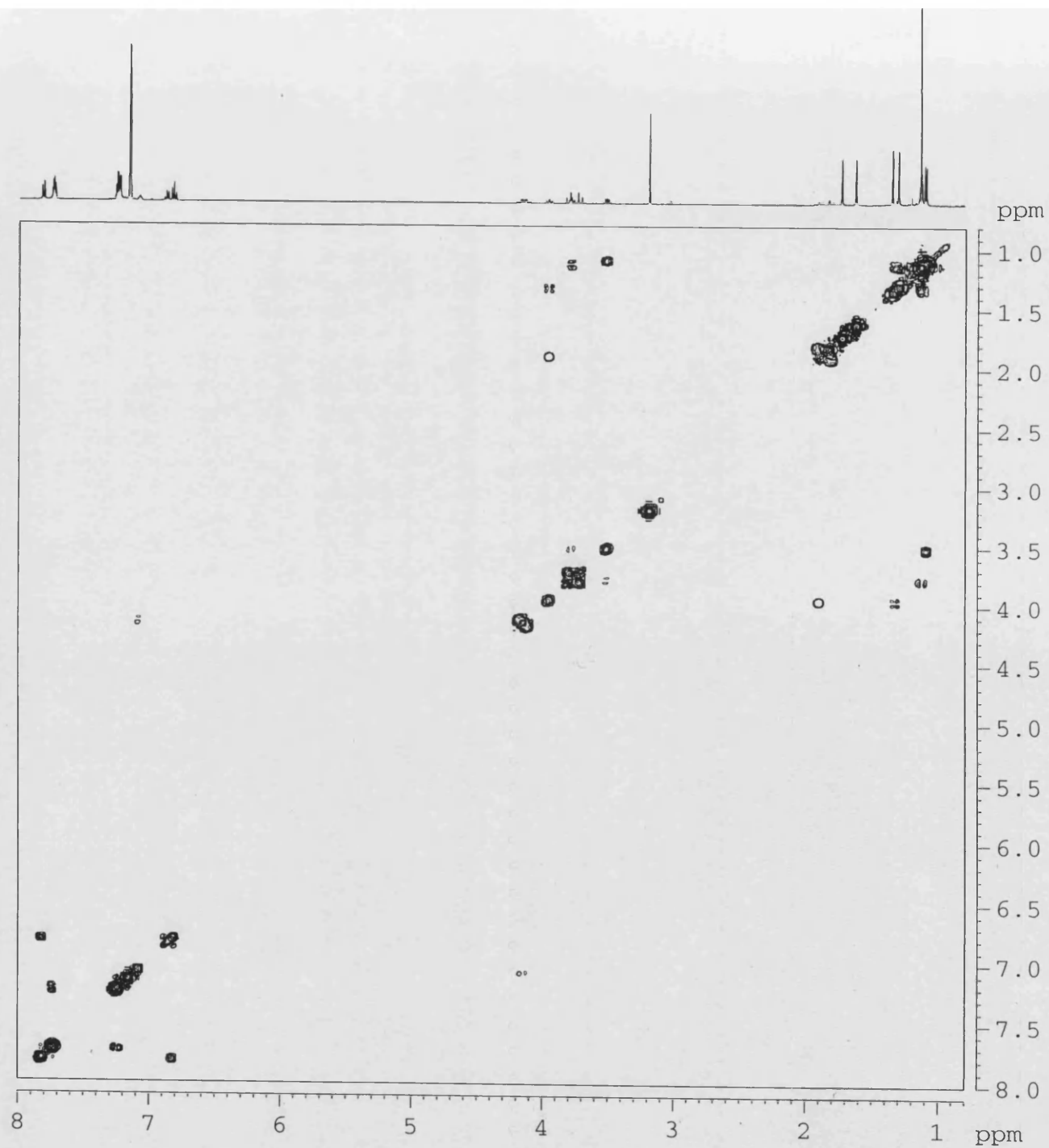
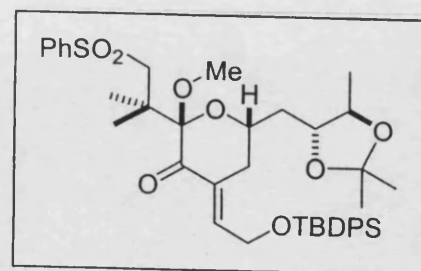
IV-MF-39
CARBON
C6D6



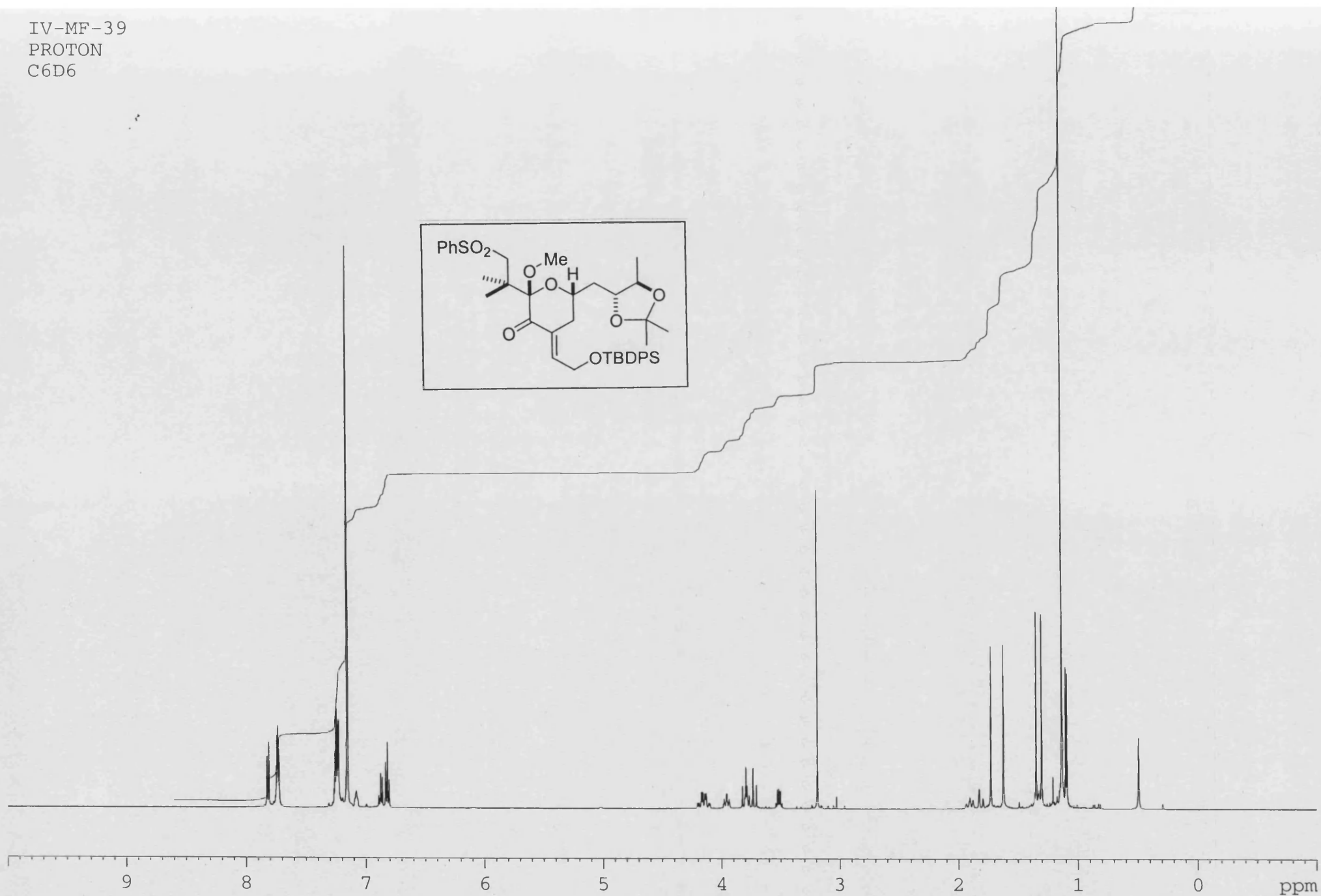
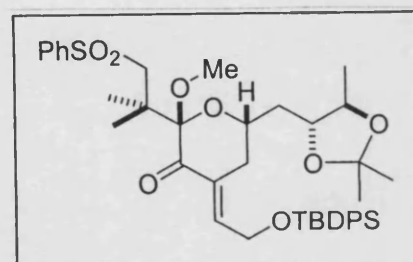
IV-MF-39

COSY

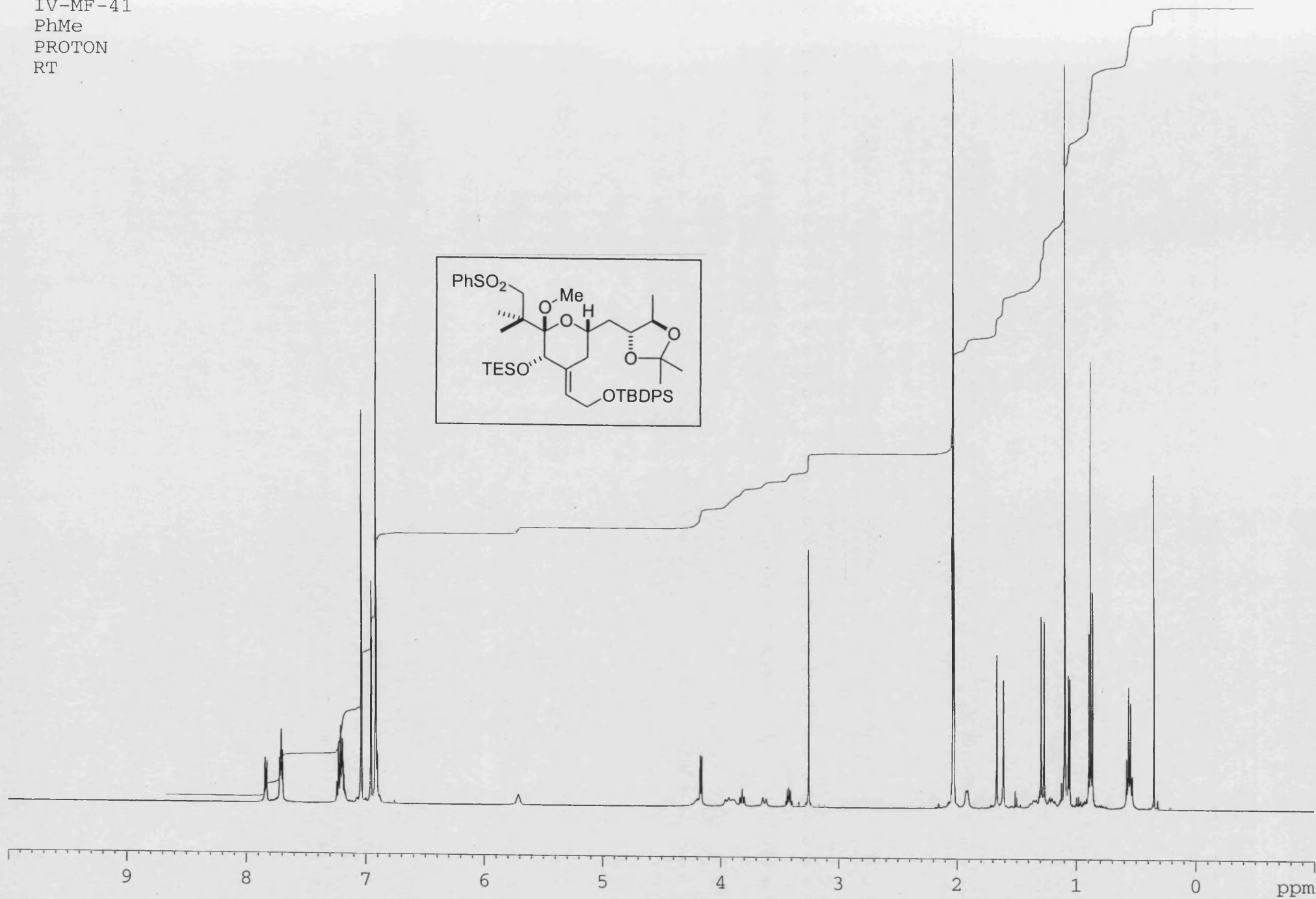
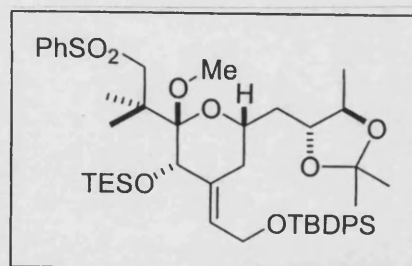
C6D6



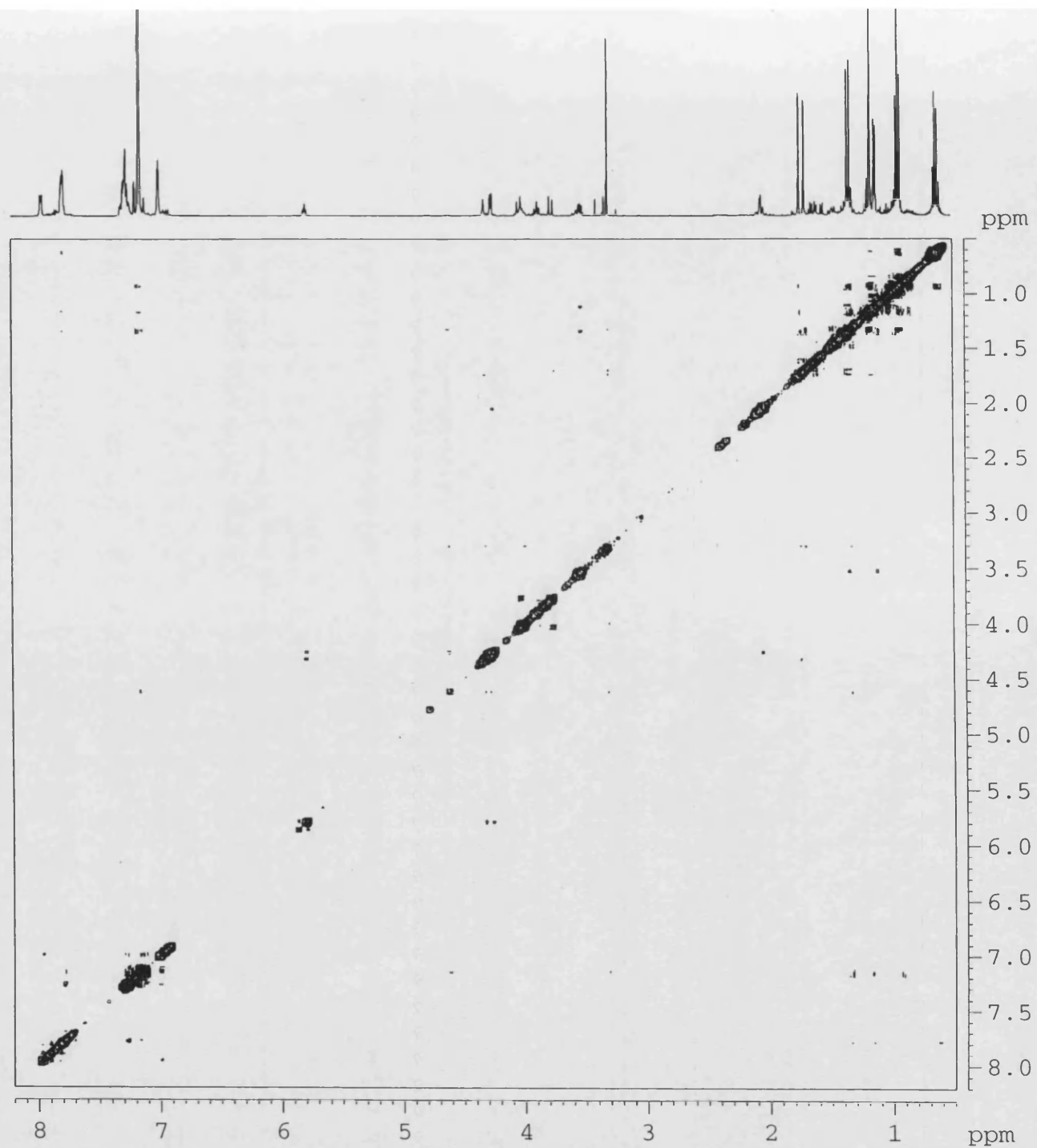
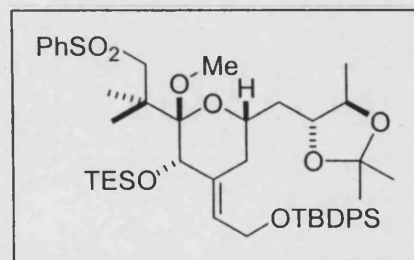
IV-MF-39
PROTON
C6D6



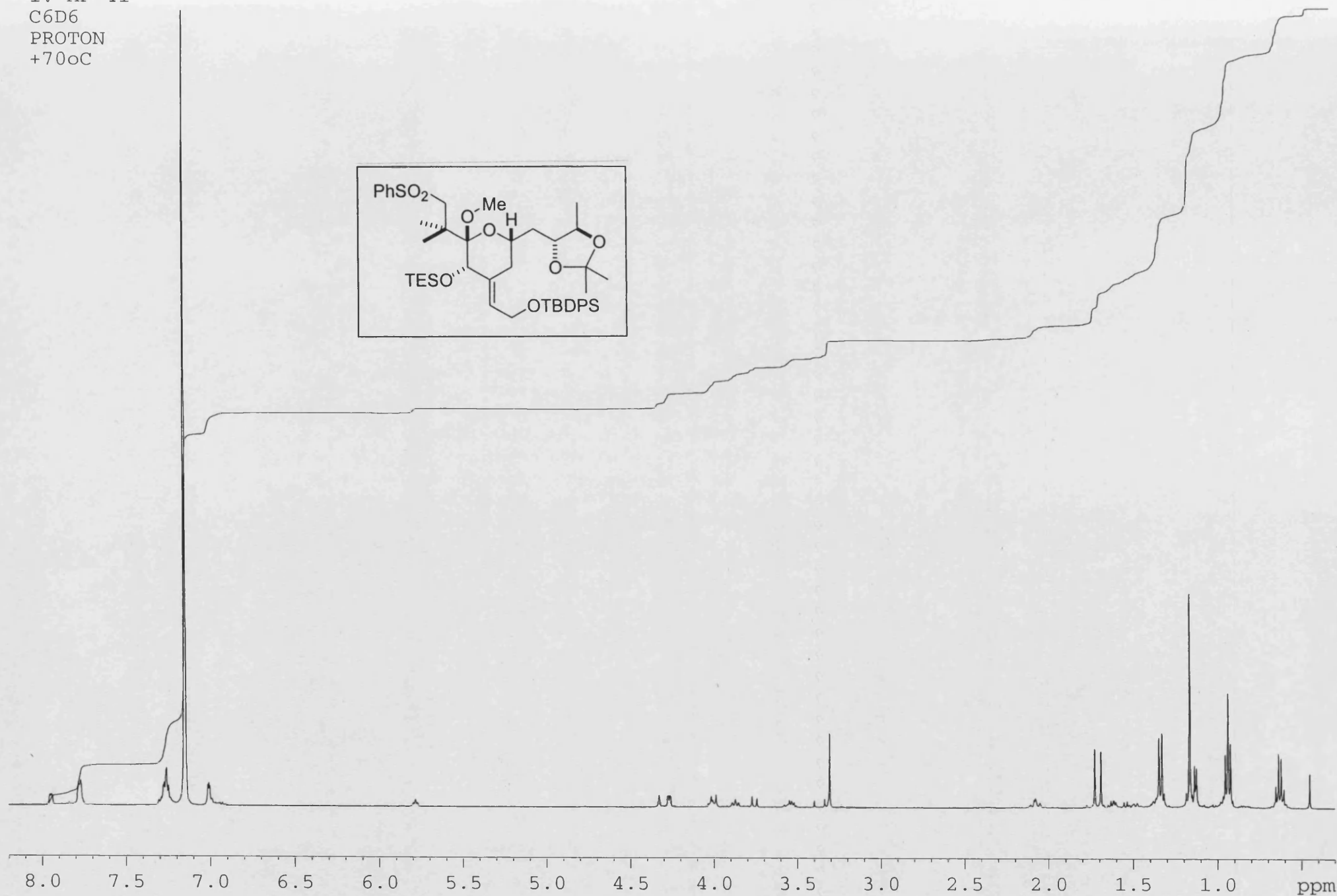
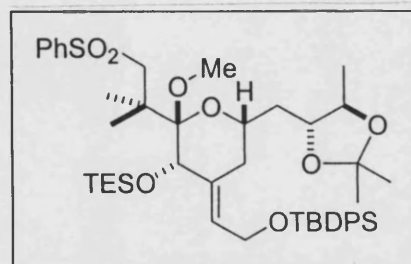
IV-MF-41
PhMe
PROTON
RT



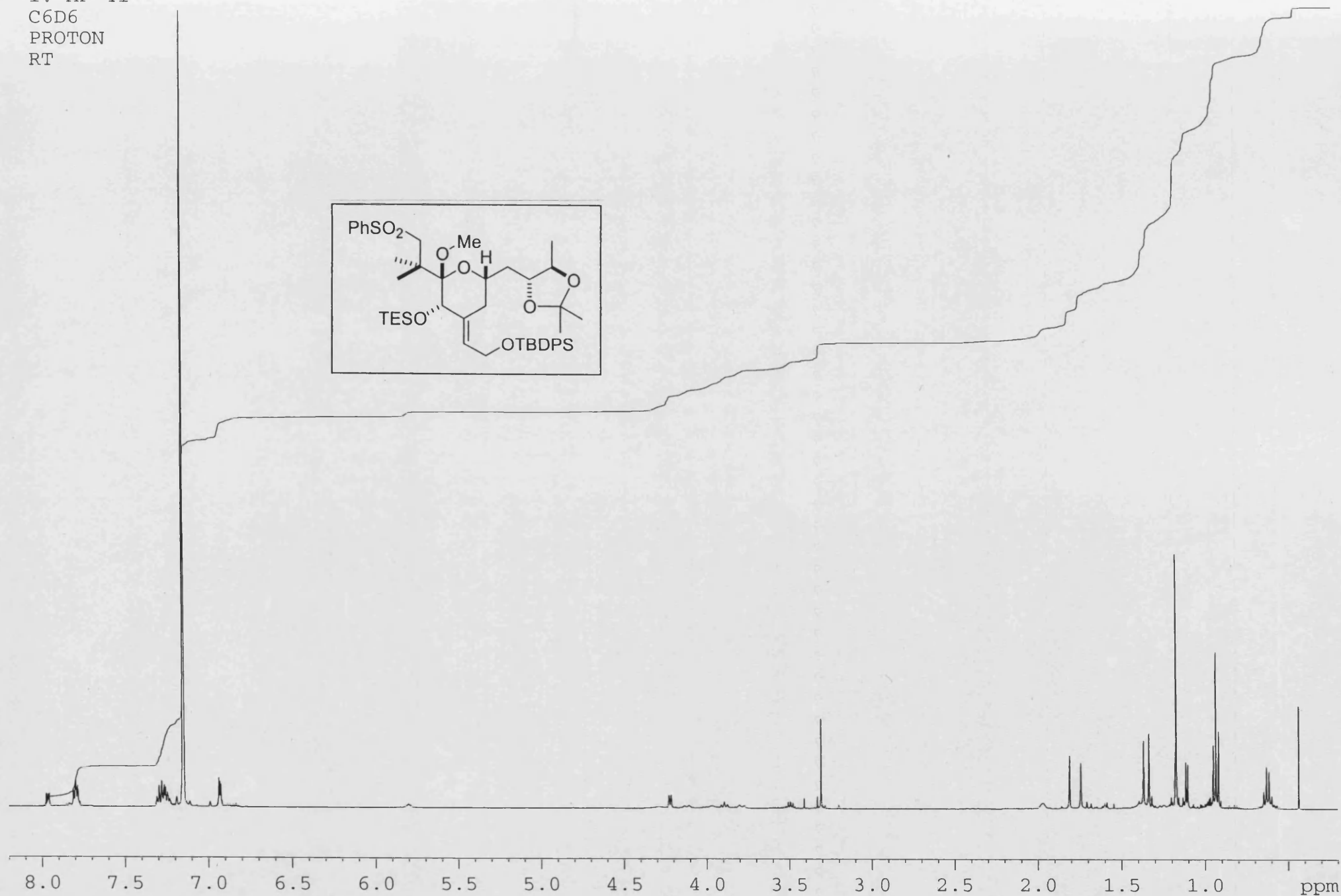
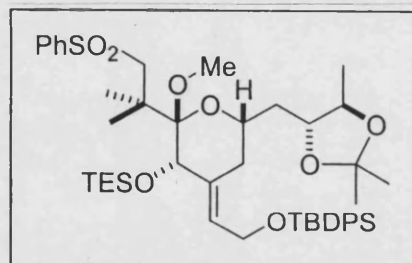
IV-MF-41
C6D6
NOESY
+60°C



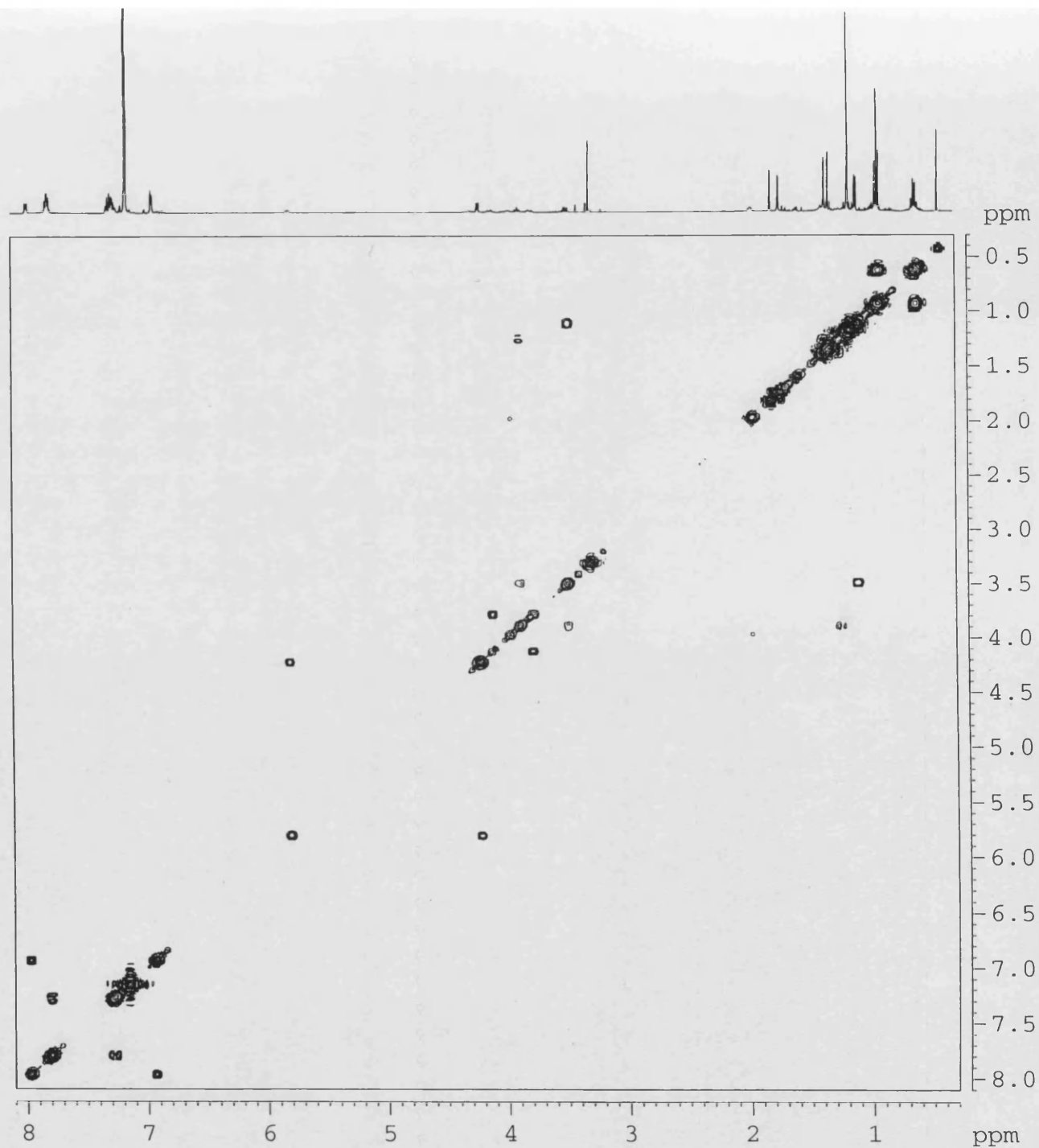
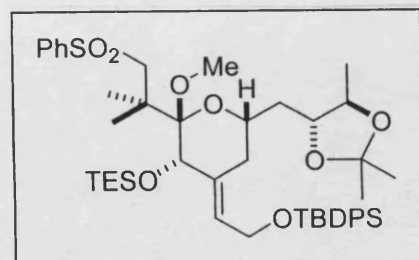
IV-MF-41
C6D6
PROTON
+70oC



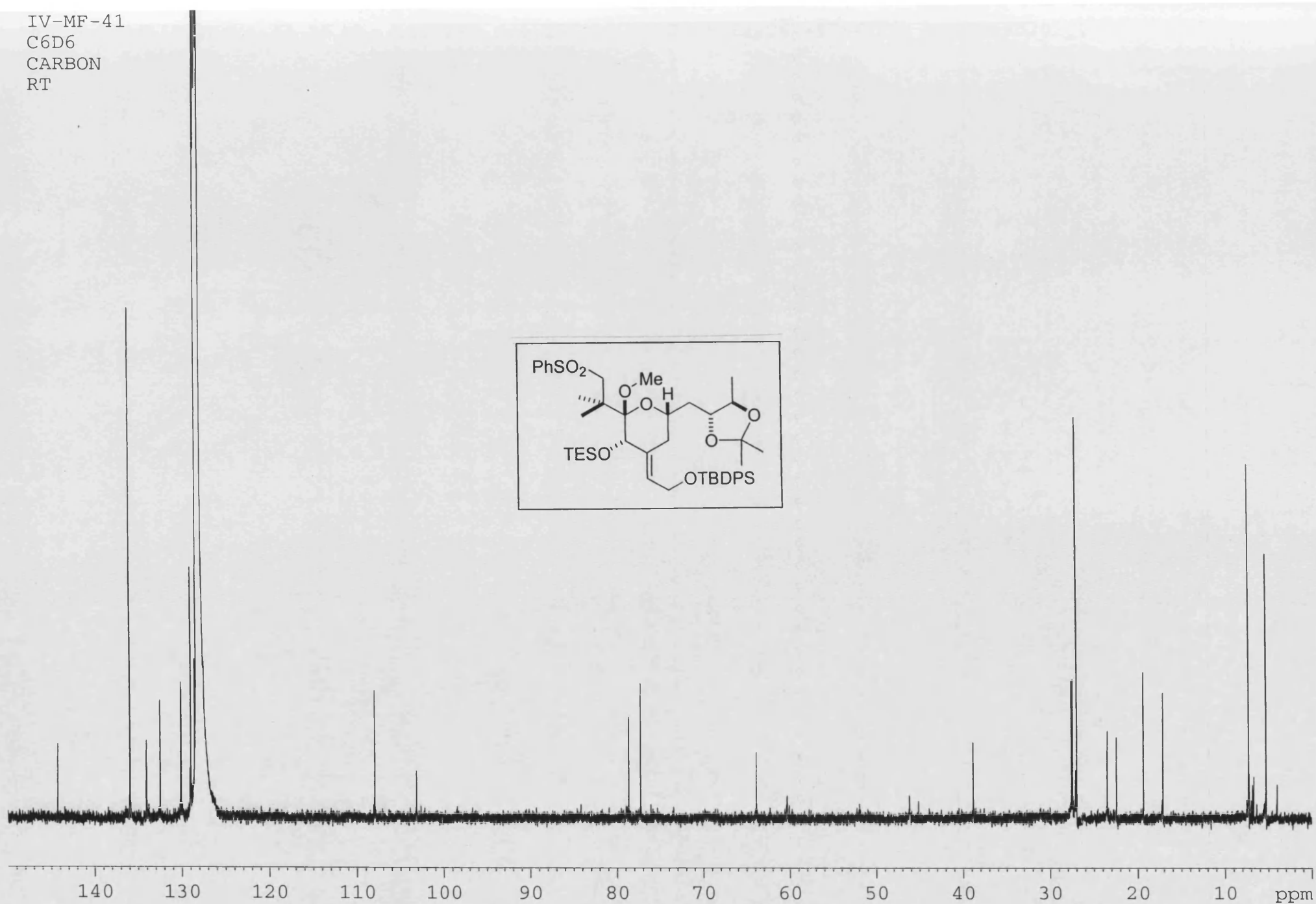
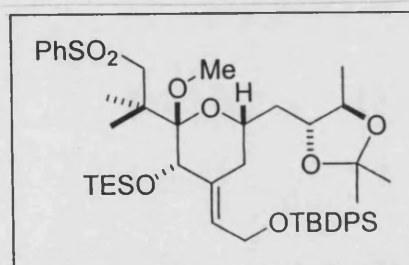
IV-MF-41
C6D6
PROTON
RT



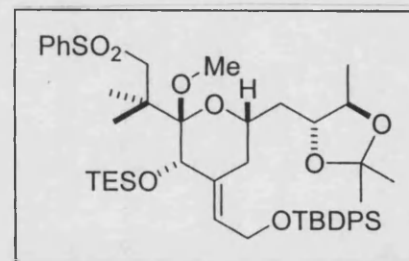
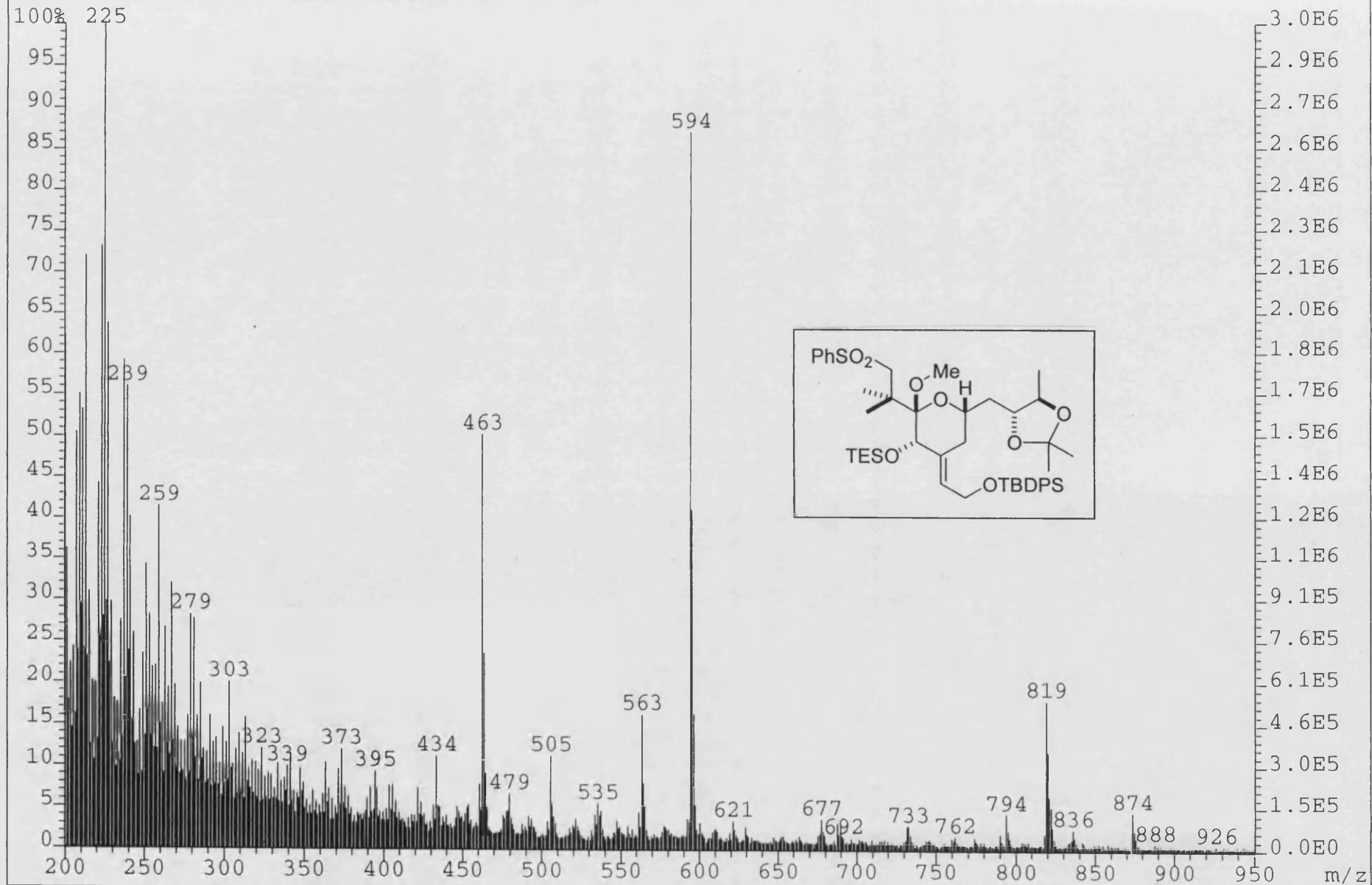
IV-MF-41
C6D6
COSY
RT



IV-MF-41
C6D6
CARBON
RT



100% 225

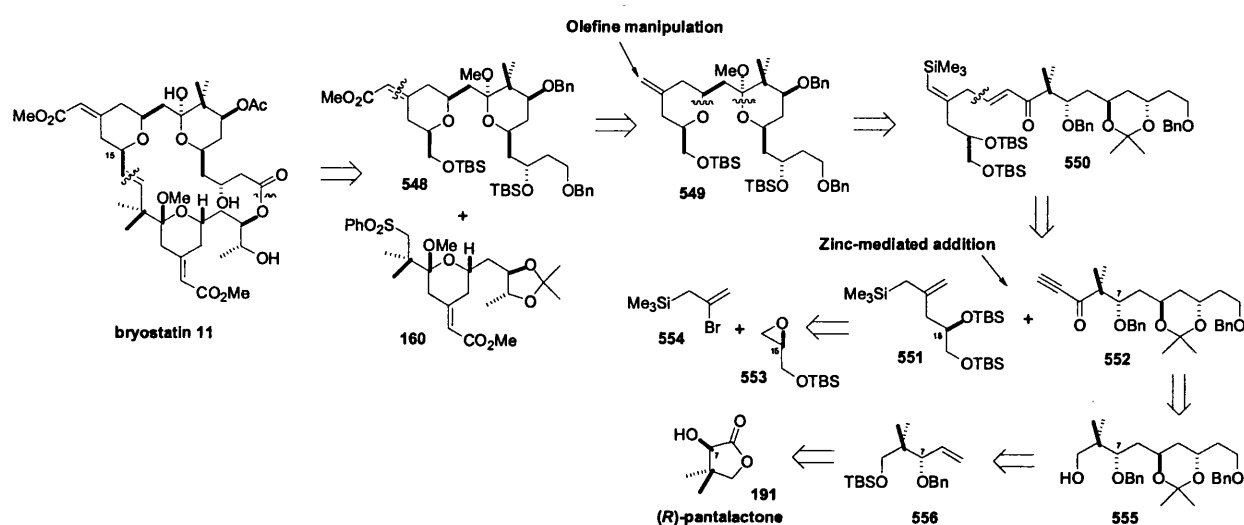


Appendix 2

This includes an update of the work carried out in the bryostatin field.

Thomas's synthesis of a C(1)-C(16) "Northern Hemisphere" fragment (2002) ¹³⁹

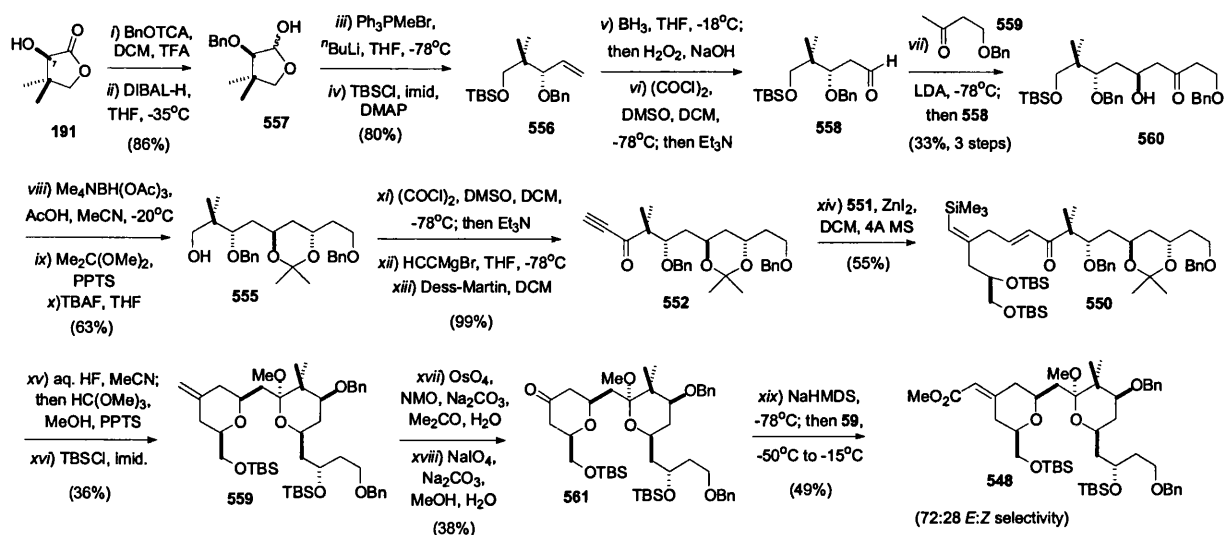
The development of a C(1)-C(16) Bryostatin A and B ring synthon **548** was undertaken by Thomas, in an alteration to his previous efforts using individual pyran rings (schemes 22 to 25). The formation of **548** constitutes a marked improvement over the synthesis of the bryostatin B-ring sections **159** and **181**, to subsequently feed into his total synthesis of bryostatin **11** via the coupling with a "southern hemisphere" bryostatin segment **160** (Scheme 22).



Scheme 91 Thomas's retrosynthetic plan for the bryostatin **11** A-B ring intermediate **548**.

The crux of this improved synthesis relied on the tandem acid-catalysed conjugate addition/*bis*-cyclisation of the linear chain **550** to the bis-pyran **549** (Scheme 91), followed by exocyclic olefination to the requisite methyl ester **548**. Disconnection of **550** releases the C(11)-C(1) synthon **552** and the C(16)-C(12) synthon **551**. The latter would be formed via the copper-catalysed addition of the vinyl Grignard intermediate of **554** and protected glycidol **553**. The propargyl ketone **552** would be formed via a number of successive chain elongation steps, initiated from the ring-opened intermediate **556** of (*R*)-pantalactone **191**.

The protection of **191** as its benzyl ether (Scheme 92) was carried out using its trichloroacetimidate (BnOTCA), which then underwent lactone reduction to the lactols **557**. The Wittig ring-opening was performed with the methylene phosphonium salt, and subsequent protection as its TBS ether gave **556** in good yields. Hydroboration of the terminal olefin and ensuing Swern oxidation to aldehyde **558** permitted the aldol condensation with the enolate of **559** to deliver the C(5) hydroxyl centre of **560** in excellent stereocontrol, albeit in diminished yields, which were attributed to the competing deprotonation of **559**.



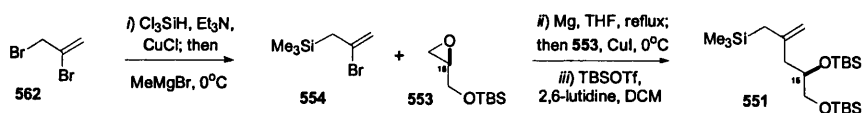
Scheme 92

Thomas's formation of the C(1)-C(16) intermediate **548**.

A Saksena-Evans reduction of **560** presented the C(3)-C(5) *anti*-hydroxyl array, which was protected as its acetonide, and desilylation with TBAF furnished **555** in reasonable yields. The formation of alkynone **552** began from the Swern oxidation of **555**, treatment with the acetylenic Grignard reagent, and final oxidation with Dess-Martin periodinane in excellent overall conversion. A zinc-mediated reduction of **552** was completed with the (*R*)-allyl silane **551** (see Scheme 93) in a formal “ene” reaction, to form the requisite C(1)-C(16) carbon backbone in excellent stereocontrol. This allowed the critical deprotection/*bis*-cyclisation to be carried out with aqueous HF, followed by an in-situ trapping of the C(9) acetal as its methyl glycoside, with trimethyl orthoformate. A bis-silylation of the resulting hydroxyls furnished **559**, and all that remained was to complete the C(13) olefin to methyl enoate transmutation.

A two-step procedure was employed to first access the exocyclic ketone, with an initial hydroxylation of **559** followed by a periodate cleavage. Once the ketone **561** was in place, a selective olefination using Fuji's chiral phosphanoacetate **59** was employed, delivering the enoate in a 2.6:1 mixture of epimers in favour of the desired (*E*) form. In comparison, Evans' found that his olefination on the exocyclic ketone of **58** using **59** (Scheme 15) was effected in a 5.5:1 ratio in favour of the desired isomer, and Nishiyama and Yamamura found that their olefination of **157** with **59** (Scheme 21) was completed in a 9:1 mixture in favour of the desired isomer.

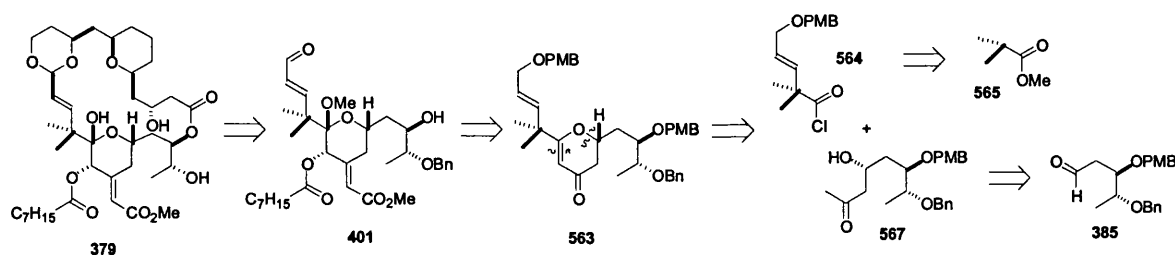
The intermediate **551** began with the conversion of the allylic bromide **562** to the allylsilane **554** (Scheme 93). This was followed by the copper-catalysed reaction of the Grignard component of **554** with the silyl protected (*S*)-glycidol **553** intermediate, and the synthesis of **551** was completed by the silyl etherification at C(16).



Scheme 93 Thomas's synthesis of the allylsilane intermediate **551**.

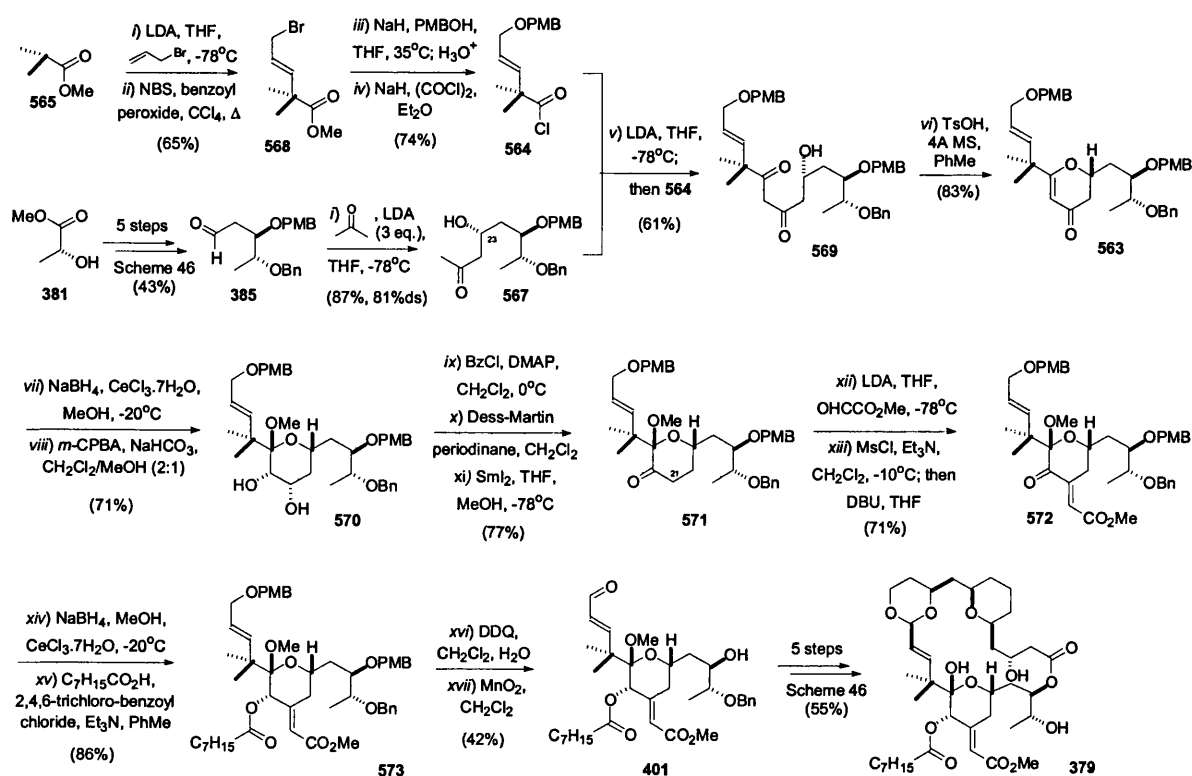
Wender's convergent synthesis of bryostatin analogue **379** ¹⁴⁰

During the course of his analogue programme, Wender found that the C(17)-C(27) bryostatin C-ring was of central importance for compounds possessing potent activity. In a second generation synthesis, Wender has shown that the analogue **379** (see Scheme 46) could be accessed via a more expedient route, using a more convergent synthesis (Scheme 94). This was carried out by the synthesis of the hydropyranone **563** that underwent elaboration to the known C(17)-C(27) C-ring **401**. Disconnection of the pyran revealed the acid chloride **564**, formed from the alkylation of methyl isobutyrate **566**, and the ketone **567**, formed via the addition of the enolate of acetone to the known aldehyde **385**. The major significant enhancement of this route is the reduction in the number of steps required, and the selectivity achieved at C(23) of 81% ds, compared to its racemate. More elaborate schemes were also attempted utilising this more convergent strategy, however they resulted only in a greater number of transformations and reduced the selectivity achieved at C(23).



Scheme 94 Wender's updated synthesis of the analogue **379**.

The redesigned synthesis began with the alkylation of methyl isobutyrate **565** (Scheme 95) using allyl bromide, and subsequent radical bromination to yield **568**, which then underwent conversion to the PMB ether by displacement with the alkoxide ion, derived via the deprotonation with sodium hydride. It was fortuitously found that with an aqueous quench, the reaction delivered the acid in good overall yield, and this then underwent treatment with oxalyl chloride to form the acid chloride **564**.



Scheme 95

Wender's convergent route to analogue **379**.

The requisite C(27)-C(20) synthon **567** commenced with the first 5 steps of the previously reported synthesis (see Scheme 46) to produce the aldehyde **385** in 43% overall yield. This then underwent condensation with the enolate derived from acetone and LDA to deliver **567** in a much improved 81% ds for the C(23) hydroxyl, in comparison to a racemic mixture achieved in Scheme 46. Completion of the carbon backbone was generated from the *bis*-anion of **567** with the acid chloride **564**, which then underwent ring closure and dehydration to the hydropyranone **569** under mildly acidic conditions.

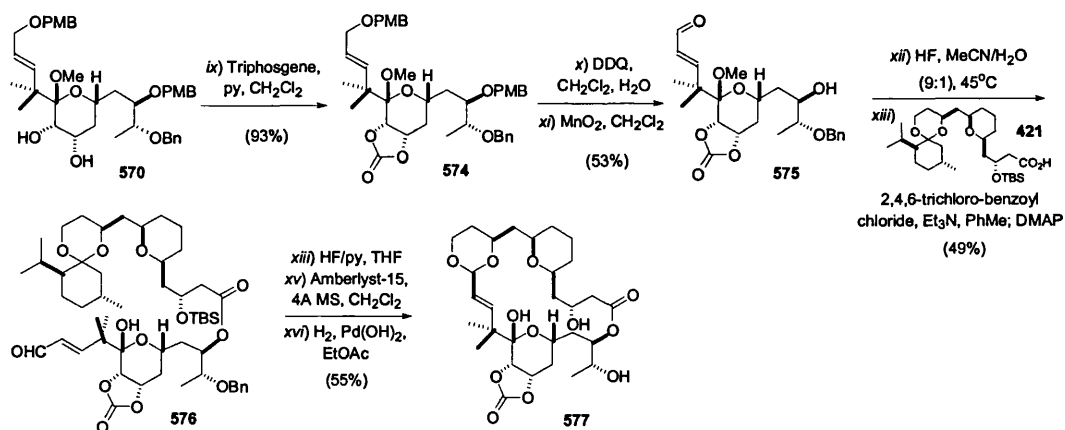
The following transformations to **573** were a repetition of the work previously reported (steps *ix* to *xviii* in Scheme 46), although they are shown above for clarity, with the only difference being the in-situ base-mediated dehydration to yield the exocyclic olefin **572**. Once **573** was in-hand, the PMB ether protecting groups were cleaved with DDQ, allowing the selective oxidation at C(15) with manganese dioxide to take place, thereby yielding the known α,β -unsaturated aldehyde **401**. This could then in-turn be converted to the analogue **379** using the previously reported transformations in 5 steps.

The significance of this second generation synthesis has been to reduce the number of overall steps from 43 to 38, with the longest linear sequence reduced to 23 from 29 steps. It has also served to incorporate an increased selectivity at C(23), thus making possible future commercial exploitation.

Wender's synthesis of novel bryostatin analogue 577

In continuation of his convergent strategy, Wender has developed analogue **577** to demonstrate the effectiveness of producing much simplified bryostatin scaffolds. In the case of **577** the spacer domain has been altered to incorporate a carbonate at C(20)-C(21), thereby dispensing with the exocyclic olefin and lipophilic side chain.

By treating diol **570** with triphosgene (Scheme 96) the hydroxyls were locked as their carbamate in, good yield. Removal of the PMB ether of **574** with DDQ and subsequent allylic oxidation yielded the α,β -unsaturated aldehyde **575**, which then underwent hydrolysis of the methyl glycoside under the optimised conditions of aqueous HF at 45°C. This allowed the esterification under Yamaguchi conditions with the acid **421** (Schemes 47 and 48), and final ring closure of **576** under acidic conditions. The novel analogue **577** was completed by hydrogenation of the benzyl protecting group at C(26) in a significantly reduced 18 step synthesis.



Scheme 96

Wender's synthesis of the novel analogue **577**.

The advancements which Wender has achieved are most notable, and in particular the activity of the new analogue are awaited in due course. This has shown the utility of a convergent strategy to reveal targets that are commercially viable, and sets a precedent in the field of bryostatin drug research. These results have been complemented by a number of patents describing the research, and are forerunners to developing meaningful drug candidates.

Advancements in the bryostatin biosynthesis and biological research field

Bryostatin 1 is currently undergoing a significant number of clinical trials in man, including treatments for recurrent epithelial ovarian carcinoma ¹⁴¹, renal cancer ¹⁴², and human myeloid leukaemia cells ¹⁴³. These have included the administration of bryostatin 1 as a singular candidate, but most often in co-administration with a second candidate. There have been some encouraging results, especially in the treatment of human breast cancer ¹⁴⁴, where it has been shown that bryostatin 1 causes up-regulation of the apoptotic p53 enzyme.

Further research into B-cell malignancies ¹⁴⁵ has demonstrated that bryostatin 1, in conjunction with vincristine, activates PKC with a short-term exposure, but on prolonged exposure leads to a depletion of PKC. This has meant an increase in apoptotic frequency, leading to a clinical response or stable disease condition in a number of patients, although more investigation into the process is ongoing to understand the precise mechanism of action.

A greater understanding in the geographical differences of bryostatin natural production has also been established ¹⁴⁶. This has investigated the fact that bryostatin may deter predators of its animal hosts, and that bryostatin biosynthesis is more likely to result not from a local adaptation of species, but as a response to bacterium produced as protection against predators. This has been carried out by studying mitochondrial cytochrome oxidase sequences, and their geographical distributions within *Bugula neritina* showing differences in individuals south of Cape Hatteras compared to its more northern counterparts.

There has also been significant investigation by the Haygood laboratory ¹⁴⁷ into the role of the bacterium that live in the larvae of the host *Bugula neritina*, which play a part in the synthesis of bryostatin. The hope is to isolate or clone these microorganisms, to develop an economical process for bryostatin synthesis. Some initial work carried out has shown that laboratory cultured *Bugula neritina*, treated with antibiotics to decrease the levels of the bacteria within, has showed a decrease in bryostatin content. Continuation in this area has significance in the aquaculture of bryostatin in complementary efforts of meaningful amounts of bryostatin production.

-
- 139 O'Brien, M.; Taylor, N. H.; Thomas, E. J.; *Tet. Lett.*, **2002**, *43*, 5491-94
- 140 i) Wender, P.A.; Koehler, M. F.T.; Sendzik, M.; *Org. Lett.*, **2003**, *5*, 24, 4549; ii) Wender, P. A.;
Lippa, B.; Park, C. M.; Hinkle, K. W.; *U.S. Pat. Appl. Publ.*, **2003**, 91 pp; iii) Wender, P. A.;
Lippa, B.; Park, C. M.; Hinkle, K. W.; *PCT Int. Appl.*, **2003**, 154 pp.
- 141 Clamp, A. R.; Blackhall, F. H.; Vasey, P.; Soukop, M.; Coleman, R.; Halbert, G.; Robson, L.;
Jayson, G. C.; *British J. Cancer*, **2003**, *89*, 7, 1152.
- 142 Madhusudan, S.; Protheroe, A.; Propper, D.; Han, C.; Corrie, P.; Earl, H.; Hancock, B.; Vasey,
P.; Turner, A.; Balkwill, F.; Hoare, S.; Harris, A. L.; *British J. Cancer*, **2003**, *89*, 8, 1418.
- 143 Wang, S.; Wans, Z.; Grant, S.; *Mol. Pharm.* **2003**, *63*, 1, 232.
- 144 Ali, S.; Aranha, O.; Li, Y.; Pettit, G. R.; Sakar, F. H.; Philip, A. A.; *Cancer Chem. Pharm.* **2003**,
52, 3, 235.
- 145 Dowlati, A.; Lazarus, H. M.; Hartman, P.; Jacobberger, J. W.; Whitacre, C.; Gerson, S. L.;
Ksenich, P.; Cooper, B. W.; Frisa, P. S.; Gottlieb, M.; Murgo, A. J.; Remick, S. C.; *Clin. Cancer*
Res. **2003**, *9*, 16(1), 5929.
- 146 McGovern, T. M.; Hellberg, M. E.; *Mol. Ecology*, **2003**, *12*, 5, 1207.
- 147 Haygood, M.; Hildebrand, M.; Anderson, C.; Waggoner, L. E.; Sherman, D. H.; Liu, H.; *PCT Int.*
Appl., **2003**, 342 pp.